Université catholique de Louvain

Institute of NeuroScience

# THE DYSREGULATION OF MICRORNAS IN MULTIPLE SCLEROSIS AND THEIR INVOLVEMENT IN THE DIFFERENTIATION OF OLIGODENDROCYTE PROGENITOR CELLS

Océane Perdaens

Promoter: Vincent van Pesch

November 2023

**Promoter**

Prof. Vincent VAN PESCH, UCLouvain, Belgium

**Assessment committee**

Prof. Emmanuel HERMANS (president), UCLouvain, Belgium

Prof. Marie-Cécile NASSOGNE (secretary), UCLouvain, Belgium

Prof. Laure DUMOUTIER, UCLouvain, Belgium

Prof. Miikka VIKKULA, UCLouvain, Belgium

Dr. Evgenia SALTA, Netherlands Institute for Neuroscience, The Netherlands

Prof. Marcin MYCKO, University of Warmia and Mazury, Poland

*We delight in the beauty of the butterfly, but rarely admit the changes it has gone through to achieve that beauty.*

Maya Angelou

Table of content

List of figures

*INTRODUCTION*



*CHAPTER 1*



*CHAPTER 2*

*CHAPTER 3*

*DISCUSSION*

List of tables

*INTRODUCTION*



*CHAPTER 1*



*CHAPTER 2*

*CHAPTER 3*

List of abbreviations

| Abbreviation | Definition |
|---|---|
| 3'UTR | 3’ untranslated region |
| 5'UTR | 5’ untranslated region |
| ABL | Abelson gene |
| AD | Alzheimer's disease |
| adj.p/padj | adjusted p-value |
| AGO | Argonaute protein/Argonaute RISC catalytic component |
| AKAP13 | A-kinase anchoring protein 13 |
| ALDOC | aldolase fructose-bisphosphate C |
| AMS | active MS |
| AP1 | activator protein 1 |
| ARHGAP5 | Rho GTPase activating protein 5 |
| ASCL1 | Achaete-Scute family bHLH transcription factor 1 |
| BBB | Blood-brain barrier |
| BCR | B cell receptor |
| BDNF | brain derived neurotrophic factor |
| bHLH | basic helix-loop-helix |
| BMP | bone morphogenetic protein |
| BNIP3L | Bcl2 interacting protein 3 like |
| Breg | regulatory B cell |
| BTK | Bruton’s tyrosine kinase |
| CCL | C-C motif chemokine ligand |
| CCND1 | cyclin D1 |
| CCR7 | C-C motif chemokine receptor 7 |
| CD40L | CD40 ligand |
| CDC42 | cell division cycle 42 |
| CDK5/6 | cyclin dependent kinase 5/6 |
| CDKN1A | cyclin dependent kinase inhibitor 1A |
| c-FOS | c-FOS proto-oncogene, subunit activator protein 1 (AP1) complex |
| CIS | clinically isolated syndrome |
| c-JUN | c-JUN proto-oncogene, subunit activator protein 1 (AP1) complex |
| c-MYB | c-MYB proto-oncogene, transcription factor |
| c-MYC | c-MYC proto-oncogene, bHLH transcription factor |
| CNP | 2',3'-cyclic nucleotide 3' phosphodiesterase |
| CNS | central nervous system |
| CPEB1 | cytoplasmic polyadenylation element binding protein 1 |

| | |
|---|---|
| CSF | cerebrospinal fluid |
| Ct | cycle threshold |
| CTLA4 | cytotoxic T lymphocyte associated protein 4 |
| CXCL | C-X-C motif chemokine ligand |
| CXCR | C-X-C motif chemokine receptor |
| DEG | differentially expressed gene |
| DGCR8 | DiGeorge syndrome critical region gene 8 |
| DIFF | differentiation medium |
| DIS | dissemination in space |
| DIT | dissemination in time |
| DMT | disease modifying therapy |
| DRG | dorsal root ganglia |
| EAE | experimental autoimmune encephalomyelitis |
| EDSS | Expanded Disability Status Scale |
| EGFR | epidermal growth factor receptor |
| EIF4 | eukaryotic translation initiation factor 4 |
| EIF4EBP | eukaryotic translation initiation factor 4E binding protein 1 |
| ELMO1 | engulfment and cell motility 1 |
| ELOVL7 | elongation of very long chain fatty acids protein 7 |
| EMSA | electrophoretic mobility shift assay |
| ERBB | ErbB tyrosine kinase receptor family member |
| ERK | extracellular signal-regulated protein kinase |
| ERRFI1 | Erbb receptor feedback inhibitor 1 |
| EV | extracellular vesicle |
| FAR1 | fatty acyl-coA reductase 1 |
| FC | fold change |
| FDR | false discovery rate |
| FGF | fibroblast growth factor |
| FGFR | fibroblast growth factor receptor |
| FKLC | free kappa light chain |
| FOXP3 | forkhead box protein P3 |
| FPKM | fragments per kilobase million |
| GA | glatiramer acetate |
| Galc | galactocerebroside |
| GEL | gadolinium enhancing lesion |
| GFAP | glial fibrillary acidic protein |
| GM-CSF | granulocyte-macrophage colony-stimulating factor |
| GO | Gene Ontology |

| | |
|---|---|
| GPR17 | G-protein-coupled receptor 17 |
| GPT2 | glutamic-pyruvic transaminase 2 |
| GRB2 | growth factor receptor-bound protein 2 |
| GSK3B | glycogen synthase kinase 3b |
| HC | healthy control |
| HDAC1/2 | histone deacetylase complex 1/2 |
| HES1/5 | Hes family bHLH transcription factor 1/5 |
| HLA | human leukocyte antigen |
| hnRNP | heterogeneous nuclear ribonucleoprotein |
| Hprt1 | hypoxanthine phosphoribosyltransferase 1 |
| hsa | homo sapiens |
| ICAM1 | intercellular cell adhesion molecule 1 |
| ID2/4 | inhibitor of DNA binding 2/4 |
| IFNb | interferon beta treatment |
| IFNg | interferon gamma |
| Ig | immunoglobulin |
| IGF | insulin like growth factor |
| IKK | inhibitor of nuclear factor kappa B kinase |
| IL | interleukin |
| IMS | inactive MS |
| Infect-ND | infectious neurological disorder |
| Inflam-ND | inflammatory neurological disorder |
| IRAK1/4 | interleukin 1 receptor associated kinase 1/4 |
| IRES | internal ribosome entry site |
| JAK | Janus kinase |
| JNK | c-Jun N-terminal kinase |
| KAT5 | Lysine acetyltransferase 5 |
| KEGG | Kyoto Encyclopaedia of Genes and Genomes |
| L2K | Lipofectamine™ 2000 |
| LFA1 | Lymphocyte function-associated antigen 1 (integrin alpha L/beta 2) |
| LINGO1 | Leucine-rich repeat and immunoglobulin domain-containing 1 |
| lncRNA | long non-coding RNA |
| LPS | lipopolysaccharide |
| LRP5/6 | lipoprotein receptor related protein 5/6 |
| MAG | myelin associated glycoprotein |
| MAPK | mitogen-activated protein kinase |
| MAPKAPK | MAPK-activated protein kinases |
| max | maximum |

| | |
|---|---|
| MBP | myelin basic protein |
| MCT1 | monocarboxylate transporter 1 |
| MHC | major histocompatibility complex |
| min | minimum |
| miRISC | microRNA-induced silencing complex |
| miRNA | microRNA |
| miR-NC | microRNA negative control mimic |
| MMP | matrix metalloproteinase |
| mmu | mus musculus |
| MOBP | myelin oligodendrocyte basic protein |
| MOG | myelin oligodendrocyte glycoprotein |
| MRI | magnetic resonance imaging |
| mRNA | messenger RNA |
| MS | multiple sclerosis |
| mTOR | mammalian target of rapamycin kinase |
| MXA | human myxovirus resistance protein 1 |
| MYD88 | myeloid differentiation innate immune signal transduction adaptor |
| MYRF | myelin regulatory factor |
| NA | not applicable |
| ND | not done |
| Ndel1 | nude neurodevelopment protein 1 like 1 |
| Nebl | nebulette |
| NF-kB | nuclear factor of kappa light polypeptide gene enhancer in B cells |
| NKX2.2 | NK2 homeobox 2 |
| NLRP3 | NLR family pyrin domain containing 3 |
| NMDA | N-methyl-D-aspartate |
| No. / n | number |
| NOTCH | Notch receptor |
| NR4A2 | nuclear receptor subfamily 4 group A member 2 |
| ns | non-significant |
| Ntrk2 | neurotrophic receptor tyrosine kinase 2 |
| nt | nucleotide |
| OCB | oligoclonal immunoglobulin G band |
| OL | oligodendrocyte |
| OLIG1/2 | oligodendrocyte transcription factor 1/2 |
| OMGP | oligodendrocyte-myelin glycoprotein |
| OND | other neurological disorders |
| OPC | oligodendrocyte progenitor cell |

| | |
|---|---|
| p | p-value |
| PABP | polyadenylate [poly(A)] binding protein |
| PAK | p21 activated kinase |
| PBMC | peripheral blood mononuclear cell |
| PCA | principal component analysis |
| PCNA | proliferating cell nuclear antigen |
| PD | Parkinson's disease |
| PDCD4 | programmed cell death 4 |
| PDGFA | platelet-derived growth factor A |
| PDGFRA | platelet-derived growth factor receptor A |
| PI3K | phosphatidylinositol-4,5-bisphosphate 3-kinase |
| PIRA | progression independent of relapse activity |
| PLP1 | proteolipid protein 1 |
| PMS | progressive multiple sclerosis |
| PPMS | primary progressive multiple sclerosis |
| pre-microRNA | precursor microRNA |
| pre-OL | premyelinating oligodendrocyte |
| pri-microRNA | primary microRNA |
| PROL | proliferation medium |
| PTEN | phosphatase and tensin homolog |
| PTK2 | protein tyrosine kinase 2 |
| PTPRJ | protein tyrosine phosphatase receptor type J |
| RAC1 | Rac family small GTPase 1 |
| RAW | relapse-associated worsening |
| Rel MS | relapsing MS patients |
| Rem MS | remitting MS patients |
| RHEB | Ras homologue enriched in brain |
| RHOA | Ras homolog family member A |
| RICTOR | RPTOR independent companion of mTORC2 |
| RIPK1 | receptor interacting protein kinase 1 |
| RIS | radiologically isolated syndrome |
| RNAseq | RNA sequencing |
| rno | rattus norvegicus |
| RNS | reactive nitrogen species |
| RNU6 | small nuclear ribonucleoprotein U6 |
| ROC | receiver operating characteristic |
| ROCK | Rho associated coiled-coil containing protein kinase |
| RORC/RORgT | RAR Related Orphan Receptor C / gamma T |

| | |
|---|---|
| ROS | reactive oxygen species |
| RPS6 | ribosomal protein S6 |
| RPS6KB1 | ribosomal protein S6 kinase B1 |
| RPTOR | regulatory associated protein of mTORC1 |
| RRAS2 | Ras related 2 |
| RRMS | relapsing-remitting multiple sclerosis |
| RT-qPCR | real time quantitative polymerase chain reaction |
| SC | symptomatic control |
| SD | standard deviation |
| SEMA3A/3F | semaphorin 3A/3F |
| SHC | Src homology 2 domain containing transforming protein |
| SHH | Sonic hedgehog |
| siRNA | small interfering RNA |
| SMAD | small mother's against decapentaplegic homolog family member |
| sNfL | serum neurofilament light chain |
| SOCS1 | suppressor of cytokine signalling 1 |
| SOX | SRY box transcription factor |
| SPMS | secondary progressive multiple sclerosis |
| SREBP2 | sterol regulatory element-binding protein 2 |
| STAT | signal transducer and activator of transcription |
| SYNM | synemin |
| TBX21 / TBET | T-box transcription factor 21 |
| TCF7L2 | transcription factor 7 like 2 |
| $T_{CM}$ cell | central memory T cell |
| TCR | T cell receptor |
| $T_{EM}$ cell | effector memory T cell |
| TGFb | transforming growth factor beta |
| Th | T helper cell |
| TLR | Toll-like receptor |
| TNFa | tumour necrosis factor alpha |
| TNFR | tumour necrosis factor receptor |
| Tr1 | type 1 regulatory T cells |
| TRAF6 | TNF receptor associated factor 6 |
| TRBP | TAR RNA binding protein |
| Treg | regulatory T cell |
| TSC1/2 | tuberous sclerosis complex, subunit 1 and 2 |
| VAMP2 | vesicle associated membrane protein 2 |
| VCAM1 | vascular cell adhesion molecule 1 |

| | |
|---|---|
| VehCo | vehicle control |
| VIM | vimentin |
| VLA4 | very late activation 4 (integrin alpha 4/beta 1) |
| vs. | versus |

# INTRODUCTION

# I. Multiple sclerosis

## i. A little bit of history

A woman from Iceland, called Halla, experienced at some point between 1293-1323 acute bilateral optic neuritis and severe dysarthria. She progressively recovered over a two-week time span [1]. Lidwina (1380-1433) from Schiedam, Holland fell while ice-skating at the young age of 15. She fractured a rib and developed an abscess. Hereafter she experienced difficulty in walking and what would be characterised as paresis of the right upper limb, facial paresis, trigeminal neuralgia, and right optic neuritis, with transient partial remission but finally progressive worsening [2]. Lidwina accepted her illness that was said to come directly from God and was canonised in 1890. Those two stories of the fourteenth century are speculated to be the first described cases of multiple sclerosis (MS), although, as historically originating from the popular culture, they cannot be verified scientifically [3]. Supported by verified sources, Auguste d'Este (1794-1848), illegitimate grandson of George III of England and cousin of Queen Victoria, autobiographically described the 26-year progressive course of his affection that had started with optic neuritis in 1823 of which he recovered but relapsed three years later. He also suffered of lower limb paresis, paraesthesia, bladder and bowel control problems and Uhthoff's phenomenon [3]. While there are other examples, Charles-Prosper Ollivier d'Angers (1796-1845) probably published the first case report of MS in his treatise (*Maladie de la moelle épinière* [Diseases of the spinal cord], 1824) [4].

In the nineteenth century, diseases were rather classified based on an overlapping semiology in large symptom clusters, such as paralysis, paraplegia or chorea. Herein, two independent anatomical drawings by Robert Carswell (1793-1857) in 1838, who was studying atrophy, and Jean Cruveilhier (1791-1874) in 1841, who was attempting to localise the sensory and motor tracts within the spinal cord, have retrospectively been accredited as multiple sclerosis or at least as a demyelinating disorder, although for Carswell's case any clinical information is largely missing [5]. Shortly after, in 1857 Karl von Rokitansky (1804-1878) offered a first description of fatty corpuscules (corresponding to myelin debris) in lesions. In 1863, Eduard von Rindfleisch (1836-1908) acknowledged the perivascular distribution of plaque lesions [4,5].

Contemporaneous German physicians, Friedrich Theodor von Frerichs (1819-1885) and his pupil Wilhelm Valentiner (1830-1893), described, in 1849 and 1856 respectively, *Hirnsklerose* (brain sclerosis) with some provisional clinical and pathological characteristics, although probably lacking the institutional and research facilities of the French physicians to obtain broader recognition [4–6].

In 1868, Jean Martin Charcot (1825-1893) offered in "*Histologie de la sclérose en plaques*" a detailed description of the histopathological features of the disease, which he could precisely link to its clinical symptomatology, as a result of his intensive research with his colleague, clinical physician Doctor Edmé Félix Alfred Vulpian (1826-1887), and with his doctoral fellow, Doctor Leopold Ordenstein (1835-1902) who clinically and anatomopathologically confronted Parkinson's disease, then-called paralysis agitans, with multiple sclerosis [5,6]. In the mid-nineteenth century in France the reorganisation of smaller hospitals into bigger centralised and specialised institutions, as La Salpêtrière, allowed Charcot, Vulpian and their team to have a stable and large cohort of patients for long term clinical observations, easily followed by anatomohistological studies after the patient had deceased, thanks to the proximity of the autopsy room and to the use of new German microscopic technologies (e.g. tissue staining techniques). Hence, thanks to this accurate and comprehensive clinicopathological approach, they historically set MS as a distinct disease entity [5].

Interestingly, in 1903 Raymond Cestan (1872-1933) and Claudien Philippe (1866-1903) as first acknowledged the vulnerability of the grey matter to the disease process. They described cortical lesions and neurodegeneration, which they linked to cognitive impairment and psychological symptoms [7].

Hereafter, the diagnosis of multiple sclerosis remained challenging for multiple reasons [8]. Firstly, medicine only started to be "compartmentalised" into specialties, which required some time to establish the expertise, but also to set the postgraduate programme and training of new candidates as well as to open specialised wards. Medical perceptions needed to evolve, as differential diagnoses as neurosyphilis and hysteria were primarily considered. Furthermore, for many years multiple sclerosis remained exclusively a clinical diagnosis. While physicians were aware of its relapsing-remitting course from as early as Charcot's description (and even before), this also meant that sometimes years could pass by in between relapses before the diagnosis was properly documented. This changed with the

introduction of new, and still evolving, imaging techniques and biomarkers [9,10]. Brain lesions were first described on magnetic resonance imaging (MRI) in 1981, that was found to be superior to computed tomography, and gadolinium enhancing lesions, reflecting leakage of the blood-brain barrier (BBB), in 1986. It would take at least one more decade to set it as a diagnostic tool in clinical routine while it was included in the diagnostic criteria only in 2001 [9,11,12]. Research on MRI techniques currently evolves quickly, allowing the detection of cortical lesions, chronic active paramagnetic rim lesions, leptomeningeal enhancement, microstructural tissue integrity, among others, although this is not yet set in clinical practice.[13–15] Oligoclonal immunoglobulin G bands (OCBs), produced by B cell clones in the cerebrospinal fluid (CSF), were first detected in 1959 by Karcher, van Sande and Lowenthal at the Institute of Tropical Medicine in Antwerp (Belgium) and named this way by the Belgian neurologist Emile-Christian Laterre [16–18]. CSF-specific OCBs are present in about 90% of MS patients. Although they can also be detected in other inflammatory disorders, they are an important additional diagnostic criterion in case of a clinical suspicion of MS [19,20].

### ii. Natural history

Multiple sclerosis is a chronic inflammatory, demyelinating and neurodegenerative disorder of the central nervous system (CNS) [21–23]. MS can follow a relapsing-remitting (RRMS) or a progressive (PMS) course (figure 0.1). Lublin e.a. [24] offered to specify the disease course by its activity, i.e. inactive versus (vs.) active RRMS/PMS based on clinical and/or radiological evidences, as well as by its progression in PMS.

MS diagnosis was fully clinical before the advent of MRI. Several have offered clinical diagnostic criteria, as the historical symptoms triad of Charcot (nystagmus, intention tremor, scanning speech), but these symptoms were often not specific to MS, as they are the functional translation of active/chronic MS lesions [5,25]. The diagnosis of MS hinges on two principles, namely the clinical and/or radiological evidence that lesions occur in at least two characteristic areas of the CNS and develop over time, referred to as dissemination in space and time (DIS/DIT), first implied in 1954 by Allison and Millar, then stated in 1965 by Broman e.a. [26,27]. The modern diagnostic criteria, including paraclinical tests (mainly MRI and CSF analysis), have been revised several times since Poser in 1983 until McDonald in

2017, in order to facilitate and quicken an accurate diagnosis. However, this also limits the comparison of MS cohorts over time, especially for epidemiological studies [27–29]. In the current diagnostic criteria, DIS is supported by the presence of T2-hyperintense MRI lesions in different characteristic areas (periventricular, (juxta)cortical, infratentorial or spinal cord) if needed with an additional clinical history of an event incriminating distinct CNS sites. DIT is supported by the occurrence of multiple clinical events, by the concomitant presence of active (gadolinium enhancing T1-weighted) lesions (reflecting the breakdown of the blood-brain barrier) and inactive (T2-weighted) lesions or by the presence of CSF-specific OCBs [29].

RRMS affects a majority of patients, with an increasing female-to-male ratio of 2-3 to 1 and age of onset on average within the third-fourth decade of life, although it can already occur in children and adolescents [30–34]. Herein, patients present with acute relapses, in which the confined inflammatory assault within the CNS clinically translates into new or exacerbating neurological symptoms lasting for more than 24 hours and up to 3 months, and radiologically into gadolinium enhancing lesions [24,35]. These relapses alternate with longer periods of remission characterised by complete/incomplete recovery of the neurological deficits. Remarkably, the relapse rate and the number of gadolinium enhancing lesions is higher in women and the decline in relapse activity is related to patient's age rather than disease duration [36,37].

Most patients will evolve within approximately 20 years after disease onset into secondary progressive MS (SPMS), while a minority of patients immediately present with a progressive phenotype, with no history of relapses, called primary progressive MS (PPMS). Age of progression onset is within the fifth-sixth decade of life for both SPMS and PPMS [30,38,39]. The female-to-male ratio decreases for PMS as compared to RRMS. Thus, men are more at risk to develop PMS and to reach certain disability landmarks, which is mirrored by the accelerated grey matter atrophy in men, impacting especially cognitive functions [40,41]. PMS is characterised by a steady progression of the disease, marked by continuous worsening of the neurological deficits, especially regarding ambulation and cognitive function, clinically evidenced by the Expanded Disability Status Scale (EDSS) [35,42–44]. As specified by the descriptors of Lublin, PMS can have plateau-phases of non-progression but also

superimposed acute phases of disease activity, although the latter is more frequent in SPMS [24].

In fact, MS is rather a single disease continuum of neuroinflammation and neurodegeneration reflected by disability worsening due to relapses and underlying, initially silent, disease progression. Age is a critical factor, marked not only by premature immunosenescence in MS but also by changes in the pathophysiology of MS with ageing (neurodegeneration, chronic inflammation, lack of remyelination) [23,45,46]. The impact of relapses on long-term disability worsening and progression is still debated, and might be more evident in women and when occurring early, within the first two years of disease onset, but vanishes at higher disability landmarks (EDSS ≥ 4) [40,47–51]. On the contrary, progression independent of relapse activity (PIRA), i.e. the worsening of EDSS and other functional tests without any (mainly) clinical evidence of relapse, seems to be a bigger burden than relapse-associated worsening (RAW), starting already very early in the disease, increasing with age and occurring more frequently in men [45,52]. The ongoing neurodegeneration occurs silently from disease onset until it becomes clinically evident as disease progression when the compensatory CNS mechanisms are exhausted [53]. Hence, reaching a certain level of disability and onset of disease progression are rather depending on age than on any other factor [30,54]. Radiologically, silent disease progression is seen within chronic active, slowly expanding lesions with smouldering inflammation [55,56].

The evolution in the diagnostic criteria gave rise to two new disease categories, clinically and radiologically isolated syndrome (CIS/RIS). CIS patients present with a first demyelinating event suggestive of MS, that does not fulfil the criteria of DIS and/or DIT. However, the presence of CSF-specific OCBs replaces the DIT criterion, as these patients are at risk of converting to MS [24,29,57,58]. About 20% of patients without MRI lesions and 60-80% of patients with MRI lesions will eventually convert to MS. Other risk factor include young age and female gender [57]. RIS relies on the, often incidental, discovery of MRI lesions suggestive of a demyelinating disease with no record of neurological events [59,60]. Young age, male gender and spinal cord lesions predicted conversion to MS in a multivariate model. Moreover, up to one third of RIS patients have signs of cognitive impairment [61,62].

The latest McDonald criteria categorise a higher proportion of patients with a first demyelinating event as RRMS by the presence of OCBs, substituting for the need to

demonstrate DIT on a further MRI scan. This possibly results in more patients diagnosed with a milder disease course [29,63,64]. Attempts have been made to define benign MS, especially to support decision making for treatment. However, a non-negligible 20-35% of patients with so-called benign MS will have progressed at 20 years of disease onset under the most common definition of EDSS ≤ 3 at 10 years of disease onset [65–67]. Defining benign MS as EDSS ≤ 2 or even ≤ 1 at 10 years might be more accurate [66,67]. This remains however a retrospective observation and should be considered with caution. No prognostic model can reliably predict disease course at disease onset, while reducing relapse rate in the first two years of disease course is critical as it increases the risk of converting to SPMS and of accumulating disability [51,68].

Paediatric onset MS (POMS) has received increasing awareness because of its challenging differential diagnosis and its singular management [69,70]. There are at least 30.000 children younger than 18 diagnosed with MS worldwide (3-5% of MS patients), although it is rare before the age of 10 (<1%) [69,71,72]. Children present, even more than adults, with RRMS (98%) with a very active disease course (high relapse rate), but recover remarkably better [73–76]. It is difficult to differentiate POMS from acute demyelinating encephalomyelitis, especially in children younger than 10 presenting more frequently with polyfocal deficits and encephalopathy [69,70,77,78]. A primary progressive course is extremely rare, thus mitochondrial, neoplastic, and neurodegenerative disorders must be firmly excluded [69,79]. Although it takes longer for children to reach a certain disability landmark, they will still be on average 10 years younger than adult-onset MS patients when reaching them. In POMS, SPMS settles after a median disease duration of 28.1 years at a median age of 41.4 years [80]. Children with MS are also at risk of faster cognition decline due to impaired maturation of the cortical and deep grey structures driven by inflammatory and early neurodegenerative phenomena [81,82]. This may affect their academic, emotional and social functioning, and thus their perception on quality of life [83,84]. It is further predictive of earlier long-term cognitive impairment and worse socio-professional attainment in adulthood [85].

*Figure 0.1 Disease course*

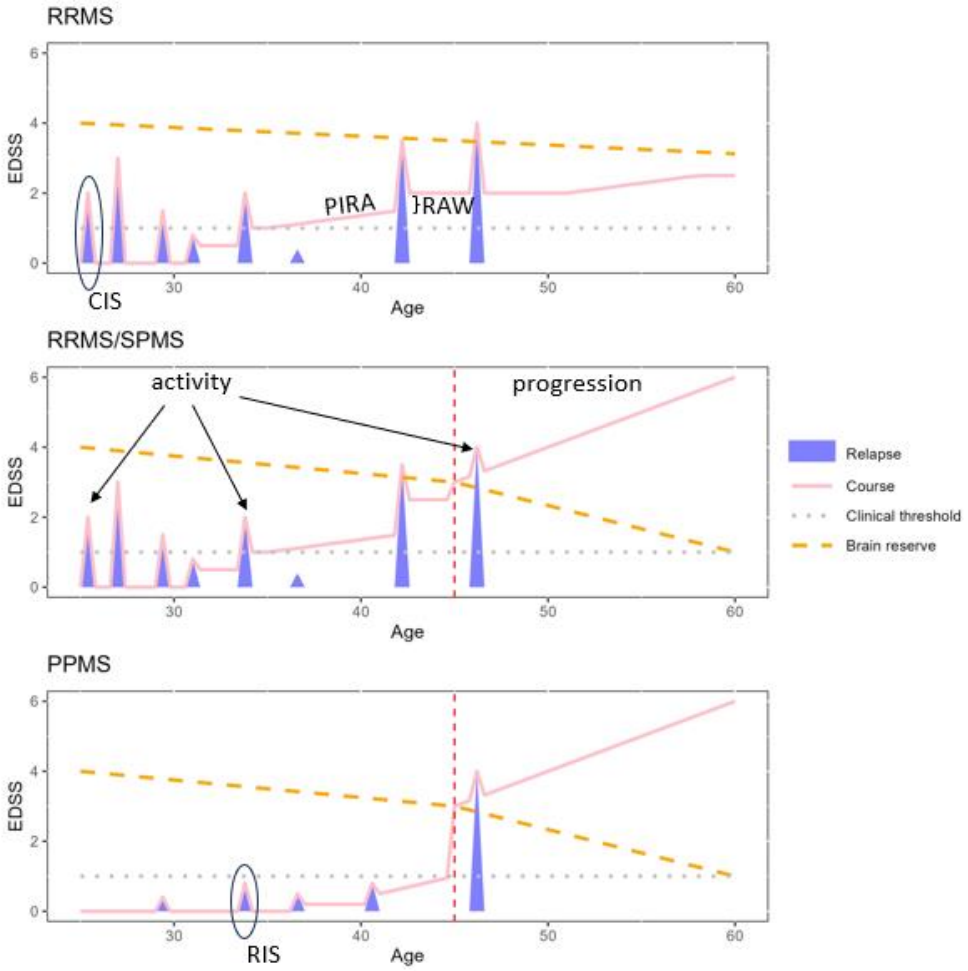


*These plots show the disease course (pink solid line) clinically evidenced by the Expanded Disability Status Scale (EDSS) score (y-axis) according to the patient's age (x-axis), for relapsing-remitting MS (RRMS), secondary progressive MS (SPMS) and primary progressive MS (PPMS). MS disease course is characterised by its activity and progression. Most patients present with a relapsing-remitting course. Hereby, relapses (blue pyramids) corresponding to acute demyelinating events are translated clinically by acute neurological symptoms and intermediate worsening of EDSS. They alternate with extended periods of remission. At the beginning, patients may recover completely, but with time, they might accumulate disabilities, as sequelae of the relapses, which is called relapse associated worsening (RAW). Patients may also progress independently of relapse activity (PIRA) as can be highlighted by*

*different functional tests, which can happen already early in the disease. Some RRMS patients will develop a progressive phenotype after a relapsing/remitting course, called secondary progressive MS. In progressive MS, patients suffer of progressive worsening, without necessarily having relapses, although they might occur at the beginning. A minority of patients develop the disease from onset as a progressive phenotype, which is then called primary progressive. Patients may also suffer from relapses remaining under the clinical threshold (grey dotted line). The brain reserve (orange dashed line) also decreases over time, due to ageing, neuroinflammatory and demyelinating processes. It contributes to neurodegeneration and may determine the transition into a progressive phenotype. A clinically isolated syndrome (CIS) corresponds to an isolated demyelinating event with neurological symptoms. Oppositely, a radiologically isolated syndrome (RIS) is a radiologically (MRI) evidenced demyelinating event without any history of related neurological symptoms, which might have been a relapse compensated by the brain reserve and thus not reaching the clinical threshold.*

### iii. Epidemiology

In 2020, 2.8 million people worldwide lived with multiple sclerosis, corresponding to a global prevalence of 35.9/100,000 people, an increase by 30% as compared to 2013 (Atlas of MS, www.atlasofms.org) [72]. To date, the prevalence reaches 100 to 300/100,000 people in most North American and European countries as well as in Australia, but is much lower, reaching <1-20/100,000 people in most Latin American, African and South-East Asian countries, although data coverage is low for Africa (56%) (www.atlasofms.org) [72,86–88]. According to the Viking hypothesis, the high prevalence areas coincide with the raiding, conquest and trading routes of the Vikings and their descendants (from the 9th century on) [1].

The important female preponderance of MS manifests in adolescence and is thus suggestive of a hormonal influence on MS risk. While in paediatric MS female-to-male ratio is around 1, especially before the age of 10, it largely increases post-puberty and slightly decreases in PMS, or after the age of 50, which is approximately around menopause [89–91]. A younger age of menarche correlates with an increased risk of MS and/or a younger age at first symptoms [92–95]. There is no clear explanation to this phenomenon, although it has been evidenced that women exhibit a more robust adaptive immune response, especially of encephalitogenic T helper cells [96–99]. The male hormones testosterone and dihydroxytestosterone (its

metabolite) are protective against MS through an immunosuppressive effect on T cells and macrophages [37,90,99–102]. On the contrary, the female hormone oestradiol is protective at higher levels, which explains that less relapses occur during the third trimester of pregnancy, while it is immunostimulatory at the lowest end of the physiological range on T cell immunity, but promotes humoral immunity at any dose [90,103–106]. Remarkably, parity has a cumulative protective effect on MS risk [107]. Prolactin, another female sex hormone, promotes T cell response and supports B cell autoreactivity [90,108,109].

Acknowledged risk factors include vitamin D deficiency, obesity in childhood, and possibly even in young adulthood (up to age 30), Epstein-Barr virus infection after early childhood, especially if symptomatic (as infectious mononucleosis), as well as smoking. Vitamin D deficiency and smoking can also increase the risk of disease progression [86]. Remarkably, vitamin D3 has a stronger immunomodulatory effect in women [110]. On the contrary, circulating levels of leptin, an immunostimulatory hormone linked to adipose inflammation, are higher in female, and adiposity advances the age of menarche, another risk factor of MS [92,93,111]. Interestingly, people migrating to a high prevalence country during childhood acquire a risk of MS close to the risk in their new country, on the contrary, if they migrate during adulthood, their risk remains similar to the risk in their country of origin [86].

Moreover, different populations living in a same country do not necessarily have the same risk, as seen for example by the lower prevalence (24.2/100,000 people) in the smaller indigenous Māori population as compared to the general disease prevalence (73.1/100,000 people) in New Zealand in which a majority of the population is of Scottish ancestry, hence implying a genetic susceptibility next to the environmental factors [112]. This is also supported by familial aggregation showing an increased risk of MS of 25-30% among monozygotic twins versus 2-5% among dizygotic twins or other first-degree relatives [113–115]. The genetic susceptibility of MS is polygenic, meaning that everyone possibly carries risk variants, and the combination of these determines the individual's total genetic risk [116]. A genome-wide association study by the International Multiple Sclerosis Genetics Consortium identified 233 susceptibility variants, of which 32 within the major histocompatibility complex (MHC) region [117]. Notably, the association of the human leukocyte antigen HLA-DRB1*15:01 haplotype, an major histocompatibility complex class II (MHC-II) allele promoting antigen presentation, with MS is long-

established in Caucasians only [118–121]. Remarkably, these candidate genes are largely involved in innate and adaptive immune cells as well as in microglia but barely or not in other CNS cell types, supporting the role of the immune system in the disease pathogenicity [114,116,117,122,123]. However, MS-associated genes in cerebral non-myeloid cells were linked to myelinating oligodendrocytes [124].

### iv. Treatment

Although multiple sclerosis is not curable, its management has remarkably improved over the last three decades and resides in three pillars: the rapid dampening of acute relapses by corticosteroids, the long-term modulation of the disease course by disease modifying therapies (DMTs), and the symptomatic treatment of MS-associated sequelae and comorbidities (neuropathic pain, bowel/bladder dysfunction etc.) [125].

The first DMTs, interferon beta and glatiramer acetate, were approved in the mid-1990s [126]. Since then, research in the field has expanded, resulting in a large panel of DMTs available today. Currently, all DMTs are effective in reducing the relapse rate and the lesion load and thus possibly slowing down disease progression in RRMS [125,127]. It is in fact acknowledged that the natural history of MS has changed since the introduction of DMTs, although DMTs are probably not the single drivers of this change, changes in diagnostic criteria and environmental factors play a role as well [128,129]. From disease onset, the median time to conversion to SPMS was 12 vs. 23 years and to EDSS score 6.0 was 22 vs. 30.4 years in a Swedish cohort of DMT naïve MS patients diagnosed between 1950 and 1964 vs. a predominantly treated MS cohort from the Swedish MS register assessed in July 2015 [38,129]. In the latter cohort, DMTs delayed the average age of sustained EDSS score 6.0 by 1.6 years [38].

Current DMTs target the inflammatory processes of the disease. They have an immunomodulatory effect on dendritic cells, T and/or B cells (interferon beta, glatiramer acetate, dimethyl fumarate), prevent lymphocyte egress from lymph nodes (sphingosine-1-phosphate receptor modulators as fingolimod, siponimod, ozanimod, ponesimod), prevent leukocyte transmigration into the CNS (natalizumab, an anti-a4-integrin monoclonal antibody), deplete B cells (rituximab, ocrelizumab and ofatumumab, anti-CD20 monoclonal antibodies) or activated T and B cells (alemtuzumad, an anti-CD52 monoclonal antibody), induce the

apoptosis of proliferating T and B cells by disrupting DNA synthesis (teriflunomide, an inhibitor of dihydroorotate dehydrogenase blocking pyrimidine synthesis) or DNA repair (cladribine, a purine analogue causing DNA strand breakage) [130,131].

Seen the large panel of DMTs, treatment choice is driven by efficacy, safety, and tolerability criteria. Although neurologists often start with a first line, less toxic DMT (interferon beta, glatiramer acetate, teriflunomide) and escalate to more effective DMTs in the event of ongoing activity, there is growing evidence that treating from the beginning with high-efficacy DMTs more effectively decreases the risk of progression [127,132,133]. Treatment options are still sparse for PMS. Overall, DMTs are more effective in PMS in younger patients with clinical or radiological signs of disease activity over the past 2 years [134]. To date, ocrelizumab is approved for active PPMS, siponimod for active SPMS [134–136].

New therapeutic classes that also target CNS resident cells, might expand the panel of DMTs in a near future. Clinical trials are ongoing for Bruton's tyrosine kinase (BTK) inhibitors (tolebrutinib, evobrutinib, fenebrutinib, remibrutinib, orelabrutinib) [137] in relapsing and/or progressive MS (phase 2 or 3 ongoing), for a receptor interacting protein kinase 1 (RIPK1) inhibitor (phase 1 completed, NCT04982991), and for a second generation CD40 ligand antagonist monoclonal antibody in RRMS and active SPMS (frexalimab, phase 2 ongoing, NCT04879628) (https://clinicaltrials.gov). BTK is a non-receptor tyrosine kinase downstream of the B cell receptor and Toll-like receptor (TLR) in B cells, participating in their development and maturation (from central pre-B cells up to the activation and terminal differentiation of circulating B cells) [137–140]. It also mediates microglia and macrophage activation via IgG-specific Fc receptor III and TLR signalling [137]. Phosphorylated BTK is increased in blood memory B cells of RRMS and SPMS patients [141]. Its expression level is also increased in B cells and in microglia in MS brain lesion samples [142]. Different from B cell depletion therapy, BTK inhibitors alter B cell function as antigen presenting cells for the development of encephalitogenic T cells without affecting their frequency and functional integrity [139]. The BTK inhibitor reduces the severity of secondary progressive autoimmune demyelination in an in vivo mice model [143]. RIPK1, increased in brain samples of MS patients and correlating with disease progression, induces a detrimental neuroinflammatory programme in microglia and astrocytes and mediates microglial cell death [144]. RIPK1 inhibition could also promote the proliferation of oligodendrocyte progenitor cells

(OPCs) by increasing the transcription of platelet derived growth factor receptor alpha via NFkB pathway [145]. The costimulatory receptor CD40 and its ligand (CD40L) can activate T, B and innate immune cells. Anti-CD40L antibody reduced the number of new lesions in MS patients vs placebo [146].

Stem cell transplantation has been considered as a therapeutic approach in aggressive MS, irresponsive to DMTs. Autologous hematopoietic stem cell transplantation can, by resetting the immune system, significantly increase relapse- and progression-free survival, yet especially in patients with RRMS and mild to moderate disability [147–151]. Bone marrow mesenchymal stem cell infusion lowers the severity of experimental autoimmune encephalomyelitis (EAE) by reducing immune cell infiltration, demyelination, and axonal damage, although this is not yet clearly established by clinical trials in MS patients [151–155]. Other yet experimental stem cell based strategies aim to promote remyelination via OPC differentiation and to possibly reduce neuroinflammation using neuronal stem cells, mesenchymal stem cell neuronal progenitors, human embryonic stem cell-derived neural precursors or induced pluripotent stem cells [151,156–160].

The neurodegenerative process in MS pathogenesis, resulting from primary and secondary axonal damage, due to neuroinflammation and demyelination, conceivably starts early in the disease and sustains progression and even silent progression that has been evidenced in absence of relapse [23,45]. Therefore, promoting remyelination, especially as it is inadequate and gradually insufficient, is a rational though unmet therapeutic strategy. Several agents that had proven promising in vitro and in vivo on the differentiation of oligodendrocyte progenitor cells and remyelination, have been tested in phase I and phase II studies over the past decades [161]. Neither erythropoietin (a phase 3 study in optic neuritis) nor opicinumab, an anti-LINGO1 monoclonal antibody (a phase 2 study in RRMS/SPMS) (for the function of LINGO1, cf. Introduction II.i) did show any functional improvement [162,163]. Clinical trials are currently ongoing for clemastine, an oral antihistamine drug with anti-muscarinic properties (as M1 muscarinic receptors possibly negatively regulate OPC differentiation[164,165] (NCT05131828/ NCT02521311/phase 2, NCT05338450/phase 3), Metformin, an activator of AMP-activated kinase pathway with anti-inflammatory effects on peripheral immune cells and proregenerative effects on OPCs by increasing the mitochondrial function[166,167] (NCT05131828/phase 2), CNM-Au8, an oral suspension of

catalytically active, clean-surfaced gold nanocrystals (NCT03993171/phase2, NCT04626921/phase 2-3), bazedoxifene, an oral selective oestrogen receptor modulator (NCT04002934/phase 2), and testosterone (NCT03910738/phase 2) (https://clinicaltrials.gov). Testosterone, that can be aromatised in oestradiol but not dihydoxytestosterone, and oestrogens are neuroprotective during EAE [168–170]. For the many others, further clinical trials seemed to have been delayed (https://clinicaltrials.gov) [161].

### v. Physiopathology

Multiple sclerosis is an immune-mediated demyelinating disorder of the CNS characterised by a focal inflammatory assault resulting in lesions of primary demyelination and gliosis in the white and grey matter, as well as by diffuse neurodegeneration resulting in brain and spinal cord atrophy [21–23]. The principal dogma states MS as a primary inflammatory disease with an activation of CNS-resident cells by invading immune cells from the periphery that jointly injure oligodendrocytes, their progenitor cells and the myelin sheaths causing secondary neuroaxonal damage [21,171]. Another, less defended concept of its pathogenesis sets it as a primary neurodegenerative disease by loss of glial support to axons amplified by secondary inflammatory demyelination [23,172,173].

Neuroinflammation is ongoing throughout the entire disease. Herein, two types of inflammation, although occurring in parallel, distinctively prevail at the relapsing and the progressive stage of the disease (figure 0.2) [21,22,174,175]. In the early phase of the disease, naïve CD4+ T cells are primed against myelin antigens in the periphery and differentiate towards encephalitogenic CD4+ T helper cells (Th1 and Th17). These activated cells migrate through an abnormally disrupted BBB by the interplay with endothelial cells involving chemokines and adhesion molecules and focally invade the CNS in a limited perivenular area [176–180]. By secreting inflammatory mediators as cytokines and chemokines, they then attract other peripheral immune cells, as CD8+ cytotoxic T cells, CD20+ B cells and macrophages, and activate CNS-resident cells, namely microglia and astrocytes [181–189]. CD8+ T cells become eventually predominant [190–192]. This inflammatory environment harms the homeostasis of oligodendrocytes and destroys the myelin sheaths, whereas

demyelinated axons are longer preserved although axonal transection has been evidenced early in the disease [171,193–200].

*Figure 0.2: Pathophysiology of multiple sclerosis*

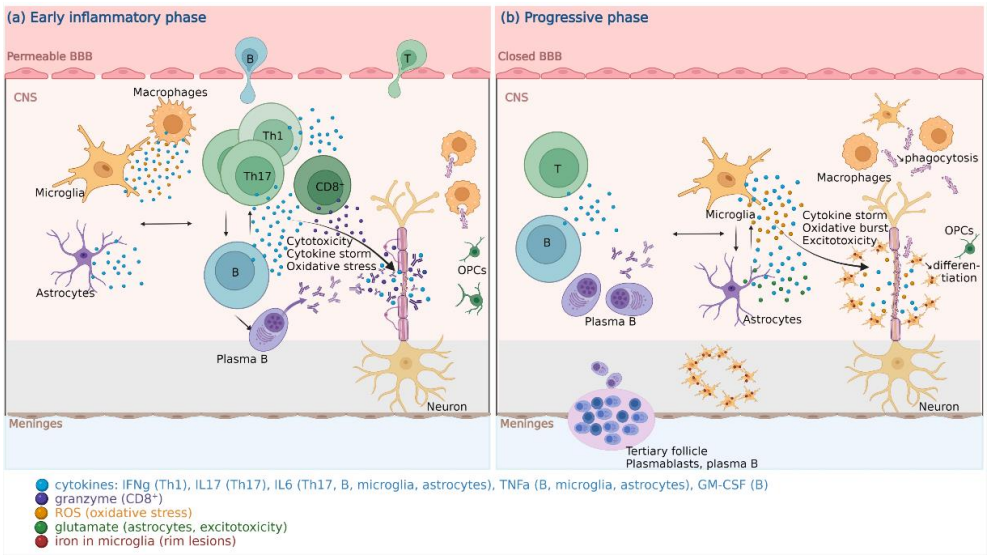


*(A) In the early inflammatory phase of MS, peripheral adaptive immune cells infiltrate the CNS through a disrupted BBB. These activated cells interact with each other and the resident cells of the CNS. They secrete cytokines (e.g., IFNg by Th1, IL6/17 by Th17, GM-CSF, IL6, TNFa by B cells) and cytotoxic molecules (e.g., granzyme B by CD8+ T cells). B cells can further evolve into autoantibody-producing plasma cells. As a consequence, T and B cells activate macrophages and microglia, which produce cytokines, nitric oxide, and ROS. This cytotoxic pro-inflammatory environment breaks down the myelin sheaths around axons and induces energy failure in the axon. Macrophages and microglia can still clear the myelin debris, allowing for the recruitment of OPCs that will partially remyelinate the lesion. (B) In the progressive phase of MS, T and B cell infiltrates are reduced. Remarkably, plasmablasts and plasma B cells form tertiary follicle-like structures in the meninges. The BBB is closed and the inflammation is sustained by innate CNS-resident cells, i.e., microglia and astrocytes. They produce cytokines (TNFa, IL6) and release ROS, causing myelin damage. Although microglia are primed into a pro-inflammatory phenotype, their phagocytic capacities are reduced. These features also characterise the senescence-associated phenotype of microglia and astrocytes. Myelin debris are improperly cleared, OPCs are less recruited and fail to differentiate. TNFa-mediated glutamate release from astrocytes results in excitotoxicity causing axonal damage. The ferrous iron released from the myelin, where it accumulates*

*with age, is oxidized, which produces ROS, and incorporated by microglia, forming a phenotypical rim around the demyelinating lesions, both in the white and grey matter. These successive events are self-sustained and enhanced by senescent processes, resulting in a major oxidative burst, causing mitochondrial dysfunction, mitochondrial DNA damage, energy failure and axonal loss. BBB = blood-brain barrier; B = B cell; CNS = central nervous system; GM-CSF = granulocyte-macrophage colony-stimulating factor; IFN = interferon; IL, interleukin; MS = multiple sclerosis; OPC = oligodendrocyte progenitor cell; ROS = reactive oxygen species; T = T cell; Th = T helper cell; TNF = tumour necrosis factor. Created in BioRender.com.*

In a second phase, when the focal inflammatory burst dampens due to the programmed cell death of the lymphocytes, microglia and macrophages will ensure their anti-inflammatory role by phagocyting myelin debris, allowing the process of remyelination by oligodendrocyte progenitor cells (OPCs) and surviving oligodendrocytes [201–204]. This acute phenomenon repeats itself at each relapse. The chronic stage of the disease, which is pathophysiologically similar for PPMS and SPMS, is characterised by a meningeal inflammation and microglial activation within a compartmentalised reaction seen the integrity of the BBB [174,175]. T and B cells, accounting mainly plasmablasts and plasma cells, relocate to the large perivascular spaces and in the meninges, eventually forming tertiary follicle-like structures in the more aggressive forms of the disease, which can be visualised with new MRI techniques as leptomeningeal enhancement. Interestingly, these meningeal and perivascular infiltrates release inflammatory mediators (mainly by B cells) and contribute hereby directly or indirectly through microglial activation to slowly expanding pre-existing white matter lesions and subpial cortical demyelination [205–211]. Microglia and astrocytes further supply the neurotoxic environment with inflammatory mediators and reactive oxygen species causing a major oxidative burst and excitotoxicity [181,212–217]. Chronically demyelinated axons finally degenerate due to the loss of oligodendroglial trophic support and energy shortage with ionic imbalance secondary to mitochondrial dysfunction causing a state of virtual hypoxia [218–222]. The neurodegenerative processes eventually become self-perpetuating. Moreover, ageing causes functional changes in all the involved cell types that further support the pathophysiological differences observed in chronic MS [46].

Anatomopathological features of the different MS lesion types translate these pathophysiological events [56,223]. Active lesions are typically centred on a venule, corresponding to the central vein sign on high resolution MRI, with a perivenular lymphocytic cuff; as well as a majority of microglia and macrophages throughout the lesion, containing myelin debris [56,224,225]. Contrariwise, in slow-expanding lesions, characteristic to PMS, the lesion edge of microglia (and macrophages) surrounds an inactive demyelinated centre [56]. Due to oxidative changes of iron molecules in the myelin debris phagocytised by the microglia, these edges appear as paramagnetic rim lesions on specific MRI sequences [226–228]. Features of axonal injury can be seen in both lesions [229]. Inactive lesions are sharply demarcated and characterised by reactive astrocytes forming a gliotic scar in the centre of the lesion while other immune cells have largely deserted the lesion, although a few microglia/macrophages can be present at the lesion edge. These lesions are depleted of oligodendrocytes and have a low degree of ongoing axonal injury [56,224,229]. Shadow plaques contain remyelinated axons with typically thinner myelin [230]. Cortical lesions and cortical, mainly subpial, demyelination occur already early in the disease. They are typically depopulated from lymphocytes but can have a rim of activated microglia [231–233]. Remyelination is more effective in the cortex [234]. Normal appearing white and grey matter, that is more frequent in PMS, is only normal in appearance, since it shows diffuse changes as perivascular inflammatory infiltrates, microglial activation, astrocytic gliosis and diffuse axonal injury with secondary demyelination (meaning that the demyelination is a consequence of axonal injury, while it is the opposite in primary demyelination) [235,236]. Axonal injury results partially from anterograde (Wallerian) and retrograde degeneration secondary to neuronal and axonal damage, and is thus not caused by a focal lesion [195,237]. This occurs already early in the disease [195,198].

*Immune cells*

Briefly, the immune system comprises the innate immunity (granulocytes, macrophages, natural killer cells and dendritic cells), providing an immediate response against a pathogen, and the adaptive immunity (lymphocytes), that generates a specific cellular response selectively targeting a pathogen within a few days [238]. Short-lived and blood-resident neutrophils, the major subtype of granulocytes, trap and kill a pathogen by phagocytosis and NETosis [239]. Tissue-

resident macrophages, deriving from monocytes, act through phagocytosis, secretion of inflammatory mediators and antigen presentation. In the adaptive immune system, antigen presenting cells (macrophages, dendritic cells, B cells) present a peptide fragment of a pathogen bound to MHC-II at their cellular surface (signal 1) alongside costimulatory molecules, such as CD80, CD86 and CD40 (signal 2) and activate naïve CD4+ T cells by binding with the T cell receptor (TCR) and its costimulatory receptor [238,240]. Contrariwise, naïve CD8+ T cells are activated by MHC-I, present on nucleated cells [241]. Activated T cells will then differentiate towards effector T cells, requiring active antigenic stimulation, and finally a fraction persist as central memory (lymph node homing C-C motif chemokine receptor (CCR) 7+ $T_{CM}$) and effector memory T cells (tissue homing CCR7- $T_{EM}$), able to survive without antigenic stimulation and to expand rapidly upon a secondary challenge, whereby $T_{CM}$ stimulate dendritic cells and differentiate into $T_{EM}$ while $T_{EM}$ display immediate effector functions [242–244]. CD4+ T helper (Th) cells produce cytokines promoting macrophages, CD8+ T cells and B cells. Depending on the cytokines involved, we identify several Th cells, namely Th1, Th2, Th9, Th17, Th22, each with partially distinctive functions (table 0.1). Effector CD8+ T cells are cytolytic. They adhere to the infected target cells to form an immune synapse in which they secrete granzyme B and perforin inducing the apoptosis of the targeted cell [240]. The stepwise development of B-cells (pre-/pro-/immature B cells) in the bone marrow is marked by the successive rearrangements of immunoglobulin heavy and light chain gene segments until the surface expression of the B cell receptor (BCR). Transitional B cells will then migrate to the secondary immune organs (lymph nodes, spleen) and integrate follicles until they encounter a pathogen which they will internalise to present its antigen on MHC-II to Th cells. This cognate T/B cell interaction activates the B cells as well, allowing their further development in the germinal centres, marked by immunoglobulin class switch recombination, with support of follicular Th cells, where they finally differentiate into memory B cells expressing surface immunoglobulins or into long-lived plasma cells secreting the antibodies [245,246]. Finally, the extent of the immune reaction is carefully controlled and counterbalanced, mainly by the release of anti-inflammatory mediators, although other mechanisms have been described. In this function, the well acknowledged regulatory CD4+ T cells (Tregs), characterised by the expression of transcription factor forkhead box P3 (FOXP3) and interleukin 2 (IL2) receptor CD25 (table 0.1), are accompanied by subsets of other CD4+ Tregs, namely, type 1

regulatory T cells (Tr1), IL17-producing Tregs, RAR related orphan receptor (ROR)gT-expressing inducible Tr3 Tregs and follicular CD4+ Tregs, as well as CD8+ Tr2 Tregs and regulatory B cells (Bregs) [247–252].

*Table 0. 1: CD4+ T cell differentiation and function*

| Th subtype | Inductor cytokines | Key transcription factors | Effector cytokines | Functions | Pro/anti-inflammatory |
|---|---|---|---|---|---|
| **Th1** | IL12 | STAT4, TBX21 | IFNg | Cellular immunity (intracellular pathogen) | Pro-inflammatory |
| **Th2** | IL4, IL25, IL33 | STAT5, STAT6, GATA3 | IL4, IL5, IL13 | Parasitic immunity, Allergic reaction | Pro-inflammatory counterbalance to Th1 |
| **Th9** | IL4, TGFb | PU.1, IRF4 | IL9, IL10 | Parasitic immunity, Allergic reaction | Pro-inflammatory |
| **Th17** | TGFb, IL6 IL21, IL23 | STAT3, RORC | IL17, IL21, IL22 | Tissue inflammation (extracellular pathogen) | Pro-inflammatory |
| **Th22** | TNFa, IL6 | AHR, RORC | IL22, IL13 | Tissue inflammation | Pro-inflammatory |
| **Treg** | TGFb, IL2 | STAT5, FOXP3 | IL10 | Suppression of immune response Tolerance to self-antigen | Anti-inflammatory |

*This table summarises the key mediators of CD4+ T cell differentiation and activation[253–257], the cytokines inducing their differentiation and the transcription factors involved in their activation resulting in the expression of their effector cytokines via which they fulfil their function, as well as their overall pro- or anti-inflammatory character. AHR = aryl hydrocarbon receptor, FOXP3 = forkhead box P3, GATA3 = GATA binding protein 3, IFNg = interferon gamma, IL: interleukin, IRF4 = interferon regulatory factor 4, PU.1 = PU.1 transcription factor, RORC = RAR Related Orphan Receptor C (also called RORgT), STAT = signal transducer and activator of transcription, TBX21 = T-box transcription factor 21 (also called TBET), TGFb = transforming growth factor beta, Th = T helper cell, TNFa = tumour necrosis factor alpha, Treg = regulatory T cell*

The activation of CD4+ T cells, especially Th1 and Th17 cells, and their infiltration in the CNS triggers the further inflammatory cascade in MS. Through the release of cytokines and chemokines, they recruit other peripheral immune cells and activate CNS resident cells, microglia and astrocytes, resulting in the damage of oligodendrocytes and myelin sheaths [21,176,183,185,188]. Peripheral immune cells, expressing chemokine receptors (CCR7, CXCR4/5) and integrins (alpha-4/beta-1 (VLA4), alpha-L/beta-2 (LFA1)), are more prone to cross the BBB, due to the increased expression of chemokines (CCL19/21, CXCL12/13) and adhesion molecules (vascular and intercellular cell adhesion molecule 1 (VCAM1 and ICAM1)) on endothelial cells, induced by pro-inflammatory cytokines as TNFa, IL1b and IL17, thereby contributing to the permeability of the BBB and the invasion of the CNS [258–265].

IL12, a heterodimer of IL12p35 and IL12p40, and IL23, a heterodimer of IL23p19 and IL12p40, induce respectively encephalitogenic Th1 and Th17 cells [266–269]. Th17 cells induced by IL6, transforming growth factor beta (TGFb), and IL21 but in the absence of IL23 are less pathogenic [270,271]. Remarkably, IL12p40 or IL23p19 deficient mice are resistant, while IL12p35 deficient mice are still highly susceptible to EAE, suggesting the importance of Th17 cells [272]. In fact, interferon gamma (IFNg)-producing Th17 cells, also referred to as Th17/1 cells, inducible by both IL12 and IL23, preferentially cross the BBB and are increased in the blood of relapsing MS patients [178,273]. Moreover, the production of granulocyte-macrophage colony stimulating factor (GM-CSF) by both activated subsets seems important towards their encephalitogenicity, given that GM-CSF is sufficient to induce EAE in the absence of IFNg and IL17 [177,266,274]. It is involved in the proliferation, survival and migration of leukocytes within the CNS, but it is also neurotrophic, it induces the phagocytosis of myelin debris and regulates astrogliosis [275]. Interestingly, a signature subset of Th cells, characterised by the expression of GM-CSF, tumour necrosis factor (TNF), IL2 and C-X-C motif chemokine receptor 4 (CXCR4), and mainly consisting of Th1 cells, are increased in the blood and CSF of RRMS patients [276]. In fact, Th cells contributed substantially more to the production of GM-CSF in RRMS patients than any other cell type, namely CD8+, γδ T cells or B cells. Moreover, these CXCR4-expressing cells have a greater migration potential towards C-X-C motif chemokine ligand 12 (CXCL12), that has previously been involved in CNS invasion [259,276]. Furthermore, Th1 and Th17 associated cytokines, such as IFNg, IL1b, IL17, TNFa, are involved in the disruption of the BBB (also by inducing the

expression of adhesion molecules on endothelial cells) and the recruitment and activation of other peripheral immune cells as well as CNS-resident cells, microglia and astrocytes [180,183,186,277]. Notably, IL6 and IFNg have also anti-inflammatory effects, IL6 by inducing IL10 producing T cells, IFNg by counterbalancing GM-CSF production and by upregulating IL18 binding protein in microglia [177,278,279].

The molecular trigger causing T cells to act against the own CNS is still unknown. Autoreactive CD4+ T cells recognising myelin proteins as myelin basic protein (MBP), proteolipid protein (PLP), and myelin oligodendrocyte glycoprotein (MOG) were found in MS patients but also in controls [280,281]. Hence a dominant T cell antigen is still missing in MS and nourishing the etiological debate.

Research has long been focused on CD4+ T cells. However, it has been evidenced that clonally expanded CD8+ T cells outnumber CD4+ T cells in MS lesions, and the CSF of MS patients, where they also display a higher cytotoxicity (measured by granzyme levels) during relapses [190,282–284]. MHC-I is constitutively expressed on microglia and endothelial cells, and its expression is furthermore upregulated on astrocytes, oligodendrocytes and neurons in response to disease severity, while CD8+ T cells can target each of these cell types and cause axonal transection correlating positively with the extent of axonal damage [285–288,288–290]. Moreover, a subset of non-cytotoxic CD8+ T cells secrete IL17, noticeably to the same amount as CD4+ T cells in active MS lesions [188,285]. Tissue-resident memory T cells are more prominent in MS than naïve T cells and actively contribute to the disease pathogenesis, in particular memory CD8+ T cells in the compartmentalized inflammatory response [174,291–294].

Tregs in MS, especially in RRMS, are functionally impaired, causing an imbalance in the immune response [295–300].The thymic output of naïve Tregs is reduced, whereas changes in the number of circulating Tregs in MS (subtypes) vs healthy controls (HC) are disputed [295,298,301]. Additionally, T effector cells are resistant to Tregs via the signal transducer and activator of transcription 3 (STAT3)/IL6 signalling pathway wherein IL6 signalling is dominant in inhibiting T cell conversion towards Tregs and suppress Treg function, partly by inducing the secretion of non-apoptotic granzyme B by CD4+ T cells [302–304]. IL12 and IL6/IL1b can induce respectively Th1-like Tregs (secreting IFNg) and Th17-like Tregs (secreting IL17) with reduced suppressive activity [305,306]. Moreover, Tr1 exhibit a defective secretion of IL10 [307]. Several subsets of regulatory CD8+ T cells have been evidenced in EAE [308,309]. While less

CD8+ Tregs recognising myelin-reactive CD4+ T cells were found in the CSF and peripheral blood of relapsing MS patients, glatiramer acetate treatment induces them [310–312].

Children with MS have a lower proportion of circulating naïve T cells, and a higher proportion of memory T cells, suggesting a premature deficit T cell development in the thymus. Moreover, the peripheral response of IL17-producing $T_{CM}$ cells to myelin-derived antigens is increased while the suppressive capacity of Tregs is decreased in POMS [313,314].

The contribution of B cells to MS pathogenesis is not negligible, as antigen presenting cells and antibody producing cells, as well as in modulating the response of other immune cells [315]. Clonally expanded plasma cells produce antibodies within the CSF, which is reflected by the detection of CSF-specific OCBs [316]. Antibodies against MBP or MOG were detected in CNS tissues of MS patients rather than in the CSF or serum [317–319]. However, the presence of anti-MOG antibodies is characteristic of another disease category, called MOG antibody-associated disease, and is a criterion against the diagnosis of MS [320]. Patient-derived plasma/serum antibodies could further cause complement-derived demyelination by specifically targeting terminally differentiated oligodendrocytes in vitro in 30% of the cases [321]. Molecular mimicry was evidenced between the EBV nuclear antigen 1 (EBNA1, an EBV transcription factor) and glial cell adhesion molecule (GlialCAM), while MS patients have CSF/plasma antibodies against EBNA1/GlialCAM as well as EBNA1-specific clonally expanded T and B cells [322,323]. Memory B cells of RRMS patients but not of healthy controls, can further induce autoreactive T cells by acting as antigen presenting cells in response to myelin antigens, characterized by the overexpression of costimulatory molecules as CD80 and CD86, wherein MCH-II and BCR are indispensable [324–326]. Furthermore, memory B cells of MS patients secrete proinflammatory cytokines as TNFa and lymphotoxin (LT) supporting CD4+ (both Th1 and Th17) and CD8+ T cell responses as well as GM-CSF supporting myeloid cells, both of which are reversed by B cell depletion treatment (namely anti-CD20) [327–329]. B cells of RRMS patients have a direct or indirect (through activation of microglia or astrocytes) cytotoxic effect on oligodendrocytes and neurons that is independent of immunoglobulins and cytokines. The secreted cytotoxic factor is yet not identified [209,330]. In children with incomplete recovery the transcriptional profile of PBMCs is characterised by B cell activation [76].

The chronic disease is marked by a meningeal inflammation wherein B cells, alongside plasmablasts, plasma cells, T cells and follicular dendritic cells can aggregate to form follicle-like structures with the architecture of germinal centres. The presence of these tertiary follicles was associated with microglial activation, cortical demyelination and neuronal loss [210,211,331]. Leptomeningeal enhancement, although not specific to MS, is the radiological translation of these follicles, visualised by new MRI acquisition techniques. It is associated with lower cortical volume and variably associated with higher numbers of cortical lesions [208,332] Remarkably, subsets of the several stages of B cell development typically encountered in secondary lymphoid organs were detected in the CSF of patients with MS and other neurological inflammatory disorders.

Finally, Bregs, secreting IL10, IL35 and/or TGFb, are potentially supportive of Tregs while opposing Th1, Th17 and myeloid cells, but reports regarding their numerical and functional integrity in MS are largely contradictory [333–336].

*Microglia*

Microglia are the primary resident myeloid cells of the CNS, deriving from mesodermal progenitors in the embryonic yolk sac [337]. These progenitors migrate early towards and spread out in the developing brain, proliferate, and differentiate to form this unique cell population with a large range of functions. During CNS development they sustain myelination (by releasing insulin like growth factor (IGF)), and phagocyte apoptotic neurons and overproduced oligodendrocytes. Microglia are guardian of the CNS homeostasis, ensuring synaptic integrity and plasticity, they also provide a trophic support to reduce the risk of excitotoxicity [338]. While microglia were first considered quiescent cells scrutinising their environment through their ramifications to shift towards a so-called proinflammatory M1 (IL1b, IL6, IL23) or anti-inflammatory M2 (IL10, TGFb) phenotype upon encountering an activator mainly via Toll-like receptor signalling, they are now regarded as a heterogenous population rapidly changing within a phenotypic spectrum in between these two extremes depending on the type of stimulus and the microenvironment [338]. This is further supported by single-cell approaches, identifying a diversity of microglial populations within the CNS contributing to neuroinflammation, neurodegeneration and/or oxidative stress, but also to

recovery, with distinct molecular hallmarks and cellular kinetics [339–343]. Thus, the developmentally proliferative and postnatally myelination-supportive microglia turns into an adult homeostatic phenotype with regional differences depending on functional requirements [343]. Moreover, human microglia have a long lifespan and divide on an average of 4.2 to 20 years [344].

Microglia and macrophages play similar roles in MS, although some differences appear with ageing as ageing macrophages are impaired in producing a functional pro-inflammatory response [343]. Both are involved in active lesions, expressing genes related to phagocytosis, oxidative stress and antigen presentation [345]. Th1 and Th17 cells induce proinflammatory microglia/macrophages, expressing MHC-II and secreting proinflammatory cytokines and reactive oxygen and nitrogen species (ROS/RNS). These ROS/RNS cause mitochondrial DNA mutations and mitochondrial dysfunction within glial cells, neurons and axons enhancing the oxidative burst, resulting in energy deficiency and ionic imbalance, and triggering axonal degeneration by accumulation of calcium as well [181,183,186,346–349]. Via pro-inflammatory cytokines, as IL1b and TNFa, they contribute to the glutamate excitotoxicity, causing oligodendrocyte death and synaptic degeneration [212,350]. Moreover, the oxidation of $Fe^{2+}$, accumulating in the extracellular space from harmed oligodendrocytes and myelin debris, to $Fe^{3+}$ produces hydroxyl radicals, increasing the oxidative stress. The uptake of oxidized iron by microglia causes dystrophy and a second wave of $Fe^{2+}$ release [228]. This iron accumulation in microglia can be seen on brain MRI as a paramagnetic rim at the edge of slowly expanding lesions [226,227]. Myeloid cells at the chronic lesion edge are mainly TMEM119+, a specific marker of microglia [345]. Remarkably, two distinct microglia clusters have been identified, a foamy cluster characterised by foam-cell differentiation and lipid storage, thus involved in myelin phagocytosis, and an iron cluster characterised by MHC-II and inflammatory (especially IL1b and complement 1, Q subcomponent (C1q), involved in microglial activation and reactive microgliosis) markers as well as iron-related genes [351]. Other cells at the lesion edge correspond to inflamed astrocytes, stressed oligodendrocytes and immunological OPCs, expressing genes involved in antigen presentation (MHC-I/II) and in immunoprotection, as well as some immune susceptibility genes of MS [351–353]. Activated microglia can further induce neurotoxic astrocytes [354].

Microglia/macrophages play an important role in recovery by stimulating OPC survival and proliferation via IL1b and TNFa, that is profitable by binding to TNF receptor 2 (TNFR2) whereas its binding to TNFR1 is accompanied by a proinflammatory Th1 response [355–357]. Furthermore, microglia/macrophages are indispensable to clear myelin debris that inhibit OPC differentiation as well as remyelination [202,204,358,359]. Herein, macrophages seem to be rather involved in myelin destruction and microglia in myelin clearance [360]. In this process, microglia/macrophages must switch to an immunoregulatory phenotype for the release of growth/neurotrophic factor such as Igf1 and activin-A that support OPC differentiation [203,361]. Rather than switching between phenotypes, an immunoregulatory phenotype might in fact repopulate the lesion area following necroptosis of the inflammatory phenotype [362]. Remarkably, in vitro MS-derived myelin is preferentially phagocytised by microglia/macrophages as compared to myelin of healthy controls, thus changes in myelin might precede demyelination and phagocytosis [363].

*Astrocytes*

Astrocytes derive embryogenically from radial glial cells, originating themselves from neuronal stem cells [364]. They are highly ramified cells expressing numerous receptors to sense and make contact with their environment [365,366]. Astrocytes actively participate to ensure CNS homeostasis. They regulate synaptic formation, activity and plasticity, and control the composition of the extracellular milieu (pH, electrolytes) and the neuronal microenvironment as part of the panglial syncytium (a network between oligodendrocytes/astrocytes/ependymal cells) [366–370]. They provide energy substrates, trophic factors and cholesterol to neurons and oligodendrocytes [366,371]. They support the integrity and functionality of the BBB (formed by the astrocyte endfeet, the pericytes, the basement membrane and the tightly joint endothelial cells) and are an intermediate for the neurovascular coupling within the neurovascular unit [372,373].

Astrocytes represent a very heterogenous cell population with a dual role, protective and degenerative, in the setting of MS [365]. Astrocytes are activated early in the disease, even before the massive CNS invasion. By the production of cytokines, chemokines, matrix metalloproteinases (MMPs), and ROS/RNS, they

contribute to the disruption of the BBB (reduction in tight junction proteins, endothelial cell apoptosis, retraction of the astrocytic endfeet), to the attraction (expression of CXCL12, induction of expression of adhesion molecules on endothelial cells) and activation of peripheral immune cells and microglia [365]. They may express MCH-I and/or MCH-II, but their expression of costimulatory molecules is disputed. They support the differentiation of CD4+ T cells towards Th1/Th17, they produce IL15 which activate CD8+ T cells and B cells, as well as IL6 and lymphotoxin-alpha, stimulating microglia. Moreover, CNS-restricted production of IL23 by astrocytes has been evidenced in progressive chronic EAE and induces pronounced neuroinflammation and demyelination, accompanied by multilocular infiltrates of B cells [374]. Astrocytes massively produce ROS/RNS, which is further sustained by pro-inflammatory cytokines resulting in oxidative stress, mitochondrial dysfunction and energy deficits [215,216,375,376]. Activated astrocytes form a glial scar in order to contain the inflammatory assault, and release several molecules (hyaluronan, fibronectin, chondroitin sulfate proteoglycans, fibroblast-growth factor) that hinder OPC migration, maturation and differentiation [377–380]. They can also promote TNF-mediated OPC cell death [381]. Finally, astrocytes contribute to excitotoxicity when their glutamate buffering capacity is exceeded, partly by reduced glutamate metabolism and increased glutamate release [350,382,383].

Even in light of all these adverse effects supporting MS pathogenesis, ablation of reactive astrocytes increased the leukocyte infiltration in the CNS, resulting in a fulminant EAE course indicating the indispensable role of astrocytes in containing the inflammatory assault [384]. Moreover, they express anti-inflammatory cytokines as IL4, IL10, IL27 and induce the expression of ectoendonucleases CD39 and CD73 in activated CD4+ T cells possibly partially reversing the balance towards an immunoregulatory response [385–387]. Although they produce ROS/RNS, they can also produce several antioxidant enzymes [365]. Furthermore, astrocytes can restore the integrity of the BBB by releasing several molecules (retinoic acid, peroxiredoxin 6, sonic hedgehog) that silence the inflammatory and oxidative burst around the endothelial cells [388–390]. They can finally promote remyelination, axonal regeneration and neurogenesis by secreting several neurotrophic factors and growth factors (that act on both neurons and oligodendrocytes), and recruit microglia/macrophages to remove myelin debris [365,391].

*Oligodendrocytes*

Oligodendrocytes (OLs) are postmitotic cells differentiating from oligodendrocyte progenitor cells (OPCs), originating themselves from neuroepithelial cells of the neural tube giving rise to a common progenitor for neurons, oligodendrocytes and astrocytes [392]. OPCs are uniformly distributed across the adult brain and spinal cord, although more abundant in the white matter, as well as in germinative areas, especially in the subventricular zone [393–396]. They form a pool for OL/myelin remodelling throughout life in case of physiological turnover or local injury [397–399].

In MS, OLs and myelin sheaths are directly harmed by the cytotoxic, inflammatory and oxidative environment, as explained in previous sections, due to the presence of proinflammatory cytokines, auto-antibodies against myelin proteins, ROS/RNS and other molecules secreted by the peripheral and/or CNS-resident immune cells as well as by the direct cytotoxicity of CD8+ T cells, resulting in mitochondrial dysfunction, metabolic imbalance and apoptosis, although microglia/macrophages and astrocytes can eventually shift to an anti-inflammatory remyelination-supportive phenotype [400]. A primary oligodendrogliopathy with loss of myelin associated glycoprotein (MAG) expression but a prominent nuclear expression of hypoxia inducible factor 1a (HIF1a), that characterises the early degeneration of most distal, periaxonal oligodendrocyte processes, has been described as well [401,402].

Following demyelination, OPCs are activated, migrate to the site of harm and differentiate into remyelinating OLs in response to respectively cytokines, mitogens (platelet derived growth factor), chemoattractants (semaphorin 3F (Sema3F)) and trophic factors (IGF, ciliary neurotrophic factor) released by microglia and astrocytes, whereby an axon-OL interaction is indispensable as well to engage remyelination (figure 0.3), with a notion of critical window of time for remyelination, beyond which axonal damage and thus functional loss can't possibly totally recover [403–409]. Moreover, surviving OLs that reversibly retract myelin processes to favour cell survival under metabolic stress, at least to a critical point, could possibly form new myelin sheaths, as carbon dating of genomic DNA evidenced an increase of newly generated OLs in normal appearing white matter only in subjects with aggressive MS but not in shadow plaques [193,410,411].

Single-cell RNA sequencing identified similar OPC/OL subcluster in MS patients and controls, although at different frequency highlighting changes in their transcriptional signatures. OPC and intermediate OL subclusters were reduced in MS lesions and normal appearing white matter. One end state OL subcluster was notably reduced while other subclusters were enriched in MS, namely a mature actively myelinating with increased myelin gene expression, another end state and an immune OL subcluster, the latter being closely associated with microglia. Hence, the loss of this end state OL subcluster, that was transcriptionally directed towards signalling, cell-to-cell adhesion and viability rather than myelination, might be important in the understanding of MS pathogenesis [412]. The transcriptional signature of OPC/OL clusters also significantly differs at the peak of EAE with among others, alternative splicing of myelin genes and increased expression of neuroprotective serpin family A member 3 (Serpina3), a serine protease inhibitor, and of immunoprotective serpin family G member 1 (Serping1), an inhibitor of complement activation. Remarkably, specific subsets of OPCs/OLs have immunomodulatory capacities as they express MS susceptibility genes (as interferon responsive genes), MHC-I genes, making them direct targets of cytotoxic CD8+ T cells, or MHC-II genes induced by Ifng thereby promoting CD4+ T cells. Furthermore, certain immunocompetent OPCs are also capable of phagocytosis, even of myelin [353].

Remyelination efficiency declines with age and disease progression and is often incomplete as only approximately 20% of chronic lesions are completely remyelinated [413–417]. Moreover, myelin sheaths coming from remyelination are thinner with shorter internodes, but still sufficient to ensure nerve conduction [230]. There are multiple reasons explaining remyelination failure in MS, both intrinsic and extrinsic to OPCs/OLs, due to the toxic neuroinflammation and an inhibitory lesion microenvironment [418]. OPC densities decrease in chronic lesions but whether this is due to OPC depletion, especially after successive episodes of demyelination, is still debated [419–423]. However, OPCs might be more fragile and susceptible to the inflammatory and oxidative assault and be directly targeted by cytotoxic CD8+ T cells [194,352,424,425]. OPC migration might further be impaired [426–428]. Herein, group 3 semaphorins, normally absent, are re-expressed in MS lesions. Notably, the overexpression of chemoattractant Sema3F in active inflammatory lesions correlates with higher numbers of OPCs, and the overexpression of chemorepellent Sema3A in chronic active lesions correlates with lower numbers of OPCs [408,429].

Netrin 1 is progressively upregulated upon OPC recruitment to arrest their migration and favour their differentiation. However, early expression of Netrin 1 by reactive astrocytes in demyelinated lesions, limits periplaque OPC recruitment, while chemokine Cxcl1 (interacting with Cxcr2 expressed on OPCs), is upregulated at the periphery of demyelinated lesions and promotes OPC proliferation but inhibits their differentiation [430–432]. Oppositely, Cxcl12 expressed by microglia and astrocytes during demyelination, supports the maturation and differentiation of Cxcr4-expressing OPCs [433]. Endothelin 1 induced jagged 1 expression in reactive astrocytes which induces Notch signalling in OPCs, inhibiting its differentiation in lysolecithin demyelinated rats [434]. Myelin itself as well as the altered composition of the extracellular matrix, partly resulting from deposition of reactive astrocytes and microglia, inhibit OPC differentiation [202,358,435] Hereby, inhibitory aggregates of fibronectin persist in chronic lesions because of the reduced microglial secretion of metalloproteinases (MMP) such as MMP7, that cleave these aggregates [436]. Furthermore, OLIG2 that is sufficient to induce OPC differentiation, was more detected in maturing OPCs in active lesion borders than in chronic silent lesions, shadow plaques and periplaque white matter of chronic MS suggesting a differentiating block, further supported by an impaired migration and differentiation capacity of ageing OPCs and their reduced response to pro-differentiation compounds [167,428,437,438]. Finally, premyelinating OLs in chronic lesions extended processes to demyelinated axons but radial ensheathment was rare, suggesting an axonal irresponsiveness to remyelination [419].

Hence, in MS, the demyelination/remyelination balance tilts towards demyelination overtime, due to (1) the loss of OLs and myelin sheaths, (2) the impaired migration and differentiation of OPCs, (3) the impaired remyelination capacity of surviving/newly formed OLs, contributing to the axonal damage and neuronal loss and thus to neurodegeneration [422,439].

### vi. What's still to explore?

MS is characterised by neuroinflammation, demyelination and neurodegeneration. Despite decades of research, that has however historically focused primarily on the inflammatory aspect, none of these aspects is completely understood and the causal character of each, by means of primary or secondary, is still debated [440].

Nevertheless, since they occur simultaneously, they are probably intertwined and not mutually exclusive.

Neurodegeneration (figure 0.3) that is mainly driving disease progression, remains a major burden we still fail to control in today's disease management. Moreover, axonal transection and Wallerian degeneration have been detected early in the disease course [195,198,199]. However, delaying Wallerian degeneration did not reduce axonal damage that was further sustained by axonal transport disturbances [198].

Focal axonal damage can occur with intact myelin sheaths, initiated by intra-axonal mitochondrial pathology [349]. Therefore, neuroinflammation has been incriminated in direct axonal damage, possibly by the cytotoxicity of CD8+ T cells (exocytosis of granzyme B/perforin-containing granules), and the oxidative stress induced by microglia and astrocytes [349,440–447]. Mitochondrial dysfunction, partly resulting from oxidative stress, causes axonal energy deficiency and major ionic imbalance, mainly of sodium and calcium, due to the decreased activity of the sodium/potassium ATPase, and the reversing of the sodium/calcium exchanger, leading further to the degradation of structural proteins by calcium-activated neutral proteases (calpains), and the disruption of axonal transport, microscopically seen as axonal swelling [218,222,448,449]

Furthermore, excitotoxicity, mediated by an astrocytic-microglial interplay, largely contributes to neuronal damage and OL death. The synaptic concentration of glutamate, the major excitatory neurotransmitter, is finely regulated, especially by astrocytic uptake [450]. Increased levels of glutamate are observed in the CSF and in active lesions and normal appearing white matter of MS patients, and cause excessive synaptic excitation [450–452]. Herein, the reduced expression of proteins involved in the uptake and degradation of glutamate by activated astrocytes, as well as the release of ATP by activated microglia and of TNFa and IL1b by activated microglia, T and B cells potentiate excitotoxicity [212,350,382,453–457].

Demyelination is not solely causing neurodegeneration, but its contribution is undeniable. While demyelination results from the inflammatory and oxidative burst in acute lesions and from the oxidative environment nourished by microglial activity and iron toxicity in chronic active lesions, directly exposing the axon to the hostile environment, demyelination also occurs in the normal appearing white and grey matter, secondary to axonal injury [21,22,171,228,237].

*Figure 0.3: Remyelination and neurodegeneration*

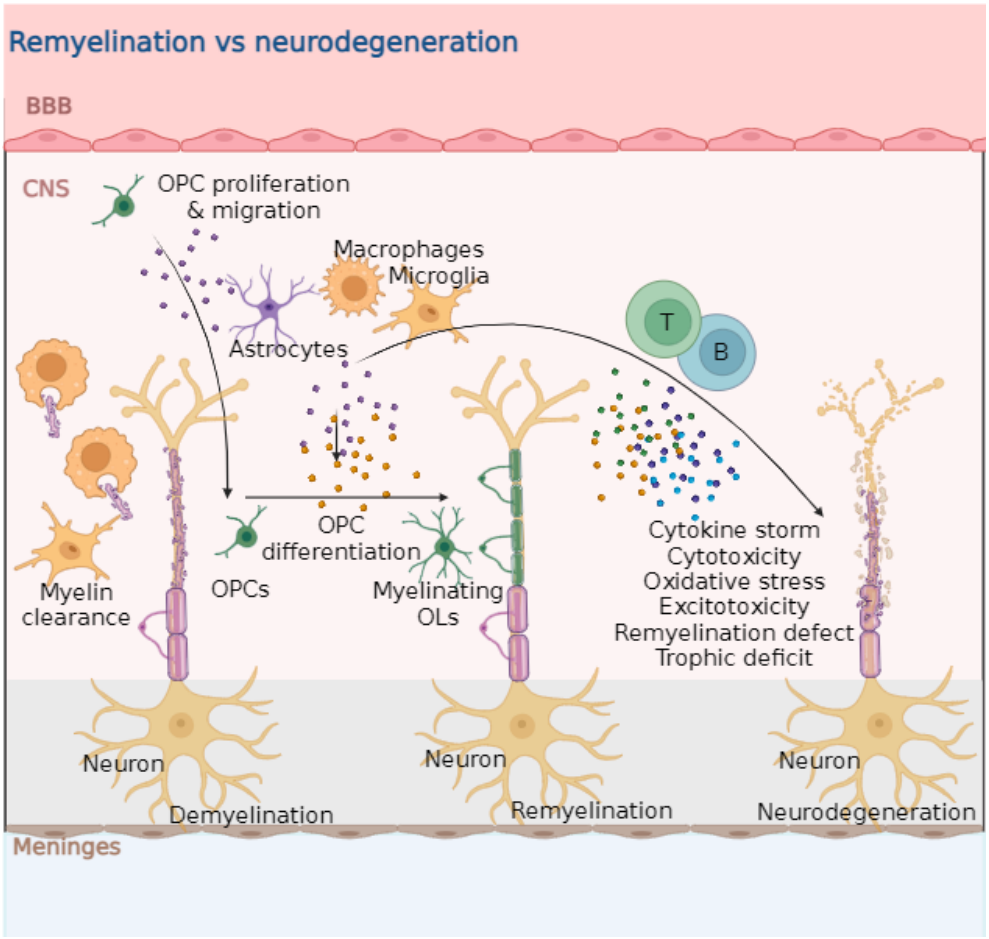


*At the beginning of the disease remyelination is possible by surviving OLs or by OPCs proliferating, migrating, and differentiating at the site of injury, in response to cytokines, chemokines (Cxcl1, Cxcl12), mitogens (platelet derived growth factor), chemoattractants (semaphorin 3F) and trophic factors (insulin like growth factor, ciliary neurotrophic factor) released by microglia and astrocytes. Moreover, myelin debris clearance by microglia/macrophages, recruited by astrocytes, is indispensable as myelin debris inhibit OPC differentiation and collocate myelin-associated factors inhibiting axonal growth and regeneration. However, remyelination decreases with disease progression due to the impaired migration and differentiation of OPCs, the impaired remyelination capacity of surviving/newly formed OLs and the reduced phagocytosis capacity of*

*microglia/macrophages, contributing to the axonal damage, neuronal loss and thus to neurodegeneration. Neurodegeneration is further driven by the cytokine storm, cytotoxicity, oxidative stress, excitotoxicity of microglia, astrocytes, T and B cells as well as the lack of trophic support by the loss of oligodendrocytes. BBB = blood-brain barrier, CNS = central nervous system, OPC = oligodendrocyte progenitor cell, OL = oligodendrocyte. Created in BioRender.com*

Moreover, primary OL apoptosis alongside microglial activation has been suggested in myelinated tissue without any consistent lymphocyte/myelin-containing phagocyte infiltration [458]. This is further supported by a mouse model of toxin-induced focal subpial demyelination, resulting in the selective degeneration and functional impairment of a normally myelinated interneuron subtype (characterised by the staining of calcium-binding protein parvalbumin), possibly with a subsequent microglial/astrocytic contribution. This interneuron subtype is particularly ATP-demanding and thus depending on nutrient supply by OLs. Noticeably, excitatory neurons, that can be variably myelinated, remained unaffected. The selective loss of these interneurons was also observed in MS brains [459]. Moreover, myelin debris clearance by microglia/macrophages is essential as myelin debris inhibit OPC differentiation and remyelination, but also collocate myelin-associated inhibitory factors, such as reticulon 4, previously known as neurite outgrowth inhibitory factor (NogoA) as well as MAG and oligodendrocyte-myelin glycoprotein (OMGP), inhibiting axonal growth and regeneration by binding to Nogo receptor 1 expressed on axons [460–462].

Oligodendrocytes are essential for the axonal integrity and vice versa. First, myelin ensures the insulation of axons facilitating the proper saltatory, electrical conduction relying on highly organised Ranvier nodes, enriched in voltage-gated sodium channels, and paranodal axo-glial junctions where several adhesion molecules anchor the myelin loops to the axon [463]. Demyelination results in a diffuse distribution of the nodal/paranodal/juxtaparanodal ion channels and molecules, whereas aggregation of these molecules is necessary in the process of remyelination to restore nerve conduction and possibly prevent or lessen secondary axonal degeneration [229,464,465]. Oppositely, neurofascin-specific (a nodal protein) antibodies, detected in the serum of MS patients, exacerbated the clinical course of MOG-induced EAE by causing axonal injury without demyelination nor

enhanced CNS-inflammation [466]. Moreover, elongated and disorganised paranodes on myelinated axons at the border of chronic lesions, could contribute to axonal degeneration and impend further myelin loss [467]. Remarkably, the extent of paranodal axoglial disruption was found to be correlated with the local degree of microglial inflammation and axonal injury in MS normal appearing white matter, but was independent of demyelinating lesions and of infiltrating lymphocytes. Moreover, paranodal alteration persisted along microglial inflammation in chronic EAE [468]. On the contrary, while remyelinated lesions could still present with signs of inflammation, acute axonal injury was significantly less pronounced [229]

Secondly, OLs are, myelin-independently, a major trophic (prostaglandin D) and metabolic (lactate and ATP, required for membrane repolarization and axonal transport of organelles and vesicles) support to the adjacent axon, ensuring mitochondrial function and transport within the axon [469]. To illustrate this, Mbp null mice are severely dysmyelinated with functional axons whereas Plp null mice are fully myelinated with extended axonal degeneration [469–472]. Moreover, peroxisome-deficiency in OLs resulted in axonal degeneration, progressive subcortical demyelination and generated a proinflammatory milieu attracting CD8+ T and B cells [473].

In a noteworthy study, spatial transcriptomics and high-sensitivity proteomics performed on cortical brain tissues of SPMS patients vs controls identified a pseudotemporal pattern of early grey matter neurodegeneration despite active myelination pathways, mainly driven by local failure of trophic and anti-inflammatory cellular interactions, that were correlated with both immune-related and CNS-related groups of genes whereas pro-inflammatory interactions appeared more ambiguous and were narrowly linked to immune-related components. Remarkably trophic interactions were already reduced in intact grey matter of MS patients as compared to controls but further reduced in degenerating MS grey matter [474].

The current DMTs mechanistically target and lessen the neuroinflammatory events, although mostly without directly affecting CNS resident immune cells, but still fail to control neurodegeneration, which remains the major burden of disease progression we are still not able to modulate in patients' disease management [134,475–478]. While trophic failure appears to strongly underlie neurodegeneration, OPCs/OLs could still prove to be an indirect counteractant, both by the newly

formed myelin protecting physically the axonal integrity, and by the trophic support of OLs. This remains so far an unmet need in the current therapeutic strategies.

Thus, exploring inflammation, demyelination and neurodegeneration could help further understand their concomitant and joint involvement in MS pathogenesis as well as unravel the primary and secondary mechanisms to their self-maintenance and mutual interaction [22,23,440].

## II. Oligodendrocyte progenitor cells and oligodendrocytes

### i. Physiology

Oligodendrocytes, first described as neuroglia in the nineteenth century by Rudolf Virchow (1856), Otto Deiters (1865) and Camillo Golgi (1886), were initially considered as connective tissue, or nerve glue, in between neurons [479–482]. Since their first description, the appreciation of their functional importance has been largely upgraded. Next to myelinating axons in the CNS, thereby ensuring their insulation for rapid and efficient saltatory conduction of the action potential, they grant a trophic and metabolic support (by lactate supply) to the axons sustaining their integrity [219,220,483].

Myelination is a dynamically active process in the first two decades of life and neocortical myelination is protracted beyond late adolescence [396,484,485]. OPCs are equally distributed in the CNS, although more abundant in the white than in the grey matter in the adult brain. Throughout adult life, OPCs can differentiate in mature OLs to replace lost OLs and renew myelin sheaths [397,399].

*OPC/OL development*

Neurons, OLs and astrocytes sequentially arise from multipotent neuroepithelial progenitor cells in neurogenic niches in the developing and adult CNS by a tightly orchestrated epigenetic programme of transcriptional control [486,487]. In the developing forebrain/prosencephalon, OPCs are generated in 3 sequential waves, first ventrally in the medial ganglionic eminence and anterior entopeduncular area,

of which most OPCs do not survive, secondly in the lateral and caudal ganglionic eminences, and thirdly within the postnatal cortex [488]. OPCs develop similarly in 3 waves in the spinal cord, although herein, ventral-derived OPCs predominate in the end [489,490].

*OPC fate determination*

After neurogenesis, neural progenitor cells are specified towards the oligodendroglial fate by extrinsic factors, namely Sonic hedgehog (Shh), along Notch signalling, or fibroblast growth factor (Fgf) 2, binding to Fgf receptor (Fgfr) 1/2 (with downstream phosphorylation of extracellular signal-regulated protein kinase (Erk) 1/2 of mitogen-activated protein kinase (Mapk) signalling), antagonising bone morphogenetic protein (Bmp)/small mother's against decapentaplegic homolog family member (Smad) and Wnt/beta-catenin signalling [491–496]. The spinal cord is impregnated by opposite gradients of ventrally expressed Shh and dorsally expressed Bmp, whereby Bmp at low concentration enhances astroglial lineage specification at the expense of OL lineage by favouring global histone acetylation [494,495,497]. This results in the expression of transcription factors NK2 homeobox 2 (Nkx2.2) and Nkx6.1 collaborating with the basic helix-loop-helix (bHLH) oligodendrocyte transcription factor Olig2, key to OPC specification [498–501]. Serine-147 phosphorylation of Olig2, resulting in its homodimerization, promotes the generation of motoneurons, while its dephosphorylation with resulting sequestration of proneural transcription factor neurogenin 2 (Neurog2/Ngn2) is necessary for OPC development [502]. Olig2 can be compensated by the closely related Olig1, although Olig1 has a more important role in OL maturation [500]. Moreover, Achaete-Scute family bHLH transcription factor 1 (Ascl1/Mash1) promotes OPC specification at the expense of neurons at early stages and at the expense of astrocytes at later stages by repressing proneural transcription factors distal-less homeobox 1/2 (Dlx1/2) [503–505]. SRY box transcription factor 9 (Sox9) is key for initial glial specification as well, both OPCs and astrocytes, by inducing nuclear factor I/A (Nfia), a proglial/antineuronal transcription factor [506,507]. Sox9 ablation in neural stem cells reduces astrocyte numbers, while OPCs will recover at later stages due to compensation by Sox8/10 (Sox10 is induced by Olig2), but the double ablation of Sox9/10 will further reduce their numbers [507]. Oppositely, Sox9 ablation in established OPCs does not affect their further development, while double

Sox9/10 deletion results in the loss of platelet-derived growth factor receptor A (Pdgfra) expression in OPCs, displaying an increased apoptotic rate and a reduced migratory capacity [508].

*OPC proliferation and migration*

After glial cell fate decision, OPCs proliferate and migrate throughout the CNS, keeping the differentiation programme on hold. The two most important mitogens are Pdgf, binding to tyrosine kinase receptor Pdgfra, its only isoform expressed in OPCs, and Fgf2 binding to Fgfr, which can also act in synergy with Igf1. These mitogens induce downstream of these tyrosine kinase receptors ERK/MAPK and PI3K/Akt/mTOR signalling pathway and promote cell cycle transition by inducing cyclin D1 [509–512]. Furthermore, transcription factors inhibiting OPC differentiation, as Sox5, Sox6, Hes family bHLH transcription factor 5 (Hes5), inhibitor of DNA binding 2 (Id2), Id4, are upregulated in OPCs in response to extracellular signalling through the transmembrane protein, Leucine-rich repeat and immunoglobulin domain-containing 1 (Lingo1), G-protein-coupled receptor 17 (Gpr17), transmembrane glycoprotein receptor Notch1, and Wnt [487]. The SoxD proteins, Sox5/6 interfere with the SoxE proteins (Sox9/10) [513].

Lingo1, by binding in trans to its own ectodomain or by dimerizing with ErbB tyrosine kinase receptor family member 2 (Erbb2), activates small GTPase, Ras homolog family member A (RhoA) and represses Fyn tyrosine kinase, a negative regulator of RhoA signalling by inducing Rho GTPase activating protein 5 (Arhgap5). Thereby Lingo1 supports active, GTP-binding, RhoA that inhibits morphologic OPC differentiation [514–517]. Gpr17 signalling is mediated by Id2/Id4, that bind and inhibit Olig1 [518]. Notch1 is cleaved by a gamma-secretase upon binding to axonally expressed jagged-1 and delta-1, which releases the notch intracellular domain (Nicd) that enters the nucleus, forms a complex with recombination signal binding protein for immunoglobulin kappa J region (Rbpj) and induces the expression of Hes1 and Hes5 [519,520]. Hes5 represses Ascl1 expression and competes with Sox10 whereby the most abundant of both factors sequestrates its opponent [521–523]. Oppositely, its non-canonical pathway launched by axonally expressed F3/contactin, a glycosyl phosphatidylinositol (GPI)-anchored neural cell adhesion molecule of the immunoglobulin superfamily, promotes OPC differentiation

through the distinctively cleaved Nicd binding to downstream Deltex1 which induces Mag expression [524]. In the canonical, differentiation inhibiting, Wnt signalling pathway, upon binding of Wnt to the receptor Frizzled, beta-catenin moves to the nucleus where it recruits transcription factor 7 like 2 (Tcf7l2, also called Tcf4) to its target genes, delaying OPC differentiation [525–527].

OPC migration is guided by proteins that are secreted (chemoattractant Pdgfaa, Fgf2, Cxcl12/Cxcr4, Sema3f vs. chemorepellent astrocytic Cxcl1/Cxcr2, Sema3a) or presented in the extracellular matrix (chemoattract fibronectin vs. chemorepellent tenascin C, anosmin 1) and on the surface of other cells (chemoattract polysialylated neuronal cell adhesion molecule (Psa-Ncam), claudin 11 – oligodendrocyte specific protein vs. chemorepellent membrane-bound Sema4d, Ephrins/Eph, N-cadherin) [489]. Moreover, the OPCs mutually repel each other to ensure a homogenous distribution [528].

*OPC differentiation*

Once at destination, OPCs will stepwise pass through a transient stage of premyelinating OLs and then terminally differentiate into post-mitotic mature myelinating OLs in a controlled, timely scheduled manner (figure 0.4) [528]. Tcf7l2, expressed at late OPC/premyelinating OL stage, acts as a molecular switch of OPC differentiation, as histone deacetylase complex 1/2 (Hdac1/2) disrupts it from beta-catenin, when beta-catenin levels are low, by decreased Wnt signalling or by increased beta-catenin proteasomal degradation mediated by Sox17 [529,530]. Moreover to promote OPC differentiation and subsequent myelination, Tcf7l2 interacts with zinc finger and BTB domain containing 33 (Zbtb33), which blocks beta-catenin, at differentiation onset, and recruits Sox10 during OL maturation [531]. Ascl1, alongside Nkx2.2, and Olig2, both involved in OPC specification, also play an active role in OPC differentiation [503,532,533]. Herein, Nkx2.2 binds to the promoter of Pdgfra to repress its expression [534]. Although Nkx2.2 is required for OPC differentiation, it can inhibit Mbp expression and is thus transiently downregulated at the onset of myelination alongside re-expression of Nkx6.2 needed for the expression of paranodal molecules [535–537]. Of note, the binding sites of Olig2, Sox10 and myelin regulatory factor (Myrf) display a substantial overlap. Hereby, Olig2 recruits chromatin-remodelling enzyme Smarca4 (SWI/SNF related, matrix

associated, actin dependent regulator of chromatin, subfamily A, member 4, also called Brg1) to regulatory regions of key differentiation genes, making them accessible to transcription factors Sox10 and Myrf, that act synergistically on a subset of myelin genes, but not for all [487,538–540]. Remarkably, unlike the other transcription factors that are expressed throughout OPC/OL development, Myrf is specifically induced by Sox8/10 and Olig2/Smarca4 chromatin remodelling complex at the early stages of differentiation and is needed for both initiation and maintenance of myelination, by inducing many genes encoding cytoskeletal, (para)nodal, lipid metabolism and myelin proteins (Mbp, Plp) as well as other transcription factors (Smad7, Nkx6.2) and receptors (Fgfr2, Gpr37) [538]. Smad7, induced by zinc finger E-box binding homeobox 2 (Zeb2) inhibits Bmp and Wnt/beta-catenin signalling [541].

Although Olig1 is already expressed early in OPC development. Olig1 knockout does not affect OPCs but abrogates OL myelination resulting in axonal degeneration, hence highlighting its importance at the onset of myelination [542]. Olig1 promotes Mbp transcription in synergy with Sox10 [543]. More strikingly, as OLs mature, the relocation of phosphorylated Olig1 to the cytosol is mandatory to promote membrane expansion [544].

*Myelination*

For the process of myelination itself (figure 0.4), immature OLs extend numerous cytoplasmic protrusions mediated by actin polymerization, called filipodia, that are enlarged by the invasion of microtubules to form lamellipodia, adopting a highly branched morphology enabling them to sense their environment searching for myelin-competent axons. These cytoskeletal changes are dynamically modulated [545,546]. Hereby, extracellular matrix proteins as laminin alpha 2 or fibronectin bind with alpha-6 beta-1 integrins. Hereafter, these integrins can associate at the inner leaflet with integrin-linked kinase (ILK) that can activate PI3K/Akt and is involved in the actin cytoskeleton assembly by complexing with parvin and LIM zinc finger domain containing 1 to recruit paxillin and protein tyrosine kinase (linking it to Fyn) [547–549]. Moreover, non-receptor tyrosine kinase Fyn, is also activated by these integrins, resulting in the dephosphorylation of an inhibitory site on Fyn.

*Figure 0.4 OPC differentiation and myelination*

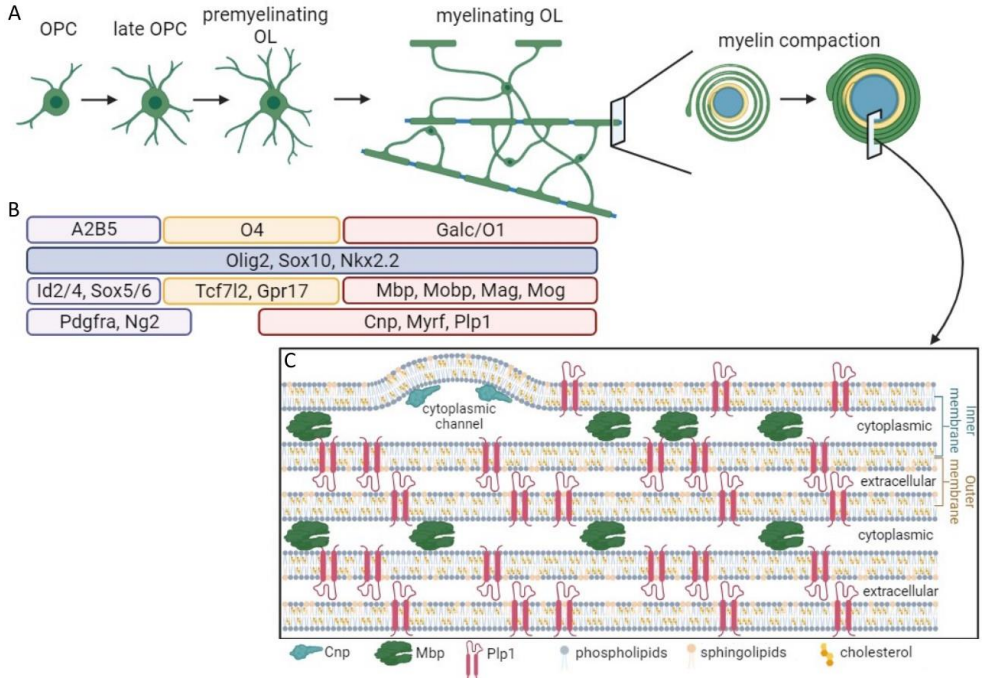


*(A) OPCs differentiate into myelinating OLs and enwrap an axon (blue) at the inner tongue whereafter the myelin is compacted. (B) OPC differentiation can be staged by the expression of distinctive genes ((late) OPC markers (purple), premyelinating OL markers (yellow), myelinating OL markers (red), overall markers (blue)). A2B5, O4 and O1 are not themselves expressed by OPCs/OLs but recognise surface proteins and are typically used in immunocytochemistry. Of note, markers do not switch abruptly but progressively overlap at stage transition. (C) This figure shows the structure of compacted myelin with key myelin proteins (Cnp, Mbp and Plp) and the distribution of cholesterol, phospholipids (phosphatidylcholine in the outer leaflet, plasmalogens and other phospholipids in the inner leaflet), and sphingolipids (galactocerebrosides and sphingomyelin in the outer leaflet). Myelin compaction by zippering via Mbp results in the apposition of the inner/cytoplasmic and outer/extracellular membrane leaflets (corresponding respectively to the major-dense lines, and intraperiod lines in electron microscopy). Cnp hinders myelin compaction and forms cytoplasmic channels for molecule transport. Adapted from Jackman et al (2009), Kister and Kister (2023), Poitelon et al (2020)[550–552] and from the master thesis of Pauline Pauss. Created in BioRender.com. OPC = oligodendrocyte progenitor cell, OL = oligodendrocyte.*

Activated Fyn induces ERK signalling pathway and acts on several small GTPases of the Rho subfamily by the inhibition of RhoA, through phosphorylation of Arhgap5, and by the activation of cell division cycle 42 (Cdc42) and Rac family small GTPase 1 (Rac1), through phosphorylation of protein tyrosine kinase 2 (Ptk2) [515,553,554]. By activating downstream Rho associated coiled-coil containing protein kinase (Rock), active GTP-binding RhoA favours the formation and contraction of stress fibres, that inhibit both process expansion and differentiation in OPCs. This negative effect is further abided by phosphorylated myosin II, also acting as an actin-depolymerizing agent, enhanced by Rock [545,555,556]. Moreover, morphological deficits in Ilk-deficient OLs was caused by increased RhoA activity [549]. The synergistic contribution of Cdc42 and Rac1 to myelination requires tight regulation of their expression as both Cdc42 and Rac1 knockout result in an abnormal accumulation of cytoplasm at the inner tongue of OL processes and outfolding of myelin [557]. Cdc42 and Rac1 can bind to and activate p21 activated kinase (Pak), an actin regulator, by inducing a conformational change and the autophosphorylation of Pak [558–560]. Pak1, a member of the group 1 PAKs that is particularly enriched in OL, promotes morphologic changes in OL and myelination [561,562] Furthermore, Cdc42 activates neural Wiskott-Aldrich syndrome protein (WASP) like actin nucleation promoting factor (Wasl, also known as Nwasp), involved in the formation of filipodia, while Rac1 activates WASP family member 1 (Wasf1, also known as Wave1), involved in the formation of lamellipodia [563,564]. Both Wasl and Wasf1 act on actin polymerization within the cell processes and are necessary for myelin ensheathment [565–567]. There is possibly an additional link between the pathways downstream Ilk and Fyn as Ilk and paxillin potentially regulate Wasl and Wasf, but this remains to be explored in OLs [545,549,568].

### ii. Myelin and nodes – ultrastructure and function

Differently from the Schwann cells, that only myelinate a segment of a single axon in the peripheral nervous system, OLs extend flattened membrane processes to 40-60 axons to enwrap an internodal segment of each axon, thereby myelinating several axons to a different extent depending on their diameter, and enhancing its surface up to 2 $mm^2$ [551,569]. Myelin sheaths are thus the extension of the OL cell membrane that is however remarkably different from a typical cell membrane (figure 0.4). Myelin has a low water content versus a high proportion of lipids (70-

85% of its dry weight), and a low proportion of proteins (15-30%), contrarily to the 50/50 lipid/protein-ratio in a typical cell membrane. Although no lipids are uniquely specific to myelin, the composition of the major lipid components is unique to myelin, consisting of 40% cholesterol, 40% phospholipids (mainly ethanolamine plasmalogens and phosphatidylcholines) and 20% glycosphingolipids (particularly galactocerebroside and galactosulfatide) (versus 25%/65%/10% in a typical cell membrane). Phospholipids are more abundant in the inner and glycolipids in the outer layer of the membrane. This highly hydrophobic, poorly permeable, insulating bilayer membrane has thus a high proportion of saturated, long-chain fatty acids, to ensure its tight packing [552,570–573]. Myelin lipid biosynthesis is finely modulated at the level of the enzymes involved in their metabolism [574]. Moreover, astrocytes are an important cholesterol supplier [371]. Myelin-associated proteins are also very specific and strongly contribute to the ultrastructure and function of the myelin sheath [575]. Proteolipid protein (PLP), a transmembrane protein and the most abundant myelin protein of the CNS with 38% of its total protein mass, fixes the apposition of the outer leaflets by its hydrophilic extracellular domain [576,577]. *PLP1* gene gives 2 isoforms by alternative splicing, the shorter, less abundant but functional DM20 (25kDa) and the longer PLP (30kDa) [577–579]. PLP safeguards myelin and axonal integrity [578]. Duplication and missense mutations in the *PLP1* gene, causing Pelizaeus-Merzbacher disease, result in OL cell death due to the toxicity of accumulated mutated PLP, myelin swelling and abnormal folding, and hypomyelination of the cerebral and cerebellar white matter [580–583]. Contrarily, PLP null mutations are associated with noticeably less myelin loss and large areas with normal myelination, but with more axonal swelling and degeneration, which is also observed in PLP knockout mice [470,584]. Myelin basic protein (MBP), the second most abundant protein of the CNS (30%) existing as different isoforms by alternative splicing and different isomers by posttranslational modifications, is a positively charged intracellular protein bridging by electrostatic forces two apposing negatively charged cytoplasmic leaflets of the myelin sheath, indispensable for its compaction [576,585–590]. Mbp is also involved in cytoskeletal turnover, calcium homeostasis, membrane expansion and Fyn-mediated signalling [589]. Remarkably, while the average cholesterol content of myelin is 40%, it has been measured that a cholesterol content of 44% is thermodynamically the most optimal for MBP interaction [552,591]. Moreover, after transcription, *MBP* mRNA binds to heterogeneous nuclear ribonucleoproteins (e.g. hnRNPA2, hnRNPF) and is

transported in granules to the distal end of membrane processes where hnRNPA2 is phosphorylated by activated Fyn kinase upon which *MBP* mRNA is released, and locally translated by free polysomes to be directly incorporated into the myelin sheath [592–595]. Myelin oligodendrocyte basic protein (MOBP) is quite similar to MBP. It is dispensable for myelin compaction but reinforces the apposition of the cytoplasmic leaflets. Moreover, it increases the expansion of the membrane processes. It is also transported in granules bound to hnRNPA2 and translated close to the cell membrane upon Fyn activation [596,597]. Other proteins are quantitatively minor. 2',3'-cyclic nucleotide 3' phosphodiesterase (CNP) associates with the actin cytoskeleton forming struts to oppose MBP-mediated membrane zippering and form cytoplasmic channels to allow the transportation of molecules [598]. Myelin-associated glycoprotein (MAG), a transmembrane protein, member of the immunoglobulin superfamily, with a heavily glycosylated extracellular part, is located in the periaxonal myelin membrane, where it interacts with neuronal gangliosides establishing the axon-myelin spacing [599–601]. MAG can induce signalling through Fyn tyrosine kinase in OLs and is thereby involved in myelination [602,603]. MAG can also bind to the Ngr1-Lingo1-Troy/p75 complex on axons inhibiting axonal outgrowth by activating downstream RhoA signalling [461]. MAG further contributes to the maturation of the axonal cytoskeleton by inducing the phosphorylation of neurofilaments and microtubule associated proteins through cyclin dependent kinase 5 (CDK5) and ERK1/2 activation [604].

Myelin ensheathment occurs in a bidirectional movement allowing its radial and longitudinal growth. First, the flattened membrane extension wraps spirally around the axon, whereby the newly formed myelin membrane is added at the inner tongue, crawling underneath the previously deposited membrane thanks to dynamic actin remodelling [605,606]. After a few wraps, myelin compaction, driven by the electrostatic interaction and folding of MBP with two adjacent cytoplasmic leaflets of the myelin bilayer membrane, progresses from the outermost layer on inwards [585,588,606]. Electron microscopy shows this multilayered periodic structure of alternating major-dense lines, representing the condensed cytoplasmic surfaces, and intraperiod lines, corresponding to the tightly apposed outer membranes, with a periodicity of approximately 12 nm [588].

Myelin also grows at the lateral edges longitudinally towards the future node [606,607]. When it is close to the growing myelin sheath of the opposite internode, up to 40

terminal loops of the myelin sheath are anchored to the axon by the paranodal proteins (contactin-associated protein Caspr and contactin-1 at the axonal side, neurofascin at the glial side, bound to the cytoskeleton), forming the axon-glial junction [463,608–611]. Except of the very narrow junctional gaps for diffusion of nutrients and metabolites, this paranodal barrier (4 µm) tightly separates clusters of sodium channels and other proteins of the node (1 µm) from the potassium channels in the juxtaparanode segment (10-15 µm), preventing any current leakage, as high potassium levels cause repetitive depolarization and lead to conduction block by inactivation of the sodium channels [370,569,612–614]. Moreover, myelin also ensures potassium siphoning as gap junctions, composed of connexins, connect the periaxonal space to the inner myelin sheath and further at the outer layer to a network of interconnected glial cells. Astrocytes are further connected to ependymal cells and to the pericapillary and subpial space, forming thus the panglial syncytium (between oligodendrocytes/astrocytes/ependymal cells) allowing an osmotic and ionic homeostatic regulation of the periaxonal space [370,615–618].

The myelin sheaths effectively insulate the internode region of the axon, but also separate it from the extracellular nutrient-rich environment. Therefore, axons are metabolically supported by OLs [619,620]. OLs sense their metabolic needs through N-methyl-D-aspartate (NMDA) receptors at the inter/paranodal membrane and produce lactate by glycolysis which they transfer to axons through the solute carrier family 16 member 1 (*Slc16a1*, also known as monocarboxylate transporter 1 (*Mct1*)) at the adaxonal membrane [621,622]. Hereby, cytoplasmic channels, formed by CNP, connect the OL cell body to the innermost myelin layer allowing molecule and organelle transport in between the surrounding compacted myelin [598,623]. Remarkably, OL-specific Slc16a1/Mct1-deletion in mice causes axonal degeneration with normal myelination [621].

### iii. Key signalling pathways

Several signalling pathways are concomitantly or successively involved in OPC proliferation and/or differentiation (figure 0.5).

*Wnt/beta-catenin signalling pathway*

In the canonical Wnt/beta-catenin signalling pathway, an extracellular Wnt family member binds to a seven-transmembrane domain frizzled receptor and a single-transmembrane domain coreceptor, the low density lipoprotein receptor related protein (LRP5/6). LRP5/6 is thereby phosphorylated and recruits axin, which is mediated by a cytoplasmic signalling molecule, dishevelled segment polarity protein (DVL). This results in the dissociation of the intracellular beta-catenin destruction complex, formed by axin, adenomatous polyposis coli (APC), glycogen synthase kinase 3b (GSK3B), and casein kinase 1 (CK1) and responsible for the proteasome-mediated degradation of beta-catenin. Beta-catenin, that has no DNA binding site, can then translocate to the nucleus and interact with one of the four transcription factors of the TCF/LEF family (TCF7, TCF7L1, TCF7L2, lymphoid enhancer binding factor 1 (LEF1), of which TCF7L2 is specific to OLs). Canonical Wnt signalling mediates cell fate via its target genes that are cell type and developmental stage specific [624,625]. Id2, an inhibitor of OPC differentiation, is induced by Wnt/beta-catenin/Tcf7l2 [626].

The role of the canonical Wnt/beta-catenin pathway in OPCs during development is still not completely understood. Some controversies remain from the different experimental models as they do not exclude involvement of parallel pathways [625]. Overall, forced Wnt/beta-catenin activation can both inhibit OPC generation and promote postnatal/adult OPC generation/proliferation from the subventricular/subependymal zone. Therefore endogenous Wnt/beta-catenin activity might rather modulate the timing of OPC specification from embryonic neuronal progenitor cells depending on the microenvironment [625,627–629]. Tcf7l2 is not expressed in adult normal white matter, but the Wnt/beta-catenin signalling pathway is (re)activated during developmental myelination and remyelination. Herein, low levels of Wnt/beta-catenin/Tcf7l2 promote the transition from OPCs to immature OLs, whereas a forced activation of Wnt/beta-catenin/Tcf7l2 delays OPC differentiation and myelination with however progressive partial normalisation into adult life, without affecting OPC proliferation, apoptosis or adoption of another cell fate [525,526,530,628,630]. The same was evidenced during remyelination with constitutively active Wnt/beta-catenin signalling in mice models of demyelination [525]. Unexpectedly, Tcf7l2 knockdown in mice is lethal soon after birth and marked by a decreased expression of myelin gene [631,632]. Tcf7l2 is mainly expressed in CNP+

premyelinating (pre-)OLs and promotes timely OL maturation by a two-modal action, wherein beta-catenin/Tcf7l2 complex inhibits OPC differentiation (as a transcriptional activator), but when beta-catenin levels are low, Tcf7l2 is caught by Hdac1/2 and promotes OPC differentiation (as a transcriptional repressor) [530,631]. Tcf7l2 can also bind to the regulatory element of Bmp4, thereby repressing it and allowing OPC differentiation and remyelination as Bmp4 opposes this by inducing its target genes, such as Id2/4 via phosphorylation of Smad1/5 [633,634]. Interestingly, TCF7L2, undetectable in normal adult white matter, is expressed in early but not in chronic MS lesions. While one study colocalised it with Olig2 within active lesions, another found it aside Nogoa at the periplaque white matter and in remyelinating areas, rather than in demyelinating/demyelinated lesions. Whether it hereby promotes or affects remyelination remains to be determined [525,635].

In the noncanonical Wnt signalling pathway, Wnt still binds to a frizzled receptor and phosphorylates DVL, but it does not involve downstream beta-catenin nor its degradation complex. Hereby, it can increase intracellular calcium which leads to the activation of calcium/calmodulin-dependent kinase and protein kinase C, or induce a planar cell polarity pathway involving small GTPases or c-Jun N-terminal kinase to modulate the cytoskeleton [636]. Noncanonical Wnt signalling seems to prompt neurodegeneration by microglial induction in neurons but has not been investigated directly in OPCs/OLs [637].

*Mitogen-activated protein kinases signalling pathways*

Mitogen-activated protein kinases (MAPK) are one of the components of a three-kinase cascade, activated by subsequent phosphorylation events starting from MAPKKKs to MAPKKs (MAP2K) and finally MAPKs, downstream a wide range of receptors (receptor tyrosine kinases (RTKs), G-protein coupled receptors (GPRs), cytokine receptors etc). There are three major families of MAPKs with multiple partners underlying the cell- and context-dependent diversity of actions. The effect of MAPKs results from their phosphorylation of downstream cellular and nuclear targets, directly or via MAPK-activated protein kinases (MAPKAPKs, consisting of ribosomal S6 kinases (RSKs), mitogen- and stress-activated kinases (MSKs), MAPK-interacting kinases (MNKs), MAPKAPK2/3) [638].

(1) The mainly stress-induced c-Jun N-terminal kinase (JNK) is encoded by 3 genes, with each existing as multiple isoforms by alternative splicing, influencing their substrate specificity, JNK1 or MAPK8 and JNK2/MAPK9, ubiquitously expressed, and JNK3/MAPK10, only expressed in the brain, heart, and testis. JNK is activated by MAP2K4/7 [638,639]. Moreover, Ras can induce the activation of Jnk in a Raf/Erk-independent pathway, possibly via Ras p21 protein activator 1 (Rasa1) [640]. Among many others, the key downstream substrates of JNK are the transcription factors JUN proto-oncogene (mainly JUN/c-JUN but also JUNB, JUND) and FOS proto-oncogene (FOS, FOSB, FOS like (FOSL) 1, and FOSL2) that dimerize to form the active activator protein 1 (AP1) complex. JNK signalling pathway is involved in the regulation of cell proliferation, differentiation, survival and apoptosis [638,639,641].

In vitro proliferation of OPCs promoted by the conditioned medium of B104 neuroblastoma cells, containing both Pdgfaa and basic Fgf depends on the phosphorylation of Jnk (as well as Erk1/2) and the expression of downstream c-Jun, c-Fos and c-Myc [642,643]. Jnk1 knockout mice are postnatally marked by hypomyelination resulting from the impaired morphological maturation of OPCs exhibiting a reduced branching morphology. These OPCs are however highly proliferative and do not fail to differentiate into Mbp-expressing OLs [644]. On the contrary, phosphorylated c-Jun was found to downregulate Mbp and Cnp expression in a Sox10-independent manner by binding at a AP1-like site at Mbp promoter only after inhibition of p38MAPK activity [645,646]. This binding was however lost when the cells differentiated as Sox10 can interact with and sequestrate c-Jun to attenuate AP1 activity [646,647]. Moreover, Jnk1 maintains the cytoskeletal integrity by regulating microtubule dynamics through phosphorylation of microtubule associated protein 1b (Map1b) as evidenced in neuronal cells and Map1b is expressed in myelinating OLs [648,649]. However, Jnk, rather Jnk3, also transduces the signalling for oligodendroglial apoptosis [650,651]. In Schwann cells, c-Jun blocks myelination and promotes their dedifferentiation [652,653].

(2) The extracellular signal-regulated kinases (ERK) ERK1/MAPK3 and ERK2/MAPK1, are phosphorylated by MAP2K1/2, themselves activated by MAP3Ks, mainly of the Raf family, and upstream MAP4K such as Ras signal transduction proteins. Their extracellular signals can be of many types, as growth factors, transforming growth factors, neurotrophic factors, cytokines, cell stressors etc, and bind to receptors as

RTK, GPR, that transduce the signal to the ERK/MAPK signalling pathway through adapter proteins as growth factor receptor-bound protein 2 (GRB2), Src homology 2 domain containing transforming proteins (SHC), and SOS Ras/Rac guanine nucleotide exchange factor. c-Fos and c-Myc are downstream targets of ERK1/2, among others [638,654].

Although in vitro inhibition of Erk1/2 potentiated AMPA-induced excitotoxicity, in vivo data point towards a negligible role of Erk1/2 in OL survival [655–657]. Nevertheless, Erk1/2 plays a temporally specific role in OPC proliferation, promoting it in the earliest stages (evidenced by Olig1/2-Cre driven genetic manipulation) while being dispensable in later stages (evidenced by Ng2-Cre drivers or in $O4^+$-OPCs) [656–659]. In vitro proliferation of OPCs promoted by the conditioned medium of B104 neuroblastoma cells depends on the phosphorylation of Erk1/2 (as well as Jnk) resulting in the expression of c-Jun, c-Fos, Id2 and cyclins D1, D2, E [642,643]. The involvement of ERK/MAPK signalling in OPC differentiation (based on O4/O1/Galc staining or Plp expression) is still debated [654,656,657,659–661,661]. Erk1/2 was suggested to promote the transition from early to late progenitors and immature OLs but to be dispensable thereafter [660,661]. On the contrary OL-specific ablation or constitutive activation of Erk1/2 signalling in vivo did not affect Plp expression and thus OPC differentiation [656,657]. Notably, Erk1/2 activation temporally coincides with active myelination. Hereby, in vivo and in vitro constitutively active Map2k1 increases while Erk1/2 knockout decreases myelination (based on Mbp expression) and myelin thickness (based on electron microscopy) without affecting numbers of OL and of myelinated axons [656,657,659,660]. The loss of Erk2 is more critical and is only partially compensated by Erk1 [660]. ERK/MAPK signalling is on longer terms needed to ensure myelin maintenance and axonal integrity [662]. Its sustained activity fastens myelin repair and increases myelin thickness in lysolecithin lesions [663]. On the contrary, in vitro pharmacological inhibition of MAP2K/ERK pathway in neuronal progenitor cell-derived OPCs enhanced OPC differentiation and myelination. In vivo, it reduced EAE severity and accelerated remyelination after cuprizone withdrawal [664].

Brain-derived neurotrophic factor, by binding to the neurotrophic receptor tyrosine kinase 2 (Ntrk2), induces non-receptor tyrosine kinase Fyn, that then phosphorylates Ras and launches the ERK cascade, promoting myelination [665]. Fyn can also be activated by extracellular matrix proteins that interact with

transmembrane beta-1 integrins. It is further involved in cytoskeletal dynamics, OPC differentiation and myelination by modulating small GTPase activity of RhoA, Rac1 and Cdc42, but also by regulating Mbp translation in membrane processes through hnRNPA2/F (as largely detailed in Introduction II.i.) [515,553,555,557,594,595].

(3) p38MAPKs consist of p38MAPK alpha and beta, both ubiquitously expressed, gamma and delta, respectively MAPK14/11/12/13. p38MAPK is mainly stress-induced and is activated by MAP2K3/6. It can be activated upstream through Rac1 and Cdc42 that bind to and activate group I PAKS (PAK1/2/3). It is also involved in cell growth, differentiation, apoptosis, and inflammation [638,666].

p38MAPK induces the transition from OPCs to pre-OL and further as well as the initial establishment of axonal contact necessary for myelination, marked by an early increase of phosphorylated MAPKAPK2 and an upregulation of differentiation and myelin genes (Cnp, Mbp, Plp, Mag). [645,667–669]. Hereby, it promotes Sox10 DNA-binding activity to *Mbp*, without changing its transcriptional levels [645]. The inhibition of p38MAPK pathway is remarkably most effective early after mitogen withdrawal, thereby emphasising its role in the transition to pre-OL. p38MAPK inhibition decreases their morphological differentiation, overall without affecting OPC proliferation or survival, although a decrease in proliferation capacity has been described as well [645,668,669]. p38MAPK antagonises ERK, Jnk and c-Jun phosphorylation and vice versa, Jnk and Erk mediate p38MAPK inhibition, suggesting that this reciprocal relationship could tightly coordinate OPC differentiation [645]. Hereby p38MAPK may block Ras-induced Jnk activation via Mapkapk2 and block Erk activation by inducing dual specificity phosphatase 6 (DUSP6) [645,670,671]. Moreover, c-Jun inhibits Mbp expression by binding to an AP1-like site in its promoter, but this is only possible after inhibition of p38MAPK activity [645,646].

*PI3K/AKT/mTOR signalling pathway*

In the PI3K/Akt/mTOR pathway, phosphatidylinositol-4,5-bisphosphate 3-kinase (PI3K), induced upon binding of a growth factor to a RTK, phosphorylates phosphatidylinositol-4,5-biphosphate (PIP2) into phosphatidylinositol-3,4,5-

triphosphate (PIP3). Hereby, AKT serine/threonine kinase (AKT, also known as protein kinase B) and 3-phosphoinositide dependent protein kinase 1 (PDPK1) are recruited to the cell membrane, allowing PDPK1 to partially phosphorylate AKT. AKT phosphorylates and inhibits tuberous sclerosis complex, subunit 1 and 2 (TSC1/2), GTPase-activating proteins, which releases Ras homologue enriched in brain (RHEB). RHEB activates mTOR complex 1 (mTORC1), formed by mammalian target of rapamycin kinase (mTOR) and regulatory associated protein of mTORC1 (RPTOR), that phosphorylates its downstream targets ribosomal protein S6 kinase B1 (RPS6KB1, an inducer of translation through phosphorylation of RPS6 and EIF4B), and eukaryotic translation initiation factor 4E binding protein 1 (EIF4EBP1, a repressor of translation by binding EIF4E that is released upon its phosphorylation). Contrariwise, mTORC2, formed by mTOR and RPTOR independent companion of mTORC2 (RICTOR), is directly activated downstream PI3K and TSC1/2 in a RHEB-independent manner. mTORC2 reinforces the pathway by phosphorylating AKT [672,673].

mTOR signalling is determinant for the differentiation from immature to mature OLs [661,674]. PI3K/Akt/mTOR signalling pathway is further involved in lipid biogenesis, initiation of myelination, and myelin thickness [675]. Forced activation of the pathway, by knockout of phosphatase and tensin homolog (Pten), a negative regulator of PI3K, or constitutively activated Akt, resulted in hypermyelination [676–678]. Similarly, mTOR inactivation, by rapamycin (pharmacologically), by mTOR knockout, and more specifically by Rptor, rather than by Rictor knockout, decreased OPC differentiation (evidenced by reduction in Galc+ OLs) and myelination, indicating the prominent role of mTORC1 in CNS myelination, while none of these affected the total numbers of OPCs and OLs [674,679–681]. Remarkably, these effects persist throughout life [676,681]. PI3K/Akt/mTOR signalling pathway involves phosphorylation of Rps6kb1, Rps6 and Eif4ebp through mTORC1 and of Akt through mTORC2 [674,678,679,682]. Notably, Rptor knockout was not compensated by mTORC2 and Rictor knockout reduced mTORC1 signalling [679]. The pathway induces the expression of myelin protein genes (Cnp, Mbp, Plp, and possibly to a lesser extent Mag and Mog), genes related to lipid biosynthesis, both cholesterol (sterol regulatory element binding protein 2 (Srebp2), 3-hydroxy-3-methylglutaryl-coenzyme A reductase (Hmgcr) and isopentenyl-diphosphate delta isomerase 1 (Idi1)) and fatty acid synthesis (fatty acid synthase (Fasn) and stearoyl-CoA desaturase-1 (Scd1) levels, two targets of Srebp1 that was itself not affected) [679–681,683]. Rapamycin treatment

further decreased cytoskeletal proteins and factors (sirtuin 2 (Sirt2), modulating microtubule stability) and positive mediators of OPC differentiation (Fyn and quaking I (QKI6/7)), while it elevated a negative regulator, G-protein coupled receptor 17 (Gpr17), mRNA processing factors and carrier proteins [683].

*Crosstalk*

The Erbb tyrosine kinase receptor family has four members, Erbb1 or epidermal growth factor receptor (EGFR), and Erbb2/3/4 that are activated upon homo- or heterodimerization with another family member, and thereby involved in OPC specification, proliferation, survival and differentiation as well as myelination, depending on their ligand, their dimerization partner and the downstream pathway induced [684,685]. Homodimers of Erbb1/1-2/2-4/4 as well as heterodimers of Erbb1/2-2/3-2/4 can induce the Ras/Raf/MAP2K/ERK cascade through adapters as Shc, Grb2, Sos. Erbb1/1 and Erbb1/2 can further induce Jnk and p38MAPK pathways, as well as Src family tyrosine kinase/PTK2. Finally Erbb2/3 and 2/4, through binding of a neuregulin, induce the PI3K/Akt/mTOR signalling pathway [685]. Hereby Erbb1 and Errb2 are expressed in immature astrocytes and OPCs during their development whereas, Erbb1 inhibition promotes Mbp expression and OPC differentiation [686,687]. Moreover, axonal neuregulin 1 (NRG1) modulates OPC differentiation and/or myelin thickness via Erbb2, Erbb3 and/or Erbb4. Erbb3 colocalises with Cnp [686,688–690]. However, sustained Erbb activation induced apoptosis in OPCs and newly formed OLs leading to non-inflammatory hypomyelination whereas it caused necroptosis in mature OLs resulting in hypermyelination followed by inflammatory demyelination [691].

Regarding OPC proliferation, Pdgf and Fgf2 are two major mitogens, whereby Pdgf delays the differentiation from early to late progenitors and Fgf2 hinders late progenitors to enter terminal differentiation [509,692]. Likewise, Pdgfra heterozygote knockout reduces OPC proliferation and OL regeneration in cuprizone-fed mice, while Fgf2 knockout mice had more differentiated OLs. Therefore, the combination of both rescued impaired OL regeneration and thus restored lesion repopulation after cuprizone feeding [511]. Their mitogenic effect within OPCs are mediated by ERK, p38MAPK and mTOR signalling [509,693]. Fgf2 further acts synergistically with Igf1, whereby Fgf2 enhances via Erk signalling cyclin D1 (Ccnd1) expression to promote

cell cycle transition, and Igf1 phosphorylates and inactivates Gsk3b via PI3K/Akt which reduces the proteasomal degradation of Ccnd1 and increases the abundance of beta-catenin [510,694,695]. Pdgf can also induce Ccnd1 by transducing its signal through PI3K/Akt/Gsk3b or through Map2k1-2/Erk/Lrp6, a coreceptor of Wnt ligands), and is thereby linked to activation of Wnt/beta-catenin signalling [529]. Pdgfa is further involved in OPC migration, partly in combination with the extracellular matrix protein fibronectin, by the phosphorylation of Erk1/2 that then interacts with PTK2 (also known as focal adhesion kinase) and paxillin resulting in actin reorganization allowing OPC migration [696,697]. Pdgfaa is involved in OPC migration by stimulating, via Fyn, cyclin dependent kinase 5 (Cdk5) activity, that phosphorylates Wasp2 [698]. Notably, Cdk5 inhibition/ablation reduced OPC differentiation and myelination and also delayed myelin repair in lysolecithin lesions, by reducing Akt pathway while enhancing Gsk3b pathway [699,700].

Erk and PI3K/AKT/mTOR have been suggested to act sequentially on OPC differentiation, wherein Erk signalling is required for the transition from early to late progenitors whereas mTOR signalling promotes the differentiation from immature to mature OLs [661]. However, Rptor knockout was accompanied by an increase in Erk phosphorylation, although this was not evidenced elsewhere [679,680]. Therefore, it appears that both pathways converge unidirectionally at two crossing points, insulin receptor substrate 1 (Irs1) and Rps6kb1. The inhibition of Erk had little impact on PI3K/Akt/mTOR. Oppositely, by the inhibition of mTOR, the less active/phosphorylated Rps6 reduced its negative feedback on Irs1, an upstream regulator common to both pathways, whereas Irs1 could then induce the Ras/Raf/Map2k/Erk pathway [701]. Herein, Igf1 binds to Igf1 receptor which phosphorylates Irs1/2 and hereby, Igf1 induces both PI3K/Akt/mTOR, and downstream Rps6 and Eif4ebp, as well as Erk signalling pathway [702,703]. Secondly, Erk2 knockout was found to decrease the activation/phosphorylation of Rps6kb1, a downstream target of mTORC1 as well, resulting in reduced Rps6 phosphorylation and Mbp translation (without affecting its transcription) while mTOR expression and activation was unaffected. The timing of myelination is thus tightly controlled, as Mbp translation is induced upon a critical threshold of Rps6kb1 activity, coordinated by both pathways [704]. Moreover, the differentiation of OPCs, cultured in vitro without mitogens, was arrested at an early progenitor stage when inhibiting p38MAPK, but at a later stage when inhibiting ERK or mTOR signalling [509].

Interestingly, OL-specific Pten ablation increases myelin thickness with no change in OL numbers in a mTOR-dependent manner, while OPC-specific Pten ablation resulted in enhanced myelination and OL accumulation by increased OPC proliferation and differentiation to OL in a mTOR-independent manner. Herein, Pten inactivation promoted the inhibitory phosphorylation of Gsk3b by Akt in OPCs [705]. Inhibition of Gsk3b induces OPC proliferation and survival by increasing the nuclear translocation of beta-catenin. However, oppositely to the Wnt/beta-catenin signalling pathway, the inhibition of Gsk3b can also support myelination by stimulating Creb and by reducing Notch1 signalling [706]. Moreover, ERK can phosphorylate and inhibit GSK3B, resulting in increased beta-catenin levels while inhibited GSK3B reduced RPS6KB1 phosphorylation, although this has not directly been evidenced in OPCs/OLs [707,708]. Reduced Rps6kb1 can induce ERK signalling by reduced negative feedback on Irs1 [701].

*Figure 0.5: Signalling pathways involved in OPC proliferation and differentiation*

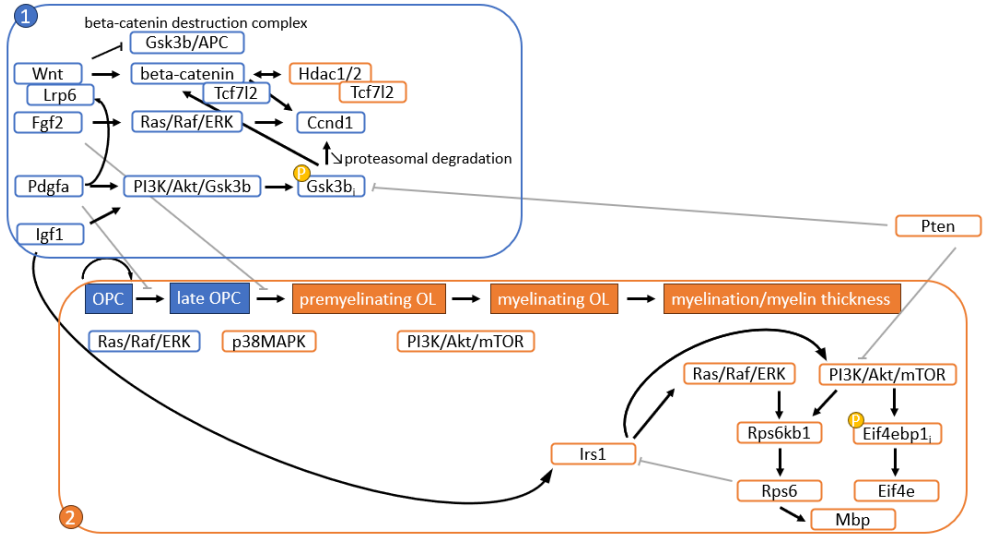


*Several pathways are involved in the (1) proliferation (blue) and/or (2) differentiation (orange) of OPCs. (1) Pdgfa and Fgf2 are two key growth factors to OPC proliferation via the expression of cyclin D1 (Ccnd1), a promoter of cell cycle transition. Fgf2 induces the Ras/Raf/ERK signalling pathway and acts synergistically with Igf1, whereby Igf1*

*phosphorylates and inactivates (i) Gsk3b via PI3K/Akt reducing the proteasomal degradation of Ccnd1 and beta-catenin. Pdgfa induces PI3K/Akt/Gsk3b signalling pathway as well as the phosphorylation of Lrp6, coreceptor of Frizzled in Wnt signalling, via Map2k1/2. The canonical Wnt signalling pathway inhibits the beta-catenin destruction complex (Gsk3b, APC, axin, Ck1), and thus increases beta-catenin levels whereby beta-catenin complexes with Tcf7l2, a transcriptional activator, to promote OPC proliferation. Oppositely, Tcf7l2 can be caught by Hdac1/2 and will then promote OPC differentiation (as a transcriptional repressor). (2) OPC to OL differentiation can be conceptualised stepwise, whereby different signalling pathways are predominantly involved at each transition. ERK signalling pathway supports transition of OPCs to late progenitors and p38MAPK signalling pathway from late progenitors to premyelinating OLs, which are respectively inhibited by Pdgfa and Fgf2. PI3K/Akt/mTOR signalling pathway promotes the final differentiation to mature myelinating OLs. Finally, myelination and myelin thickness depend on Ras/Raf/ERK and PI3K/Akt/mTOR signalling pathways, which both act through downstream Rps6kb1/Rps6 to induce Mbp expression. Rps6 further acts via a negative feedback loop on Irs1, while Igf1-induced Irs1 activates Ras/Raf/ERK and PI3K/Akt/mTOR signalling pathways. mTOR also phosphorylates downstream Eif4bp1, which then unbinds from Eif4e, promoting the translation of myelin protein genes. Pten inhibits both OPC proliferation and differentiation, by dephosphorylating respectively Gsk3b and PI3K. OPC = oligodendrocyte progenitor cell, OL = oligodendrocyte, i (subscript) = inactive form.*

iv. What's still to explore?

There is a major heterogeneity in remyelination capacity between lesions of a single MS patients and even more between MS patients [234,417,709,710]. OPCs become functionally heterogenous with regional and age-dependent differences [711]. Moreover, the tissue transcriptional signature suggests an OPC deficit in chronic lesions of cuprizone-induced demyelination as compared to acute lesions as well as differences between brain lesions in chronic cuprizone-induced demyelination [712]. Remyelination of MS lesions is more extensive in the cortex than in the white matter [234]. Age is an important factor, as the capacity of myelin clearance by macrophages (rather than microglia) decreases with age, and OPCs/OLs themselves manifest a functional decline as seen in their reduced capacity to respond to extracellular factors, to migrate or to differentiate [46,167,416,428,713]. Herein, an increased mTOR activity was accompanied by the expression of genes associated to cellular senescence as well as increased DNA damage and reduced cellular

respiration in ageing OPCs [167]. However, this OPC heterogeneity is already observed in young patients [411].

Moreover, recent findings have opened many doors to new research areas in the field. While OL were long seen as passive bystanders in remyelination, a recent study evidenced by carbon dating of genomic DNA that shadow plaques contained "old" rather than newly generated OLs. Hereby it suggests the inefficient integration of new OLs in lesions, and the remyelination by surviving OLs. Oppositely, shadow plaques might be partly demyelinated rather than thinly remyelinated lesions [411]. Furthermore, single cell RNA sequencing evidenced changes in OPC/OL heterogeneity and their transcriptional signature in MS patients as compared to controls, especially with a decrease in an OPC, intermediate OL and an end stage OL subcluster while actively myelinating OLs were present, suggesting that enhancing remyelination might not be enough to reverse MS pathogenesis [412].

Hence, the physiology and pathophysiology of OPCs/OLs is complicated and intricated as the same signalling pathways appear to be involved in OPC proliferation and differentiation, possibly determined by the ligand and receptor dimerization. Moreover, the underlying cellular changes are probably vaster than expected and multifaceted as evidenced by single cell RNA sequencing [353,412].

Thus, exploring OPC/OL physiology and pathophysiology could help further understand demyelination and (defective) remyelination processes and the underlying pathways as well as unravel ways to counter this.

## III. microRNAs

### i. Biogenesis

Microribonucleic acids (microRNAs) are small non-coding RNAs of approximately 21-24 nucleotides (nt) [714]. In 1993, Lee et al. and Wightman et al. first described a small RNA of *Caenorhabditis elegans* (*C. elegans*), *Lin-4*, not coding for a protein but with an antisense complementarity to *Lin-14* in its 3' untranslated region (3'UTR) that negatively regulated the expression level of the latter [715,716]. It is only in 2001, after the discovery of approximately a hundred similar genes encoding these short

transcripts in *Drosophila melanogaster, C. elegans* and humans, that the name "microRNA" was introduced [714,717,718]. They are distinct from the many other non-coding RNA species (small interfering (si)RNAs, Piwi-interacting RNAs, yRNA, small nuclear RNA, small nucleolar RNA, vault RNA, long non-coding (lnc)RNAs, and all derived non-canonical small non-coding RNAs) that may differ in their biogenesis and/or function [719].

MicroRNA genes are independent genes (with their own promoters) or enclosed within the introns of a coding gene (and thus coordinated with the expression of a protein) (figure 0.6). They are transcribed by RNA polymerase II, mainly (in rare cases by RNA polymerase III), and fold into an imperfect double-stranded hairpin, the primary (pri-)microRNA. It is hereafter processed successively by two RNase III type endonucleases, containing each two RNase III domains for a separate cut of each strand, leaving a 2-nt 3' overhang. DROSHA, complexed with DiGeorge syndrome critical region gene 8 (DGCR8, containing double stranded RNA binding domains) cleave the pri-microRNA into the precursor (pre-)microRNA, a 70-nt hairpin, in the nucleus, which is then exported to the cytoplasm by exportin 5. In the cytoplasm, the hairpin-end is cleaved by DICER, complexed with TAR RNA binding protein (TRBP), leaving a 21-24 base-pair microRNA duplex. The strand with the 5' terminus located at the thermodynamically less stable end of the microRNA duplex is selected as "guide" single stranded mature microRNA and loaded onto the microRNA-induced silencing complex (miRISC) containing an Argonaute protein (AGO 1 to 4 in mammals) and other regulatory/effector proteins. The other "passenger" strand is degraded, although sometimes both strands can be selected and functionally active [720,721]. Alternately, a few spliced out introns fold into a hairpin corresponding to a pre-microRNA, and these miRtrons are, without cleavage by DROSHA, further processed by exportin 5 and DICER [722]. All the steps of microRNA biogenesis can be finely regulated by accessory proteins [723]. To note, microRNAs have been numbered in order of discovery. To date, miRbase has 1917 human microRNA entries (https://mirbase.org/browse/results/?organism=hsa). Previously the less abundant functional strand was indicated by an asterisk, but to avoid any confusion seen the amount of microRNAs, both strands are now denoted with the suffix -3p or -5p [724].

*Figure 0.6 microRNA biogenesis*

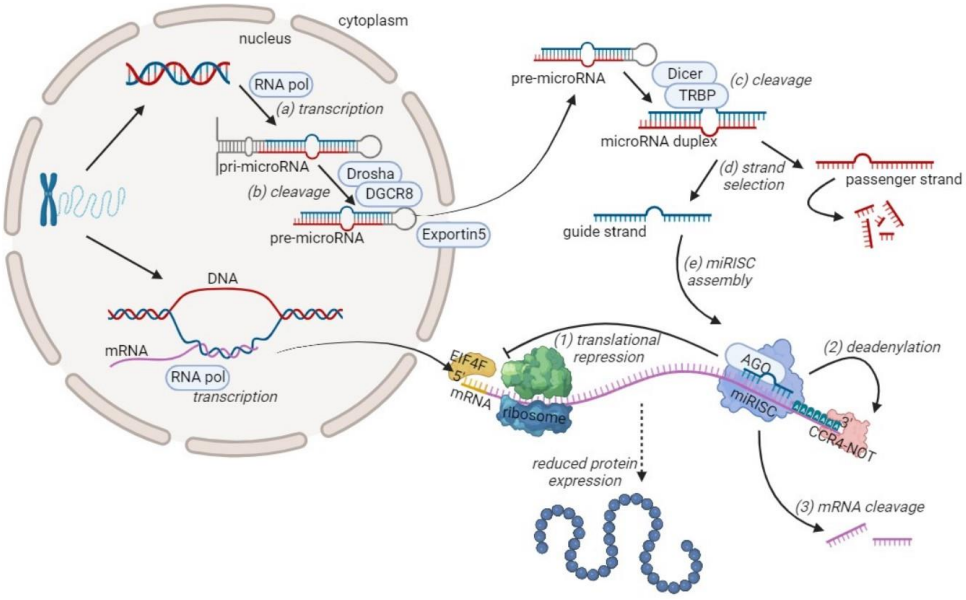


*RNA polymerase (RNA pol) II (a) transcribes DNA into a primary microRNA (pri-microRNA) which is further (b) cleaved by endonuclease Drosha, complexed with DiGeorge syndrome critical region gene 8 (DGCR8) into a precursor microRNA (pre-microRNA). The pre-microRNA is exported from the nucleus into the cytoplasm by exportin 5 where it is (c) cleaved by endonuclease Dicer, complexed with TAR RNA binding protein (TRBP), into a microRNA duplex. Hereafter, the guide strand is (d) selected from the passenger strand, the latter is usually degraded (although in some cases it can be selected as guide strand as well), the former is (e) loaded with an Argonaute (AGO) protein onto the microRNA-induced silencing complex (miRISC). This complex binds by complementarity to its seed region in the 3' untranslated region and (1) represses translation by competing with the eukaryotic initiation factor 4F (EIF4F) complex at the 5' cap region or by dissociating the ribosomes. It can also (2) destabilise the mRNA by inducing deadenylation by the CCR4-NOT deadenylase complex. Both result in reduced protein expression. In the rare case of perfect mRNA/microRNA complementarity AGO2 can (3) cleave the mRNA via its catalytically active RnaseH-like domain. Created in BioRender.com*

ii. Mechanism of action

MicroRNAs mainly negatively regulate gene expression post-transcriptionally by binding by complementarity to the 3'UTR of their target messenger RNA (mRNA) [725]. Hereby, microRNAs regulate an estimated 30-60% of protein-coding genes, hence participating in the regulation of almost every cellular process and implicated in pathologies by changes in their expression [721,726].

MicroRNAs bind to the 3'UTR of their target mRNA by base pairing, although complete complementarity is rare in animals. Instead, a perfect and contiguous 6-8 oligomer base pairing (the longest, the strongest), centred on their seed (nt 2-8) is mandatory, and stabilized by a reasonable complementarity to the 3' half of the microRNA (particularly to nt 13-16). Moreover, microRNA seeds are remarkably conserved between species [721,725,727,728]. Binding to the open reading frame and 5'UTR of the mRNA has been reported as well but is less frequent and less effective as the silencing complexes would be displaced by the translation machinery, up to approximately the 15$^{th}$ nt after the stop codon [725,729,730]. A mRNA can have multiple seed regions of a single microRNA or the seed region of several microRNAs, that act cooperatively if they are close (<40 nt) and independently if not to repress the mRNA [729]. Therefore, one microRNA can potentially target hundreds of mRNAs and each mRNA can be targeted by several microRNAs. Since they are not all expressed within one cell, the cell-specific microRNA milieu finely tunes the mRNA expression [725].

Regarding mRNAs, translation is initiated by recognition of the mRNA 5'-terminal 7-methylguanosine ($m^7G$) cap by the precedingly phosphorylated eukaryotic translation initiation factor (EIF) 4E, part of the multi-subunit complex EIF4F containing EIF4A (an RNA helicase), and EIF4G (a scaffold protein for the assembly of the complex) as well. Upon interaction of EIF4G with EIF3 and polyadenylate [poly(A)] binding protein 1 (PABP1, associated with the poly(A) tail), the latter allowing circularisation of the mRNA, the 40S ribosomal subunit is recruited, and attracts the 60S ribosomal subunit at the start codon for translation elongation until the stop codon where both subunits are dissociated again and easily recycled due to the circular conformation of the mRNA. EIF6 participates to the 60S ribosomal subunit biogenesis and might inhibit its recruitment. Less frequently, the ribosomal subunits are recruited at the internal ribosome entry site (IRES), independently of cap and the translation initiation complex [721].

In the rare cases of perfect complementarity, AGO2, the only Argonaute protein with a catalytically active RnaseH-like within the P-element induced wimpy testis (Piwi) domain, cleaves the mRNA in the centre of the microRNA-mRNA duplex, between nt 10-11 [731,732]. More often, however, protein synthesis is lessened by repressing translation initiation or by destabilising the mRNA (figure 0.6) [721].

Cap-initiated translation can be repressed by miRISC by promoting the dissociation of EIF4A1 and EIF4A2 before releasing the other complexed proteins [733]. Argonaute proteins can bind to $m^7$G-cap, although with lower affinity than EIF4E, and thus compete with the latter especially if there are several microRNA binding sites whereby multiple Argonaute proteins can be recruited. This impedes the recruitment of the 40S ribosomal subunit and the mRNA circularisation, possibly rendering the poly(A) tail more vulnerable to deadenylation [734–736]. Alternately, EIF6 can associate with miRISC in a multiprotein complex and hereby reduces the 60S ribosomal subunit recruitment [737]. Furthermore, instead of reducing translation initiation, microRNAs could induce premature dissociation of ribosomes or decelerate the translation elongation, as repressed mRNAs with actively translating polyribosomes have been reported. These mechanisms are still unclear but could explain the repression of IRES-mediated translation [738–740]. Finally, microRNAs can destabilise a mRNA by inducing deadenylation by the CCR4-NOT deadenylase complex. Within the CCR4-NOT complex, CCR4 interacts with trinucleotide repeat containing adaptor 6A (TNRC6A, better known as GW182) through CCR4-NOT transcription complex subunit 9 (CNOT9), and both CCR4 and CNOT9 are scaffolded to CNOT1, that recruits DEAD-box helicase 6 (DDX6, a translational inhibitor) and modulates its ATPase activity [741–743]. This can be followed by a 3'-to-5' decay by an RNA exosome complex containing several 3'-5' exoribonucleases or by a 5'-to-3' decay by the 5'-3' exoribonuclease 1 (XRN1) following decapping by decapping mRNA proteins (DCP1/2) [741,744,745]. Moreover, GW182 can dissociate EIF4G and PABP from respectively the 5' and 3' end of the targeted mRNA, which is independent of deadenylation [746]. The deadenylation of the poly(A) tail might as well impede the synergy between the 5' cap and 3' poly(A) tail by disrupting the EIF4G-mediated mRNA circularisation [743,747]. MicroRNA-targeted mRNA repression is initiated in the cytosol. Hereafter, Argonaute proteins interact with GW182 to load onto mRNA ribonucleoproteins that accumulate in discrete granules, called GW- or P-bodies, enriched in these proteins involved in mRNA catabolism, to be degraded or to be stored [748–750].

### iii. microRNA dysregulation in MS

The expression of microRNAs has been largely investigated in the setting of MS and over 500 microRNAs have been found dysregulated in MS, with however only 9% consistency in at least 3 studies [751–755]. Interestingly, the microRNA biogenesis machinery, namely DROSHA, DGCR8 and DICER, was upregulated in the blood of RRMS patients as compared to healthy controls (HC) [756]. miR-146a-5p and miR-155-5p are well-known immuno-microRNAs found upregulated in serum, peripheral blood mononuclear cells (PBMCs) and monocytes of RRMS patients and in active lesions of RR/PMS patients, as is miR-21-5p, found upregulated in PBMCs and active lesions as well [757–761]. The effect of DMTs on microRNA expression has also been investigated in order to look for potential biomarkers of response to treatment [751]. miR-146a-5p was downregulated and miR-150-5p was upregulated in response to glatiramer acetate and natalizumab respectively [760,762]. Furthermore, the microRNA expression profile appears to be slightly different between MS phenotypes [763–767]. Herein, miR-15b, miR-23a and miR-223 were downregulated in serum exosomes of PMS vs RRMS and in serum of PPMS vs HCs [764,765]. Several microRNAs have been proposed as biomarkers of MS or MS phenotypes, but with almost no concordance in between studies and none has been validated by a systematic and comprehensive study so far [763,768,769]. Moreover, some microRNAs are also dysregulated in other inflammatory and neurodegenerative disorders of the CNS, although not necessarily in the same direction [763,770,771]. Therefore, a microRNA signature compelling several microRNAs might offer a better discrimination [763,764,772]. However, the many studies on microRNA dysregulation in MS have shown some discrepancies and have revealed to be hard to unify due to differences in (1) methodology (small RNA sequencing, microarray, PCR array, RT-qPCR), (2) population characteristics (patients not always grouped according to disease activity/progression or treatment course), (3) sample type (mainly in the periphery: whole blood, serum, plasma, PBMCs, specific cell subtypes; to a lesser extent centrally: different types of brain tissues and lesions, CSF) [755,763].

iv. Functional impact of microRNAs on immune cells, microglia, astrocytes, and OPCs/OLs

Some of these microRNAs linked to MS have been functionally investigated to explore their physiological and pathophysiological role in MS and other diseases. Remarkably, TGFb signalling topped in a pathway enrichment analysis on the predicted targets of the most consistently reported dysregulated microRNAs in MS among 61 studies. TGFb, an important cytokine for the differentiation of Th17 and Tregs [773], can induce the expression of several microRNAs and is itself modulated by several microRNAs as well, epitomising the filigree conjunction between microRNAs and mRNAs. This might however be biased as the majority of studies was conducted in the immune compartment [755].

Since so many microRNAs have been linked to MS, this section will focus on a few microRNAs of interest of this thesis, in order to briefly summarise their known functional involvement in peripheral immune cells, microglia, astrocytes and oligodendrocytes in and outside the scope of MS.

*Dicer ablation*

Dicer knockout is lethal early in the development due to the depletion of stem cells [774]. However, as Drosha/Dicer ablation impairs microRNA biogenesis, its experimental ablation in a specific cell type is a way to appreciate the general involvement of microRNAs in the cellular homeostasis and function.

A CD4-driven Drosha ablation causes a spontaneous and lethal inflammatory disorder marked by lymphopenia, whereby the remaining T cells can still differentiate in IFNg and IL17 secreting T cells but fail to induce a Treg response [775]. Dicer ablation in early effector CD8+ T cells reduces their expansion while in B cells it hinders germinal centre formation, reduces antibody diversity and increases their apoptosis [776–778]. In microglia, Dicer ablation results prenatally in a spontaneous microglial activation and postnatally in an excessive microglial responsiveness to endotoxin exposure, reflecting the need of microRNAs to modulate microglial activation [779]. Dicer ablation in postnatal astrocytes impedes OPC differentiation and myelination without impacting neuronal integrity [780]. However, in another study it severely affected the maturation and function of postnatal astrocytes

resulting in impaired glutamate uptake and antioxidant pathways causing a lethal, fulminant neurological decline due to neuronal dysfunction and degeneration [781]. Dicer ablation in OPCs does not affect their proliferation/survival but severely delays their differentiation. Herein, Dicer knockout in mice causes early severe tremor and ataxia, whereby CNP and Olig1-driven Dicer knockout mice die at 3-4 weeks postnatal, while Olig2-driven knockout results in delayed myelination, but the mice eventually recover [782,783]. Contrarily, OL-specific Plp-driven Dicer knockout is accompanied by demyelination, peroxisomal and oxidative damage, inflammatory astrogliosis/microgliosis and neuronal degeneration [784].

*miR-21-5p*

Both pro- and anti-inflammatory properties have been attributed to miR-21-5p. miR-21-5p is known to target STAT3 and SMAD7, hereby impeding Th17 while promoting Treg development [785,786]. It can induce CD8+ Tregs as well [787]. However, it has also been described as inducing T cell proliferation and enhancing the secretion of pro-inflammatory cytokines as IL6/17/21/23 and IFNg by targeting programmed cell death 4 (PDCD4) [788,789]. On the contrary, lipopolysaccharide (LPS) induces miR-21-5p via myeloid differentiation innate immune signal transduction adaptor (MYD88) and nuclear factor of kappa light polypeptide gene enhancer in B cells (NFkB), whereafter miR-21-5p targets Pdcd4, that blocks NFkB activity and enhances IL10 expression in macrophages [790]. miR-21-5p is upregulated in malignant T cells through STAT3 and STAT5, while its silencing causes apoptosis [791,792]. In microglia, miR-21-5p overexpression dampens the proinflammatory response after intracerebral haemorrhage, and averts microglia-mediated neuronal apoptosis through the downregulation of Fas ligand during hypoxia [793,794]. Furthermore, exosomes derived from injured neuron cells (PC12) containing miR-21-5p polarized microglia towards a proinflammatory “M1” phenotype which in return induced apoptosis of the PC12 cells [795]. It is also upregulated in neurons and astrocytes after an ischaemic event (oxygen and glucose deprivation/spinal cord injury), while oppositely its silencing promotes synaptic formation, nerve growth and the transformation of neurotoxic reactive astrocytes to anti-inflammatory “A2” astrocytes [796–798]. Finally, miR-21-5p can reduce OPC apoptosis and improve myelination by targeting Pten [799].

*miR-27a-3p/miR-27b-3p*

Optimal miR-27 levels are mandatory to insure Treg homeostasis [800]. miR-27b-3p impairs Treg differentiation through the TGFb signalling pathway, without impacting the suppressor function of the cells that could differentiate, it induces a Th2 to Th1 shift, and worsens EAE [801,802]. Similarly, miR-27a-3p overexpression in CD4+ T cells during relapsing MS was accompanied by the overexpression of Th17 mediators. Oppositely, miR-27a-3p was found to reduce dendritic cell mediated differentiation of Th1 and Th17 cells allowing the accumulation of Tregs [803–805]. miR-27a-3p is also overexpressed in exosomes of IL1b-induced astrocytes [806]. On the contrary, miR-27a-3p is downregulated in LPS-induced microglia, while its overexpression negatively modulates this pro-inflammatory response by targeting Toll like receptor 4 (*Tlr4*) and interleukin 1 receptor associated kinase 4 (*Irak4*) [807]. Contrarily, miR-27b-3p was induced in LPS-treated macrophages and contributed to the pro-inflammatory response by targeting peroxisome proliferator activated receptor gamma (*PPARg*) [808]. Finally, miR-27a-3p impeded OPC proliferation and differentiation as well as myelination by activating the Wnt/beta-catenin signalling pathway. Remarkably, miR-27a-3p could hinder miR-219-5p induced OPC differentiation [809]. Oppositely, miR-27a-3p overexpression in neurons is neuroprotective [810].

*miR-145-5p*

miR-145-5p is downregulated in Tregs from HCs, as it can target cytotoxic T lymphocyte associated protein 4 (*CTLA4*), a co-inhibitory molecule that sustains Treg suppression [811,812]. It however promotes a Th2 response over a Th1 response [813]. miR-145-5p is overexpressed in vitro in microglia under oxygen/glucose deprivation conditions, accompanied by the downregulation of its target nuclear receptor subfamily 4 group A member 2 (*Nr4a2*, also known as *Nurr1*), which releases the expression of Tnfa. Furthermore, miR-145-5p overexpression in microglia causes neuronal cell death in cocultures with neurons [814]. Oppositely, it was upregulated in anti-inflammatory “M2” polarized microglia (by IL4 stimulation), but not in pro-inflammatory “M1” microglia (by LPS stimulation) [815]. miR-145-5p overexpression in vivo in astrocytes affects their proliferation and migration and reduces their cell density and morphology (size and number of cell

processes) by targeting *Gfap* and Myc proto-oncogene (*Myc*), a bHLH transcription factor promoting cell growth. Therefore, the downregulation of miR-145-5p one week after spinal cord injury is critical to induce astrogliosis [816]. Furthermore, LPS downregulates its expression in astrocytes, while oppositely, it is upregulated in exosomes of IL1b-treated astrocytes [806,816]. Finally, miR-145-5p was found highly expressed in OPCs and its silencing allowed their spontaneous differentiation by releasing the expression of its target *Myrf* [817] miR-145-5p was still highly expressed in a cuprizone-fed mice, but downregulated as compared to the control mice [818].

*miR-146a-5p*

The activation of the pro-inflammatory NFkB signalling pathway, involved in both innate and T cell response, induces miR-146a-5p. miR-146a-5p targets *IRAK1* and TNF receptor associated factor 6 (*TRAF6*), subsequent factors in the TLR/MYD88 signalling pathway that activate inhibitor of nuclear factor kappa B kinase (IKK), needed for the activation of NFkB, thereby acting as a negative feedback on its inflammatory stimulus [819–822]. Alternately, IRAK1 phosphorylates STAT3 involved in Th17 differentiation [823,824]. *STAT1*, involved in Th1 differentiation, is another target of miR-146a-5p [825]. miR-146a-5p is thus an anti-inflammatory microRNA. In T cells it promotes Tregs instead of Th1 and Th17 cells, while its silencing does the opposite resulting in the loss of immunotolerance [821,825,826]. Moreover, miR-146a-5p overexpression in brain endothelial cells hinders cytokine-stimulated adhesion of T cells [827]. IL1b treatment in astrocytes induces the expression of miR-146a-5p as well as the upregulation of pro-inflammatory cytokines as IL6 and TNFa, but also of upstream mediators cyclooxidase 2 and high mobility group box 1 (HMGB1). However the specific overexpression of exogenous miR-146a-5p in IL1b stimulated astrocytes completely reverses the pro-inflammatory signature [820]. Likewise in microglia/macrophages, it promotes the anti-inflammatory phenotype [819,828,829]. Similarly, miR-146a-5p overexpression in microglial BV2 cells resulted in the downregulation of genes involved in TLR signalling pathway, Fcγ receptor-mediated phagocytosis and in the oxidative burst phenomenon [830]. Interestingly, exogenous miR-146a-5p, that was detected in microglia/macrophages and OPCs after intravenous injection and intracerebral infusion respectively, improved both EAE and cuprizone demyelination by promoting an anti-inflammatory phenotype of microglia/macrophages as well as OPC differentiation and myelination [831,832].

Microglia isolated from miR-146a knockout mice and stimulated by LPS acquired a pro-inflammatory phenotype however with reduced proliferation and migration [833]. When cuprizone-fed, these knockout mice had less induced CD11c+ microglia with moreover a reduced sensome protein signature to perceive their environment [833]. Contrarily, cuprizone-fed miR-146a-5p knockout mice were protected against demyelination and axonal loss [834].

*miR-150-5p*

miR-150-5p is expressed in mature T and B cells but not in their progenitors and thereby tightly controls their development, i.a. by targeting MYB proto-oncogene transcription factor. Its premature or ectopic expression hampers B cell development [835,836]. Its overexpression also represses memory CD8+ T cell differentiation by reducing anti-apoptic factors, Bcl2 apoptosis regulator and Bcl2 like 1, downstream of c-Myb, hereby regulating the balance between terminal effector and memory CD8+ T cells [837]. It promotes the differentiation to effector and effector memory T cells by inhibiting FOXP1 and increases the secretion of proinflammatory cytokines [838]. EAE severity and demyelination are reduced in miR-150 knockout mice [839]. Finally, miR-150-5p overexpression in microglial BV2 cells reversed the LPS-induced expression of pro-inflammatory cytokines IL1b, IL6, and TNFa [840].

*miR-155-5p*

Suppressor of cytokine signalling 1 (*SOCS1*) is a well-established target of miR-155-5p [841,842]. SOCS1 is a negative regulator of T helper cell differentiation and microglia/macrophage response by inhibiting the JAK/STAT signalling pathway, involved in cytokine production and signalling [843–845]. miR-155-5p inhibition of *SOCS1* results in an increased phosphorylation of STAT3 and STAT5, important for Th17 and Treg cells respectively [842]. It thereby promotes Th17 development and IL17 production, and it even potentialises their encephalitogenicity by targeting *Ets1*, a negative regulator of Th17 differentiation that is contrarily indispensable for proper Th1 and Treg development [842,846–849]. miR-155 knockdown mice presented with a milder EAE course [850]. miR-155-5p further ensures Treg homeostasis. It is

induced by FOXP3 and promotes Treg development, but not IL10/TGFb production, by increasing STAT5 phosphorylation in response to IL2 [842,851,852]. miR-155 deficient mice have less, but functional Tregs [853]. miR-155-5p is involved in B cell activation and its silencing reduces the production of antibodies [854]. It also supports IL10 production by Bregs which suppresses TNFa and IFNg production by monocytes and Tregs. However, in Bregs isolated from Crohn patients, miR-155-5p induces an impaired response, marked by the production of TNFa instead of IL10 and subsequently its inability to induce Tregs and suppress T effector cells [855]. miR-155-5p expression in brain endothelial cells contributes to the cytokine-induced (TNFa/IFNg) disruption of the BBB by targeting components of focal adhesion and of the interendothelial junctional complex [856]. miR-155-5p has been linked to the pro-inflammatory phenotype of microglia/macrophages and astrocytes as well [815,841,857–861]. In microglia and macrophages, it can subsequently promote CD4+ T cell proliferation and activation and neuronal cell death [841,857]. Its silencing promotes their polarization towards the anti-inflammatory M2 phenotype and reduces their phagocytic activity [862,863]. Hereby, it can target *SOCS1* (a JAK/STAT inhibitor), *RACK1* (a negative regulator of NFkB), SMAD2 (a mediator of TGFb signalling), inositol polyphosphate-5-phosphatase D (*INPP5D*, a negative regulator of PI3K pathway and suppressor of inflammatory cytokines and iNOS) or CCAAT enhancer binding protein beta (*CEBPB*, a transcription factor indispensable for "M2" cytokines) [857,863–868]. Finally, miR-155-5p is upregulated during EAE and cuprizone demyelination [818,869,870].

p53 activation in microglia, induced by ROS and the accumulation of DNA damage linked to oxidative stress, promotes miR-34a-5p, miR-145-5p and miR-155-5p in microglia. miR-155-5p targets the anti-inflammatory transcription factor Maf, while the other 2 microRNAs target Twist2, a transcriptional activator of Maf, resulting in a proinflammatory response and reduced tissue repair [871]. Moreover, miR-34a-5p and miR-155-5p, upregulated in active MS lesions and found in astrocytes, target CD47 and could thereby promote the phagocytosis of myelin, as CD47 interacts with signal regulatory protein alpha (SIRPa) on macrophages/microglia to trap them and withhold them from their phagocytic activity [758].

*miR-219-5p, miR-338-3p/5p and others in OPCs/OLs*

miR-219-5p and miR-338-3p/5p are key microRNAs in promoting strongly and cooperatively OPC differentiation, even in human-induced pluripotent stem cells [782,783,872–874]. Shared targets are *Hes5*, *Sox6* (OPC differentiation inhibitors) and zinc finger and BTB domain containing 18 *(Zbtb18)*, a transcriptional repressor promoting neurogenesis but repressing OL differentiation [782,783,875]. miR-338, as well as miR-155, target pre-OL transcription factor *Tcf7l2*, as part of a feedforward loop as Sox10 induces both microRNAs and *Tcf7l2,* thereby finely tuning oligodendrogenesis [876]. Both (miR-338 and miR-155) also target neurosteroidogenic enzymes of which the biosynthetic machinery was found downregulated in normal appearing white matter of MS patients [877]. miR-338 further targets *Sox9* [878]. Other targets of miR-219-5p include *Pdgfra, and Lingo1*. It further tailors very long chain fatty acid biosynthesis by targeting elongation of very long chain fatty acids protein 7 (*Elovl7*) to avoid the pejorative effects of its accumulation. miR-219-5p is therefore also involved in later stages of OL maturation and myelination [782,784,879]. Correspondingly, miR-219-5p overexpression enhances differentiation in Dicer knockout OPCs in vitro, as well as OL maturation and remyelination in vivo after lysolecithin-induced demyelination and EAE [782,879]. miR-219-5p reduces cuprizone-induced demyelination as well by inducing OL maturation. Hereby it upregulates solute carrier family 16 member 1 (*Slc16a1*, also known as monocarboxylate transporter 1 (*Mct1*)) via targeting of *Hes5* and *Sox6*. Interestingly, MCT1 inhibitor is sufficient to reverse the effects of miR-219-5p [880]. Contrarily, miR-138-5p promotes early stages of OPC differentiation, but will delay later stages [782]. Interestingly, exogenous miR-219-5p is able to suppress microglia and astrocyte activation alone or jointly with miR-338-3p/5p, but also to promote Tregs and decrease Th17 cell percentages [881–883].

Furthermore, microRNA expression changes dynamically along OPC development [884,885]. Hereby, miR-219 and miR-338 are among the most compelling upregulated microRNAs during OL maturation [884]. Moreover, miR-145-5p and miR-214-3p strongly increase in the earliest OPC stage, then decrease during the developing OPC stages and slightly increase again in mature OLs. Hereby miR-214-3p was proposed to target Mobp [885]. miR-214-3p further induces Tregs by targeting PTEN [886]. miR-297a-5p was found to arrest cell cycle and induce OPC differentiation [887]. miR-297 is downregulated in astrocytes suffering of oxidative injury due to iron

exposure or overexpression of heme oxygenase 1 which promoted iron deposition [888]. miR-20a-5p, part of the miR-17-92 cluster that induces OPC proliferation, is upregulated in both OPC and OL, along the other members of the clusters, although it was also found downregulated in mature OLs as an inhibitor of Plp, it seemingly decreases along OPC differentiation [872,889,890].

v. What's still to explore?

The interest in microRNAs has boomed over the past 15 years leading to the discovery of over 500 dysregulated microRNAs in several biological compartments in MS patients with however substantial differences between studies complicating their interpretation. Likewise, several microRNAs have been proposed separately or conjointly as potential biomarkers of disease, of disease subtype/progression or of response to treatment, but none has been confirmed so far due to the same issue of study heterogeneity [755]. Moreover, their functional characterisation is quite limited, proportionally to this high number of dysregulated microRNAs linked to MS, with some discrepancies but also a redundant focus on a few of them [751,769,891]. Identifying the cellular source of circulating microRNAs might also be challenging [892]. However, since microRNAs can potentially target a hundred of mRNAs, their cell- and condition-specific expression finely tunes cellular signalling pathways. They are thereby a unique mirror of the cell's physiological or pathophysiological state, substantiating their interest in research.

The therapeutic opportunities of microRNAs, mainly as personalised precision medicine, are currently explored in order to restore their physiological expression levels directly with synthetically modified microRNA mimics or inhibitors. However, there is concern regarding the stability, safety and target-specificity of the delivered microRNA(s). Circulating microRNAs are bound to lipoproteins or enclosed within extracellular vesicles. Research is ongoing on producing extracellular vesicles or nanoparticles, manipulating their content and their composition, the latter in order to improve their stability and delivery to the cell/tissue of interest to avoid off-target effects [893–896].

Thus, exploring microRNAs could help further understand the cellular signalling pathways and their regulation as well as unravel new therapeutic strategies based on the microRNAs themselves or their key targets.

## IV. Hypothesis and aims

microRNAs are undeniably dysregulated in MS. Instead of a single microRNA, we expected that the expression profile of several microRNAs could be more accurate to characterise MS, while still keeping in mind that DMTs, disease activity and phenotype are major confounding factors. We further hypothesised that MS dysregulated microRNAs are actively involved in the pathophysiology of the disease, and that they might in particular partially orchestrate the contribution of each involved cell population to MS pathogenesis.

Therefore, we first aimed to explore the expression of microRNAs that had been related to immunological, neurodegenerative and/or lipidic processes, in the CSF of treatment naïve RRMS patients, with regard to their disease activity, as compared to symptomatic controls, but also of patients with other infectious, inflammatory and non-inflammatory disorders of the CNS, in order to verify the specificity of the identified dysregulated microRNAs to MS. We focused on the CSF as it had not been largely explored so far, while it is the site of the ongoing pathophysiological events. We further investigated the expression of a selection of these dysregulated microRNAs in the peripheral compartments, namely the serum and PBMCs, of treatment naïve RRMS patients, considering relapse and remission separately, vs healthy controls.

Our second purpose was to link these dysregulated microRNAs with the peripheral immunological T cell signature in a clinic's routine-based MS population. We investigated the expression of these microRNAs as well as T cell mediators and markers of interferon beta response in the PBMCs of MS patients vs HC, and further looked for their mutual correlation as well as their correlation with serum neurofilament light chain levels. In this population, MS patients were not characterised by their MS phenotype (relapsing vs remitting), but by their radiological disease activity (based on brain MRI), and were rather untreated or treated with first line DMTs, namely interferon beta or glatiramer acetate.

We then initially aimed to explore the functional impact of the less characterised microRNAs on the Th17/Treg balance and to identify potential mRNA targets in this scope. We tried to transfect and nucleofect an exogenous microRNA mimic and to nucleofect a plasmid expressing a pre-microRNA in PBMCs, but unfortunately, we failed to obtain a satisfactory transfection rate to allow an effective mRNA (by RT-

qPCR) or protein (by flow cytometry) readout, even after fluorescence activated cell sorting (FACS, when transfecting a fluorescent-labelled microRNA mimic). We further had major issues with the stability of the microRNA mimic after its transfection, and with cell viability after nucleofection of a pre-microRNA expressing plasmid, which we could not solve.

Therefore, we decided to shift our focus to oligodendrocyte progenitor cells. Failure of OPC differentiation and remyelination is one of the key events in MS pathogenesis. Herein, the microRNA involvement is even less explored. We first wanted to screen for the effect of several of the initially identified dysregulated microRNAs on the differentiation of OPCs. Hereafter, we aimed to investigate in detail how the microRNAs with the strongest effect in the first screening, could functionally affect OPC cell fate by RNA sequencing, confirming our independent RT-qPCR analysis. Therefore, we transfected the microRNA mimics separately in an OPC cell line called CG-4, cultured in a medium promoting their differentiation after the transfection. We wanted to confirm their effect by transfecting sequentially the corresponding microRNA inhibitor as well. We finally attempted to identify mRNA targets that could support the observed changes in cell fate, characterised by gene enrichment analysis on RNA sequencing, and verified their downregulation by RT-qPCR. We are confident that this strategy could draw broader attention to known pathways involved in OPC physiology/pathophysiology or even unravel so far unexplored pathways.

# CHAPTER 1: CSF MICRORNAS DISCRIMINATE MS ACTIVITY AND SHARE SIMILARITY TO OTHER NEUROINFLAMMATORY DISORDERS

Océane Perdaens, Hong Anh Dang, Ludovic D'auria, Vincent van Pesch

*Neurology: Neuroimmunology & Neuroinflammation*, *2020 Feb 7;7(2):e673*

We first aimed to screen for microRNAs differentially expressed in the CSF of relapsing and remitting MS patients versus controls and hereafter verify their specificity in RRMS vs other neurological disorders as well as their dysregulation in peripheral compartments (serum and peripheral blood mononuclear cells) as part of our hypothesis that microRNA dysregulation is involved in MS pathogenesis.

*Figure 1.1 Graphical abstract*

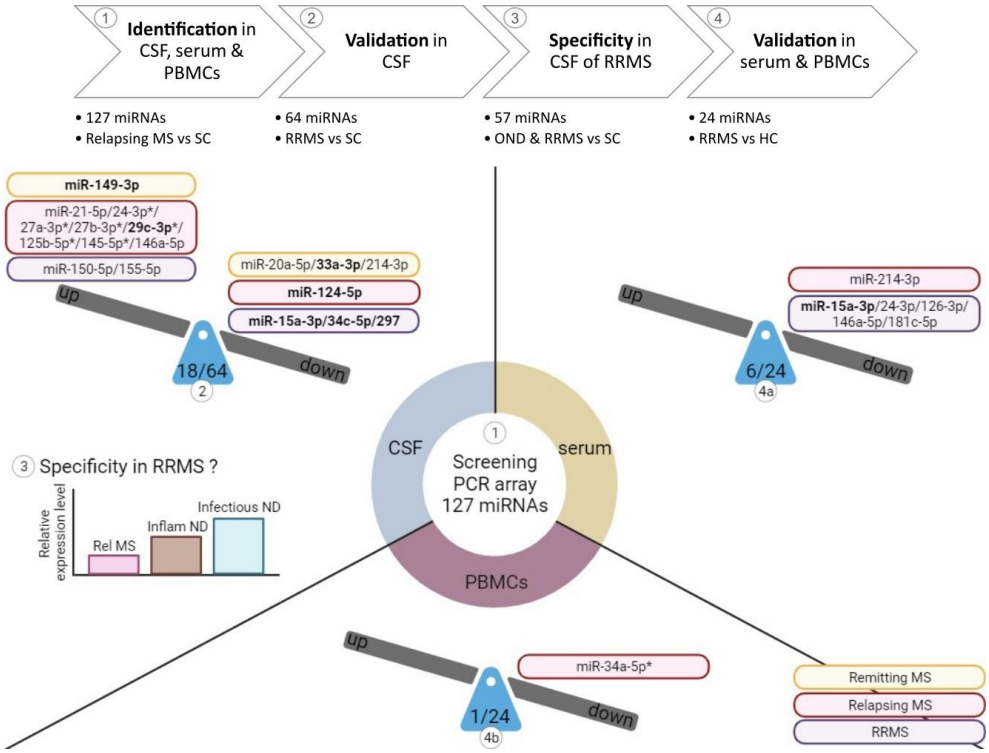


*We first aimed to analyse (1) the expression of 127 microRNAs by PCR array on pooled cerebrospinal fluid (CSF), serum or peripheral blood mononuclear cell (PBMC) samples of relapsing MS patients vs controls. Hereafter, we verified (2) the dysregulation of 64 microRNAs with a higher fold change in individual CSF samples of relapsing and remitting MS (RRMS) patients separately vs symptomatic controls (SC) by RT-qPCR and we verified (3) the specificity of this dysregulation in the CSF in RRMS vs other neurological disorders (OND). Based on these first results, we finally explored (4) the expression of 24 more promising microRNAs in individual serum and PBMC samples of RRMS patients vs healthy controls (HC) by RT-qPCR. We identified (2) 18 microRNAs in the CSF, (4a) 6 microRNAs in the serum and*

*(4b) 1 microRNA in PBMCs that were differentially expressed (up- or downregulated) in relapsing MS (red), remitting MS (yellow) or both (purple) vs the controls at least, or remitting MS only (*). We also identified 7 microRNAs, indicated in bolt, that had not been linked to MS before, although in the meantime, miR-29c-3p and miR-149-3p have* [897]*. Some microRNAs are commonly (3) upregulated in the CSF of relapsing MS patients (Rel MS, red) and patients with inflammatory (Inflam ND, brown) and infectious neurological disorders (Infectious ND, blue), with however an increased relative expression level.*

## I. Abstract

*Objective* - To perform a comprehensive multicompartment analysis of microRNA (miRNA) expression in multiple sclerosis (MS) linked to disease activity and compared with other neuroinflammatory diseases through a retrospective cross-sectional study.

*Methods* - One hundred twenty-seven miRNAs were measured by PCR arrays on pooled CSF, serum, and peripheral blood mononuclear cell (PBMC) samples of 10 patients with relapsing MS and 10 controls. Sixty-four miRNAs were then measured by quantitative PCR on individual CSF samples of patients with relapsing or remitting MS and controls (n = 68). Fifty-seven miRNAs were analysed in the CSF from a second cohort (n = 75), including patients with MS, neuroinfectious, or neuroinflammatory diseases and controls. MiRNAs significantly dysregulated in the CSF were analysed on individual serum/PBMC samples (n = 59/48) of patients with relapsing or remitting MS and controls. Post-hoc analysis consisted of principal component analysis (PCA), gene set, and pathway enrichment analysis.

*Results* - Twenty-one miRNAs were differentially expressed, mainly upregulated in the CSF during MS relapses. Relapsing MS and neuroinfectious/inflammatory diseases exhibited a partially overlapping CSF miRNA expression profile. Besides confirming the association of miR-146a-5p/150-5p/155-5p with MS, 7 miRNAs uncharacterised for MS emerged (miR-15a-3p/29c-3p/33a-3p/34c-5p/124-5p/149-3p/297). PCA showed that distinct miRNA sets segregated MS from controls and relapse from remission. In silico analysis predicted the involvement of these miRNAs in cell cycle, immunoregulation, and neurogenesis, but also revealed that the signalling pathway pattern of remitting MS is more akin to controls rather than patients with relapsing MS.

*Conclusions* - This study highlights the CSF-predominant dysregulation of miRNAs in MS by identifying a signature of disease activity and intrathecal inflammation among neuroinflammatory disorders.

## II. Introduction

Multiple sclerosis (MS) is characterized by multifocal inflammatory lesions inducing myelin sheath damage and axonal degeneration. MS results from a complex interplay between genetic susceptibility and environmental and epigenetic factors, but its molecular determinants remain elusive. A predominance of patients present initially with a relapsing-remitting disease course [898].

MicroRNAs (miRNAs) are single-stranded noncoding RNAs regulating post-transcriptionally the expression of a large spectrum of genes during various biological processes [899]. Several miRNAs have been associated with MS, but only few were linked to disease activity [753,900]. Most studies were performed in small cohorts, in single biological compartments, rarely compared with other neurologic disorders or were not replicated, due to large heterogeneity between study populations and analysis methods. Few studies have focused on CSF miRNAs [901], although these might be more relevant to understanding disease regulation.

We sought to characterise miRNA expression in 3 biological compartments, i.e., CSF, serum, and peripheral blood mononuclear cells (PBMCs) of patients with MS according to disease activity compared with that of controls and other neurologic disorders in the CSF. MiRNAs known for their involvement in immunity, inflammation, neurodegeneration, and lipid metabolism were measured by quantitative PCR (qPCR). Finally, a principal component analysis (PCA) and a pathway enrichment analysis were performed, altogether leading to a comprehensive multicompartment characterisation of the miRNA expression profile in MS.

## III. Methods

### i. Patients

CSF and blood samples were collected at the Cliniques universitaires Saint-Luc (Brussels) between March 2005 and March 2018, processed according to international guidelines within 1 hour before storage at −80°C until miRNA extraction [902,903]. PBMCs paired with serum were processed as previously described [904]. The study was conducted stepwise (figure 1.2).

*Figure 1.2: Workflow summary of different study steps*

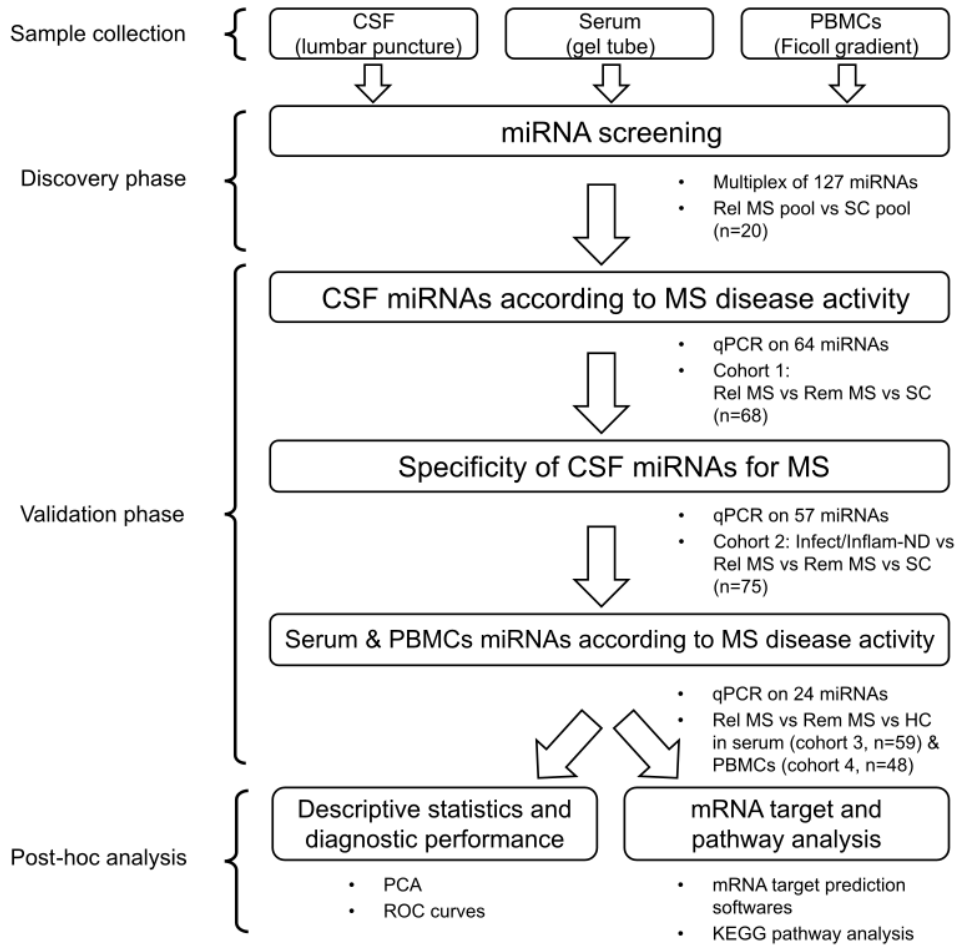

*AUC = area under the curve; HC = healthy control; Infect/Inflam-ND = patients with infectious or inflammatory neurologic disorders; KEGG = Kyoto Encyclopaedia of Genes and Genomes; mRNA = messenger RNA; miRNA = microRNA; MS = multiple sclerosis, PBMC = peripheral blood mononuclear cell; PCA = principal component analysis; qPCR = quantitative PCR; Rel MS = relapsing MS; Rem MS = remitting MS; ROC = receiver operating characteristic; RRMS = relapsing-remitting MS; SC = symptomatic control.*

A group size of at least 9 patients was calculated using the CSF fold changes of relapsing MS vs controls in the 2 miRNA arrays, with alpha error at 0.05 and power of 0.80. Patient cohorts were classified according to the BioMS-eu consortium definitions (supplementary table 1.1) [905]. The 2017 McDonald criteria were used for MS diagnosis [29]. Relapse was defined clinically and/or by the presence of gadolinium-enhancing lesions (GELs) on MRI for 93% - 100% of patients, depending on the cohort [24]. Remitting patients were clinically stable for 1 month up to 21 years. To reduce bias, patients were age and sex matched to controls, and none of the patients with MS were under any disease-modifying treatment (DMT). None of the relapsing patients had received high-dose IV methylprednisolone before sample collection. Clinical and paraclinical features of the patients are summarised in table 1.1 and supplementary table 1.1 [906,907]. Diagnoses of other disease categories are listed in supplementary table 1.2. Data were collected between February 2015 and July 2018.

ii. MiRNA isolation

MiRNAs were isolated from CSF (400 µL) and serum (200 µL) using the miRNeasy Serum/Plasma Kit, and from 11 - 13.$10^6$ PBMCs using the miRNeasy Mini Kit, following the manufacturer's protocol (Qiagen, Hilden, Germany). Caenorhabditis elegans miR-39 mimic (Qiagen) was added to CSF and serum samples as spike-in control for relative quantification. MiRNA extraction, reverse transcription (RT), and PCR were performed sequentially.

*Table 1.1: Baseline characteristics of patients and controls included in the CSF microRNA study*

| | CSF MS vs SC | | |
|---|---|---|---|
| n (%♀) | 68 (64.7) | | |
| Mean age (±SD) | 35.1 (±10.8) | | |
| | **Rel MS** | **Rem MS** | **SC** |
| n (%♀) | 40 (72.5) | 13 (46.2) | 15 (60) |
| Mean age (±SD) | 34.5 (±11.7) | 38.2 (±11.5) | 33.1 (±7.1) |
| Disease duration in months: mean (±SD) | 5 (±16) | 65 (±83) | NA |
| Relapse phenotype (%) | | | |
| 1: Spinal | 32.5 | | |
| 2: Brainstem/cerebellum | 20 | | |
| 3: Optic neuritis | 27.5 | NA | NA |
| 4: Supratentorial | 10 | | |
| 5: Multifocal | 10 | | |
| EDSS score: median [range] | 2.25 [0-3.5] | 2.0 [0-3] | NA |
| No. of relapses since disease onset: median [range] | 1 [1-2] | 2 [0-3] | NA |
| Proportion of patients with a 1st clinical event (%) | 75 | 30.8 | NA |
| Barkhof criteria[a] scores 3 and 4 (%) | 85.0 | 75.0, n = 12 | NA |
| GELs on brain MRI: mean (±SD) | 2 (±1.7), n = 35 | 0, n = 8 | NA |
| Proportion of patients with spinal cord lesions on MRI (%) | 82.5, n = 33 | 81.8, n = 11 | NA |
| GELs on spinal cord MRI: mean (±SD) | 0.3 (±0.6), n = 19 | 0, n = 8 | NA |
| Proportion of patients with at least 1 GEL on brain and spinal cord MRI (%) | 94.6, n = 37 | 0, n = 9 | NA |
| No. of CSF cells/mm³: mean (±SD) [range] | 5.6 (±5.3) [0-22] | 3.8 (±2.9) [0-8] | 0.8 (±1.3) [0-4] |
| Proportion of patients with CSF-specific IgG OCBs or CSF FKLCs (%) | 87.5 | 92.3 | 0 |
| Proportion of patients with IgG intrathecal synthesis (%) | 67.5 | 53.8 | 0 |
| % IgG intrathecal synthesis[b]: mean (±SD) | 24.9 (±23.4) | 26.8 (±30.5) | 0 |
| Proportion of patients with IgM intrathecal synthesis (%) | 37.5 | 38.5 | 0 |
| % IgM intrathecal synthesis[b]: mean (±SD) | 15.1 (±23.3) | 19.5 (±28.3) | 0 |

*Number of patients for which data are available is indicated by "n." [a]Barkhof criteria[907] was assessed to reflect the lesion load. [b]IgG and IgM intrathecal fractions were calculated using Reiber formulas[906] (normal value is 0%). Patients with relapsing-remitting MS were disease-modifying treatment naive. Furthermore, none of the patients had received high-dose IV methylprednisolone. According to the consensus definition[905], SCs are patients with neurologic symptoms, but without any objective clinical or paraclinical findings to support the diagnosis of a specific neurologic disease. % ♀ = percentage of female; EDSS = Expanded Disability Status Scale; FKLC = free kappa light chain; GEL = gadolinium-enhancing lesion; IgG = immunoglobulin G; IgM = immunoglobulin M; NA = not applicable; OCB = oligoclonal band; SC = symptomatic control, SD = standard deviation.*

iii. MiRNA PCR array

MiRNA profiling was kindly performed by the manufacturer with "Inflammatory Response & Autoimmunity" and "T-cell & B-cell Activation" miScript miRNA PCR Arrays (Qiagen) on a pool of 10 patients with relapsing MS and 10 symptomatic controls (SCs) (for CSF) or 10 healthy controls (HCs) (for serum and PBMCs).

iv. RT, preamplification, and qPCR

RT was performed on 5 µL of miRNA using the miScript II RT Kit. One microliter of complementary DNA was preamplified using the miScript PreAmp PCR Kit following the manufacturer's recommendations (Qiagen). The spike-in control C. elegans miR-39 mimic was not preamplified. qPCR reactions were performed in duplicate, except for miR-24-3p in CSF, a putative internal reference gene [908], which was assayed in triplicate. Patients' subgroups and controls were equally distributed across each run to minimise inter-run bias for a single miRNA target.

v. qPCR analysis

Sample selection was based on Ct variability within duplicates of a same sample and between samples, as well as melt curve morphology. Ct was set at 40 in case of inefficient amplification. The miRNA transcripts were normalised using references (exogenous miR-39 for CSF/serum or intracellular RNU6B [small nuclear ribonucleoprotein U6B, later referred to as RNU] for PBMCs). Relative expression

was determined by the comparative Ct method to the mean of the SCs or HCs ($2^{-\Delta\Delta Ct}$ with $\Delta\Delta Ct = \Delta Ct\ [target\text{-}reference]_{sample} - \Delta Ct\ [target\text{-}reference]_{mean\ of\ controls}$) [909]. Extraction efficiency was considered by comparing the mean Ct of miR-39 or RNU amplification between subgroups and miRNA extraction series. When extraction efficiency appeared variable, results were expressed relative to the mean of controls extracted using the same RT enzyme lot.

vi. Gene target prediction and pathway enrichment analysis

Kyoto Encyclopaedia of Genes and Genomes (KEGG) pathways were investigated for miRNAs displaying a statistically significant relative expression difference above 1.5-fold between disease categories. MiRNAs were grouped in sets according to the disease subgroup and biological compartment. Two (supplementary table 1.6) or three (figure 1.6) databases were combined comprising predicted and validated miRNA targets, namely mirPath v.3 by DIANA TOOLS based on TarBase v7.0 (filtered with Pathway Union and false discovery rate [FDR] correction), miRNet (filtered with a 2.0 cutoff degree and using a hypergeometric Fisher exact test algorithm; mirnet.ca), and enrichment using the Cytoscape stringApp (with data set from the filtered miRNet analysis and a confidence score cutoff set at 0.6). The miRNA-gene network was generated from the miRNet database, filtered (2.0 cutoff degree of analysis and 40.0 betweenness) and sketched in the Cytoscape stringApp to show the most representative genes.

vii. Statistical analysis

For statistical analysis, a nonparametric one-way analysis of variance Kruskal-Wallis test of all relative miRNA expression levels across subgroups was performed using GraphPad Prism 5.0, followed by a Dunn's post-test for a 2-by-2 comparison of the subgroups. Dunn's p values, with a significance threshold set at ≤ 0.05, were calculated and corrected by the Benjamini-Hochberg FDR method (astatsa.com/KruskalWallisTest/). Differential expression of miRNAs was considered only if statistically significant for both post-tests.

PCA of continuous variables obtained from the CSF miRNAs screening was performed using the R FactoMineR program. The presence/absence of oligoclonal

bands (OCBs), MRI lesion load, presence/absence of GELs, and diagnostic category were analysed as illustrative qualitative variables. The missing values were replaced by the mean value of the subgroup to which the sample belonged to [910]. Results were plotted using Rcmdr (cran.r-project.org/web/packages/Rcmdr/index.html). For miR-146a-5p, -150-5p, and -155-5p in CSF, the receiver operating characteristic (ROC) curves were calculated providing a cutoff with an optimal compromise between sensitivity and specificity to discriminate MS from SC.

### viii. Standard protocol approvals, registrations, and patient consents

Patients sign a charter upon hospital admission stating that the residual CSF and serum samples, collected for routine diagnostic procedures or patient care, can be used for retrospective academic research, without an additional informed consent (ethical approval 2007/10SEP/233). PBMCs and paired serum were collected separately under a distinct research protocol upon signature of an informed consent (ethical approval 2007/31AOUT/222).

### ix. Data availability

Raw PCR files and detailed in silico and statistical outputs are not included in this article. Any unpublished and anonymised data will be shared upon request from a qualified investigator. Strengthening the Reporting of Observational Studies in Epidemiology guidelines have been respected.

## IV. Results

### i. Multicompartment screening of immune related miRNAs from a pool of patients with relapsing MS vs SCs/HCs

To investigate whether miRNA expression was modified in MS, particularly during relapses, we first performed a screening on a pool of CSF, serum, or PBMCs obtained from 10 patients with MS in relapse and 10 age- and sex-matched SCs or

HCs (supplementary table 1.1A). The expression of 168 miRNAs was assessed using the "Human Inflammatory Response & Autoimmunity" and the "T-Cell & B-Cell Activation" miScript miRNA PCR Arrays. Forty-one miRNAs were assayed in both arrays, thus 127 different miRNAs were ultimately assessed. Absolute expression differences ranging between 3- (ΔCt = 1.59) and 148-fold (ΔCt = 7.21) were observed for 49 miRNAs, of which 35 originated from CSF, 9 from serum, and 8 from PBMCs. Of note, some miRNAs were found dysregulated in 2 compartments (miR-181c-5p and miR-210-3p in CSF and PBMCs; miR-34c-5p and miR-184 in PBMCs and serum). Most CSF miRNAs were overexpressed in the relapsing MS pool in comparison to the SC pool (ΔCt < 0), except miR-101-3p and miR-17-5p. Twenty-three miRNAs were discarded from subsequent analysis because of low expression levels (Ct ≥ 30) (supplementary figure 1.1).

ii. Quantification of miRNAs in the CSF of patients with relapsing and remitting MS vs SCs

As most miRNAs were found dysregulated in the CSF, we aimed to confirm these trends in individual CSF samples of patients with MS, according to disease activity (n = 40 in relapse and n = 13 in remission) and compared with age- and sex-matched SCs (n = 15) (table 1.1). In total, 64 miRNAs were amplified from individual CSF samples (supplementary table 1.3). Those were either selected from the differentially expressed targets identified in the screening arrays, from previously published studies in MS or for their involvement in immunity, inflammation, lipid metabolism, or neurodegeneration.

Eighteen miRNAs were differentially expressed in at least 1 subgroup, with statistically significant ($p \leq 0.05$) median fold changes ranging from −4.17 to 5.41 (figure 1.3A, supplementary figure 1.2A and supplementary table 1.4A). MiR-150-5p and miR-155-5p were upregulated, whereas miR-15a-3p, -34c-5p, and -297 were downregulated in patients with MS, irrespective of disease activity in comparison to SCs. Most miRNAs (n = 8) were upregulated in patients with relapsing MS compared with patients with remitting MS or SCs, except miR-124-5p, which was downregulated compared with SCs. Three miRNAs (miR-20a-5p, -33a-3p, and -214-3p) were downregulated in patients with remitting MS compared with patients with relapsing MS and/or SCs, whereas miR-149-3p was upregulated. In addition, miR-

24-3p was differentially regulated in patients with MS and could therefore not be used as an internal reference gene in this setting.

*Figure 1.3: miRNA expression fold change in MS according to disease activity*

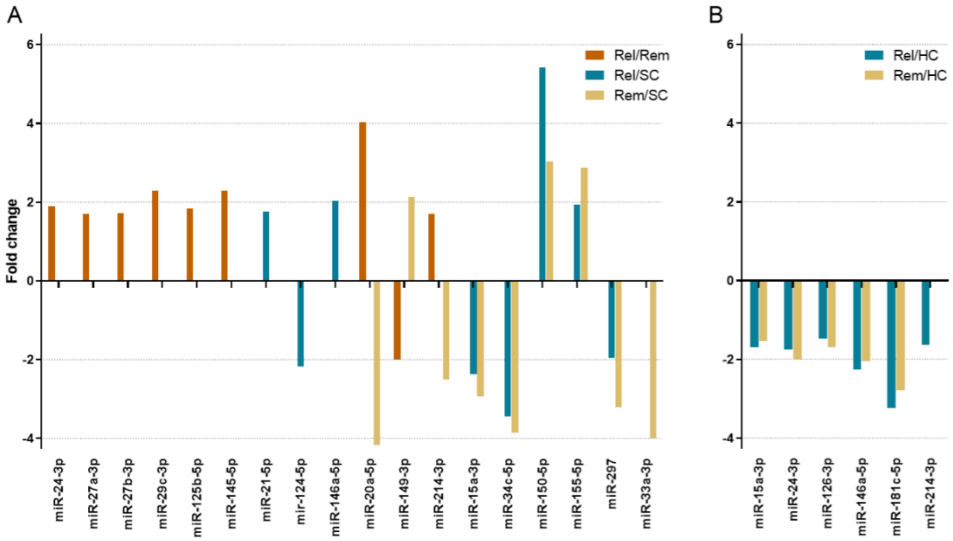


*Differences in CSF (A) and serum (B) miRNA expression levels. The fold change is calculated as the ratio between the median of the relative miRNA expression level of the respective subgroups. HC = healthy control; miRNA = microRNA; Rel = relapsing MS; Rem = remitting MS; SC = symptomatic control.*

iii. Specificity of the differentially expressed CSF miRNAs for MS

qPCR was performed for 57 miRNAs (supplementary table 1.3) on individual CSF samples of 14 patients having infectious neurologic disorders (Infect-NDs), 12 patients having inflammatory neurologic disorders (Inflam-NDs), 15 patients with relapsing MS, 9 patients with remitting MS, and 25 SCs.

Twenty-four miRNAs were differentially expressed in at least 1 subgroup reaching a statistically significant threshold of 0.05 following Benjamini-Hochberg correction (supplementary table 1.4B). These were all upregulated in Infect-ND compared with SC except miR-22-3p.

*Figure 1.4: Comparative CSF miRNA expression profile of MS vs neuroinfectious/neuroinflammatory diseases and controls*

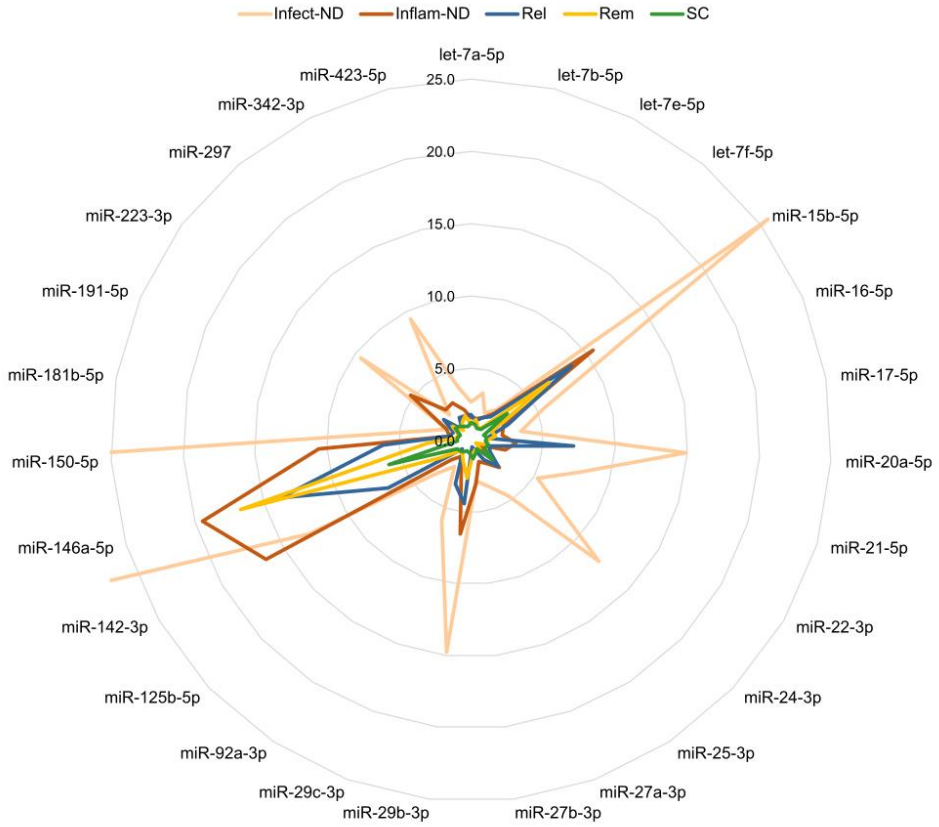


*Relative CSF miRNA expression levels in the different subgroups. Of note, values exceeding the graph scale were of 25.66, 61.48, and 85.94 for miR-15b-5p, -146a-5p, and -150-5p, respectively. Infect-ND = infectious neurologic disorder; Inflam-ND = inflammatory neurologic disorder; miRNA = microRNA; Rel = relapsing MS; Rem = remitting MS; SC = symptomatic control.*

The levels of miR-21-5p, -142-3p, -223-3p, -342-3p, -423-5p, and let-7f-5p were increased in the CSF of both Infect- and Inflam-ND vs SC, whereas miR-15b-5p, -29b-3p, and -29c-3p were upregulated in Infect-ND, Inflam-ND, and relapsing MS compared with SC. miR-150-5p was the only miRNA upregulated in all disease subgroups in comparison to SC. The profile of overexpressed miRNAs in these

disease categories was strikingly similar except for the expression levels that were 2- to 6-fold higher in the Infect-ND subgroup and even 14-fold higher for miR-150-5p compared with relapsing MS (figure 1.4).

In addition, 46 of these miRNAs were investigated on CSF samples of 16 patients having neurodegenerative disorders and 17 patients with peripheral nervous system disorders, but no differences in expression levels were found, except compared with Infect-ND (data not shown).

iv. Quantification of miRNAs in the serum of relapsing and remitting MS vs HCs

To determine whether the dysregulated miRNAs identified in the CSF were also differentially expressed in peripheral compartments, qPCR was performed for 24 miRNAs (supplementary table 1.3) on individual serum samples of 20 patients with relapsing MS, 19 patients with remitting MS, and 20 HCs.

Relative quantification of 6 miRNAs reached statistical significance, with fold change in the median miRNA expression level ranging between −3.23 and −1.47 (figure 1.3B, supplementary figure 1.2B and supplementary table 1.4A). Five miRNAs (miR-15a-3p, -24-3p, -126-3p, -146a-5p, and -181c-5p) were downregulated in both relapsing and remitting MS compared with HC, whereas miR-214-3p was downregulated in relapsing MS compared with HC only.

v. Quantification of miRNAs in PBMCs of patients with relapsing and remitting MS vs HCs

qPCR was performed for 24 miRNAs (supplementary table 1.3) on individual PBMC samples of 18 patients with relapsing MS, 16 patients with remitting MS, and 14 HCs. Only 1 miRNA, miR-34a-5p, was significantly downregulated in relapsing MS compared with remitting MS with a fold change of −1.89 (supplementary figure 1.2C and supplementary table 1.4A).

vi. PCA and correlation with CSF parameters

To identify the combination of variables that best explain the differences between patients with MS and SCs, we performed a PCA on upregulated CSF miRNAs that showed more than 1.5-fold variation between these groups. Significantly upregulated miRNAs in patients with MS (miR-150-5p, -155-5p, -146a-5p, -21-5p, and -149-3p) accounted for 40.32% of the sample population variance, whereas other numerical variables such as the immunoglobulin G (IgG) or immunoglobulin M intrathecal fractions and CSF pleocytosis accounted for 18.43% of the variance, allowing an excellent discrimination between patients with MS and SCs (figure 1.5, A and B). The relative contribution of selected miRNAs to the variability of the population was significant as indicated by their $cos^2$ value, with the most significant miRNAs being miR-146a-5p and miR-150-5p (supplementary table 1.5A). Conversely, the analysis performed with the miRNAs that were significantly downregulated in MS vs SC (miR-15a-3p, -20a-5p, -33a-3p, -34c-5p, -124-5p, -214-3p, and -297) accounted only for 31.95% of the sample population variance (data not shown). ROC curves were plotted for miR-150-5p, -146a-5p, and -155-5p, with an area under the curve of 0.88, 0.82, and 0.80, respectively ($p < 0.0001$). Relative cutoff value for miR-150-5p was 1.9, with a sensitivity of 80% and a specificity of 81% for MS diagnosis (figure 1.5C). In addition, miR-150-5p expression levels were moderately correlated with CSF pleocytosis, but not with other CSF parameters, both in the MS vs control cohort and in the cohort of different Infect-NDs/Inflam-NDs (Spearman $r = 0.47$ and $r = 0.58$, respectively, $p < 0.0001$). miR-150-5p levels were also significantly upregulated in patients with CSF-specific IgG OCBs (data not shown).

PCA on miRNAs whose expression was modified in patients with relapsing vs remitting MS (miR-20a-5p, -145-5p, -214-3p, -27a-3p, -27b-3p, -24-3p, and -29c-3p), using the presence/absence of GELs as illustrative variable for disease activity, showed a good separation between patients with relapsing and remitting MS. This miRNA combination accounted for 77.52% of the population variance (figure 1.5, D and E), with the most representative miRNAs being miR-24-3p, -27a-3p, and -145-5p (supplementary table 1.5B). Adding miR-149-3p, which is decreased 2-fold in relapsing vs remitting MS, did not improve disease activity discrimination (data not shown).

*Figure 1.5: Patient stratification according to diagnosis or disease activity by PCA*

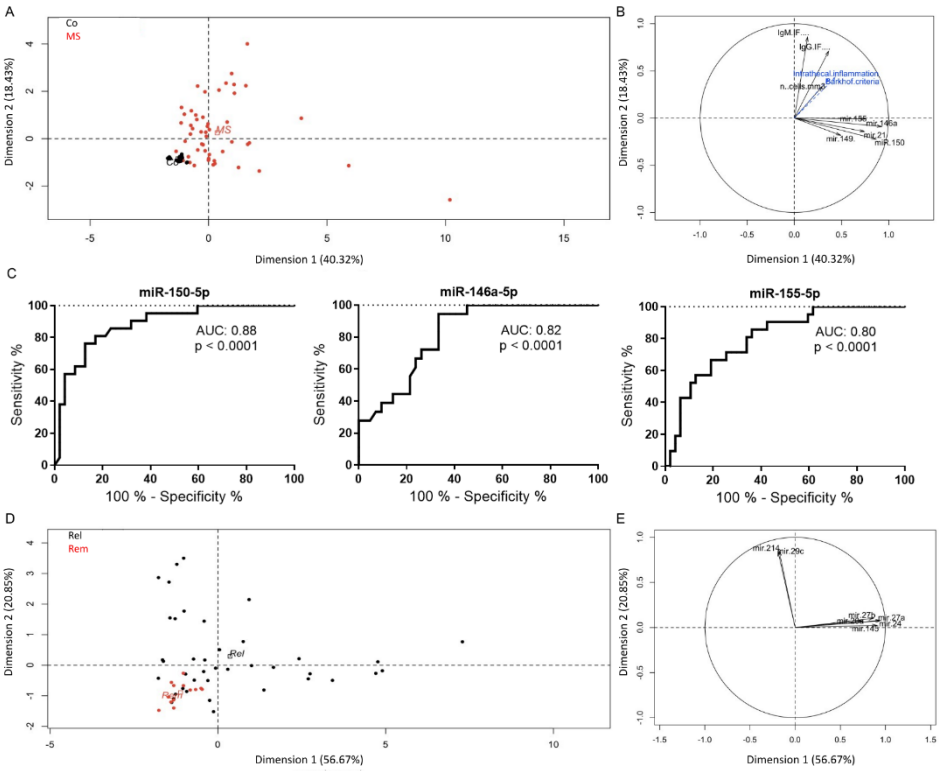


*PCA was applied using the significantly upregulated CSF miRNAs in patients with MS and other CSF parameters (IgG or IgM IF, CSF pleocytosis). PCA can distinctly separate MS from SC (A) in a 2-dimensional representation comprising in total 58.75% of sample population variability. The upregulated miRNA panel (i.e., miR-21-5p, -146a-5p, -149-3p, -150-5p, and -155-5p) segregates from other diagnostic criteria (Barkhof imaging criteria, IgM and IgG IF). Cos² values for each variable are plotted in abscissa and ordinate (B). They represent the strength of the individual variables in indicating population variability according to each dimension (significant above 0.5). ROC curves are plotted (C) for miR-150-5p, -146a-5p, and -155-5p as diagnostic biomarkers for MS with respective areas under the curve of 0.88, 0.82, and 0.80, respectively (p < 0.0001). PCA can also partially separate patients with Rel MS from patients with Rem MS (D) in a 2-dimensional representation comprising in total 77.52% of sample population variability. MiR-20a-5p, -24-3p, -27a-3p, -27b-3p, and -145-5p segregate from miR-29c-3p and miR-214-3p (E). AUC = area under curve; GEL = gadolinium-enhancing lesion; IF = intrathecal fraction; IgG = immunoglobulin G; IgM = immunoglobulin*

*M; miRNA = microRNA; PCA = principal component analysis; Rel = relapsing MS; Rem = remitting MS; ROC = receiver operating characteristic; SC = symptomatic control.*

vii. Biological significance and targeted genes of the differentially expressed miRNAs in MS

To obtain insight regarding the functions of the dysregulated miRNAs, we performed pathway enrichment analysis for the differentially expressed miRNA sets (more than 1.5-fold difference with corrected p value ≤ 0.05) between subgroups, as defined below and in figure 1.6. Some pathways were affected, independently from disease activity, such as cancer (p53 signalling pathway, glioma, or chronic myeloid leukaemia), cell cycle and proliferation (Wnt), immune (transforming growth factor beta and FoxO), cellular adhesion (focal adhesion and adherens junction) signalling pathways. We nevertheless observed that the enrichment score (defined as the -log10[p value])[755] was always stronger for the relapsing vs remitting (Rel/Rem) subgroup compared with the 2 other subgroups. More strikingly, some pathways were found specifically in relapsing patients (neurotrophin, mTOR, and ErbB) compared with the 2 other groups, suggesting some relevance of these pathways in modulating disease activity. On the other hand, nuclear factor kappa-light chain-enhancer of activated B cells (NFkB) was shown as general signalling for relapsing-remitting MS (RRMS). Some pathways were only affected in the Rel/Rem subgroup (axon guidance and insulin) or specifically in the Rel/SC subgroup (tumour necrosis factor alpha) (figure 1.6A). The comparison between up- and downregulated miRNAs in the different compartments showed a parallelism between pathways targeted by miRNAs upregulated in the CSF of relapsing MS and downregulated in the CSF of remitting MS (supplementary table 1.6). In addition, the most representative genes retrieved from the analysis of all differentially expressed miRNAs in the CSF were introduced in a miRNA-gene interaction network. Several genes (MYC, VEGFA, MKN2, BCL2, PMAIP1, KIAA1551, XIAP, NFAT5, E2F3, WEE1, STAT3, CCND1, SMAD4, TMEM167A, and LRRC58) were targeted by at least 4 miRNAs species from the 3 different sets, revealing possibly important miRNA-related genes affected in MS (figure 1.6B).

.

*Figure 1.6: Predicted signalling pathways and genes targeted by dysregulated CSF miRNAs in MS*

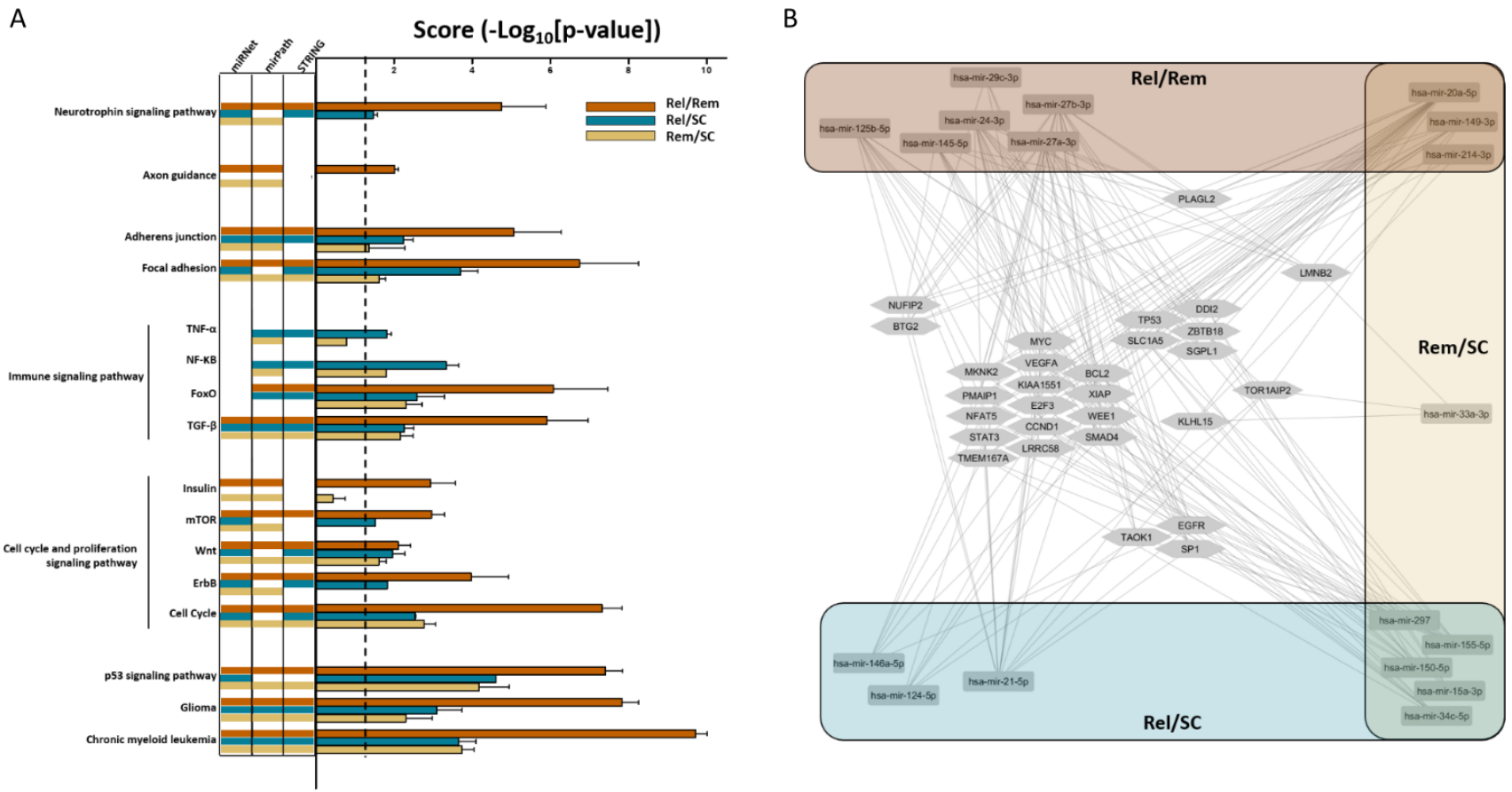

*(A) Top enriched canonical pathways associated with the differentially expressed CSF miRNAs between each subgroup (Rel/Rem [orange bars], Rel/SC [blue bars], or Rem/SC [yellow bars]) are illustrated. Indicated pathways were found by performing Kyoto Encyclopaedia of Genes and Genomes (KEGG) analysis using the miRNet, mirPath, or Cytoscape stringApp databases. The columns on the left side of the graph indicate the number of databases from which a determined pathway was retrieved. The pathways retrieved by specific databases are indicated by the aforementioned colour code (a void line indicates that a pathway was not found in the database from the corresponding column). On the right side, results are expressed as mean ± standard error of the enrichment score (−log10 of adjusted p value) obtained from the 3 databases, giving a score for the relative weight of a given signalling pathway between experimental subgroups; the dotted line designates the threshold of 1.3 (representing p value at 0.05). We identified signalling pathways consistent with MS pathogenesis such as cell cycle or apoptosis (Insulin, mTOR, Wnt, and ErbB signalling pathways with the following gene targets: MYC, CCND1, LMNB2, CDKN1A, MDM2, E2F3, TP53, NRAS, WEE1, MKNK2, BTG2, PMAIP1, TAOK1, DDI2, and NUFIP2), immunoregulation (TNF-α, NF-κB, TGF-β, FoxO signalling pathways, and gene targets: SMAD4, NFAT5, SP1, MYC, CCND1, SLC1A5, STAT3, BCL2, and XIAP), neuroprotective and neurodegenerative processes (axon guidance, ErbB, and neurotrophin signalling pathways with BCL2, TP53, VEGFA, EGFR, ZBTB18, PLAGL2, and TOR1AIP2 as targeted genes), and cancer-related signalling pathways (only glioma and myeloid leukaemia were selected). (B) Cytoscape network representation of interactions between the 18 MS-associated miRNAs in the CSF and a panel of targeted genes extracted from the miRNet database. The resulting network comprises 47 nodes (the 18 dysregulated miRNAs with the 29 most represented genes) and 176 direct edges. The colour code refers to the sets of miRNAs according to their differential expression across subgroups, as in A. miRNA = microRNA; NF-κB = nuclear factor kappa-light-chain-enhancer of activated B; Rel = relapsing MS; Rem = remitting MS; SC = symptomatic control; TGF-β = transforming growth factor beta; TNF-α = tumour necrosis factor alpha*

## V. Discussion

### i. CSF-predominant miRNA dysregulation and miRNA species newly associated with MS

This study sought to perform a comprehensive analysis of the differential expression of carefully preselected miRNAs in patients with RRMS, according to

disease activity, vs controls in 3 different biological compartments. Patients were free of DMT and devoid of high-dose steroids. A second CSF cohort was analysed to compare the MS miRNA profile with that of other neurologic diseases. Strikingly, we observed 18 significantly dysregulated miRNAs in the CSF vs 6 in the serum and only 1 in PBMCs, pointing toward specific intrathecal processes ongoing in MS and confirming the results of the preliminary miRNA array analysis performed on pooled samples. We have identified 7 miRNAs, namely miR-15a-3p, -29c-3p, -33a-3p, -34c-5p, -124-5p, -149-3p, and -297 that have not yet been described in MS to the best of our knowledge, but rather found in cancer either as tumour suppressors or as oncogenes [911]. Other miRNA species (miR-21-5p, -27b-3p, -145-5p, -146a-5p, -150-5p, -155-5p, -20a-5p, -214-3p, -24-3p, -27a-3p, and -125b-5p) were previously described as differentially expressed in RRMS in at least 1 of the following sample types: PBMCs or immune cell subpopulations, serum, whole blood, or active brain lesions [753]. Moreover, this study suggests that a specific set of miRNAs could serve as potential biomarkers for MS disease activity.

ii. The CSF miRNA profile parallels the extent of intrathecal inflammation, but is not specific to MS

Although studies on CSF miRNAs in MS are sparse, several miRNAs identified in this study were previously described by other groups either in the CSF or other sample types [900]. Our work emphasises, however, the predominance of CSF miRNA dysregulation in MS, in concordance with its pathogenesis. Furthermore, our results highlight the partially overlapping profile of CSF-upregulated miRNAs in infectious and inflammatory CNS disorders compared with relapsing MS. The CSF miRNA expression level was related to pleocytosis, as it was higher in Infect-NDs than in relapsing MS, especially regarding miR-150-5p expression, which was also associated with the presence of OCBs.

The upregulation of CSF miR-150-5p in MS is in agreement with the previously published studies by Quintana et al. and Bergman et al [768,912]. The expression of this miRNA is also increased in serum and exosomes from activated lymphocytes and is therefore considered as a sensor for activation of adaptive immunity [913]. In this study, however, miR-150-5p was not upregulated in peripheral compartments, again suggesting the predominance of intrathecally mediated immune processes.

We illustrated by PCA that miR-150-5p, -146a-5p, and -155-5p could significantly segregate patients with RRMS from controls. ROC curve analysis was the strongest for miR-150-5p, with a sensitivity and specificity of 80% and 81%, respectively, an even stronger result than previously shown [912] and comparable to ROC curves of kappa free light chains for MS diagnosis [903].

The set of miRNAs (miR-20a-5p, -145-5p, -214-3p, -27a-3p, -27b-3p, -24-3p, and -29c-3p) whose expression was modified according to disease activity could be sufficient to segregate patients with relapsing MS from patients with remitting MS. Further studies, in larger independent cohorts, should investigate whether these miRNAs could serve as biomarkers of disease activity.

iii. MiRNA profile in the serum and PBMCs of patients with MS

Five miRNAs were downregulated in the serum of both relapsing and remitting MS (miR-15a-3p, -24-3p, -126-3p, -146a-3p, and -181c-5p), whereas miR-214-3p was downregulated in the serum of relapsing MS only. Remarkably, only downregulation of miR-15a-3p was consistent in both serum and CSF, whereas miR-24-3p, -146a-5p, and -214-3p were found upregulated in the CSF. Comparably, miR-126-3p was downregulated in whole blood MS samples [914]. Other miRNAs (miR-122-5p, -196b-5p, -301a-3p, and -532-5p) found in extracellular vesicles were also decreased in the serum of patients with relapsing MS [915]. This discrepancy between the CSF and peripheral compartments was also shown in Alzheimer disease and intracerebral haemorrhage, but is yet not understood [916,917]. The expression patterns of miR-181c-5p remain controversial, as some have described its upregulation in the CSF and in active MS lesions [758,901]. In our hands, the levels of miR-181c-5p were however too low to allow quantification in the CSF, but it was downregulated in the serum of patients with MS compared with controls. Finally, in agreement with the decrease of miR-34a-5p levels in CD4+ T cells of patients with MS, we found its expression significantly downregulated in the PBMCs of patients with relapsing MS [918].

iv. Target analysis of miRNAs dysregulated in MS

To generate hypothesis regarding the functional role of the identified miRNAs in CSF, we performed a pathway enrichment analysis on several KEGG pathway databases to reveal the most affected signalling pathways according to disease activity, but also in serum and PBMCs. As a single miRNA species is not sufficient to account solely for the disease, as discussed above, we grouped the different miRNAs in sets. For CSF miRNAs, we first observed the highest enrichment score for several cancer signalling pathways, but we only presented the results for glioma and chronic myeloid leukaemia because (1) these pathways are relevant for the (neuro)immunopathologic aspect of MS disease and (2) most of the miRNAs were extensively investigated in cancer research, which naturally biases most analyses toward cancer-related pathways. Besides cancer-related signalling pathways, the score comparison of the different subgroups of patients (relapsing, remitting MS and SC vs each other) and the Cytoscape miRNA-messenger RNA (mRNA) network representation obtained from CSF showed pathways consistent with MS pathogenesis such as cell cycle or apoptosis, immunoregulation, neuroprotective, and neurodegenerative processes.

MiRNA molecular function prediction by gene ontology provided the highest score to several negative regulators of transcriptional activity through targeting of CCND1, STAT3, the E2F family, MYC, SP1, ZBTB18, and PLAGL2 among others (findings obtained by miRNet; data not shown). This result confirms previous studies on the impact of miRNAs on the transcriptional network in MS pathogenesis [915,919–922]. Our research demonstrates for the first time that the CSF profile of remitting MS (Rem) is more closely related to the profile of controls than relapsing MS (Rel) because (1) the signalling pathways target analysis scores were the lowest (if not absent) for the miRNAs differentially expressed between Rem vs SC (Rem/SC), whereas the scores were the highest for the ones between Rel/Rem and (2) that no common signalling pathways specifically stood out for the dysregulated miRNAs in Rel and Rem compared with controls. At the mRNA level, it is worth noting that, unlike most of the genes regulated by miRNAs from all groups, PLAGL2 and LMNB2 were specifically clustered to the Rel/Rem and Rem/SC subgroups. Of interest, LMNB2 was related to 2 miRNAs not previously associated with MS, namely miR-149-3p and miR-33a-3p. PLAGL2 is a transcription factor regulating Wnt signalling, and thus leading to the inhibition of neural stem cell

differentiation[923]. It could therefore be relevant for reparative processes during remission. LMNB2 codes for a member of the lamin family and was found 5-fold downregulated in CD4+ T cells of patients with remitting MS compared with HCs [924]. Altogether, the pathway enrichment analysis with the miRNA sets identified in this study remarkably pinpoints to important pathways and miRNA-gene interactions pertinent to MS pathogenesis, as evidenced in earlier studies. The differentially expressed miRNAs have relevant mRNA interactions, especially in regard to the modulation of the immune response. For instance, miR-155-5p promotes Th17 and regulatory T-cell (Treg) differentiation, Th17 function, and microglia-mediated immune responses, through expression of interleukin (IL) 6, tumour necrosis factor alpha, and iNOS, by targeting SOCS1 [842,857]. MiR-155-5p also alters blood-brain barrier permeability and enhances leukocyte adhesion to endothelial cells, whereas miR-126-3p and miR-146a-5p counteract this by modulating the expression of brain endothelial ICAM1, VCAM1 [827,856,925]. Moreover, miR-146a-5p exerts its immunoregulatory effect by blocking Th17 differentiation through repression of TRAF6 and IRAK1, which are transducers of nuclear factor kappa-light-chain-enhancer of activated B cells and thus reduces IL-6 and IL-21 expression [821]. MiR-27b-3p inhibits Treg differentiation but not their function, by downregulating SMAD4 and TGFBR1 [802]. MiR-21-5p represses lymphocyte migration through STAT3 regulation [926]. The deletion of miR-150-5p in experimental autoimmune encephalomyelitis (EAE) mice affects CD3+, CD4+, and CD8+ cells and mRNA expression of proinflammatory cytokines compared with wild-type EAE, likely by regulating CMYB [839].

v. Cellular source and carriers of CSF miRNAs

Although our study did not investigate the cellular source of the CSF-associated miRNAs, according to the cell-specific miRNA catalogue, nearly all immune cell subpopulations express the miRNAs found in our study [927]. Yet, some miRNA species might be more specific of certain cell types, as extracellular vesicles (EVs) of Treg cells were specifically enriched with miR-21-5p, -146a-5p, and -150-5p, whereas those of Th1 and Th17 cells preferentially expressed miR-155-5p [928].

Whether miRNAs are carried exclusively by EVs such as exosomes in the CSF is still an open question. However, miRNAs were enriched in exosomal fractions of CSF[929].

The number of CSF EVs increases during MS relapses and GELs on brain or spinal cord MRIs were associated with an increase in CSF EVs expressing markers of CD8+ memory T cells, Th2 and Th1 cells [930]. The cellular source of miRNAs from the CSF and their carriers should be further investigated in the setting of MS.

vi. Study limitations

The strength of this study resides in the comprehensive stepwise strategy used, the large CSF sample size, the use of a confirmatory cohort for the CSF, the comparison between compartments, and finally the comparison with miRNA expression in other disease categories. Moreover, patients were systematically sex- and age-matched to controls. However, there is inevitable heterogeneity between reports on miRNA expression analysis in MS due to discrepancies in sample numbers, collection and storage procedures, patient characteristics, study design, molecular biology techniques (microarray or qPCR, with or without preamplification, TaqMan vs SYBR Green), data analysis (quantification method, choice of reference gene), and finally the type of statistical tests. These factors, altogether or separately, possibly affect results. In this study, qPCRs from CSF and serum were normalised with an external reference, as an internal reference could not be identified. Future studies could possibly combine a panel of non-significantly altered miRNAs as normalizers. Some selected miRNAs were below the PCR detection level, preventing further analysis. The targeted selection of miRNAs based on the literature and immune-related miRNA PCR arrays does not exclude that other miRNA species are also dysregulated in MS. Finally, the patient cohort from a single academic centre may not be representative of a more global MS cohort. An international and multicentric study that includes miRNA sequencing could provide novel miRNA targets that would refine our current results.

In conclusion, we have demonstrated that 21 miRNAs were differentially expressed in RRMS, mostly in the CSF, which is at the core of the inflammation, 7 of which were never associated with MS so far. The miRNA expression profile varied according to disease activity. It was associated with the extent of intrathecal inflammation, notably CSF pleocytosis, not only in MS but also in neuroinfectious and other neuroinflammatory diseases. Considering this, a single miRNA is unlikely

to be considered as a MS biomarker, but a set of miRNAs could rather be investigated for that purpose. The strength of this work resides in (1) the study of different disease categories, (2) the comprehensive miRNA analysis performed on 3 biological compartments in patients with MS, and (3) the validation of CSF results by our second cohort and some miRNAs already described in other studies. Our work emphasises the potential of a miRNA set to reflect intrathecal inflammation and MS disease activity. The miRNA expression profile was in concordance with their known effects on immune and neuroinflammatory processes at play in MS. In silico analysis provided a view on affected signalling pathways, warranting further studies into their function, cellular source, and carriers, especially for the newly found miRNAs associated with MS. Ultimately, the present report will help fundamental research on MS by paving the way for the functional characterisation of miRNAs and unravelling novel pathways for possible therapeutic intervention.

## VI. Supplementary material

*Supplementary figure 1.1: Heatmap representation of the multi-compartment miRNA screening performed in relapsing MS versus controls*

*Differences in miRNA expression in CSF, serum and PBMCs on a pool of ten relapsing MS patients versus ten controls were measured by two 84-plex PCR arrays for inflammatory response and autoimmunity (left) or T- and B-cell activation (right). miRNA species indicated in bold were subsequently measured by RT-qPCR in individual samples. $\triangle Ct$ corresponds to the difference in Ct (inversely related to the amount of target miRNA in the sample) between relapsing MS versus controls. They are indicated by a colour graduation for absolute values ≥ 1.59, corresponding to a 3-fold change in expression (calculated as $2^{-\triangle Ct}$). Significantly different $\triangle Ct$ values are indicated in numeric values in the graph. Underscored values correspond to miRNAs of low abundance with Cts > 30. Ct = cycle threshold; hsa = Homo sapiens; PBMC = peripheral blood mononuclear cells; Rel = relapsing MS.*

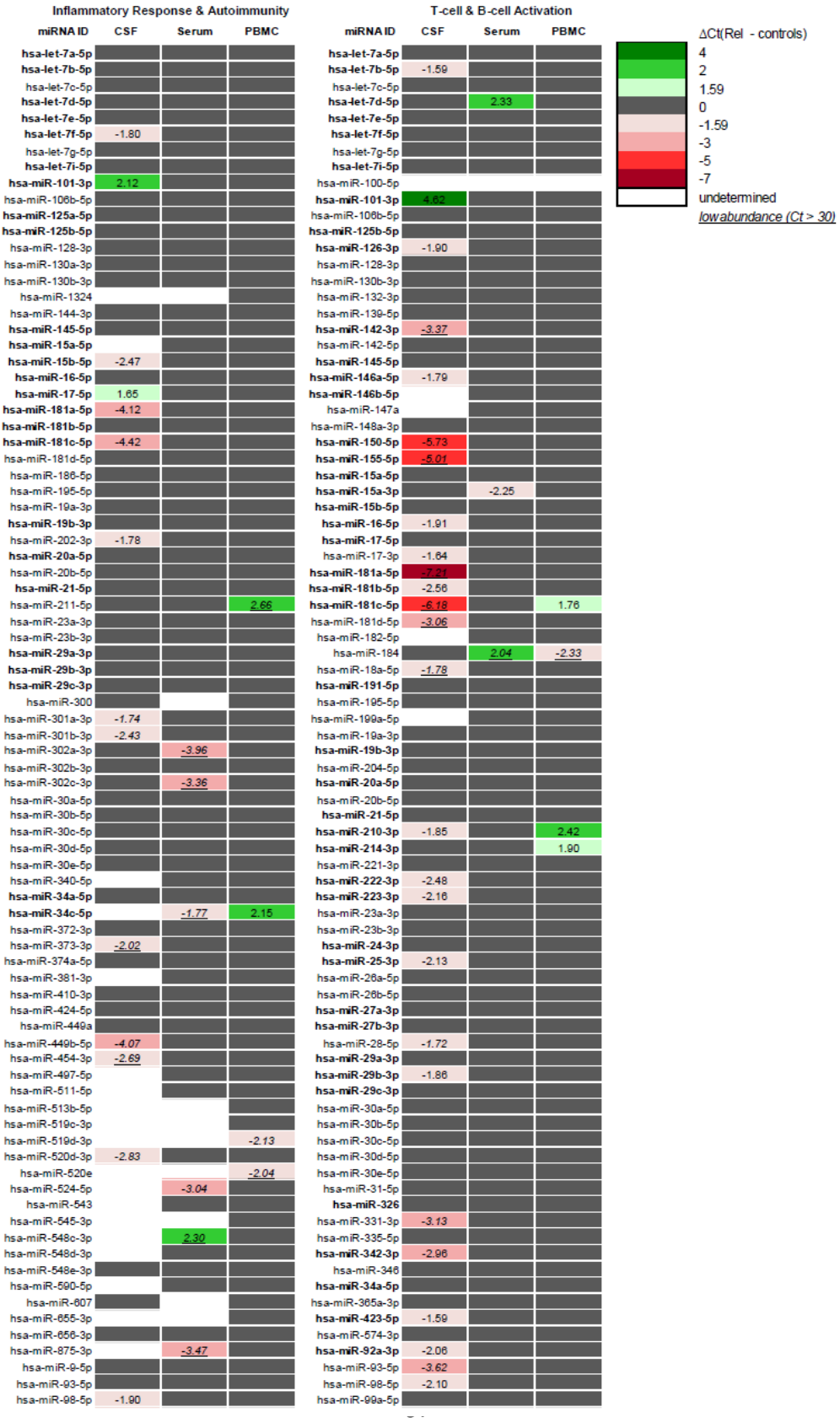
Inflammatory Response & Autoimmunity
miRNA ID
CSF
Serum
PBMC
hsa-let-7a-5p
hsa-let-7b-5p
hsa-let-7c-5p
hsa-let-7d-5p
hsa-let-7e-5p
hsa-let-7f-5p
-1.80
hsa-let-7g-5p
hsa-let-7i-5p
hsa-miR-101-3p
2.12
hsa-miR-106b-5p
hsa-miR-125a-5p
hsa-miR-125b-5p
hsa-miR-128-3p
hsa-miR-130a-3p
hsa-miR-130b-3p
hsa-miR-1324
hsa-miR-144-3p
hsa-miR-145-5p
hsa-miR-15a-5p
hsa-miR-15b-5p
-2.47
hsa-miR-16-5p
hsa-miR-17-5p
1.65
hsa-miR-181a-5p
-4.12
hsa-miR-181b-5p
hsa-miR-181c-5p
-4.42
hsa-miR-181d-5p
hsa-miR-186-5p
hsa-miR-195-5p
hsa-miR-19a-3p
hsa-miR-19b-3p
hsa-miR-202-3p
-1.78
hsa-miR-20a-5p
hsa-miR-20b-5p
hsa-miR-21-5p
hsa-miR-211-5p
2.66
hsa-miR-23a-3p
hsa-miR-23b-3p
hsa-miR-29a-3p
hsa-miR-29b-3p
hsa-miR-29c-3p
hsa-miR-300
hsa-miR-301a-3p
-1.74
hsa-miR-301b-3p
-2.43
hsa-miR-302a-3p
-3.96
hsa-miR-302b-3p
hsa-miR-302c-3p
-3.36
hsa-miR-30a-5p
hsa-miR-30b-5p
hsa-miR-30c-5p
hsa-miR-30d-5p
hsa-miR-30e-5p
hsa-miR-340-5p
hsa-miR-34a-5p
hsa-miR-34c-5p
-1.77
2.15
hsa-miR-372-3p
hsa-miR-373-3p
-2.02
hsa-miR-374a-5p
hsa-miR-381-3p
hsa-miR-410-3p
hsa-miR-424-5p
hsa-miR-449a
hsa-miR-449b-5p
-4.07
hsa-miR-454-3p
-2.69
hsa-miR-497-5p
hsa-miR-511-5p
hsa-miR-513b-5p
hsa-miR-519c-3p
hsa-miR-519d-3p
-2.13
hsa-miR-520d-3p
-2.83
hsa-miR-520e
-2.04
hsa-miR-524-5p
-3.04
hsa-miR-543
hsa-miR-545-3p
hsa-miR-548c-3p
2.30
hsa-miR-548d-3p
hsa-miR-548e-3p
hsa-miR-590-5p
hsa-miR-607
hsa-miR-655-3p
hsa-miR-656-3p
hsa-miR-875-3p
-3.47
hsa-miR-9-5p
hsa-miR-93-5p
hsa-miR-98-5p
-1.90
T-cell & B-cell Activation
miRNA ID
CSF
Serum
PBMC
hsa-let-7a-5p
hsa-let-7b-5p
-1.59
hsa-let-7c-5p
hsa-let-7d-5p
2.33
hsa-let-7e-5p
hsa-let-7f-5p
hsa-let-7g-5p
hsa-let-7i-5p
hsa-miR-100-5p
hsa-miR-101-3p
4.62
hsa-miR-106b-5p
hsa-miR-125b-5p
hsa-miR-126-3p
-1.90
hsa-miR-128-3p
hsa-miR-130b-3p
hsa-miR-132-3p
hsa-miR-139-5p
hsa-miR-142-3p
-3.37
hsa-miR-142-5p
hsa-miR-145-5p
hsa-miR-146a-5p
-1.79
hsa-miR-146b-5p
hsa-miR-147a
hsa-miR-148a-3p
hsa-miR-150-5p
-5.73
hsa-miR-155-5p
-5.01
hsa-miR-15a-5p
hsa-miR-15a-3p
-2.25
hsa-miR-15b-5p
hsa-miR-16-5p
-1.91
hsa-miR-17-5p
hsa-miR-17-3p
-1.64
hsa-miR-181a-5p
-7.21
hsa-miR-181b-5p
-2.56
hsa-miR-181c-5p
-6.18
1.76
hsa-miR-181d-5p
-3.06
hsa-miR-182-5p
hsa-miR-184
2.04
-2.33
hsa-miR-18a-5p
-1.78
hsa-miR-191-5p
hsa-miR-195-5p
hsa-miR-199a-5p
hsa-miR-19a-3p
hsa-miR-19b-3p
hsa-miR-204-5p
hsa-miR-20a-5p
hsa-miR-20b-5p
hsa-miR-21-5p
hsa-miR-210-3p
-1.85
2.42
hsa-miR-214-3p
1.90
hsa-miR-221-3p
hsa-miR-222-3p
-2.48
hsa-miR-223-3p
-2.16
hsa-miR-23a-3p
hsa-miR-23b-3p
hsa-miR-24-3p
hsa-miR-25-3p
-2.13
hsa-miR-26a-5p
hsa-miR-26b-5p
hsa-miR-27a-3p
hsa-miR-27b-3p
hsa-miR-28-5p
-1.72
hsa-miR-29a-3p
hsa-miR-29b-3p
-1.86
hsa-miR-29c-3p
hsa-miR-30a-5p
hsa-miR-30b-5p
hsa-miR-30c-5p
hsa-miR-30d-5p
hsa-miR-30e-5p
hsa-miR-31-5p
hsa-miR-326
hsa-miR-331-3p
-3.13
hsa-miR-335-5p
hsa-miR-342-3p
-2.96
hsa-miR-346
hsa-miR-34a-5p
hsa-miR-365a-3p
hsa-miR-423-5p
-1.59
hsa-miR-574-3p
hsa-miR-92a-3p
-2.06
hsa-miR-93-5p
-3.62
hsa-miR-98-5p
-2.10
hsa-miR-99a-5p
ΔCt(Rel - controls)
4
2
1.59
0
-1.59
-3
-5
-7
undetermined
low abundance (Ct > 30)

*Supplementary figure 1.2: MiRNA expression levels in CSF, serum and PBMCs of relapsing/remitting MS and controls*

*Box plots of relative expression for indicated miRNA are presented by Tukey's method. p-value (* ≤ 0.05; ** ≤ 0.01; *** ≤ 0.001) are calculated by Benjamini-Hochberg's correction. HC = healthy controls; PBMCs = peripheral blood mononuclear cells; Rel = relapsing MS; Rem = remitting MS; SC = symptomatic controls.*

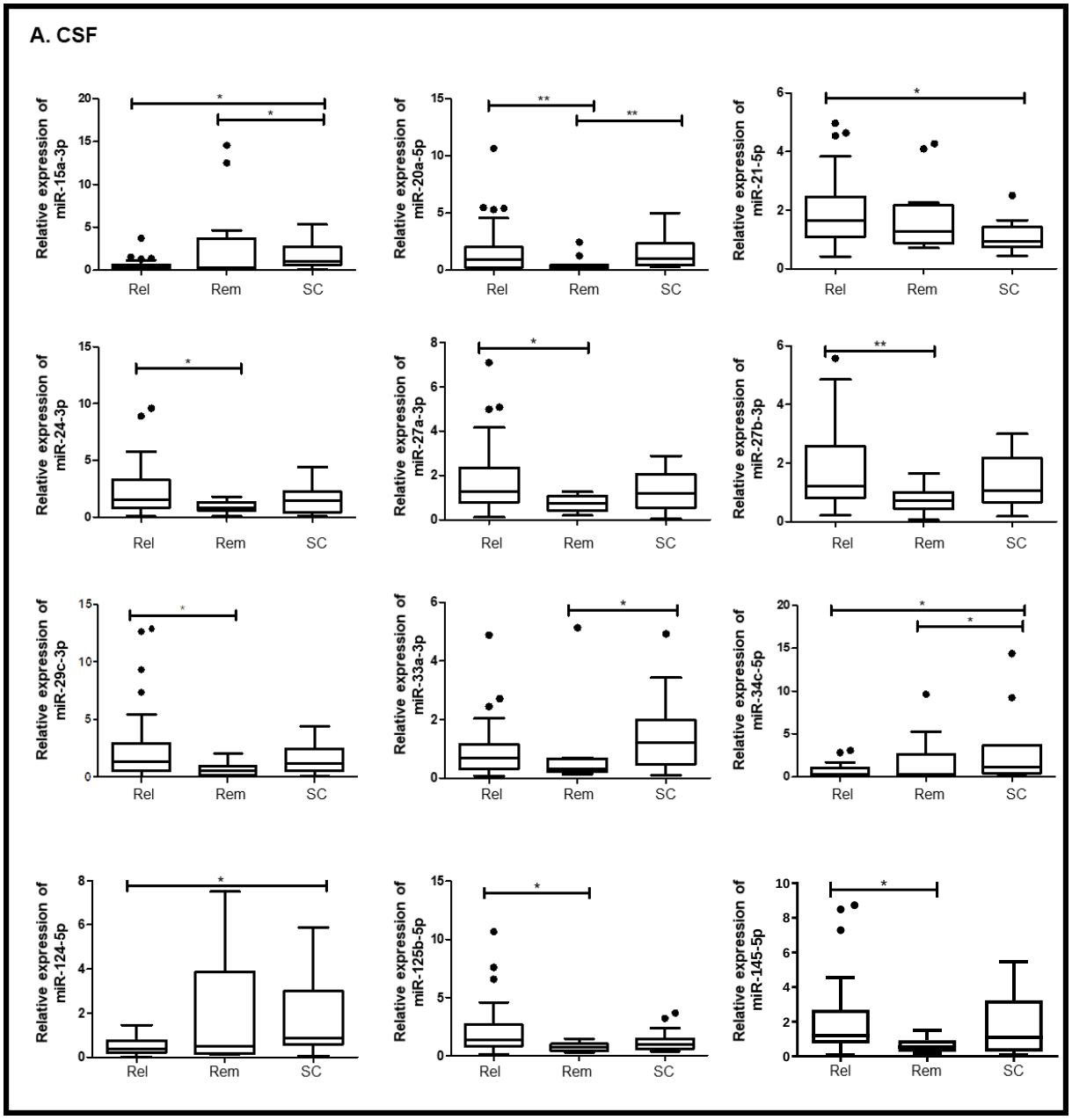

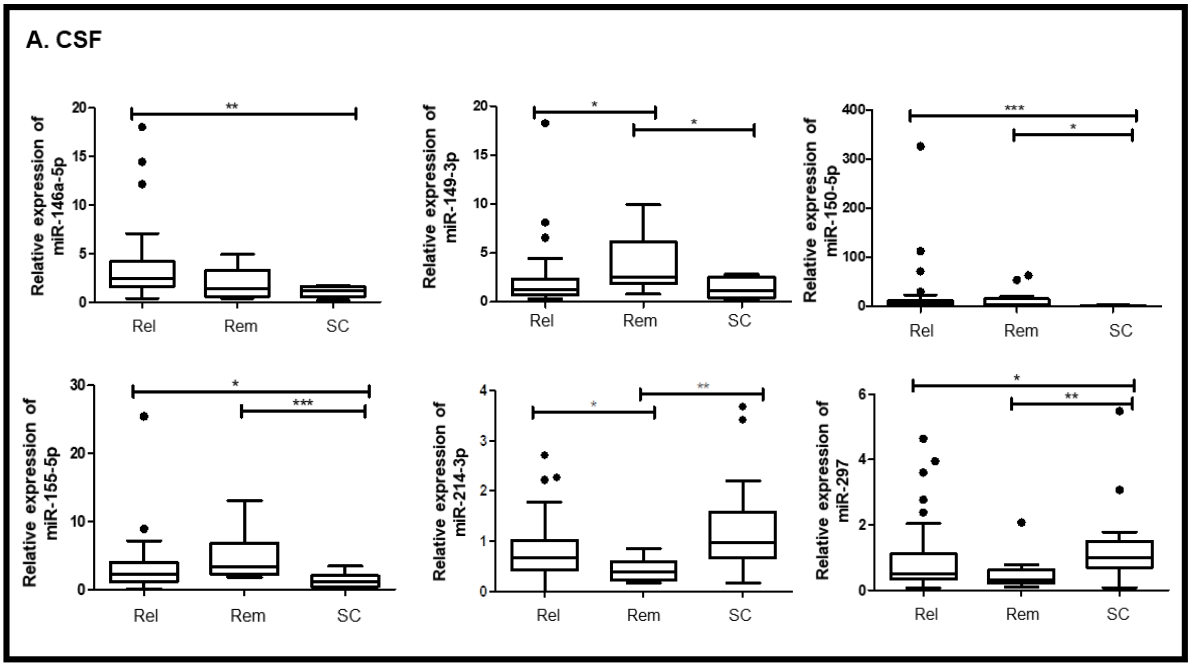
A. CSF
Relative expression of miR-146a-5p
Relative expression of miR-149-3p
Relative expression of miR-150-5p
Relative expression of miR-155-5p
Relative expression of miR-214-3p
Relative expression of miR-297
Rel
Rem
SC

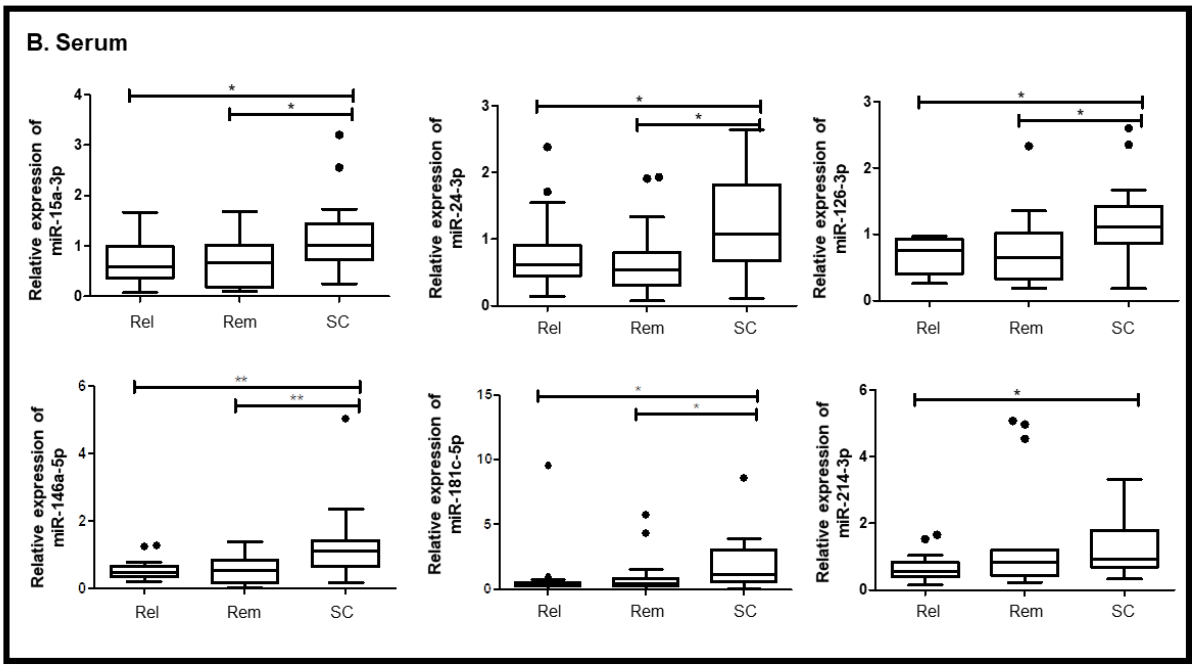
B. Serum
Relative expression of miR-15a-3p
Relative expression of miR-24-3p
Relative expression of miR-126-3p
Relative expression of miR-146a-5p
Relative expression of miR-181c-5p
Relative expression of miR-214-3p
Rel
Rem
SC

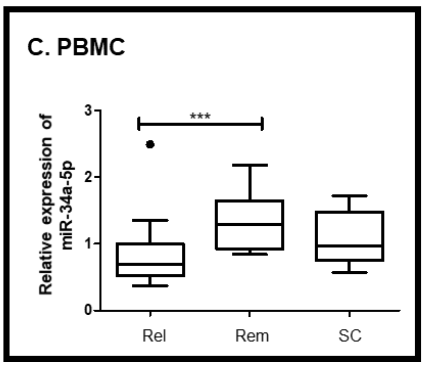
C. PBMC
Relative expression of miR-34a-5p
Rel
Rem
SC

*Supplementary table 1.1: Baseline characteristics of patients and controls included in the several cohorts*

*Number of patients for which data is available is indicated by "n". [a]Barkhof criteria[907] was assessed to reflect the lesion load. [b]IgG and IgM intrathecal fractions were calculated using Reiber's formulas[906] (normal value is 0%). All CSF RRMS patients were disease modifying treatment (DMT)-naïve. Only 7 out of 38 relapsing and 6 out of 35 remitting MS patients had stopped DMT three months to 13 years prior to serum or PBMCs sampling, with the remainder being treatment naïve. Furthermore, none of the patients had received high dose intravenous methylprednisolone. According to the consensus definition[905], inflammatory neurological disease controls include all inflammatory neurological diseases that have abnormal CSF findings (pleocytosis and/or elevated QAlb) except if other findings support the inflammatory nature. Symptomatic controls (SCs) are patients with neurological symptoms, but without any objective clinical or paraclinical findings to support the diagnosis of a specific neurological disease, whereas healthy controls are subjects without any medical complaint or condition. EDSS = expanded disability status score; FKLC = free kappa light chains; GEL = gadolinium-enhancing lesions; HC = healthy controls; Infect-ND = infectious neurological disorders; Inflam-ND = inflammatory neurological disorders; n = number; NA = not applicable; OCB = oligoclonal bands; PBMCs = peripheral blood mononuclear cells; Rel MS = relapsing MS; Rem MS = remitting MS; RRMS = relapsing-remitting MS;* SC = symptomatic controls; *SD = standard deviation*, *% ♀= percentage of female*.

*Supplementary table 1.1A: CSF, serum and PBMCs cohorts of miRNA arrays of relapsing MS vs SC/HC*

| | **CSF** | | **Serum/PBMCs** | | |
|---|---|---|---|---|---|
| | MS vs SC array | | MS vs SC array | | |
| n (% ♀) | 20 (90.0) | | 20 (90.0) | | |
| Mean age (±SD) | 31.1 (±8.8) | | 33.3 (±8.9) (PBMCs)<br>33.5 (± 9.6) (serum) | | |
| | **Rel MS** | **SC** | **Rel MS** | **HC (serum)** | **HC (PBMCs)** |
| n (% ♀) | 10 (100) | 10 (80.0) | 10 (90.0) | 10 (90.0) | 10 (90.0) |
| Mean age (±SD) | 31.9 (±10.9) | 30.2 (±4.2) | 33.1 (±9.8) | 33.8 (± 9.9) | 33.4 (±8.3) |
| Disease duration in months: mean (±SD) | 5 (±11) | NA | 14 (±31) | NA | NA |
| Relapse phenotype (%) | | | | | |
| 1: Spinal | 20.0 | NA | 30.0 | NA | NA |
| 2: Brainstem/cerebellum | 10.0 | | 0.0 | | |
| 3: Optic neuritis | 40.0 | | 40.0 | | |
| 4: Supratentorial | 10.0 | | 10.0 | | |
| 5: Multifocal | 20.0 | | 20.0 | | |
| EDSS: median [range] | 2.25 [2-3.5] | NA | 2 [2-3.5] | NA | NA |
| Number of relapses since disease onset: median [range] | 1 [1-2] | NA | 1 [1-2] | NA | NA |
| Proportion of patients with a 1st clinical event (%) | 70.0 | NA | 70.0 | NA | NA |
| Barkhof criteria[a] score 3 and 4 (%) | 90.0 | NA | 90.0 | NA | NA |
| GELs on brain MRI: mean (±SD) | 2.6 (±1.7)<br>*n = 9* | NA | 2.6 (±2.5) | NA | NA |
| Proportion of patients with spinal cord lesions on MRI (%) | 80.0 | NA | 80.0 | NA | NA |
| GELs on spinal cord MRI: mean (±SD) | 0.3 (±0.5)<br>*n = 4* | NA | 0<br>*n = 3* | NA | NA |
| Proportion of patients with at least one GEL on brain or spinal cord MRI (%) | 100 | NA | 100 | NA | NA |
| Number of CSF cells/mm³: mean (±SD) [range] | 4.4 (±4.4)<br>[0-14] | 0.8 (±1.4)<br>[0-4] | 9.6 (±10.6)<br>[0-34] | NA | NA |
| Proportion of patients with CSF-specific IgG OCBs or CSF FKLCs (%) | 100 | 10 | 100 | NA | NA |
| Proportion of patients with IgG intrathecal synthesis (%) | 90.0 | 0 | 90.0 | NA | NA |
| % IgG intrathecal synthesis[b]: mean (±SD) | 34.7 (±19.1) | 0 | 33.4 (±21.5) | NA | NA |
| Proportion of patients with IgM intrathecal synthesis (%) | 30.0 | 0 | 50.0 | NA | NA |
| % IgM intrathecal synthesis[b]: mean (±SD) | 16.6 (±27.6) | 0 | 25.4 (±30.9) | NA | NA |

*Supplementary table 1.1B: CSF cohort of Infect-/Inflam-ND and RRMS vs SC*

| | CSF<br>**Infect- & Inflam-ND vs MS vs SC** | | | | |
|---|---|---|---|---|---|
| n (% ♀) | 75 (57.3) | | | | |
| Mean age (±SD) | 39.7 (±14.9) | | | | |
| | **Infect-ND** | **Inflam-ND** | **Rel MS** | **Rem MS** | **SC** |
| n (% ♀) | 14 (57.1) | 12 (33.3) | 15 (73.3) | 9 (44.4) | 25 (64.0) |
| Mean age (±SD) | 41.2 (±15.0) | 32.8 (±20.2) | 32.5 (±10.6) | 40.1 (±10.8) | 46.3 (±13.1) |
| Disease duration in months: mean (±SD) | 0.7 (±0.5) | 7.7 (±13.4) | 33 (±65) | 38 (±60) | NA |
| Relapse phenotype (%)<br>1: Spinal<br>2: Brainstem/cerebellum<br>3: Optic neuritis<br>4: Supratentorial<br>5: Multifocal | NA | NA | 53.3<br>20.0<br>6.7<br>16.3<br>6.7 | NA | NA |
| EDSS: median [range] | NA | NA | 2 [0-3] | 2 [1-3] | NA |
| Number of relapses since disease onset: median [range] | NA | NA | 1 [1-6] | 2 [0-3] | NA |
| Proportion of patients with a 1st clinical event (%) | NA | NA | 53.3 | 33.3 | NA |
| Barkhof criteria[a] score 3 and 4 (%) | NA | NA | 93.3 | 44.4 | NA |
| GELs on brain MRI: mean (±SD) | NA | NA | 5.4 (±8.9)<br>*n = 13* | 0<br>*n = 6* | NA |
| Proportion of patients with spinal cord lesions on MRI (%) | NA | NA | 85.7<br>*n = 14* | 75.0<br>*n = 8* | NA |
| GELs on spinal cord MRI: mean (±SD) | NA | NA | 0.5 (±0.5)<br>*n = 10* | 0<br>*n = 3* | NA |
| Proportion of patients with at least one GEL on brain or spinal cord MRI (%) | NA | NA | 100<br>*n=14* | 0<br>*n=8* | NA |
| Number of CSF cells/mm³: mean (±SD) [range] | 80.9 (±133.5) [0-470] | 23.8 (±30.5) [2-102] | 6.8 (±6.4) [0-18] | 4.4 (±3.7) [0-11] | 1.2 (±1.8) [0-6] |
| Proportion of patients with CSF-specific IgG OCBs or CSF FKLCs (%) | 46.2<br>*n = 13* | 50 | 93.3 | 100 | 0<br>*n = 24* |
| Proportion of patients with IgG intrathecal synthesis (%) | 30.8<br>*n = 13* | 25.0 | 80.0 | 66.7 | 4.2<br>*n = 24* |
| % IgG intrathecal synthesis[b]: mean (±SD) | 13.3 (±23.4)<br>*n = 13* | 3.7 (±7.0) | 32.0 (±26.8) | 17.4 (±21.1) | 0.3 (±1.4)<br>*n = 24* |
| Proportion of patients with IgM intrathecal synthesis (%) | 53.8<br>*n = 13* | 25.0 | 33.3 | 22.2 | 0<br>*n = 24* |
| % IgM intrathecal synthesis[b]: mean (±SD) | 24.8 (±29.8) | 4.5 (±11.2) | 14.7 (±23.2) | 7.6 (±15.5) | 0; *n = 24* |

*Supplementary table 1.1C: Serum and PBMCs cohorts of RRMS vs HC*

| | Serum | | | PBMCs | | |
|---|---|---|---|---|---|---|
| | **MS vs HC** | | | **MS vs HC** | | |
| n (% ♀) | 59 (76.3) | | | 48 (83.3) | | |
| Mean age (±SD) | 40.8 (±11.2) | | | 41.5 (±13.3) | | |
| | **Rel MS** | **Rem MS** | **HC** | **Rel MS** | **Rem MS** | **HC** |
| n (% ♀) | 20 (80.0) | 19 (79.0) | 20 (70.0) | 18 (77.8) | 16 (93.8) | 14 (78.6) |
| Mean age (±SD) | 32.8 (±7.8) | 47.3 (±8.9) | 42.7 (±11.6) | 31.8 (±10.4) | 50.9 (±10.5) | 43.3 (±11.4) |
| Disease duration in months: mean (±SD) | 51 (±60) | 173 (±115) | NA | 52 (±77) | 133 (±97) | NA |
| Relapse phenotype (%) | | | | | | |
| 1: Spinal | 45.0 | NA | NA | 27.8 | NA | NA |
| 2: Brainstem/cerebellum | 15.0 | | | 16.7 | | |
| 3: Optic neuritis | 15.0 | | | 22.2 | | |
| 4: Supratentorial | 15.0 | | | 33.3 | | |
| 5: Multifocal | 10.0 | | | 0 | | |
| EDSS: median [range] | 2.5 [0-3.5] | 2 [0-3.5] | NA | 2.75 [0-3.5] | 2 [0-3.5] | NA |
| Number of relapses since disease onset: median [range] | 2 [1-11] | 2 [1-9] *n = 18* | NA | 2 [1-9] | 1 [0-4] | NA |
| Proportion of patients with a 1st clinical event (%) | 35.0 | 36.8 | NA | 35.0 | 62.5 | NA |
| Barkhof criteria[a] score 3 and 4 (%) | 84.2, *n = 19* | 84.2 | NA | 82.4, *n = 17* | 93.8 | NA |
| GELs on brain MRI: mean (±SD) | 2.5 (±2.3) *n = 17* | 0 *n = 11* | NA | 3.6 (±4.5) *n = 14* | NA | NA |
| Proportion of patients with spinal cord lesions on MRI (%) | 88.2 *n = 17* | 84.6 *n = 13* | NA | 87.5 *n = 16* | 78.6 *n = 14* | NA |
| GELs on spinal cord MRI: mean (±SD) | 0, *n = 4* | NA | NA | 0.4 (±0.5) *n = 5* | NA | NA |
| Proportion of patients with at least one GEL on brain or spinal cord MRI (%) | 93.8 *n = 16* | NA | NA | 92.9 *n = 14* | NA | NA |
| Number of CSF cells/mm³: mean (±SD) [range] | 11.3 (±9.3) [0-34] *n = 13* | NA | NA | 5.64 (±7.1) [0-22] *n = 11* | NA | NA |
| Proportion of patients with CSF-specific IgG OCBs or CSF FKLCs (%) | 100 *n=18* | 94.4 *n=18* | NA | 100 | 93.8 | NA |
| Proportion of patients with IgG intrathecal synthesis (%) | 100 *n = 11* | NA | NA | 77.8 *n = 9* | NA | NA |
| % IgG intrathecal synthesis[b]: mean (±SD) | 34.9 (±20.0) *n = 11* | NA | NA | 27.1 (±20.1) *n = 9* | NA | NA |
| Proportion of patients with IgM intrathecal synthesis (%) | 45.5 *n = 11* | NA | NA | 33.3 *n = 9* | NA | NA |
| % IgM intrathecal synthesis[b]: mean (±SD) | 15.4 (± 22.6) *n = 11* | NA | NA | 16.0 (±27.1) *n = 9* | NA | NA |

*Supplementary table 1.2: Diagnoses of infectious and inflammatory neurological disorders*

| | **Diagnosis** | **n** |
|---|---|---|
| **Infect-ND** | Bacterial meningitis (unidentified pathogen) | 2 |
| | Pneumococcal meningitis with subdural empyema | 1 |
| | Presumptive tuberculous meningitis | 1 |
| | Focal meningitis consecutive to otitis media (by H. *influenzae* and S. *pneumoniae*) | 1 |
| | Unspecified meningitis | 2 |
| | HSV meningo-encephalitis | 2 |
| | HIV meningitis | 1 |
| | Progressive Multifocal Leukoencephalopathy | 1 |
| | Viral meningitis and cerebellitis | 1 |
| | Meningo-encephalitis of unknown origin | 1 |
| | Lepto-meningitis of unknown origin | 1 |
| **Inflam-ND** | Neuro-Behçet's disease | 3 |
| | Neurosarcoidosis | 2 |
| | Hashimoto's encephalopathy | 1 |
| | Susac syndrome | 1 |
| | Idiopathic CNS vasculitis | 1 |
| | Primary granulomatous CNS vasculitis | 1 |
| | Post-infectious meningo-encephalitis | 1 |
| | Isolated optical neuritis | 1 |
| | HaNDL syndrome | 1 |

*HaNDL = headache and neurologic deficits with CSF lymphocytosis; HSV = Herpes Simplex Virus; Infect-ND = infectious neurological disorders, Inflam-ND = inflammatory neurological disorders.*

*Supplementary table 1.3: List of miRNAs selected for individual amplification by quantitative PCR in the different cohorts*

| **CSF of MS vs SC** | | **CSF of Infect- & Inflam-ND vs MS vs SC** | | **Serum & PBMCs of MS vs HC** |
|---|---|---|---|---|
| **64 targets** | | **57 targets** | | **24 targets** |
| **Immunological (n=34)** | | **Immunological (n=35)** | | **Immunological (n=18)** |
| let-7a-5p | miR-133b | let-7a-5p | miR-145-5p | let-7e-5p |
| let-7b-5p | miR-145-5p | let-7b-5p | miR-146a-5p | let-7d-5p |
| let-7d-5p | miR-146a-5p | let-7e-5p | miR-150-5p | miR-15a-3p |
| let-7e-5p | miR-150-5p | let-7f-5p | miR-155-5p | miR-16-5p |
| let-7f-5p | miR-155-5p | miR-15a-3p | miR-181a-5p | miR-17-5p |
| miR-15a-3p | miR-181b-5p | miR-15b-5p | miR-181b-5p | miR-20a-5p |
| miR-15b-5p | miR-206 | miR-16-5p | miR-210-3p | miR-24-3p |
| miR-16-5p | miR-210-3p | miR-17-5p | miR-222-3p | miR-29b-3p |
| miR-17-5p | miR-223-3p | miR-20a-5p | miR-223-3p | miR-34c-5p° |
| miR-18b-5p° | miR-326 | miR-22-3p | miR-326 | miR-124-3p |
| miR-20a-5p | miR-342-3p | miR-24-3p | miR-342-3p | miR-126-3p |
| miR-24-3p | miR-423-5p | mir-25-3p | miR-423-5p | miR-145-5p |
| mir-25-3p | miR-96-5p° | miR-29b-3p | let-7d-5p° | miR-146a-5p |
| miR-29b-3p | miR-181c-5p° | miR-34c-5p | let-7i-5p° | miR-150-5p |
| miR-34c-5p | miR-493-3p° | miR-92a-3p | miR-15a-5p° | miR-155-5p |
| miR-92a-3p | miR-599° | miR-124-3p | miR-18b-5p° | miR-181c-5p |
| miR-124-3p° | | miR-126-3p | miR-96-5p° | miR-210-3p |
| miR-126-3p | | miR-133b | | miR-223-3p |
| **Immunological & lipidic (n=11)** | **Lipidic (n=15)** | **Immunological & lipidic (n=8)** | **Lipidic (n=10)** | **Immunological & lipidic (n=3)** |
| miR-19b-3p | miR-33a-3p | miR-21-5p | miR-122-5p | miR-34a-5p |
| miR-21-5p | miR-122-5p | miR-27a-3p | miR-192-5p | miR-142-3p |
| miR-27a-3p | mir-124-5p | miR-27b-3p | miR-297 | miR-214-3p |
| miR-27b-3p | miR-125a-3p° | miR-34a-5p | miR-338-3p | |
| miR-34a-5p | miR-147b° | miR-101-3p | miR-378a-5p | **Lipidic (n=1)** |
| miR-101-3p | miR-149-3p | miR-125b-5p | miR-422b | miR-297 |
| miR-125a-5p | miR-192-5p | miR-142-3p | (= miR-378a-3p) | |
| miR-125b-5p | miR-297 | miR-214-3p | miR-32-5p° | |
| miR-142-3p | miR-338-3p | | miR-33a-5p° | |
| miR-146b-5p | miR-378a-5p | | miR-138-5p° | |
| miR-214-3p | miR-422b | | miR-219a-5p° | |
| | (= miR-378a-3p) | | | |
| | miR-32-5p° | | | |
| | miR-33a-5p° | | | |
| | miR-138-5p° | | | |
| | miR-219a-5p° | | | |
| **Immunological & neuro-degenerative (n=3)** | **Neuro-degenerative (n=1)** | **Immunological & neuro- degenerative (n=3)** | **Neuro-degenerative (n=1)** | **Immunological & neuro-degenerative (n=2)** |
| miR-29a-3p | miR-107 | miR-29a-3p | miR-107 | miR-29c-3p |
| miR-29c-3p | | miR-29c-3p | | miR-191-5p |
| miR-191-5p | | miR-191-5p | | |

*The miRNAs were selected based on the results of the screening arrays or identified from bibliographic search. They are grouped according to their involvement in immunity/inflammation, lipid metabolism or neurodegeneration. MiRNAs that could not be analysed for technical reasons (qPCR melt curve with several peaks, heterogeneous melt curves, low miRNA levels resulting in a flat amplification curve) are indicated by °. HC = healthy controls; Infect-ND = infectious neurological disorders; Inflam-ND = inflammatory neurological disorders; PBMCs = peripheral blood mononuclear cells; SC = symptomatic controls.*

*Supplementary table 1.4: Differentially expressed miRNAs in MS and other inflammatory/infectious neurological disorders*

*Median fold change and statistical significance are listed for miRNAs amplified from CSF, serum and PBMCs of relapsing or remitting MS vs. SC/HC (A) and in the CSF of inflammatory and infectious neurological diseases and relapsing or remitting MS vs. SC (B). Values significant according to Dunn's post-test with (bold) or without (italic) confirmation by Benjamini-Hochberg's correction are shown. qPCR inclusion criteria described in the material and methods section allowed the inclusion of over 90% of CSF samples, over 96% of serum samples and 100% of PBMCs samples in the analysis, except for (A) [1]88.2% and [2]86.4% and for (B) [3]74.7% and [4]81.3%. ND = neurological disorders; PBMCs = peripheral blood mononuclear cells; SC = symptomatic controls*

*Supplementary table 1.4A: Differentially expressed miRNAs in MS*

| A | | Relapsing vs Remitting | | | Relapsing vs Controls | | | Remitting vs Controls | | |
|---|---|---|---|---|---|---|---|---|---|---|
| ID miRNA | ANOVA p-value | Fold change | Dunn's p-value | Adjusted p-value | Fold change | Dunn's p-value | Adjusted p-value | Fold change | Dunn's p-value | Adjusted p-value |
| **CSF** | | | | | | | | | | |
| **miR-15a-3p** | 0,0215 | 1,25 | 0,9779 | 0,9779 | **-2,38** | **0,0071** | **0,0212** | **-2,94** | **0,0330** | **0,0494** |
| **miR-20a-5p** | 0,0077 | **4,03** | **0,0045** | **0,0076** | -1,01 | 0,6242 | 0,6242 | **-4,17** | **0,0051** | **0,0076** |
| **miR-21-5p** | 0,0231 | 1,29 | 0,4872 | 0,4872 | **1,76** | **0,0061** | **0,0182** | 1,37 | 0,1080 | 0,1619 |
| **miR-24-3p** | 0,0484 | **1,90** | **0,0158** | **0,0474** | 1,04 | 0,2764 | 0,2764 | -1,82 | 0,2446 | 0,2764 |
| **miR-27a-3p** | 0,0323 | **1,69** | **0,0092** | **0,0276** | 1,09 | 0,6875 | 0,6875 | -1,56 | 0,0610 | 0,0915 |
| **miR-27b-3p** | 0,0125 | **1,72** | **0,0032** | **0,0095** | 1,15 | 0,3247 | 0,3247 | -1,49 | 0,0892 | 0,1337 |
| **miR-29c-3p** | 0,0359 | **2,29** | **0,0102** | **0,0305** | 1,13 | 0,6645 | 0,6645 | -2,04 | 0,0650 | 0,0975 |
| **miR-33a-3p** | 0,0311 | 2,26 | 0,1047 | 0,1047 | -1,78 | 0,1006 | 0,1047 | **-4,00** | **0,0087** | **0,0260** |
| **miR-34c-5p** | 0,0269 | 1,13 | 0,9096 | 0,9096 | **-3,44** | **0,0108** | **0,0324** | **-3,85** | **0,0305** | **0,0457** |
| **mir-124-5p** | 0,016 | -1,28 | 0,3427 | 0,3427 | **-2,17** | **0,0041** | **0,0124** | -1,23 | 0,1513 | 0,2270 |
| **miR-125b-5p** | 0,0198 | **1,83** | **0,0067** | **0,0202** | 1,49 | 0,1656 | 0,2402 | -1,23 | 0,2402 | 0,2402 |
| **miR-145-5p** | 0,0257 | **2,28** | **0,0070** | **0,0209** | 1,07 | 0,6187 | 0,6187 | -2,13 | 0,0608 | 0,0911 |
| **miR-146a-5p**[1] | 0,0018 | 1,75 | 0,0854 | 0,1281 | **2,04** | **0,0005** | **0,0016** | 1,17 | 0,1519 | 0,1717 |
| **miR-149-3p** | 0,0115 | **-2,00** | **0,0092** | **0,0138** | 1,06 | 0,4114 | 0,4114 | **2,12** | **0,0057** | **0,0138** |
| **miR-150-5p** | <0,0001 | 1,79 | 0,2007 | 0,2007 | **5,41** | **0,0000** | **0,0000** | **3,03** | **0,0116** | **0,0173** |
| **miR-155-5p** | 0,001 | -1,47 | 0,0659 | 0,0659 | **1,94** | **0,0081** | **0,0122** | **2,87** | **0,0002** | **0,0007** |
| **miR-214-3p** | 0,0035 | **1,69** | **0,0175** | **0,0340** | -1,47 | 0,0951 | 0,1225 | **-2,50** | **0,0008** | **0,0063** |
| **miR-297** | 0,0073 | 1,62 | 0,0930 | 0,0930 | **-1,96** | **0,0307** | **0,0460** | **-3,22** | **0,0020** | **0,0060** |
| **SERUM** | | | | | | | | | | |
| **miR-15a-3p** | 0,0175 | -1,11 | 0,9922 | 0,9922 | **-1,69** | **0,0140** | **0,0209** | **-1,54** | **0,0136** | **0,0209** |
| **miR-24-3p** | 0,0099 | 1,14 | 0,4974 | 0,4974 | **-1,75** | **0,0250** | **0,0374** | **-2,00** | **0,0038** | **0,0115** |
| **miR-126-3p** | 0,0069 | 1,14 | 0,8050 | 0,8050 | **-1,47** | **0,0043** | **0,0128** | **-1,69** | **0,0100** | **0,0150** |
| **miR-146a-5p** | 0,0010 | -1,10 | 0,7851 | 0,7851 | **-2,27** | **0,0007** | **0,0022** | **-2,04** | **0,0021** | **0,0032** |
| **miR-181c-5p**[2] | 0,0192 | -1,16 | 0,5588 | 0,5588 | **-3,23** | **0,0074** | **0,0223** | **-2,78** | **0,0326** | **0,0488** |
| **miR-214-3p** | 0,0318 | -1,46 | 0,1093 | 0,1640 | **-1,64** | **0,0093** | **0,0279** | -1,11 | 0,3339 | 0,3339 |
| **PBMCs** | | | | | | | | | | |
| **miR-34a-5p** | 0,0013 | **-1,89** | **0,0003** | **0,0008** | -1,41 | 0,0621 | 0,0931 | 1,32 | 0,1086 | 0,1086 |

*Supplementary table 1.4B: Differentially expressed miRNAs in MS and other inflammatory/infectious neurological disorders*

| B.1 | | Infectious ND vs Inflammatory ND | | | Infectious ND vs Relapsing MS | | | Infectious ND vs Remitting MS | | | Infectious ND vs SC | | | Inflammatory ND vs Relapsing MS | | |
|---|---|---|---|---|---|---|---|---|---|---|---|---|---|---|---|---|
| **ID miRNA** | **ANOVA p-value** | **Fold change** | **Dunn's p-value** | **Adjusted p-value** | **Fold change** | **Dunn's p-value** | **Adjusted p-value** | **Fold change** | **Dunn's p-value** | **Adjusted p-value** | **Fold change** | **Dunn's p-value** | **Adjusted p-value** | **Fold change** | **Dunn's p-value** | **Adjusted p-value** |
| **let-7a-5p** | 0,0019 | 1,72 | 0,0869 | 0,1538 | 1,51 | 0,1077 | 0,1538 | **2,47** | **0,0023** | **0,01132** | **2,16** | **0,0002** | **0,00186** | -1,14 | 0,8450 | 0,8836 |
| **let-7b-5p** | 0,0045 | 2,14 | 0,1699 | 0,2831 | 2,41 | 0,0539 | 0,1348 | *2,29* | *0,0207* | *0,10374* | **2,96** | **0,0002** | **0,00189** | 1,13 | 0,6490 | 0,6490 |
| **let-7e-5p** | 0,0066 | 1,24 | 0,4876 | 0,6095 | 1,24 | 0,3227 | 0,4610 | *2,10* | *0,0176* | *0,07410* | **2,27** | **0,0013** | **0,01301** | 1,00 | 0,7980 | 0,8867 |
| **let-7f-5p** | 0,006 | 1,16 | 0,8269 | 0,8269 | 1,32 | 0,3740 | 0,5342 | 2,56 | 0,0610 | 0,1525 | **2,76** | **0,0016** | **0,01569** | 1,13 | 0,5281 | 0,5868 |
| **miR-15b-5p** | <0,0001 | 2,45 | 0,2053 | 0,2933 | *2,96* | *0,0307* | *0,06144* | **3,80** | **0,0185** | **0,04635** | **8,31** | **0,0000** | **0,00002** | 1,21 | 0,4315 | 0,4795 |
| **miR-16-5p** | 0,0008 | 2,22 | 0,1193 | 0,2241 | 1,92 | 0,1344 | 0,2241 | *3,57* | *0,0157* | *0,05217* | **5,76** | **0,0000** | **0,00038** | -1,15 | 0,8839 | 0,8839 |
| **miR-17-5p** | 0,0147 | 1,59 | 0,4741 | 0,5926 | **3,29** | **0,0092** | **0,04596** | 2,04 | 0,0951 | 0,1902 | **3,12** | **0,0024** | **0,02395** | 2,07 | 0,0764 | 0,1902 |
| **miR-20a-5p**[3] | 0,0067 | 4,84 | 0,0605 | 0,1513 | 2,09 | 0,1611 | 0,3223 | *14,43* | *0,0119* | *0,05937* | **14,42** | **0,0004** | **0,00384** | -2,31 | 0,5717 | 0,6352 |
| **miR-21-5p** | <0,0001 | 3,20 | 0,2286 | 0,3266 | **5,62** | **0,0010** | **0,00330** | **7,07** | **0,0003** | **0,00142** | **6,28** | **0,0000** | **0,00005** | 1,76 | 0,0527 | 0,0879 |
| **miR-22-3p** | 0,0163 | *8,67* | *0,0229* | *0,11468* | 3,62 | 0,0808 | 0,1347 | **14,38** | **0,0009** | **0,00906** | 4,93 | 0,0587 | 0,1347 | -2,39 | 0,4437 | 0,4930 |
| **miR-24-3p** | 0,0008 | *4,50* | *0,0472* | *0,09158* | *4,64* | *0,0168* | *0,05612* | **14,88** | **0,0001** | **0,00076** | **6,15** | **0,0005** | **0,00269** | 1,03 | 0,7553 | 0,7553 |
| **miR-25-3p** | 0,001 | 2,41 | 0,0798 | 0,1585 | *2,92* | *0,0393* | *0,13096* | **5,68** | **0,0011** | **0,00561** | **6,57** | **0,0001** | **0,00088** | 1,21 | 0,8427 | 0,8427 |
| **miR-27a-3p** | 0,0063 | 2,13 | 0,2912 | 0,4160 | **4,90** | **0,0026** | **0,01412** | **4,73** | **0,0042** | **0,01412** | **3,69** | **0,0042** | **0,01412** | 2,30 | 0,0689 | 0,1379 |

| | | | | | | | | | | | | | | | | |
|---|---|---|---|---|---|---|---|---|---|---|---|---|---|---|---|---|
| **miR-27b-3p** | 0,0417 | -1,06 | 0,8956 | 0,8956 | *6,11* | *0,0303* | *0,10348* | *2,99* | *0,0233* | *0,10348* | *2,19* | *0,0493* | *0,10348* | 6,50 | 0,0517 | 0,1035 |
| **miR-29b-3p** | <0,0001 | 2,26 | 0,8830 | 0,8830 | 3,36 | 0,0782 | 0,1304 | *5,58* | *0,0258* | *0,06442* | **16,21** | **0,0000** | **0,00007** | 1,48 | 0,1235 | 0,1765 |
| **miR-29c-3p** | 0,0001 | 2,79 | 0,1858 | 0,2654 | 1,84 | 0,0619 | 0,1237 | **3,72** | **0,0048** | **0,01745** | **7,31** | **0,0000** | **0,00011** | -1,52 | 0,6301 | 0,6301 |
| **miR-92a-3p** | 0,0241 | 1,61 | 0,2168 | 0,4335 | *1,89* | *0,0358* | *0,17913* | 1,87 | 0,0750 | 0,2201 | **2,24** | **0,0012** | **0,01153** | 1,17 | 0,4477 | 0,5596 |
| **miR-125b-5p** | 0,0106 | 1,73 | 0,5982 | 0,6320 | *3,84* | *0,0319* | *0,06750* | **3,01** | **0,0074** | **0,03721** | **3,19** | **0,0041** | **0,03721** | 2,22 | 0,1277 | 0,2128 |
| **miR-142-3p** | <0,0001 | -1,27 | 0,5725 | 0,6361 | *1,95* | *0,0272* | *0,07703* | *5,39* | *0,0308* | *0,07703* | **11,47** | **0,0000** | **0,00014** | 2,47 | 0,1148 | 0,1640 |
| **miR-146a-5p**[4] | 0,0001 | 3,16 | 0,0740 | 0,1234 | *4,47* | *0,0206* | *0,05324* | *3,69* | *0,0182* | *0,05324* | **10,34** | **0,0000** | **0,00002** | 1,41 | 0,6988 | 0,7764 |
| **miR-150-5p** | <0,0001 | 8,10 | 0,1990 | 0,2842 | *14,03* | *0,0380* | *0,06333* | **28,64** | **0,0184** | **0,03689** | **86,82** | **0,0000** | **0,00000** | 1,73 | 0,4824 | 0,5360 |
| **miR-181b-5p** | 0,0115 | 2,44 | 0,2004 | 0,2552 | 2,44 | 0,1185 | 0,2370 | **3,73** | **0,0090** | **0,04515** | **3,80** | **0,0011** | **0,01057** | 1,00 | 0,8435 | 0,9372 |
| **miR-191-5p** | 0,0275 | 1,02 | 0,8328 | 0,9099 | 1,37 | 0,1054 | 0,2109 | *1,91* | *0,0424* | *0,14121* | *2,32* | *0,0067* | *0,06718* | 1,35 | 0,1806 | 0,3009 |
| **miR-223-3p** | 0,0001 | 1,83 | 0,5104 | 0,5672 | *3,94* | *0,0379* | *0,07588* | **5,81** | **0,0046** | **0,01545** | **6,86** | **0,0000** | **0,00025** | 2,15 | 0,1859 | 0,2655 |
| **miR-297** | 0,033 | -1,20 | 0,7353 | 0,7910 | *2,28* | *0,0326* | *0,08500* | 2,53 | 0,1783 | 0,2972 | *1,84* | *0,0340* | *0,08500* | *2,73* | *0,0167* | *0,08334* |
| **miR-342-3p** | 0,0002 | 3,24 | 0,1737 | 0,2481 | **5,24** | **0,0126** | **0,03146** | **6,82** | **0,0072** | **0,02394** | **8,69** | **0,0000** | **0,00007** | 1,62 | 0,3005 | 0,3406 |
| **miR-423-5p** | 0,0003 | 1,72 | 0,0942 | 0,1569 | **2,13** | **0,0133** | **0,04430** | **2,15** | **0,0055** | **0,02749** | **3,91** | **0,0000** | **0,00010** | 1,24 | 0,4994 | 0,5280 |

| B.2 | | Inflammatory ND vs Remitting MS | | | Inflammatory ND vs SC | | | Relapsing MS vs Remitting MS | | | Relapsing MS vs SC | | | Remitting MS vs SC | | |
|---|---|---|---|---|---|---|---|---|---|---|---|---|---|---|---|---|
| **ID miRNA** | **ANOVA p-value** | **Fold change** | **Dunn's p-value** | **Adjusted p-value** | **Fold change** | **Dunn's p-value** | **Adjusted p-value** | **Fold change** | **Dunn's p-value** | **Adjusted p-value** | **Fold change** | **Dunn's p-value** | **Adjusted p-value** | **Fold change** | **Dunn's p-value** | **Adjusted p-value** |
| **let-7a-5p** | 0,0019 | 1,44 | 0,1525 | 0,1906 | 1,26 | 0,1021 | 0,1538 | 1,64 | 0,0937 | 0,1538 | *1,43* | *0,0467* | *0,15381* | -1,14 | 0,8836 | 0,8836 |
| **let-7b-5p** | 0,0045 | 1,07 | 0,3096 | 0,4423 | *1,39* | *0,0443* | *0,13480* | -1,05 | 0,5192 | 0,5769 | 1,23 | 0,1045 | 0,2091 | 1,29 | 0,5062 | 0,5769 |
| **let-7e-5p** | 0,0066 | 1,69 | 0,0877 | 0,1753 | *1,83* | *0,0222* | *0,07410* | 1,69 | 0,1256 | 0,2094 | *1,83* | *0,0353* | *0,08837* | 1,08 | 0,9436 | 0,9436 |
| **let-7f-5p** | 0,006 | 2,20 | 0,1052 | 0,2104 | **2,37** | **0,0058** | **0,02888** | 1,95 | 0,2649 | 0,4415 | *2,10* | *0,0264* | *0,08809* | 1,08 | 0,5120 | 0,5868 |
| **miR-15b-5p** | <0,0001 | 1,55 | 0,2496 | 0,3120 | **3,40** | **0,0020** | **0,00996** | 1,28 | 0,6300 | 0,6300 | **2,81** | **0,0166** | **0,04635** | 2,19 | 0,1343 | 0,2239 |
| **miR-16-5p** | 0,0008 | 1,61 | 0,3411 | 0,4068 | *2,60* | *0,0288* | *0,07192* | 1,85 | 0,2585 | 0,3693 | *2,99* | *0,0117* | *0,05217* | 1,62 | 0,3661 | 0,4068 |
| **miR-17-5p** | 0,0147 | 1,28 | 0,3278 | 0,5464 | *1,96* | *0,0371* | *0,12379* | -1,61 | 0,5454 | 0,6060 | -1,06 | 0,8890 | 0,8890 | 1,53 | 0,4395 | 0,5926 |
| **miR-20a-5p**[3] | 0,0067 | 2,98 | 0,5347 | 0,6352 | 2,98 | 0,2264 | 0,3235 | 6,90 | 0,2225 | 0,3235 | *6,89* | *0,0448* | *0,14943* | 1,00 | 0,6437 | 0,6437 |
| **miR-21-5p** | <0,0001 | **2,21** | **0,0146** | **0,02917** | **1,97** | **0,0029** | **0,00732** | 1,26 | 0,4383 | 0,4870 | 1,12 | 0,3671 | 0,4588 | -1,13 | 0,9339 | 0,9339 |
| **miR-22-3p** | 0,0163 | 1,66 | 0,3442 | 0,4917 | -1,76 | 0,4108 | 0,4930 | 3,97 | 0,0682 | 0,1347 | 1,36 | 0,9941 | 0,9941 | -2,92 | 0,0512 | 0,1347 |
| **miR-24-3p** | 0,0008 | *3,31* | *0,0330* | *0,08247* | 1,37 | 0,2704 | 0,3380 | 3,21 | 0,0549 | 0,0916 | 1,33 | 0,4259 | 0,4732 | -2,42 | 0,1571 | 0,2245 |
| **miR-25-3p** | 0,001 | 2,35 | 0,1109 | 0,1585 | 2,72 | 0,0774 | 0,1585 | 1,95 | 0,1376 | 0,1720 | 2,25 | 0,0962 | 0,1585 | 1,16 | 0,8313 | 0,8427 |
| **miR-27a-3p** | 0,0063 | 2,22 | 0,0664 | 0,1379 | 1,73 | 0,1245 | 0,2075 | -1,04 | 0,8033 | 0,8033 | -1,33 | 0,6136 | 0,6818 | -1,28 | 0,4874 | 0,6093 |
| **miR-27b-3p** | 0,0417 | *3,18* | *0,0374* | *0,10348* | 2,33 | 0,0843 | 0,1406 | -2,04 | 0,6965 | 0,7739 | -2,79 | 0,6759 | 0,7739 | -1,37 | 0,4406 | 0,6295 |

| | | | | | | | | | | | | | | | | |
|---|---|---|---|---|---|---|---|---|---|---|---|---|---|---|---|---|
| **miR-29b-3p** | <0,0001 | *2,46* | *0,0425* | *0,08491* | **7,16** | **0,0000** | **0,00021** | 1,66 | 0,4794 | 0,5326 | **4,82** | **0,0098** | **0,03264** | 2,91 | 0,1606 | 0,2008 |
| **miR-29c-3p** | 0,0001 | 1,33 | 0,1055 | 0,1758 | **2,62** | **0,0052** | **0,01745** | 2,02 | 0,2151 | 0,2689 | **3,97** | **0,0177** | **0,04422** | 1,97 | 0,5430 | 0,6034 |
| **miR-92a-3p** | 0,0241 | 1,16 | 0,5333 | 0,5926 | 1,39 | 0,0880 | 0,2201 | -1,01 | 0,9633 | 0,9634 | 1,19 | 0,3504 | 0,5596 | 1,20 | 0,4040 | 0,5596 |
| **miR-125b-5p** | 0,0106 | *1,74* | *0,0337* | *0,06750* | *1,84* | *0,0327* | *0,06750* | -1,27 | 0,4116 | 0,5880 | -1,21 | 0,6242 | 0,6320 | 1,06 | 0,6320 | 0,6320 |
| **miR-142-3p** | <0,0001 | 6,84 | 0,1071 | 0,1640 | **14,57** | **0,0003** | **0,00164** | 2,77 | 0,8130 | 0,8130 | *5,90* | *0,0462* | *0,09243* | 2,13 | 0,1561 | 0,1951 |
| **miR-146a-5p**[4] | 0,0001 | 1,17 | 0,5549 | 0,6936 | *3,27* | *0,0213* | *0,05324* | -1,21 | 0,8079 | 0,8079 | *2,31* | *0,0455* | *0,09093* | 2,80 | 0,1260 | 0,1800 |
| **miR-150-5p** | <0,0001 | 3,54 | 0,2496 | 0,3120 | **10,72** | **0,0000** | **0,00014** | 2,04 | 0,5763 | 0,5763 | **6,19** | **0,0002** | **0,00082** | **3,03** | **0,0133** | **0,03327** |
| **miR-181b-5p** | 0,0115 | 1,53 | 0,1653 | 0,2552 | 1,56 | 0,0932 | 0,2370 | 1,53 | 0,2042 | 0,2552 | 1,56 | 0,1162 | 0,2370 | 1,02 | 0,9542 | 0,9542 |
| **miR-191-5p** | 0,0275 | 1,88 | 0,0753 | 0,1883 | *2,28* | *0,0191* | *0,09558* | 1,39 | 0,5287 | 0,6609 | 1,69 | 0,3465 | 0,4949 | 1,21 | 0,9099 | 0,9099 |
| **miR-223-3p** | 0,0001 | *3,17* | *0,0311* | *0,07588* | **3,75** | **0,0011** | **0,00545** | 1,47 | 0,2984 | 0,3730 | 1,74 | 0,0520 | 0,0866 | 1,18 | 0,6136 | 0,6136 |
| **miR-297** | 0,033 | 3,03 | 0,1083 | 0,2167 | *2,20* | *0,0167* | *0,08334* | 1,11 | 0,6031 | 0,7910 | -1,24 | 0,7910 | 0,7910 | -1,38 | 0,7329 | 0,7910 |
| **miR-342-3p** | 0,0002 | 2,11 | 0,1589 | 0,2481 | **2,69** | **0,0043** | **0,02130** | 1,30 | 0,6015 | 0,6015 | 1,66 | 0,0620 | 0,1241 | 1,27 | 0,3065 | 0,3406 |
| **miR-423-5p** | 0,0003 | 1,25 | 0,2314 | 0,3306 | **2,27** | **0,0190** | **0,04749** | 1,01 | 0,5280 | 0,5280 | 1,83 | 0,0846 | 0,1569 | 1,82 | 0,4403 | 0,5280 |

*Supplementary table 1.5: Strength of individual variables in representing population variability in the principal component analysis*

| **A** | $Cos^2$ | | **B** | $Cos^2$ | |
|---|---|---|---|---|---|
| | Dimension 1 | Dimension 2 | | Dimension 1 | Dimension 2 |
| Cells/$mm^3$ | 0.088 | 0.113 | miR-20a-5p | **0.546** | 0.006 |
| IgG IF | 0.133 | **0.507** | miR-24-3p | **0.896** | 0.006 |
| IgM IF | 0.020 | **0.742** | miR-145-5p | **0.821** | 0.001 |
| miR-146a-5p | **0.862** | 0.008 | miR-29c-3p | 0.031 | **0.719** |
| miR-150-5p | **0.755** | 0.050 | miR-214-3p | 0.036 | **0.712** |
| miR-155-5p | **0.569** | 0.000 | miR-27a-3p | **0.884** | 0.006 |
| miR-149-3p | 0.242 | 0.033 | miR-27b-3p | **0.752** | 0.011 |
| miR-21-5p | **0.566** | 0.021 | | | |

*(A) PCA was applied between MS and controls, using the significantly upregulated CSF miRNAs in MS subjects and other quantitative CSF parameters (IgG or IgM IF, CSF pleocytosis). (B) PCA was also applied using differentially expressed miRNAs between relapsing and remitting MS patients. $Cos^2$ values, representing the strength of the individual variables in indicating population variability according to each dimension, are shown (see figure 1.4). Significant $cos^2$ values (>0.5) are indicated in bold. IF = intrathecal fractions; PCA = principal component analysis.*

*Supplementary table 1.6: Pathway enrichment analysis for differentially expressed miRNAs in all biological compartments associated to MS*

*This table shows the most commonly targeted KEGG pathways and genes by the miRNAs reaching statistical significance among the different groups and biological compartments. Up- and down-regulated miRNAs were grouped as sets according to the biological compartment and the disease category. These miRNA sets were then introduced into two databases, namely miRNet and mirPath. Only KEGG pathways significant in both databases for at least two miRNA sets have been selected (top part of the table). MiRNAs identified by both databases are shown in the middle part of the table, miRNAs common in at least two miRNA sets are indicated by 'X', those appearing in only one miRNA set by 'o'. Genes from top enriched canonical pathways identified by both databases and targeted at least (i) by two miRNAs, (ii) in one database and (iii) in two miRNA sets are shown in the lower part of the table. Genes have been ranked from top to bottom based on the number of miRNAs targeting them in both databases. Genes indicated in bold are common to four or five pathways. KEGG = Kyoto Encyclopaedia of Genes and Genomes, MS = multiple sclerosis, PBMCs = peripheral blood mononuclear cells, Rel = relapsing MS, Rem = remitting MS.*

| KEGG pathways | | Cell cycle | ErbB signalling | mTOR signalling | Insulin signalling | p53 signalling | TGFβ signalling | Adherens junction | Endocytosis | Neurotrophin signalling | Chronic Myeloid Leukaemia | Glioma |
|---|---|---|---|---|---|---|---|---|---|---|---|---|
| **miRNA sets** | | | | | | | | | | | | |
| CSF | Up Rel MS | X | X | X | X | X | X | X | | X | X | X |
| | Down Rem MS | X | X | X | X | X | X | X | X | X | X | X |
| | Down Rel MS | | | | | | | | | | | X |
| Serum | Down Rel MS | X | X | | | | | | X | | X | X |
| | Down Rem MS | X | X | | | | | | X | | X | X |
| PBMCs | Down Rel MS | | | | | X | | X | | | X | X |
| **miRNAs** | | | | | | | | | | | | |
| hsa-miR-20a-5p | | X | X | X | o | X | X | o | o | o | X | X |
| hsa-miR-21-5p | | o | o | o | | o | o | | | | o | o |
| hsa-miR-24-3p | | X | o | | | o | o | o | X | | X | o |
| hsa-miR-27a-3p | | o | o | o | X | o | X | o | | o | o | o |
| hsa-miR-27b-3p | | o | | o | | | o | | | o | o | o |
| hsa-miR-29c-3p | | | | o | | | | | | o | X | o |
| *hsa-miR-33a-3p°* | | | | | | | | o | | | | |
| *hsa-miR-34a-5p°* | | o | | | | o | | o | | | o | o |
| *hsa-miR-34c-5p°* | | | | | | | | | | | | o |
| hsa-miR-125b-5p | | o | X | o | o | o | | o | | o | o | o |
| hsa-miR-126-3p | | | | | | | | | | | X | X |
| hsa-miR-145-5p | | | o | | | | | o | | | | o |
| hsa-miR-146a-5p | | X | X | | | | | | | o | | |
| *hsa-miR-150-5p°* | | | | o | | | | | | | | |

| | | | | | | | | | | | |
|---|---|---|---|---|---|---|---|---|---|---|---|
| *hsa-miR-155-5p°* | o | | o | o | | o | o | | | | |
| hsa-miR-181c-5p | | | | | | | | | | | X |
| hsa-miR-214-3p | | | | | X | | | o | X | o | |
| **Targeted genes** | | | | | | | | | | | |
| | **MYC** | **MYC** | VEGFA | MKNK2 | **TP53** | **MYC** | CTNND1 | **TP53** | **TP53** | **TP53** | |
| | **TP53** | NRAS | HIF1A | FOXO1 | PTEN | BMPR2 | EGFR | BCL2 | **MYC** | **CDK6** | |
| | E2F3 | **CDKN1A** | RPS6KA3 | GSK3B | THBS1 | TGFBR2 | SMAD2 | | E2F3 | E2F1 | |
| | **CDK6** | ERBB3 | | PRKAR1A | **CDK6** | THBS1 | **SMAD4** | | **CDK6** | NRAS | |
| | E2F1 | EGFR | | | SESN1 | **SMAD4** | CTNNB1 | | E2F1 | PTEN | |
| | **SMAD4** | AKT1 | | | **CCND1** | SP1 | SSX2IP | | TGFBR2 | E2F3 | |
| | E2F2 | CDKN1B | | | CCNG1 | TGFBR1 | | | NRAS | **CCND1** | |
| | CCNA2 | | | | **CDKN1A** | SMAD2 | | | E2F2 | MDM2 | |
| | **CCND1** | | | | RRM2 | ID4 | | | RUNX1 | **CDKN1A** | |
| | CDKN2A | | | | MDM4 | SMAD5 | | | **CDKN1A** | EGFR | |
| | WEE1 | | | | CCNB1 | | | | MAPK1 | CDK4 | |
| | CDK4 | | | | | | | | **CCND1** | AKT1 | |
| | **CDKN1A** | | | | | | | | TGFBR1 | KRAS | |
| | GSK3B | | | | | | | | CDKN2A | PIK3R1 | |
| | CCNB1 | | | | | | | | **SMAD4** | | |
| | SMAD2 | | | | | | | | CDK4 | | |
| | YWHAZ | | | | | | | | NFKBIA | | |
| | CDKN1B | | | | | | | | AKT1 | | |
| | TGFB1 | | | | | | | | CDKN1B | | |
| | | | | | | | | | CRKL | | |
| | | | | | | | | | NFKBIA | | |
| | | | | | | | | | TGFB1 | | |

# CHAPTER 2: MICRORNAS ARE DYSREGULATED IN PERIPHERAL BLOOD MONONUCLEAR CELLS IN MULTIPLE SCLEROSIS AND CORRELATE WITH T CELL MEDIATORS

Océane Perdaens, Vincent van Pesch

*Journal of Neuroimmunology, 2023, 578196*

We then aimed to verify in PBMCs of a different MS patient cohort, whether disease activity based on brain MRI and/or treatment status (untreated/interferon beta/glatiramer acetate) could affect the expression of promising microRNAs identified in the first screening as compared to healthy controls. Hereafter, we first focused on the inflammatory aspect by exploring the correlation of the expression of microRNAs and of T cell mediator mRNAs and by confronting their prediction as a microRNA target to their expression and correlation profiles.

*Figure 2.1: Graphical abstract*

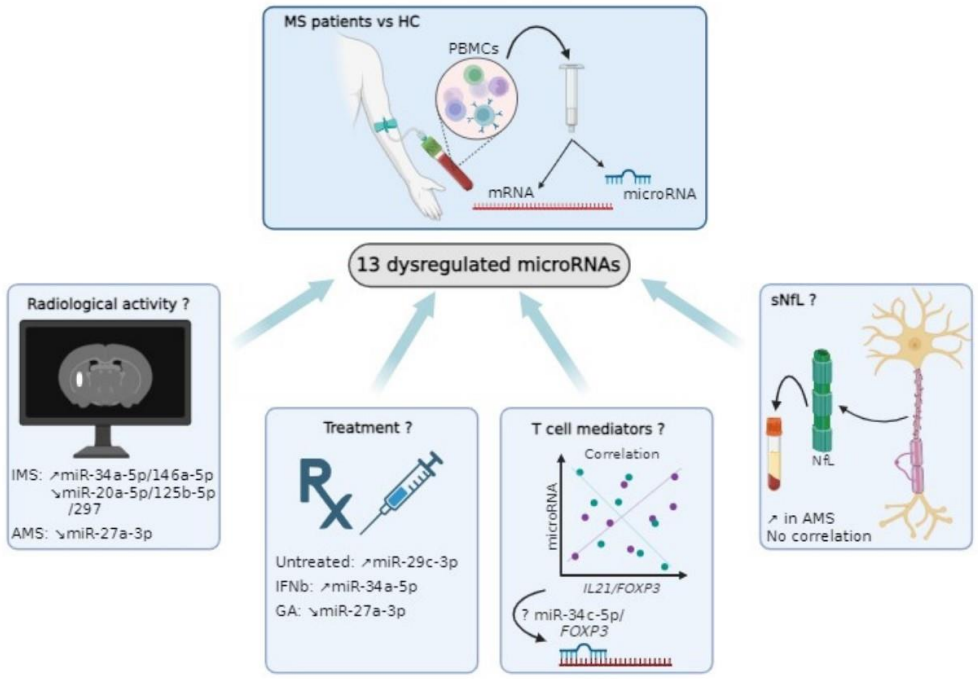


*We aimed to investigate the expression of microRNAs and mRNAs of T cell mediators in PBMCs of MS patients and controls and whether they were differentially expressed depending on disease activity status, determined on brain MRI, or treatment status (none, IFNb, GA). We further showed a positive or negative correlation between several microRNAs and IL21 and/or FOXP3. In silico analysis consistently predicted the interaction of miR-34c-5p and FOXP3, but most of the other (mainly positive) correlations rather suggest an indirect targeting of a T cell mediator by a microRNA. Finally, neurofilament light chain (sNfL) levels were upregulated in the serum of active MS patients, but did not correlate with any*

*microRNA or T cell mediator. AMS = active multiple sclerosis, GA = glatiramer acetate, HC = healthy controls, IFNb = interferon beta therapy, IMS = inactive multiple sclerosis, miR = microRNA, MS = multiple sclerosis, PBMCs = peripheral blood mononuclear cells, sNfL = serum neurofilament light chain, ↗ = upregulation/increased levels, ↘ = downregulation. Created in BioRender.com*

## I. Abstract

T cell mediators and microRNAs are involved in the pathogenesis of multiple sclerosis (MS), but their interaction largely remains undetermined. We investigated by RT-qPCR the dysregulation of microRNAs in peripheral blood mononuclear cells of MS patients versus healthy controls, according to radiological disease activity or treatment. Several microRNAs correlated positively/negatively with *IL21*/*FOXP3* mRNA expression, but not with serum neurofilament light chain levels. Cytokine expression is conceivably balanced by several regulators, whereas microRNAs possibly target upstream transcription factors rather than directly cytokine mRNAs. Functional studies are needed to investigate their interaction, notably for the predicted targeting of *FOXP3* by miR-34c-5p.

## II. Introduction

Multiple sclerosis (MS), a chronic inflammatory disorder of the central nervous system (CNS), is characterised by acute demyelination, and concomitant neurodegeneration. Although the role of the immune system in its pathophysiology is indisputable, the elementary mechanisms and triggers underlying it are only partially elucidated [21].

Both pro-inflammatory T helper (Th) 1 cells induced by interleukin (IL)12, a heterodimer of IL12p35 and IL12p40, and Th17 cells, induced by IL23, a heterodimer of IL23p19 and IL12p40, play an important role in acute MS-related inflammatory disease activity [931]. On the other hand, forkhead box (FOX) P3-expressing regulatory T cells (Treg) are functionally impaired in MS [932], leading to an imbalance of the immune system favouring pro-inflammatory processes.

MicroRNAs are small non-coding RNAs of 18 to 22 nucleotides. They are recognised players in immune cell fating by directly or indirectly inhibiting the expression of transcription factors or cytokines, or by being themselves directed by these proteins [933]. Several microRNAs are dysregulated in MS, whether it be in brain lesions, cerebrospinal fluid (CSF), serum or plasma, peripheral blood mononuclear cells (PBMCs), or in specific cell subtypes. Some microRNAs are proposed as biomarkers predicting or confirming the response to a disease modifying treatment, as for interferon beta (IFNb) or glatiramer acetate (GA) [751,753]. The role of microRNAs on the expression of cytokines, that are important in the acute neuroinflammatory events occurring in MS, is, however, largely unknown. We aimed to analyse the expression of microRNAs, of cytokines and transcription factors participating in Th and Treg cell activation and differentiation and of the markers of IFNb response in PBMCs of MS patients either treated (IFNb or GA) or untreated and according to disease activity on brain magnetic resonance imaging (MRI), compared to healthy controls (HC). In parallel, serum neurofilament light chain (sNfL) levels were measured. We then investigated the possible correlation between the expression of microRNAs and T cell mediators as well as sNfL levels in MS patients and HC.

## III. Methods

### i. Patients

Blood and serum samples of MS patients and HC were collected at the Cliniques universitaires Saint-Luc (Brussels, Belgium). PBMCs were isolated by Ficoll-Paque PLUS (GE Healthcare) density gradient centrifugation within one hour and stored in Qiazol at −80°C until RNA/microRNA extraction. MS diagnosis was revised with the 2017 McDonald criteria [29].

Patients were enrolled during a regular outpatient visit at the neurology department, after signing informed consent (ethical approval 2007/31AOUT/222). They were classified according to disease activity based on the presence of gadolinium-enhancing lesions on brain MRI [24], performed concomitantly to blood sampling. None of the patients were clinically in relapse. Patients were either

untreated or treated with IFNb or GA, and had no concomitant infection. The subjects' characteristics are summarised in figure 2.2.

*Figure 2.2: Study population characteristics*

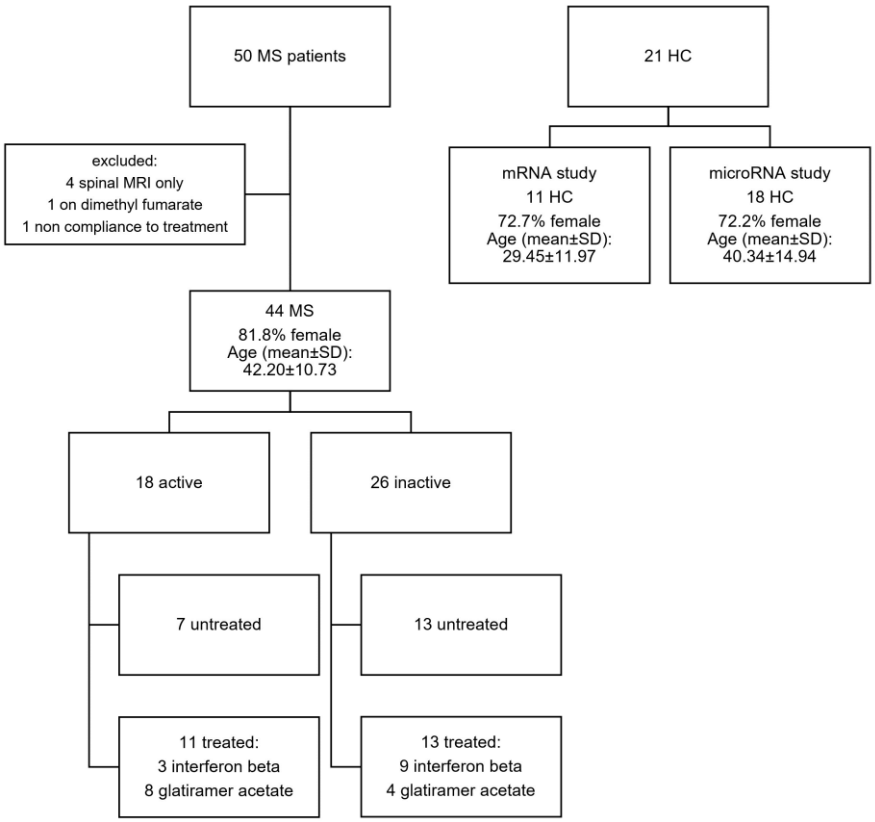


*This chart shows the subjects' characteristics (age and sex distribution) as well as the subdivision of MS patients according to disease activity (based on the presence of gadolinium-enhancing lesions on brain MRI), and treatment. HC = healthy controls, MS = multiple sclerosis, SD = standard deviation*

ii. mRNA and microRNA extraction, reverse transcription, preamplification, and real time quantitative polymerase chain reaction (RT-qPCR)

Messenger RNAs (mRNAs) and microRNAs were isolated separately from 11-13.$10^6$ PBMCs using the miRNeasy Mini Kit, following the manufacturer's protocol (Qiagen). Extracted mRNAs and microRNAs were stored at -80°C until reverse transcription (RT). Total mRNA was quantified with Qubit and reverse transcribed using SuperScript™ III Reverse Transcriptase (Invitrogen). ABsolute qPCR SYBR Green Mix (ThermoScientific) was used for RT-qPCR. Primers are listed in supplementary table 2.1 (IL12p35, IL12p40, IL17A, IL21, IL22, IL23p19, FOXP3, TGFB1, IL10, IL27p28, MXA, JAK2).

MicroRNAs were reverse transcribed using the miScript II RT Kit (Qiagen). For the complementary DNA preamplification and the RT-qPCRs we used the miScript PreAmp PCR Kit and the miScript SYBR® Green PCR Kit (Qiagen) respectively with the miScript Primer Assays (Qiagen, see supplementary table 1: miR-15a-3p, miR-20a-5p, miR-21-5p, miR-24-3p, miR-27a-3p, miR-27b-3p, miR-29c-3p, miR-33a-3p, miR-34a-5p, miR-34c-5p, miR-124-5p, miR-125b-5p, miR-126-3p, miR-145-5p, miR-146a-5p, miR-149-3p, miR-150-5p, miR-155-5p, miR-181c-5p, miR-214-3p, miR-297) following the manufacturer's recommendations. The microRNAs were selected based on their differential expression within the CSF, serum or PBMCs of relapsing-remitting MS patients in our previous study [892]. All PCRs were performed on Rotor-Gene Q (Qiagen).

iii. RT-qPCR analysis

All samples were run in duplicates and the specificity was verified with the melt curves. The mRNA transcripts were normalised to Abelson gene (ABL) and their relative expression was determined by the $2^{-\Delta\Delta Ct}$ method (with $\Delta\Delta Ct = \Delta Ct$ [target mRNA-ABL]$_{sample}$ − mean $\Delta Ct$ [target mRNA-ABL]$_{HC}$) [909]. Cycle thresholds (Cts) of ABL were within a close range for all samples. The microRNA transcripts were normalised by the global mean method ($\Delta Ct$ = Ct [target microRNA]$_{sample}$ – mean Cts [all target microRNAs]$_{sample}$) [934]. The fold change was calculated as $2^{-\Delta(\Delta)Ct}{}_{target,sample}$ / median of $2^{-\Delta(\Delta)Ct}{}_{target,HC}$.

iv. In silico analysis

We searched in six databases whether the investigated microRNAs were predicted to target the T cell mediator mRNAs of this study:

miRNet (https://www.mirnet.ca/),
miRDB (http://www.mirdb.org/index.html),
RNA22 (https://cm.jefferson.edu/rna22/Precomputed),
DIANA-microT-CDS (http://www.microrna.gr/microT-CDS),
miRWalk 3 (http://mirwalk.umm.uni-heidelberg.de/), and
miRMAP (https://mirmap.ezlab.org/app/) [935–940].

v. Serum neurofilament light chain

sNfL levels were measured in duplicate using the highly sensitive immunoassay Single Molecule Array technology (NF-LIGHT™ (SR-X version), SIMOA®, Quanterix) following the manufacturer's protocol.

vi. Statistical analysis

We used GraphPad Prism 5.0 for all statistical analyses on the relative mRNA ($2^{-\Delta\Delta Ct}$) and microRNA (ΔCt) expression levels: a nonparametric one-way analysis of variance (ANOVA) Kruskal-Wallis test, followed by a Dunn's multiple comparison post-test, across subgroups; a Mann-Whitney t-test (MW t-test) between MS and HC, as well as a nonparametric Spearman's correlation test. P values were corrected by the Benjamini-Hochberg false discovery rate (FDR) method (https://tools.carbocation.com/FDR) and considered significant if the adjusted p-value (adj.p) was ≤ 0.05 following correction. Principal component analysis (PCA) on the relative expression levels (-ΔCt) of microRNAs of MS patients and HC as continuous variables was performed in R using the *FactoMineR* package. Results were plotted using the *factoextra* package. Heatmaps, correlogram and linear regression were also built in R using the packages *pheatmap, corrplot, Hmisc* and *ggplot2* (https://cran.r-project.org/).

## IV. Results

### i. FOXP3 and JAK2 mRNA are differentially expressed in PBMCs of MS patients

*Figure 2.3: Relative mRNA expression of T cell mediators and IFNb markers in PBMCs of MS patients and HC (activity)*

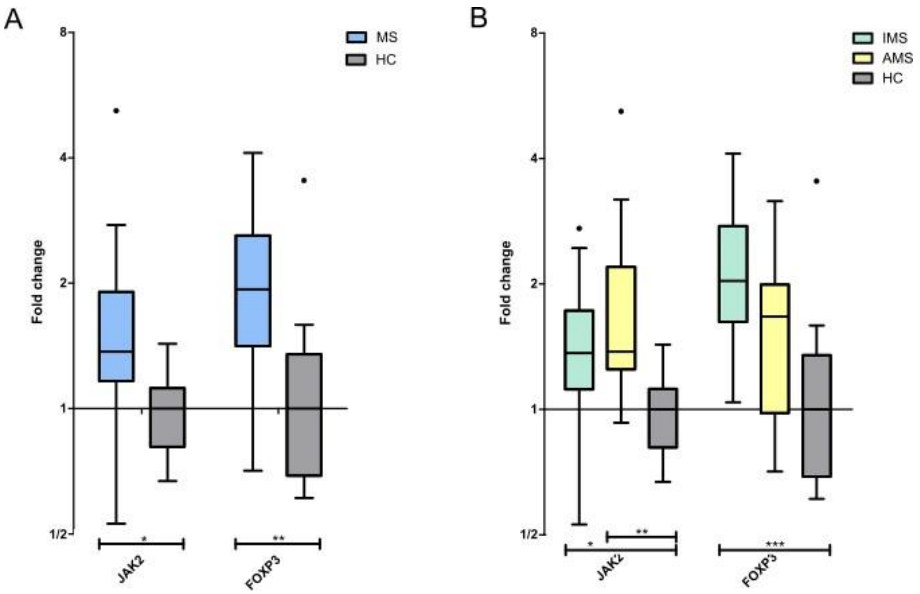


*The box plots, following the Tukey method, show the fold change ($2^{-\Delta\Delta Ct}_{target,sample}$ / median of $2^{-\Delta\Delta Ct}_{target,HC}$) between the relative expression of the significantly dysregulated mRNAs of interest of this study and their median relative expression in HC for (A) MS patients vs HC and (B) IMS and AMS patients vs HC. The y-axis is log2-scaled. Statistical significance was determined by (A) a Mann-Whitney t-test and (B) a one-way ANOVA Kruskal-Wallis test followed by a Dunn's post-test in between the subgroups. The p-values of the t-test and the one-way ANOVA have been corrected by the Benjamini-Hochberg method. p≤0.05: *; p≤0.01: **; p≤0.001: ***. AMS = active multiple sclerosis, HC = healthy controls, IMS = inactive multiple sclerosis, MS = multiple sclerosis.*

We first aimed to explore the differential mRNA expression of markers of T cell activity (cytokines and transcription factors) and of IFNb response in PBMCs of MS patients and HC. *FOXP3* was significantly upregulated in PBMCs of MS patients compared to HC, in particular in inactive MS (IMS) (figure 2.3, supplementary table 2.2), but independently of treatment status (data not shown). Janus kinase *(JAK2)*

was significantly upregulated in MS patients, to the same extent in both active (AMS) and IMS.

*Figure 2.4: Relative mRNA expression of T cell mediators and IFNb markers in PBMCs of MS patients and HC (treatment)*

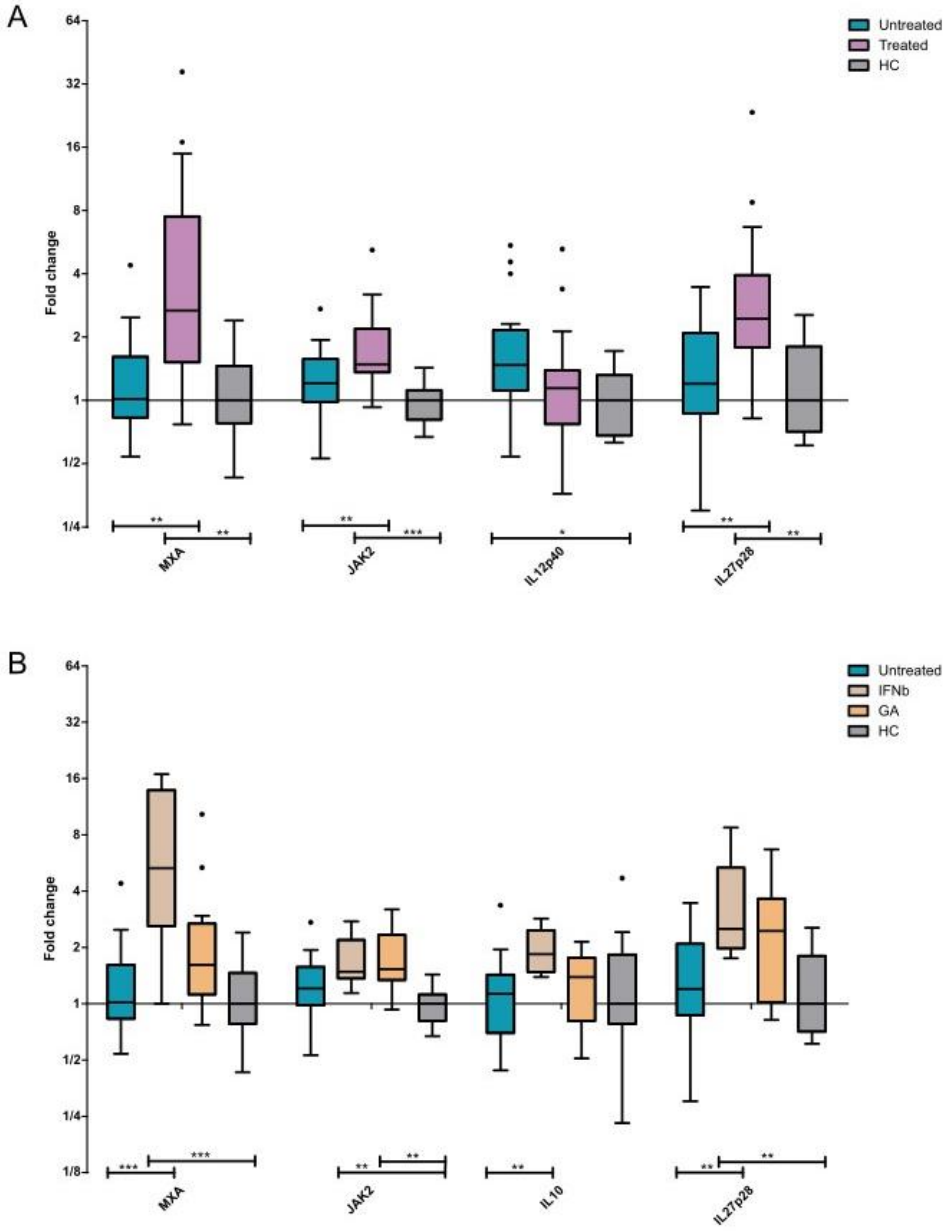

*The box plots, following the Tukey method, show the fold change ($2^{-\Delta\Delta Ct}_{target,sample}$ / median of $2^{-\Delta\Delta Ct}_{target,HC}$) between the relative expression of the significantly dysregulated mRNAs of interest of this study and their median relative expression in HC for (A) untreated and treated MS patients vs HC and (B) untreated, IFNb- and GA-treated MS patients vs HC. The y-axis is log2-scaled. Statistical significance was determined by a one-way ANOVA Kruskal-Wallis test followed by a Dunn's post-test in between the subgroups. The p-values of the one-way ANOVA have been corrected by the Benjamini-Hochberg method. p≤0.05: *; p≤0.01: **; p≤0.001: ***., GA = glatiramer acetate, HC = healthy controls, IFNb = interferon beta.*

The mRNAs of the interferon-induced antiviral protein, human myxovirus resistance protein 1 (*MXA),* as well as of *IL10* and *IL27p28* were significantly upregulated in IFNb-treated patients compared to untreated patients and/or HC (figure 2.4B, supplementary table 2.2). *JAK2* was the only marker increased in both IFNb- and GA-treated patients as compared to HC. Conversely *IL12p40* was significantly upregulated in untreated patients versus (vs) HC (figure 2.4A). These markers were, however, not affected by disease activity (data not shown).

ii. MicroRNAs are differentially expressed in PBMCs of MS patients

We quantified 21 microRNAs, previously found dysregulated in the CSF, serum or PBMCs of relapsing and/or remitting MS patients [892]. Of these, miR-15a-3p/20a-5p/27a-3p/34c-5p/125b-5p/181c-5p/297 were significantly downregulated in MS vs HC, and miR-21-5p/29c-3p/34a-5p/146a-5p/150-5p/155-5p were upregulated (figure 2.5A). This differential expression was independent of disease activity for miR-21-5p/34c-5p/155-5p/181c-5p, while it was more strongly directed by IMS than AMS for the other microRNAs, except for miR-27a-3p (figure 2.5B, supplementary table 2.3). Interestingly, up- and downregulated microRNAs consistently correlated with each other (figure 2.5C).

*Figure 2.5: Relative microRNA expression in PBMCs of MS patients and HC (activity)*

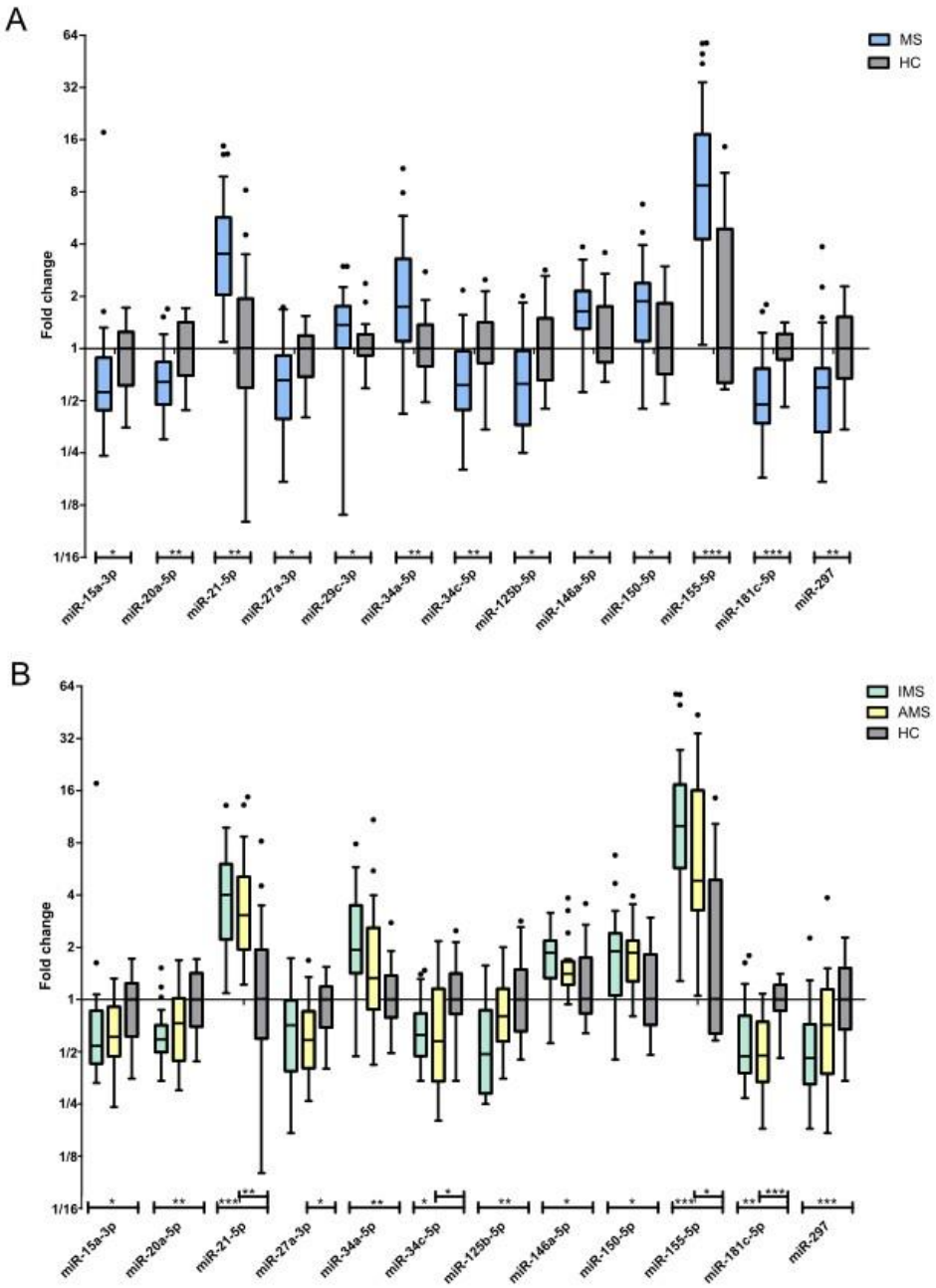

C

| Spearman r / p-value | | Downregulated | | | | | | | Upregulated | | | | | |
|---|---|---|---|---|---|---|---|---|---|---|---|---|---|---|
| | | miR-15a-3p | miR-20a-5p | miR-27a-3p | miR-34c-5p | miR-125b-5p | miR-181c-5p | miR-297 | miR-21-5p | miR-29c-3p | miR-34a-5p | miR-146a-5p | miR-150-5p | miR-155-5p |
| Downregulated | miR-15a-3p | | 0.3035 | | 0.4972 | 0.3215 | 0.2628 | 0.4589 | -0.5129 | -0.3011 | -0.5242 | -0.4804 | | -0.5084 |
| | miR-20a-5p | 0.0165 | | 0.7073 | 0.4887 | 0.3945 | 0.5854 | | -0.6334 | | -0.3161 | -0.3551 | -0.5403 | -0.7910 |
| | miR-27a-3p | | < 0.0001 | | | 0.2517 | 0.3368 | | -0.4766 | 0.2859 | | | -0.3484 | -0.6032 |
| | miR-34c-5p | < 0.0001 | < 0.0001 | | | | 0.5522 | 0.4859 | -0.6553 | -0.3645 | -0.3701 | -0.4234 | -0.3597 | -0.5836 |
| | miR-125b-5p | 0.0108 | 0.0015 | 0.0485 | | | | 0.2641 | -0.4400 | | -0.3647 | -0.2733 | | -0.5024 |
| | miR-181c-5p | 0.0390 | < 0.0001 | 0.0074 | < 0.0001 | | | | -0.5158 | -0.3900 | -0.3702 | | -0.3022 | -0.6528 |
| | miR-297 | 0.0002 | | | < 0.0001 | 0.0380 | | | -0.5765 | -0.6091 | -0.5160 | -0.5347 | -0.2589 | -0.4010 |
| Upregulated | miR-21-5p | < 0.0001 | < 0.0001 | < 0.0001 | < 0.0001 | 0.0003 | < 0.0001 | < 0.0001 | | 0.3001 | 0.5380 | 0.4103 | 0.2843 | 0.8189 |
| | miR-29c-3p | 0.0174 | | 0.0243 | 0.0036 | | 0.0017 | < 0.0001 | 0.0178 | | | 0.6165 | 0.3118 | 0.2981 |
| | miR-34a-5p | < 0.0001 | 0.0123 | | 0.0031 | 0.0036 | 0.0031 | < 0.0001 | < 0.0001 | | | | | 0.5480 |
| | miR-146a-5p | < 0.0001 | 0.0046 | | 0.0006 | 0.0316 | | < 0.0001 | 0.0009 | < 0.0001 | | | 0.3787 | 0.3514 |
| | miR-150-5p | | < 0.0001 | 0.0055 | 0.0041 | | 0.0170 | 0.0421 | 0.0251 | 0.0136 | | 0.0024 | | 0.3318 |
| | miR-155-5p | < 0.0001 | < 0.0001 | < 0.0001 | < 0.0001 | < 0.0001 | < 0.0001 | 0.0012 | < 0.0001 | 0.0186 | < 0.0001 | 0.0051 | 0.0084 | |

*The box plots, following the Tukey method, show the fold change ($2^{-\Delta Ct}_{target,sample}$ / median of $2^{-\Delta Ct}_{target,HC}$) between the relative expression of the significantly dysregulated microRNAs of interest of this study and their median relative expression in HC for (A) MS patients vs HC and (B) IMS and AMS patients vs HC. The y-axis is log2-scaled. Statistical significance was determined by (A) a Mann-Whitney t-test and (B) a one-way ANOVA Kruskal-Wallis test followed by a Dunn's post-test in between the subgroups. The p-values of the t-test and the one-way ANOVA have been corrected by the Benjamini-Hochberg method. p≤0.05: *; p≤0.01: **; p≤0.001: ***. (C) The table shows the nonparametric correlation analysis between the relative expression (-ΔCt) of microRNAs, grouped as significantly down- and upregulated, with the colour-scaled Spearman r coefficient in the upper right (dark blue for the lowest value to dark yellow for the highest value) and the respective unadjusted p-value in the lower left of the table. AMS = active multiple sclerosis, HC = healthy controls, IMS = inactive multiple sclerosis, MS = multiple sclerosis.*

Treatment status did not affect microRNA expression, except for miR-29c-3p that was upregulated in untreated MS patients compared to treated MS patients and HC (figure 2.6A). Interestingly, when analysing the data according to treatment, miR-27a-3p was significantly downregulated for GA-treated patients vs HC, miR-34a-5p was significantly upregulated for IFNb-treated vs GA-treated patients and HC. Moreover, miR-150-5p and miR-297 were respectively up- and downregulated in untreated MS patients vs HC and tended to be similarly dysregulated in GA- and IFNb-treated patients respectively (figure 2.6B, supplementary table 2.3).

*Figure 2.6: Relative microRNA expression in PBMCs of MS patients and HC (treatment)*

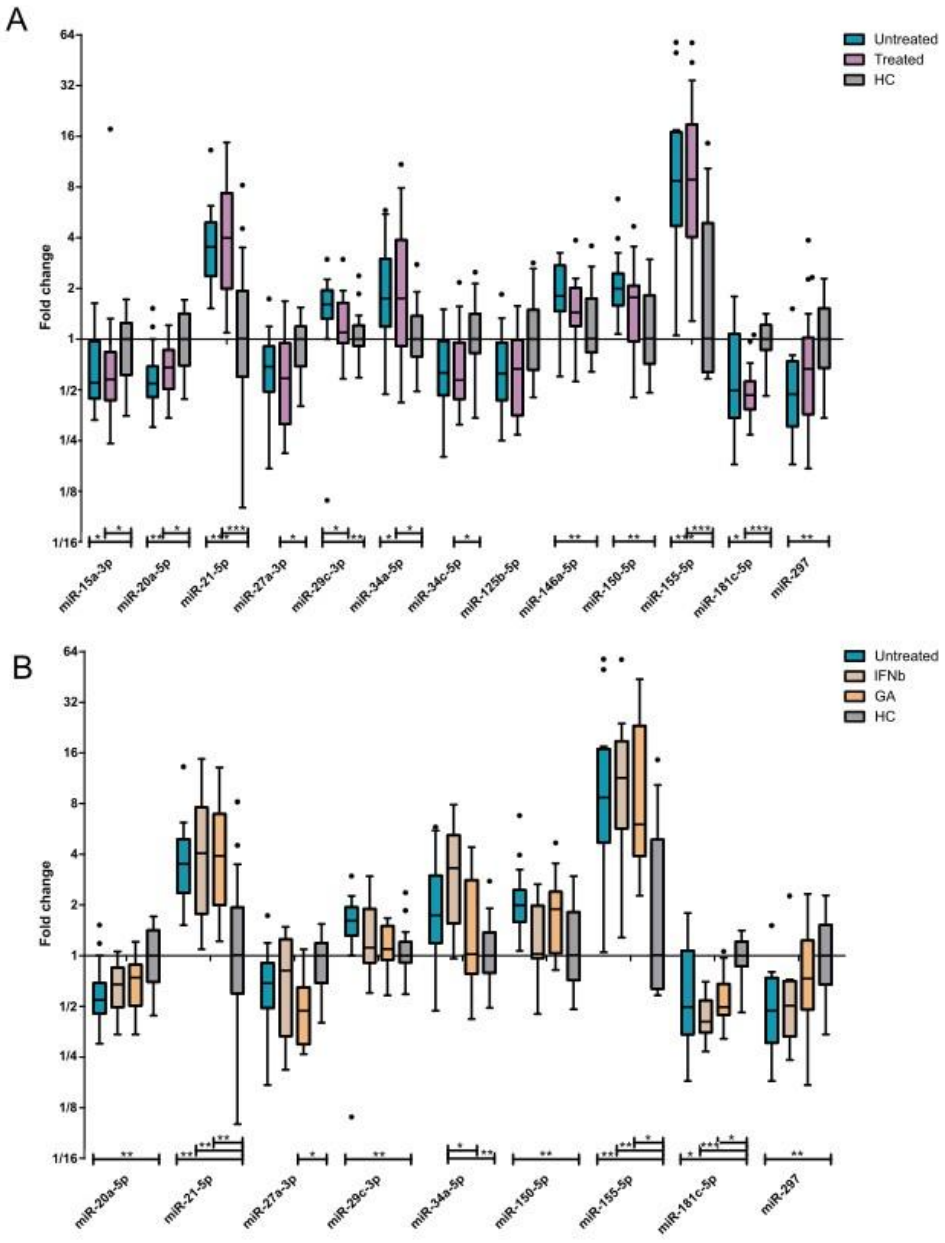


*The box plots, following the Tukey method, show the fold change ($2^{-\Delta Ct}_{target,sample}$ / median of $2^{-\Delta Ct}_{target,HC}$) between the relative expression of the significantly dysregulated microRNAs of*

*interest of this study and their median relative expression in HC for (A) untreated and treated MS patients vs HC and (B) untreated, IFNb- and GA-treated MS patients vs HC. The y-axis is log2-scaled. Statistical significance was determined by a one-way ANOVA Kruskal-Wallis test followed by a Dunn's post-test in between the subgroups. The p-values of the one-way ANOVA have been corrected by the Benjamini-Hochberg method. p≤0.05: *; p≤0.01: **; p≤0.001: ***. GA = glatiramer acetate, HC = healthy control, IFNb = interferon beta.*

In PCA on all significantly dysregulated microRNAs, the first two principal components explained 57.40 % of the sample population's variance, while separately, on the significantly up- and downregulated microRNAs, they represented 68.61% and 62.17% respectively (data not shown). Interestingly, for miR-21-5p, miR-155-5p and miR-181c-5p, the three most significantly dysregulated microRNAs, they accounted for 93.26% of the population's variance (figure 2.7A). However, they segregated only partially MS patients from HC (figure 2.7B).

*Figure 2.7: Principal component analysis of the relative expression of microRNAs*

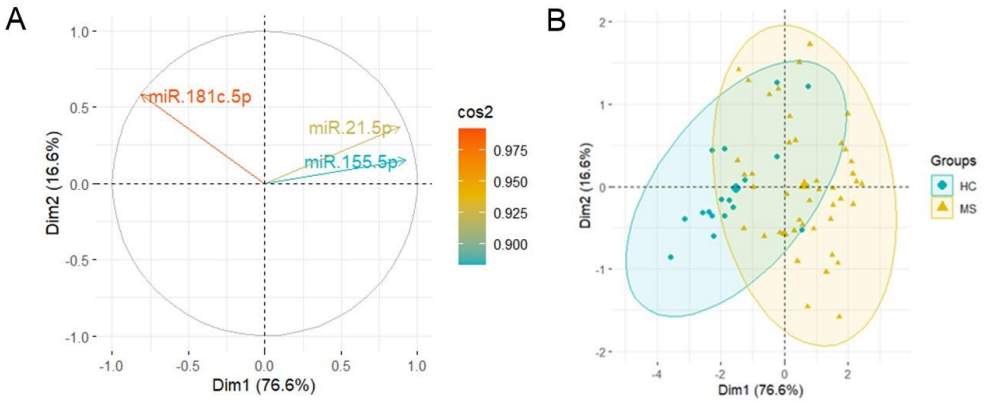


*The relative expression (-ΔCt) of the three most significantly dysregulated microRNAs (miR-21-5p/155-5p/181c-5p) are reduced to the first two principal components of the PCA to explain the population's variance (%) in these two dimensions (Dim1/Dim2). The loadings plot (A) represents the correlation of each variable (-ΔCt of the microRNA) to each component and is colour-scaled according to its cos2 value. The score plot (B) helps to cluster both populations, HC (yellow) and MS (blue), as illustrated by the ellipses. HC = healthy controls, MS = multiple sclerosis.*

iii. MicroRNAs mainly correlated with *IL21* and *FOXP3*

*Figure 2.8: Nonparametric correlation analysis between the relative expression of the mRNAs ($2^{-\Delta\Delta Ct}$) and the microRNAs (-ΔCt)*

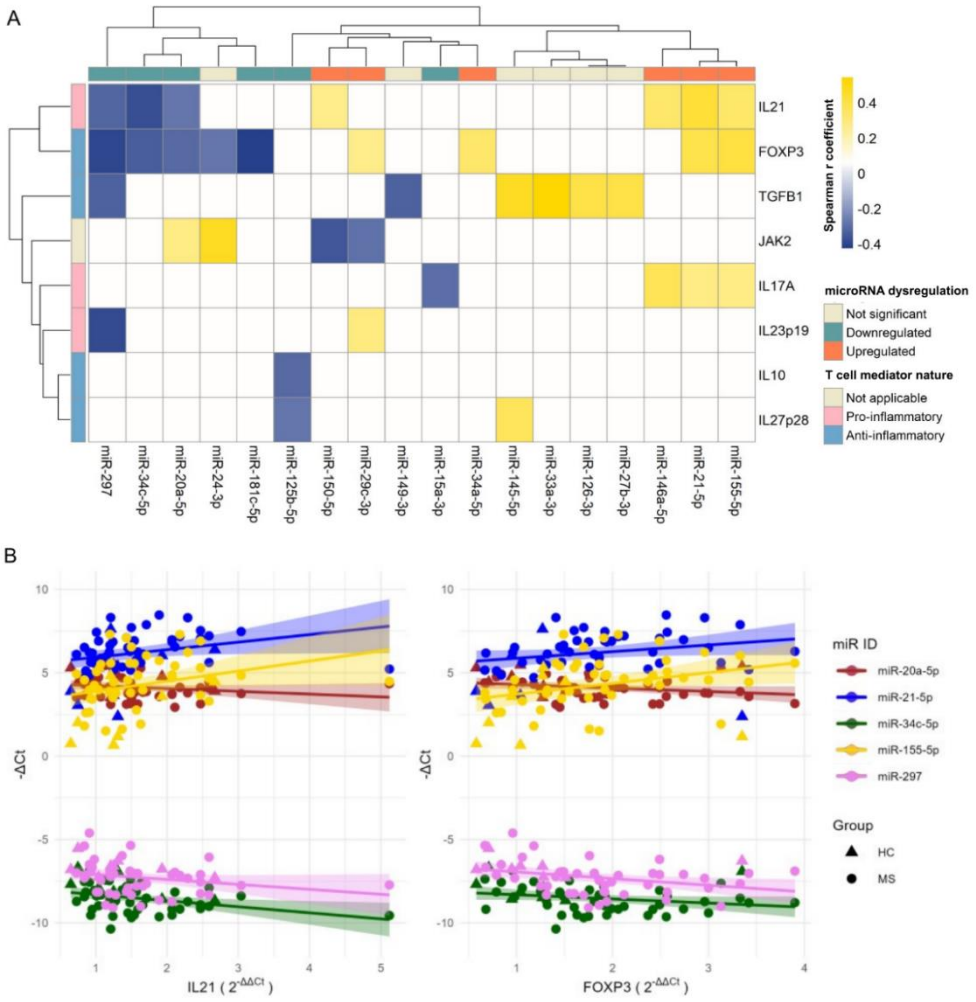


*(A) This heatmap with unsupervised hierarchical clustering, horizontally among the mRNAs, vertically among the microRNAs, displays the significant correlations between both, represented by the Spearman r coefficient in a blue-to-yellow colour scale, blue corresponding to a negative correlation, yellow to a positive. The horizontal colour bar on top of the heatmap indicates the dysregulation of each microRNA (not*

*significant/downregulated/upregulated) and the vertical colour bar on the left side of the heatmap informs about the nature of each T cell mediator (not applicable/pro-inflammatory/anti-inflammatory) correspondingly to the colours in the plot legend. (B) miR-21-5p/155-5p and miR-20a-5p/34c-5p/297 correlate, respectively, positively and negatively with IL21 (left) and FOXP3 (right) as further highlighted by this linear regression (line) with confidence interval of 95% (shaded area), wherein each colour corresponds to one of these microRNAs as specified in the plot legend. Moreover, the shape of the dots allows to visualise the distribution of samples of healthy controls (HC, ▲) and multiple sclerosis patients (MS, ●).*

In a nonparametric correlation analysis between the mRNA ($2^{-\Delta\Delta Ct}$) and microRNA (-ΔCt) levels of expression in this study, significantly down- and upregulated microRNAs correlated, respectively, negatively and positively with the T cell mediators, independently of their pro- or anti-inflammatory character, while the opposite was noticed with *JAK2* (with regard to the significant correlations only) (figure 2.8A, figure 2.9A). Furthermore, microRNAs with similar dysregulation and T cell mediators of similar nature were not strictly grouped together by the unsupervised hierarchical cluster analysis (figure 2.8A).

We identified most correlations with *IL21* and *FOXP3* (figures 2.8A-B, figure 2.9A-B-D). miR-21-5p and miR-155-5p corelated positively with both *IL21* and *FOXP3*; miR-146a-5p and miR-150-5p with *IL21* and miR-29c-3p and miR-34a-5p with *FOXP3*. On the contrary, miR-20a-3p, miR-34c-5p and miR-297 correlated negatively with *IL21* and *FOXP3*, and miR-24-3p and miR-181c-5p with *FOXP3* only. Interestingly, miR-150-5p/29c-3p and miR-20a-5p/24-3p were also negatively and positively correlated with *JAK2* respectively. Furthermore, miR-125b-5p correlated negatively with *IL10* and *IL27p28*. Of note, miR-27b-3p/33a-3p/126-3p/145-5p and miR-149-3p/297 were respectively positively and negatively correlated with transforming growth factor beta 1 *(TGFB1)*, but these microRNAs, except miR-297, were not significantly dysregulated in our MS population (figure 2.8A, figure 2.9A-B-D).

*Figure 2.9: Nonparametric correlation analysis and in silico analysis between the investigated mRNAs and microRNAs*

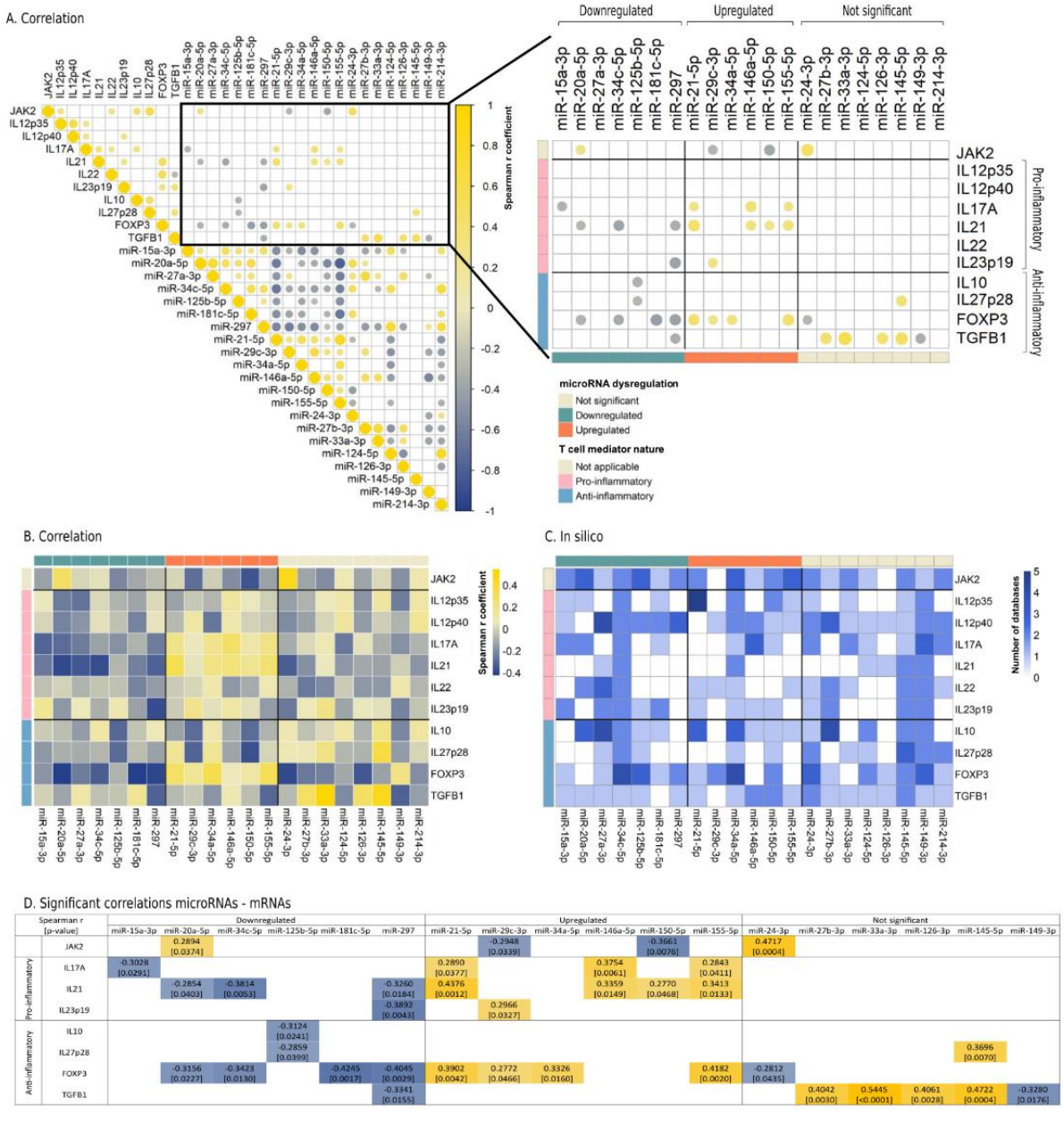

*(A) The correlogram displays the significant Spearman r coefficients by a blue-to-yellow colour scale of the correlation analysis of the microRNAs and mRNAs with a magnification on the significant correlations between the microRNAs (columns) and mRNAs (rows), wherein blue corresponds to a negative correlation, yellow to a positive. The size of the dots increases with the strength of the p-value. (B) This heatmap shows all the correlations, both significant and not significant for which can be referred to (A), between the microRNAs (columns) and mRNAs (rows) based on the Spearman r coefficient in a blue-to-yellow colour scale, blue negative, yellow positive. (C) This heatmap shows the number of databases predicting the mRNAs (rows) to be targeted by the investigated microRNAs (columns), in a white-to-blue scale from 0 to maximum 5 databases out of the 6 interrogated. In (A), (B), (C) the horizontal colour bar at the bottom of the magnified correlogram or on top of the heatmaps indicates the dysregulation of each microRNA (not significant/downregulated/ upregulated) and the vertical colour bar on the left side of the plots informs about the nature of each T cell mediator (not applicable/pro-inflammatory/anti-inflammatory) correspondingly to the colours in the plot legend in (A). Moreover, the microRNAs and mRNAs have been plotted in the same order on all plots to allow an easier comparison between the correlation analysis and the in silico analysis, of all correlations (B) or in light of the significant correlations (A). Finally, (D) this heatmap shows the Spearman r coefficient and corresponding unadjusted p-value (in between [ ]) of the significant correlations between microRNAs (columns) and mRNAs (rows) with a blue-to-yellow colour scale based on the Spearman r coefficient, blue negative, yellow positive.*

All investigated microRNAs were predicted to target several T cell mediators of this study, although these predictions were mostly limited to one or two out of the six explored databases, except for miR-21-5p/*IL12p35*, miR-27a-3p/*IL12p40*, miR-27a-3p/*IL10*, miR-34a/c-5p/*FOXP3* (figure 2.9C), However, this in silico analysis was overall variably consistent with the mRNA expression profile and the correlation analysis, except for miR-34c-5p/*FOXP3*. Moreover, it did not identify any pattern between the up- and downregulated microRNAs and the pro- and anti-inflammatory T cell mediators (figure 2.9A-B-C).

iv. Serum neurofilament light chain levels increase with radiological disease activity

AMS patients had significantly higher sNfL levels than MS patients with inactive disease or HC, independently of treatment status (figure 2.10). sNfL levels did not, however, correlate with any of the microRNAs and mRNAs of interest of this study.

*Figure 2.10: Serum neurofilament light chain levels of MS and HC*

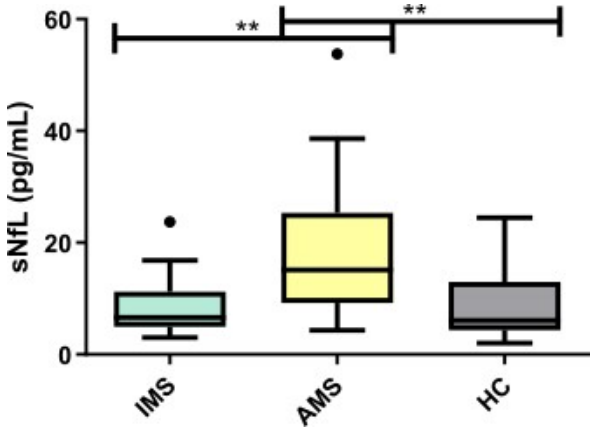


*The box plot, following the Tukey method, shows the concentration (pg/mL) of neurofilament light chain in the serum (sNfL) of IMS, AMS patients and HC, measured by single molecule immunoassay (SIMOA, Quanterix). The one-way ANOVA Kruskal-Wallis test results in an unadjusted p-value of 0.0017, the Dunn's post-test shows a significant difference between the subgroups, p≤0.01: **. AMS = active multiple sclerosis, HC = healthy controls, IMS = inactive multiple sclerosis.*

## V. Discussion

We investigated the expression of microRNAs and of markers of T cell activation (cytokines and transcription factors), and of IFNb response in PBMCs of treated (IFNb or GA) and untreated MS patients, according to their disease activity, based

on the presence/absence of gadolinium-enhancing lesions on brain MRI, compared to HC.

We confirmed the upregulation of interferon-induced proteins *MXA* and *JAK2* in MS patients treated with IFNb independently of disease activity [941,942], while only *JAK2* was upregulated with GA. MXA strongly monitors IFNb response, but its potential as a biomarker of relapse risk is disputed [943–947]. We did not detect differences in *MXA* expression levels between AMS and IMS, but only 25% of IFNb-treated patients had AMS vs 67% of GA-treated patients. Moreover, anti-IFNb neutralising antibodies, which can affect levels of *MXA* expression, were not measured in IFNb-treated patients [948]. Cytokine expression and cytokine-induced signalling occur through the Janus kinase/signal transducer and activator of transcription (JAK/STAT) signalling pathway, and JAK2/STAT3 signalling is especially involved in Th17 differentiation [949]. Interestingly, JAK2 stabilises IFNg receptor 2 on Th17 cells and IFNb therapy induces an antiproliferative response through IFNg signalling [950]. The effect of GA on JAK2 is unknown, however GA was proven to inhibit JAK2 and STAT3 phosphorylation in experimental autoimmune encephalomyelitis, possibly by means of suppressor of cytokine signalling (SOCS) 7 as it was found upregulated in PBMCs of GA-treated MS patients [951,952]. Nevertheless, we did not measure the level of phosphorylated JAK2 in this study.

We further highlighted that *IL27p28* (a subunit of IL27) was upregulated in PBMCs of treated MS patients, in particular with IFNb. Its expression was found to be induced by both GA and IFNb [953,954]. IFNb inhibits the proliferation and differentiation of Th17 cells, directly, or indirectly through its effect on dendritic cells, and in correlation with *IL27p28* overexpression [954].

In our cohort *FOXP3* was overexpressed in MS vs HC, independently of treatment status as seen by others [955,956]. *FOXP3* was previously found upregulated in relapsing vs remitting MS [957]. Conversely, unstimulated PBMCs of newly diagnosed MS patients expressed in vitro lower levels of *FOXP3* compared to HC [958].

Regarding the microRNAs, we highlight the dysregulation of several microRNA species in PBMCs of MS patients, independently of radiological disease activity for miR-21-5p/34c-5p/155-5p/181c-5p and more pronounced in AMS for miR-27a-3p only. Moreover, the three most significantly dysregulated microRNAs, miR-21-5p/155-5p/181c-5p, described 93.26% of the population's variance as shown by

PCA. miR-21-5p/146a-5p/155-5p were previously found upregulated in PBMCs of RRMS, while miR-34a was found downregulated in CD4+ T cells and miR-297a in B cells of RRMS patients, and miR-150/181c in PBMCs of MS (Huang et al., 2016; Ma et al., 2014; Martin and Illes, 2014) (table 1). Conversely, miR-27a-3p was previously found upregulated in CD4+ T cells of relapsing MS patients and was thus postulated to target negative Th17 regulators [803]. Yet on the contrary miR-27a-3p modulates dendritic cell maturation resulting in its mediated accumulation of Tregs instead of the mediated Th1/Th17 differentiation [804,959]. These apparently contradictory pro- and anti-inflammatory effects of miR-27a-3p were further observed in our in silico analysis. Herein, miR-27a-3p was predicted to target both *IL12p40* and *IL10*. Hence, the discrepancy between total PBMCs and CD4+ T cell microRNA expression for miR-34a-5p and miR-27a-3p highlights the difficulty in interpreting the pathophysiological significance of these changes, and should therefore be further functionally explored.

In our study treatment status did not significantly affect microRNA dysregulation, except for miR-29c-3p that was upregulated in untreated MS patients. Similarly, miR-29c-3p expression decreased after one month of IFNb therapy as compared to baseline [960]. Furthermore, in GA-treated patients, miR-27a-3p was significantly downregulated and miR-150-5p tended to be upregulated, while in IFNb-treated patients, miR-34a-5p was significantly upregulated and miR-297 tended to be downregulated. Conversely, others highlighted the upregulation of miR-146a-5p and the downregulation of miR-20a-5p in untreated RRMS patients, but their expression level was comparable to HC in GA- and in IFNb-treated patients respectively [760,961].

Several microRNAs of this study correlated with the mRNA levels of *IL21* and/or *FOXP3* or with *TGFB1*. We could however not identify a general and consistent pattern between the microRNAs and mRNAs of this study by in silico analysis, except for miR-34c-5p/*FOXP3*. The direct interaction of miR-34c-5p and *FOXP3* remains so far unexplored but has been evidenced for miR-34a-5p, although our correlation analysis was contrary to this [962]. An integrated view on cytokine regulation by microRNAs is missing as many studies have been investigating their interaction in a single setting. Cytokine expression conceivably results from a balanced effect of several microRNAs and other regulators. Moreover, chemokines and cytokines are rarely predicted as targets, but might be indirectly, positively or

negatively, affected by microRNA regulation dependent whether the upstream target is a promoter or a repressor [963,964], which supports the positive and negative correlations found in our study as well as the difficulties identifying a causal interaction. The expression level of upregulated microRNAs of this study correlated only positively with the T cell mediators, independently of their pro-/anti-inflammatory nature. Given the mainly inhibitory effect of a microRNA on its direct target, we could hypothesise that these microRNAs rather target an upstream negative regulator. On the contrary, the expression level of downregulated microRNAs of this study correlated negatively with the T cell mediators and they might thus rather target them directly or an upstream positive regulator. Consistently with our correlation results, miR-125b-5p inhibition in macrophages increases the expression of *IL10,* and miR-24 and miR-149-3p target *FOXP3* [811,965,966]. The latter could support our negative correlation between *TGFB1* and miR-149-3p. miR-27b-3p and miR-126-3p were both positively correlated with *TGFB1*. Accordingly miR-126-3p preferentially induced Treg differentiation over Th17 in a sepsis model [967]. In contrast, miR-27b inhibited inducible Treg development in vitro by targeting TGFb receptor 1 and *SMAD4* [802]. In accordance with the positive correlations we observed with *IL17A*, *IL21* and *FOXP3*, miR-155-5p promotes Th17 (IL6/STAT3/IL21/IL17) and Treg differentiation (IL2/STAT5/FOXP3), mainly through the JAK/STAT signalling pathway [968], as reported as well for miR-21-5p although with some discrepancies probably due to the experimental setting [786,969,970]. Our in silico analysis further predicted miR-21-5p to target *IL12p35*, of which the interaction has already been proven by luciferase assay, but it was not significant in our correlation analysis [971,972]. On the contrary, miR-146a-5p induces Treg differentiation at the expense of Th17 cells, which was also not reflected by our correlation analysis [973].

We acknowledge the limitations of this study in investigating the dysregulation of microRNAs in PBMCs of MS patients as well as their interplay with pathogenic cytokines and their related transcription factors. Firstly, the microRNA dysregulation was overall independent of radiological disease activity and treatment status, with a few exceptions. Although the size of our entire MS cohort was reasonable, the numbers of patients per subgroup when considering both parameters together were rather small, limiting the power of further statistical analyses. Furthermore we chose a relatively small amount of microRNAs (21) based on the results of our previous study, that however investigated 64 microRNAs,

selected from PCR array data on 127 microRNAs [892]. Many other microRNAs have been linked to MS before, and are still being identified by indiscriminate techniques with a higher discovery power such as small RNA sequencing [751,753,763]. Therefore, this study offers a partial vision on the mutual involvement of microRNAs and T cell mediators in MS. We are aware that other unexplored microRNAs could be uncovered as stronger functional players in the regulation of T cell mediator/cytokine expression.

It is also challenging to draw an overall conclusion on T cell mediators' expression or a peculiar profile of microRNA dysregulation in MS due to differences between studies regarding the population's characteristics and size, the type of sample analysed (serum, plasma, PBMCs, T cell subtypes) and the methodologies used (microarray, sequencing or RT-qPCR for microRNA and mRNA levels, ELISA or flow cytometry for protein levels). Moreover, PBMCs might not be the best surrogate for disease activity markers, since the CNS is the site of active inflammation. Interestingly, as compared to our previous study on microRNA expression in CSF of relapsing-remitting MS patients (table 2.1), miR-15a-3p/20a-5p/21-5p/29c-3p/34c-5p/146a-5p/150-5p/155-5p/297 were similarly dysregulated, while miR-27a-3p and miR-125b-5p were dysregulated in the opposite direction [892]. CSF-dysregulated miR-24-3p/27b-3p/33a-3p/124-5p/145-5p/149-3p/214-3p were not confirmed in PBMCs of this MS population.

*Table 2.1: Comparison of microRNA dysregulation in MS of this current study on PBMCs with our previous study and with the literature*

| microRNA ID | PBMCs study | CSF study [892] | | | Literature |
|---|---|---|---|---|---|
| | | CSF | serum | PBMCs | |
| miR-15a-3p | **down in MS** | down in RRMS | down in RRMS | ns | NA |
| miR-20a-5p | **down in MS** | down in RemMS | ns | ns | down in whole blood of MS (RR/PP/SP) [914]<br>down in grey matter lesions of PP/SPMS[897] |
| miR-21-5p | **up in MS** | up in RelMS | ND | ND | up in active lesions of MS (RR/PP/SP) [758]<br>ns/up in PBMCs of RelMS[757,766] |
| miR-24-3p | ns | up in RelMS | down in RRMS | ns | up in serum of RR/PPMS[974,975] |
| miR-27a-3p | **down in (A)MS** | up in RelMS | ND | ND | up in active lesions of MS (RR/PP/SP)[758] |
| miR-27b-3p | ns | up in RelMS | ND | ND | up in naive CD4⁺ of RemMS[801] |
| miR-29c-3p | **up in MS** | up in RelMS | ns | ns | down in grey matter lesions of PP/SPMS[897] |
| miR-33a-3p | ns | down in RemMS | ND | ND | NA |
| miR-34a-5p | **up in (I)MS** | Ns | ns | down in RelMS | up in active lesions of MS (RR/PP/SP) [758]<br>down in CD4⁺ of RRMS[918] |
| miR-34c-5p | **down in MS** | down in RRMS | ns | ns | NA |
| miR-124-5p | ns | down in RelMS | ND | ND | NA |
| miR-125b-5p | **down in (I)MS** | up in RelMS | ND | ND | down in PBMCs of RRMS[976] |
| miR-126-3p | ns | Ns | down in RRMS | ns | up in inactive lesions of MS (RR/PP/SP)[758]<br>up in CD4⁺ of RRMS[918] |
| miR-145-5p | ns | up in RelMS | ns | ns | up in PBMCs/serum of RemMS[977] |
| miR-146a-5p | **up in (I)MS** | up in RelMS | down in RRMS | ns | up in active lesions of MS (RR/PP/SP) [758]<br>up in PBMCs of RRMS[760] |
| miR-149-3p | ns | up in RemMS | ND | ND | up in grey matter lesions of PP/SPMS[897] |
| miR-150-5p | **up in MS** | up in RRMS | ns | ns | down in PBMCs of MS (RR/PP/SP) [978]<br>ns in PBMCs of RelMS[757]<br>up in CSF of RRMS[768] |
| miR-155-5p | **up in MS** | up in RRMS | ns | ns | up in active lesions of MS (RR/PP/SP) [758]<br>ns/up in PBMCs of RRMS[757,760] |
| miR-181c-5p | **down in MS** | Ns | down in RRMS | ns | down in active lesions of MS (RR/PP/SP) [758]<br>down in PBMCs of MS (RR/PP/SP) [978]<br>up in CSF of RRMS[901] |
| miR-214-3p | ns | down in RemMS | down in RRMS | ns | up in active/inactive lesions of MS (RR/PP/SP) [758] |
| miR-297 | **down in (I)MS** | down in RRMS | ns | ns | down in B cells of RRMS[762] |

*The significantly dysregulated microRNAs of this study are in bold. Matching dysregulations are highlighted in blue. CSF = cerebrospinal fluid, ns = non-significant, NA = not applicable, ND = not done, PBMCs = peripheral blood mononuclear cells, MS = multiple sclerosis, AMS = active MS, IMS = inactive MS, RelMS = relapsing MS, RemMS = remitting MS, RRMS = relapsing-remitting MS, PPMS = primary progressive MS, SPMS = secondary progressive MS.*

To conclude, in PBMCs of MS patients on platform injectable therapies or untreated, with radiologically active or inactive disease, T cell mediators were not dysregulated at the mRNA level, except for *FOXP3* and *JAK2*. We investigated microRNAs previously linked to MS and confirmed for several their dysregulation in PBMCs, although they could only partially segregate MS patients from HC. Interestingly, the expression level of some of them correlated positively or negatively with *IL21* and/or *FOXP3* mRNA expression. In particular, the predicted direct interaction of miR-34c-5p and *FOXP3*, supported by our findings on their opposite dysregulation and negative correlation, should be further explored. Cytokine expression conceivably results from the balanced effect of several regulators, of which microRNAs possibly do not target directly the mRNAs of cytokines but rather of their transcription factors. Their dysregulation in MS patients versus HC might not only reflect disease status but possibly contribute substantially to understanding MS pathogenicity, advocating further functional studies.

## VI. Supplementary material

*Supplementary table 2.1: mRNA and microRNA primers*

| mRNA target | Primers Sequence 5' - 3' | microRNA target | miScript Primer Assay (Qiagen) name - *MIMAT code* - sequence 5' - 3' |
|---|---|---|---|
| ABL | Forward: 5' - AAA ACC TTC TCG CTG GAC CC - 3'<br>Reverse: 5' - TTT GGG CTT CAC ACC ATT CC - 3' | hsa-miR-15a-3p | Hs_miR-15a*_1 *MIMAT0004488*<br>5' - CAGGCCAUAUUGUGCUGCCUCA - 3' |
| FOXP3 | Forward: 5' - CAA CAT GGA CTA CTT CAA GTT C - 3'<br>Reverse: 5' - ACT TGT GCA GAC TCA GGT TGT - 3' | hsa-miR-20a-5p | Hs_miR-20a_1 *MIMAT0000075*<br>5' - UAAAGUGCUUAUAGUGCAGGUAG - 3' |
| IL10 | Forward: 5' - CCC CAA GCT GAG AAC CAA GAC - 3'<br>Reverse: 5' - CGG CCT TGC TCT TGT TTT CAC - 3' | hsa-miR-21-5p | Hs_miR-21_2 *MIMAT0000076*<br>5' - UAGCUUAUCAGACUGAUGUUGA - 3' |
| IL12p35 | Forward: 5' - GAA TGT TCC CAT GCC TTC AC - 3'<br>Reverse: 5' - GAG TTT GTC TGG CCT TCT GG - 3' | Hsa-miR-24-3p | Hs_miR-24_1 *MIMAT0000080*<br>5' - UGGCUCAGUUCAGCAGGAACAG - 3' |
| IL12p40 | Forward: 5' - CAC CTG CTG GTG GCT GAC GAC - 3'<br>Reverse: 5' - CCA CTG AGT ACT CAT ACT CC - 3' | hsa-miR-27a-3p | Hs_miR-27a_1 *MIMAT0000084*<br>5' - UUCACAGUGGCUAAGUUCCGC - 3' |
| IL17A | Forward: 5' - AAC AAC GAT GAC TCC TGG GAA - 3'<br>Reverse: 5' -GTT ATG GAT GTT CAG GTT GAC - 3' | hsa-miR-27b-3p | Hs_miR-27b_2 *MIMAT0000419*<br>5' - UUCACAGUGGCUAAGUUCUGC - 3' |
| IL21 | Forward: 5' - GCT GAA GAG GAA ACC ACC TTC - 3'<br>Reverse: 5' - GAA TCA CAT GAA GGG CAT GTT - 3' | hsa-miR-29c-3p | Hs_miR-29c_1 *MIMAT0000681*<br>5' - UAGCACCAUUUGAAAUCGGUUA - 3' |
| IL22 | Forward: 5' - AGG CTC AGC AAC AGG CTA AG - 3'<br>Reverse: 5' - TTT GCT CTG GTC AAA TGC AG - 3' | hsa-miR-33a-3p | Hs_miR-33a*_1 *MIMAT0004506*<br>5' - CAAUGUUUCCACAGUGCAUCAC - 3' |
| IL23p19 | Forward: 5' - GGA TCC ACC AGG GTC TGA TTT - 3'<br>Reverse: 5' - GCT TGG AAT CTG CTG AGT CTC - 3' | hsa-miR-34a-5p | Hs_miR-34a_1 *MIMAT0000255*<br>5' - UGGCAGUGUCUUAGCUGGUUGU - 3' |
| IL27p28 | Forward: 5' - TGA TGT TTC CCT GAC CTT CC - 3'<br>Reverse: 5' - AGC TGC ATC CTC TCC AGT TT - 3' | hsa-miR-34c-5p | Hs_miR-34c_1 *MIMAT0000686*<br>5' - AGGCAGUGUAGUUAGCUGAUUGC - 3' |
| JAK2 | Forward: 5' -CAG GCA ACA GGA ACA AGA TG - 3'<br>Reverse: 5' - CCA TTC CCA TGC AGA GTC TT - 3' | hsa-miR-124-5p | Hs_miR-124*_1 *MIMAT0004591*<br>5' - CGUGUUCACAGCGGACCUUGAU - 3' |
| MXA | Forward: 5' - ACC TGA TGG CCT ATC ACC AG - 3'<br>Reverse: 5' - GCC AGC TGT AGG TGT CCT TG - 3' | hsa-miR-125b-5p | Hs_miR-125b_1 *MIMAT0000423*<br>5' - UCCCUGAGACCCUAACUUGUGA - 3' |
| TGFB1 | Forward: 5' - CCA GAG TGG TTA TCT TTT GAT G - 3'<br>Reverse: 5' - GGC CAT GAG AAG CAG GAA AG - 3' | hsa-miR-126-3p | Hs_miR-126_1 *MIMAT0000445*<br>5' - UCGUACCGUGAGUAAUAAUGCG - 3' |
| | | hsa-miR-145-5p | Hs_miR-145_1 *MIMAT0000437*<br>5' - GUCCAGUUUUCCCAGGAAUCCCU - 3' |
| | | hsa-miR-146a-5p | Hs_miR-146a_1 *MIMAT0000449*<br>5' - UGAGAACUGAAUUCCAUGGGUU - 3' |
| | | hsa-miR-149-3p | Hs_miR-149*_3 *MIMAT0004609*<br>5' - AGGGAGGGACGGGGGCUGUGC - 3' |
| | | hsa-miR-150-5p | Hs_miR-150_1 *MIMAT0000451*<br>5' - UCUCCCAACCCUUGUACCAGUG - 3' |
| | | hsa-miR-155-5p | Hs_miR-155_2 *MIMAT0000646*<br>5' - UUAAUGCUAAUCGUGAUAGGGGU - 3' |
| | | hsa-miR-181c-5p | Hs_miR-181c_2 *MIMAT0000258*<br>5' - AACAUUCAACCUGUCGGUGAGU - 3' |
| | | hsa-miR-214-3p | Hs_miR-214_2 *MIMAT0000271*<br>5' - ACAGCAGGCACAGACAGGCAGU - 3' |
| | | hsa-miR-297 | Hs_miR-297_2 *MIMAT0004450*<br>5' - AUGUAUGUGUGCAUGUGCAUG - 3' |

*Supplementary table 2.2: Median fold change and adjusted p-value of the relative expression of mRNAs*

| | **MS vs HC** | | **Activity** | Inactive vs HC | | Active vs HC | | **Treatment** | Untreated vs Treated | | Untreated vs HC | | Treated vs HC | | **Treatment (IFNb/GA)** | Untreated vs IFNb | | Untreated vs HC | | INFb vs HC | | GA vs HC | |
|---|---|---|---|---|---|---|---|---|---|---|---|---|---|---|---|---|---|---|---|---|---|---|
| mRNA target | Median FC | t-test (adj.p) | ANOVA (adj.p) | Median FC | Dunn's | Median FC | Dunn's | ANOVA (adj.p) | Median FC | Dunn's | Median FC | Dunn's | Median FC | Dunn's | ANOVA (adj.p) | Median FC | Dunn's | Median FC | Dunn's | Median FC | Dunn's | Median FC | Dunn's |
| IL12p35 | 1,46 | 0,0804 | 0,0945 | 1,40 | | 1,61 | * | 0,0677 | 1,12 | | 1,51 | * | 1,35 | | 0,1284 | 1,17 | | 1,51 | | 1,29 | | 1,35 | |
| IL12p40 | 1,32 | 0,1653 | 0,1357 | 1,21 | | 1,40 | | **0,0456** | 1,29 | | **1,47** | * | 1,14 | | 0,0878 | 1,38 | | 1,47 | | 1,07 | | 1,16 | |
| IL17A | 1,62 | 0,5234 | 0,8634 | 1,62 | | 1,63 | | 0,4606 | 1,49 | | 2,18 | | 1,47 | | 0,5764 | 1,37 | | 2,18 | | 1,59 | | 1,28 | |
| IL21 | 1,34 | 0,1058 | 0,1560 | 1,43 | | 1,19 | | 0,2253 | 0,96 | | 1,31 | | 1,37 | | 0,3020 | 1,08 | | 1,31 | | 1,22 | | 1,37 | |
| IL22 | 2,60 | 0,2198 | 0,0984 | 3,45 | | 1,71 | | 0,3306 | 0,83 | | 2,18 | | 2,61 | | 0,2181 | 0,64 | | 2,18 | | 3,38 | | 1,96 | |
| IL23p19 | 1,05 | 0,6453 | 0,9153 | 1,01 | | 1,08 | | 0,4396 | 1,18 | | 1,13 | | 0,96 | | 0,1692 | 0,99 | | 1,13 | | 1,14 | | 0,78 | |
| **FoxP3** | 1,93 | **0,0078** | **0,0060** | **2,03** | *** | 1,67 | | **0,0159** | 0,94 | | **1,88** | ** | **1,99** | * | **0,0262** | 0,89 | | **1,88** | * | **2,10** | * | 1,82 | |
| TGFB1 | 1,06 | 0,3651 | 0,3991 | 0,93 | | 1,14 | | 0,2267 | 1,32 | | 1,21 | | 0,92 | | 0,3108 | 1,25 | | 1,21 | | 0,97 | | 0,91 | |
| IL10 | 1,43 | 0,8006 | 0,9471 | 1,42 | | 1,43 | | 0,0608 | 0,74 | * | 1,13 | | 1,54 | | **0,0297** | **0,62** | ** | 1,13 | | 1,84 | | 1,39 | |
| IL27p28 | 1,98 | 0,0828 | 0,1207 | 1,59 | | **2,34** | * | **0,0016** | **0,49** | ** | 1,20 | | **2,45** | ** | **0,0032** | **0,48** | ** | 1,20 | | **2,51** | ** | 2,45 | |
| MXA | 1,62 | 0,0981 | 0,1479 | 1,42 | | 1,65 | | **0,0012** | **0,38** | ** | 1,02 | | **2,67** | ** | **0,0006** | **0,19** | *** | 1,02 | | **5,31** | *** | 1,62 | |
| **JAK2** | 1,37 | **0,0132** | **0,0210** | **1,36** | * | **1,38** | ** | **0,0006** | **0,81** | ** | 1,20 | | **1,48** | *** | **0,0012** | 0,81 | | 1,20 | | **1,48** | ** | **1,53** | ** |

*Median fold change and adjusted p-value of the relative expression of mRNAs, determined by a Mann-Whitney t-test or a one-way ANOVA Kruskal-Wallis test followed by Dunn's multiple comparison post-test. The p-values of the Mann-Whitney t-test and the one-way ANOVA have been corrected by the Benjamini-Hochberg method. p≤0.05: *; p≤0.01: **; p≤0.001: ***. Data of non-significant mRNAs are greyed, data of mRNAs that are significant for all analyses are in bold. Adj.p = adjusted p-value, AMS = active multiple sclerosis, FC = fold change, GA = glatiramer acetate, HC = healthy controls, IFNb = interferon beta therapy, IMS = inactive multiple sclerosis, MS = multiple sclerosis, vs = versus*

*Supplementary table 2.3: Median fold change and adjusted p-value of the relative expression of microRNAs*

| | **MS vs HC** | | **Activity** | Inactive vs HC | | Active vs HC | | **Treat-ment** | Untreated vs Treated | | Untreated vs HC | | Treated vs HC | | **Treatment (IFNb/GA)** | Untreated vs HC | | IFNb vs GA | | INFb vs HC | | GA vs HC | |
|---|---|---|---|---|---|---|---|---|---|---|---|---|---|---|---|---|---|---|---|---|---|---|
| microRNA ID | Median FC | t-test (adj.p) | ANOVA (adj.p) | Median FC | Dunn | Median FC | Dunn | ANOVA (adj.p) | Median FC | Dunn | Median FC | Dunn | Median FC | Dunn | ANOVA (adj.p) | Median FC | Dunn | Median FC | Dunn | Median FC | Dunn | Median FC | Dun n |
| miR-15a-3p | **0,56** | **0,0126** | **0,0336** | **0,54** | * | 0,61 | | **0,0342** | 0,95 | | **0,55** | * | **0,58** | * | 0,0725 | 0,55 | | 0,88 | | 0,58 | | 0,67 | |
| **miR-20a-5p** | **0,64** | **0,0053** | **0,0109** | **0,59** | ** | 0,73 | | **0,0084** | 0,81 | | **0,55** | ** | **0,68** | * | **0,0189** | **0,55** | ** | 0,92 | | 0,68 | | 0,74 | |
| **miR-21-5p** | **3,52** | **0,0011** | **0,0011** | **4,01** | *** | **3,06** | ** | **0,0011** | 0,90 | | **3,52** | *** | **3,98** | *** | **0,0063** | **3,52** | ** | 1,04 | | **4,06** | ** | **3,91** | ** |
| miR-24-3p | 0,95 | 0,8402 | 0,9780 | 0,96 | | 0,90 | | 0,3242 | 0,85 | | 0,84 | | 0,99 | | 0,4651 | 0,84 | | 0,96 | | 0,97 | | 1,02 | |
| miR-27a-3p | **0,65** | **0,0128** | **0,0359** | 0,71 | | **0,58** | * | **0,0343** | 1,17 | | 0,68 | | **0,58** | * | **0,0369** | 0,68 | | 1,77 | | 0,82 | | **0,47** | * |
| miR-27b-3p | 0,96 | 0,7757 | 0,7862 | 0,97 | | 0,94 | | 0,3964 | 1,21 | | 1,05 | | 0,87 | | 0,3375 | 1,05 | | 1,29 | | 1,06 | | 0,82 | |
| miR-29c-3p | **1,37** | **0,0250** | 0,0817 | 1,41 | | 1,33 | | **0,0100** | 1,47 | * | **1,61** | ** | 1,10 | | **0,0168** | **1,61** | ** | 1,02 | | 1,12 | | 1,10 | |
| miR-33a-3p | 1,21 | 0,3788 | 0,5480 | 1,25 | | 1,16 | | 0,1860 | 1,23 | | 1,36 | | 1,10 | | 0,3405 | 1,36 | | 1,06 | | 1,10 | | 1,05 | |
| **miR-34a-5p** | **1,74** | **0,0098** | **0,0108** | **1,93** | ** | 1,33 | | **0,0297** | 1,00 | | **1,74** | * | **1,74** | * | **0,0047** | 1,74 | | **3,27** | * | **3,31** | ** | 1,02 | |
| miR-34c-5p | **0,61** | **0,0093** | **0,0318** | **0,62** | * | **0,58** | * | **0,0264** | 1,10 | | 0,63 | | **0,57** | * | 0,0569 | 0,63 | | 1,05 | | 0,61 | | 0,57 | |
| miR-124-5p | 0,78 | 0,3871 | 0,6269 | 0,80 | | 0,69 | | 0,4936 | 0,90 | | 0,72 | | 0,81 | | 0,4691 | 0,72 | | 0,71 | | 0,78 | | 1,11 | |
| miR-125b-5p | **0,62** | **0,0160** | **0,0092** | **0,48** | ** | 0,80 | | **0,0489** | 0,94 | | 0,62 | | 0,66 | | 0,0529 | 0,62 | | 0,65 | | **0,52** | * | 0,80 | |
| miR-126-3p | 0,61 | 0,1257 | 0,3030 | 0,58 | | 0,62 | | 0,2502 | 1,41 | | 0,69 | | 0,49 | | 0,3240 | 0,69 | | 1,80 | | 0,74 | | 0,41 | |
| miR-145-5p | 1,00 | 0,4740 | 0,1784 | 0,97 | | 1,18 | | 0,4759 | 0,88 | | 0,98 | | 1,12 | | 0,3302 | 0,98 | | 0,75 | | 0,94 | | 1,24 | |
| miR-146a-5p | **1,64** | **0,0201** | **0,0340** | **1,86** | * | 1,41 | | **0,0269** | 1,26 | | **1,80** | ** | 1,43 | | 0,0582 | **1,80** | * | 0,93 | | 1,40 | | 1,50 | |
| miR-149-3p | 0,81 | 0,3050 | 0,4228 | 0,81 | | 0,84 | | 0,4148 | 0,92 | | 0,76 | | 0,81 | | 0,5358 | 0,76 | | 0,77 | | 0,81 | | 1,11 | |
| **miR-150-5p** | **1,87** | **0,0128** | **0,0389** | **1,90** | * | 1,86 | | **0,0105** | 1,13 | | **1,99** | ** | 1,77 | | **0,0147** | **1,99** | ** | 0,54 | | 1,03 | | 1,89 | |
| **miR-155-5p** | **8,69** | **0,0004** | **0,0005** | **9,99** | *** | **4,84** | * | **0,0005** | 0,99 | | **8,69** | *** | **8,83** | *** | **0,0021** | **8,69** | ** | 1,90 | | **11,35** | ** | **6,02** | * |
| **miR-181c-5p** | **0,47** | **0,0005** | **0,0021** | **0,47** | ** | **0,47** | *** | **0,0014** | 1,06 | | **0,49** | * | **0,46** | *** | **0,0031** | **0,49** | * | 0,81 | | **0,40** | *** | **0,50** | * |
| miR-214-3p | 0,81 | 0,2150 | 0,4340 | 0,83 | | 0,74 | | 0,3792 | 0,96 | | 0,81 | | 0,84 | | 0,5009 | 0,81 | | 1,21 | | 0,93 | | 0,77 | |
| **miR-297** | **0,59** | **0,0055** | **0,0074** | **0,46** | *** | 0,71 | | **0,0084** | 0,70 | | **0,47** | ** | 0,67 | | **0,0143** | **0,47** | ** | 0,69 | | 0,50 | | 0,73 | |

*Supplementary table 2.3*

*Median fold change and adjusted p-value of the relative expression of microRNAs, determined by a Mann-Whitney t-test or a one-way ANOVA Kruskal-Wallis test followed by Dunn's multiple comparison post-test. The p-values of the Mann-Whitney t-test and the one-way ANOVA have been corrected by the Benjamini-Hochberg method. p≤0.05: *; p≤0.01: **; p≤0.001: ***. Data of non-significant microRNAs are greyed, data of microRNAs that are significant for all analyses are in bold. Adj.p = adjusted p-value, AMS = active multiple sclerosis, FC = fold change, GA = glatiramer acetate, HC = healthy controls, IFNb = interferon beta therapy, IMS = inactive multiple sclerosis, MS = multiple sclerosis, vs = versus*

# CHAPTER 3: MICRORNAS DYSREGULATED IN MULTIPLE SCLEROSIS AFFECT THE DIFFERENTIATION OF CG-4 CELLS, AN OLIGODENDROCYTE PROGENITOR CELL LINE

Océane Perdaens, Pauline Bottemanne, Vincent van Pesch

We finally aimed to investigate whether several microRNAs dysregulated in relapsing-remitting MS patients in our initial screening affect the differentiation of CG-4 oligodendrocyte progenitor cells. We then focused on 5 microRNAs of which miR-33-3p, miR-34c-5p, miR-124-5p, and miR-145-5p impede and miR-214-3p promotes their differentiation into mature oligodendrocytes, in order to detail the differential expression of OPC/OL stage markers and Gene Ontology enrichment analysis by RT-qPCR and RNA sequencing. We finally sought potential mRNA targets and molecular mechanisms to support the change in cell fate they induce.

*Figure 3.1: Graphical abstract*

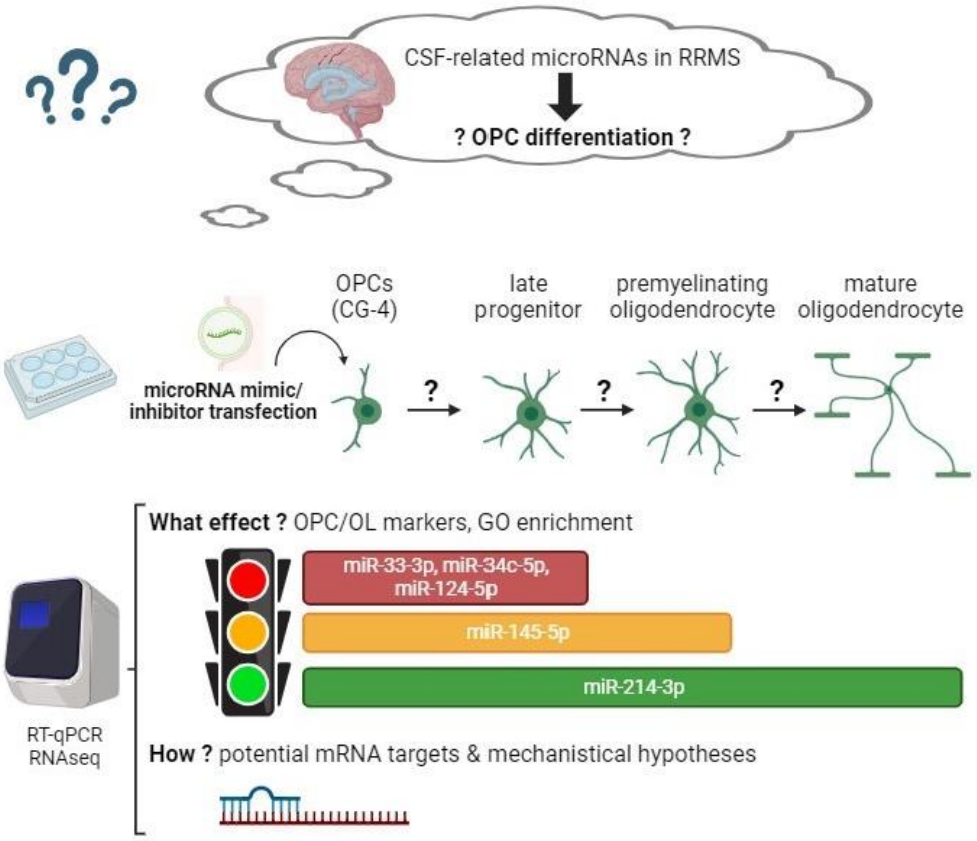


*We investigated the effect of microRNAs previously found dysregulated in the cerebrospinal fluid (CSF) of patients with relapsing and/or remitting multiple sclerosis (RRMS) by transfecting their microRNA mimic (with or without the inhibitor) in CG-4 cells, an oligodendrocyte progenitor cell line. By exploring by RT-qPCR and RNA sequencing (RNAseq)*

*the expression of several markers of oligodendrocyte progenitor cells (OPC) and oligodendrocytes (OL) as well as the enrichment of Gene Ontology (GO) terms, we evidenced that miR-33-3p, miR-34c-5p and miR-124-5p arrested their differentiation at a late progenitor stage and miR-145-5p at an early premyelinating oligodendrocyte stage, while miR-214-3p promoted oligodendrocyte maturation. We further sought potential mRNA targets to propose mechanistical hypotheses supporting the changes in cell fate. Created in BioRender.com*

## I. Abstract

Remyelination in multiple sclerosis (MS) is from the start of the disease imperfect, and strongly decreases with its progression, mainly due to the harm on oligodendrocyte progenitor cells (OPCs), causing neurodegeneration and resulting in irreversible neurological deficits. Therapeutic strategies promoting remyelination are still very preliminary and lack within the current treatment panel of MS. In a previous study we have identified 21 microRNAs dysregulated mostly in the CSF of relapsing and/or remitting MS patients. Here, we observed that among these, the majority of 13 transfected microRNA mimics decreased the differentiation of an OPC cell line called CG-4. Herein we support by RNA sequencing and independent RT-qPCR analyses that miR-33-3p, miR-34c-5p, miR-124-5p, and miR-145-5p impede OPC differentiation as evidenced by the downregulation of premyelinating oligodendrocyte (OL) (*Tcf7l2, Cnp* [except for miR-145-5p]) and mature OL (*Plp1, Mbp, Mobp*) markers, whereas only miR-214-3p promotes OPC differentiation. We further propose a comprehensive exploration of their change in cell fate through Gene Ontology enrichment analysis. We finally confirm by RT-qPCR analysis the downregulation of several predicted mRNA targets for each microRNA that possibly support their effect on OPC differentiation by very distinctive mechanisms, of which some are still unexplored in OPC/OL physiology. We hereby open new perspectives in the research on OPC differentiation and the pathophysiology of demyelination/remyelination, and possibly even in the research on new remyelinating therapeutic strategies in the scope of MS.

## II. Introduction

Multiple sclerosis (MS) is a chronic inflammatory demyelinating disorder of the central nervous system. Although remyelination occurs, mainly during the early phase of the disease, it remains incomplete and even declines with disease duration and ageing, underpinning neurodegeneration [400,411].

The myelin sheath is a lipid membrane formed by mature oligodendrocytes (OLs) that spirally wraps around axons, in order to facilitate neuronal conduction and protect axonal integrity [620]. OLs originate from oligodendrocyte progenitor cells (OPCs). The adult brain has a pool of OPCs in the subventricular zone as well as in the surrounding intact grey and white matter that can migrate to the site of myelin turnover and differentiate into mature OLs [392,394,396,399,528]. However, in MS, over time OPCs are depleted and fail to migrate and/or differentiate properly as demonstrated by the presence of fewer and often undifferentiating OPCs alongside the loss of mature OLs and the apparent unreceptiveness of axons to remyelination within chronic MS lesions [419,422,437,439,979]. Moreover, the myelin sheath formed by remyelination is thinner and extends over a shorter internode distance [230]. Demyelination or unproper remyelination results in neuro-axonal degeneration, in turn leading to brain and spinal cord atrophy [980]. Additionally, ongoing demyelination within chronic active (slowly expanding) lesions, characteristic of smouldering MS, is clinically associated with relapse-free disability worsening and disease progression, a process referred to as progression independent of relapse activity (PIRA) [40,45,981]. While the number of disease-modifying therapies (DMTs) has gradually increased over the last two decades, all of them target the immune system and clinical research on remyelination-enhancing agents is still very preliminary [161]. So far there is no DMT directly sustaining remyelination, while this can contribute to slow down neurodegeneration and disease progression [982].

MicroRNAs are small non-coding RNAs that regulate gene expression post-transcriptionally by binding to a complementary seed of their target messenger RNA (mRNA), mostly located in its 3' untranslated region (3'UTR) [720]. MicroRNAs play a largely acknowledged role in physiological as well as pathophysiological processes [983], as evidenced as well in central nervous system myelination. Dynamic changes in the microRNA expression profile presumably finely tunes OPC/OL development [884,885,984]. miR-219, miR-338 and miR-138 promote early OPC differentiation into OLs by targeting OPC proliferation genes. Yet, while miR-219

plays a supporting role up to the late stage of differentiation, miR-138 delays it [782,783]. Transgenic mice with OPC/OL-specific Dicer1 ablation, an indispensable endonuclease in microRNA biogenesis, develop tremor and ataxia due to myelination defects [720,782,783]. miR-219, the strongest induced microRNA in differentiating OLs, can partially rescue Dicer1 ablation and improve both lysolecithin-induced demyelination and experimental autoimmune encephalomyelitis [782,985]. Furthermore, miR-219 and miR-338 have been found upregulated in normal appearing white matter but downregulated in inactive white matter lesions of MS patients and miR-219 is more often undetectable in the cerebrospinal fluid (CSF) of MS patients than controls [986,987]. Finally, microRNA dysregulation has been linked to MS [753]. We have previously found 18 microRNAs dysregulated in the CSF of relapsing and/or remitting MS patients, of which 5 have still not been described in MS so far (miR-15a-3p, miR-33-3p, miR-34c-5p, miR-124-5p, miR-297) [892].

Therefore, we hypothesise that these MS-related microRNAs possibly affect OPC differentiation. We thus aimed to screen the effect of a series of these microRNAs on the differentiation of CG-4 cells, a bipotential OPC cell line. We then selected the microRNAs exhibiting the most effect - miR-33-3p, miR-34c-5p, miR-124-5p, miR-145-5p, miR-214-3p - to further characterise their action on CG-4 differentiation both at the mRNA and protein level. We finally aimed to identify potential microRNA targets by crossing the data of in silico analysis and RNA sequencing, which we confirmed by independent RT-qPCR analyses.

## III. Methods

### i. Cell culture

We kindly received the Central Glia-4 (CG-4) cells, a permanent cell line derived from rat bipotential oligodendrocyte-type 2-astrocyte (O-2A) progenitor cells [988], and the B104 neuroblastoma cells from Dr. M. Grãos (University of Coimbra, Portugal). For CG-4 cell culture, T175 culture flasks or 6-well plates were coated with poly-L-lysine (P2636, Sigma-Aldrich) at 0.04 mg/mL for 30 minutes at 37°C and washed twice with autoclaved deionized water and once with sterile Dulbecco's

phosphate buffered saline (DPBS, L0615-500, BioWest). Cells were first plated for 30-60 minutes in Dulbecco's Modified Eagle Medium (DMEM, L0101-500, BioWest) containing 100 UI/mL penicillin, 100 µg/mL streptomycin (15140-122, Gibco) and 2.5 µg/mL amphotericin B (15290-018, Gibco) (PSA-DMEM) supplemented with 5% foetal bovine serum (FBS, S15898S181H, Gibco), 5 µg/mL human insulin (I9278, Sigma-Aldrich), 2 mM sodium pyruvate (11360-039, Gibco) and 10 mM Hepes (15630-056, Gibco), called recovery medium. Hereafter, CG-4 cells were cultured in a proliferation medium, consisting of PSA-DMEM supplemented with 30% B104 conditioned medium containing the essential mitogens, 50 µg/mL human apo-transferrin (T2036, Sigma-Aldrich), 9.8 ng/mL biotin (B4639, Sigma-Aldrich), 40 ng/mL sodium selenite (S5261, Sigma-Aldrich), 5 µg/mL human insulin and 10 mM Hepes in order to allow OPC proliferation [989]. To promote their differentiation into OLs, they were cultured in DMEM containing penicillin-streptomycin, and 1% GlutaMAX™ supplement (35050-061, Gibco), and supplemented with 5 µg/mL bovine insulin (I6634, Sigma-Aldrich), 50 µg/mL human holo-transferrin (T0665, Sigma-Aldrich), 2% B-27™ supplement (080085-SA, Gibco), 0.5% FBS, 0.05 µg/mL recombinant rat ciliary neurotrophic factor (CNTF, 450-50, PeproTech), 1% OL-supplement and 10 mM Hepes, called differentiation medium [990].

B104 conditioned medium was recovered from the culture medium of B104 cells cultured in uncoated T175 flasks at a cell density of 15,000 cells/cm² for 24 hours in PSA-DMEM-F12 medium (L0090-500, BioWest) supplemented with 10% FBS and for 72 hours in PSA-DMEM-F12 medium supplemented with 10 µg/mL human holo-transferrin, 5 ng/mL sodium selenite, 16 µg/mL putrescine dihydrochloride (P5780, Sigma-Aldrich) and 6.3 ng/mL progesterone (P8783, Sigma-Aldrich). The latter medium was recovered and centrifuged at 1000 x g for 10 minutes. The supernatant was filtered (0.22 µm) with 1 µg/mL phenylmethylsulfonyl fluoride (a protease inhibitor, 36978, Thermo Fisher Scientific) and stored add -20°C upon use [989].

### ii. MicroRNA mimic and inhibitor transfection

*Double transfection of microRNA mimics*

CG-4 cells were plated (day -1) overnight in the proliferation medium at a cell density of 250,000 cells per well in a pre-coated 6-well plate and were separately transfected on day 0 for 6h and on day 4 for 48h following the manufacturer's

recommendations. In brief, the miRCURY LNA microRNA mimic or negative control (miR-NC) (Qiagen, supplementary table 1) was diluted in 50 µl Opti-MEM™ reduced serum medium (51985026, Thermo Fisher Scientific) for a final concentration of 40 nM (in culture well) and added on top of 50 µl Opti-MEM™ containing 3µl Lipofectamine™ 2000 Transfection Reagent (Thermo Fisher Scientific), mixed gently by reverse pipetting (15x) and incubated at room temperature for 5-10 minutes. This 100 µl transfection mix was then added dropwise to 900 µl of proliferation medium for 6h. After 6h, the medium was replaced by 1.5 ml of proliferation medium. On day 1, the proliferation medium was replaced by 1.5 ml of differentiation medium, of which two third was refreshed on day 4 before the second transfection, that was processed likewise in 1000 µl total volume, but after 6h of transfection, 500µl of fresh differentiation medium was added for an additional 48h, leaving the transfection mix in the culture wells. Cells were collected on day 6 for RNA extraction.

*Single transfection of microRNA mimics*

On day -1, CG-4 cells were plated at a cell density of 75,000 cells on a pre-coated glass coverslip placed in a 24-well plate (for immunocytochemistry analysis) or at a cell density of 250,000 cells per well in a pre-coated 6-well plate (for RT-qPCR analysis) for one hour in the recovery medium and for approximately 20 hours in the proliferation medium. On day 0, the cells were transfected with 40 nM miRCURY LNA microRNA mimic or miR-NC (final concentration in culture well) for 6h (Qiagen) using Lipofectamine™ 2000 according to the manufacturer's protocol (40 nM mimic/1.2 µl Lipofectamine in 40 µl Opti-MEM™ added to 360 µl of proliferation medium in 24-well plate and 40 nM mimic/3 µl Lipofectamine in 100 µl Opti-MEM™ added to 900 µl of proliferation medium in 6-well plate). After 6 hours, the medium was replaced by the differentiation medium (respectively 500 µl and 1.5 ml) and cells were kept in culture for 48 hours.

*Sequential transfection of microRNA mimics and inhibitors*

Cells were plated likewise in pre-coated 6-well plates (day-1) and transfected on day 0 with 40 nM LNA miRCURY microRNA mimic for 4h followed by a second

transfection without (mock transfection with Lipofectamine™ 2000 only) or with 40 nM of the corresponding miRCURY LNA microRNA inhibitor (Qiagen) for 4h (without refreshing the medium) using Lipofectamine™ 2000 (40 nM mimic or inhibitor/2 µl Lipofectamine in 50 µl Opti-MEM™ added to 900 µl of proliferation medium in 6-well plate). The medium was hereafter replaced by 1.5 ml of differentiation medium to culture the cells for an additional 48h.

In all transfection protocols, the proliferation and differentiation vehicle control conditions were processed likewise but transfected with Lipofectamine™ 2000 alone, without microRNA mimic/inhibitor. The proliferation vehicle control was cultured similarly in proliferation medium only. For each transfection method, 3 independent experiments were performed with each condition in triplicate.

For endogenous microRNA analysis, cells were plated at a cell density of 100,000 cells per well in a pre-coated 6-well plate. The cells were cultured for 3 days in total in proliferation with/without differentiation medium following the same timing as in section 2.2.2. and did not undergo any other treatment. Four independent experiments were performed with each condition in triplicate.

iii. RNA and microRNA extraction and PCR

The culture medium was removed from the 6-well plates and the wells were washed with 1 ml DPBS. For RNA extraction, TriPure™ Isolation Reagent (Roche) was added to the wells and the plates were stored for minimum 30 minutes at -80°C to help with the cell lysis. RNA was hereafter extracted following the manufacturer's protocol except for the precipitation step, samples were stored for 2h in isopropanol at -20°C to help with RNA precipitation before being centrifuged. RNA concentration and purity were verified by spectrophotometry (Shimadzu BioSpec-nano Spectrophotometer) and 500 ng RNA were reverse transcribed using iScript™ cDNA Synthesis Kit (Bio-Rad). MicroRNAs were extracted with QIAzol lysis reagent (Qiagen) following the miRNeasy Mini Kit protocol with RPE and RWT buffer (Qiagen), but we used Enzymax RNA Mini spin columns (EZCR101, Enzymax) instead. RNA concentration and purity was verified by spectrophotometry and set at an equal concentration of 50 ng/µL for all samples. MicroRNAs were reverse

transcribed using miRCURY LNA RT (Qiagen). We performed the real time quantitative polymerase chain reactions (RT-qPCR) using Takyon™ No ROX Probe 2X MasterMix Blue dTTP (Eurogentec) for mRNAs and miRCURY LNA SYBR Green PCR kit (Qiagen) for microRNAs on a RotorGene (Qiagen). Primers are listed in supplementary table 1A-B. The specificity was verified with the melt curves. The relative expression was determined by the $2^{-\Delta\Delta Ct}$ method (with ΔΔCt = ΔCt [target m(i)RNA-reference]$_{sample}$ − mean ΔCt [target m(i)RNA-reference]$_{differentiation\ (vehicle)\ control}$) [909]. We used hypoxanthine phosphoribosyltransferase 1 *(Hprt1)* as reference gene for the mRNAs and miR-103a-3p for the microRNAs.

iv. RNA sequencing

RNA sequencing (by synthesis) and the primary bio-informatic analyses were performed by Novogene UK. All samples of a single experiment with each condition in triplicate (proliferation and differentiation vehicle control, miR-33-3p, miR-34c-5p, miR-124-5p, miR-145-5p, miR-214-3p and miR-NC cultured in the differentiation medium) passed the pre-sequencing sample quality control with an RNA integrity number between 9 and 9.4 (Agilent 5400), as well as the post-sequencing data quality control with an average of 98.67% clean reads [98.15-98.93% (min-max)], 97.43% Q20 [96.28-97.97%] and 93.04% Q30 [91.23-94.30%]. However, one miR-NC replicate was finally excluded from the analysis as it appeared as an outlier. This sample had the lowest Q20 and Q30 percentage.

For library preparation, mRNA was purified from total RNA using poly-T oligo-attached magnetic beads. After fragmentation, the first cDNA strand was synthesised using random hexamer primers, the second using either dUTP for directional library or dTTP for non-directional library, followed by end repair, A-tailing, adapter ligation, size selection, USER enzyme digestion (for the directional library only), amplification, and purification. The libraries, quantified with Qubit and real-time PCR and verified by bioanalyzer for size distribution, were pooled and sequenced on Illumina NovaSeq 6000 to generate 150 bp paired-end reads. Twelve gigabytes of raw data (fastq format) were yielded per sample and processed through fastp software. Clean reads were obtained by removing low quality reads and reads containing adapter or ploy-N. Paired-end clean reads were aligned to the improved rat reference genome (mRatBN7.2) using HISAT2 v2.0.5. The mapped

reads of each sample were assembled by StringTie (v1.3.3b) and the reads numbers mapped to each gene were counted with featureCounts v1.5.0-p3. Fragments per kilobase million (FPKM) of each gene was calculated based on the length of the gene and reads count mapped to this gene.

Differential expression analysis between two conditions was performed using the DESeq2 R package (1.20.0). Gene Ontology enrichment analysis of differentially expressed genes was implemented with the cluster Profiler R package, with correction of gene length bias. The p-values were corrected for the false discovery rate by the Benjamini and Hochberg's approach. Differentially expressed genes (DEG) and enriched GO terms were significant if the adjusted p-value was ≤ 0.05.

v. Immunocytochemistry

Cells were fixed a first time with 4% homemade paraformaldehyde (PFA; 1.04005.1000, Merck) while still in the culture medium (1:2 volumes) for 10 minutes. The medium was discarded, and cells were fixed a second time in plain 4% PFA at room temperature for 10 minutes. There were two staining conditions: (1) surface staining of O4 (hybridoma supernatant, AK3203/01, In Vivo BioTech) or A2B5 (hybridoma supernatant, CRL-1520, ATCC), (2) intracellular staining of Gfap (ab16997, Abcam) and Mbp (ab7349, Abcam). For the surface staining of O4 (dilution 1/15) and A2B5 (dilution 1/25), cells were first blocked for 1 hour with 5% bovine serum albumin (BSA; A7906, Sigma-Aldrich), then incubated for 1 hour with the primary antibody and for 2 hours with the secondary antibody (dilution 1/1000; goat anti-mouse IgM Alexa Fluor (AF) 488 [A21042, Thermo Fisher Scientific] and AF647 [A21238, Thermo Fisher Scientific] respectively) in 1% BSA. Hereafter, cells were fixed again. For the intracellular staining of Gfap (dilution 1/500) and Mbp (dilution 1/500), cells were blocked and permeabilised with 0.3% Triton X-100 (T8787, Sigma-Aldrich) and 5% BSA for 1 hour. Cells were hereafter incubated overnight at 4°C with the primary antibodies and 2 hours with the secondary antibody (dilution 1/1000; AF488 goat anti-rabbit IgG (A11008, Thermo Fisher Scientific) and AF555 goat anti-Rat IgG (A21434, Thermo Fisher Scientific) respectively) in 0.3% Triton X-100 and 1% BSA. Hereafter, the coverslips were mounted on VWR® Superfrost® Plus Micro Slide using ProLong™ Gold Antifade Mountant with DAPI (Thermo Fisher Scientific). All buffers were prepared with

DPBS containing calcium and magnesium (14080-055, Gibco). All steps were performed at room temperature, except the overnight incubation, and cells were washed 3 times in between steps, but not after blocking. The mounted coverslips were scanned by the Zeiss Axio Scan.z1 and the QuPath open source software (version 0.4.0.) was trained to count distinctively the marked cells, except for Gfap [991]. Gfap expression was estimated to the total number of cells by visualising grid-wise each coverslip, and scored as 0 = no Gfap-positive ($Gfap^+$) cells, 1 = a few $Gfap^+$ cells scattered over the whole coverslip, 2 = a few $Gfap^+$ cells congregated in a few grids of the coverslip, 3 = a few $Gfap^+$ cells in several grids of the coverslip, 4 = many $Gfap^+$ cells in several grids of the coverslip, 5 = many $Gfap^+$ cells over the whole coverslip. The evaluator was blinded to the experimental conditions.

Each staining was performed on a single replicate per condition within each experiment, repeated 3-5 times. The specificity of the primary antibodies was verified by staining a differentiation vehicle control condition with the secondary antibody/antibodies only, correspondingly to each staining condition within each experiment.

vi. In silico analysis

We interrogated 4 databases for the predicted mRNA targets of each investigated microRNA separately: miRDB (http://www.mirdb.org/index.html), TargetScanHuman 8.0 (https://www.targetscan.org/), DIANA-microT-CDS (http://www.microrna.gr/microT-CDS), and miRWalk 3 (http://mirwalk.umm.uni-heidelberg.de/) [936,938,939,992]. We preselected targets predicted by at least 3 databases for both Rattus norvegicus and Homo sapiens, and also found downregulated by the RNA sequencing analysis as compared to the differentiation vehicle control and miR-NC conditions. We checked by a PubMed search ("mRNA name + oligodendrocyte") if these were involved accordingly in OPC differentiation, *i.e.* if their downregulation could explain the effect of the microRNA, or checked if they were listed in the gene annotations of downregulated Gene Ontology/Biological Process terms of interest.

### vii. Statistical Analysis

We used Graphpad Prism 8.0.2 for all statistical analyses. Outliers identified by Grubb's test were excluded (max 1/condition). Normality was verified by the D'Agostino & Pearson test, and a parametric (ordinary or Brown-Forsythe in case of significantly different standard deviations) or a non-parametric (Kruskal-Wallis) one-way ANOVA was performed accordingly. Dunnett's (parametric analysis) and Dunn's (non-parametric analysis) multiple comparison post-tests were used to compare all conditions to the differentiation vehicle control or the differentiation miR-NC, Sidak's, Tamhane's T2 or Dunn's multiple comparisons post-test was used as recommended to compare the mimic condition to its inhibitor. A non-parametric Mann-Whitney U-test, was performed for the statistical analysis of the relative expression of endogenous microRNAs between the proliferation and differentiation control conditions. For plots built in R, we used the packages "cowplot", "gplots", "ggplot2", "grid", "gridExtra", "patchwork", and "stringr".

## IV. Results

### i. microRNA mimics affect the differentiation of CG-4 cells

We have previously identified 21 microRNAs dysregulated in the cerebrospinal fluid, serum and/or peripheral blood mononuclear cells of relapsing and/or remitting MS patients as compared to symptomatic/healthy controls [892]. Therefore, we aimed to investigate whether these microRNAs could affect the differentiation of OPCs, using the CG-4 cell line. The microRNAs were chosen based on the strength of their dysregulation or their uniqueness in the setting of MS. As a preliminary screening, CG-4 cells were transfected on day 0 and day 4 separately with one of the 13 microRNA mimics (miR-15a-3p, miR-20a-5p, miR-29c-3p, miR-33-3p, miR-34a-5p, miR-34c-5p, miR-124-5p, miR-145-5p, miR-146a-5p, miR-155-5p, miR-181c-5p, miR-214-3p, miR-297) and cultured in the differentiation medium from day 1 until day 6. We used miR-219a-5p as a positive control of differentiation, as well as the negative control microRNA mimic (miR-NC). Most of these microRNAs significantly reduced the expression of the differentiation markers myelin basic protein *(Mbp)* and proteolipid protein 1 *(Plp1)* at the mRNA level. miR-214-3p was

the only microRNA that increased their expression but to a lower extent than miR-219a-5p (figure 3.2, supplementary figure 3.1).

*Figure 3.2: The effect of 13 microRNA mimics on the differentiation of CG-4 cells in RT-qPCR (screening)*

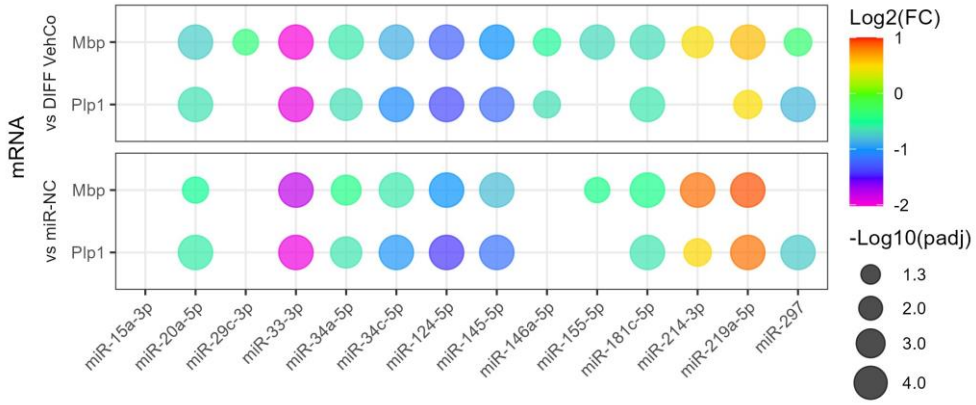


*This dot plot shows the fold change (FC) of the relative expression of the differentiation markers Mbp and Plp1 to the differentiation vehicle control (DIFF VehCo) and the microRNA mimic negative control (miR-NC) resulting from the double transfection of each microRNA mimic, as labelled on the x-axis, in CG-4 cells in differentiation culture conditions. The colour of each dot represents the fold change (expressed in logarithm base 2 [Log2(FC)]) of the relative expression, scaled by the rainbow colour gradient from -2 to 1, and its size represents the adjusted p-value (padj) (expressed as minus logarithm base 10 [-Log10(padj)]) as indicated in the plot legend. The adjusted p-value was calculated by Tukey's multiple comparison test, as recommended following a parametric one-way ANOVA on each microRNA separately with both controls. Only the significant data is depicted. -Log10(padj) ≥ 1.3 corresponds to the significance level of p ≤ 0.05, -Log10(padj.) of 2.0 corresponds to p = 0.01, -Log10(padj.) of 3.0 to p = 0.001, -Log10(padj.) of 4.0 to p = 0.0001. Data of 3 experiments for each microRNA with each condition in triplicate*.

From here on, we decided to focus on the microRNA species reducing the expression of the differentiation markers by at least a factor 2 as compared to the differentiation vehicle control, i.e. miR-33-3p, miR-34c-5p, miR-124-5p, and miR-145-5p. miR-214-3p was also selected as it was the only microRNA significantly

increasing the expression of *Plp1* and *Mbp*, although by less than a factor 2. We used a simplified protocol with a single transfection followed by 48h culture in the differentiation medium. We further aimed to stage each of the transfected cells by measuring the relative expression of several OPC/OL markers (figure 3.3, supplementary figure 3.2) [489]. miR-33-3p, miR-34c-5p, miR-124-5p and miR-145-5p significantly downregulated the expression of mature OL markers - myelin regulatory factor *(Myrf)*, *Plp1*, *Mbp,* and myelin associated oligodendrocyte basic protein *(Mobp)* - as compared to the differentiation vehicle control and miR-NC, except for *Mbp* with miR-34c-5p and miR-145-5p when compared to miR-NC. miR-33-3p was the strongest inhibitor for all markers, except *Myrf*. On the contrary, miR-214-3p promoted CG-4 differentiation, remarkably to an even greater extent than miR-219a-5p, as seen by the significant upregulation of these markers (figure 3.3, supplementary figure 3.2).

Interestingly, these microRNAs affected the differentiation already at an early premyelinating stage, as seen by the significant downregulation of transcription factor 7 like 2 *(Tcf7l2)* and 2',3'-cyclic nucleotide 3'phosphodiesterase *(Cnp)* by miR-33-3p and miR-124-5p, and their upregulation by miR-214-3p vs. both controls, while miR-34c-5p significantly downregulated *Tcf7l2* only. The OPC marker, inhibitor of DNA binding 4 *(Id4)* was significantly upregulated by miR-33-3p, miR-34c-5p, miR-124-5p and miR-NC as well vs. the differentiation vehicle control and significantly downregulated by miR-214-3p and miR-219a-5p vs. miR-NC. Moreover, miR-214-3p significantly increased the expression of oligodendrocyte transcription factor 2 *(Olig2)*, that is involved in oligodendroglial specification, highly expressed in myelinating OLs and sufficient to promote OPC differentiation by inducing SRY-box transcription factor 10 (Sox10) and other differentiation genes through chromatin remodelers (figure 3.3, supplementary figure 3.2) [540,993,994]. Given the bipotentiality of CG-4 progenitor cells that can differentiate into type-2 astrocytes or mature OLs, depending on the culture medium, we explored this axis as well and found that miR-124-5p increased and miR-219a-5p decreased the expression of glial fibrillary acidic protein *(Gfap)*, while cultured in the OL-differentiation medium (figure 3.3, supplementary figure 3.2).

*Figure 3.3: The effect of 5 microRNA mimics on the differentiation of CG-4 cells in RT-qPCR (confirmation)*

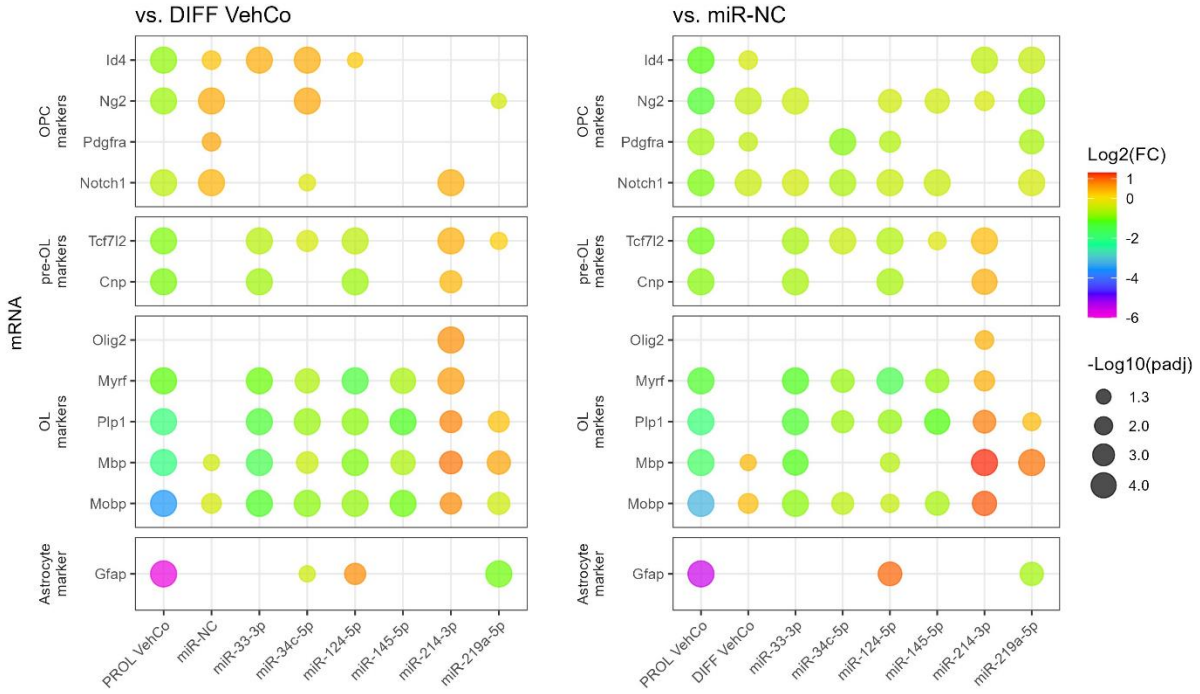


*This dot plot shows the fold change (FC) of the relative expression of several OPC, pre-OL, OL and astrocyte markers as labelled on the y-axis, to the differentiation vehicle control (DIFF VehCo) and the microRNA mimic negative control (miR-NC), resulting from the single transfection of each microRNA mimic, as labelled on the x-axis, in CG-4 cells in differentiation culture conditions, as well as the proliferation vehicle control (PROL VehCo). The colour of each dot represents the fold change (expressed in logarithm base 2 [Log2(FC)]) of the relative expression, scaled by the rainbow colour gradient from -6 to 1, and its size represents the adjusted p-value (padj) (expressed as minus logarithm base 10 [-Log10(padj)]) as indicated in the plot legend. The adjusted p-value was calculated by Dunn's or Dunnett's multiple comparison test to each control separately, i.e. the differentiation vehicle control and miR-NC, as recommended following a parametric/nonparametric one-way ANOVA on all conditions. Only the significant data is depicted. -Log10(padj) ≥ 1.3 corresponds to the significance level of p ≤ 0.05, -Log10(padj.) of 2.0 corresponds to p = 0.01, -Log10(padj.) of 3.0 to p = 0.001, -Log10(padj.) of 4.0 to p = 0.0001. Data of 3 experiments with each condition in triplicate. OPC = oligodendrocyte progenitor cells, pre-OL = premyelinating oligodendrocytes, OL = oligodendrocytes.*

Hereafter, we phenotypically characterised the transfected CG-4 cells at the protein level by immunocytochemistry. Cells transfected with miR-33-3p, miR-34c-5p and miR-124-5p tended to show a higher proportion of A2B5$^{+}$ cells, a progenitor cell marker, as compared to the differentiation vehicle control. A trend towards a higher proportion of O4$^{+}$ cells, an early differentiation marker, was observed in miR-214-3p-transfected cells (figure 3.4A-B) [995]. miR-33-3p, miR-34c-5p, miR-124-5p and miR-145-5p did not affect O4-positivity as compared to the differentiation vehicle control but tended to decrease the proportion of Mbp-expressing cells, while miR-214-3p tended to increase it (figure 3.4B-C). None of these differences reached the statistical significance level. Finally, miR-124-5p transfected cells expressed significantly more Gfap, based on a visual score (figure 3.4D).

*Figure 3.4: The effect of 5 microRNA mimics on the differentiation of CG-4 cells in immunocytochemistry*

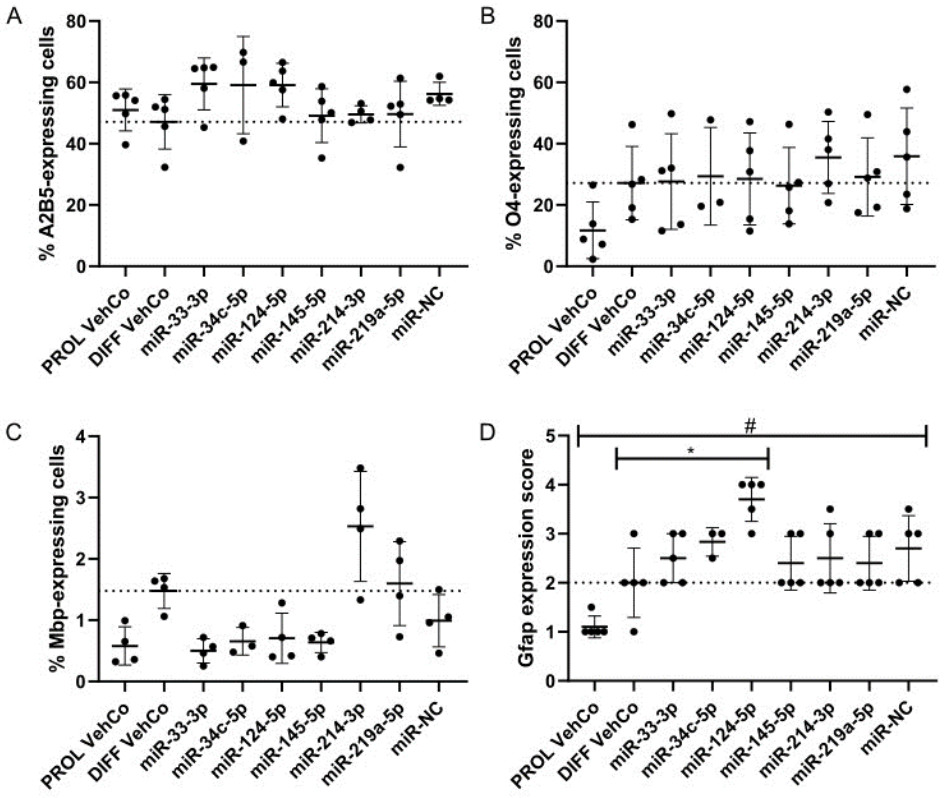

*The plots show the percentage of cells expressing (A) the OPC marker A2B5, (B) the early differentiation marker O4 and (C) the late differentiation marker Mbp, as well as (D) the score of Gfap expression (mean with SD), calculated (A-B-C)/estimated (D) to the total number of cells (based on the detections of the nucleus), resulting from the single transfection of each microRNA mimic (as labelled on the x-axis) in CG-4 cells in differentiation culture conditions, as well as the proliferation vehicle control (PROL VehCo). The score for Gfap expression ranges from 0 = none to 5 = abundant (namely 0 = no Gfap-positive ($Gfap^+$) cells, 1 = a few $Gfap^+$ cells on the whole coverslip, 2 = a few $Gfap^+$ cells in a few grids of the coverslip, 3 = a few $Gfap^+$ cells in several grids of the coverslip, 4 = many $Gfap^+$ cells in several grids of the coverslip, 5 = many $Gfap^+$ cells on the whole coverslip). The dotted line represents the mean value of the differentiation vehicle control. One-way ANOVA on all conditions was not significant, except for Gfap: adjusted p-value = 0.0148 (*) for miR-124-5p vs. the differentiation vehicle control, and adjusted p-value = 0.0261 (#) for PROL VehCo vs miR-NC on Dunn's multiple comparison test. Data of 3-5 experiments, in single replicate for each experimental and staining condition within each experiment. OPC = oligodendrocyte progenitor cells, SD = standard deviation*.

From these results at mRNA and protein level, we can thus conclude that miR-33-3p, miR-34c-5p, miR-124-5p and miR-145-5p impeded to a certain extent the differentiation of CG-4 cells into more mature OLs by retaining the cells within a late progenitor (miR-33-3p, miR-34c-5p, miR-124-5p) - early premyelinating (miR-145-5p) stage, while miR-214-3p induced their differentiation to a further stage.

### ii. microRNA inhibitors antagonise their corresponding exogenous microRNA in differentiating CG-4 cells

In order to verify the specificity of the microRNA mimics, we sought to counter their effect by transfecting the cells first with the microRNA mimic, followed by a second transfection with the respective microRNA inhibitor. This was compared to the transfection of the mimic followed by a mock transfection (without its inhibitor), which yielded, similarly to the single transfection, the expected dysregulation of *Id4*, *Myrf*, *Plp1*, *Mbp* and *Mobp* for all microRNAs when compared to the differentiation vehicle control, reaching the significance level for all except for miR-34c-5p on *Myrf*. On the other hand, the microRNA inhibitors significantly antagonised the effect of their corresponding exogenous microRNA on the

expression of 3 to 4 of these markers, depending on the microRNA species (figure 3.5, supplementary figure 3.3).

*Figure 3.5: The effect of 5 microRNA mimics and their inhibitors on the differentiation of CG-4 cells in RT-qPCR*

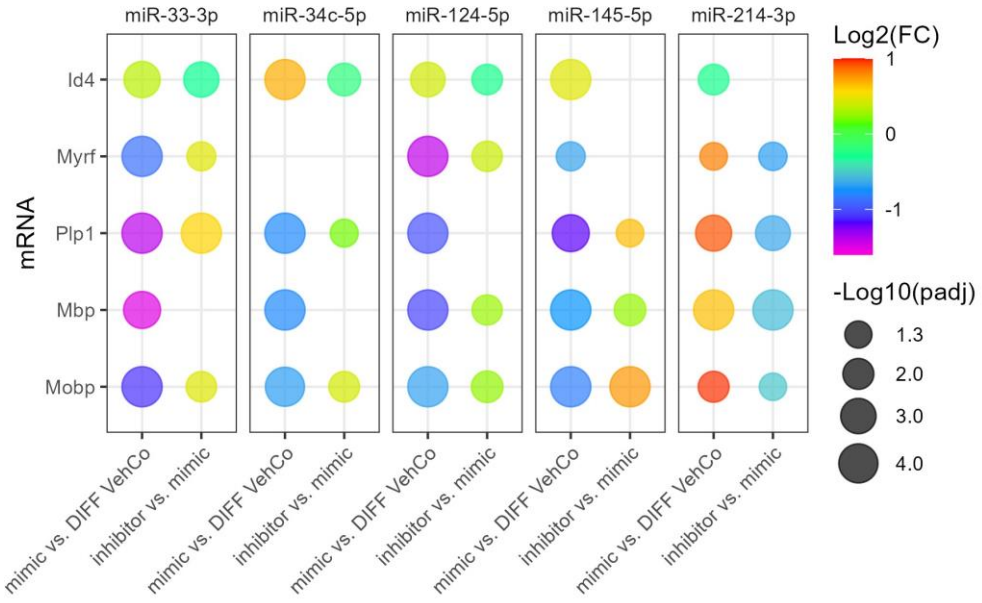


*This dot plot shows the fold change (FC) of the relative expression of the OPC marker (Id4) and OL markers (Myrf, Plp1, Mbp, and Mobp) as labelled on the y-axis, resulting from the sequential transfection of each microRNA mimic followed or not by its inhibitor in CG-4 cells in differentiation culture conditions. For each microRNA mimic the fold change was calculated to the differentiation vehicle control (DIFF VehCo), while for each microRNA inhibitor it was calculated to its corresponding microRNA mimic, as labelled on the x-axis. The colour of each dot represents the fold change (expressed in logarithm base 2 [Log2(FC)]) of the relative expression, scaled by the rainbow colour gradient from -1.6 to 1, and its size represents the adjusted p-value (padj) (expressed as minus logarithm base 10 [-Log10(padj)]) as indicated in the plot legend. The adjusted p-value was calculated by Dunn's or Dunnett's multiple comparison test of each condition to the differentiation vehicle control and by Sidak's, Tamhane's T2 or Dunn's multiple comparison test between the mimic and its inhibitor, as recommended following a parametric/nonparametric one-way ANOVA on all conditions, including the proliferation vehicle control (not shown). Only the significant data*

*is depicted. -Log10(padj) ≥ 1.3 corresponds to the significance level of p ≤ 0.05, -Log10(padj.) of 2.0 corresponds to p = 0.01, -Log10(padj.) of 3.0 to p = 0.001, -Log10(padj.) of 4.0 to p = 0.0001. Data of 3 experiments for each microRNA with each condition in triplicate. OPC = oligodendrocyte progenitor cells, OL = oligodendrocytes.*

iii. The endogenous microRNA expression is partially consistent with their effect on CG-4 cell differentiation

We verified the endogenous microRNA expression in CG-4 cells cultured for 24h in the proliferation medium followed by an additional 48h in either proliferation or differentiation medium. While miR-33-3p was not significantly dysregulated, miR-34c-5p and miR-124-5p were significantly downregulated in differentiating CG-4 cells. miR-145-5p was upregulated under differentiation culture conditions, which is inconsistent with the observed effect of the microRNA mimic, and miR-214-3p was undetectable in both conditions (figure 3.6A). miR-124-5p and miR-145-5p were moreover the least abundant, as evidenced by their higher ΔCt, with miR-103a-3p as reference (figure 3.6B).

*Figure 3.6: Endogenous microRNAs in proliferating and differentiating CG-4 cells*

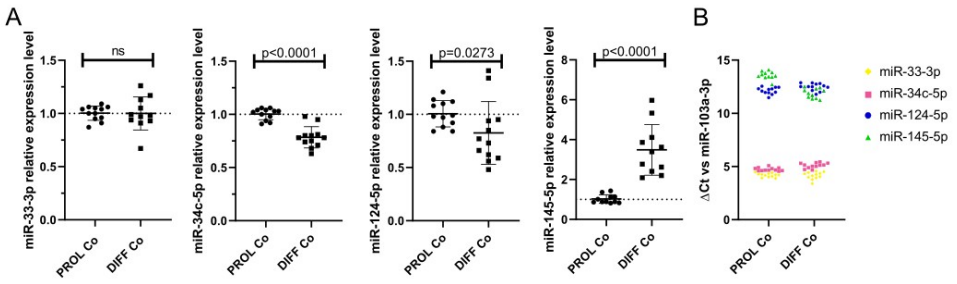


*The plots show (A) the relative expression in RT-qPCR (mean with SD of $2^{-\Delta\Delta Ct}$) of each endogenous microRNA in CG-4 cells cultured in the proliferation or differentiation medium, as well as (B) the ΔCt of each microRNA with miR-103a-3p as reference (ΔCt = Ct(target microRNA)$_{sample}$ – Ct(reference miR-103a-3p)$_{sample}$), which is representative of the relative abundance of each microRNA. Each colour in (B) corresponds to a microRNA species as indicated in the plot legend. The p-value (p) was calculated by a Mann-Whitney U-test, ns*

*for not significant. Data of 4 experiments with each condition in triplicate. PROL Co = proliferation control, DIFF Co = differentiation control, SD = standard deviation.*

iv. RNA sequencing reveals the changes of cell fate directed by each microRNA

RNA sequencing was performed on all conditions in triplicates. One miR-NC replicate was excluded from the final analysis as it appeared to be an outlier masking the effects of the other conditions (see Methods). Principal component analysis (PCA), performed on the gene expression value (Fragments Per Kilobase Million [FPFM]) of all samples, segregated well the different conditions, especially miR-33-3p, miR-124-5p, and miR-214-3p from the differentiation vehicle control and miR-NC conditions, and the proliferation vehicle control was distinctly segregated from all other conditions (figure 3.7A). The first and second principal components covered respectively only 38.06 % and 10.95% of the conditions' variance. The gene expression, illustrated by the heatmap, was partially different between the microRNAs and the controls (figure 3.7B). In accordance with the PCA analysis, miR-145-5p clustered the closest to the differentiation vehicle control and miR-33-3p the furthest.

The significant dysregulation, vs. the differentiation vehicle control and miR-NC, induced by each microRNA on genes involved in the different stages of OPC-to-OL differentiation is illustrated in figure 3.8 [489]. These differentially expressed genes (DEG) evidenced the upregulation of OPC markers nestin (*Nes*) and/or *Id4* and the downregulation of premyelinating OL (pre-OL) markers NK2 homeobox 2 (*Nkx2-2*), *Tcf7l2, Cnp* and G protein-coupled receptor 17 *(Gpr17)* and of mature OL markers (*Plp1, Myrf, Mbp, Mobp*, myelin associated glycoprotein *[Mag],* myelin oligodendrocyte glycoprotein *[Mog]*) by miR-33-3p, miR-34c-5p miR-124-5p and miR-145-5p, although the downregulation of the pre-OL markers by miR-145-5p was less pronounced, especially vs. miR-NC (figure 3.8). The opposite dysregulation of these markers was driven by miR-214-3p.

*Figure 3.7: The effect of 5 microRNA mimics on the differentiation of CG-4 cells in RNA sequencing (clustering)*

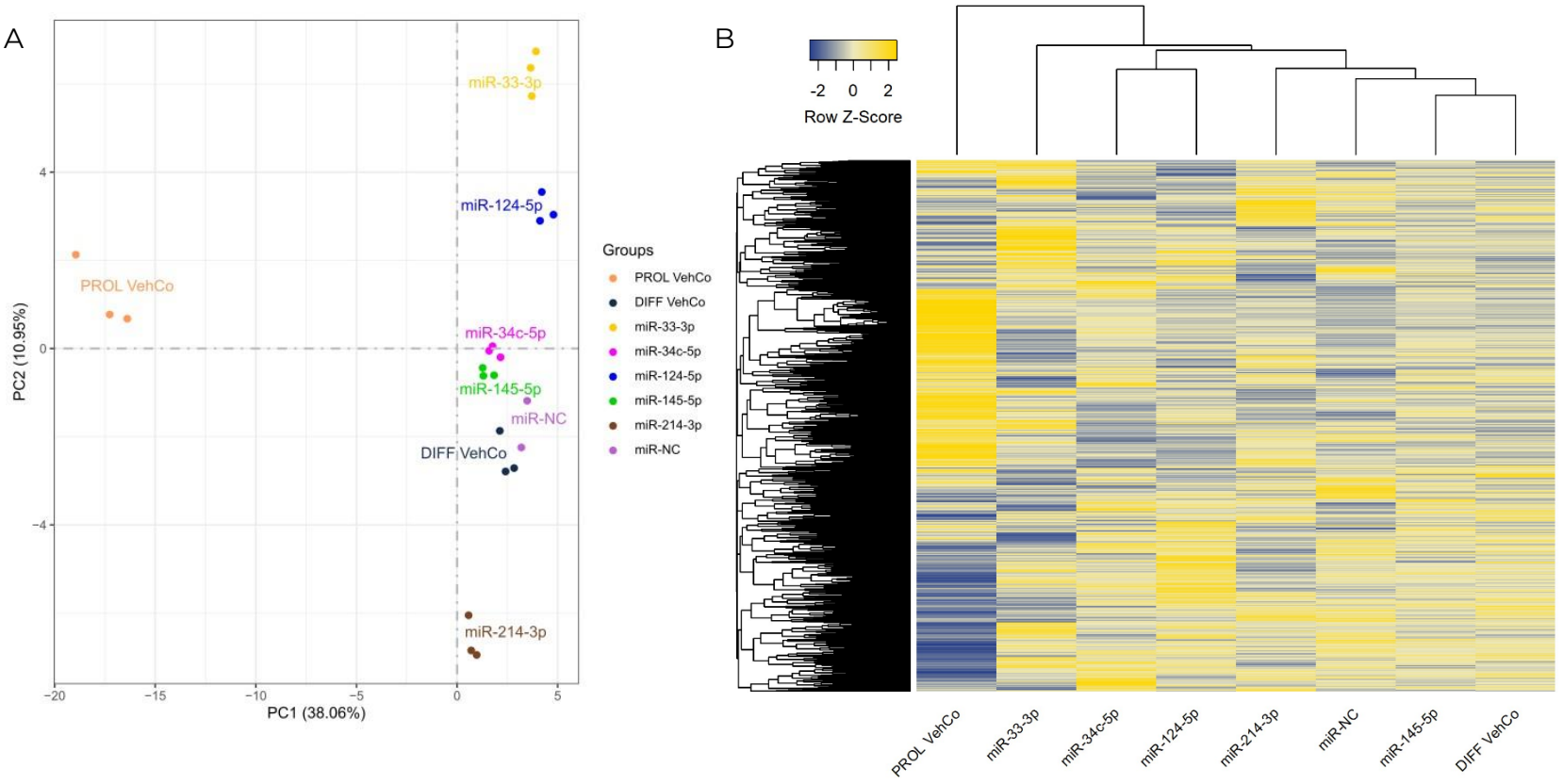

*(A) Principal component analysis was performed on the gene expression value (Fragments Per Kilobase Million [FPKM]) of all samples. In this plot, each sample is dispersed to the first and second principal component (PC1/2). The colour of the dots corresponds to the microRNA species and controls as indicated in the plot legend. (B) The heatmap shows the cluster analysis horizontally on the row-wise homogenised gene expression value (z-score of FPKM, represented by the blue-to-yellow colour gradient from -2 to 2) and vertically on the different experimental conditions as labelled at the bottom of the heatmap. Data of 1 experiment with each condition in triplicate, except microRNA negative control (miR-NC) in duplicate. PROL VehCo = proliferation vehicle control, DIFF VehCo = differentiation vehicle control.*

Interestingly, miR-33-3p and miR-124-5p induced the expression of several astrocyte markers, as aldolase fructose-bisphosphate C *(Aldoc),* glutamic-pyruvic transaminase 2 (*Gpt2*) and nebulette (*Nebl*). Immature astrocyte markers, vimentin (*Vim*) and *Gfap*, were upregulated by miR-124-5p but downregulated by miR-33-3p [364,996]. All, except *Gpt2*, were downregulated by miR-214-3p as well (figure 3.8). Finally, proliferating cell nuclear antigen (*Pcna*), an auxiliary protein regulating DNA replication/repair, cell cycle control etc and hence a marker of the early G1 and S phase of the cell cycle, was downregulated by miR-33-3p and miR-124-5p in RNA sequencing but upregulated by miR-34c-5p, as compared to the differentiation vehicle control (figure 3.8) [997].

*Figure 3.8: The effect of 5 microRNA mimics on the differentiation of CG-4 cells in RNA sequencing (staging)*

*This dot plot shows the fold change (FC) of the gene expression value of several proliferation, OPC, pre-OL, OL and astrocyte markers, as labelled on the y-axis, to the differentiation vehicle control (DIFF VehCo) and the microRNA mimic negative control (miR-NC), resulting from the single transfection of each microRNA mimic, as labelled on the x-axis, in CG-4 cells in differentiation culture conditions. The colour of each dot represents the fold change (expressed in logarithm base 2 [Log2(FC)]) of the relative expression, scaled by the rainbow colour gradient from -1.7 to 1.3, and its size represents the adjusted p-value (padj) (expressed as minus logarithm base 10 [-Log10(padj)]) as indicated in the plot legend. Only the significant data is depicted. -Log10(padj) ≥ 1.3 corresponds to the significance level of p ≤ 0.05. The adjusted p-value ranges up to approximately 10-220 for certain targets. Data of 1 experiment with each condition in triplicate, except miR-NC in duplicate.*

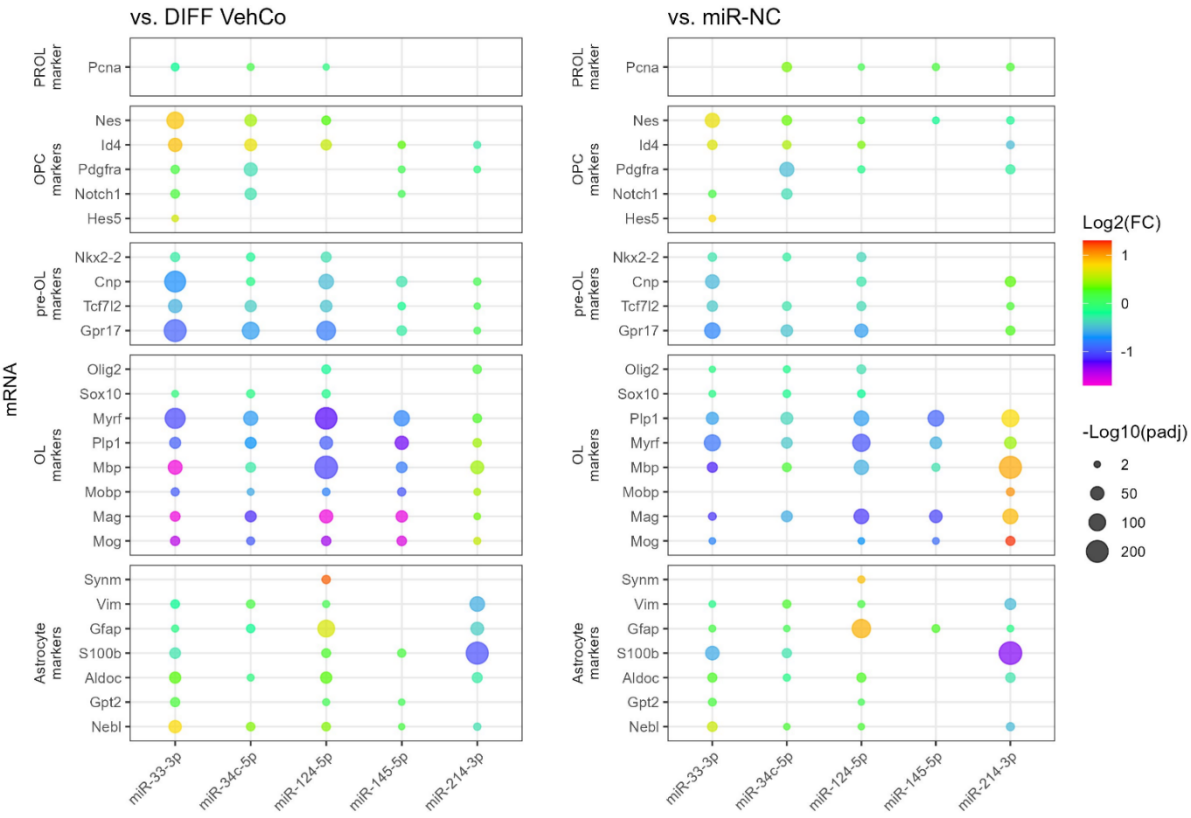


*PROL = proliferation, OPC = oligodendrocyte progenitor cells, pre-OL = premyelinating oligodendrocytes, OL = oligodendrocytes.*

We comprehensively compared the gene enrichment analysis of each microRNA vs. both the differentiation vehicle control and miR-NC conditions within Gene Ontology (GO)/Biological Process (figure 3.9). OPC differentiation and myelination were supported by miR-214-3p, but countered by miR-33-3p, miR-34c-5p, miR-124-5p and miR-145-5p. The GO term "oligodendrocyte differentiation" was however upregulated by miR-33-3p vs. the differentiation vehicle control, although genes annotated to this GO term support OPC rather than OL physiology, such as *Notch1*, Hes family BHLH transcription factor *(Hes) 1, Hes5, Id2, Id4,* and Leucine rich repeat and immunoglobulin domain containing 1 *(Lingo1)*. Note that the GO term "myelination" was not significantly dysregulated by miR-214-3p vs. the differentiation vehicle control, neither by miR-34c-5p vs. miR-NC. Additionally,

astrocyte differentiation and glial cell differentiation with annotated genes rather linked to astrocytic physiology were upregulated by miR-33-3p and/or miR-124-5p, but downregulated by miR-34c-5p and miR-214-3p. miR-33-3p upregulated signalling pathways involved in OPC/OL physiology, either in its proliferation (i.e. Wnt, Notch signalling pathway) or in both its proliferation and differentiation (i.e. mitogen-activated protein kinase (MAPK) and p38MAPK cascade [645]); as well as the platelet derived growth factor (Pdgfr) (proliferation) and extracellular signal-regulated kinase (ERK) and phosphoinositide-3-kinase (PI3K) (proliferation/differentiation [509,998]) signalling pathways, but also the negative regulation of these signalling pathways, when compared to the differentiation vehicle control only. The other microRNAs affected fewer signalling pathways. miR-34c-5p downregulated the Wnt signalling pathway, while miR-124-5p induced the Notch signalling pathway and ERK cascade. miR-145-5p downregulated Ras protein signal transduction, and miR-214-3p downregulated the "negative regulation of ERBB signalling pathway" (epidermal growth factor receptor (Egfr) tyrosine kinase family), both involved in differentiation.

Lipid metabolism was barely affected vs. miR-NC, except for miR-214-3p that downregulated phospholipid/glycerolipid metabolism vs. both controls. Conversely, as compared to the differentiation vehicle control only, lipid metabolism was curtailed by miR-33-3p at the level of fatty acid, phospholipid and cholesterol biosynthesis, by miR-34c-5p at the level of triglyceride/glycerolipid biosynthesis and phospholipid/cholesterol metabolism, and by miR-214-3p at the level of lipid/fatty acid catabolism and lipid/cholesterol storage, while miR-124-5p supported lipid/sterol transport.

Energy metabolism was affected by miR-33-3p and miR-214-3p vs. the differentiation vehicle control, but supported by miR-34c-5p, miR-124-5p and miR-145-5p vs miR-NC, as seen by the dysregulation of oxidative phosphorylation, aerobic respiration, ATP biosynthesis and the generation of precursor metabolites. The energy homeostasis appeared however still safeguarded with miR-33-3p. miR-214-3p reduced autophagy and cell death in response to oxidative stress as well, while GO terms within autophagy and apoptosis were less consistent vs. both controls for the other microRNAs.

Cell cycle processes (cell division and cell cycle transition) were upregulated by all microRNAs vs. miR-NC, but only by miR-34c-5p vs. the differentiation vehicle

control and downregulated by miR-124-5p. Remarkably, the cyclin-dependent protein kinase activity was upregulated by miR-34c-5p vs. both controls. miR-33-3p impeded DNA biosynthesis, replication and repair as well as telomere maintenance and supported the cell cycle transition only until G1/S phase vs. the differentiation vehicle control. Regarding gene expression, miR-145-5p and miR-214-3p supported (m)RNA processing and splicing vs. both controls while miR-124-5p downregulated these vs. the differentiation vehicle control only. Furthermore, miR-145-5p supported the negative regulation of (m)RNA processing and splicing and miR-214-3p negatively regulated translation and increased gene silencing vs. the differentiation vehicle control.

---

*Figure 3.9: The effect of 5 microRNA mimics on the differentiation of CG-4 cells in RNA sequencing (Gene Ontology enrichment)*

*This dot plot shows the significant down- and upregulated Gene Ontology (GO) terms within Biological Process for each microRNA to the differentiation vehicle control (DIFF VehCo) and the microRNA mimic negative control (miR-NC). The GO terms have been grouped by classes of biological processes as labelled on the right side of the plot. The gene ratio, which is the number of genes annotated to the GO term divided by the total number of down-/upregulated genes in the condition, is depicted on the x-axis, positively for upregulated GO terms, negatively for downregulated GO terms, separated by the vertical dotted line. The colour of the dots corresponds to the microRNA species, the transparency to the absolute gene count and the size to the adjusted p-value (expressed as minus logarithm base 10 [-Log10(padj)]) as indicated in the plot legend. Data of 1 experiment with each condition in triplicate, except miR-NC in duplicate.*


vs. DIFF VehCo
vs. miR-NC
DOWN
UP
GO Term
Wnt signaling pathway
negative regulation of Wnt signaling pathway
Notch signaling pathway
neurotrophin signaling pathway
platelet-derived growth factor receptor signaling pathway
response to platelet-derived growth factor
ERBB signaling pathway
negative regulation of ERBB signaling pathway
regulation of Rac protein signal transduction
Ras protein signal transduction
Rho protein signal transduction
JNK cascade
ERK1 and ERK2 cascade
negative regulation of ERK1 and ERK2 cascade
negative regulation of MAPK cascade
positive regulation of MAPK cascade
p38MAPK cascade
phosphatidylinositol 3-kinase signaling
negative regulation of phosphatidylinositol 3-kinase signaling
regulation of cyclin-dependent protein kinase activity
insulin receptor signaling pathway
Cell signaling
regulation of timing of cell differentiation
astrocyte differentiation
oligodendrocyte differentiation
negative regulation of oligodendrocyte differentiation
glial cell differentiation (OL)
glial cell differentiation (OPC/astrocyte)
negative regulation of glial cell differentiation
myelination
myelin assembly
myelin maintenance
Cell differentiation
regulation of lipid metabolic process
negative regulation of lipid metabolic process
positive regulation of lipid metabolic process
lipid catabolic process
lipid storage
regulation of lipid transport
fatty acid metabolic process
fatty acid elongation
fatty acid catabolic process
very long-chain fatty acid biosynthetic process
regulation of triglyceride biosynthetic process
(regulation of) phospholipid biosynthetic/metabolic process
glycerolipid metabolic/biosynthetic process
cholesterol metabolic/biosynthetic process
positive regulation of cholesterol efflux
cholesterol storage
Lipid metabolism
energy homeostasis
generation of precursor metabolites and energy
glucose homeostasis
glucose metabolic process
glucose catabolic process
pyruvate metabolic process
aerobic respiration
oxidative phosphorylation
fatty acid beta-oxidation
ATP biosynthetic process
Energy metabolism
autophagy
organelle disassembly
negative regulation of protein catabolic process
positive regulation of protein catabolic process
intrinsic apoptotic signaling pathway
negative regulation of intrinsic apoptotic signaling pathway
cell death in response to oxidative stress
(regulation of) necrotic cell death
Cell catabolism
DNA biosynthetic process
DNA replication
DNA repair
chromosome segregation
mitotic spindle organization
telomere maintenance
cytokinesis
cell division
cell cycle checkpoint
mitotic cell cycle phase transition
negative regulation of mitotic cell cycle phase transition
G1 to G0 transition
G1/S transition of mitotic cell cycle
negative regulation of G1/S transition of mitotic cell cycle
G2/M transition of mitotic cell cycle
metaphase/anaphase transition of mitotic cell cycle
negative regulation of mitotic metaphase/anaphase transition
Cell cycle
gene silencing
transcription by RNA polymerase I
ribosome biogenesis
mRNA processing
negative regulation of mRNA processing
mRNA catabolic process
negative regulation of mRNA catabolic process
mRNA stabilization
RNA splicing
negative regulation of RNA splicing
ribonucleoprotein complex assembly
mRNA-containing ribonucleoprotein complex export from nucleus
cytoplasmic translation
negative regulation of translation
Gene expression
-0.05
0.00
0.05
0.10
GeneRatio
Count
2
50
100
150
miR ID
miR-33-3p
miR-34c-5p
miR-124-5p
miR-145-5p
miR-214-3p
-Log10(padj)
1.3
5.0
15.0
30.0

In conclusion, the RNA sequencing data supported our results obtained by RT-qPCR on independent experiments, phenotyping miR-33-3p, miR-34c-5p and miR-124-5p transfected cells as late OPCs while miR-33-3p and miR-124-5p induced to a certain extent some astrocytic features as well. miR-145-5p transfected cells shifted closer to a pre-OL stage. All of these inhibited OPC differentiation and myelination, which was also supported by the decrease of the metabolism of different lipid species by both miR-33-3p and miR-34c-5p. miR-33-3p restrained DNA biosynthesis and energy metabolism, and miR-34c-5p sustained cell division while miR-124-5p prevented cell cycle and gene expression as compared to the differentiation vehicle control. GO enrichment analysis was overall poorer for miR-145-5p, but it downregulated Ras protein signal transduction. On the contrary, miR-214-3p promoted OPC differentiation into a mature OL phenotype, although it affected energy and lipid metabolism, but it orchestrated Erbb signalling.

v. Several predicted mRNA targets possibly support the effect of each microRNA on OPC differentiation

In order to identify potential targets of each microRNA, we crossed the data of the in silico analysis and RNA sequencing and verified their corresponding involvement in OPC differentiation by a PubMed search. For each microRNA, we identified 2 to 7 potential targets that were also significantly downregulated in the RNA sequencing (vs. differentiation vehicle control and miR-NC) (supplementary table 3.2A). Their dysregulation by the other microRNAs was variable (data not shown). Interestingly, among these, Bcl2 interacting protein 3 like *(Bnip3l),* neurotrophic receptor tyrosine kinase 2 *(Ntrk2)* and *Rab10,* a member of the Ras oncogene family, for miR-33-3p, heterogeneous nuclear ribonucleoprotein F *(Hnrnpf)* for miR-124-5p, *Myrf* for miR-145-5p and Erbb receptor feedback inhibitor 1 *(Errfi1)* for miR-214-3p were also genes annotated to downregulated GO terms of interest (supplementary table 3.2B). This latter strategy offered more potential targets verified in silico, of which engulfment and cell motility 1 *(Elmo1)* for miR-145-5p, A-kinase anchoring protein 13 *(Akap13)*, cytoplasmic polyadenylation element binding protein 1 (Cpeb1) and protein tyrosine phosphatase receptor type J (Ptprj) for miR-214-3p (supplementary table 2B). Regarding miR-34c-5p, Notch receptor 1 *(Notch1)* and platelet derived growth factor receptor A (*Pdgfra)* were predicted by both strategies. However, this was not in favour of the phenotype observed in miR-

34c-5p-transfected CG-4 cells, as both Notch1 and Pdgfra support OPC proliferation and are expected to decrease during differentiation. Their downregulation by miR-34c-5p was verified by RNA sequencing and RT-qPCR analysis on 3 independent experiments (figure 3.8, supplementary figure 3.4A).

Hereafter, we confirmed the downregulation of several targets by RT-qPCR on 3 independent experiments: *Bnip3l*, eukaryotic translation initiation factor 4E *(Eif4e), Rab10* (miR-33-3p), vesicle associated membrane protein 2 *(Vamp2)* (miR-34c-5), Ras related 2 *(Rras2)* (miR-34c-5p, miR-124-5p), *Hnrnpf* (miR-124-5p) *Myrf* and *Elmo1* (miR-145-5p) were significantly downregulated vs. both controls (figure 3.10A, supplementary figure 3.4A). Note that *Vamp2* and *Rras2* were predicted in silico by 3 databases in rats, but by only 2 or less in humans. For miR-34c-5p *Rras2* was not significantly downregulated vs. miR-NC in RNA sequencing, but it was on independent RT-qPCR analysis. Furthermore, on independent RT-qPCR analysis, *Ntrk2* (miR-33-3p), *Akap13*, *Cpeb1*, and *Errfi* (miR-214-3p) were significantly downregulated vs. miR-NC only, but their expression was also significantly upregulated by miR-NC vs. the differentiation vehicle control, except for *Ntrk2*. Notably, *Akap13* showed a tendency toward downregulation vs. the differentiation vehicle control (figure 3.10A, supplementary figure 3.4A). Finally, *Ptprj* (miR-214-3p) was not significantly downregulated vs. neither of the controls in RT-qPCR although it was in RNA sequencing (supplementary figure 3.4A)

The downregulation of these predicted targets was also corroborated by the sequential transfection of the microRNA mimic followed by a mock transfection, except for the miR-145-5p target *Elmo1* (supplementary figure 3.4B). However, only the expression of *Eif4e* and *Rab10* was significantly antagonised by the microRNA inhibitor as compared to the miR-33-3p mimic (figure 3.10B). For all the other investigated predicted targets, the microRNA inhibitor slightly, but non-significantly, tended to reverse or did not change the target's expression level vs. its corresponding mimic (supplementary figure 3.4B).

*Figure 3.10: Potential mRNA targets of each microRNA verified in RT-qPCR*

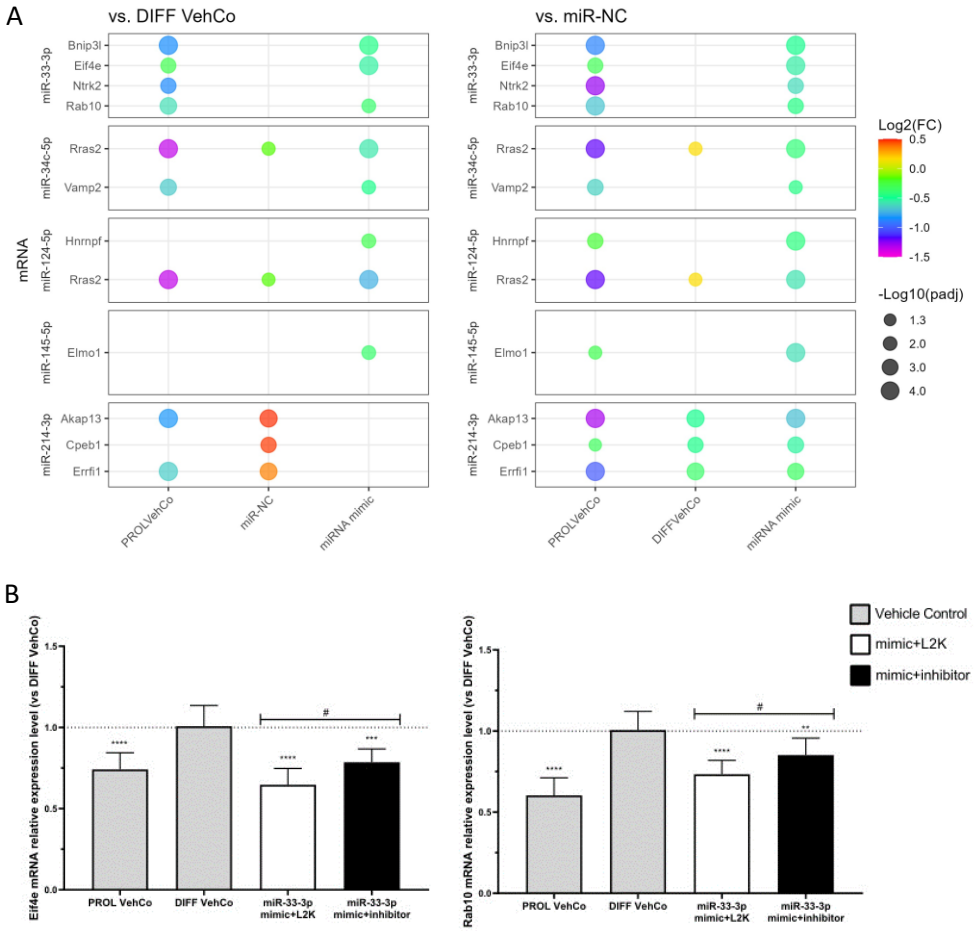


*(A) This dot plot shows the fold change (FC) of the relative expression of potential mRNA targets of each microRNA as labelled on the y-axis, to the differentiation vehicle control (DIFF VehCo) and the microRNA mimic negative control (miR-NC), resulting from the single transfection of each microRNA mimic in CG-4 cells in differentiation culture conditions, as well as the proliferation vehicle control (PROL VehCo). The colour of each dot represents the fold change (expressed in logarithm base 2 [Log2(FC)]) of the relative expression, scaled by the rainbow colour gradient from -1.5 to 0.5, and its size represents the adjusted p-value (padj) (expressed as minus logarithm base 10 [-Log10(padj)]) as indicated in the plot legend. The adjusted p-value was calculated by Dunn's or Dunnett's multiple comparison test to each control separately, i.e. the differentiation vehicle control and miR-NC, as recommended*

*following a parametric/nonparametric one-way ANOVA on all conditions. Only the significant data is depicted. -Log10(padj) ≥ 1.3 corresponds to the significance level of p ≤ 0.05, -Log10(padj.) of 2.0 corresponds to p = 0.01, -Log10(padj.) of 3.0 to p = 0.001, -Log10(padj.) of 4.0 to p = 0.0001. Data of 3 experiments with each condition in triplicate. (B) The plots show the relative expression (mean with SD of $2^{-\Delta\Delta Ct}$) of Eif4e and Rab10 to the differentiation vehicle control (DIFF VehCo, grey bar), resulting from the sequential transfection of miR-33-3p mimic followed (black bar) or not (white bar) by its inhibitor (as labelled on the x-axis) in CG-4 cells in differentiation culture conditions, as well as the proliferation vehicle control (PROL VehCo, grey bar). The dotted line represents the mean relative expression of the differentiation vehicle control to which the relative expression ($2^{-\Delta\Delta Ct}$) of each sample was calculated. The adjusted p-value was calculated by Dunnett's multiple comparison test to the differentiation vehicle control (*) and by Sidak's multiple comparison test between the microRNA mimic and its inhibitor (#), as recommended following a parametric one-way ANOVA on all conditions: */# for p ≤ 0.05, ** for p ≤ 0.01, *** for p ≤ 0.001, **** for p ≤ 0.0001. Data of 3 experiments with each condition in triplicate. L2K = Lipofectamine™ 2000, SD = standard deviation.*

## V. Discussion

We have investigated the effect of 13 microRNAs previously identified as dysregulated in relapsing and/or remitting MS [892] on the differentiation of an OPC cell line, called CG-4. Most of the screened microRNAs decreased OPC differentiation, while Dicer ablation in mice, which impedes microRNA maturation, markedly affects myelination, thereby suggesting that microRNAs would rather promote differentiation by inhibiting OPC proliferation [782,783,999]. We then focused on 5 microRNAs - miR-33-3p, miR-34c-5p, miR-124-5p, miR-145-5p, and miR-214-3p – that exhibited the strongest dysregulation of the differentiation markers. Interestingly, miR-33-3p, miR-34c-5p and miR-124-5p have not been investigated functionally in the scope of multiple sclerosis so far. Only miR-214-3p promoted OPC differentiation into more mature OLs, while the other 4 microRNAs arrested it, each to a different extent, at a late OPC (miR-33-3p, miR-34c-5p, miR-124-5p) - pre-OL (miR-145-5p) stage. We have further explored the phenotype of these CG-4 cells transfected with different microRNAs through the significant DEG and GO terms in RNA sequencing. We have identified several potential targets by in silico analysis,

that were also downregulated in RNA sequencing (DEG and/or GO terms) and confirmed some by RT-qPCR analyses on independent experiments. Their involvement in OPC differentiation is not known for all of them. Based on our data, we finally sought to propose mechanistical hypotheses for the observed effects (figure 3.11).

*Figure 3.11: Hypotheses on the mechanistical/functional involvement of each microRNA and its potential mRNA targets on OPC differentiation*

*We have evidenced that miR-33-3p, miR-34c-5p, miR-124-5p and miR-145-5p impede OPC differentiation, while miR-214-3p promotes it in CG-4 cells, an OPC cell line. Herein, we hypothesise that miR-33-3p (yellow) targets: (1) Eif4e, a translation initiation factor, part of the Eif4f complex, that once phosphorylated recognizes the mRNA 5'-terminal 7-methylguanosine (m7G) cap on OPC differentiation and myelin genes downstream PI3K/mTOR and ERK/MAPK signalling; (2) Rab10, a small GTPase involved in intracellular vesicle trafficking allowing plasma membrane elongation important for myelin ensheathment; (3) Bnip3l regulating mitochondrial function by mitophagy and (4) more hypothetically Ntrk2 upstream of the Ras/ERK/MAPK cascade [702,1000–1004]. miR-34c-5p possibly targets Vamp2 (pink), involved in intracellular vesicle targeting to the membrane, leading to its expansion, and potentially Rras2 (purple), a small GTPase involved in OPC differentiation by inducing ERK/MAPK and PI3K/Akt/mTOR signalling pathways. Rras2 is also a predicted target of miR-124-5p [998,1005–1007]. miR-124-5p is further predicted to target Hnrnpf (blue), a ribonucleoprotein that upon phosphorylation by Fyn tyrosine kinase within Mbp transport granules, releases Mbp mRNA, allowing its translation within the cellular processes and its local interaction with the cytoplasmic membrane leaflets inducing myelin compaction.[585,595] miR-145-5p (green) has already been proven to target Myrf, a key transcription factor of myelin genes, and possibly targets Elmo1 as well, an activator of Rac1, a small GTPase (which is itself induced by Fyn tyrosine kinase by integrin engagement) inducing morphological OPC differentiation by acting on actin organisation, or possibly via p21 activated kinase 1 (Pak1) [515,559,561,817,1008]. Finally, miR-214-3p (brown), the only microRNA of our study inducing OPC differentiation, hypothetically targets (1) Akap13, a scaffolder of protein kinase A (Pka) that inhibits mTORC1 and an inducer of RhoA (which is itself inhibited by Fyn but induced by Lingo1) that was found to inhibit OPC differentiation by favouring stress fibre formation and actin depolymerization, or potentially by inducing Pten, an inhibitor of PI3K/Akt/mTOR signalling; (2) Cpeb1, acting as a translational repressor until it is phosphorylated or degraded, with its consensus binding sequence on several OPC/OL-related genes; (3) Errfi1, an Erbb receptor feedback inhibitor, and (4) Ptprj, a protein tyrosine phosphatase, both inhibiting Erbb signalling that can be involved in OPC*

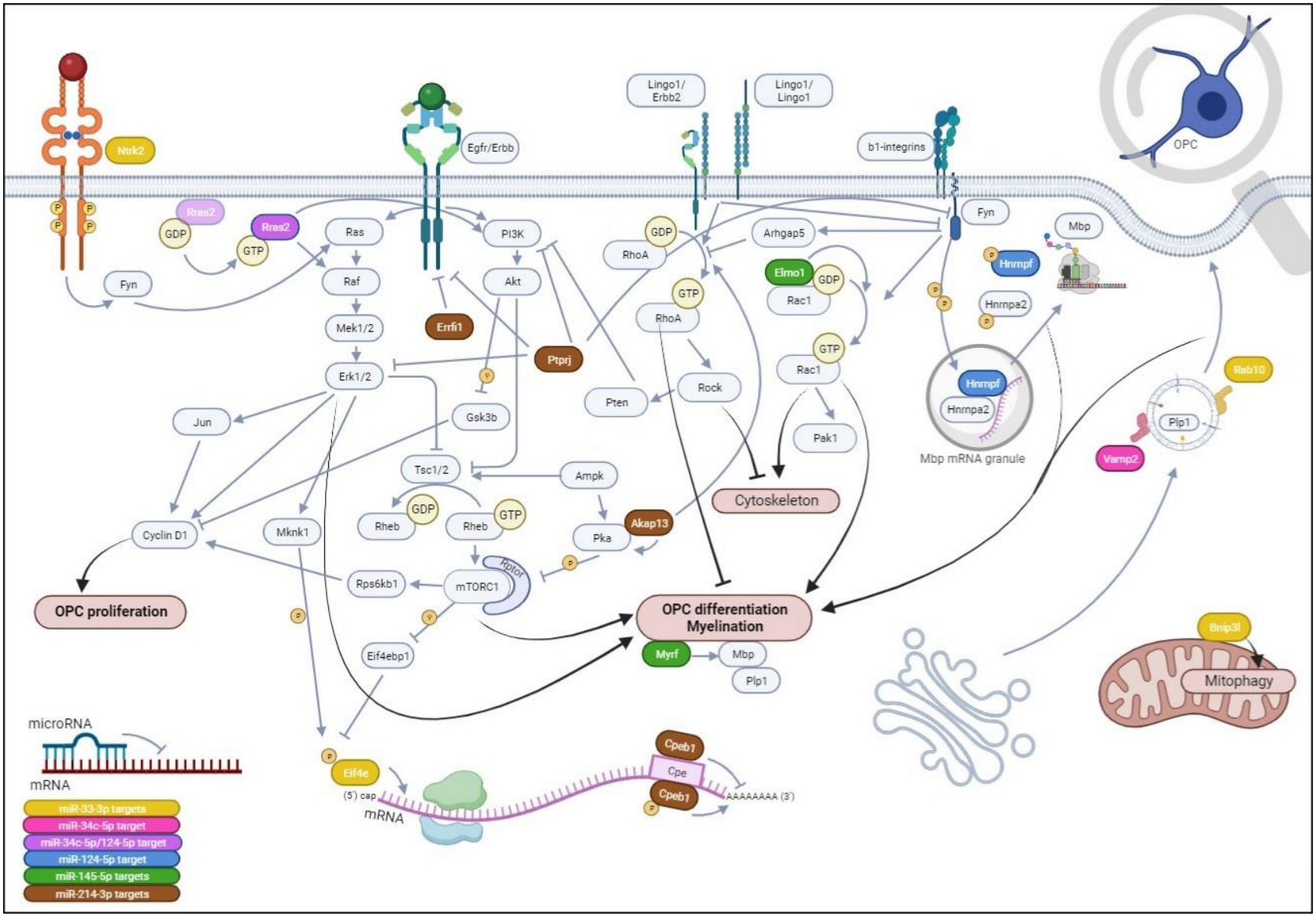
Ntrk2
Egfr/Erbb
Lingo1/
Erbb2
Lingo1/
Lingo1
b1-integrins
OPC
Rras2
GDP
GTP
Ras
PI3K
Fyn
Raf
Akt
Mek1/2
Erfi1
Ptprj
Erk1/2
Gsk3b
Jun
Tsc1/2
Ampk
Cyclin D1
Mknk1
Rheb
Pka
Akap13
Rptor
mTORC1
Rps6kb1
Eif4ebp1
OPC proliferation
RhoA
Rock
Pten
Arhgap5
Elmo1
Rac1
Pak1
Cytoskeleton
Hnrnpf
Hnrnpa2
Mbp mRNA granule
Mbp
Rab10
Plp1
Vamp2
OPC differentiation
Myelination
Myrf
Bnip3l
Mitophagy
microRNA
mRNA
miR-33-3p targets
miR-34c-5p target
miR-34c-5p/124-5p target
miR-124-5p target
miR-145-5p targets
miR-214-3p targets
Eif4e
(5') cap
Cpeb1
Cpe
AAAAAAAA (3')

*differentiation. Ptprj can dephosphorylate ERK/MAPK, PI3K and Fyn tyrosine kinase as well* [515,517,555,1009–1018]*. Notably, Erbb receptor tyrosine kinase family, existing of 4 isoforms, is important in OPC/OL physiology* [685]*.Upon dimerization of two receptors within the Erbb family, which will determine the downstream signalling of the receptor tyrosine kinase, the signal will mainly be transduced intracellularly to the PI3K/Akt/mTOR signalling pathway, inducing OPC differentiation and myelination, or to the ERK/MAPK cascade, enhancing myelin thickness, although both have also been described as playing a role in OPC proliferation upon Pdgf induction through cyclin D1 (Ccnd1)* [509,645,998,1019]*. OPC = oligodendrocyte progenitor cells, OL = oligodendrocytes. Created in BioRender.com*

i. miR-33-3p strongly inhibits OPC differentiation, possibly by altering PI3K/mTOR signalling, membrane trafficking and/or mitochondrial function

miR-33-3p unveiled the strongest inhibitory effect on OPC differentiation as seen by the downregulation of *Mbp* and *Plp1*, although "oligodendrocyte differentiation" was upregulated vs. the differentiation vehicle control in GO enrichment analysis but downregulated vs. miR-NC, whereas its negative regulation was commonly upregulated. In fact, OPC-related genes as *Notch1, Hes1, Hes5, Id4, Lingo1* etc. were annotated to these GO terms [489]. Furthermore, myelination was downregulated in GO vs. both controls. Herein, miR-33-3p potentially targets *Rab10* and *Eif4e*, as supported by in silico analysis and by their significant downregulation in RNA sequencing and independent RT-qPCR analyses. Moreover, they were the only predicted targets significantly antagonized by the microRNA inhibitors. They could thus directly affect OPC differentiation and/or myelination. Rab10, a small GTPase of the Rab family, is involved in the addition of proteins and lipids to the plasma membrane by regulating intracellular vesicle trafficking necessary for OPC maturation and myelin sheath formation [1002,1004]. Its inactivation has been involved in neurodegeneration due to lysosomal dysfunction in Parkinson's disease [1020]. On the contrary, in the context of Alzheimer's disease, the knockdown of *RAB10* is protective by decreasing amyloid beta 42 levels [1021]. Translation initiation factor Eif4e is released downstream of PI3K/mammalian target of rapamycin (mTOR) signalling by phosphorylation of its repressor binding protein Eif4ebp1, conceivably increasing the translation of myelin proteins [702,1000]. Furthermore, Ntrk2 signalling promotes via the Ras/ERK cascade OPC

differentiation and remyelination in the demyelinating cuprizone mice model [665,1001,1022]. *Ntrk2* downregulation was however only confirmed vs. miR-NC by independent RT-qPCR analysis. In GO enrichment analysis, "neurotrophin TRK receptor signalling pathway" was upregulated vs. differentiation vehicle control, although it did not annotate *Ntrk2*.

Wnt and Notch signalling, supporting OPCs, were the only pathways upregulated vs. both differentiation vehicle control and miR-NC [523,629]. Of note, the ERK/MAPK cascade and PI3K signalling pathway, that have been linked to both OPC proliferation (downstream Pdgfra) and differentiation, as well as their negative regulation, were upregulated vs. the differentiation vehicle control only [509,998]. Accordingly, a higher proportion of miR-33-3p-transfected cells seemed A2B5$^+$, although this was not statistically significant. Cell division was downregulated in GO, mainly due to reduced DNA biosynthesis/repair and telomere maintenance. miR-33-3p has not been studied in OPC differentiation so far and the literature on miR-33-3p is sparse, possibly because it is the minor product of the mir-33 precursor. Conversely, it arrests the proliferation of rat pheochromocytoma PC12 cells in favour of their differentiation toward choline acetyltransferase-positive neuron-like cells [1023].

Myelin has a high content of cholesterol and very long-chain fatty acid, and fatty acids are structural elements of all other myelin lipid species [552]. GO indicated that very long-chain fatty acid, acyl-coA, phospholipid and cholesterol biosynthesis were downregulated in miR-33-3p-transfected cells. Herein, fatty acyl-coA reductase 1 (*Far1*), a predicted target of miR-33-3p we did not further investigate, is involved in glycerophospholipid (plasmalogen) synthesis [1024]. Moreover, the more abundant product miR-33-5p reduces cholesterol efflux and fatty acid degradation but induces mitochondria-dependent apoptosis [1025,1026]. Interestingly, the mir-33 precursor is located in an intron of the sterol regulatory element-binding protein 2 (*SREBP2*) locus, a sterol-sensing transcription factor [1025].

Energy metabolism is important in the myelination process [1027]. Although energy homeostasis, especially through glucose homeostasis, appeared safeguarded in miR-33-3p-transfected cells, the generation of precursor metabolites was downregulated, which paralleled the downregulation of oxidative phosphorylation and aerobic respiration vs. the differentiation vehicle control, resulting in ATP biosynthesis deficiency. Additionally, we confirmed the downregulation of *Bnip3l*,

another predicted target of miR-33-3p identified by our selection strategy, that is upregulated in differentiating OPCs and induces mitophagy to allow proper mitochondrial function [1003,1028]. Interestingly, *Bnip3l* was also annotated to downregulated GO terms as "organelle disassembly" (vs. both controls) and "autophagy" (vs. miR-NC).

Finally, miR-33-3p-transfected CG-4 cells arrested for OPC differentiation acquired astrocytic features as supported by the upregulation of GO term "astrocyte differentiation" and of several astrocytic markers (*Aldoc, Gpt2, Nebl*) in RNA sequencing, while immature astrocytic markers *Vim* and *Gfap* were downregulated. Herein, miR-33-3p is predicted to target nude neurodevelopment protein 1 like 1 (*Ndel1*), which is critical for neuronal migration but was also found to inhibit astrocyte differentiation, although to a much lesser extent than its ohnologue, Nde1 [1029].

ii. miR-34c-5p sustains cell division although it targets Pdgfra and Notch1 and may affect signal transduction in differentiation pathways as well as membrane expansion

miR-34c-5p downregulated the differentiation markers *Mbp* and *Plp1*, although to a much lesser extent than miR-33-3p. This was supported by the downregulated GO term "oligodendrocyte differentiation".

We verified the downregulation of miR-34c-5p target *Vamp2* by RNA sequencing and by independent RT-qPCR analyses. Vamp2 is a soluble N-ethylmaleimide sensitive factor attachment protein receptor (SNARE) protein involved in exocytosis by guiding the fusion of the vesicular and target (plasma) membrane. Herein, Vamp2/3 was necessary for membrane expansion but not for OPC differentiation, although it was experimentally inactivated in premyelinating OLs through *Cnp*-dependency [1006]. On the contrary, in another study Vamp2/3-cleavage arrested OPC at a premyelinating, early stage, which was also seen in our study as *Cnp* was already downregulated in miR-34c-5p-transfected CG-4 cells in RNA sequencing, but not on independent RT-qPCR analyses [1005]. Hence, its involvement in OPC differentiation might warrant further research. The interaction of miR-34c-5p and *Vamp2* has previously been validated by luciferase assay and Vamp2 was found significantly less expressed at the protein level in the brain of Alzheimer patients

and in amyloid beta-42-treated rat hippocampal neurons [1030,1031]. Overexpression of miR-34c-5p impairs dendritic length, branching morphology and synaptic function in neurons [1030,1032]. On the contrary, it has also been positively linked to neurogenesis and it is neuroprotective by reducing mitochondrial dysfunction, oxidative stress and neuronal apoptosis [1033–1035].

GO enrichment analysis was further mainly marked by the upregulation of GO terms related to the cell cycle (cell division, cell cycle phase transition, DNA replication, chromosome segregation). Accordingly, miR-34c-5p-transfected cells tended to be more A2B5$^+$ and, the cell cycle marker *Pcna* was significantly upregulated in RNA sequencing. Herein, the cyclin-dependent protein kinase activity (e.g. cyclin D1 *(Ccnd1),* a cell cycle coordinator) was upregulated vs. both differentiation vehicle control and miR-NC [1036]. Cyclin D1 is induced by several pathways, namely Wnt/beta-catenin, ERK/MAPK/Jun (Jun proto-oncogene, AP-1 transcription factor subunit), PI3K/Akt/Gsk3b (glycogen synthase kinase 3 beta) and PI3K/Akt/mTOR, which can all be induced by Pdgfa in OPCs [509,529,645,1019]. Moreover, Wnt, Pdgfra and Notch1 signalling support OPC proliferation and their downregulation accompanies OPC differentiation [523,629,1037]. However, in our study, the Wnt signalling pathway was downregulated by miR-34c-5p in GO, and both *Notch1* and *Pdgfra*, recognised mRNA targets of miR-34c-5p [1038,1039], were significantly downregulated in RNA sequencing and in RT-qPCR analyses on independent experiments. Of note, *Hes5*, the downstream transcription factor of Notch1 was not differentially expressed (figure 6C). It is therefore not clear which pathway supports their proliferation. This should be further explored as, for example, Jun N-terminal kinase (Jnk) interacting protein 1 (also called mitogen-activated protein kinase 8 interacting protein 1 (*Mapk8ip1*)) and *Jun*, elements of the Jnk signalling pathway involved in OPC proliferation, were slightly but significantly upregulated, as well as *Ntrk3*, that has been linked to both OPC proliferation/survival and differentiation (data not shown) [645,1040,1041]. miR-34c-5p was also identified as anti-proliferative in glioblastoma and osteosarcoma cells [1042,1043]. However, *Nkx2-2* that induces early differentiation by directly repressing *Pdgfra* [534], was downregulated as well in our experimental condition.

Hence, to potentially explain that miR-34c-5p-transfected cells do not engage in differentiation, we demonstrated the downregulation of *Rras2* mRNA, a small GTPase of the Ras-related subfamily, that supports OPC differentiation through the

PI3K/Akt/mTOR and ERK1/2-MAPK signalling pathways, of which both GO terms were downregulated as compared to miR-NC. *Rras2* knockout results in an increase of immature OLs [1007,1044].

Finally, the metabolism of specific lipid species, i.e. phospholipids, glycerolipids and cholesterol, was downregulated as well, compared to the differentiation vehicle control only.

iii. miR-124-5p possibly impedes signal transduction in differentiation pathways as well as Mbp mRNA granule transport

miR-124-5p caused the second strongest downregulation of differentiation markers *Mbp* and *Plp1*, supported by the downregulated GO term "oligodendrocyte differentiation". In miR-124-5p-transfected cells, insulin receptor signalling pathway was downregulated vs. both differentiation vehicle control and miR-NC, while Notch and Ntrk signalling were upregulated as compared to the former only. Insulin like growth factor 1 is seemingly involved at all stages of OPC development, proliferation, survival and differentiation [694]. All cell cycle processes were also reduced as compared to the differentiation vehicle control. Lipid biosynthesis was not affected, and energy metabolism was overall positively balanced.

Little is known about miR-124-5p, while increased neuronal levels of miR-124-3p, the major product of mir-124 precursor, accompanied hippocampal demyelination in MS brains [1045]. miR-124-3p also promotes neurogenesis [1046,1047]. Contrarily, the downregulation of miR-124-5p has been linked to angiogenesis and endothelial cell migration/invasion [1048,1049]. In rats failing on stress coping, its downregulation in the amygdala was negatively, and indirectly, correlated with the expression of genes involved in nucleosome assembly and chromatin remodelling [1050]. These genes were however not oppositely dysregulated in our study.

We confirmed by RNA sequencing and RT-qPCR analysis on independent experiments, the downregulation of *Hnrnpf*, a predicted target of miR-124-5p. Hnrnpf, alongside Hnrnpa2, binds *Mbp* mRNA in RNA transport granules and silences its translation along transport to the cell periphery, where the phosphorylation of Hnrnpf by Fyn proto-oncogene 1 Src family tyrosine kinase (Fyn)

releases Mbp mRNA allowing its on-site translation in the cellular processes whereafter it can easily interact with the apposing cytoplasmic leaflets for myelin compaction [585,595]. Hnrnpab is similarly involved in the RNA transport of Mbp and Mbp mRNA was localised in the cell body instead of cellular processes by its silencing [1051]. Interestingly, RNA sequencing in our study showed a bigger negative fold change for *Hnrnpab*, however, while it met our selection criteria as a predicted target of miR-124-5p in rats, it was only predicted by 2 databases in humans.

Similarly to miR-34c-5p, *Rras2* is a predicted target of miR-124-5p but in rats only. We evidenced its downregulation by RNA sequencing and by independent RT-qPCR analyses.

Finally, we evidenced the overexpression of *Gfap* by miR-124-5p at the mRNA level by independent RT-qPCR analyses and at the protein level by immunocytochemistry, which was further supported by the upregulation of both immature (synemin (*Synm*), *Vim*, *Gfap*) and general/mature (*Aldoc, Gpt2, Nebl*) astrocytic markers in RNA sequencing. miR-124-5p is predicted to target Lysine acetyltransferase 5 *(Kat5)* in rats and Kat5-defiency induces a neurogenesis-to-gliogenesis switch in vivo and an increase of $Gfap^+$ astrocytes in vitro [1052].

iv. miR-145-5p targets a key transcription factor for OPC differentiation but might also indirectly affect signal transduction by a small GTPase

miR-145-5p inhibited the differentiation of CG-4 cells as well, as evidenced by the downregulation of *Mbp* and *Plp1* and of the GO terms “oligodendrocyte differentiation” and “myelination”. Hereby we confirmed by other techniques and in another cell model what was previously demonstrated [817]. They validated *Myrf* as a direct target of miR-145-5p on primary OPCs using its microRNA inhibitor. We showed its downregulation in RNA sequencing and independent RT-qPCR analyses, although it was downregulated by the other differentiation-impeding microRNAs as well. Myrf is indispensable for OL development and myelin maintenance. Along with its inducer Sox10, it separately or cooperatively activates OL genes and blocks the expression of Sox10-dependent OPC genes [538,539,1053].

Unexpectedly, miR-145-5p-transfected cells were clustered the closest to the controls, the differentiation vehicle control and miR-NC, as seen by the PCA and the

heatmap of the RNA sequencing. GO dysregulation was also limited. Ras and Rho protein signal transduction was downregulated versus both controls. Herein, we demonstrated the downregulation of *Elmo1*, a predicted target of miR-145-5p and an activator of Rac family small GTPase 1 (Rac1) [1008]. Rac1 supports morphological OPC differentiation and is also involved in the organization of actin within the cytoskeleton [515].

Overall, lipid metabolism was not affected. Energy metabolism and cell cycle processes were upregulated vs. miR-NC only, while mRNA processing was upregulated vs. both controls. Conversely, the downregulation of miR-145-5p in glioblastomas supports tumour growth and tumour cell invasion [1054,1055].

v. miR-214-3p unexpectedly promotes the differentiation of CG-4 cells, a matter of timing ?

In our study we repeatedly (by single, double, and sequential transfection) demonstrated that miR-214-3p induced CG-4 cell differentiation, as seen by the upregulation of *Plp1, Mbp* and *Mobp*. miR-214-3p has however long been postulated to hinder OPC differentiation as it is predicted to target *Mobp*, an important protein for myelin compaction and structure, although this has never been investigated functionally [885,1056]. Interestingly, miR-214-3p promoted the migration and myelination of Schwann Cell-like cells, derived from human amniotic mesenchymal stem cells, by targeting *Jun* and could improve peripheral nerve regeneration [1057]. Furthermore, miR-214-3p promotes the differentiation of neural progenitor cells, while the opposite has been described as well. It is neuroprotective and reduces both neuronal apoptosis and autophagy via several mRNA targets [1058–1062]. Notably, its effect on neural progenitor cell proliferation and neuronal apoptosis was found to be mediated by targeting *Pten*, an inhibitor of PI3K/Akt signalling and thus inducing this pathway, which is involved in both OPC proliferation and differentiation [509,998,1058,1060,1063]. *Pten* was however not downregulated by miR-214-3p in CG-4 cells, according to our RNA sequencing data. It has also been characterized as tumour suppressor in gliomas [1064,1065].

GO enrichment analysis was further challenging to understand the changes in cell fate induced by miR-214-3p. The “negative regulation of Erbb signalling” was downregulated vs. both controls, with *Errfi1* and *Ptprj* as genes annotated to this

GO term. Erbb receptors are involved in OPC proliferation and differentiation, depending on their dimerization partner [685]. Other pathways as Pdgfr signalling, Ras signal transduction and ERK1/2 cascade, were downregulated vs. miR-NC only. Phospholipid and glycerolipid metabolism as well as autophagy were downregulated, but cell division was upregulated vs. both controls, while energy metabolism was largely and negatively affected as compared to the differentiation vehicle control only.

We hypothesized that miR-214-3p targets *Errfi1* and growth factor receptor bound protein 2 *(Grb2)*, as predicted by in silico analysis and as seen by their downregulation in RNA sequencing. Errfi1 inhibits Egfr signalling while Grb2 binds to Egfr and induces Erk/Jun signalling. A similar microRNA-mRNA target mechanism has been described for miR-200a, resulting in a shift of Egfr/Erk/Jun signalling towards Egfr/PI3K/Akt/mTOR signalling and enhanced OPC differentiation [1014]. Additionally, Ptprj dephosphorylates and inactivates receptor tyrosine kinases as Egfr and possibly other Erbb receptors, ERK1/2, PI3K and Fyn tyrosine kinase as well [1013,1015,1016,1066,1067]. Therefore, the downregulation of *Ptprj* may maintain the activity of these tyrosine kinases and thus subsequently promote OPC differentiation through ERK/MAPK and/or PI3K/Akt/mTOR signalling and by facilitating *Mbp* translation in RNA transport granules [595,685,998].

Alternately, Cpeb1 binds to a consensus sequence, called cytoplasmic polyadenylation element (CPE), within the 3'UTR of a mRNA and represses the translation of this mRNA until it is itself phosphorylated or degraded [1011]. Cpeb1 contributes to dendritic branching and synaptic plasticity in neurons and induces the differentiation of glioma stem cells by binding to *Hes1* [1068,1069]. We have however identified the CPE consensus sequence (5'-UUUUUAU-3') within the 3'UTR of several mRNAs related to OPC proliferation (*Notch1, Hes1, Id2, Id4*) and differentiation (*Olig1, Tcf7l2, Yy1* transcription factor*, Mbp*), all of which were confirmed by the bioinformatic resource (https://genome.crg.eu/CPE) in human and/or mice (no data available for rats), except for *Yy1*. Therefore, if miR-214-3p targets *Cpeb1*, it would increase their translation. Finally, Akap13 inhibits mTORC1 by scaffolding protein kinase A, and induces Ras homolog family member A (RhoA) activity, both of which impede OPC differentiation [515,998,1009,1010,1012,1018]. Interestingly, RhoA activation favours the formation and contraction of stress fibres and the depolymerization of actin, via downstream Rho associated coiled-coil

containing protein kinase (Rock), thereby inhibiting process expansion and differentiation in OPCs [555]. RhoA/Rock can also possibly inhibit PI3K/Akt through induction of Pten, although this hasn't yet been evidenced in OPCs [1017,1070,1071]. Remarkably, the role of Akap13 as well as Ptprj and Cpeb1, in OPCs/OLs remains unexplored.

*Akap13*, *Cpeb1, Errfi1, Grb2* and *Ptprj* are therefore strong candidates to mechanistically support OPC differentiation induced by miR-214-3p. Although their downregulation was evidenced by RNA sequencing, we could not confirm it by RT-qPCR analyses on independent experiments, except vs. miR-NC for *Akap13*, *Cpeb1* and *Errfi1* (data not shown for *Grb2*). Nonetheless, it is still possible that the expression of a direct target remains unaffected at the mRNA level as the microRNA might not degrade its target mRNA [725]. Notably, only the expression of *Akap13* tended to be slightly decreased as compared to the differentiation vehicle control. In fact, as it was not downregulated in only one of the 3 independent experiments, in which *Plp1* and *Mbp* were also slightly less, but still significantly, upregulated, possibly due to a later passage of the cells, we verified and confirmed by RT-qPCR its downregulation in the experiment sent for RNA sequencing (data not shown). Therefore, it might still be interesting to explore the expression of these candidates and the pathways they are involved in at a protein level or test whether miR-214-3p indeed interacts with the 3'UTR of *Akap13* by a dual luciferase assay.

The induction of OPC differentiation might, however, be a matter of timing. The differentiation markers were more potently induced by miR-214-3p than miR-219a-5p in the short, single transfection protocol (1+2 days), while their upregulation by miR-214-3p was lower than by miR-219a-5p in the long, double transfection protocol (1.5+6 days). Therefore, miR-214-3p could induce initial OPC differentiation, whereas it might not be able to maintain it on long terms as its effect seemed to slow down. Similarly, miR-138-5p was found to induce early phases of OPC differentiation but it inhibited it at later stages [782]. This remains largely hypothetic as both protocols are very different and should be further investigated by precise kinetics.

vi. Does endogenous microRNA expression mirror the effect of the transfected microRNAs?

miR-33-3p was endogenously not differentially expressed both in basal proliferating and differentiating CG-4 cells (without any other treatment than the medium change), which may not directly imply its endogenous involvement in OPC differentiation.

Endogenous miR-34c-5p and miR-124-5p were downregulated in differentiating CG-4 cells which is consistent with their inhibitory effect on OPC differentiation identified in our study. On the contrary, endogenous miR-145-5p was upregulated in differentiating CG-4 cells, while we showed that its transfection interfered with OPC differentiation. Finally, miR-214-3p was not detectable in proliferating nor in differentiating CG-4 cells.

The expression of miR-33-3p and miR-124-5p has not been described in OPC differentiation/development so far, possibly because they are the minor product of their corresponding precursor microRNA. miR-219-5p, miR-145-5p and miR-214-3p were found upregulated and miR-34c-5p slightly downregulated during OL maturation from primary rat A2B5$^+$ OPCs to premyelinating Galc$^+$ OLs [884]. Contrarily, miR-145-5p decreased gradually within a few hours of differentiation induction in rat OPCs and remained low up to 5 days of differentiation [817]. Similarly, during the maturation of human embryonic stem cells, miR-145-5p and miR-214-3p, even more strongly, increased at early O4$^+$ OPC stage, but already decreased from the mid Galc$^+$ OPC stage and slightly increased again in mature OLs [885].

Thus, the endogenous downregulation of miR-34c-5p and miR-124-5p possibly mirrors their inhibition of OPC differentiation, while the endogenous expression of miR-145-5p could be variable according to time and cell-stage. However, these microRNAs might also be expressed differently by OPCs/OLs or by other cell types in physiological and/or pathophysiological conditions of the central nervous system. Determining their cellular source could therefore further inform on their physiological and pathophysiological role.

vii. Does MS-related microRNA dysregulation mirror the effect of the transfected microRNAs?

In our previous study on microRNA dysregulation in the CSF, miR-33-3p and miR-214-3p were downregulated in remitting MS patients, and miR-34c-5p and miR-124-5p in relapsing MS patients, while miR-145-5p was upregulated in relapsing patients [892]. As miR-33-3p and miR-145-5p both inhibited OPC differentiation, their respective downregulation during remission and upregulation during relapse possibly supports the pathogenesis of MS within the CSF, while this is less equivocal considering the dysregulation of miR-34c-5p and miR-124-5p. On the contrary, the downregulation of miR-214-3p, a promoter of OPC differentiation, in the CSF of remitting MS patients could underpin remyelination defects. However, it might still be a matter of compartment differences, as for miR-214-3p that was also found upregulated in active and even more in inactive white matter lesions of MS patients [758].

miR-33-3p and miR-124-5p have not been linked to MS so far, except in our previous study [892]. An extended bioinformatic analysis linked miR-34c-5p, only identified by our previous study so far, to many MS-related genes, among which *MAPK1*, therefore characterising it as a risk microRNA in MS [1072], thus possibly supporting its inhibitory effect on OPC differentiation, as demonstrated by our results. However, in the CSF, miR-34c-5p was downregulated during relapses. miR-145-5p that was also found upregulated in plasma, serum and peripheral blood mononuclear cells of MS patients [977,1073], has been characterized as a pro-inflammatory (by targeting immune response limiting factors semaphorin 3A and cytotoxic T lymphocyte associated protein 4 *(CTLA4*)) and an anti-OPC differentiation (by targeting *Myrf*) microRNA, and is thus potentially supportive of MS pathogenesis [811,817,1074]. Oppositely, a bioinformatic-based network established the sponging of miR-145-5p by an upregulated long-non-coding RNA, taurine upregulated 1 (*TUG1*), in the periplaque regions in MS brains, leading to the upregulation of catenin delta *(CTNND1)*, a potential MBP-interacting protein [1075,1076].

Hence data of our study and of the literature suggest a possible link between the dysregulation and a pathophysiological role of miR-33-3p and miR-145-5p in MS. Furthermore, the opposite dysregulation of miR-214-3p in the CSF (downregulated) and the white matter lesions (upregulated) could be related to repair mechanisms

potentially supporting initial OPC differentiation (by its upregulation) or oppositely to their impairment resulting in remyelination defects (by its downregulation).

Moreover, since demyelination underpins neurodegeneration, miR-214-3p has been described as neuroprotective against cognitive impairment by reducing the expression of neurodegenerative proteins involved in apoptosis [1077]. Contrarily, miR-145-5p might support neurodegeneration as it targets the neuroprotective and anti-inflammatory nuclear receptor subfamily 4 group A member 2 (*NR4A2*) [1078,1079]. *NR4A2* knockout worsens EAE [1080]. *NR4A2* was however found upregulated in the motor cortex on brain autopsies of MS patients, correlating positively with neuronal densities [1081].

### viii. Limitations of the study

Although we showed comparable effects of the investigated microRNAs on the differentiation of CG-4 cells by three different transfection strategies (with microRNA mimics and their inhibitors as well), we are fully aware that (a) microRNA mimics were transfected at supraphysiological levels, and that (b) our investigation was restricted to an in vitro cell line model and should thus be verified by other experimental models. We have therefore comprehensively balanced the interpretation versus both the differentiation vehicle control and miR-NC. Furthermore, we proposed several mRNA targets based on in silico and RNA sequencing data and verified their downregulation by independent RT-qPCR analyses, but only for two predicted targets the effect of the microRNA mimic was significantly antagonised by its microRNA inhibitor. Hence, the interaction of each microRNA with its predicted targets should ideally be validated by a dual luciferase assay. Mechanistically, it would be interesting to investigate the key pathways involved in OPC and OL physiology (Notch, Wnt, ERK/MAPK, Akt/mTOR signalling pathways) to further clarify the effect of each microRNA and its potential mRNA target(s) both in vitro and in vivo.

### ix. Conclusions

We have screened the effect of several MS-dysregulated microRNAs on the differentiation of CG-4 cells. Herein we support by independent RT-qPCR analyses

and RNA sequencing that miR-33-3p, miR-34c-5p, miR-124-5p, and miR-145-5p impede OPC differentiation and one microRNA, miR-214-3p, promotes (initial) OPC differentiation. In this study we propose a deeply comprehensive investigation of their effect on OPC differentiation. Moreover, for each microRNA, we confirmed the downregulation of several predicted mRNA targets that supposedly support the cell fate changes induced by each microRNA by very distinctive mechanisms, of which some are still unexplored in OPC/OL physiology. Many microRNAs are intricated in MS pathogenesis, possibly at different intra- and intercellular levels, of which we currently master only a very limited part. microRNA-based therapeutic strategies could target these different levels at once, but might also cause undesired on- and off-target effects as a single microRNA potentially targets hundreds of mRNAs and as a single mRNA is finely tuned by several microRNAs. However, further elucidating the role of the microRNAs, the proposed mRNA targets and their respective pathways could open the way for developing new remyelinating treatment strategies, an unmet need to counteract chronic neurological disability in MS.

## VI. Supplementary material

*Supplementary figure 3.1: The effect of 13 microRNA mimics on the differentiation of CG-4 cells in RT-qPCR (screening)*

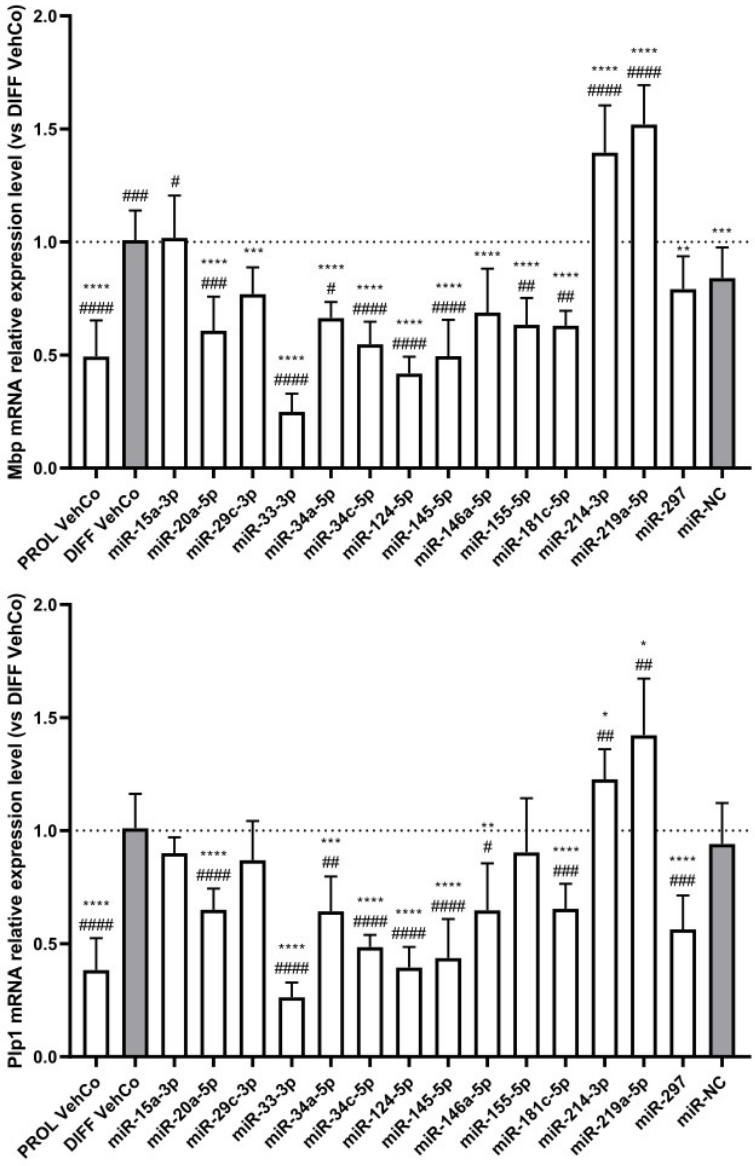

*Supplementary figure 3.1: The effect of 13 microRNA mimics on the differentiation of CG-4 cells in RT-qPCR (screening)*

The plots show the relative expression (mean with SD of $2^{-\Delta\Delta Ct}$) of the differentiation markers *Mbp* and *Plp1* to the differentiation vehicle control (DIFF VehCo) resulting from the double transfection of each microRNA mimic (as labelled on the x-axis) in CG-4 cells in differentiation culture conditions, as well as the proliferation vehicle control (PROL VehCo). The dotted line represents the mean relative expression of the differentiation vehicle control to which the relative expression ($2^{-\Delta\Delta Ct}$) of each sample was calculated. The adjusted p-value was calculated by Dunnett's multiple comparison test to each control separately (grey bars), i.e. the differentiation vehicle control (*) and the microRNA mimic negative control (miR-NC, #), as recommended following a parametric one-way ANOVA on all conditions: ns for not significant, */# for $p \leq 0.05$, **/## for $p \leq 0.01$, ***/### for $p \leq 0.001$, ****/#### for $p \leq 0.0001$. Data of 3 experiments for each microRNA with each condition in triplicate. SD = standard deviation.

*Supplementary figure 3.2: The effect of 5 microRNA mimics on the differentiation of CG-4 cells in RT-qPCR (confirmation)*

The plots show the relative expression (mean with SD of $2^{-\Delta\Delta Ct}$) of several OPC, pre-OL, OL and astrocyte markers to the differentiation vehicle control (DIFF VehCo) resulting from the single transfection of each microRNA mimic (as labelled on the x-axis) in CG-4 cells in differentiation culture conditions, as well as the proliferation vehicle control (PROL VehCo). The dotted line represents the mean relative expression of the differentiation vehicle control to which the relative expression ($2^{-\Delta\Delta Ct}$) of each sample was calculated. The adjusted p-value was calculated by Dunn's or Dunnett's multiple comparison test to each control separately (grey bars), i.e. the differentiation vehicle control (*) and the microRNA mimic negative control (miR-NC, #), as recommended following a parametric/nonparametric one-way ANOVA on all conditions: ns for not significant, */# for $p \leq 0.05$, **/## for $p \leq 0.01$, ***/### for $p \leq 0.001$, ****/#### for $p \leq 0.0001$. Data of 3 experiments with each condition in triplicate. OPC = oligodendrocyte progenitor cells, OL = oligodendrocytes, SD = standard deviation.

*Supplementary figure 3.2: The effect of 5 microRNA mimics on the differentiation of CG-4 cells in RT-qPCR (confirmation)*

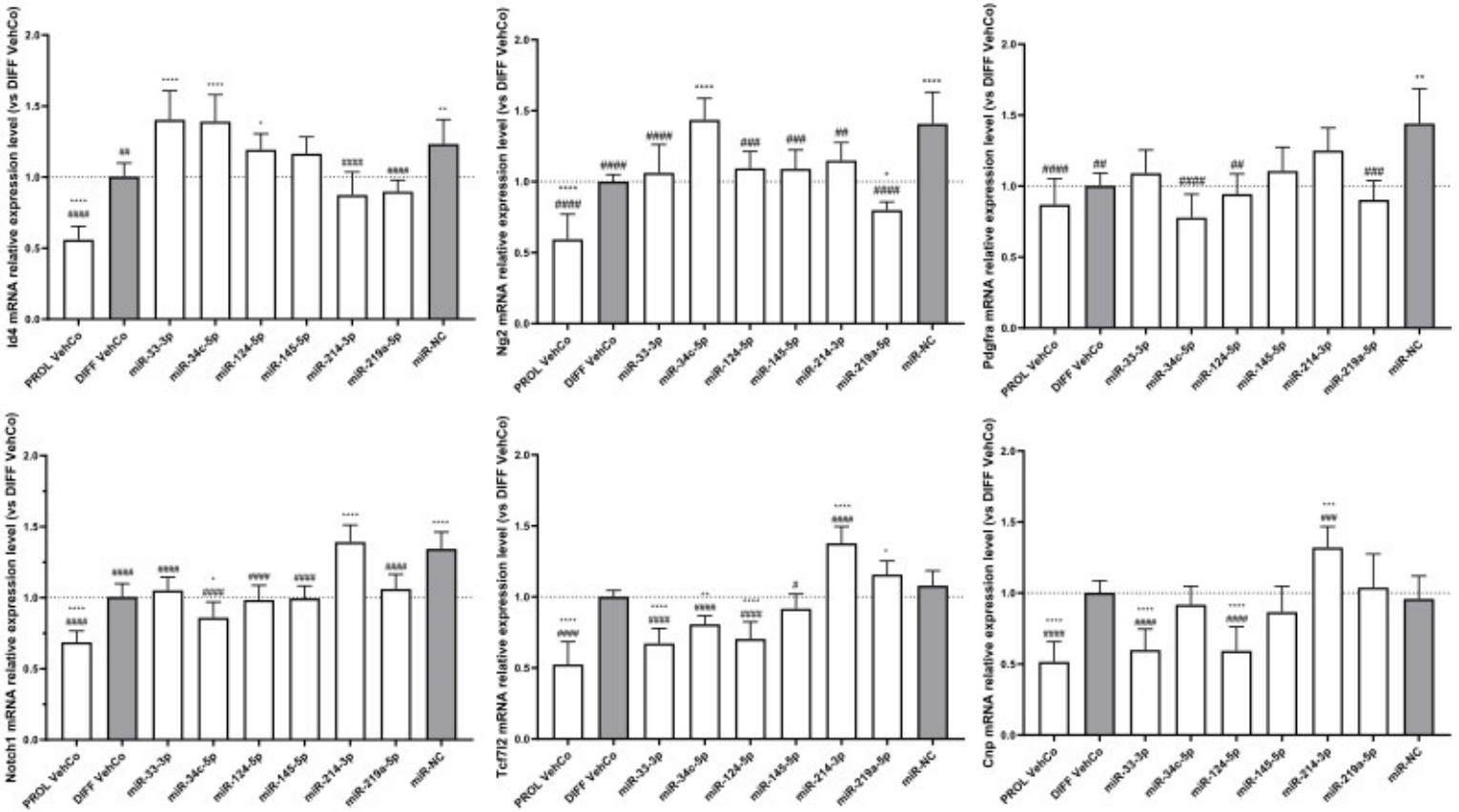

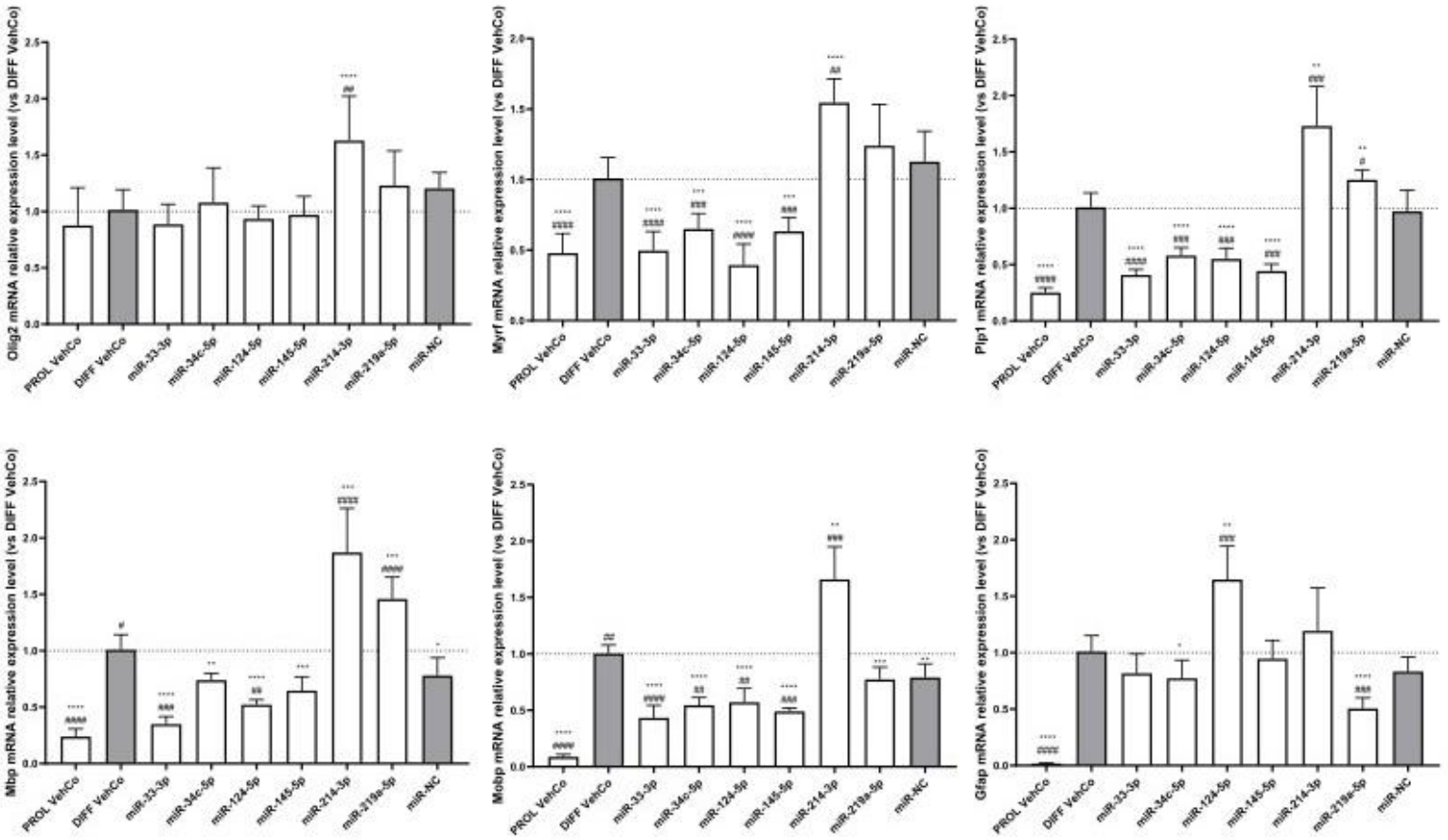
Olig2 mRNA relative expression level (vs DIFF VehCo)
Myrf mRNA relative expression level (vs DIFF VehCo)
Plp1 mRNA relative expression level (vs DIFF VehCo)
Mbp mRNA relative expression level (vs DIFF VehCo)
Mobp mRNA relative expression level (vs DIFF VehCo)
Gfap mRNA relative expression level (vs DIFF VehCo)
PROL VehCo
DIFF VehCo
miR-33-3p
miR-34c-5p
miR-124-5p
miR-145-5p
miR-214-3p
miR-219a-5p
miR-NC

*Supplementary figure 3.3: The effect of 5 microRNA mimics and their inhibitors on the differentiation of CG-4 cells in RT-qPCR*

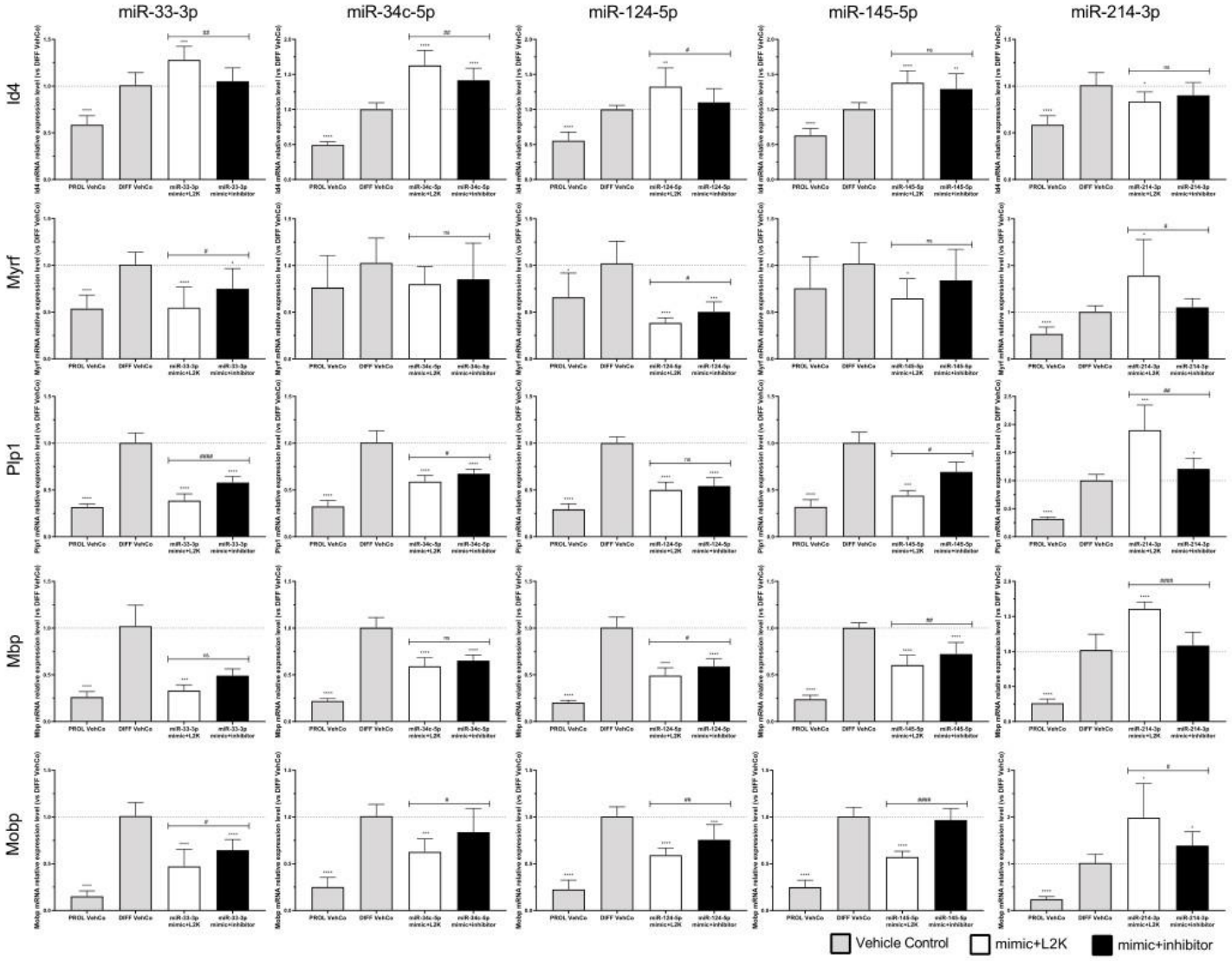

Supplementary figure 3.3: The effect of 5 microRNA mimics and their inhibitors on the differentiation of CG-4 cells in RT-qPCR

The plots show the relative expression (mean with SD of $2^{-\Delta\Delta Ct}$) of the OPC marker (*Id4*) and OL markers *(Myrf, Plp1, Mbp,* and *Mobp)* to the differentiation vehicle control (DIFF VehCo, grey bar), resulting from the sequential transfection of each microRNA mimic followed (black bar) or not (white bar) by its inhibitor (as labelled on the x-axis) in CG-4 cells in differentiation culture conditions, as well as the proliferation vehicle control (PROL VehCo, grey bar). The dotted line represents the mean relative expression of the differentiation vehicle control to which the relative expression ($2^{-\Delta\Delta Ct}$) of each sample was calculated. The adjusted p-value was calculated by Dunn's or Dunnett's multiple comparison test to the differentiation vehicle control (*) and by Sidak's, Tamhane's T2 or Dunn's multiple comparison test between the microRNA mimic and its inhibitor (#), as recommended following a parametric/nonparametric one-way ANOVA on all conditions: ns for not significant, */# for $p \leq 0.05$, **/## for $p \leq 0.01$, ***/### for $p \leq 0.001$, ****/#### for $p \leq 0.0001$. Data of 3 experiments for each microRNA with each condition in triplicate. L2K = Lipofectamine™ 2000. SD = standard deviation.

*Supplementary figure 3.4: Potential mRNA targets of each microRNA verified in RT-qPCR by (A) the microRNA mimic and (B) by the microRNA mimic and its inhibitor*

The plots show the relative expression (mean with SD of $2^{-\Delta\Delta Ct}$) of the potential mRNA targets of each microRNA to the differentiation vehicle control (DIFF VehCo, grey bar), resulting (A) from the single transfection of each microRNA mimic, or (B) from the sequential transfection of each microRNA mimic followed (black bar) or not (white bar) by its inhibitor (as labelled on the x-axis) in CG-4 cells in differentiation culture conditions, as well as the proliferation vehicle control (PROL VehCo). The dotted line represents the mean relative expression of the differentiation vehicle control to which the relative expression ($2^{-\Delta\Delta Ct}$) of each sample was calculated. The adjusted p-value was calculated (A) by Dunn's or Dunnett's multiple comparison test to the differentiation vehicle control (*) and to the microRNA negative control mimic (miR-NC, #), and (B) by Dunnett's multiple comparison test to the differentiation vehicle control and by Sidak's or Tamhane's T2 multiple comparison test between the microRNA mimic and its inhibitor (#), as recommended following a parametric/nonparametric one-way ANOVA on all conditions: ns for not significant, */# for $p \leq 0.05$, **/## for $p \leq 0.01$, ***/### for $p \leq 0.001$, ****/#### for $p \leq 0.0001$. Data of 3 experiments for each microRNA with each condition in triplicate. L2K = Lipofectamine™ 2000. SD = standard deviation.

*Supplementary figure 3.4A: Potential mRNA targets of each microRNA verified in RT-qPCR by the microRNA mimic*

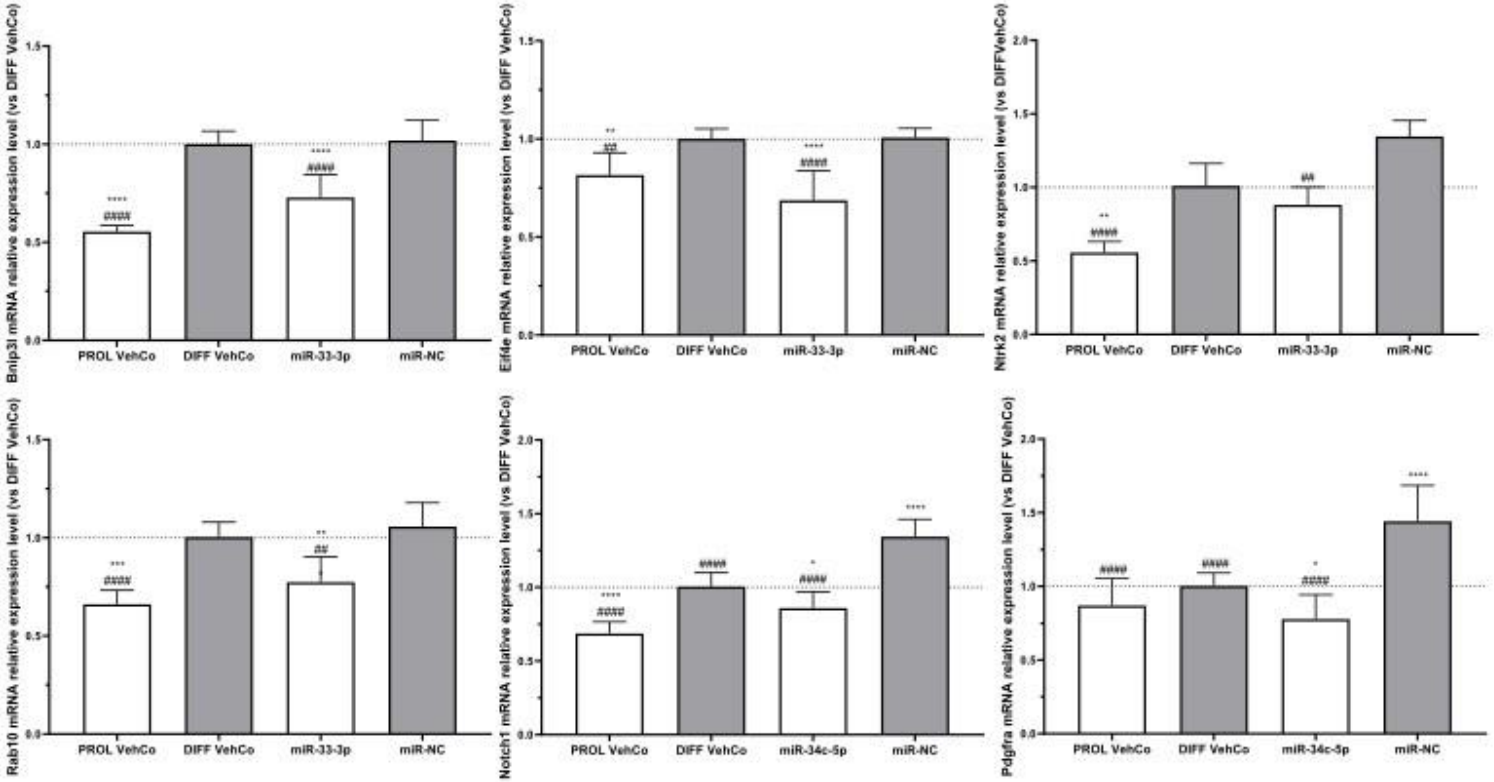

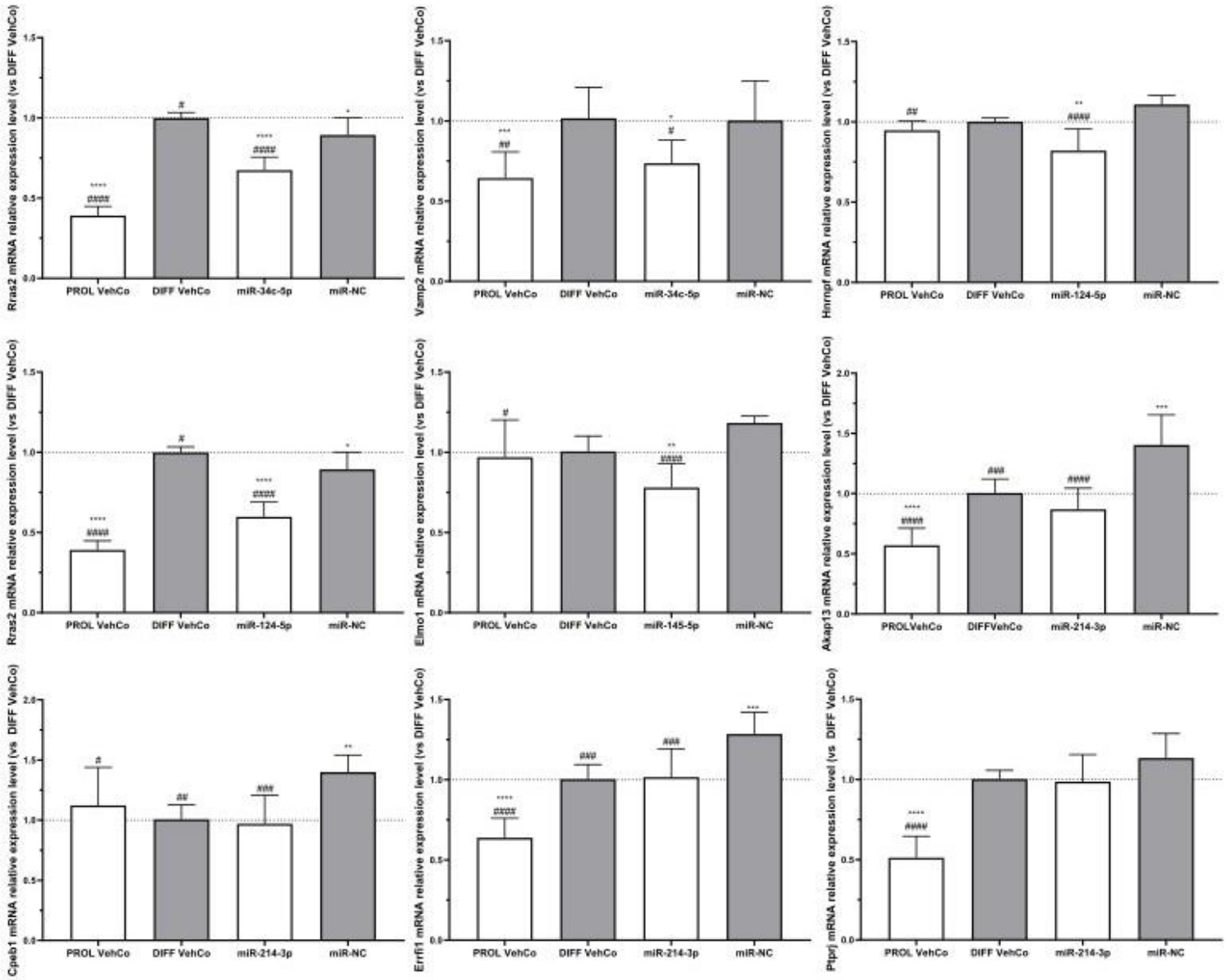
Rras2 mRNA relative expression level (vs DIFF VehCo)
PROL VehCo
DIFF VehCo
miR-34c-5p
miR-NC
Vamp2 mRNA relative expression level (vs DIFF VehCo)
PROL VehCo
DIFF VehCo
miR-34c-5p
miR-NC
Hnrnpf mRNA relative expression level (vs DIFF VehCo)
PROL VehCo
DIFF VehCo
miR-124-5p
miR-NC
Rras2 mRNA relative expression level (vs DIFF VehCo)
PROL VehCo
DIFF VehCo
miR-124-5p
miR-NC
Elmo1 mRNA relative expression level (vs DIFF VehCo)
PROL VehCo
DIFF VehCo
miR-145-5p
miR-NC
Akap13 mRNA relative expression level (vs DIFF VehCo)
PROLVehCo
DIFFVehCo
miR-214-3p
miR-NC
Cpeb1 mRNA relative expression level (vs DIFF VehCo)
PROL VehCo
DIFF VehCo
miR-214-3p
miR-NC
Errfi1 mRNA relative expression level (vs DIFF VehCo)
PROL VehCo
DIFF VehCo
miR-214-3p
miR-NC
Ptprj mRNA relative expression level (vs DIFF VehCo)
PROL VehCo
DIFF VehCo
miR-214-3p
miR-NC

*Supplementary figure 3.4B: Potential mRNA targets of each microRNA verified in RT-qPCR by the microRNA mimic and its inhibitor*

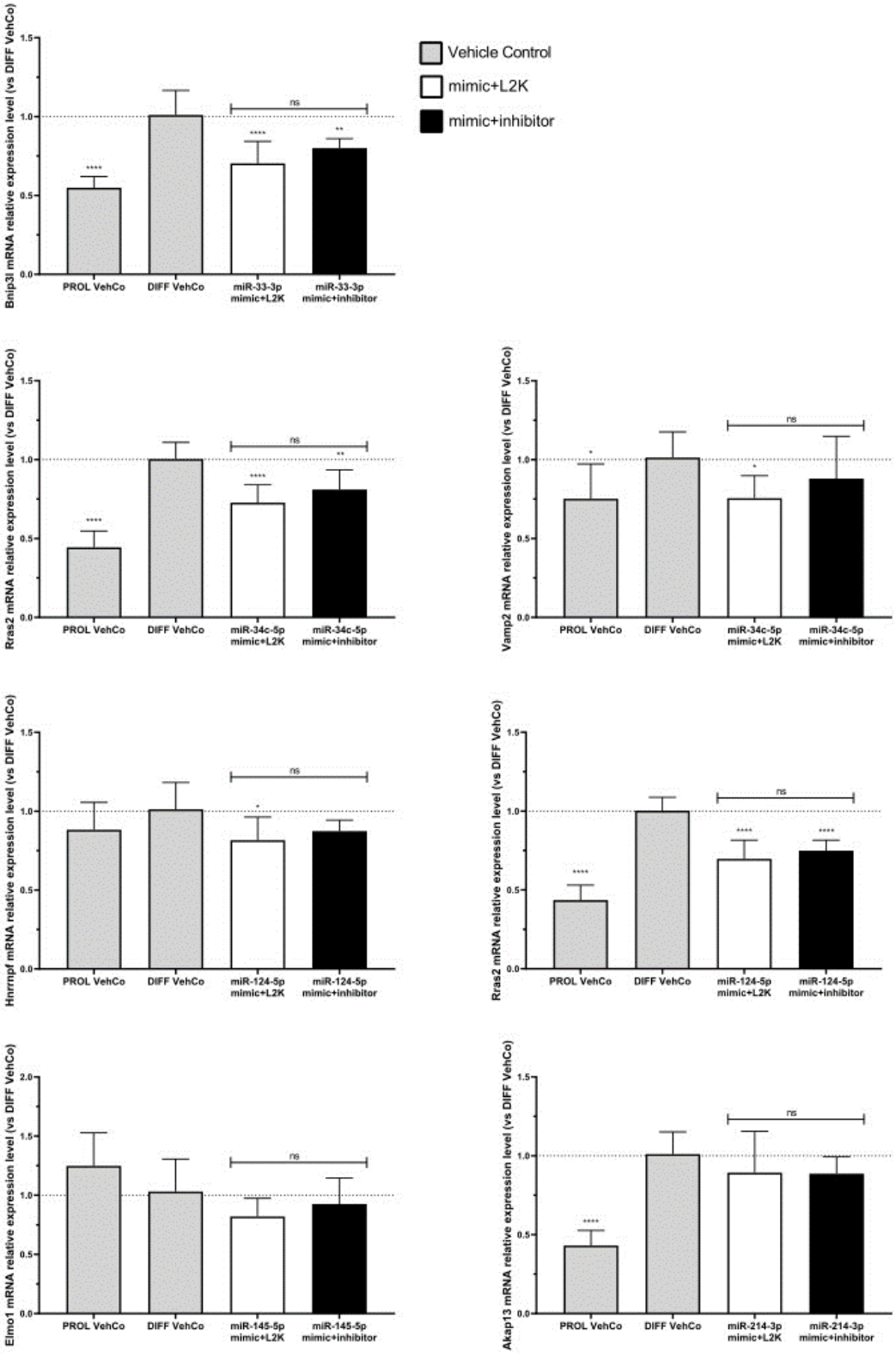

*Supplementary table 3.1: Sequences of mRNA primers, microRNA mimics and microRNA primers*

3.1A

| mRNA | Forward primer - sequence 5'-3' | Reverse primer - sequence 5'-3' |
|---|---|---|
| rno_Akap13 | TGCAGAAATGAACCAGCGGA | GGGACACCAGCTCATACTTCT |
| rno_Bnip3l | TGTCTCACTTAGTCGAGCCGC | CTCCACCCAGGAACTGTTGA |
| rno_Cnp | GAGCTTCGACACTTCATTTCTGG | TGGCCTTCCCGTAGTCACAG |
| rno_Cpeb1 | CTCTGGAAGAAGAATCAGGAAGGA | CCAGTGAATCATCCAAAATGGCA |
| rno_Eif4e | AGATGGCGACTGTGGAACCG | CCAGAGTGCCCACCTGTTCT |
| rno_Elmo1 | TGATGAGAGGAGACAGGAGATGG | GTGCTCGGATGACATGGGTTA |
| rno_Errfi1 | GGGGCAGTCGCAATGAGTT | AGAAGCACATCCGAGGGTTG |
| rno_Gfap | GGGATGGCGAGGTCATTAAG | TCTGAGGAGGGAGCTTTAGG |
| rno_Grb2 | TCTCCCTGTCAGTCAAGTTTGG | CTTCACCACCCACAGGAAGTAC |
| rno_Hnrnpf | GCATCTGTGGTGGTTCTTTAAGC | ATTGAGCAGGACCAGGGTAG |
| rno_Hprt1 | GTCATGTCGACCCTCAGTCC | GCAAGTCTTTCAGTCCTGTCC |
| rno_Id4 | CGTTGTGACAAGCGAACTGT | AAAAGTTCCCCGCCCTGTTA |
| rno_Mbp | GTGGGGGTAAGAGAAACGCA | CGAACACTCCTGTGGAACGA |
| rno_Mobp | CAGAGCACTTCAGCATCCACT | CTCCTCCTTCTCAATCTGGTCTTC |
| rno_Myrf | TGCCAACAACATGCGGAAGAAG | GGGTTAGAGGCCCGAACAATGA |
| rno_Ng2 | AGGCCCTCAGGGGAATAGAC | CAGGGCTCCTCTGTGTGAGA |
| rno_Notch1 | TGCGTGGACAAGATCAACGA | GGTCCCCGTGTAACCTTCTG |
| rno_Ntrk2 | CGGGAGCATCTCTCGGTCTA | CCTTTCATGCCAAACTTGGAATG |
| rno_Olig2 | TCAAATCGAATTCACATTCGGAAG | CGTGGATGAGGACACGGTTC |
| rno_Pdgfra | TCTTATGGCGTTCTGCTCTG | CCATCCTGTATCCGCTCTTG |
| rno_Plp1 | GGCGACTACAAGACCACCAT | AATGACACACCCGCTCCAAA |
| rno_Ptprj | CCAAGTTAATCCGAGTGGAGA | TCCAATCAGCTTCAGATCCTCA |
| rno_Rab10 | GAAAGGCAAAGGAGAGCAGATTG | TCAGCTAATGTGAGGAACGCC |
| rno_Rras2 | GACCATCAGAGACAGGTAACGC | AACTCGGACAAGTTCGTGGAA |
| rno_Sox10 | AGGTTGCTGAACGAGAGTGAC | CGCCGAGGTTGGTACTTGTAG |
| rno_Tcf7l2 | ATGGTTAGTACCACAGCAAGGT | AGAGTGTGATGGGGAGGGAC |
| rno_Vamp2 | CCCTGCACCTCCTCCAAATC | GATGTCCACCACCTCATCCAC |

(A) List of forward and reverse primers of the investigated mRNAs. (B) List of microRNAs mimics, inhibitors and PCR Assay primers (miRCURY LNA miRNA, Qiagen) with corresponding GeneGlobe ID (Qiagen database), sequence and MIMAT ID (miRbase database). Interspecies compatibility was strictly verified. hsa = homo sapiens, mmu = mus musculus, rno = rattus norvegicus, NA = not applicable.

*Supplementary table 3.1B*

| miRCURY LNA miRNA (Qiagen) microRNA ID | Mimic (Cat No. 339173) | Inhibitor (Cat. No. 339121) GeneGlobe ID | PCR Assay (Cat. No. 339306) | sequence 5'-3' | miRBase MIMAT ID |
|---|---|---|---|---|---|
| hsa-miR-15a-3p | YM00471094 | NA | NA | CAGGCCAUAUUGUGCUGCCUCA | MIMAT0004488 |
| hsa-miR-20a-5p | YM00472205 | NA | NA | UAAAGUGCUUAUAGUGCAGGUAG | MIMAT0000075 |
| hsa-miR-29c-3p | YM00470481 | NA | NA | UAGCACCAUUUGAAAUCGGUUA | MIMAT0000681 |
| rno-miR-33-3p | YM00471597 | YI04100217 | YP02113481 | CAAUGUUUCCACAGUGCAUCA | MIMAT0017104 |
| hsa-miR-34a-5p | YM00473212 | NA | NA | UGGCAGUGUCUUAGCUGGUUGU | MIMAT0000255 |
| hsa-miR-34c-5p | YM00472810 | YI04101981 | YP00205659 | AGGCAGUGUAGUUAGCUGAUUGC | MIMAT0000686 |
| hsa-miR-103a-3p | NA | NA | YP00204063 | AGCAGCAUUGUACAGGGCUAUGA | MIMAT0000101 |
| hsa-miR-124-5p | YM00470547 | YI04101111 | | CGUGUUCACAGCGGACCUUGAU | MIMAT0004591 |
| hsa-miR-145-5p | YM00470014 | YI04102423 | YP00204266 | GUCCAGUUUUCCCAGGAAUCCCU | MIMAT0000437 |
| hsa-miR-146a-5p | YM00472124 | NA | YP00204483 | UGAGAACUGAAUUCCAUGGGUU | MIMAT0000449 |
| mmu-miR-155-5p | YM00470919 | NA | NA | UUAAUGCUAAUUGUGAUAGGGGU | MIMAT0000165 |
| hsa-miR-181c-5p | YM00471280 | NA | NA | AACAUUCAACCUGUCGGUGAGU | MIMAT0000258 |
| rno-miR-214-3p | YM00472862 | YI04105003 | NA | ACAGCAGGCACAGACAGGCAG | MIMAT0000885 |
| hsa-miR-214-3p | NA | NA | YP00205512 | ACAGCAGGCACAGACAGGCAGU | MIMAT0000271 |
| hsa-miR-219a-5p | YM00470876 | NA | NA | UGAUUGUCCAAACGCAAUUCU | MIMAT0000276 |
| rno-miR-297 | YM00470075 | NA | NA | AUGUAUGUGUGCAUGUAUGCAUG | MIMAT0000899 |
| Negative Control | YM00479902 | NA | NA | UCACCGGGUGUAAAUCAGCUUG | NA |

*Supplementary table 3.2: Potential mRNA targets of each microRNA*

| **3.2A** | vs. DIFF VehCo | | vs. miR-NC | |
|---|---|---|---|---|
| mRNA | padj | log2(FC) | padj | log2(FC) |
| **miR-33-3p targets** | | | | |
| Ntrk2 | 2.41E-08 | -0.18 | 2.73E-14 | -0.34 |
| Rab10 | 4.28E-05 | -0.15 | 2.96E-06 | -0.19 |
| Eif4e | 5.57E-21 | -0.36 | 6.28E-06 | -0.25 |
| Bnip3l | 3.78E-10 | -0.22 | 1.96E-05 | -0.18 |
| Stim2 | 1.69E-02 | -0.14 | 4.45E-03 | -0.20 |
| Fam168b | 5.15E-03 | -0.10 | 2.11E-03 | -0.13 |
| Sec63 | 1.37E-08 | -0.23 | 1.25E-12 | -0.34 |
| **miR-34c-5p targets** | | | | |
| Vamp2* | 5.08E-28 | -0.43 | 8.74E-17 | -0.38 |
| Vdr* | 1.05E-24 | -0.59 | 6.85E-13 | -0.53 |
| Rras2* | 1.23E-03 | -0.30 | | |
| **miR-124-5p targets** | | | | |
| Rras2* | 8.31E-16 | -0.67 | 2.93E-02 | -0.28 |
| Cdon* | 5.43E-07 | -0.55 | 1.86E-05 | -0.60 |
| Hnrnpab* | 1.76E-28 | -0.44 | 2.57E-21 | -0.50 |
| Hnrnpf | 1.91E-04 | -0.11 | 2.24E-02 | -0.10 |
| **miR-145-5p targets** | | | | |
| Myrf | 2.96E-76 | -0.77 | 6.53E-32 | -0.56 |
| Snx27 | 4.45E-09 | -0.22 | 1.59E-03 | -0.18 |
| **miR-214-3p targets** | | | | |
| Id4$^{+}$ | 3.05E-04 | -0.28 | 1.24E-06 | -0.50 |
| Errfi1 | 2.71E-04 | -0.26 | 1.17E-05 | -0.37 |
| Grb2* | 1.19E-04 | -0.14 | 7.59E-06 | -0.22 |
| Fgfr1$^{+}$ | 3.10E-06 | -0.15 | 9.30E-11 | -0.28 |

Search strategy in 3.2A

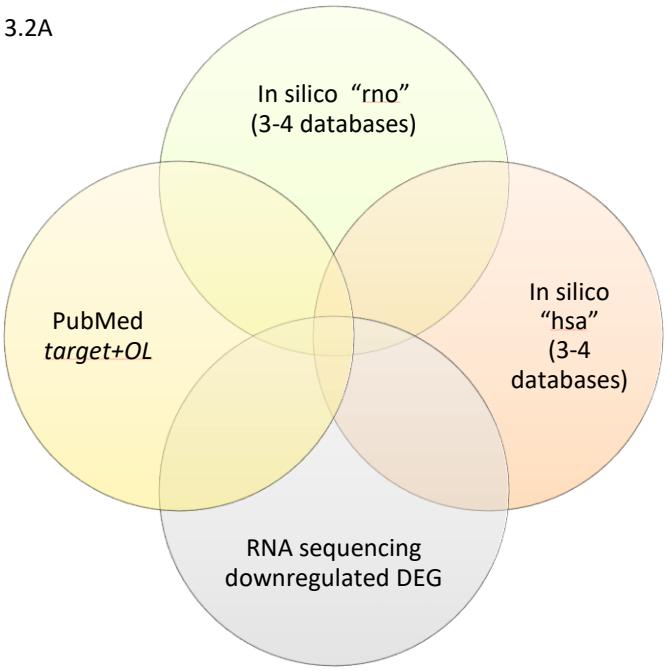


Search strategy in 3.2B

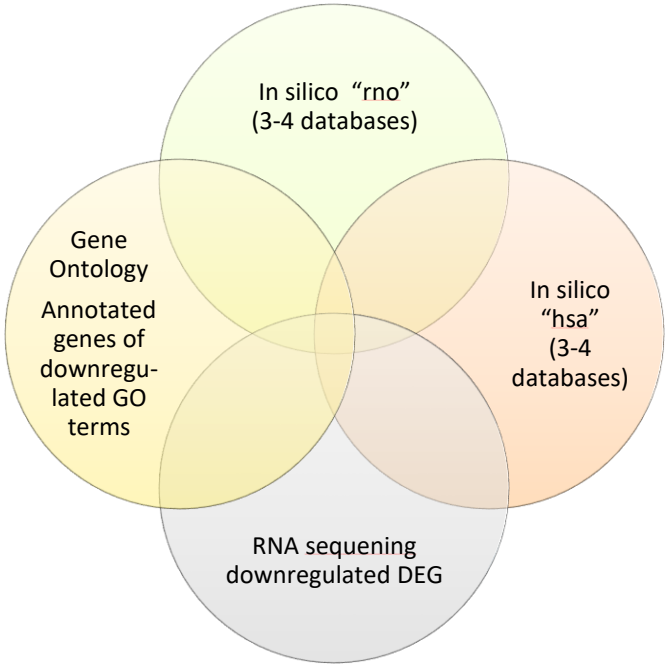

| **3.2B** | vs. DIFF VehCo | | vs. miR-NC | | Gene Ontology terms (Biological Process) |
|---|---|---|---|---|---|
| mRNA | padj | log2(FC) | padj | log2(FC) | |
| **miR-33-3p targets** | | | | | |
| Calm2 | 4.68E-07 | -0.16 | 1.36E-02 | -0.11 | cell division |
| Etnk1 | 4.15E-02 | -0.08 | 4.01E-02 | -0.11 | phospholipid biosynthetic process |
| Far1 | 2.67E-21 | -0.40 | 6.05E-12 | -0.40 | phospholipid biosynthetic process<br>long-chain fatty-acyl-CoA metabolic process |
| Ndel1 | 2.75E-04 | -0.19 | 4.09E-03 | -0.20 | chromosome segregation |
| Ntrk2 | 2.41E-08 | -0.18 | 2.73E-14 | -0.34 | myelination<br>axon ensheathment |
| Rab10 | 4.28E-05 | -0.15 | 2.96E-06 | -0.19 | cell division |
| Slc1a3 | 1.51E-02 | -0.12 | 3.91E-13 | -0.41 | generation of precursor metabolites and energy |
| Ube2j1 | 2.79E-02 | -0.13 | 6.40E-05 | -0.27 | regulation of protein catabolic process |
| Ube2n | 8.00E-30 | -0.46 | 1.32E-10 | -0.35 | DNA repair |
| **miR-34c-5p targets** | | | | | |
| Ago4 | 4.62E-07 | -0.46 | 2.69E-04 | -0.44 | ribonucleoprotein complex assembly |
| Atg4b | 3.59E-03 | -0.13 | 2.92E-02 | -0.13 | regulation of protein catabolic process |
| Dixdc1 | 7.73E-03 | -0.14 | 5.39E-03 | -0.17 | Wnt signaling pathway<br>stress-activated MAPK cascade<br>axonogenesis |
| Dll1 | 3.24E-04 | -0.29 | 5.77E-10 | -0.54 | astrocyte differentiation<br>glial cell differentiation |
| Erc1 | 1.09E-21 | -0.31 | 4.33E-02 | -0.11 | synapse organization |
| Erlin1 | | | | | regulation of lipid biosynthetic process<br>cholesterol metabolic process |
| Map1a | 6.31E-13 | -0.23 | 6.03E-05 | -0.16 | regulation of protein catabolic process<br>axonogenesis |
| Notch1 | 1.54E-28 | -0.32 | 6.11E-21 | -0.34 | Wnt signaling pathway<br>Ras protein signal transduction<br>astrocyte differentiation<br>oligodendrocyte differentiation<br>negative regulation of gliogenesis<br>axonogenesis |
| Pdgfra | 7.60E-47 | -0.34 | 7.92E-60 | -0.50 | positive regulation of kinase activity<br>regulation of phospholipid metabolic process |
| Pip5k1a | 1.16E-09 | -0.26 | 7.49E-08 | -0.29 | glycerolipid biosynthetic process |
| Ppp2r5a | 8.38E-06 | -0.23 | 9.80E-05 | -0.29 | regulation of lipid metabolic process |
| Synj1 | 1.67E-02 | -0.14 | 6.32E-04 | -0.22 | regulation of gliogenesis |
| Vcl | 2.86E-06 | -0.37 | 4.27E-07 | -0.47 | axonogenesis |

| | | | | | |
|---|---|---|---|---|---|
| **miR-124-5p targets** | | | | | |
| Atxn2 | 1.42E-04 | -0.17 | 5.32E-03 | -0.17 | ribonucleoprotein complex biogenesis |
| Hnrnpf | 1.91E-04 | -0.11 | 2.24E-02 | -0.10 | mRNA processing |
| | | | | | RNA splicing |
| **miR-145-5p targets** | | | | | |
| Adpgk | 1.75E-02 | -0.15 | 2.49E-02 | -0.17 | pyruvate metabolic process |
| Arl6ip5 | 7.97E-06 | -0.19 | 9.17E-03 | -0.15 | stress-activated protein kinase signaling cascade |
| Elmo1 | 2.10E-06 | -0.29 | 5.30E-09 | -0.40 | Ras protein signal transduction |
| Map4k4 | 3.37E-13 | -0.20 | 5.96E-03 | -0.13 | Ras protein signal transduction |
| | | | | | stress-activated protein kinase signaling cascade |
| Myrf | 2.96E-76 | -0.77 | 6.53E-32 | -0.56 | oligodendrocyte differentiation |
| | | | | | gliogenesis |
| | | | | | myelination |
| | | | | | axon ensheathment |
| Rtkn | 7.52E-16 | -0.35 | 3.17E-14 | -0.42 | Ras protein signal transduction |
| | | | | | Rho protein signal transduction |
| | | | | | cell division |
| **miR-214-3p targets** | | | | | |
| Akap13 | 4.54E-26 | -0.35 | 9.44E-30 | -0.49 | positive regulation of kinase activity |
| Atg13 | 1.97E-03 | -0.18 | 2.81E-02 | -0.17 | autophagy |
| Atp2a2 | 1.25E-56 | -0.41 | 9.92E-28 | -0.38 | autophagy |
| Cdip1 | 2.05E-06 | -0.23 | 2.09E-02 | -0.16 | intrinsic apoptotic signaling pathway |
| Cpeb1 | 3.74E-03 | -0.83 | 6.65E-04 | -1.13 | cytoplasmic translation |
| Csf1 | 3.21E-03 | -0.26 | 5.09E-06 | -0.45 | positive regulation of kinase activity |
| | | | | | gliogenesis |
| Errfi1 | 2.71E-04 | -0.26 | 1.17E-05 | -0.37 | response to platelet-derived growth factor |
| | | | | | negative regulation of ERBB signaling pathway |
| Gpd1 | 2.23E-14 | -1.10 | 1.72E-17 | -1.35 | glycerolipid metabolic process |
| | | | | | generation of precursor metabolites and energy |
| | | | | | pyruvate biosynthetic process |
| | | | | | carbohydrate catabolic process |
| | | | | | ATP biosynthetic process |
| Ifnar1 | 1.18E-08 | -0.23 | 4.03E-11 | -0.32 | generation of precursor metabolites and energy |
| Mtmr3 | 6.38E-03 | -0.11 | 2.89E-02 | -0.12 | phospholipid metabolic process |
| | | | | | glycerolipid metabolic process |
| | | | | | autophagy |
| Mtmr4 | 5.09E-03 | -0.13 | 1.23E-02 | -0.15 | phospholipid metabolic process |
| | | | | | glycerolipid metabolic process |
| | | | | | autophagy |

| | | | | | |
|---|---|---|---|---|---|
| Plec | 1.18E-26 | -0.38 | 8.89E-08 | -0.26 | glial cell differentiation<br>myelin maintenance<br>generation of precursor metabolites and energy |
| Ptprj | 3.88E-15 | -0.29 | 2.55E-17 | -0.39 | insulin receptor signaling pathway<br>negative regulation of ERBB signaling pathway<br>glial cell differentiation |

The potential mRNA targets were predicted by in silico analysis, by their downregulation in RNA sequencing and by (A) a Pubmed search of their involvement in OPC/OL physiology or (B) the gene annotation to downregulated gene ontology terms of interest as illustrated by the Venn diagrams. We selected the targets predicted by 3-4 databases in both rats and humans, except for (*) only in rats and (+) only in humans and predicted by 0-2 databases in the other species. Each table contains the fold change (FC, expressed as logarithm base 2 [Log2(FC)] and highlighted by a blue-colour scale [dark blue for a bigger negative fold change, to light blue for a smaller negative fold change]) of the expression gene value of the potential mRNA targets to the differentiation vehicle control (DIFF VehCo) and to the microRNA negative control mimic (miR-NC) as well as the adjusted p-value (padj) in RNA sequencing. DEG: differentially expressed genes, GO = Gene Ontology, hsa = homo sapiens, OPC = oligodendrocyte progenitor cells, OL = oligodendrocytes, rno = rattus norvegicus.

Furthermore, we will briefly highlight other targets we did not investigate, but that might deserve further attention, namely Fyn related Src family tyrosine kinase (*Frk*) and vitamin D receptor (*Vdr*) (mir-34c-5p), as well as fibroblast growth factor receptor 1 (*Fgfr1,* miR-214-3p). *Frk* (miR-34c-5p) has not been described in OPCs, but it is related to Fyn tyrosine kinase. Fyn tyrosine kinase regulates morphological OPC differentiation by activation of Rac1 and inactivation of RhoA, involved in stress fibre formation and actin polymerization, and allows Mbp translation in RNA transport granules by phosphorylating Hnrnpa2/Hnrnpf.[515,555,595] *Vdr* (miR-34c-5p) was only predicted by one database in humans. However, vitamin D treatment, both in vitro and in vivo, as well as Vdr signaling induce OPC differentiation [1082–1085]. Herein, vitamin D inhibits OPC proliferation by downregulating Myc proto-oncogene BHLH transcription factor, and upregulates Ras protein signal transduction, that has been linked to OPC differentiation [1084,1085]. Finally, *Fgfr1*, a target of miR-214-3p predicted in humans but not in rats, is involved in OPC specification and proliferation [509,1086].

*Research is the irrational belief in colourless magic.*

Océane Perdaens

# DISCUSSION

# I. microRNA dysregulation in MS: a truth or a myth?

## i. MS-related microRNA dysregulation lacks specificity

We have evidenced the dysregulation of 21 microRNAs in the CSF/serum/PBMCs of relapsing and/or remitting MS patients as compared to symptomatic/healthy controls, of which 18 were remarkably dysregulated in the CSF, mainly upregulated in relapsing MS patients. The CSF has been less thoroughly explored as compared to the peripheral compartments, although it directly surrounds the site where the pathology occurs. In our study, the microRNAs found in the peripheral compartments were all downregulated, namely 6 in the serum of relapsing and/or remitting MS vs HC and one in PBMCs of relapsing vs remitting MS. Furthermore, 5 microRNAs had not been linked to MS before (miR-15a-3p, miR-33a-3p, miR-34c-5p, miR-124-5p, and miR-297, while miR-29c-3p and miR-149-3p have been linked to grey matter atrophy in MS since our publication [897]). However, in the second CSF cohort of our first study, we could only confirm the upregulation of miR-146a-5p in relapsing MS vs SC and of miR-150-5p in relapsing and remitting MS vs SC, while in this cohort three other microRNAs (miR-15b-5p, miR-16-5p, and miR-29b-3p) were upregulated in relapsing MS vs SC.

In this second CSF cohort, we also verified the MS-specificity of the dysregulated microRNAs by including patients with other neurological disorders (infectious and inflammatory CNS disorders, non-inflammatory and peripheral neurological disorders). Herein, 23 out of the 25 significantly dysregulated microRNAs were upregulated in infectious CNS disorders, 10 in inflammatory CNS disorders and 4 in relapsing MS vs SC, whereby miR-15b-5p, miR-29b-3p and miR-29c-3p were in common to the 3 groups, and miR-150-5p was in common to these 3 groups and remitting MS as well vs SCs, non-inflammatory (mainly dementia) and peripheral inflammatory neurological disorders. The microRNA expression profile was thus partially similar between the infectious and inflammatory CNS disorders and relapsing MS, but with a much greater positive fold change in infectious CNS disorders. miR-223-3p, miR-342-3p and miR-423-5p were common to infectious and inflammatory CNS disorders vs SCs and were noticeably also upregulated in infectious CNS disorders vs non-inflammatory and peripheral neurologic disorders, remitting (the 3 microRNAs) and relapsing (except miR-223-3p) MS. However, only miR-423-5p does not seem to have been linked to MS elsewhere, as miR-223-3p and miR-342-3p have been found upregulated in serum EVs of RRMS patients vs

PMS patients [764]. Both miR-223-3p and miR-342-3p inhibit pyroptosis (i.e. pro-inflammatory programmed cell death) by targeting respectively NLR family pyrin domain containing 3 (*NLRP3*) inflammasome and caspase 1 [1087,1088]. miR-223-3p and NLRP3 were found upregulated in activated microglia and macrophages surrounding injured myelin [1089]. Dexamethasone-induced miR-342-3p also targets Rictor (mTORC2 subunit) in Tregs, thereby promoting their immune regulatory function [1090]. An anti-inflammatory effect has also been alleged to miR-423-5p in several disease models, but it was also proven to alter the intestinal barrier by targeting claudin, thereby aggravating inflammatory bowel disease in mice [1091–1095]. Furthermore, 8 upregulated microRNAs were common to the infectious CNS disorder group of the second cohort and the relapsing MS group of the first cohort.

The discrepancies between the two cohorts are probably mostly due to the variability in group sizes and the low abundance of microRNAs in the CSF reducing the sensitivity of RT-qPCR analysis. In the CSF, a pre-amplification step was needed after reverse transcription and before the microRNA-specific PCR assay, in order to increase their detection, while this can possibly affect the linearity of the final assay [1096]. Even with this pre-amplification, the Cts of most microRNAs were still high, thereby complicating the interpretation of some PCR analyses.

Pathway enrichment analysis within KEGG (Kyoto Encyclopaedia of Genes and Genomes) was the strongest on the sets of CSF-dysregulated microRNAs in relapsing MS (vs remitting MS and SC) which were rather upregulated in the CSF, although several of them were also linked to remitting MS vs SC which were rather downregulated in the CSF (as indicated in supplementary table 1.6). It highlighted pathways involved in cell cycle and signalling, immune signalling, cell adhesion, axon guidance and neurotrophic support. The most commonly annotated genes were linked to cell cycle progression (cyclin D1 (CCND1), cyclin dependent kinase 6 (CDK6), MYC Proto-Oncogene bHLH Transcription Factor (MYC)) or cell cycle arrest (cyclin dependent kinase inhibitor 1A (CDKN1A), TP53) and signal transduction of TGFb signalling (SMAD4).

ii. MS-related microRNAs and T cell mediators presumably correlate via indirect pathways

Hereafter, we verified the expression of 21 dysregulated microRNAs, identified in our first study, in PBMCs of a different MS population, characterised by the absence or presence of radiological activity on brain MRI (without a clinical overt relapse) and of an ongoing first line DMT (none/IFNb/GA). In this population we evidenced the dysregulation of 13 microRNAs in the PBMCs of all MS patients, that was overall slightly stronger in inactive MS, except for miR-27a-3p, although with no significant differences between active and inactive MS. The treatment status affected a minority of the microRNAs, miR-29c-3p was significantly upregulated in untreated patients vs treated patients and HC, miR-27a-3p was downregulated in GA-treated patients and miR-34a-5p was upregulated in IFNb-treated patients. PCA did not segregate well patients from HC.

We also measured the mRNA expression level of several T cell mediators (mainly Th1, Th17 and Treg cytokines and transcription factors). We observed the upregulation of *FOXP3* (more strongly in inactive MS) and *JAK2* (more strongly in treated MS) in PBMCs of MS patients vs HC, of MXA and IL27p28 in IFNb-treated, and of IL12p40 in untreated patients vs HC.

The correlation analysis, when considering the significant correlations only, showed only positive correlations between the significantly upregulated microRNAs and the T cell mediator mRNAs (except with *JAK2*), indicating that these microRNAs may not target them directly but rather an upstream negative regulator. The opposite was seen with the significantly downregulated microRNAs, that were negatively correlated with T cell mediator mRNAs, and could thus target them directly or indirectly via an upstream positive regulator. We further highlighted the positive or negative correlation of several significantly dysregulated microRNAs with *IL21* and/or *FOXP3*, and also of a few non-significantly dysregulated microRNAs with *TGFB1*, except miR-297 that was significantly downregulated and negatively correlated with *TGFB1*. We aimed to verify by in silico analysis whether these T cell mediators were predicted targets of one of these microRNAs. The predictions were however mostly limited to one or two databases and were not always consistent with the microRNA expression profile and the correlation analysis, further suggesting that the microRNAs might not target them directly, except for miR-34c-5p and *FOXP3*.

The in silico analysis in both studies were not conducted with the same purpose and are therefore difficult to compare. In the first study, we aimed to identify the pathways in which a set of dysregulated microRNAs were involved, while in the second we wanted to verify whether a T cell mediator could be specifically targeted by the microRNAs of the study. TGFb signalling was identified in the first study and TGFB1 was investigated in the second, however, different microRNAs were prominently linked to each in each study.

### iii. MS-related microRNA dysregulation shows some consistency despite technical challenges

We acknowledge the differences in the microRNA expression in PBMCs between these two studies (1 microRNA significantly dysregulated in the first study, 13 in the second), although 14 microRNAs were measured in both. The study population was very different, but inherent technical issues might also be involved. Although there was no reason to doubt on the quality of the PCR runs in neither study (based on the melt curves), the Cts were overall smaller in the second study, suggesting that the reverse transcription might have worked better on this cohort (more active enzyme). Moreover, in the second study, we first aimed to apply the commonly used $2^{-\Delta\Delta Ct}$ method (with $\Delta\Delta Ct$ = $\Delta Ct$ [target-reference]$_{sample}$ − $\Delta Ct$ [target-reference]$_{mean\ of\ controls}$), which normalises the data first to a reference gene and secondly to the mean of the controls[909]. However, the Cts of *RNU6*, frequently used as internal reference gene, were too variable with significant differences within (especially in the HCs) and between the groups. The use of RNUs as reference gene has been questioned by others as well. Moreover, RNUs are small non-coding RNAs with a distinct biogenesis of that of microRNAs [1097]. None of the investigated microRNAs, neither another microRNA tested as potential reference, namely miR-103a-3p, were within a close range for all samples to allow for normalisation. Therefore, we decided to use the global mean method (with $\Delta Ct$ = Ct [target microRNA]$_{sample}$ – mean Cts [all target microRNAs]$_{sample}$), whereby the Ct of the investigated microRNA is normalised to the mean expression value of all expressed microRNAs within the same sample [1098]. This method was initially developed to normalise the data of a big set of microRNAs (e.g. in a microarray) but does not specify the minimal number of microRNAs needed for normalisation [934]. However, while in the $2^{-\Delta\Delta Ct}$ method part of the normalisation is across the control samples,

in the global mean method the normalisation is within the sample. Therefore, we reasonably assumed that the global mean would help balance the variability across (control) samples as seen for *RNU6*. When applying this global mean method on the data of the PBMC cohort of our first study, there was still only one significantly downregulated microRNA, namely miR-191-5p in relapsing MS vs HC, while with the $2^{-\Delta\Delta Ct}$ method vs *RNU6* miR-34a-5p was solely downregulated in relapsing vs remitting MS, which with the global mean was only significant on a Mann-Whitney U-test between the two groups, but not on a one-way ANOVA. While I cannot rationally argument in favour or against one or the other method, this, as well as the partial lack of concordance between the two CSF cohorts of our first study, clearly illustrates how differences in the study design (study population characteristics and size, type of samples and method of sampling, quantification technology employed, analytical and statistical methods applied etc.) can lead to the large variability in the reported dysregulated microRNAs as well as the difficulties to harmonise these data.

However, a comparison between our two studies and the literature (see table 2.1) shows some discrepancies, but also several consistencies between the studies, supporting the reliability of both studies. Herein, miR-15a-3p/20a-5p/21-5p/29c-3p/34c-5p/146a-5p/150-5p/155-5p/297 in the CSF and miR-181c-5p in the serum of relapsing and/or remitting MS patients were similarly dysregulated in the PBMCs of active/inactive treated/untreated MS patients, while miR-27a-3p and miR-125b-5p were dysregulated in the opposite direction. miR-34a-5p, was upregulated in PBMCs of remitting vs relapsing MS in our first study and of inactive MS vs HC in our second study. miR-24-3p/27b-3p/33a-3p/124-5p/145-5p/149-3p/214-3p dysregulated in the CSF and miR-126-3p dysregulated in the serum of relapsing and/or remitting MS in our first study, were however not confirmed in PBMCs of the second MS population.

microRNA dysregulation is undeniably present, but possibly overestimated in MS and potentially involved in MS pathogenesis. The interest in the field has led to a high number of studies reporting with much disparity over 500 microRNAs as dysregulated in MS, of which a few have been functionally characterised, while only 1917 microRNAs have been assigned to humans. Moreover, with only 9% of consistency in at least 3 studies, these reported microRNAs should be considered with caution [755]. Reviews have so far not been conclusive on a MS-specific

microRNA signature due to the many differences in study design. Therefore, a large study with a multicentric recruitment of MS patients and controls with detailed records, and a centralised analysis by a single technique could help confirm the microRNA expression profile characteristic of MS (depending on disease subtype, activity, progression, treatment etc.) and could even be more powerful in identifying (clinically applicable) biomarkers, as many have been proposed so far, but none has been confirmed.

iv. microRNAs are dysregulated in other neurodegenerative diseases

Many studies have reported dysregulated microRNAs in Alzheimer's (AD) and Parkinson's disease (PD), that are, as seen for MS, sometimes difficult to reconcile between studies or between the peripheral and central compartments [1099–1104]. Both diseases are characterised by neurodegeneration, alongside neuro-inflammation in particular by the activation of the inflammasome in microglia [1105]. Although the microRNAs more strongly linked to both diseases differ from the ones we have investigated in the scope of MS, a few, such as miR-27a-3p, miR-29b-3p, miR-29c-3p, miR-34a-5p, miR-34c-5p, miR-145-5p and miR-146a-5p are mutual. Of note, miR-27a-3p, miR-29b-3p,miR-29c-3p, miR-34a-5p, and miR-145-5p were all identified as part of a competing endogenous RNA axis in the periplaque region in SPMS spinal cords, whereby they are sponged by an upregulated lncRNA [1075]. miR-27a-3p is seemingly downregulated and miR-27b-3p upregulated in PBMCs of PD patients [1106]. Both contribute to mitochondrial damage by preventing mitophagy [1107]. In MS, miR-29b-3p may contribute to chronic inflammation as it is upregulated in memory CD4+ T cells, and decreases upon their activation while it remains stable in control [1108]. The latter suggests an impaired feedback loop, as miR-29b-3p regulates Th1/Th17 response by repressing TBET and RORgT, is itself induced by IFNg and increases the fraction of Tregs [1108,1109]. In the second patient cohort of our first study, miR-29b-3p was the only microRNA significantly upregulated in the CSF of patients with non-inflammatory neurological disorders (dementia) vs SCs (within a one-way ANOVA on all groups of that patient cohort), while it was found downregulated in the blood of AD patients and in the serum of PD patients with mild cognitive impairment and even more in PD patients with dementia [1110,1111]. Serum levels of miR-29c-3p are decreased in PD patients vs controls [1112,1113]. miR-29c-3p is anti-inflammatory by inhibiting microglial inflammasome *NLPR3*

activation, while its sequestration/decrease contributes to apoptosis and autophagy of dopaminergic neurons [1114–1116]. miR-29c-3p downregulation in the brain of AD patients accompanies the upregulation of beta secretase 1 and the accumulation of amyloid beta [1117]. In fact, by targeting tumour necrosis factor alpha-inducible protein-1 (*TNFAIP1*) miR-29c-3p decreases NFkB signalling and reduces amyloid beta induced neurotoxicity [1118]. miR-29c-3p was further found downregulated in grey matter lesions of PMS patients' brain [897]. miR-34c-5p was downregulated in several brain areas of PD patients which was in vitro associated with a reduction in cell viability of a neuroblastoma cell line (SH-SY5Y) alongside altered mitochondrial function and oxidative stress [1034,1119]. Oppositely, miR-34c-5p is upregulated in the hippocampus of AD patients [1120]. Its overexpression, mediated by oxidative stress through ROS/JNK/p53 pathway, alters the dendritic and synaptic integrity (by targeting synaptotagmin 1) and thereby supports cognitive decline [1032,1121]. miR-145-5p was downregulated in the CSF of PD patients vs SCs [1122]. miR-145-5p downregulation resumes the expression of its direct target, nuclear receptor subfamily 4 group A member 2 (*NR4A2*), which mediates the BMP2-induced differentiation of dopaminergic neurons but also reduces TNFa expression in microglia thereby improving neuronal survival after ischaemia/reperfusion [814,1123]. Oppositely, miR-145-5p could mediate anti-inflammatory mechanisms by facilitating macrophages/microglia towards a M2 phenotype or by blocking astrocyte proliferation, while it is downregulated in extracellular vesicles of LPS-induced microglia [815,1124]. Interestingly, NR4A2 is considered neuroprotective [1125]. It is important in the differentiation, survival and integrity of dopaminergic neurons [1126–1128]. *NR4A2* is downregulated in PBMCs of PD patients, and mutations reducing its expression are associated with familial PD [1129,1130]. In AD, NR4A2 is highly co-expressed with amyloid beta early in the disease, but its expression declines with disease progression and accumulation of amyloid beta [1131]. Finally, in MS patients, *NR4A2* was found downregulated in PBMCs but upregulated in T cells of MS [1132,1133]. It is however upregulated in the motor cortex on brain autopsies of MS patients, correlating positively with neuronal densities [1081]. Its knockout precipitates EAE severity, oppositely its activation lowers EAE by repressing NFkB [1080,1134]. The role of miR-146a-5p in PD and AD seems contradictory to its anti-inflammatory properties described in MS/EAE [821,827]. miR-146a-5p, downregulated in the serum and PBMCs of PD patients, induces ROS production in a PD cell line model [1135–1137]. miR-146a-5p is upregulated in the hippocampus of AD patients, which was in vitro

and in vivo linked to several pathophysiological processes as apoptosis/pyroptosis, oxidative stress, amyloid beta deposition, and cytoskeletal instability aggravating cognitive impairment [1138–1142]. Moreover, EV-mediated transfer of miR-146a-5p from microglia to neurons decreases the dendritic spine density in hippocampal neurons by targeting presynaptic synaptotagmin and postsynaptic neuroligin 1 [1143]. However, an AD transgenic mice model with microglial miR-146a-5p overexpression exhibited the opposite (reduced cognitive deficits, attenuated neuroinflammation, reduced Aβ levels, reduced neuronal loss associated with a microglial anti-inflammatory phenotypic switch) [1144]. miR-155-5p was upregulated in PBMCs of PD patients, in hippocampal brain tissue of AD patients as well as in the hippocampus/cortex of an AD mice model [1136,1142,1145]. miR-155-5p is proactively involved in neuroinflammation, microglial activation, oxidative stress and apoptosis in both diseases [1145–1149]. miR-155-5p enhances amyloid beta deposition, partly by inhibiting its microglial catabolism [1150,1151]. Finally, miR-214-3p has been described as neuroprotective [1077]. It is decreased in serum of PD patients vs controls [1113,1152]. Its downregulation in in vitro and in vivo PD models accompanies microglial activation, neuroinflammation, cell apoptosis and oxidative stress [1153,1154]. It was also decreased in the CSF of AD patients [1062]. miR-214-3p overexpression decreases autophagy and neuronal apoptosis and improves cognition in a mice model of AD[1062].

## II. May MS-related microRNAs condition the differentiation of OPCs?

We next aimed to study the functional involvement of these microRNAs in OPC differentiation. Hereby, we first observed that several MS-related microRNAs impeded the differentiation of CG-4 cells, while OPC/OL-directed Dicer knockout experiments suggested a supportive role of microRNAs in OPC differentiation [782,783,999].

Hereafter we showed, with a great consistency between independent RT-qPCR and the RNA sequencing results, the negative impact of miR-33-3p, miR-34c-5p, miR-124-5p on OPC differentiation, arresting it at a late OPC stage, while miR-145-5p halted it rather at a late OPC/early pre-OL stage. miR-214-3p, that has long been postulated to inhibit OPC differentiation by targeting *Mobp* [885] (on the basis of an

in silico analysis only), on the contrary promoted OPC differentiation to mature OLs in our experimental setting.

i. The predicted mRNA targets remain to be confirmed

We proposed for each microRNA several potential mRNA targets supporting its observed effect on the cell fate, that were significantly downregulated on RT-qPCR analysis and RNA sequencing, except for the predicted targets of miR-214-3p. However, as a microRNA may not cause the degradation of its targeted mRNA, its expression might not change at the mRNA level [725].

The predicted targets should ideally be verified by electrophoretic mobility shift assay (EMSA) or by a reporter gene assay (e.g. dual luciferase assay) and confirmed by mutagenesis. EMSA can evidence the interaction between the microRNA of interest and the seed region of the predicted mRNA, using radio- or fluorescent-labelled (fluorescent-based RNA EMSA [FREMSA]) probes of both. The interacting microRNA/mRNA couple will move more slowly through the gel during electrophoresis, resulting in a shift of the detection band as compared to the probes loaded separately or with a probe mutated in the seed region of the mRNA [1155,1156]. The dual luciferase assay explores the regulatory effect of the microRNA by binding to its predicted seed. Hereby, the 3'UTR of the predicted mRNA target, or a part of it containing the seed region, is cloned in a plasmid in between the restriction sites downstream of the open reading frame of the firefly luciferase. The cloned plasmid contains a second luciferase, Renilla luciferase, relying on a strong promoter and thus constitutively expressed. Recipient cells, for example HEK293T that are easy to transfect, are co-transfected with the uncloned or cloned plasmid and the microRNA mimic of interest or the miR-NC. Hereafter, the cells are lysed, the reagents of both luciferases are added sequentially, and the luminescence induced by each luciferase is measured separately after each step. If the microRNA recognises its seed region in the cloned 3'UTR downstream of the firefly luciferase, it will repress the translation of the firefly luciferase. This results in a decreased activity of the firefly luciferase, evidenced by the decreased relative luminescence, normalised to the luminescence induced by the Renilla luciferase, as compared to a control condition (miR-NC). By introducing a mutation in the predicted seed region (mutagenesis), the effect of the microRNA on the activity of the firefly

*Figure 4.1: mRNA target prediction of miR-33-3p to Eif4e and miR-214-3p to Akap13*

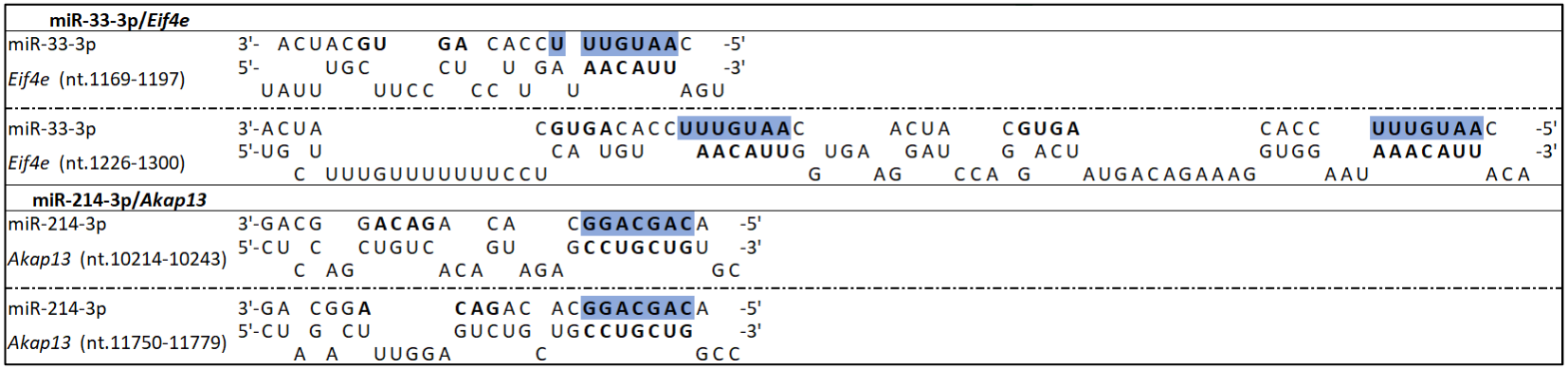


*The 3'UTR of Eif4e and of Akap13 is aligned to the sequence of miR-33-3p and miR-214-3p respectively with complementarity to the seed region highlighted in blue and to the 3' supplementary pairing site (microRNA nucleotides 13 to 16), which enhances binding specificity and affinity [725], highlighted in bolt. Incompatible nucleotides of the 3'UTR are shifted down a line. The 3'UTR site region is indicated by the nucleotide (nt.) numbering in between the brackets.*

luciferase should be abolished with relative values returning to those of the controls [1157,1158]. One could further verify if transfecting a small interfering RNA (siRNA) of the target mRNA [809] in CG-4 cells, which would inhibit it, could mirror the effect of the microRNA mimic, and on the contrary, if co-transfecting a plasmid expressing the target alongside its microRNA mimic could rescue the effect of the microRNA.

ii. The involvement of these predicted mRNA targets in MS is largely unknown

The majority of the predicted mRNA targets of the 5 investigated microRNAs of this study have not been linked to MS so far. It is thus unknown whether or how they are involved in MS pathogenesis, while for a minority of these targets this matter is still ambiguous.

Translation initiation factor *EIF4E* (miR-33-3p), is activated downstream of mTORC1. In a genome wide association study meta-analysis, *RPS6K* was identified as a risk factor for MS, but the plasmatic levels of other mTOR-dependent genes (*EIF4EBP* and EIF4F complex subunits *EIF4A, EIF4E*, and *EIF4G*) were not significantly associated, while *mTOR, RPS6KB* and *EIF4EBP1* were also found upregulated at the mRNA level in whole blood samples of newly diagnosed RRMS patients [1159,1160]. However, MAPK interacting protein kinase/EIF4E pathway is also activated via p38MAPK signalling pathway, which is critically involved in Th17 differentiation and response in both EAE and MS [1161,1162]. *NTRK2* (miR-33-3p) is positively linked to lncRNA *TUG1* in the periplaque region in SPMS spinal cord as part of a competing endogenous RNA axis whereby the lncRNA sponges the intermediate microRNA (here miR-22-3p) [1075]. Remarkably, brain derived neurotrophic factor (Bdnf)-induced Ntrk2 signalling was protective in a mild form of EAE but not in a more severe form [1163]. Finally, deletion polymorphisms of *VAMP2* (miR-34c-5p) were significantly more frequent in MS patients than in controls [1164]. No report was found linking the other predicted targets to MS.

Regarding hnRNPF, the cytoplasmic mislocalisation and altered expression of hnRNPA1, another RNA-binding protein, in neurons and oligodendrocytes is involved in both neurodegeneration and demyelination in MS and EAE by stress granule formation, and necroptosis [1165–1168].

iii. The underlying signalling pathways could bring further insight

The gene enrichment analysis allowed to further detail the cell fate directed by each microRNA in the transfected CG-4 cells, although the significant differences were more noticeable versus the differentiation vehicle control than versus the differentiation microRNA negative control. Gene Ontology consistently reflected the effect of each microRNA on OPC differentiation and myelination. Furthermore, miR-34c-5p supported DNA biosynthesis and cell cycle processes even with downregulation of Wnt signalling pathway and *Pdgfra* and *Notch1* mRNAs, both targets of miR-34c-5p involved in OPC proliferation, but cyclin-dependent kinase activity was upregulated [523,629,1036–1039]. It is thus unclear what upstream signalling pathway and receptor tyrosine kinase guides this cell fate [1019]. Jun N-terminal kinase (Jnk) interacting protein 1 (also called mitogen-activated protein kinase 8 interacting protein 1 (*Mapk8ip1*)) and *Jun*, elements of the Jnk signalling pathway involved in OPC proliferation, were slightly but significantly upregulated for example, as well as *Ntrk3*, that has been linked to both OPC proliferation/survival and differentiation (data not shown) [645,1040,1041]. miR-124-5p negatively regulated cell cycle processes (vs. the differentiation vehicle control) and RNA processing. Remarkably, miR-145-5p had the least affected GO terms, but Ras protein signal transduction was downregulated. miR-33-3p both positively and negatively affected several signalling pathways involved in OPC and OL physiology. Remarkably, both miR-33-3p and miR-214-3p negatively affected the biosynthesis/metabolism of fatty acids and/or specific lipid species as well as the energy metabolism (vs the differentiation vehicle control). This is strikingly opposite to the differentiation promoting effect of miR-214-3p [552,1027]. However, miR-214-3p also downregulated the negative regulation of Erbb signalling, involved in OPC proliferation/differentiation depending on its ligand and its dimerization pair [685].

The gene enrichment analysis thus highlighted the involvement of key signalling pathways in OPC/OL physiology, in particular ERK/MAPK and PI3K/Akt/mTOR signalling pathways, however with some difficulties in interpretation as for some conditions both the positive and negative regulation of a pathway could be enriched. Given that these pathways can vary very subtly during their regulation of OPC proliferation and differentiation [998], it would be of greatest interest to further explore these pathways for a more detailed understanding of the functional impact

of these microRNAs. Therefore, one could establish by Western blot or by a multiplex immunoassay a phosphorylation map of key members of each pathway, since it determines their activation, namely Jnk/c-Jun (JNK signalling pathway), Erk1/2 (ERK/MAPK signalling pathway), Akt, mTOR or Rptor, Rps6kb1, Eif4ebp1, Gsk3b (PI3K/Akt/mTOR signalling pathway) [998]. OPC/OL-specific genes targeted downstream of these pathways could be identified by chromatin immunoprecipitation or electrophoretic mobility shift assay. Furthermore, by pharmacologically inhibiting one of these kinases (Jnk, Map2k1/2 (upstream Erk1/2), p38Mapk, PI3K, mTOR), one might also evaluate if this reverses/blocks the effect of the microRNA of interest (following transfection of the microRNA mimic, or lentiviral transduction/plasmid transfection of the primary microRNA (cf Discussion III.i)).

iv. Determining the microRNAs' cellular source is key to understanding their (patho-)physiology

The endogenous microRNA expression in CG-4 cells, cultured in a proliferation or differentiation medium only, was not totally comprehensive of their effect on OPC differentiation observed when transfecting the corresponding microRNA mimic. Herein, miR-34c-5p and miR-124-5p were downregulated in differentiating CG-4 cells, consistent with their negative effect on OPC differentiation. Oppositely, miR-145-5p, that negatively affected OPC differentiation as well, was however significantly upregulated in differentiating CG-4 cells. miR-33-3p was not differentially expressed between both conditions while miR-214-3p was undetectable in neither condition. Therefore, it is difficult to conclusively support their physiological involvement in OPC differentiation, although it is the precisely regulated expression profile of a series of microRNAs and not of a single one that finely tunes cellular physiology [725]. Moreover, these microRNAs could be expressed differently in OPCs/OLs under pathological conditions or originate from another cell type. miR-34c-5p, miR-145-5p, miR-214-3p have for example been linked to neurons, microglia, astrocytes and/or brain endothelial cells [816,1035,1059,1124,1154,1169–1173]. It would thus be of great value to determine their cellular origin under physiological and pathophysiological conditions to help understand their involvement in OPC differentiation and MS pathogenesis.

v. microRNA-based therapies could be part of the future

Research on microRNA-based and other non-coding RNA-based therapies have gain a lot of interest over the past years, with potential advantages as microRNAs are processed by the intracellular machinery, they target a wide range of transcripts, even within one pathway, and can be quite easily and widely engineered, modified, and generated. However, they are also challenging regarding stability, tolerability, delivery, and specificity [1174,1175]. Chemical modifications or carrier systems as ligand-oligonucleotide conjugates, virus-based approaches or lipid-, polymer- or metal-based nanoparticles with possibly bio-engineered surface modifications can increase their stability and the cell-/organ-specific delivery [1174–1182]. Extracellular vesicle (EV-)mediated delivery is another interesting option, as it follows the natural path of EV-based intercellular communication and can bypass the endocytic pathway [1183]. The biodistribution of EVs can be determined by the genetic modification of membrane proteins, by the route of administration and by the cells used for their production (preference for self-tissue delivery), but this cell-based production is also the limiting factor for large scale applications of EV-based strategies [1174,1184–1186]. Tolerability is another concern. A phase I clinical trial using a liposomal miR-34 mimic RNA therapeutic on solid tumours was stopped prematurely due to severe immune-mediated adverse events suspected to be due to the mimic itself rather than its carrier [1187]. Hereby, small RNA molecules (single- more than double-stranded) can induce a pro-inflammatory immune response mediated via endosomal Toll-like receptors inducing the NFkB pathway (TLR/MyD88/NFkB) [1188–1190]. Moreover, as a microRNA possibly targets over a hundred mRNAs, microRNA-based therapeutics could also affect targets outside the scope of the therapeutic strategy. Undesired on-target effects, on its defined targets but in another cell than the cell of interest, and off-target effects, caused by the recognition of a similar target sequence, by the loading of the passenger strand or by the induction of non-specific gene expression, are intimately linked to the dosing and route of administration of the RNA therapeutics [1174,1187,1191–1195]. This can be abrogated by chemical modifications of the RNA molecules [1191]. Overdosing can more largely affect the endogenous microRNA targetome by competing with other endogenous microRNA species or by altering their processing by saturation of the system [1192,1193]. Next to microRNA mimics and inhibitors, which could be used to restore the physiological levels of functionally active and dysregulated microRNAs, several other therapeutic molecules are currently being developed namely small-

molecule inhibitors of microRNAs (e.g. small molecules interfering with Drosha/Dicer), peptide nucleic acid polymers (targeting a pre-microRNA), microRNA sponges that trap and sequester complementary microRNA (e.g. endogenous circular RNAs), or microRNA masks that hide the seed region of the microRNA within the mRNA [1174,1196–1199]. Most of them are still explored experimentally, some have been launched in phase I/II trials (e.g. RG-125, a N-acetylgalactosamine-conjugated antimiR-103/107 for the treatment of diabetes and nonalcoholic fatty acid disease; Remlarsen, a cholesterol-conjugated miR-29 mimic for the treatment of keloid fibrosis; Miravirsen, a β-D-oxy-locked nucleic acid-modified phosphorothioate antisense oligonucleotide targeting miR-122 in hepatitis C treatment. Other clinical trials have been interrupted due to safety/tolerability issues (RG-101, an antimiR-122 in hepatitis C treatment, MRX34, a miR-34 mimic tested in several cancers) [1174].

Furthermore, in the scope of MS, an antisense oligonucleotide targeting human *CD49d* RNA transcript, the alpha subunit of very late antigen 4 (VLA4, *i.e.* integrin alpha 4/beta 1 involved in the crossing of the BBB), could reduce disease activity in a phase 2 trial but further clinical trials aren't planned so far [1200]. Similarly to microRNAs, small interfering RNAs (siRNAs) inhibit the expression of their target mRNA, with greater selectivity than microRNAs as complete complementarity is necessary. Several siRNAs, targeting *TBX21, NR4A2, CD40, IL23p19, Lingo 1, NogoA* among others, have been studied in vitro or in vivo in EAE showing promising results in reducing neuroinflammation or increasing remyelination and axonal recovery [1201–1206]. Aptamers are small stable RNA or DNA oligonucleotides folding in a three-dimensional structure fitting with high affinity and specificity to its target molecule, in particular a protein. A 40-nucleotide single-stranded DNA aptamer binding multiple myelin components could promote remyelination of CNS lesions in mice infected by Theiler's virus [1206,1207]. No clinical trial with an siRNA or aptamer has been conducted so far in MS.

Research is progressing on microRNA- and non-coding RNA-based therapeutics and offers innovating bio-engineering strategies to face the challenges linked to them. However, the biggest challenge might be to select the right microRNA candidate, especially as several microRNAs can be dysregulated in a disease, without being specific to this disease [1175].

In our case, we could imagine a therapeutic strategy to promote OPC differentiation by an inhibitor (antimiR/antagomiR) of the OL-inhibitory microRNAs (miR-33-3p, miR-34c-5p, miR-124-5p and miR-145-5p) that would reverse their effect, or by a mimic of miR-214-3p. However, an antimiR/antagomiR can only restrain a microRNA that is endogenously expressed. In our first screening of the microRNA expression in the CSF, these microRNAs were all downregulated (or tended to be) in the CSF of relapsing or remitting MS patients, except miR-145-5p (figure 1.3 and supplementary figure 1.2). The downregulation of miR-214-3p in the CSF of remitting MS patients may already suggest a deficit of remyelination. Thus, inhibiting endogenous miR-145-5p or increasing miR-214-3p could be reasonable therapeutic approaches to boost OPC differentiation, although deeper functional characterisation of these microRNAs, in OPCs but also in the other cell types involved in MS, is first needed.

Regarding the 3 other OL-inhibitory microRNAs, even if they were downregulated in the CSF, an antimiR/antagomiR-based therapeutic approach is not absolutely rejected as they might be differently dysregulated in another compartment. This was for example evidenced for miR-214-3p that we found downregulated in the CSF of remitting MS patients, but others found upregulated in active and inactive MS lesions [758]. Otherwise, exploring these microRNAs, their potential targets, and the signalling pathways they affect, might unravel new mechanisms and lead towards other, not necessarily microRNA-based, therapeutic targets.

## III. Further limitations and perspectives

We have investigated the effect of several microRNA species in vitro by transfecting their mimic, with or without their inhibitor, in CG-4 cells. This experimental model has multiple limitations calling for caution in the interpretation of the results and calling for confirmation by other experimental models.

i. Transfection of a microRNA mimic/inhibitor

We perceive the artificial character of transfecting a synthetic microRNA mimic in a cell line to study its physiological/pathophysiological effect. First of all, Lipofectamine™ 2000, a cationic lipid transfection reagent, has some toxicity and can induce genes involved in cellular stress response, cellular metabolism and cell cycle control, thereby impacting the cellular physiology [1208,1209].

*Figure 4.2: The effect of the vehicle, Lipofectamine™ 2000, on the proliferation and differentiation of CG-4 cells in RT-qPCR*

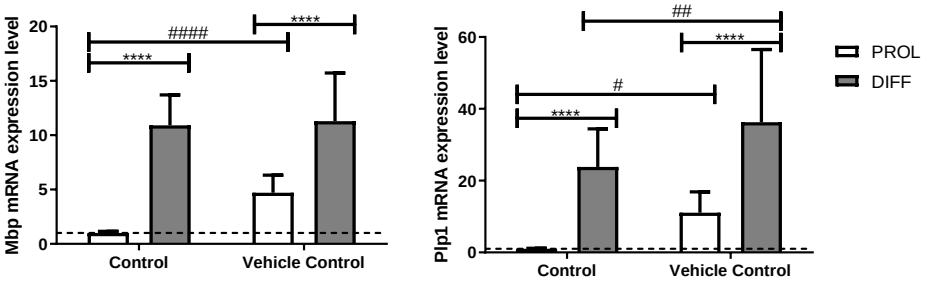


*The plots show the relative expression (mean with SD of $2^{-\Delta\Delta Ct}$) of the differentiation markers Mbp and Plp1 to the proliferation control (PROL Control). CG-4 cells were cultured in 6-well plates in proliferation (PROL, white bars) or differentiation medium (DIFF, grey bars) without or with addition of the vehicle, Lipofectamine™ 2000, as indicated on the x-axis (control vs vehicle control respectively), following the timing of the double transfection protocol. The dotted line represents the mean relative expression of the proliferation control to which the relative expression ($2^{-\Delta\Delta Ct}$) of each sample was calculated. The p-value was calculated by Sidak's multiple comparison test following a two-way ANOVA according to the absence/presence of the vehicle (#) and the type of medium (*). # for p ≤ 0.05, ## for p ≤ 0.01, ****/#### for p ≤ 0.0001. Data of 7 experiments with each condition in triplicate. SD = standard deviation.*

We have cultured in parallel CG-4 cells in proliferation and differentiation medium with or without Lipofectamine™ 2000, and noticed indeed that Lipofectamine™ 2000 induced the expression of the differentiation markers, *Mbp* and *Plp1*, especially in the cells cultured in proliferation medium. However, there was still a

significant difference in their expression between the proliferation and differentiation condition both without and with the vehicle (figure 4.2). Therefore, we have always normalised our results to the differentiation vehicle control.

Furthermore, the synthetic microRNA mimic is transfected at a supraphysiological concentration in order to be able to visualise distinctively its effect under the experimental conditions. However, exogenous microRNAs at a supraphysiological concentration may alter the processing of endogenous microRNAs and in fine affect cellular physiological processes by competing for the use of the intracellular resources for gene expression or possibly by saturating the system [1192,1193]. Moreover, transient expression of a microRNA mimic leads to the accumulation of high molecular RNA species generated by the concatemerisation (continuous molecules with multiple copies of the microRNA), and by the 5'- and 3'-end tailing of the microRNA mimic, and causes non-specific alterations in gene expression as well [1210]. Although microRNA mimics are largely used, the expression of the microRNA of interest can also be induced following lentiviral transduction or plasmid transfection, with the sequence of the primary microRNA, whereby it is processed by the endogenous machinery and expressed at a more physiological level [1210].

We might harbour some reservations about the negative control microRNA (miR-NC), which is a mature microRNA of C. elegans (cel-miR-39-3p), said to have no mRNA target in mammals. Some of the investigated mRNA markers were significantly up- (*Id4, Ng2, Pdgfra, Notch1*; all markers of OPCs) or downregulated (*Mbp* and *Mobp*; both markers of mature OLs) by miR-NC as compared to the differentiation vehicle control. However, the differentiation vehicle control and miR-NC clustered closely on principal component analysis of the RNA sequencing and segregated strongly from the proliferation vehicle control, but the Gene Ontology enrichment analyses of each microRNA mimic compared to each differentiation control (vehicle control and miR-NC) were hard to unify. Herein, cell cycle processes in GO were upregulated in all microRNA conditions as compared to the miR-NC, while this was only seen for miR-34c-5p vs. the differentiation vehicle control. Likewise, the expression of Pcna, a cell cycle marker, tended to be reduced in immunocytochemistry by miR-NC vs the proliferation vehicle control only (figure 4.3). We have however not verified the cell mortality linked to each condition. For

all these reasons, I have been very cautious in balancing the interpretation of the data towards both the differentiation vehicle control and the miR-NC.

*Figure 4.3: Pcna expression in vehicle control and transfected cells (immunocytochemistry)*

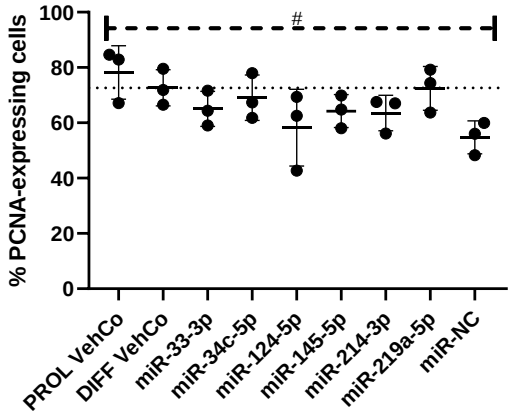


*The plot shows the percentage of cells expressing the proliferation marker Pcna (mean with SD), calculated to the total number of cells (based on the detections of the nucleus), resulting from the single transfection of each microRNA mimic (as labelled on the x-axis) in CG-4 cells in differentiation culture conditions, as well as the proliferation vehicle control (PROL VehCo). The dotted line represents the mean value of the differentiation vehicle control (DIFF VehCo). One-way ANOVA on all conditions was not significant but Dunn's multiple comparison test was significant for PROL VehCo vs miR-NC, adjusted p-value = 0.0318 (#, dashed bracket), suggesting the tendency of miR-NC to decrease cell proliferation. Data of 3 experiments, in single replicate within each experiment. SD = standard deviation*

Finally, we acknowledge that our transfection strategy regarding the microRNA inhibitors is rather uncommon. We transfected sequentially the microRNA mimic and 4 hours later the microRNA inhibitor, while normally the microRNA inhibitor is transfected on its own to block the endogenous microRNA [817]. However, when we transfected the microRNA inhibitor only at two timepoints, following the double transfection protocol, the expression levels of *Mbp* and *Plp1* were similar for all differentiation conditions (vehicle control and microRNA/miR-NC inhibitors) thereby providing no evidence of the effect of the microRNA inhibitor itself (figure 4.4).

*Figure 4.4: Mbp and Plp1 expression in cells transfected with the microRNA inhibitor only*

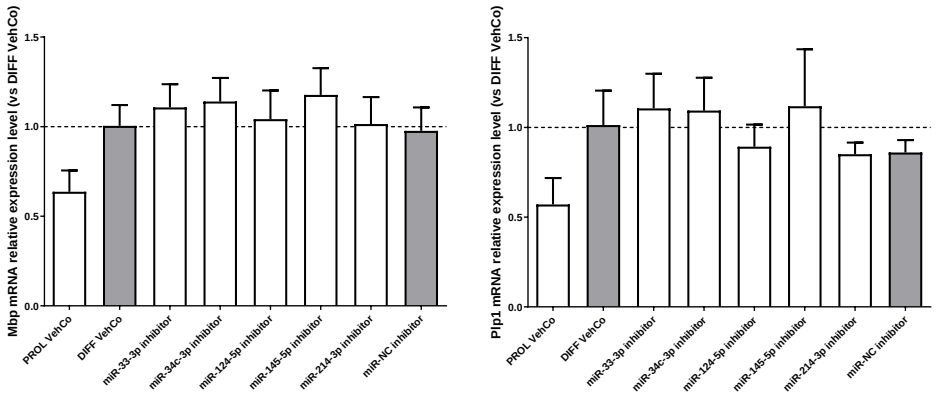


*The plots show the relative expression (mean with SD of $2^{-\Delta\Delta Ct}$) of the differentiation markers Mbp and Plp1 to the differentiation vehicle control (DIFF VehCo) resulting from the double transfection of each microRNA inhibitor (as labelled on the x-axis) in CG-4 cells in differentiation culture conditions, as well as the proliferation vehicle control (PROL VehCo). The dotted line represents the mean relative expression of the differentiation vehicle control to which the relative expression ($2^{-\Delta\Delta Ct}$) of each sample was calculated. The relative expression was roughly similar in each condition, therefore not allowing to evidence a specific effect of each microRNA inhibitor. Data of one experiment for each microRNA inhibitor with each condition in triplicate. SD = standard deviation*

We did not try to increase the concentration of the microRNA inhibitor. However, with the sequential transfections, the microRNA inhibitor was sufficient to antagonise its corresponding microRNA mimic transfected at equal concentration. Therefore, this brings us back to the questions surrounding the endogenous microRNAs. The endogenous microRNAs do not seem to be abundant enough to have any effect on their own on the differentiation of OPCs that can be antagonised by transfecting the corresponding microRNA inhibitor. However, it does not rule out that these microRNAs might be part of a broader network finely tuning OPC/OL physiology.

ii. Experimental model

We are aware that results emanating from an in vitro model with a cell line should be regarded with caution as it is an isolated system of a (almost) homogenous, single cell population, and should be further validated by other models. CG-4 cells are a permanent cell line, spontaneously generated from primary cultures of rat bipotential oligodendrocyte-type 2-astrocyte (O-2A) progenitor cells by passaging them in medium supplemented for 30% with the conditioned medium of B104 (B104-CM) neuroblastoma cells containing the needed mitogens. These CG-4 cells can keep on proliferating in the continuous presence of the B104-CM for several weeks. They are morphologically and immunochemically undistinguishable from primary O-2A cells, 95% of these cells are A2B5-positive (recognising a cell surface tetraganglioside) but galactocerebroside (Galc-) and Gfap-negative. They can differentiate into oligodendrocytes (expressing Galc and a fraction also Mbp) when cultured in the absence of serum (for 2 days) and B104-CM, or into type-2 astrocytes (coexpressing A2B5 and Gfap; different from type-1 astrocytes expressing Gfap only) in the presence of 20% of serum [988]. The advantage of this cell line is that it was spontaneously generated from O-2A precursors, it was not genetically immortalized neither derived from a tumour (e.g. oligodendroglioma). However, contrarily to Louis et al. announcing approximately 100% O1-positive cells (binding to a galactocerebroside) and 50% Mbp-positive cells upon removal of the mitogens from the medium[988], we obtained approximately 50% A2B5-positive cells, 30% O4-positive cells (detected prior to O1) and 1.5% Mbp-positive cells after 2 days of differentiation in the differentiation vehicle control condition (figure 3.4A-B-C).

Therefore, confronting our results with the effect of these microRNAs on primary OPCs isolated from newborn rat brains would be a first step forward [817]. Moreover, our experiments were run on single cell cultures of CG-4 cells. Although we could investigate the effect of the microRNAs on mature myelinating OLs by measuring late myelin genes (*Mbp, Mobp, Mag, Mog*) by RT-qPCR and/or RNA sequencing, one could verify the myelinating capacity of the transfected cells in a cell culture of OPCs with axon-like nanofibers or in mixed glial neuronal cultures that produce myelinated axons in vitro [883,1211–1215]. However, by transfecting a microRNA mimic in a mixed glial culture, all cell types are possibly impacted by the microRNA mimic, depending on the cell-specific transfection efficiency. Therefore, it is possible to

isolate and culture separately OPCs (from newborns rats/mice), and embryonic dorsal root ganglia (DRG) neurons. The OPCs could then be transfected separately before being co-cultured with the DRG neurons [555,1211,1213,1216,1217]. This latter model however lacks the interaction with the other glial cells.

Ex vivo cultures of organotypic brain or spinal cord slices offer a 3-dimensional system preserving the CNS architecture and the complex electrical and biochemical pathways in and in between the different cell types, but might be less reproducible than cell cultures [555,809,1218,1219]. Hereby, the transfection mix containing the microRNA mimic or inhibitor could be added to the organotypic culture, followed by RT-qPCR analysis of the extracted RNA, immunostaining of cell-specific proteins of interest on the fixed and embedded tissue or staining of myelin by luxol fast blue [1218,1220]. However, by adding the transfection mix directly to the organotypic culture, all cells might be transfected, however not necessarily with the same efficiency. The observed effect might not be attributable to OPCs specifically.

The same experimental designs could be imagined with transfection of a plasmid or transduction of a viral vector expressing the primary microRNA instead of the microRNA mimic [1210].

Finally, the effect of the microRNAs could be proven in vivo. There are several animal models mirroring, to a certain extent, particular aspects of MS. EAE is induced in specific rat or mice strains by active immunisation with a specific myelin protein or peptide (Plp, Mbp, Mog) emulsified in complete Freund's adjuvant or by passive transfer of activated myelin-reactive CD4+ T cells. Depending on the animal strain, age and sex and the induction method used, different courses of EAE (acute non-relapsing, relapsing, chronic) can be induced, that are mainly characterised by neuroinflammation with possibly a certain extent of demyelination and axonal loss [1211]. There are however some differences with MS, as EAE is mainly driven by CD4+ T cells and poorly reflects the other involved immune cells (especially CD8+ T cells), it affects the spinal cord rather than the brain, and it does not allow to study remyelination or disease progression [1221]**.** There are also several animal models of demyelination, of which cuprizone and lysolecithin induced demyelination are more commonly used. Cuprizone (0.2%), a copper chelator is added to the food of young adult (8 weeks old) male C57BL/6 mice for 4 to 6 weeks, causing white matter demyelination most easily seen in the corpus callosum, which recovers within 4 weeks when the cuprizone is removed from their diet [1211,1222]. Lysolecithin (1%), a

detergent-like membrane solubilising agent, is stereotactically injected, e.g. unilaterally into the corpus callosum, allowing comparison with the other unaffected side. Demyelination occurs within 2-3 days and remyelination is completed within a few weeks [1223–1225]. In both models, demyelination is accompanied by the recruitment of microglia for the phagocytosis of myelin debris [1222,1225]. An innovative animal model allows to investigate the impact of neuroinflammation on the remyelination process. Herein, 8-12 weeks old male C57BL/6 mice were fed for 4 weeks on a 0.2% cuprizone diet. Hereafter, the cuprizone was withdrawn of their diet and mice were treated by adoptive transfer of MOG-reactive T cells (or specifically Th17 cells), which decreased the spontaneous remyelination seen in the classic cuprizone model up to 3 weeks after the transfer [1226]. Finally, intracerebral Theiler's murine encephalomyelitis virus (TMEV) infection in susceptible SJL/J mice causes chronic encephalomyelitis primarily driven by microglial activation and mimicking progressive forms of MS, as it is characterised by astrogliosis, demyelination and axonal degeneration. TMEV predominantly infects glial cells (oligodendrocytes, astrocytes, microglia). OL loss is due to virus-induced apoptosis, but also due to the inflammatory assault by microglia, macrophages and cytotoxic CD8+ T cells. Remyelination is incomplete (thinner, as seen in MS) due to decreased cholesterol biosynthesis and astrogliosis [1227].

Thus, for in vivo explorations, a microRNA mimic or inhibitor (chemically modified, carried by a life transfection reagent, exosomes or nanoparticles, or encoded into a viral vector) could be administered by intravenous, intrathecal, intracerebroventricular or stereotactic (e.g. in the corpus callosum) injection or by intranasal drops, to a cuprizone or lysolecithin induced demyelination mice model, to the combined adoptive transfer cuprizone model or a TMEV-induced demyelinating disease mice model [831,832,880,882,1182,1228–1232]. Otherwise, demyelination could be induced, following one of these models, in mice knocked out for the microRNA of interest [834,879]. In these models, myelin can be assessed in the animals by MRI (MRI magnetization transfer ratios (MTRs)) or on CNS tissue sections by staining with luxol fast blue, or by electron microscopy [1220,1233,1234].

## IV. Conclusions

Non-coding microRNAs regulate gene expression post-transcriptionally. We hypothesised that their dysregulation in MS is thereby involved in disease pathogenesis both in neuroinflammation, and in demyelination and defective remyelination. Thereby we evidenced the dysregulation of 21 microRNAs of which 18 in the CSF of relapsing and/or remitting MS patients vs controls. These dysregulated microRNAs are not specific to (relapsing) MS as several were also found commonly upregulated, with an increased fold change, in the CSF of patients with inflammatory and infectious neurological disorders. In a second patient cohort, we evidenced a limited effect of disease activity status, determined by brain MRI, and treatment status on microRNA expression in PBMCs of MS patients. We further evidenced positive and negative correlations of these microRNAs with T cell mediator mRNAs, especially *IL21* and/or *FOXP3*, that further suggested, especially for the positive correlations, that the microRNAs might indirectly affect the T cell mediators via an intermediate target. We finally explored the demyelinating aspect and hereby evidenced that most screened microRNAs inhibited in vitro the differentiation of CG-4 cells. We further confirmed that miR-33-3p, miR-34c-5p and miR-124-5p inhibited OPC differentiation at a late OPC stage and miR-145-5p at an early premyelinating stage, while miR-214-3p was the only microRNA strongly promoting OPC differentiation as evidenced by the expression of stage-specific markers on RT-qPCR and RNA sequencing. We further studied their cell fate changes via Gene Ontology enrichment analysis and explored potential mRNA targets, suggesting, sometimes unexplored, mechanistical pathways in OPC differentiation. We acknowledge however an inconsistency between the effect of certain microRNAs on OPC differentiation and their endogenous expression in differentiating CG-4 cells (miR-33-3p, miR-145-5p, miR-214-3p) and/or their dysregulation in the CSF of R/RMS patients (miR-33-3p, miR-34c-5p, miR-124-5p). Therefore, identifying their cellular source will help to clarify their involvement in OPC/OL physiology and in the pathogenesis of MS. Otherwise, exploring the pathways they are potentially involved in OPC differentiation via their predicted mRNA target(s) could unravel new pathophysiological mechanisms or even new therapeutic targets for the understanding and management of MS and other demyelinating diseases.

*Travelers, we're fabric of the road we go.*
*We settle, but like feathers on time's flow.*

Cecil Day-Lewis

# REFERENCES

1. Poser, C. M. The dissemination of multiple sclerosis: A Viking saga? A historical essay. *Annals of Neurology* 36, S231–S243 (1994).

2. Medaer, R. Does the history of multiple sclerosis go back as far as the 14th century? *Acta Neurol Scand* 60, 189–192 (1979).

3. Butler, M. A. & Bennett, T. L. In Search of a Conceptualization of Multiple Sclerosis: A Historical Perspective. *Neuropsychol Rev* 13, 93–112 (2003).

4. Murray, T. J. The history of multiple sclerosis: the changing frame of the disease over the centuries. *Journal of the Neurological Sciences* 277, S3–S8 (2009).

5. Talley, C. L. The Emergence of Multiple Sclerosis as a Nosological Category in France, 1838-1868. *Journal of the History of the Neurosciences* 12, 250–265 (2003).

6. Lehmann, H. C., Compston, A. & Hartung, H.-P. 150th anniversary of clinical description of multiple sclerosis: Leopold Ordenstein's legacy. *Neurology* 90, 1011–1016 (2018).

7. Walusinski, O. 1903 manuscript revived: Cerebral disturbances in multiple sclerosis (Des troubles cérébraux dans la sclérose en plaques) by Raymond Cestan (1872–1933) and Claudien Philippe (1866–1903). *Revue Neurologique* 171, 333–340 (2015).

8. Talley, C. L. The emergence of multiple sclerosis, 1870-1950: a puzzle of historical epidemiology. *Perspect Biol Med* 48, 383–395 (2005).

9. Louapre, C. Conventional and advanced MRI in multiple sclerosis. *Revue Neurologique* 174, 391–397 (2018).

10. Maroto-García, J. *et al.* Biochemical biomarkers for multiple sclerosis. *Clinica Chimica Acta* 548, 117471 (2023).

11. Grossman, R. I., Gonzalez-Scarano, F., Atlas, S. W., Galetta, S. & Silberberg, D. H. Multiple sclerosis: gadolinium enhancement in MR imaging. *Radiology* 161, 721–725 (1986).

12. Young, I. R. *et al.* Nuclear magnetic resonance imaging of the brain in multiple sclerosis. *Lancet* 2, 1063–1066 (1981).

13. La Rosa, F. *et al.* Cortical lesions, central vein sign, and paramagnetic rim lesions in multiple sclerosis: Emerging machine learning techniques and future avenues. *Neuroimage Clin* 36, 103205 (2022).

14. Granziera, C. *et al.* Quantitative magnetic resonance imaging towards clinical application in multiple sclerosis. *Brain* 144, 1296–1311 (2021).

15. Filippi, M. *et al.* Present and future of the diagnostic work-up of multiple sclerosis: the imaging perspective. *J Neurol* 270, 1286–1299 (2023).

16. Holmøy, T. The Discovery of Oligoclonal Bands: A 50-Year Anniversary. *European Neurology* 62, 311–315 (2009).

17. Karcher, D., Sande, M. van & Lowenthal, A. Micro-Electrophoresis in Agar Gel of Proteins of the Cerebrospinal Fluid and Central Nervous System. *Journal of Neurochemistry* 4, 135–140 (1959).

18. Laterre, E. C., Heremans, J. F. & Carbonara, A. Immunological comparison of some proteins found in cerebrospinal fluid, urine and extracts from brain and kidney. *Clinica Chimica Acta* 10, 197–209 (1964).

19. Ferrand, M. *et al.* Real-life evaluation of the 2017 McDonald criteria for relapsing–remitting multiple sclerosis after a clinically isolated syndrome confirms a gain in time-to-diagnosis. *J Neurol* (2023) doi:10.1007/s00415-023-11905-w.

20. Petzold, A. Intrathecal oligoclonal IgG synthesis in multiple sclerosis. *Journal of Neuroimmunology* 262, 1–10 (2013).

21. Dendrou, C. A., Fugger, L. & Friese, M. A. Immunopathology of multiple sclerosis. *Nature Reviews Immunology* 15, 545–558 (2015).

22. Lassmann, H. Pathogenic Mechanisms Associated With Different Clinical Courses of Multiple Sclerosis. *Front Immunol* 9, 3116 (2019).

23. Trapp, B. D. & Nave, K.-A. Multiple Sclerosis: An Immune or Neurodegenerative Disorder? *Annual Review of Neuroscience* 31, 247–269 (2008).

24. Lublin, F. D. *et al.* Defining the clinical course of multiple sclerosis. *Neurology* 83, 278–286 (2014).

25. Gafson, A., Giovannoni, G. & Hawkes, C. H. The diagnostic criteria for multiple sclerosis: From Charcot to McDonald. *Multiple Sclerosis and Related Disorders* 1, 9–14 (2012).

26. Broman, T. *et al.* Aspects on classification methods in multiple sclerosis. *Acta Neurol Scand Suppl* 13 Pt 2, 543–548 (1965).

27. Ntranos, A. & Lublin, F. Diagnostic Criteria, Classification and Treatment Goals in Multiple Sclerosis: The Chronicles of Time and Space. *Curr Neurol Neurosci Rep* 16, 90 (2016).

28. Poser, C. M. *et al.* New diagnostic criteria for multiple sclerosis: Guidelines for research protocols. *Annals of Neurology* 13, 227–231 (1983).

29. Thompson, A. J. *et al.* Diagnosis of multiple sclerosis: 2017 revisions of the McDonald criteria. *The Lancet Neurology* 17, 162–173 (2018).

30. Confavreux, C. & Vukusic, S. Natural history of multiple sclerosis: a unifying concept. *Brain* 129, 606–616 (2006).

31. Fisher, K. S., Cuascut, F. X., Rivera, V. M. & Hutton, G. J. Current Advances in Pediatric Onset Multiple Sclerosis. *Biomedicines* 8, 71 (2020).

32. Koch-Henriksen, N., Thygesen, L. C., Stenager, E., Laursen, B. & Magyari, M. Incidence of MS has increased markedly over six decades in Denmark particularly with late onset and in women. *Neurology* 90, e1954–e1963 (2018).

33. O'Connell, K., Tubridy, N., Hutchinson, M. & McGuigan, C. Incidence of multiple sclerosis in the Republic of Ireland: A prospective population-based study. *Multiple Sclerosis and Related Disorders* 13, 75–80 (2017).

34. Wallin, M. T. *et al.* The prevalence of MS in the United States: A population-based estimate using health claims data. *Neurology* 92, e1029–e1040 (2019).

35. Lublin, F. D. & Reingold, S. C. Defining the clinical course of multiple sclerosis: results of an international survey. National Multiple Sclerosis Society (USA) Advisory Committee on Clinical Trials of New Agents in Multiple Sclerosis. *Neurology* 46, 907–911 (1996).

36. Kalincik, T. *et al.* Sex as a determinant of relapse incidence and progressive course of multiple sclerosis. *Brain* 136, 3609–3617 (2013).

37. Tomassini, V. *et al.* Sex hormones modulate brain damage in multiple sclerosis: MRI evidence. *J Neurol Neurosurg Psychiatry* 76, 272–275 (2005).

38. Manouchehrinia, A., Beiki, O. & Hillert, J. Clinical course of multiple sclerosis: A nationwide cohort study. *Mult Scler* 23, 1488–1495 (2017).

39. Tutuncu, M. *et al.* Onset of Progressive Phase is an Age Dependent Clinical Milestone in Multiple Sclerosis. *Mult Scler* 19, 188–198 (2013).

40. Cree, B. A. C. *et al.* Silent progression in disease activity–free relapsing multiple sclerosis. *Ann Neurol* 85, 653–666 (2019).

41. Schoonheim, M. M. *et al.* Subcortical atrophy and cognition: sex effects in multiple sclerosis. *Neurology* 79, 1754–1761 (2012).

42. Katz Sand, I. Classification, diagnosis, and differential diagnosis of multiple sclerosis. *Curr Opin Neurol* 28, 193–205 (2015).

43. Kurtzke, J. F. Rating neurologic impairment in multiple sclerosis: an expanded disability status scale (EDSS). *Neurology* 33, 1444–1452 (1983).

44. Lorscheider, J. *et al.* Defining secondary progressive multiple sclerosis. *Brain* 139, 2395–2405 (2016).

45. Kappos, L. *et al.* Contribution of Relapse-Independent Progression vs Relapse-Associated Worsening to Overall Confirmed Disability Accumulation in Typical Relapsing Multiple Sclerosis in a Pooled Analysis of 2 Randomized Clinical Trials. *JAMA Neurol* 77, 1–9 (2020).

46. Perdaens, O. & van Pesch, V. Molecular Mechanisms of Immunosenescene and Inflammaging: Relevance to the Immunopathogenesis and Treatment of Multiple Sclerosis. *Front Neurol* 12, 811518 (2022).

47. Bosca, I. *et al.* Effect of relapses over early progression of disability in multiple sclerosis patients treated with beta-interferon. *Mult Scler* 14, 636–639 (2008).

48. Jokubaitis, V. G. *et al.* Predictors of long-term disability accrual in relapse-onset multiple sclerosis. *Annals of Neurology* 80, 89–100 (2016).

49. Koch-Henriksen, N., Thygesen, L. C., Sørensen, P. S. & Magyari, M. Worsening of disability caused by relapses in multiple sclerosis: A different approach. *Multiple Sclerosis and Related Disorders* 32, 1–8 (2019).

50. Kremenchutzky, M., Rice, G. P. A., Baskerville, J., Wingerchuk, D. M. & Ebers, G. C. The natural history of multiple sclerosis: a geographically based study 9: Observations on the progressive phase of the disease. *Brain* 129, 584–594 (2006).

51. Scalfari, A. *et al.* The natural history of multiple sclerosis, a geographically based study 10: relapses and long-term disability. *Brain* 133, 1914–1929 (2010).

52. Portaccio, E. *et al.* Progression is independent of relapse activity in early multiple sclerosis: a real-life cohort study. *Brain* 145, 2796–2805 (2022).

53. Bjartmar, C., Wujek, J. R. & Trapp, B. D. Axonal loss in the pathology of MS: consequences for understanding the progressive phase of the disease. *Journal of the Neurological Sciences* 206, 165–171 (2003).

54. Confavreux, C., Vukusic, S. & Adeleine, P. Early clinical predictors and progression of irreversible disability in multiple sclerosis: an amnesic process. *Brain* 126, 770–782 (2003).

55. Elliott, C. *et al.* Slowly expanding/evolving lesions as a magnetic resonance imaging marker of chronic active multiple sclerosis lesions. *Mult Scler* 25, 1915–1925 (2019).

56. Frischer, J. M. *et al.* Clinical and pathological insights into the dynamic nature of the white matter multiple sclerosis plaque. *Annals of Neurology* 78, 710–721 (2015).

57. Miller, D. H., Chard, D. T. & Ciccarelli, O. Clinically isolated syndromes. *The Lancet Neurology* 11, 157–169 (2012).

58. Masjuan, J. *et al.* Clinically isolated syndromes: a new oligoclonal band test accurately predicts conversion to MS. *Neurology* 66, 576–578 (2006).

59. De Stefano, N. *et al.* Improving the Characterization of Radiologically Isolated Syndrome Suggestive of Multiple Sclerosis. *PLoS ONE* 6, e19452 (2011).

60. Okuda, D. T. *et al.* Incidental MRI anomalies suggestive of multiple sclerosis: The radiologically isolated syndrome. *Neurology* 72, 800–805 (2009).

61. Amato, M. P. *et al.* Association of MRI metrics and cognitive impairment in radiologically isolated syndromes. *Neurology* 78, 309–314 (2012).

62. Lebrun, C. *et al.* Cognitive function in radiologically isolated syndrome. *Mult Scler* 16, 919–925 (2010).

63. Sormani, M. P. *et al.* Will Rogers phenomenon in multiple sclerosis. *Annals of Neurology* 64, 428–433 (2008).

64. van der Vuurst de Vries, R. M. *et al.* Application of the 2017 Revised McDonald Criteria for Multiple Sclerosis to Patients With a Typical Clinically Isolated Syndrome. *JAMA Neurology* 75, 1392–1398 (2018).

65. Ramsaransing, G. S. M. & De Keyser, J. Benign course in multiple sclerosis: a review. *Acta Neurologica Scandinavica* 113, 359–369 (2006).

66. Sartori, A., Abdoli, M. & Freedman, M. S. Can we predict benign multiple sclerosis? Results of a 20-year long-term follow-up study. *J Neurol* 264, 1068–1075 (2017).

67. Sayao, A.-L., Devonshire, V. & Tremlett, H. Longitudinal follow-up of "benign" multiple sclerosis at 20 years. *Neurology* 68, 496–500 (2007).

68. Brown, F. S. *et al.* Systematic review of prediction models in relapsing remitting multiple sclerosis. *PLOS ONE* 15, e0233575 (2020).

69. Waldman, A. *et al.* Pediatric multiple sclerosis: Clinical features and outcome. *Neurology* 87, S74–S81 (2016).

70. Jakimovski, D., Awan, S., Eckert, S. P., Farooq, O. & Weinstock-Guttman, B. Multiple Sclerosis in Children: Differential Diagnosis, Prognosis, and Disease-Modifying Treatment. *CNS Drugs* 36, 45–59 (2022).

71. Brola, W. & Steinborn, B. Pediatric multiple sclerosis – current status of epidemiology, diagnosis and treatment. *Neurologia i Neurochirurgia Polska* 54, 508–517 (2020).

72. Walton, C. *et al.* Rising prevalence of multiple sclerosis worldwide: Insights from the Atlas of MS, third edition. *Mult Scler* 26, 1816–1821 (2020).

73. Gorman, M. P., Healy, B. C., Polgar-Turcsanyi, M. & Chitnis, T. Increased relapse rate in pediatric-onset compared with adult-onset multiple sclerosis. *Arch Neurol* 66, 54–59 (2009).

74. Mowry, E. M. *et al.* Demyelinating events in early multiple sclerosis have inherent severity and recovery. *Neurology* 72, 602–608 (2009).

75. Chitnis, T. *et al.* Improved relapse recovery in paediatric compared to adult multiple sclerosis. *Brain* 143, 2733–2741 (2020).

76. Menascu, S. *et al.* Clinical and transcriptional recovery profiles in pediatric and adult multiple sclerosis patients. *Ann Clin Transl Neurol* 8, 81–94 (2021).

77. Banwell, B. *et al.* Incidence of acquired demyelination of the CNS in Canadian children. *Neurology* 72, 232–239 (2009).

78. Huppke, B. *et al.* Clinical presentation of pediatric multiple sclerosis before puberty. *Eur J Neurol* 21, 441–446 (2014).

79. Rostasy, K., Bajer-Kornek, B., Venkateswaran, S., Hemingway, C. & Tardieu, M. Differential diagnosis and evaluation in pediatric inflammatory demyelinating disorders. *Neurology* 87, S28–S37 (2016).

80. Renoux, C. *et al.* Natural history of multiple sclerosis with childhood onset. *N Engl J Med* 356, 2603–2613 (2007).

81. McKay, K. A. *et al.* Long-term Cognitive Outcomes in Patients With Pediatric-Onset vs Adult-Onset Multiple Sclerosis. *JAMA Neurol* 76, 1028–1034 (2019).

82. Meo, E. D. *et al.* Dynamic gray matter volume changes in pediatric multiple sclerosis: A 3.5 year MRI study. *Neurology* 92, e1709–e1723 (2019).

83. Mowry, E. M. *et al.* Health-Related Quality of Life is Reduced in Pediatric Multiple Sclerosis. *Pediatric Neurology* 43, 97–102 (2010).

84. Amato, M. P., Krupp, L. B., Charvet, L. E., Penner, I. & Till, C. Pediatric multiple sclerosis: Cognition and mood. *Neurology* 87, S82–S87 (2016).

85. Portaccio, E. *et al.* Long-term Cognitive Outcomes and Socioprofessional Attainment in People With Multiple Sclerosis With Childhood Onset. *Neurology* 98, e1626–e1636 (2022).

86. Ascherio, A. & Munger, K. L. Epidemiology of Multiple Sclerosis: From Risk Factors to Prevention-An Update. *Semin Neurol* 36, 103–114 (2016).

87. Corona, T. & Román, G. C. Multiple sclerosis in Latin America. *Neuroepidemiology* 26, 1–3 (2006).

88. Forouhari, A., Taheri, G., Salari, M., Moosazadeh, M. & Etemadifar, M. Multiple sclerosis epidemiology in Asia and Oceania; A systematic review and meta-analysis. *Multiple Sclerosis and Related Disorders* 54, 103119 (2021).

89. Banwell, B., Ghezzi, A., Bar-Or, A., Mikaeloff, Y. & Tardieu, M. Multiple sclerosis in children: clinical diagnosis, therapeutic strategies, and future directions. *Lancet Neurol* 6, 887–902 (2007).

90. Dunn, S. E., Gunde, E. & Lee, H. Sex-Based Differences in Multiple Sclerosis (MS): Part II: Rising Incidence of Multiple Sclerosis in Women and the Vulnerability of Men to Progression of this Disease. in *Emerging and Evolving Topics in Multiple Sclerosis Pathogenesis and Treatments* (eds. La Flamme, A. C. & Orian, J. M.) 57–86 (Springer International Publishing, 2015). doi:10.1007/7854_2015_370.

91. Kis, B., Rumberg, B. & Berlit, P. Clinical characteristics of patients with late-onset multiple sclerosis. *J Neurol* 255, 697–702 (2008).

92. Chitnis, T. *et al.* Distinct effects of obesity and puberty on risk and age at onset of pediatric MS. *Ann Clin Transl Neurol* 3, 897–907 (2016).

93. Harroud, A. *et al.* Effect of age at puberty on risk of multiple sclerosis: A mendelian randomization study. *Neurology* 92, e1803–e1810 (2019).

94. Ramagopalan, S. V. *et al.* Age of puberty and the risk of multiple sclerosis: a population based study. *Eur J Neurol* 16, 342–347 (2009).

95. Sloka, J. S., Pryse-Phillips, W. E. M. & Stefanelli, M. The relation between menarche and the age of first symptoms in a multiple sclerosis cohort. *Mult Scler* 12, 333–339 (2006).

96. Greer, J. M., Csurhes, P. A., Pender, M. P. & McCombe, P. A. Effect of gender on T-cell proliferative responses to myelin proteolipid protein antigens in patients with multiple sclerosis and controls. *J Autoimmun* 22, 345–352 (2004).

97. Moldovan, I. R., Cotleur, A. C., Zamor, N., Butler, R. S. & Pelfrey, C. M. Multiple sclerosis patients show sexual dimorphism in cytokine responses to myelin antigens. *J Neuroimmunol* 193, 161–169 (2008).

98. Pelfrey, C. M., Cotleur, A. C., Lee, J.-C. & Rudick, R. A. Sex differences in cytokine responses to myelin peptides in multiple sclerosis. *J Neuroimmunol* 130, 211–223 (2002).

99. Zhang, M. A. *et al.* Peroxisome proliferator-activated receptor (PPAR)α and -γ regulate IFNγ and IL-17A production by human T cells in a sex-specific way. *Proc Natl Acad Sci U S A* 109, 9505–9510 (2012).

100. Bebo, B. F., Schuster, J. C., Vandenbark, A. A. & Offner, H. Androgens alter the cytokine profile and reduce encephalitogenicity of myelin-reactive T cells. *J Immunol* 162, 35–40 (1999).

101. D'agostino, P. *et al.* Sex Hormones Modulate Inflammatory Mediators Produced by Macrophagesa. *Annals of the New York Academy of Sciences* 876, 426–429 (1999).

102. Voskuhl, R. R. & Palaszynski, K. Sex hormones in experimental autoimmune encephalomyelitis: implications for multiple sclerosis. *Neuroscientist* 7, 258–270 (2001).

103. Confavreux, C., Hutchinson, M., Hours, M. M., Cortinovis-Tourniaire, P. & Moreau, T. Rate of pregnancy-related relapse in multiple sclerosis. Pregnancy in Multiple Sclerosis Group. *N Engl J Med* 339, 285–291 (1998).

104. Kanda, N. & Tamaki, K. Estrogen enhances immunoglobulin production by human PBMCs. *J Allergy Clin Immunol* 103, 282–288 (1999).

105. Lélu, K. *et al.* Estrogen receptor α signaling in T lymphocytes is required for estradiol-mediated inhibition of Th1 and Th17 cell differentiation and protection against experimental autoimmune encephalomyelitis. *J Immunol* 187, 2386–2393 (2011).

106. Nakaya, M., Tachibana, H. & Yamada, K. Effect of estrogens on the interferon-gamma producing cell population of mouse splenocytes. *Biosci Biotechnol Biochem* 70, 47–53 (2006).

107. Ponsonby, A.-L. *et al.* Offspring number, pregnancy, and risk of a first clinical demyelinating event: the AusImmune Study. *Neurology* 78, 867–874 (2012).

108. Chavez-Rueda, K. *et al.* Identification of prolactin as a novel immunomodulator on the expression of co-stimulatory molecules and cytokine secretions on T and B human lymphocytes. *Clin Immunol* 116, 182–191 (2005).

109. Correale, J., Farez, M. F. & Ysrraelit, M. C. Role of prolactin in B cell regulation in multiple sclerosis. *J Neuroimmunol* 269, 76–86 (2014).

110. Correale, J., Ysrraelit, M. C. & Gaitán, M. I. Gender differences in 1,25 dihydroxyvitamin D3 immunomodulatory effects in multiple sclerosis patients and healthy subjects. *J Immunol* 185, 4948–4958 (2010).

111. Matarese, G., Procaccini, C. & De Rosa, V. The intricate interface between immune and metabolic regulation: a role for leptin in the pathogenesis of multiple sclerosis? *J Leukoc Biol* 84, 893–899 (2008).

112. Alla, S. & Mason, D. F. Multiple sclerosis in New Zealand. *J Clin Neurosci* 21, 1288–1291 (2014).

113. Ebers, G. C. A twin consensus in MS. *Mult Scler* 11, 497–499 (2005).

114. Kantarci, O. H. Genetics and Natural History of Multiple Sclerosis. *Semin Neurol* 28, 7–16 (2008).

115. Sadovnick, A. D., Ebers, G. C., Dyment, D. A. & Risch, N. J. Evidence for genetic basis of multiple sclerosis. The Canadian Collaborative Study Group. *Lancet* 347, 1728–1730 (1996).

116. Goris, A., Vandebergh, M., McCauley, J. L., Saarela, J. & Cotsapas, C. Genetics of multiple sclerosis: lessons from polygenicity. *The Lancet Neurology* 21, 830–842 (2022).

117. International Multiple Sclerosis Genetics Consortium. Multiple Sclerosis Genomic Map implicates peripheral immune cells & microglia in susceptibility. *Science* 365, eaav7188 (2019).

118. Barcellos, L. F. *et al.* Genetic basis for clinical expression in multiple sclerosis. *Brain* 125, 150–158 (2002).

119. Haines, J. L. *et al.* Linkage of the MHC to familial multiple sclerosis suggests genetic heterogeneity. The Multiple Sclerosis Genetics Group. *Hum Mol Genet* 7, 1229–1234 (1998).

120. Kelly, M. A. *et al.* An investigation of HLA-encoded genetic susceptibility to multiple sclerosis in subjects of Asian Indian and Afro-Caribbean ethnic origin. *Tissue Antigens* 45, 197–202 (1995).

121. Moutsianas, L. *et al.* Class II HLA interactions modulate genetic risk for multiple sclerosis. *Nat Genet* 47, 1107–1113 (2015).

122. McElroy, J. P. & Oksenberg, J. R. Multiple Sclerosis Genetics 2010. *Neurologic Clinics* 29, 219–231 (2011).

123. Ma, Q. *et al.* Integration of epigenetic and genetic profiles identifies multiple sclerosis disease-critical cell types and genes. *Commun Biol* 6, 342 (2023).

124. Shepard, C. J., Cline, S. G., Hinds, D., Jahanbakhsh, S. & Prokop, J. W. Breakdown of multiple sclerosis genetics to identify an integrated disease network and potential variant mechanisms. *Physiol Genomics* 51, 562–577 (2019).

125. Hauser, S. L. & Cree, B. A. C. Treatment of Multiple Sclerosis: A Review. *The American Journal of Medicine* 133, 1380-1390.e2 (2020).

126. Lublin, F. D. History of modern multiple sclerosis therapy. *J Neurol* 252, iii3–iii9 (2005).

127. Cree, B. A. C., Mares, J. & Hartung, H.-P. Current therapeutic landscape in multiple sclerosis: an evolving treatment paradigm. *Current Opinion in Neurology* 32, 365 (2019).

128. Ouallet, J.-C. Do disease-modifying drugs (DMD) have a positive impact on the occurrence of secondary progressive multiple sclerosis? Comment. *Revue Neurologique* 176, 500–504 (2020).

129. Tedeholm, H. *et al.* The outcome spectrum of multiple sclerosis: disability, mortality, and a cluster of predictors from onset. *J Neurol* 262, 1148–1163 (2015).

130. Bourque, J. & Hawiger, D. Current and Future Immunotherapies for Multiple Sclerosis. *Mo Med* 118, 334–339 (2021).

131. Rommer, P. S. *et al.* Immunological Aspects of Approved MS Therapeutics. *Front Immunol* 10, 1564 (2019).

132. Harding, K. *et al.* Clinical Outcomes of Escalation vs Early Intensive Disease-Modifying Therapy in Patients With Multiple Sclerosis. *JAMA Neurology* 76, 536–541 (2019).

133. Zilli, C. *et al.* Assessing 'no evidence of disease activity' status in patients with relapsing-remitting multiple sclerosis: a long-term follow-up. *Front Neurol* 14, 1187851 (2023).

134. Pozzilli, C. *et al.* Diagnosis and treatment of progressive multiple sclerosis: A position paper. *European Journal of Neurology* 30, 9–21 (2023).

135. Gold, R. *et al.* Siponimod vs placebo in active secondary progressive multiple sclerosis: a post hoc analysis from the phase 3 EXPAND study. *J Neurol* 269, 5093–5104 (2022).

136. Montalban, X. *et al.* Ocrelizumab versus Placebo in Primary Progressive Multiple Sclerosis. *N Engl J Med* 376, 209–220 (2017).

137. Krämer, J., Bar-Or, A., Turner, T. J. & Wiendl, H. Bruton tyrosine kinase inhibitors for multiple sclerosis. *Nat Rev Neurol* 19, 289–304 (2023).

138. Middendorp, S., Dingjan, G. M. & Hendriks, R. W. Impaired precursor B cell differentiation in Bruton's tyrosine kinase-deficient mice. *J Immunol* 168, 2695–2703 (2002).

139. Torke, S. *et al.* Inhibition of Bruton's tyrosine kinase interferes with pathogenic B-cell development in inflammatory CNS demyelinating disease. *Acta Neuropathol* 140, 535–548 (2020).

140. Cariappa, A. *et al.* The Follicular versus Marginal Zone B Lymphocyte Cell Fate Decision Is Regulated by Aiolos, Btk, and CD21. *Immunity* 14, 603–615 (2001).

141. Rijvers, L. *et al.* Human T-bet+ B cell development is associated with BTK activity and suppressed by evobrutinib. *JCI Insight* 7, e160909 (2022).

142. Gruber, R. C. *et al.* Central Effects of BTK Inhibition in Neuroinflammation (808). *Neurology* 94, (2020).

143. Evonuk, K. S. *et al.* Bruton's tyrosine kinase inhibition reduces disease severity in a model of secondary progressive autoimmune demyelination. *Acta Neuropathol Commun* 11, 115 (2023).

144. Zelic, M. *et al.* RIPK1 activation mediates neuroinflammation and disease progression in multiple sclerosis. *Cell Rep* 35, 109112 (2021).

145. Ma, X.-R. *et al.* Inhibition of RIPK1 by ZJU-37 promotes oligodendrocyte progenitor proliferation and remyelination via NF-κB pathway. *Cell Death Discov* 8, 147 (2022).

146. Carvalho, T. Anti-CD40L antibody frexalimab slows new brain lesions in multiple sclerosis. *Nature Medicine* 29, 1882–1883 (2023).

147. Muraro, P. A. *et al.* Thymic output generates a new and diverse TCR repertoire after autologous stem cell transplantation in multiple sclerosis patients. *J Exp Med* 201, 805–816 (2005).

148. Muraro, P. A. *et al.* Long-term Outcomes After Autologous Hematopoietic Stem Cell Transplantation for Multiple Sclerosis. *JAMA Neurol* 74, 459–469 (2017).

149. Burt, R. K. *et al.* Association of nonmyeloablative hematopoietic stem cell transplantation with neurological disability in patients with relapsing-remitting multiple sclerosis. *JAMA* 313, 275–284 (2015).

150. Arruda, L. C. M. *et al.* Immunological correlates of favorable long-term clinical outcome in multiple sclerosis patients after autologous hematopoietic stem cell transplantation. *Clin Immunol* 169, 47–57 (2016).

151. Cuascut, F. X. & Hutton, G. J. Stem Cell-Based Therapies for Multiple Sclerosis: Current Perspectives. *Biomedicines* 7, 26 (2019).

152. Zappia, E. *et al.* Mesenchymal stem cells ameliorate experimental autoimmune encephalomyelitis inducing T-cell anergy. *Blood* 106, 1755–1761 (2005).

153. Zhang, J. *et al.* Human bone marrow stromal cell treatment improves neurological functional recovery in EAE mice. *Exp Neurol* 195, 16–26 (2005).

154. Bai, L. *et al.* Human bone marrow-derived mesenchymal stem cells induce Th2-polarized immune response and promote endogenous repair in animal models of multiple sclerosis. *Glia* 57, 1192–1203 (2009).

155. Llufriu, S. *et al.* Randomized placebo-controlled phase II trial of autologous mesenchymal stem cells in multiple sclerosis. *PLoS One* 9, e113936 (2014).

156. Ben-Hur, T. *et al.* Transplanted multipotential neural precursor cells migrate into the inflamed white matter in response to experimental autoimmune encephalomyelitis. *Glia* 41, 73–80 (2003).

157. Aharonowiz, M. *et al.* Neuroprotective effect of transplanted human embryonic stem cell-derived neural precursors in an animal model of multiple sclerosis. *PLoS One* 3, e3145 (2008).

158. Harris, V. K. *et al.* Clinical and pathological effects of intrathecal injection of mesenchymal stem cell-derived neural progenitors in an experimental model of multiple sclerosis. *J Neurol Sci* 313, 167–177 (2012).

159. Harris, V. K., Faroqui, R., Vyshkina, T. & Sadiq, S. A. Characterization of autologous mesenchymal stem cell-derived neural progenitors as a feasible source of stem cells for central nervous system applications in multiple sclerosis. *Stem Cells Transl Med* 1, 536–547 (2012).

160. Laterza, C. *et al.* iPSC-derived neural precursors exert a neuroprotective role in immune-mediated demyelination via the secretion of LIF. *Nat Commun* 4, 2597 (2013).

161. Gingele, S. & Stangel, M. Emerging myelin repair agents in preclinical and early clinical development for the treatment of multiple sclerosis. *Expert Opinion on Investigational Drugs* 29, 583–594 (2020).

162. Biogen. *A Multicenter, Randomized, Double-Blind, Placebo-Controlled Study With Optional Open-Label Extension in Subjects With Relapsing Multiple Sclerosis to Evaluate the Efficacy and Safety of BIIB033 as an Add-On Therapy to Anti-Inflammatory Disease-Modifying Therapies*. https://clinicaltrials.gov/study/NCT03222973 (2022).

163. Küchlin, S. *et al.* Treatment With Erythropoietin for Patients With Optic Neuritis: Long-term Follow-up. *Neurol Neuroimmunol Neuroinflamm* 10, e200067 (2023).

164. Cree, B. A. C. *et al.* Clemastine rescues myelination defects and promotes functional recovery in hypoxic brain injury. *Brain* 141, 85–98 (2018).

165. Mei, F. *et al.* Accelerated remyelination during inflammatory demyelination prevents axonal loss and improves functional recovery. *Elife* 5, e18246 (2016).

166. Nath, N. *et al.* Metformin attenuated the autoimmune disease of the central nervous system in animal models of multiple sclerosis. *J Immunol* 182, 8005–8014 (2009).

167. Neumann, B. *et al.* Metformin Restores CNS Remyelination Capacity by Rejuvenating Aged Stem Cells. *Cell Stem Cell* 25, 473-485.e8 (2019).

168. Morales, L. B. J. *et al.* Treatment with an estrogen receptor alpha ligand is neuroprotective in experimental autoimmune encephalomyelitis. *J Neurosci* 26, 6823–6833 (2006).

169. Ziehn, M. O., Avedisian, A. A., Dervin, S. M., O'Dell, T. J. & Voskuhl, R. R. Estriol preserves synaptic transmission in the hippocampus during autoimmune demyelinating disease. *Lab Invest* 92, 1234–1245 (2012).

170. Ziehn, M. O. *et al.* Therapeutic testosterone administration preserves excitatory synaptic transmission in the hippocampus during autoimmune demyelinating disease. *J Neurosci* 32, 12312–12324 (2012).

171. Steinman, L. Multiple sclerosis: a coordinated immunological attack against myelin in the central nervous system. *Cell* 85, 299–302 (1996).

172. Chanaday, N. L. & Roth, G. A. Microglia and astrocyte activation in the frontal cortex of rats with experimental autoimmune encephalomyelitis. *Neuroscience* 314, 160–169 (2016).

173. Sun, D. *et al.* Role of chemokines, neuronal projections, and the blood-brain barrier in the enhancement of cerebral EAE following focal brain damage. *J Neuropathol Exp Neurol* 59, 1031–1043 (2000).

174. Machado-Santos, J. *et al.* The compartmentalized inflammatory response in the multiple sclerosis brain is composed of tissue-resident CD8+ T lymphocytes and B cells. *Brain* 141, 2066–2082 (2018).

175. Touil, H. *et al.* Cross-talk between B cells, microglia and macrophages, and implications to central nervous system compartmentalized inflammation and progressive multiple sclerosis. *EBioMedicine* 96, 104789 (2023).

176. Cao, Y. *et al.* Functional inflammatory profiles distinguish myelin-reactive T cells from patients with multiple sclerosis. *Sci Transl Med* 7, 287ra74 (2015).

177. Codarri, L. *et al.* RORγt drives production of the cytokine GM-CSF in helper T cells, which is essential for the effector phase of autoimmune neuroinflammation. *Nat Immunol* 12, 560–567 (2011).

178. Kebir, H. *et al.* Preferential recruitment of interferon-γ–expressing TH17 cells in multiple sclerosis. *Annals of Neurology* 66, 390–402 (2009).

179. Prat, A. *et al.* Migration of multiple sclerosis lymphocytes through brain endothelium. *Arch Neurol* 59, 391–397 (2002).

180. Sonar, S. A., Shaikh, S., Joshi, N., Atre, A. N. & Lal, G. IFN-γ promotes transendothelial migration of CD4+ T cells across the blood-brain barrier. *Immunol Cell Biol* 95, 843–853 (2017).

181. Fischer, M. T. *et al.* NADPH oxidase expression in active multiple sclerosis lesions in relation to oxidative tissue damage and mitochondrial injury. *Brain* 135, 886–899 (2012).

182. Guo, X. *et al.* Inhibition of glial cell activation ameliorates the severity of experimental autoimmune encephalomyelitis. *Neurosci Res* 59, 457–466 (2007).

183. Murphy, A. C., Lalor, S. J., Lynch, M. A. & Mills, K. H. G. Infiltration of Th1 and Th17 cells and activation of microglia in the CNS during the course of experimental autoimmune encephalomyelitis. *Brain Behav Immun* 24, 641–651 (2010).

184. Palanichamy, A. *et al.* Immunoglobulin class-switched B cells form an active immune axis between CNS and periphery in multiple sclerosis. *Science Translational Medicine* 6, 248ra106-248ra106 (2014).

185. Prajeeth, C. K. *et al.* Effectors of Th1 and Th17 cells act on astrocytes and augment their neuroinflammatory properties. *J Neuroinflammation* 14, 204 (2017).

186. Prajeeth, C. K. *et al.* Effector molecules released by Th1 but not Th17 cells drive an M1 response in microglia. *Brain Behav Immun* 37, 248–259 (2014).

187. Stern, J. N. H. *et al.* B cells populating the multiple sclerosis brain mature in the draining cervical lymph nodes. *Sci Transl Med* 6, 248ra107 (2014).

188. Tzartos, J. S. *et al.* Interleukin-17 production in central nervous system-infiltrating T cells and glial cells is associated with active disease in multiple sclerosis. *Am J Pathol* 172, 146–155 (2008).

189. Vogel, D. Y. S. *et al.* GM-CSF promotes migration of human monocytes across the blood brain barrier. *Eur J Immunol* 45, 1808–1819 (2015).

190. Babbe, H. *et al.* Clonal expansions of CD8(+) T cells dominate the T cell infiltrate in active multiple sclerosis lesions as shown by micromanipulation and single cell polymerase chain reaction. *J Exp Med* 192, 393–404 (2000).

191. Ji, Q., Castelli, L. & Goverman, J. M. MHC class I-restricted myelin epitopes are cross-presented by Tip-DCs that promote determinant spreading to $CD8^+$ T cells. *Nat Immunol* 14, 254–261 (2013).

192. Sasaki, K. *et al.* Relapsing-remitting central nervous system autoimmunity mediated by GFAP-specific CD8 T cells. *J Immunol* 192, 3029–3042 (2014).

193. Cui, Q.-L. *et al.* Sublethal oligodendrocyte injury: A reversible condition in multiple sclerosis? *Ann Neurol* 81, 811–824 (2017).

194. Cui, Q.-L. *et al.* Oligodendrocyte Progenitor Cell Susceptibility to Injury in Multiple Sclerosis. *The American Journal of Pathology* 183, 516–525 (2013).

195. Dziedzic, T. *et al.* Wallerian degeneration: a major component of early axonal pathology in multiple sclerosis. *Brain Pathol* 20, 976–985 (2010).

196. Patel, J. & Balabanov, R. Molecular mechanisms of oligodendrocyte injury in multiple sclerosis and experimental autoimmune encephalomyelitis. *Int J Mol Sci* 13, 10647–10659 (2012).

197. Selmaj, K. W. & Raine, C. S. Tumor necrosis factor mediates myelin and oligodendrocyte damage in vitro. *Annals of Neurology* 23, 339–346 (1988).

198. Singh, S. *et al.* Relationship of acute axonal damage, Wallerian degeneration, and clinical disability in multiple sclerosis. *J Neuroinflammation* 14, 57 (2017).

199. Trapp, B. D. *et al.* Axonal Transection in the Lesions of Multiple Sclerosis. *N Engl J Med* 338, 278–285 (1998).

200. Vartanian, T., Li, Y., Zhao, M. & Stefansson, K. Interferon-γ-Induced Oligodendrocyte Cell Death: Implications for the Pathogenesis of Multiple Sclerosis. *Mol Med* 1, 732–743 (1995).

201. Cignarella, F. *et al.* TREM2 activation on microglia promotes myelin debris clearance and remyelination in a model of multiple sclerosis. *Acta Neuropathol* 140, 513–534 (2020).

202. Kotter, M. R., Li, W.-W., Zhao, C. & Franklin, R. J. M. Myelin impairs CNS remyelination by inhibiting oligodendrocyte precursor cell differentiation. *J Neurosci* 26, 328–332 (2006).

203. Miron, V. E. *et al.* M2 microglia and macrophages drive oligodendrocyte differentiation during CNS remyelination. *Nat Neurosci* 16, 1211–1218 (2013).

204. Sosa, R. A., Murphey, C., Ji, N., Cardona, A. E. & Forsthuber, T. G. The kinetics of myelin antigen uptake by myeloid cells in the central nervous system during experimental autoimmune encephalomyelitis. *J Immunol* 191, 5848–5857 (2013).

205. Choi, S. R. *et al.* Meningeal inflammation plays a role in the pathology of primary progressive multiple sclerosis. *Brain* 135, 2925–2937 (2012).

206. Frischer, J. M. *et al.* The relation between inflammation and neurodegeneration in multiple sclerosis brains. *Brain* 132, 1175–1189 (2009).

207. Howell, O. W. *et al.* Meningeal inflammation is widespread and linked to cortical pathology in multiple sclerosis. *Brain* 134, 2755–2771 (2011).

208. Ineichen, B. V., Tsagkas, C., Absinta, M. & Reich, D. S. Leptomeningeal enhancement in multiple sclerosis and other neurological diseases: A systematic review and Meta-Analysis. *Neuroimage Clin* 33, 102939 (2022).

209. Lisak, R. P. *et al.* Secretory products of multiple sclerosis B cells are cytotoxic to oligodendroglia in vitro. *Journal of Neuroimmunology* 246, 85–95 (2012).

210. Magliozzi, R. *et al.* A Gradient of neuronal loss and meningeal inflammation in multiple sclerosis. *Ann Neurol* 68, 477–493 (2010).

211. Magliozzi, R. *et al.* Meningeal B-cell follicles in secondary progressive multiple sclerosis associate with early onset of disease and severe cortical pathology. *Brain* 130, 1089–1104 (2007).

212. Centonze, D. *et al.* Inflammation Triggers Synaptic Alteration and Degeneration in Experimental Autoimmune Encephalomyelitis. *J Neurosci* 29, 3442–3452 (2009).

213. Mossakowski, A. A. *et al.* Tracking CNS and systemic sources of oxidative stress during the course of chronic neuroinflammation. *Acta Neuropathol* 130, 799–814 (2015).

214. Perianes-Cachero, A. *et al.* Oxidative Stress and Lymphocyte Alterations in Chronic Relapsing Experimental Allergic Encephalomyelitis in the Rat Hippocampus and Protective Effects of an Ethanolamine Phosphate Salt. *Mol Neurobiol* 57, 860–878 (2020).

215. Rahman, M. H. & Suk, K. Mitochondrial Dynamics and Bioenergetic Alteration During Inflammatory Activation of Astrocytes. *Frontiers in Aging Neuroscience* 12, (2020).

216. Sheng, W. S., Hu, S., Feng, A. & Rock, R. B. Reactive Oxygen Species from Human Astrocytes Induced Functional Impairment and Oxidative Damage. *Neurochem Res* 38, 2148–2159 (2013).

217. Tanuma, N., Sakuma, H., Sasaki, A. & Matsumoto, Y. Chemokine expression by astrocytes plays a role in microglia/macrophage activation and subsequent neurodegeneration in secondary progressive multiple sclerosis. *Acta Neuropathol* 112, 195–204 (2006).

218. Bros, H., Millward, J. M., Paul, F., Niesner, R. & Infante-Duarte, C. Oxidative damage to mitochondria at the nodes of Ranvier precedes axon degeneration in ex vivo transected axons. *Experimental Neurology* 261, 127–135 (2014).

219. Fünfschilling, U. *et al.* Glycolytic oligodendrocytes maintain myelin and long-term axonal integrity. *Nature* 485, 517–521 (2012).

220. Nave, K.-A. Myelination and support of axonal integrity by glia. *Nature* 468, 244–252 (2010).

221. Trapp, B. D. & Stys, P. K. Virtual hypoxia and chronic necrosis of demyelinated axons in multiple sclerosis. *Lancet Neurol* 8, 280–291 (2009).

222. Ulshöfer, R. *et al.* Preventing Axonal Sodium Overload or Mitochondrial Calcium Uptake Protects Axonal Mitochondria from Oxidative Stress-Induced Alterations. *Oxid Med Cell Longev* 2022, 6125711 (2022).

223. Lassmann, H. Multiple Sclerosis Pathology. *Cold Spring Harb Perspect Med* 8, a028936 (2018).

224. Kuhlmann, T. *et al.* An updated histological classification system for multiple sclerosis lesions. *Acta Neuropathol* 133, 13–24 (2017).

225. Sati, P. *et al.* The central vein sign and its clinical evaluation for the diagnosis of multiple sclerosis: a consensus statement from the North American Imaging in Multiple Sclerosis Cooperative. *Nat Rev Neurol* 12, 714–722 (2016).

226. Bagnato, F. *et al.* Tracking iron in multiple sclerosis: a combined imaging and histopathological study at 7 Tesla. *Brain* 134, 3602–3615 (2011).

227. Dal-Bianco, A. *et al.* Slow expansion of multiple sclerosis iron rim lesions: pathology and 7 T magnetic resonance imaging. *Acta Neuropathol* 133, 25–42 (2017).

228. Hametner, S. *et al.* Iron and neurodegeneration in the multiple sclerosis brain. *Ann Neurol* 74, 848–861 (2013).

229. Kornek, B. *et al.* Multiple sclerosis and chronic autoimmune encephalomyelitis: a comparative quantitative study of axonal injury in active, inactive, and remyelinated lesions. *Am J Pathol* 157, 267–276 (2000).

230. Prineas, J. W., Barnard, R. O., Kwon, E. E., Sharer, L. R. & Cho, E.-S. Multiple sclerosis: Remyelination of nascent lesions: Remyelination of nascent lesions. *Annals of Neurology* 33, 137–151 (1993).

231. Bø, L., Vedeler, C. A., Nyland, H. I., Trapp, B. D. & Mørk, S. J. Subpial demyelination in the cerebral cortex of multiple sclerosis patients. *J Neuropathol Exp Neurol* 62, 723–732 (2003).

232. Bø, L., Vedeler, C. A., Nyland, H., Trapp, B. D. & Mørk, S. J. Intracortical multiple sclerosis lesions are not associated with increased lymphocyte infiltration. *Mult Scler* 9, 323–331 (2003).

233. Lucchinetti, C. F. *et al.* Inflammatory Cortical Demyelination in Early Multiple Sclerosis. *N Engl J Med* 365, 2188–2197 (2011).

234. Albert, M., Antel, J., Brück, W. & Stadelmann, C. Extensive cortical remyelination in patients with chronic multiple sclerosis. *Brain Pathol* 17, 129–138 (2007).

235. Baadsvik, E. L. *et al.* Quantitative magnetic resonance mapping of the myelin bilayer reflects pathology in multiple sclerosis brain tissue. *Sci Adv* 9, eadi0611 (2023).

236. Kutzelnigg, A. *et al.* Cortical demyelination and diffuse white matter injury in multiple sclerosis. *Brain* 128, 2705–2712 (2005).

237. Haider, L. *et al.* The topograpy of demyelination and neurodegeneration in the multiple sclerosis brain. *Brain* 139, 807–815 (2016).

238. McComb, S., Thiriot, A., Akache, B., Krishnan, L. & Stark, F. Introduction to the Immune System. in *Immunoproteomics: Methods and Protocols* (eds. Fulton, K. M. & Twine, S. M.) 1–24 (Springer, 2019). doi:10.1007/978-1-4939-9597-4_1.

239. Vorobjeva, N. V. & Chernyak, B. V. NETosis: Molecular Mechanisms, Role in Physiology and Pathology. *Biochemistry (Mosc)* 85, 1178–1190 (2020).

240. Brummelman, J., Pilipow, K. & Lugli, E. Chapter Two - The Single-Cell Phenotypic Identity of Human CD8+ and CD4+ T Cells. in *International Review of Cell and Molecular Biology* (eds. Galluzzi, L. & Rudqvist, N.-P.) vol. 341 63–124 (Academic Press, 2018).

241. Wieczorek, M. *et al.* Major Histocompatibility Complex (MHC) Class I and MHC Class II Proteins: Conformational Plasticity in Antigen Presentation. *Front Immunol* 8, 292 (2017).

242. Boyman, O., Létourneau, S., Krieg, C. & Sprent, J. Homeostatic proliferation and survival of naïve and memory T cells. *European Journal of Immunology* 39, 2088–2094 (2009).

243. Natalini, A. *et al.* OMIP-079: Cell cycle of CD4+ and CD8+ naïve/memory T cell subsets, and of Treg cells from mouse spleen. *Cytometry A* 99, 1171–1175 (2021).

244. Sallusto, F., Lenig, D., Förster, R., Lipp, M. & Lanzavecchia, A. Two subsets of memory T lymphocytes with distinct homing potentials and effector functions. *Nature* 401, 708–712 (1999).

245. Eibel, H., Kraus, H., Sic, H., Kienzler, A.-K. & Rizzi, M. B cell Biology: An Overview. *Curr Allergy Asthma Rep* 14, 434 (2014).

246. Morgan, D. & Tergaonkar, V. Unraveling B cell trajectories at single cell resolution. *Trends in Immunology* 43, 210–229 (2022).

247. Akkaya, B. & Shevach, E. M. Regulatory T cells: Master thieves of the immune system. *Cell Immunol* 355, 104160 (2020).

248. Beissert, S., Schwarz, A. & Schwarz, T. Regulatory T Cells. *J Invest Dermatol* 126, 15–24 (2006).

249. Matsushita, T. Regulatory and effector B cells: Friends or foes? *J Dermatol Sci* 93, 2–7 (2019).

250. Mishra, S., Srinivasan, S., Ma, C. & Zhang, N. CD8+ Regulatory T Cell - A Mystery to Be Revealed. *Front Immunol* 12, 708874 (2021).

251. Tan, D. *et al.* B cell-T cell interplay in immune regulation: A focus on follicular regulatory T and regulatory B cell functions. *Front Cell Dev Biol* 10, 991840 (2022).

252. Vasileiadis, G. K. *et al.* Regulatory B and T lymphocytes in multiple sclerosis: friends or foes? *Autoimmun Highlights* 9, 9 (2018).

253. Dong, C. Cytokine Regulation and Function in T Cells. *Annual Review of Immunology* 39, 51–76 (2021).

254. Saravia, J., Chapman, N. M. & Chi, H. Helper T cell differentiation. *Cell Mol Immunol* 16, 634–643 (2019).

255. Veldhoen, M. *et al.* Transforming growth factor-β 'reprograms' the differentiation of T helper 2 cells and promotes an interleukin 9–producing subset. *Nat Immunol* 9, 1341–1346 (2008).

256. Chen, J. *et al.* T Helper 9 Cells: A New Player in Immune-Related Diseases. *DNA Cell Biol* 38, 1040–1047 (2019).

257. Trifari, S., Kaplan, C. D., Tran, E. H., Crellin, N. K. & Spits, H. Identification of a human helper T cell population that has abundant production of interleukin 22 and is distinct from T(H)-17, T(H)1 and T(H)2 cells. *Nat Immunol* 10, 864–871 (2009).

258. Vajkoczy, P., Laschinger, M. & Engelhardt, B. α4-integrin-VCAM-1 binding mediates G protein–independent capture of encephalitogenic T cell blasts to CNS white matter microvessels. *J Clin Invest* 108, 557–565 (2001).

259. McCandless, E. E. *et al.* Pathological expression of CXCL12 at the blood-brain barrier correlates with severity of multiple sclerosis. *Am J Pathol* 172, 799–808 (2008).

260. McCandless, E. E. *et al.* IL-1R Signaling within the Central Nervous System Regulates CXCL12 Expression at the Blood-Brain Barrier and Disease Severity during Experimental Autoimmune Encephalomyelitis1. *The Journal of Immunology* 183, 613–620 (2009).

261. Krumbholz, M. *et al.* Chemokines in multiple sclerosis: CXCL12 and CXCL13 up-regulation is differentially linked to CNS immune cell recruitment. *Brain* 129, 200–211 (2006).

262. Alt, C., Laschinger, M. & Engelhardt, B. Functional expression of the lymphoid chemokines CCL19 (ELC) and CCL 21 (SLC) at the blood-brain barrier suggests their involvement in G-protein-dependent lymphocyte recruitment into the central nervous system during experimental autoimmune encephalomyelitis. *European Journal of Immunology* 32, 2133–2144 (2002).

263. Holman, D. W., Klein, R. S. & Ransohoff, R. M. The blood–brain barrier, chemokines and multiple sclerosis. *Biochimica et Biophysica Acta (BBA) - Molecular Basis of Disease* 1812, 220–230 (2011).

264. Nair, A. L. *et al.* Human BBB-on-a-chip reveals barrier disruption, endothelial inflammation, and T cell migration under neuroinflammatory conditions. *Front Mol Neurosci* 16, 1250123 (2023).

265. Wojkowska, D. W., Szpakowski, P. & Glabinski, A. Interleukin 17A Promotes Lymphocytes Adhesion and Induces CCL2 and CXCL1 Release from Brain Endothelial Cells. *Int J Mol Sci* 18, 1000 (2017).

266. Grifka-Walk, H. M., Giles, D. A. & Segal, B. M. IL-12-polarized Th1 cells produce GM-CSF and induce EAE independent of IL-23. *Eur J Immunol* 45, 2780–2786 (2015).

267. Lee, P. W. *et al.* IL-23R-activated STAT3/STAT4 is essential for Th1/Th17-mediated CNS autoimmunity. *JCI Insight* 2, e91663, 91663 (2017).

268. Segal, B. M. & Shevach, E. M. IL-12 unmasks latent autoimmune disease in resistant mice. *J Exp Med* 184, 771–775 (1996).

269. Thakker, P. *et al.* IL-23 is critical in the induction but not in the effector phase of experimental autoimmune encephalomyelitis. *J Immunol* 178, 2589–2598 (2007).

270. Lee, Y. *et al.* Induction and molecular signature of pathogenic TH17 cells. *Nat Immunol* 13, 991–999 (2012).

271. McGeachy, M. J. *et al.* The interleukin 23 receptor is essential for the terminal differentiation of interleukin 17–producing effector T helper cells in vivo. *Nat Immunol* 10, 314–324 (2009).

272. Cua, D. J. *et al.* Interleukin-23 rather than interleukin-12 is the critical cytokine for autoimmune inflammation of the brain. *Nature* 421, 744–748 (2003).

273. Abromson-Leeman, S., Bronson, R. T. & Dorf, M. E. Encephalitogenic T cells that stably express both T-bet and ROR gamma t consistently produce IFNgamma but have a spectrum of IL-17 profiles. *J Neuroimmunol* 215, 10–24 (2009).

274. El-Behi, M. *et al.* The encephalitogenicity of T(H)17 cells is dependent on IL-1- and IL-23-induced production of the cytokine GM-CSF. *Nat Immunol* 12, 568–575 (2011).

275. Franzen, R., Bouhy, D. & Schoenen, J. Nervous system injury: focus on the inflammatory cytokine 'granulocyte-macrophage colony stimulating factor'. *Neuroscience Letters* 361, 76–78 (2004).

276. Galli, E. *et al.* GM-CSF and CXCR4 define a T helper cell signature in multiple sclerosis. *Nat Med* 25, 1290–1300 (2019).

277. Luchtman, D. W., Ellwardt, E., Larochelle, C. & Zipp, F. IL-17 and related cytokines involved in the pathology and immunotherapy of multiple sclerosis: Current and future developments. *Cytokine & Growth Factor Reviews* 25, 403–413 (2014).

278. Jin, J.-O., Han, X. & Yu, Q. Interleukin-6 induces the generation of IL-10-producing Tr1 cells and suppresses autoimmune tissue inflammation. *Journal of Autoimmunity* 40, 28–44 (2013).

279. Millward, J. M., Løbner, M., Wheeler, R. D. & Owens, T. Inflammation in the Central Nervous System and Th17 Responses Are Inhibited by IFN-γ–Induced IL-18 Binding Protein. *The Journal of Immunology* 185, 2458–2466 (2010).

280. Bielekova, B. *et al.* Expansion and functional relevance of high-avidity myelin-specific CD4+ T cells in multiple sclerosis. *J Immunol* 172, 3893–3904 (2004).

281. Hellings, N. *et al.* T-cell reactivity to multiple myelin antigens in multiple sclerosis patients and healthy controls. *Journal of Neuroscience Research* 63, 290–302 (2001).

282. Hauser, S. L. *et al.* Immunohistochemical analysis of the cellular infiltrate in multiple sclerosis lesions. *Ann Neurol* 19, 578–587 (1986).

283. Jacobsen, M. *et al.* Oligoclonal expansion of memory CD8+ T cells in cerebrospinal fluid from multiple sclerosis patients. *Brain* 125, 538–550 (2002).

284. Malmeström, C. *et al.* Relapses in multiple sclerosis are associated with increased CD8+ T-cell mediated cytotoxicity in CSF. *J Neuroimmunol* 196, 159–165 (2008).

285. Denic, A., Wootla, B. & Rodriguez, M. CD8+ T Cells in Multiple Sclerosis. *Expert Opin Ther Targets* 17, 1053–1066 (2013).

286. Höftberger, R. *et al.* Expression of major histocompatibility complex class I molecules on the different cell types in multiple sclerosis lesions. *Brain Pathol* 14, 43–50 (2004).

287. Kuhlmann, T., Lingfeld, G., Bitsch, A., Schuchardt, J. & Brück, W. Acute axonal damage in multiple sclerosis is most extensive in early disease stages and decreases over time. *Brain* 125, 2202–2212 (2002).

288. Medana, I. *et al.* Fas ligand (CD95L) protects neurons against perforin-mediated T lymphocyte cytotoxicity. *J Immunol* 167, 674–681 (2001).

289. Pouly, S., Becher, B., Blain, M. & Antel, J. P. Interferon-gamma modulates human oligodendrocyte susceptibility to Fas-mediated apoptosis. *J Neuropathol Exp Neurol* 59, 280–286 (2000).

290. Rensing-Ehl, A. *et al.* Neurons induced to express major histocompatibility complex class I antigen are killed via the perforin and not the Fas (APO-1/CD95) pathway. *Eur J Immunol* 26, 2271–2274 (1996).

291. Tian, J. *et al.* Tissue-resident immune cells in the pathogenesis of multiple sclerosis. *Inflamm. Res.* 72, 363–372 (2023).

292. Bose, T. Role of Immunological Memory Cells as a Therapeutic Target in Multiple Sclerosis. *Brain Sciences* 7, 148 (2017).

293. Zaffaroni, M., Rossini, S., Ghezzi, A., Parma, R. & Cazzullo, C. L. Decrease of CD4+CD45+ T-cells in chronic-progressive multiple sclerosis. *J Neurol* 237, 1–4 (1990).

294. Frieser, D. *et al.* Tissue-resident CD8+ T cells drive compartmentalized and chronic autoimmune damage against CNS neurons. *Sci Transl Med* 14, eabl6157 (2022).

295. Fletcher, J. M. *et al.* CD39+Foxp3+ Regulatory T Cells Suppress Pathogenic Th17 Cells and Are Impaired in Multiple Sclerosis1. *The Journal of Immunology* 183, 7602–7610 (2009).

296. Frisullo, G. *et al.* Regulatory T cells fail to suppress CD4+ T-bet+ T cells in relapsing multiple sclerosis patients. *Immunology* 127, 418–428 (2009).

297. Haas, J. *et al.* Reduced suppressive effect of CD4+CD25high regulatory T cells on the T cell immune response against myelin oligodendrocyte glycoprotein in patients with multiple sclerosis. *Eur J Immunol* 35, 3343–3352 (2005).

298. Venken, K. *et al.* Natural Naive CD4+CD25+CD127low Regulatory T Cell (Treg) Development and Function Are Disturbed in Multiple Sclerosis Patients: Recovery of Memory Treg Homeostasis during Disease Progression. *The Journal of Immunology* 180, 6411–6420 (2008).

299. Venken, K. *et al.* Compromised CD4+ CD25high regulatory T-cell function in patients with relapsing-remitting multiple sclerosis is correlated with a reduced frequency of FOXP3-positive cells and reduced FOXP3 expression at the single-cell level. *Immunology* 123, 79–89 (2008).

300. Viglietta, V., Baecher-Allan, C., Weiner, H. L. & Hafler, D. A. Loss of functional suppression by CD4+CD25+ regulatory T cells in patients with multiple sclerosis. *J Exp Med* 199, 971–979 (2004).

301. Peelen, E. *et al.* Th17 expansion in MS patients is counterbalanced by an expanded CD39+ regulatory T cell population during remission but not during relapse. *J Neuroimmunol* 240–241, 97–103 (2011).

302. Korn, T. *et al.* IL-6 controls Th17 immunity in vivo by inhibiting the conversion of conventional T cells into Foxp3+ regulatory T cells. *Proc Natl Acad Sci U S A* 105, 18460–18465 (2008).

303. Schneider, A. *et al.* In Active Relapsing-Remitting Multiple Sclerosis, Effector T Cell Resistance to Adaptive Tregs Involves IL-6–Mediated Signaling. *Science Translational Medicine* 5, 170ra15-170ra15 (2013).

304. Bhela, S. *et al.* Non-apoptotic and extracellular activity of Granzyme B mediates resistance to Treg suppression by HLA-DRnegCD25hiCD127lo Tregs in multiple sclerosis and in response to IL-6. *J Immunol* 194, 2180–2189 (2015).

305. Beriou, G. *et al.* IL-17–producing human peripheral regulatory T cells retain suppressive function. *Blood* 113, 4240–4249 (2009).

306. Dominguez-Villar, M., Baecher-Allan, C. M. & Hafler, D. A. Identification of T helper type 1-like, Foxp3+ regulatory T cells in human autoimmune disease. *Nat Med* 17, 673–675 (2011).

307. Astier, A. L. & Hafler, D. A. Abnormal Tr1 differentiation in multiple sclerosis. *J Neuroimmunol* 191, 70–78 (2007).

308. Lee, Y.-H. *et al.* Essential role of CD8+CD122+ regulatory T cells in the recovery from experimental autoimmune encephalomyelitis. *J Immunol* 180, 825–832 (2008).

309. Najafian, N. *et al.* Regulatory functions of CD8+CD28- T cells in an autoimmune disease model. *J Clin Invest* 112, 1037–1048 (2003).

310. Correale, J. & Villa, A. Isolation and characterization of CD8+ regulatory T cells in multiple sclerosis. *J Neuroimmunol* 195, 121–134 (2008).

311. Sinha, S., Itani, F. R. & Karandikar, N. J. Immune regulation of multiple sclerosis by CD8+ T cells. *Immunol Res* 59, 254–265 (2014).

312. Tennakoon, D. K. *et al.* Therapeutic induction of regulatory, cytotoxic CD8+ T cells in multiple sclerosis. *J Immunol* 176, 7119–7129 (2006).

313. Balint, B. *et al.* T-cell homeostasis in pediatric multiple sclerosis: old cells in young patients. *Neurology* 81, 784–792 (2013).

314. Vargas-Lowy, D. *et al.* Increased Th17 response to myelin peptides in pediatric MS. *Clin Immunol* 146, 176–184 (2013).

315. Arneth, B. M. Impact of B cells to the pathophysiology of multiple sclerosis. *J Neuroinflammation* 16, 128 (2019).

316. Obermeier, B. *et al.* Matching of oligoclonal immunoglobulin transcriptomes and proteomes of cerebrospinal fluid in multiple sclerosis. *Nat Med* 14, 688–693 (2008).

317. Genain, C. P., Cannella, B., Hauser, S. L. & Raine, C. S. Identification of autoantibodies associated with myelin damage in multiple sclerosis. *Nat Med* 5, 170–175 (1999).

318. O'Connor, K. C. *et al.* Antibodies from inflamed central nervous system tissue recognize myelin oligodendrocyte glycoprotein. *J Immunol* 175, 1974–1982 (2005).

319. Owens, G. P. *et al.* Antibodies produced by clonally expanded plasma cells in multiple sclerosis cerebrospinal fluid. *Ann Neurol* 65, 639–649 (2009).

320. Weber, J. *et al.* Diagnosis of multiple sclerosis in times of MOG and AQP4 autoantibody testing - A monocentric study. *J Neurol Sci* 421, 117289 (2021).

321. Elliott, C. *et al.* Functional identification of pathogenic autoantibody responses in patients with multiple sclerosis. *Brain* 135, 1819–1833 (2012).

322. Lanz, T. V. *et al.* Clonally expanded B cells in multiple sclerosis bind EBV EBNA1 and GlialCAM. *Nature* 603, 321–327 (2022).

323. Lünemann, J. D. *et al.* EBNA1-specific T cells from patients with multiple sclerosis cross react with myelin antigens and co-produce IFN-gamma and IL-2. *J Exp Med* 205, 1763–1773 (2008).

324. Fraussen, J. *et al.* B cells of multiple sclerosis patients induce autoreactive proinflammatory T cell responses. *Clinical Immunology* 173, 124–132 (2016).

325. Harp, C. T. *et al.* Memory B cells from a subset of treatment naïve relapsing remitting multiple sclerosis patients elicit CD4+ T cell proliferation and IFN-γ production in response to MBP and MOG. *Eur J Immunol* 40, 2942–2956 (2010).

326. Molnarfi, N. *et al.* MHC class II-dependent B cell APC function is required for induction of CNS autoimmunity independent of myelin-specific antibodies. *J Exp Med* 210, 2921–2937 (2013).

327. Bar-Or, A. *et al.* Abnormal B-cell cytokine responses a trigger of T-cell-mediated disease in MS? *Ann Neurol* 67, 452–461 (2010).

328. Duddy, M. *et al.* Distinct Effector Cytokine Profiles of Memory and Naive Human B Cell Subsets and Implication in Multiple Sclerosis. *The Journal of Immunology* 178, 6092–6099 (2007).

329. Li, R. *et al.* Proinflammatory GM-CSF-producing B cells in multiple sclerosis and B cell depletion therapy. *Sci Transl Med* 7, 310ra166 (2015).

330. Lisak, R. P. *et al.* B cells from patients with multiple sclerosis induce cell death via apoptosis in neurons in vitro. *Journal of Neuroimmunology* 309, 88–99 (2017).

331. Serafini, B., Rosicarelli, B., Magliozzi, R., Stigliano, E. & Aloisi, F. Detection of ectopic B-cell follicles with germinal centers in the meninges of patients with secondary progressive multiple sclerosis. *Brain Pathol* 14, 164–174 (2004).

332. Absinta, M. & Ontaneda, D. Controversial association between leptomeningeal enhancement and demyelinated cortical lesions in multiple sclerosis. *Mult Scler* 26, 135–136 (2020).

333. Bjarnadóttir, K. *et al.* B cell-derived transforming growth factor-β1 expression limits the induction phase of autoimmune neuroinflammation. *Sci Rep* 6, 34594 (2016).

334. Rieger, A. & Bar-Or, A. B-cell-derived interleukin-10 in autoimmune disease: regulating the regulators. *Nat Rev Immunol* 8, 486–487 (2008).

335. Staun-Ram, E. & Miller, A. Effector and regulatory B cells in Multiple Sclerosis. *Clinical Immunology* 184, 11–25 (2017).

336. Wang, R.-X. *et al.* Interleukin-35 induces regulatory B cells that suppress autoimmune disease. *Nat Med* 20, 633–641 (2014).

337. Alliot, F., Godin, I. & Pessac, B. Microglia derive from progenitors, originating from the yolk sac, and which proliferate in the brain. *Developmental Brain Research* 117, 145–152 (1999).

338. Benarroch, E. E. Microglia: Multiple roles in surveillance, circuit shaping, and response to injury. *Neurology* 81, 1079–1088 (2013).

339. Ajami, B. *et al.* Single cell mass cytometry reveals distinct populations of brain myeloid cells in mouse models of neuroinflammatory and neurodegenerative diseases. *Nat Neurosci* 21, 541–551 (2018).

340. Masuda, T. *et al.* Spatial and temporal heterogeneity of mouse and human microglia at single-cell resolution. *Nature* 566, 388–392 (2019).

341. Mendiola, A. S. *et al.* Transcriptional profiling and therapeutic targeting of oxidative stress in neuroinflammation. *Nat Immunol* 21, 513–524 (2020).

342. Tay, T. L., Sagar, null, Dautzenberg, J., Grün, D. & Prinz, M. Unique microglia recovery population revealed by single-cell RNAseq following neurodegeneration. *Acta Neuropathol Commun* 6, 87 (2018).

343. Zia, S. *et al.* Microglia Diversity in Health and Multiple Sclerosis. *Front Immunol* 11, 588021 (2020).

344. Réu, P. *et al.* The Lifespan and Turnover of Microglia in the Human Brain. *Cell Rep* 20, 779–784 (2017).

345. Zrzavy, T. *et al.* Loss of 'homeostatic' microglia and patterns of their activation in active multiple sclerosis. *Brain* 140, 1900–1913 (2017).

346. Bolaños, J. P. *et al.* Nitric oxide-mediated mitochondrial damage in the brain: mechanisms and implications for neurodegenerative diseases. *J Neurochem* 68, 2227–2240 (1997).

347. Correale, J. The role of microglial activation in disease progression. *Mult Scler* 20, 1288–1295 (2014).

348. Lu, F. *et al.* Oxidative damage to mitochondrial DNA and activity of mitochondrial enzymes in chronic active lesions of multiple sclerosis. *J Neurol Sci* 177, 95–103 (2000).

349. Nikić, I. *et al.* A reversible form of axon damage in experimental autoimmune encephalomyelitis and multiple sclerosis. *Nat Med* 17, 495–499 (2011).

350. Takahashi, J. L., Giuliani, F., Power, C., Imai, Y. & Yong, V. W. Interleukin-1beta promotes oligodendrocyte death through glutamate excitotoxicity. *Ann Neurol* 53, 588–595 (2003).

351. Absinta, M. *et al.* A lymphocyte–microglia–astrocyte axis in chronic active multiple sclerosis. *Nature* 597, 709–714 (2021).

352. Kirby, L. *et al.* Oligodendrocyte precursor cells present antigen and are cytotoxic targets in inflammatory demyelination. *Nat Commun* 10, 3887 (2019).

353. Falcão, A. M. *et al.* Disease-specific oligodendrocyte lineage cells arise in multiple sclerosis. *Nat Med* 24, 1837–1844 (2019).

354. Liddelow, S. A. *et al.* Neurotoxic reactive astrocytes are induced by activated microglia. *Nature* 541, 481–487 (2017).

355. Arnett, H. A. *et al.* TNF alpha promotes proliferation of oligodendrocyte progenitors and remyelination. *Nat Neurosci* 4, 1116–1122 (2001).

356. Mason, J. L., Suzuki, K., Chaplin, D. D. & Matsushima, G. K. Interleukin-1beta promotes repair of the CNS. *J Neurosci* 21, 7046–7052 (2001).

357. Suvannavejh, G. C. *et al.* Divergent Roles for p55 and p75 Tumor Necrosis Factor Receptors in the Pathogenesis of MOG35-55-Induced Experimental Autoimmune Encephalomyelitis. *Cellular Immunology* 205, 24–33 (2000).

358. Plemel, J. R., Manesh, S. B., Sparling, J. S. & Tetzlaff, W. Myelin inhibits oligodendroglial maturation and regulates oligodendrocytic transcription factor expression. *Glia* 61, 1471–1487 (2013).

359. Syed, Y. A. *et al.* Inhibition of oligodendrocyte precursor cell differentiation by myelin-associated proteins. *Neurosurg Focus* 24, E5 (2008).

360. Yamasaki, R. *et al.* Differential roles of microglia and monocytes in the inflamed central nervous system. *J Exp Med* 211, 1533–1549 (2014).

361. Wlodarczyk, A. *et al.* A novel microglial subset plays a key role in myelinogenesis in developing brain. *EMBO J* 36, 3292–3308 (2017).

362. Lloyd, A. F. *et al.* Central nervous system regeneration is driven by microglia necroptosis and repopulation. *Nat Neurosci* 22, 1046–1052 (2019).

363. Hendrickx, D. A. E., Schuurman, K. G., van Draanen, M., Hamann, J. & Huitinga, I. Enhanced uptake of multiple sclerosis-derived myelin by THP-1 macrophages and primary human microglia. *J Neuroinflammation* 11, 64 (2014).

364. Molofsky, A. V. & Deneen, B. Astrocyte development: A Guide for the Perplexed. *Glia* 63, 1320–1329 (2015).

365. Aharoni, R., Eilam, R. & Arnon, R. Astrocytes in Multiple Sclerosis—Essential Constituents with Diverse Multifaceted Functions. *International Journal of Molecular Sciences* 22, 5904 (2021).

366. Volterra, A. & Meldolesi, J. Astrocytes, from brain glue to communication elements: the revolution continues. *Nat Rev Neurosci* 6, 626–640 (2005).

367. Clarke, L. E. & Barres, B. A. Emerging roles of astrocytes in neural circuit development. *Nat Rev Neurosci* 14, 311–321 (2013).

368. Piet, R., Vargová, L., Syková, E., Poulain, D. A. & Oliet, S. H. R. Physiological contribution of the astrocytic environment of neurons to intersynaptic crosstalk. *Proc Natl Acad Sci U S A* 101, 2151–2155 (2004).

369. Simard, M. & Nedergaard, M. The neurobiology of glia in the context of water and ion homeostasis. *Neuroscience* 129, 877–896 (2004).

370. Rash, J. E. Molecular disruptions of the panglial syncytium block potassium siphoning and axonal saltatory conduction: pertinence to neuromyelitis optica and other demyelinating diseases of the central nervous system. *Neuroscience* 168, 982–1008 (2010).

371. Camargo, N. *et al.* Oligodendroglial myelination requires astrocyte-derived lipids. *PLOS Biology* 15, e1002605 (2017).

372. Abbott, N. J., Patabendige, A. A. K., Dolman, D. E. M., Yusof, S. R. & Begley, D. J. Structure and function of the blood-brain barrier. *Neurobiol Dis* 37, 13–25 (2010).

373. Iadecola, C. The Neurovascular Unit Coming of Age: A Journey through Neurovascular Coupling in Health and Disease. *Neuron* 96, 17–42 (2017).

374. Nitsch, L. *et al.* MOG-Specific T Cells Lead to Spontaneous EAE with Multilocular B Cell Infiltration in the GF-IL23 Model. *Neuromolecular Med* 24, 415–423 (2022).

375. Lee, S. C., Dickson, D. W., Liu, W. & Brosnan, C. F. Induction of nitric oxide synthase activity in human astrocytes by interleukin-1β and interferon-γ. *Journal of Neuroimmunology* 46, 19–24 (1993).

376. Trajkovic, V. *et al.* Interleukin-17 stimulates inducible nitric oxide synthase activation in rodent astrocytes. *Journal of Neuroimmunology* 119, 183–191 (2001).

377. Back, S. A. *et al.* Hyaluronan accumulates in demyelinated lesions and inhibits oligodendrocyte progenitor maturation. *Nat Med* 11, 966–972 (2005).

378. Bannerman, P., Hahn, A., Soulika, A., Gallo, V. & Pleasure, D. Astrogliosis in EAE spinal cord: Derivation from radial glia, and relationships to oligodendroglia. *Glia* 55, 57–64 (2007).

379. Lau, L. W. *et al.* Chondroitin sulfate proteoglycans in demyelinated lesions impair remyelination. *Annals of Neurology* 72, 419–432 (2012).

380. Stoffels, J. M. J. *et al.* Fibronectin aggregation in multiple sclerosis lesions impairs remyelination. *Brain* 136, 116–131 (2013).

381. Kim, S., Steelman, A. J., Koito, H. & Li, J. Astrocytes promote TNF-mediated toxicity to oligodendrocyte precursors. *Journal of Neurochemistry* 116, 53–66 (2011).

382. Hardin-Pouzet, H. *et al.* Glutamate metabolism is down-regulated in astrocytes during experimental allergic encephalomyelitis. *Glia* 20, 79–85 (1997).

383. Kostic, M., Zivkovic, N., Cvetanovic, A., Stojanovic, I. & Colic, M. IL-17 signalling in astrocytes promotes glutamate excitotoxicity: Indications for the link between inflammatory and neurodegenerative events in multiple sclerosis. *Mult Scler Relat Disord* 11, 12–17 (2017).

384. Voskuhl, R. R. *et al.* Reactive Astrocytes Form Scar-Like Perivascular Barriers to Leukocytes during Adaptive Immune Inflammation of the CNS. *J. Neurosci.* 29, 11511–11522 (2009).

385. Filipello, F. *et al.* Ectonucleotidase activity and immunosuppression in astrocyte-CD4 T cell bidirectional signaling. *Oncotarget* 7, 5143–5156 (2016).

386. Hulshof, S., Montagne, L., De Groot, C. J. A. & Van Der Valk, P. Cellular localization and expression patterns of interleukin-10, interleukin-4, and their receptors in multiple sclerosis lesions. *Glia* 38, 24–35 (2002).

387. Lalive, P. H. *et al.* Increased interleukin-27 cytokine expression in the central nervous system of multiple sclerosis patients. *J Neuroinflammation* 14, (2017).

388. Alvarez, J. I. *et al.* The Hedgehog Pathway Promotes Blood-Brain Barrier Integrity and CNS Immune Quiescence. *Science* 334, 1727–1731 (2011).

389. Mizee, M. R. *et al.* Astrocyte-derived retinoic acid: a novel regulator of blood–brain barrier function in multiple sclerosis. *Acta Neuropathol* 128, 691–703 (2014).

390. Yun, H.-M., Park, K.-R., Kim, E.-C. & Hong, J. T. PRDX6 controls multiple sclerosis by suppressing inflammation and blood brain barrier disruption. *Oncotarget* 6, 20875–20884 (2015).

391. Skripuletz, T. *et al.* Astrocytes regulate myelin clearance through recruitment of microglia during cuprizone-induced demyelination. *Brain* 136, 147–167 (2013).

392. Miller, R. H. Regulation of oligodendrocyte development in the vertebrate CNS. *Progress in Neurobiology* 67, 451–467 (2002).

393. Dawson, M. R. L., Polito, A., Levine, J. M. & Reynolds, R. NG2-expressing glial progenitor cells: an abundant and widespread population of cycling cells in the adult rat CNS. *Molecular and Cellular Neuroscience* 24, 476–488 (2003).

394. Donega, V. *et al.* Single-cell profiling of human subventricular zone progenitors identifies SFRP1 as a target to re-activate progenitors. *Nat Commun* 13, 1036 (2022).

395. Gonzalez-Perez, O. & Alvarez-Buylla, A. Oligodendrogenesis in the subventricular zone and the role of epidermal growth factor. *Brain Research Reviews* 67, 147–156 (2011).

396. Perlman, K. *et al.* Developmental trajectory of oligodendrocyte progenitor cells in the human brain revealed by single cell RNA sequencing. *Glia* 68, 1291–1303 (2020).

397. Lytle, J. M., Chittajallu, R., Wrathall, J. R. & Gallo, V. NG2 cell response in the CNP-EGFP mouse after contusive spinal cord injury. *Glia* 57, 270–285 (2009).

398. Maki, T., Liang, A. C., Miyamoto, N., Lo, E. H. & Arai, K. Mechanisms of oligodendrocyte regeneration from ventricular-subventricular zone-derived progenitor cells in white matter diseases. *Front Cell Neurosci* 7, 275 (2013).

399. Young, K. M. *et al.* Oligodendrocyte Dynamics in the Healthy Adult CNS: Evidence for Myelin Remodeling. *Neuron* 77, 873–885 (2013).

400. Dulamea, A. O. Role of Oligodendrocyte Dysfunction in Demyelination, Remyelination and Neurodegeneration in Multiple Sclerosis. *Adv Exp Med Biol* 958, 91–127 (2017).

401. Aboul-Enein, F. *et al.* Preferential Loss of Myelin-Associated Glycoprotein Reflects Hypoxia-Like White Matter Damage in Stroke and Inflammatory Brain Diseases. *Journal of Neuropathology & Experimental Neurology* 62, 25–33 (2003).

402. Ludwin, S. K. & Johnson, E. S. Evidence for a 'dying-back' gliopathy in demyelinating disease. *Ann Neurol* 9, 301–305 (1981).

403. Duncan, G. J., Simkins, T. J. & Emery, B. Neuron-Oligodendrocyte Interactions in the Structure and Integrity of Axons. *Front Cell Dev Biol* 9, 653101 (2021).

404. Glezer, I., Lapointe, A. & Rivest, S. Innate immunity triggers oligodendrocyte progenitor reactivity and confines damages to brain injuries. *FASEB J* 20, 750–752 (2006).

405. Hinks, G. L. & Franklin, R. J. M. Distinctive Patterns of PDGF-A, FGF-2, IGF-I, and TGF-β1 Gene Expression during Remyelination of Experimentally-Induced Spinal Cord Demyelination. *Molecular and Cellular Neuroscience* 14, 153–168 (1999).

406. Webster, H. de F. Growth factors and myelin regeneration in multiple sclerosis. *Mult Scler* 3, 113–120 (1997).

407. White, R. & Krämer-Albers, E.-M. Axon-glia interaction and membrane traffic in myelin formation. *Front Cell Neurosci* 7, 284 (2014).

408. Williams, A. *et al.* Semaphorin 3A and 3F: key players in myelin repair in multiple sclerosis? *Brain* 130, 2554–2565 (2007).

409. Crawford, D. K., Mangiardi, M., Xia, X., López-Valdés, H. E. & Tiwari-Woodruff, S. K. Functional recovery of callosal axons following demyelination: a critical window. *Neuroscience* 164, 1407–1421 (2009).

410. Rone, M. B. *et al.* Oligodendrogliopathy in Multiple Sclerosis: Low Glycolytic Metabolic Rate Promotes Oligodendrocyte Survival. *J Neurosci* 36, 4698–4707 (2016).

411. Yeung, M. S. Y. *et al.* Dynamics of oligodendrocyte generation in multiple sclerosis. *Nature* 566, 538–542 (2019).

412. Jäkel, S. *et al.* Altered human oligodendrocyte heterogeneity in multiple sclerosis. *Nature* 566, 543–547 (2019).

413. Barkhof, F. *et al.* Remyelinated lesions in multiple sclerosis: magnetic resonance image appearance. *Arch Neurol* 60, 1073–1081 (2003).

414. Bramow, S. *et al.* Demyelination versus remyelination in progressive multiple sclerosis. *Brain* 133, 2983–2998 (2010).

415. Goldschmidt, T., Antel, J., König, F. B., Brück, W. & Kuhlmann, T. Remyelination capacity of the MS brain decreases with disease chronicity. *Neurology* 72, 1914–1921 (2009).

416. Hampton, D. W. *et al.* Focal immune-mediated white matter demyelination reveals an age-associated increase in axonal vulnerability and decreased remyelination efficiency. *Am J Pathol* 180, 1897–1905 (2012).

417. Patani, R., Balaratnam, M., Vora, A. & Reynolds, R. Remyelination can be extensive in multiple sclerosis despite a long disease course. *Neuropathol Appl Neurobiol* 33, 277–287 (2007).

418. Gharagozloo, M., Bannon, R. & Calabresi, P. A. Breaking the barriers to remyelination in multiple sclerosis. *Current Opinion in Pharmacology* 63, 102194 (2022).

419. Chang, A., Tourtellotte, W. W., Rudick, R. & Trapp, B. D. Premyelinating Oligodendrocytes in Chronic Lesions of Multiple Sclerosis. *N Engl J Med* 346, 165–173 (2002).

420. Ludwin, S. K. Chronic demyelination inhibits remyelination in the central nervous system. An analysis of contributing factors. *Lab Invest* 43, 382–387 (1980).

421. Penderis, J., Shields, S. A. & Franklin, R. J. M. Impaired remyelination and depletion of oligodendrocyte progenitors does not occur following repeated episodes of focal demyelination in the rat central nervous system. *Brain* 126, 1382–1391 (2003).

422. Tepavčević, V. & Lubetzki, C. Oligodendrocyte progenitor cell recruitment and remyelination in multiple sclerosis: the more, the merrier? *Brain* 145, 4178–4192 (2022).

423. Wolswijk, G. Oligodendrocyte precursor cells in the demyelinated multiple sclerosis spinal cord. *Brain* 125, 338–349 (2002).

424. Rao, V. T. S. *et al.* Distinct age and differentiation-state dependent metabolic profiles of oligodendrocytes under optimal and stress conditions. *PLoS One* 12, e0182372 (2017).

425. Schoenfeld, R. *et al.* Oligodendroglial differentiation induces mitochondrial genes and inhibition of mitochondrial function represses oligodendroglial differentiation. *Mitochondrion* 10, 143–150 (2010).

426. Chari, D. M., Crang, A. J. & Blakemore, W. F. Decline in rate of colonization of oligodendrocyte progenitor cell (OPC)-depleted tissue by adult OPCs with age. *J Neuropathol Exp Neurol* 62, 908–916 (2003).

427. Foote, A. K. & Blakemore, W. F. Repopulation of oligodendrocyte progenitor cell-depleted tissue in a model of chronic demyelination. *Neuropathol Appl Neurobiol* 31, 374–383 (2005).

428. Sim, F. J., Zhao, C., Penderis, J. & Franklin, R. J. M. The Age-Related Decrease in CNS Remyelination Efficiency Is Attributable to an Impairment of Both Oligodendrocyte Progenitor Recruitment and Differentiation. *J Neurosci* 22, 2451–2459 (2002).

429. Boyd, A., Zhang, H. & Williams, A. Insufficient OPC migration into demyelinated lesions is a cause of poor remyelination in MS and mouse models. *Acta Neuropathol* 125, 841–859 (2013).

430. Bin, J. M. *et al.* Full-Length and Fragmented Netrin-1 in Multiple Sclerosis Plaques Are Inhibitors of Oligodendrocyte Precursor Cell Migration. *The American Journal of Pathology* 183, 673–680 (2013).

431. Kerstetter, A. E., Padovani-Claudio, D. A., Bai, L. & Miller, R. H. Inhibition of CXCR2 signaling promotes recovery in models of multiple sclerosis. *Exp Neurol* 220, 44–56 (2009).

432. Tepavčević, V. *et al.* Early netrin-1 expression impairs central nervous system remyelination. *Annals of Neurology* 76, 252–268 (2014).

433. Patel, J. R., McCandless, E. E., Dorsey, D. & Klein, R. S. CXCR4 promotes differentiation of oligodendrocyte progenitors and remyelination. *Proc Natl Acad Sci U S A* 107, 11062–11067 (2010).

434. Hammond, T. R. *et al.* Astrocyte-derived Endothelin-1 inhibits remyelination through Notch activation. *Neuron* 81, 588–602 (2014).

435. Ghorbani, S. & Yong, V. W. The extracellular matrix as modifier of neuroinflammation and remyelination in multiple sclerosis. *Brain* 144, 1958–1973 (2021).

436. Wang, P. *et al.* MMP7 cleaves remyelination-impairing fibronectin aggregates and its expression is reduced in chronic multiple sclerosis lesions. *Glia* 66, 1625–1643 (2018).

437. Kuhlmann, T. *et al.* Differentiation block of oligodendroglial progenitor cells as a cause for remyelination failure in chronic multiple sclerosis. *Brain* 131, 1749–1758 (2008).

438. Wegener, A. *et al.* Gain of Olig2 function in oligodendrocyte progenitors promotes remyelination. *Brain* 138, 120–135 (2015).

439. Wolswijk, G. Oligodendrocyte survival, loss and birth in lesions of chronic-stage multiple sclerosis. *Brain* 123, 105–115 (2000).

440. Lee, J. Y., Biemond, M. & Petratos, S. Axonal degeneration in multiple sclerosis: defining therapeutic targets by identifying the causes of pathology. *Neurodegener Dis Manag* 5, 527–548 (2015).

441. Bitsch, A., Schuchardt, J., Bunkowski, S., Kuhlmann, T. & Brück, W. Acute axonal injury in multiple sclerosis: Correlation with demyelination and inflammation. *Brain* 123, 1174–1183 (2000).

442. Bjartmar, C., Kinkel, R. P., Kidd, G., Rudick, R. A. & Trapp, B. D. Axonal loss in normal-appearing white matter in a patient with acute MS. *Neurology* 57, 1248–1252 (2001).

443. Colombo, E. *et al.* Stimulation of the neurotrophin receptor TrkB on astrocytes drives nitric oxide production and neurodegeneration. *J Exp Med* 209, 521–535 (2012).

444. Haile, Y. *et al.* Granule-derived granzyme B mediates the vulnerability of human neurons to T cell-induced neurotoxicity. *J Immunol* 187, 4861–4872 (2011).

445. Meuth, S. G. *et al.* Cytotoxic CD8+ T cell-neuron interactions: perforin-dependent electrical silencing precedes but is not causally linked to neuronal cell death. *J Neurosci* 29, 15397–15409 (2009).

446. Miller, N. M. *et al.* Lymphocytes with cytotoxic activity induce rapid microtubule axonal destabilization independently and before signs of neuronal death. *ASN Neuro* 5, e00105 (2013).

447. Sauer, B. M., Schmalstieg, W. F. & Howe, C. L. Axons are injured by antigen-specific CD8(+) T cells through a MHC class I- and granzyme B-dependent mechanism. *Neurobiol Dis* 59, 194–205 (2013).

448. Fang, C., Bourdette, D. & Banker, G. Oxidative stress inhibits axonal transport: implications for neurodegenerative diseases. *Mol Neurodegener* 7, 29 (2012).

449. Li, S., Jiang, Q. & Stys, P. K. Important Role of Reverse Na+-Ca2+Exchange in Spinal Cord White Matter Injury at Physiological Temperature. *Journal of Neurophysiology* 84, 1116–1119 (2000).

450. Centonze, D. *et al.* The link between inflammation, synaptic transmission and neurodegeneration in multiple sclerosis. *Cell Death Differ* 17, 1083–1091 (2010).

451. Sarchielli, P., Greco, L., Floridi, A., Floridi, A. & Gallai, V. Excitatory amino acids and multiple sclerosis: evidence from cerebrospinal fluid. *Arch Neurol* 60, 1082–1088 (2003).

452. Srinivasan, R., Sailasuta, N., Hurd, R., Nelson, S. & Pelletier, D. Evidence of elevated glutamate in multiple sclerosis using magnetic resonance spectroscopy at 3 T. *Brain* 128, 1016–1025 (2005).

453. Gentile, A. *et al.* Peripheral T cells from multiple sclerosis patients trigger synaptotoxic alterations in central neurons. *Neuropathol Appl Neurobiol* 46, 160–170 (2020).

454. Ohgoh, M. *et al.* Altered expression of glutamate transporters in experimental autoimmune encephalomyelitis. *Journal of Neuroimmunology* 125, 170–178 (2002).

455. Rossi, S. *et al.* Tumor necrosis factor is elevated in progressive multiple sclerosis and causes excitotoxic neurodegeneration. *Mult Scler* 20, 304–312 (2014).

456. Rossi, S. *et al.* Interleukin-1β causes excitotoxic neurodegeneration and multiple sclerosis disease progression by activating the apoptotic protein p53. *Mol Neurodegener* 9, 56 (2014).

457. Pascual, O., Ben Achour, S., Rostaing, P., Triller, A. & Bessis, A. Microglia activation triggers astrocyte-mediated modulation of excitatory neurotransmission. *Proc Natl Acad Sci U S A* 109, E197-205 (2012).

458. Barnett, M. H. & Prineas, J. W. Relapsing and remitting multiple sclerosis: Pathology of the newly forming lesion. *Annals of Neurology* 55, 458–468 (2004).

459. Zoupi, L. *et al.* Selective vulnerability of inhibitory networks in multiple sclerosis. *Acta Neuropathol* 141, 415–429 (2021).

460. Cafferty, W. B. J. & Strittmatter, S. M. The Nogo–Nogo Receptor Pathway Limits a Spectrum of Adult CNS Axonal Growth. *J. Neurosci.* 26, 12242–12250 (2006).

461. Liu, B. P., Fournier, A., GrandPré, T. & Strittmatter, S. M. Myelin-associated glycoprotein as a functional ligand for the Nogo-66 receptor. *Science* 297, 1190–1193 (2002).

462. Wang, K. C. *et al.* Oligodendrocyte-myelin glycoprotein is a Nogo receptor ligand that inhibits neurite outgrowth. *Nature* 417, 941–944 (2002).

463. Peles, E. & Salzer, J. L. Molecular domains of myelinated axons. *Curr Opin Neurobiol* 10, 558–565 (2000).

464. Coman, I. *et al.* Nodal, paranodal and juxtaparanodal axonal proteins during demyelination and remyelination in multiple sclerosis. *Brain* 129, 3186–3195 (2006).

465. Smith, K. J., Blakemore, W. F. & McDonald, W. I. Central remyelination restores secure conduction. *Nature* 280, 395–396 (1979).

466. Mathey, E. K. *et al.* Neurofascin as a novel target for autoantibody-mediated axonal injury. *J Exp Med* 204, 2363–2372 (2007).

467. Wolswijk, G. & Balesar, R. Changes in the expression and localization of the paranodal protein Caspr on axons in chronic multiple sclerosis. *Brain* 126, 1638–1649 (2003).

468. Howell, O. W. *et al.* Activated microglia mediate axoglial disruption that contributes to axonal injury in multiple sclerosis. *J Neuropathol Exp Neurol* 69, 1017–1033 (2010).

469. Nave, K.-A. & Trapp, B. D. Axon-glial signaling and the glial support of axon function. *Annu Rev Neurosci* 31, 535–561 (2008).

470. Griffiths, I. *et al.* Axonal Swellings and Degeneration in Mice Lacking the Major Proteolipid of Myelin. *Science* 280, 1610–1613 (1998).

471. Readhead, C. *et al.* Expression of a myelin basic protein gene in transgenic shiverer mice: correction of the dysmyelinating phenotype. *Cell* 48, 703–712 (1987).

472. Uschkureit, T., Sporkel, O., Stracke, J., Bussow, H. & Stoffel, W. Early onset of axonal degeneration in double (plp-/-mag-/-) and hypomyelinosis in triple (plp-/-mbp-/-mag-/-) mutant mice. *J Neurosci* 20, 5225–5233 (2000).

473. Kassmann, C. M. *et al.* Axonal loss and neuroinflammation caused by peroxisome-deficient oligodendrocytes. *Nat Genet* 39, 969–976 (2007).

474. Kaufmann, M. *et al.* Identification of early neurodegenerative pathways in progressive multiple sclerosis. *Nat Neurosci* 25, 944–955 (2022).

475. Kappos, L. *et al.* Inclusion of brain volume loss in a revised measure of 'no evidence of disease activity' (NEDA-4) in relapsing-remitting multiple sclerosis. *Mult Scler* 22, 1297–1305 (2016).

476. Pandit, L. No Evidence of Disease Activity (NEDA) in Multiple Sclerosis - Shifting the Goal Posts. *Ann Indian Acad Neurol* 22, 261–263 (2019).

477. Fox, R. J. *et al.* Setting a research agenda for progressive multiple sclerosis: the International Collaborative on Progressive MS. *Mult Scler* 18, 1534–1540 (2012).

478. Weideman, A. M., Tapia-Maltos, M. A., Johnson, K., Greenwood, M. & Bielekova, B. Meta-analysis of the Age-Dependent Efficacy of Multiple Sclerosis Treatments. *Front Neurol* 8, 577 (2017).

479. Deiters, O. & Schultze, M. J. S. 1825-1874. *Untersuchungen über Gehirn und Rückenmark des Menschen und der Säugethiere*. (Braunschweig : Vieweg, 1865).

480. Golgi, C. & Royal College of Physicians of Edinburgh. *Sulla fina anatomia degli organi centrali del sistema nervoso*. (Milano : U. Hoepli, 1886).

481. Kuhn, S., Gritti, L., Crooks, D. & Dombrowski, Y. Oligodendrocytes in Development, Myelin Generation and Beyond. *Cells* 8, 1424 (2019).

482. Virchow, R. (Rudolf L. K., University of Glasgow. Library, & University of Glasgow. Library. *Gesammelte Abhandlungen zur Wissenschaftlichen Medicin [electronic resource]*. (Frankfurt A. M. : Meidinger Sohn & Comp., 1856).

483. Baba, H. *et al.* Completion of myelin compaction, but not the attachment of oligodendroglial processes triggers K+ channel clustering. *Journal of Neuroscience Research* 58, 752–764 (1999).

484. Miller, D. J. *et al.* Prolonged myelination in human neocortical evolution. *Proceedings of the National Academy of Sciences* 109, 16480–16485 (2012).

485. Yakovlev, P. I. & Lecours, A. R. The myelogenetic cycles of regional maturation of the brain. *Regional Development of the Brain in Early Life* (1967).

486. Davis, A. A. & Temple, S. A self-renewing multipotential stem cell in embryonic rat cerebral cortex. *Nature* 372, 263–266 (1994).

487. Emery, B. & Lu, Q. R. Transcriptional and Epigenetic Regulation of Oligodendrocyte Development and Myelination in the Central Nervous System. *Cold Spring Harb Perspect Biol* 7, a020461 (2015).

488. Kessaris, N. *et al.* Competing waves of oligodendrocytes in the forebrain and postnatal elimination of an embryonic lineage. *Nat Neurosci* 9, 173–179 (2006).

489. Mitew, S. *et al.* Mechanisms regulating the development of oligodendrocytes and central nervous system myelin. *Neuroscience* 276, 29–47 (2014).

490. Tripathi, R. B. *et al.* Dorsally and ventrally derived oligodendrocytes have similar electrical properties but myelinate preferred tracts. *J Neurosci* 31, 6809–6819 (2011).

491. Bilican, B., Fiore-Heriche, C., Compston, A., Allen, N. D. & Chandran, S. Induction of Olig2+ Precursors by FGF Involves BMP Signalling Blockade at the Smad Level. *PLOS ONE* 3, e2863 (2008).

492. Chandran, S. *et al.* FGF-dependent generation of oligodendrocytes by a hedgehog-independent pathway. *Development* 130, 6599–6609 (2003).

493. Kong, J. H. *et al.* Notch Activity Modulates the Responsiveness of Neural Progenitors to Sonic Hedgehog Signaling. *Dev Cell* 33, 373–387 (2015).

494. Mehler, M. F., Mabie, P. C., Zhu, G., Gokhan, S. & Kessler, J. A. Developmental changes in progenitor cell responsiveness to bone morphogenetic proteins differentially modulate progressive CNS lineage fate. *Dev Neurosci* 22, 74–85 (2000).

495. Pringle, N. P. *et al.* Determination of Neuroepithelial Cell Fate: Induction of the Oligodendrocyte Lineage by Ventral Midline Cells and Sonic Hedgehog. *Developmental Biology* 177, 30–42 (1996).

496. Robertson, C. P., Braun, M. M. & Roelink, H. Sonic hedgehog patterning in chick neural plate is antagonized by a Wnt3-like signal. *Dev Dyn* 229, 510–519 (2004).

497. Wu, M. *et al.* Differential Modulation of the Oligodendrocyte Transcriptome by Sonic Hedgehog and Bone Morphogenetic Protein 4 via Opposing Effects on Histone Acetylation. *J Neurosci* 32, 6651–6664 (2012).

498. Liu, R. *et al.* Region-specific and stage-dependent regulation of Olig gene expression and oligodendrogenesis by Nkx6.1 homeodomain transcription factor. *Development* 130, 6221–6231 (2003).

499. Lu, Q. R. *et al.* Sonic Hedgehog–Regulated Oligodendrocyte Lineage Genes Encoding bHLH Proteins in the Mammalian Central Nervous System. *Neuron* 25, 317–329 (2000).

500. Lu, Q. R. *et al.* Common Developmental Requirement for Olig Function Indicates a Motor Neuron/Oligodendrocyte Connection. *Cell* 109, 75–86 (2002).

501. Sun, T. *et al.* Olig bHLH proteins interact with homeodomain proteins to regulate cell fate acquisition in progenitors of the ventral neural tube. *Current Biology* 11, 1413–1420 (2001).

502. Li, H., Paes de Faria, J., Andrew, P., Nitarska, J. & Richardson, W. D. Phosphorylation Regulates OLIG2 Cofactor Choice and the Motor Neuron-Oligodendrocyte Fate Switch. *Neuron* 69, 918–929 (2011).

503. Nakatani, H. *et al.* Ascl1/Mash1 Promotes Brain Oligodendrogenesis during Myelination and Remyelination. *J Neurosci* 33, 9752–9768 (2013).

504. Parras, C. M. *et al.* The Proneural Gene Mash1 Specifies an Early Population of Telencephalic Oligodendrocytes. *J. Neurosci.* 27, 4233–4242 (2007).

505. Petryniak, M. A., Potter, G. B., Rowitch, D. H. & Rubenstein, J. L. R. Dlx1 and Dlx2 Control Neuronal versus Oligodendroglial Cell Fate Acquisition in the Developing Forebrain. *Neuron* 55, 417–433 (2007).

506. Kang, P. *et al.* Sox9 and NFIA coordinate a transcriptional regulatory cascade during the initiation of gliogenesis. *Neuron* 74, 79–94 (2012).

507. Stolt, C. C. *et al.* The Sox9 transcription factor determines glial fate choice in the developing spinal cord. *Genes Dev* 17, 1677–1689 (2003).

508. Finzsch, M., Stolt, C. C., Lommes, P. & Wegner, M. Sox9 and Sox10 influence survival and migration of oligodendrocyte precursors in the spinal cord by regulating PDGF receptor alpha expression. *Development* 135, 637–646 (2008).

509. Baron, W., Metz, B., Bansal, R., Hoekstra, D. & de Vries, H. PDGF and FGF-2 Signaling in Oligodendrocyte Progenitor Cells: Regulation of Proliferation and Differentiation by Multiple Intracellular Signaling Pathways. *Molecular and Cellular Neuroscience* 15, 314–329 (2000).

510. Frederick, T. J., Min, J., Altieri, S. C., Mitchell, N. E. & Wood, T. L. Synergistic induction of cyclin D1 in oligodendrocyte progenitor cells by IGF-I and FGF-2 requires differential stimulation of multiple signaling pathways. *Glia* 55, 1011–1022 (2007).

511. Murtie, J. C., Zhou, Y.-X., Le, T. Q., Vana, A. C. & Armstrong, R. C. PDGF and FGF2 pathways regulate distinct oligodendrocyte lineage responses in experimental demyelination with spontaneous remyelination. *Neurobiology of Disease* 19, 171–182 (2005).

512. Bansal, R., Magge, S. & Winkler, S. Specific inhibitor of FGF receptor signaling: FGF-2-mediated effects on proliferation, differentiation, and MAPK activation are inhibited by PD173074 in oligodendrocyte-lineage cells. *J Neurosci Res* 74, 486–493 (2003).

513. Stolt, C. C. *et al.* SoxD proteins influence multiple stages of oligodendrocyte development and modulate SoxE protein function. *Dev Cell* 11, 697–709 (2006).

514. Jepson, S. *et al.* LINGO-1, a Transmembrane Signaling Protein, Inhibits Oligodendrocyte Differentiation and Myelination through Intercellular Self-interactions. *Journal of Biological Chemistry* 287, 22184–22195 (2012).

515. Liang, X., Draghi, N. A. & Resh, M. D. Signaling from integrins to Fyn to Rho family GTPases regulates morphologic differentiation of oligodendrocytes. *J Neurosci* 24, 7140–7149 (2004).

516. Mi, S. *et al.* LINGO-1 negatively regulates myelination by oligodendrocytes. *Nat Neurosci* 8, 745–751 (2005).

517. Mi, S., Blake Pepinsky, R. & Cadavid, D. Blocking LINGO-1 as a Therapy to Promote CNS Repair: From Concept to the Clinic. *CNS Drugs* 27, 493–503 (2013).

518. Chen, Y. *et al.* The oligodendrocyte-specific G protein–coupled receptor GPR17 is a cell-intrinsic timer of myelination. *Nat Neurosci* 12, 1398–1406 (2009).

519. Luis de la Pompa, J. *et al.* Conservation of the Notch signalling pathway in mammalian neurogenesis. *Development* 124, 1139–1148 (1997).

520. Mizutani, T., Taniguchi, Y., Aoki, T., Hashimoto, N. & Honjo, T. Conservation of the biochemical mechanisms of signal transduction among mammalian Notch family members. *Proc Natl Acad Sci U S A* 98, 9026–9031 (2001).

521. Kondo, T. & Raff, M. Basic helix-loop-helix proteins and the timing of oligodendrocyte differentiation. *Development* 127, 2989–2998 (2000).

522. Liu, A. *et al.* A molecular insight of Hes5-dependent inhibition of myelin gene expression: old partners and new players. *The EMBO Journal* 25, 4833–4842 (2006).

523. Wang, S. *et al.* Notch Receptor Activation Inhibits Oligodendrocyte Differentiation. *Neuron* 21, 63–75 (1998).

524. Hu, Q.-D. *et al.* F3/Contactin Acts as a Functional Ligand for Notch during Oligodendrocyte Maturation. *Cell* 115, 163–175 (2003).

525. Fancy, S. P. J. *et al.* Dysregulation of the Wnt pathway inhibits timely myelination and remyelination in the mammalian CNS. *Genes Dev* 23, 1571–1585 (2009).

526. Feigenson, K., Reid, M., See, J., Crenshaw, E. B. & Grinspan, J. B. Wnt signaling is sufficient to perturb oligodendrocyte maturation. *Mol Cell Neurosci* 42, 255–265 (2009).

527. Schuijers, J., Mokry, M., Hatzis, P., Cuppen, E. & Clevers, H. Wnt-induced transcriptional activation is exclusively mediated by TCF/LEF. *EMBO J* 33, 146–156 (2014).

528. Hughes, E. G., Kang, S. H., Fukaya, M. & Bergles, D. E. Oligodendrocyte progenitors balance growth with self-repulsion to achieve homeostasis in the adult brain. *Nat Neurosci* 16, 668–676 (2013).

529. Chew, L.-J. *et al.* SRY-box containing gene 17 regulates the Wnt/β-catenin signaling pathway in oligodendrocyte progenitor cells. *J Neurosci* 31, 13921–13935 (2011).

530. Ye, F. *et al.* HDAC1 and HDAC2 regulate oligodendrocyte differentiation by disrupting the β-catenin–TCF interaction. *Nat Neurosci* 12, 829–838 (2009).

531. Zhao, C. *et al.* Dual regulatory switch through interactions of Tcf7l2/Tcf4 with stage-specific partners propels oligodendroglial maturation. *Nat Commun* 7, 10883 (2016).

532. Qi, Y. *et al.* Control of oligodendrocyte differentiation by the Nkx2.2 homeodomain transcription factor. *Development* 128, 2723–2733 (2001).

533. Sugimori, M. *et al.* Ascl1 is required for oligodendrocyte development in the spinal cord. *Development* 135, 1271–1281 (2008).

534. Zhu, Q. *et al.* Genetic evidence that Nkx2.2 and Pdgfra are major determinants of the timing of oligodendrocyte differentiation in the developing CNS. *Development* 141, 548–555 (2014).

535. Cai, J. *et al.* Co-localization of Nkx6.2 and Nkx2.2 homeodomain proteins in differentiated myelinating oligodendrocytes. *Glia* 58, 458–468 (2010).

536. Southwood, C. *et al.* CNS Myelin Paranodes Require Nkx6-2 Homeoprotein Transcriptional Activity for Normal Structure. *J. Neurosci.* 24, 11215–11225 (2004).

537. Wei, Q., Miskimins, W. K. & Miskimins, R. Stage-specific Expression of Myelin Basic Protein in Oligodendrocytes Involves Nkx2.2-mediated Repression That Is Relieved by the Sp1 Transcription Factor*. *Journal of Biological Chemistry* 280, 16284–16294 (2005).

538. Bujalka, H. *et al.* MYRF Is a Membrane-Associated Transcription Factor That Autoproteolytically Cleaves to Directly Activate Myelin Genes. *PLoS Biol* 11, e1001625 (2013).

539. Hornig, J. *et al.* The Transcription Factors Sox10 and Myrf Define an Essential Regulatory Network Module in Differentiating Oligodendrocytes. *PLoS Genet* 9, e1003907 (2013).

540. Yu, Y. *et al.* Olig2 targets chromatin remodelers to enhancers to initiate oligodendrocyte differentiation. *Cell* 152, 248–261 (2013).

541. Weng, Q. *et al.* Dual-mode Modulation of Smad Signaling by Smad-interacting Protein Sip1 is Required for Myelination in the CNS. *Neuron* 73, 713–728 (2012).

542. Xin, M. *et al.* Myelinogenesis and axonal recognition by oligodendrocytes in brain are uncoupled in Olig1-null mice. *J Neurosci* 25, 1354–1365 (2005).

543. Li, H., Lu, Y., Smith, H. K. & Richardson, W. D. Olig1 and Sox10 interact synergistically to drive myelin basic protein transcription in oligodendrocytes. *J Neurosci* 27, 14375–14382 (2007).

544. Niu, J. *et al.* Phosphorylated olig1 localizes to the cytosol of oligodendrocytes and promotes membrane expansion and maturation. *Glia* 60, 1427–1436 (2012).

545. Bauer, N. G., Richter-Landsberg, C. & Ffrench-Constant, C. Role of the oligodendroglial cytoskeleton in differentiation and myelination. *Glia* 57, 1691–1705 (2009).

546. Kirby, B. B. *et al.* In vivo time-lapse imaging shows dynamic oligodendrocyte progenitor behavior during zebrafish development. *Nat Neurosci* 9, 1506–1511 (2006).

547. Chun, S. J., Rasband, M. N., Sidman, R. L., Habib, A. A. & Vartanian, T. Integrin-linked kinase is required for laminin-2–induced oligodendrocyte cell spreading and CNS myelination. *J Cell Biol* 163, 397–408 (2003).

548. Legate, K. R., Montañez, E., Kudlacek, O. & Füssler, R. ILK, PINCH and parvin: the tIPP of integrin signalling. *Nat Rev Mol Cell Biol* 7, 20–31 (2006).

549. O'Meara, R. W. *et al.* Integrin-Linked Kinase Regulates Process Extension in Oligodendrocytes via Control of Actin Cytoskeletal Dynamics. *J. Neurosci.* 33, 9781–9793 (2013).

550. Jackman, N., Ishii, A. & Bansal, R. Myelin Biogenesis And Oligodendrocyte Development: Parsing Out The Roles Of Glycosphingolipids. *Physiology (Bethesda)* 24, 290–297 (2009).

551. Kister, A. & Kister, I. Overview of myelin, major myelin lipids, and myelin-associated proteins. *Frontiers in Chemistry* 10, (2023).

552. Poitelon, Y., Kopec, A. M. & Belin, S. Myelin Fat Facts: An Overview of Lipids and Fatty Acid Metabolism. *Cells* 9, 812 (2020).

553. Colognato, H., Ramachandrappa, S., Olsen, I. M. & ffrench-Constant, C. Integrins direct Src family kinases to regulate distinct phases of oligodendrocyte development. *J Cell Biol* 167, 365–375 (2004).

554. Hoshina, N. *et al.* Focal adhesion kinase regulates laminin-induced oligodendroglial process outgrowth. *Genes Cells* 12, 1245–1254 (2007).

555. Pedraza, C. E. *et al.* Induction of oligodendrocyte differentiation and in vitro myelination by inhibition of rho-associated kinase. *ASN Neuro* 6, 1759091414538134 (2014).

556. Wang, H. *et al.* Myosin II is a negative regulator of oligodendrocyte morphological differentiation. *J Neurosci Res* 90, 1547–1556 (2012).

557. Thurnherr, T. *et al.* Cdc42 and Rac1 Signaling Are Both Required for and Act Synergistically in the Correct Formation of Myelin Sheaths in the CNS. *J Neurosci* 26, 10110–10119 (2006).

558. Asrar, S. *et al.* Regulation of hippocampal long-term potentiation by p21-activated protein kinase 1 (PAK1). *Neuropharmacology* 56, 73–80 (2009).

559. Parrini, M. C., Lei, M., Harrison, S. C. & Mayer, B. J. Pak1 kinase homodimers are autoinhibited in trans and dissociated upon activation by Cdc42 and Rac1. *Mol Cell* 9, 73–83 (2002).

560. Wang, Y. & Guo, F. Group I PAKs in myelin formation and repair of the central nervous system: what, when, and how. *Biol Rev Camb Philos Soc* 97, 615–639 (2022).

561. Brown, T. L., Hashimoto, H., Finseth, L. T., Wood, T. L. & Macklin, W. B. PAK1 Positively Regulates Oligodendrocyte Morphology and Myelination. *J Neurosci* 41, 1864–1877 (2021).

562. Zhang, Y. *et al.* An RNA-sequencing transcriptome and splicing database of glia, neurons, and vascular cells of the cerebral cortex. *J Neurosci* 34, 11929–11947 (2014).

563. Miki, H., Sasaki, T., Takai, Y. & Takenawa, T. Induction of filopodium formation by a WASP-related actin-depolymerizing protein N-WASP. *Nature* 391, 93–96 (1998).

564. Miki, H., Suetsugu, S. & Takenawa, T. WAVE, a novel WASP-family protein involved in actin reorganization induced by Rac. *EMBO J* 17, 6932–6941 (1998).

565. Bacon, C., Lakics, V., Machesky, L. & Rumsby, M. N-WASP regulates extension of filopodia and processes by oligodendrocyte progenitors, oligodendrocytes, and Schwann cells—implications for axon ensheathment at myelination. *Glia* 55, 844–858 (2007).

566. Katanov, C. *et al.* N-Wasp Regulates Oligodendrocyte Myelination. *J Neurosci* 40, 6103–6111 (2020).

567. Kim, H.-J. *et al.* WAVE1 is required for oligodendrocyte morphogenesis and normal CNS myelination. *J Neurosci* 26, 5849–5859 (2006).

568. Zhang, W., Wu, Y., Wu, C. & Gunst, S. J. Integrin-linked kinase regulates N-WASp-mediated actin polymerization and tension development in tracheal smooth muscle. *J Biol Chem* 282, 34568–34580 (2007).

569. Stadelmann, C., Timmler, S., Barrantes-Freer, A. & Simons, M. Myelin in the Central Nervous System: Structure, Function, and Pathology. *Physiological Reviews* 99, 1381–1431 (2019).

570. LoPachin, R. M., Castiglia, C. M. & Saubermann, A. J. Elemental composition and water content of myelinated axons and glial cells in rat central nervous system. *Brain Res* 549, 253–259 (1991).

571. O'Brien, J. S. Stability of the Myelin Membrane. *Science* 147, 1099–1107 (1965).

572. Saher, G. *et al.* High cholesterol level is essential for myelin membrane growth. *Nat Neurosci* 8, 468–475 (2005).

573. Schmitt, S., Castelvetri, L. C. & Simons, M. Metabolism and functions of lipids in myelin. *Biochim Biophys Acta* 1851, 999–1005 (2015).

574. Chrast, R., Saher, G., Nave, K.-A. & Verheijen, M. H. G. Lipid metabolism in myelinating glial cells: lessons from human inherited disorders and mouse models. *J Lipid Res* 52, 419–434 (2011).

575. Dhaunchak, A. S. *et al.* A proteome map of axoglial specializations isolated and purified from human central nervous system. *Glia* 58, 1949–1960 (2010).

576. Jahn, O. *et al.* The CNS Myelin Proteome: Deep Profile and Persistence After Post-mortem Delay. *Front Cell Neurosci* 14, 239 (2020).

577. Ruskamo, S. *et al.* Human myelin proteolipid protein structure and lipid bilayer stacking. *Cell Mol Life Sci* 79, 419 (2022).

578. Lüders, K. A. *et al.* Maintenance of high proteolipid protein level in adult central nervous system myelin is required to preserve the integrity of myelin and axons. *Glia* 67, 634–649 (2019).

579. Spörkel, O., Uschkureit, T., Büssow, H. & Stoffel, W. Oligodendrocytes expressing exclusively the DM20 isoform of the proteolipid protein gene: Myelination and development. *Glia* 37, 19–30 (2002).

580. Inoue, K. Pelizaeus-Merzbacher Disease: Molecular and Cellular Pathologies and Associated Phenotypes. *Adv Exp Med Biol* 1190, 201–216 (2019).

581. Laukka, J. J., Kamholz, J., Bessert, D. & Skoff, R. P. Novel pathologic findings in patients with Pelizaeus-Merzbacher disease. *Neurosci Lett* 627, 222–232 (2016).

582. Nevin, Z. S. *et al.* Modeling the Mutational and Phenotypic Landscapes of Pelizaeus-Merzbacher Disease with Human iPSC-Derived Oligodendrocytes. *Am J Hum Genet* 100, 617–634 (2017).

583. Simons, M. *et al.* Overexpression of the myelin proteolipid protein leads to accumulation of cholesterol and proteolipid protein in endosomes/lysosomes: implications for Pelizaeus-Merzbacher disease. *J Cell Biol* 157, 327–336 (2002).

584. Garbern, J. Y. *et al.* Patients lacking the major CNS myelin protein, proteolipid protein 1, develop length-dependent axonal degeneration in the absence of demyelination and inflammation. *Brain* 125, 551–561 (2002).

585. Aggarwal, S. *et al.* Myelin membrane assembly is driven by a phase transition of myelin basic proteins into a cohesive protein meshwork. *PLoS Biol* 11, e1001577 (2013).

586. Boison, D., Büssow, H., D'Urso, D., Müller, H. W. & Stoffel, W. Adhesive properties of proteolipid protein are responsible for the compaction of CNS myelin sheaths. *J Neurosci* 15, 5502–5513 (1995).

587. Min, Y. *et al.* Interaction forces and adhesion of supported myelin lipid bilayers modulated by myelin basic protein. *Proc Natl Acad Sci U S A* 106, 3154–3159 (2009).

588. Raasakka, A. *et al.* Membrane Association Landscape of Myelin Basic Protein Portrays Formation of the Myelin Major Dense Line. *Sci Rep* 7, 4974 (2017).

589. Vassall, K. A., Bamm, V. V. & Harauz, G. MyelStones: the executive roles of myelin basic protein in myelin assembly and destabilization in multiple sclerosis. *Biochem J* 472, 17–32 (2015).

590. Zhang, C. *et al.* Myelin basic protein undergoes a broader range of modifications in mammals than in lower vertebrates. *J Proteome Res* 11, 4791–4802 (2012).

591. Träger, J., Widder, K., Kerth, A., Harauz, G. & Hinderberger, D. Effect of Cholesterol and Myelin Basic Protein (MBP) Content on Lipid Monolayers Mimicking the Cytoplasmic Membrane of Myelin. *Cells* 9, 529 (2020).

592. Carson, J. H. *et al.* Multiplexed RNA trafficking in oligodendrocytes and neurons. *Biochim Biophys Acta* 1779, 453–458 (2008).

593. Colman, D. R., Kreibich, G., Frey, A. B. & Sabatini, D. D. Synthesis and incorporation of myelin polypeptides into CNS myelin. *J Cell Biol* 95, 598–608 (1982).

594. White, R. *et al.* Activation of oligodendroglial Fyn kinase enhances translation of mRNAs transported in hnRNP A2–dependent RNA granules. *J Cell Biol* 181, 579–586 (2008).

595. White, R. *et al.* Heterogeneous Nuclear Ribonucleoprotein (hnRNP) F Is a Novel Component of Oligodendroglial RNA Transport Granules Contributing to Regulation of Myelin Basic Protein (MBP) Synthesis *. *Journal of Biological Chemistry* 287, 1742–1754 (2012).

596. Schäfer, I., Müller, C., Luhmann, H. J. & White, R. MOBP levels are regulated by Fyn kinase and affect the morphological differentiation of oligodendrocytes. *Journal of Cell Science* 129, 930–942 (2016).

597. Yamamoto, Y. *et al.* Myelin-associated oligodendrocytic basic protein is essential for normal arrangement of the radial component in central nervous system myelin. *Eur J Neurosci* 11, 847–855 (1999).

598. Snaidero, N. *et al.* Antagonistic Functions of MBP and CNP Establish Cytosolic Channels in CNS Myelin. *Cell Rep* 18, 314–323 (2017).

599. Pronker, M. F. *et al.* Structural basis of myelin-associated glycoprotein adhesion and signalling. *Nat Commun* 7, 13584 (2016).

600. Quarles, R. H. Myelin-associated glycoprotein (MAG): past, present and beyond. *J Neurochem* 100, 1431–1448 (2007).

601. Yang, L. J. *et al.* Gangliosides are neuronal ligands for myelin-associated glycoprotein. *Proc Natl Acad Sci U S A* 93, 814–818 (1996).

602. Montag, D. *et al.* Mice deficient for the myelin-associated glycoprotein show subtle abnormalities in myelin. *Neuron* 13, 229–246 (1994).

603. Umemori, H., Sato, S., Yagi, T., Aizawa, S. & Yamamoto, T. Initial events of myelination involve Fyn tyrosine kinase signalling. *Nature* 367, 572–576 (1994).

604. Dashiell, S. M., Tanner, S. L., Pant, H. C. & Quarles, R. H. Myelin-associated glycoprotein modulates expression and phosphorylation of neuronal cytoskeletal elements and their associated kinases. *J Neurochem* 81, 1263–1272 (2002).

605. Nawaz, S. *et al.* Actin filament turnover drives leading edge growth during myelin sheath formation in the central nervous system. *Dev Cell* 34, 139–151 (2015).

606. Snaidero, N. *et al.* Myelin membrane wrapping of CNS axons by PI(3,4,5)P3-dependent polarized growth at the inner tongue. *Cell* 156, 277–290 (2014).

607. Sobottka, B., Ziegler, U., Kaech, A., Becher, B. & Goebels, N. CNS live imaging reveals a new mechanism of myelination: The liquid croissant model. *Glia* 59, 1841–1849 (2011).

608. Çolakoğlu, G., Bergstrom-Tyrberg, U., Berglund, E. O. & Ranscht, B. Contactin-1 regulates myelination and nodal/paranodal domain organization in the central nervous system. *Proc Natl Acad Sci U S A* 111, E394-403 (2014).

609. Pedraza, L., Huang, J. K. & Colman, D. Disposition of axonal caspr with respect to glial cell membranes: Implications for the process of myelination. *J Neurosci Res* 87, 3480–3491 (2009).

610. Rasband, M. N. *et al.* Dependence of nodal sodium channel clustering on paranodal axoglial contact in the developing CNS. *J Neurosci* 19, 7516–7528 (1999).

611. Zonta, B. *et al.* Glial and neuronal isoforms of Neurofascin have distinct roles in the assembly of nodes of Ranvier in the central nervous system. *J Cell Biol* 181, 1169–1177 (2008).

612. Mierzwa, A., Shroff, S. & Rosenbluth, J. Permeability of the paranodal junction of myelinated nerve fibers. *J Neurosci* 30, 15962–15968 (2010).

613. Poliak, S. *et al.* Juxtaparanodal clustering of Shaker-like K+ channels in myelinated axons depends on Caspr2 and TAG-1. *J Cell Biol* 162, 1149–1160 (2003).

614. Rosenbluth, J. Multiple functions of the paranodal junction of myelinated nerve fibers. *J Neurosci Res* 87, 3250–3258 (2009).

615. Battefeld, A., Klooster, J. & Kole, M. H. P. Myelinating satellite oligodendrocytes are integrated in a glial syncytium constraining neuronal high-frequency activity. *Nat Commun* 7, 11298 (2016).

616. Larson, V. A. *et al.* Oligodendrocytes control potassium accumulation in white matter and seizure susceptibility. *Elife* 7, e34829 (2018).

617. Menichella, D. M. *et al.* Genetic and physiological evidence that oligodendrocyte gap junctions contribute to spatial buffering of potassium released during neuronal activity. *J Neurosci* 26, 10984–10991 (2006).

618. Nagy, J. I. & Rash, J. E. Astrocyte and oligodendrocyte connexins of the glial syncytium in relation to astrocyte anatomical domains and spatial buffering. *Cell Commun Adhes* 10, 401–406 (2003).

619. Philips, T. & Rothstein, J. D. Oligodendroglia: metabolic supporters of neurons. *J Clin Invest* 127, 3271–3280 (2017).

620. Simons, M. & Nave, K.-A. Oligodendrocytes: Myelination and Axonal Support. *Cold Spring Harb Perspect Biol* 8, a020479 (2016).

621. Lee, Y. *et al.* Oligodendroglia metabolically support axons and contribute to neurodegeneration. *Nature* 487, 443–448 (2012).

622. Saab, A. S. *et al.* Oligodendroglial NMDA Receptors Regulate Glucose Import and Axonal Energy Metabolism. *Neuron* 91, 119–132 (2016).

623. Lappe-Siefke, C. *et al.* Disruption of Cnp1 uncouples oligodendroglial functions in axonal support and myelination. *Nat Genet* 33, 366–374 (2003).

624. Clevers, H. & Nusse, R. Wnt/β-Catenin Signaling and Disease. *Cell* 149, 1192–1205 (2012).

625. Guo, F. *et al.* Canonical Wnt signaling in the oligodendroglial lineage–puzzles remain. *Glia* 63, 1671–1693 (2015).

626. Rockman, S. P. *et al.* Id2 is a target of the beta-catenin/T cell factor pathway in colon carcinoma. *J Biol Chem* 276, 45113–45119 (2001).

627. Azim, K. *et al.* Persistent Wnt/β-catenin signaling determines dorsalization of the postnatal subventricular zone and neural stem cell specification into oligodendrocytes and glutamatergic neurons. *Stem Cells* 32, 1301–1312 (2014).

628. Dai, Z.-M. *et al.* Stage-Specific Regulation of Oligodendrocyte Development by Wnt/β-Catenin Signaling. *The Journal of Neuroscience* 34, 8467 (2014).

629. Ortega, F. *et al.* Oligodendrogliogenic and neurogenic adult subependymal zone neural stem cells constitute distinct lineages and exhibit differential responsiveness to Wnt signalling. *Nat Cell Biol* 15, 602–613 (2013).

630. Shimizu, T. *et al.* Wnt signaling controls the timing of oligodendrocyte development in the spinal cord. *Dev Biol* 282, 397–410 (2005).

631. Fu, H. *et al.* A Genome-Wide Screen for Spatially Restricted Expression Patterns Identifies Transcription Factors That Regulate Glial Development. *J Neurosci* 29, 11399–11408 (2009).

632. Weng, C., Ding, M., Fan, S., Cao, Q. & Lu, Z. Transcription factor 7 like 2 promotes oligodendrocyte differentiation and remyelination. *Mol Med Rep* 16, 1864–1870 (2017).

633. Govier-Cole, A. E. *et al.* Inhibiting Bone Morphogenetic Protein 4 Type I Receptor Signaling Promotes Remyelination by Potentiating Oligodendrocyte Differentiation. *eNeuro* 6, ENEURO.0399-18.2019 (2019).

634. Zhang, S. *et al.* The Wnt Effector TCF7l2 Promotes Oligodendroglial Differentiation by Repressing Autocrine BMP4-Mediated Signaling. *J. Neurosci.* 41, 1650–1664 (2021).

635. Lürbke, A. *et al.* Limited TCF7L2 Expression in MS Lesions. *PLoS One* 8, e72822 (2013).

636. Montcouquiol, M., Crenshaw, E. B. & Kelley, M. W. Noncanonical Wnt signaling and neural polarity. *Annu Rev Neurosci* 29, 363–386 (2006).

637. Shimizu, T., Smits, R. & Ikenaka, K. Microglia-Induced Activation of Noncanonical Wnt Signaling Aggravates Neurodegeneration in Demyelinating Disorders. *Mol Cell Biol* 36, 2728–2741 (2016).

638. Roux, P. P. & Blenis, J. ERK and p38 MAPK-activated protein kinases: a family of protein kinases with diverse biological functions. *Microbiol Mol Biol Rev* 68, 320–344 (2004).

639. Davis, R. J. Signal Transduction by the JNK Group of MAP Kinases. *Cell* 103, 239–252 (2000).

640. Clark, G. J., Westwick, J. K. & Der, C. J. p120 GAP modulates Ras activation of Jun kinases and transformation. *J Biol Chem* 272, 1677–1681 (1997).

641. Zeke, A., Misheva, M., Reményi, A. & Bogoyevitch, M. A. JNK Signaling: Regulation and Functions Based on Complex Protein-Protein Partnerships. *Microbiol Mol Biol Rev* 80, 793–835 (2016).

642. Zhang, J.-X. *et al.* JNK Is Necessary for Oligodendrocyte Precursor Cell Proliferation Induced by the Conditioned Medium from B104 Neuroblastoma Cells. *J Mol Neurosci* 52, 269–276 (2014).

643. Hu, J.-G. *et al.* The molecular events involved in oligodendrocyte precursor cell proliferation induced by the conditioned medium from b104 neuroblastoma cells. *Neurochem Res* 38, 601–609 (2013).

644. Lorenzati, M. *et al.* c-Jun N-terminal kinase 1 (JNK1) modulates oligodendrocyte progenitor cell architecture, proliferation and myelination. *Sci Rep* 11, 7264 (2021).

645. Chew, L.-J., Coley, W., Cheng, Y. & Gallo, V. Mechanisms of Regulation of Oligodendrocyte Development by p38 Mitogen-Activated Protein Kinase. *J Neurosci* 30, 11011–11027 (2010).

646. Miskimins, R. & Miskimins, W. K. A role for an AP-1-like site in the expression of the myelin basic protein gene during differentiation. *Int J Dev Neurosci* 19, 85–91 (2001).

647. Wissmüller, S., Kosian, T., Wolf, M., Finzsch, M. & Wegner, M. The high-mobility-group domain of Sox proteins interacts with DNA-binding domains of many transcription factors. *Nucleic Acids Res* 34, 1735–1744 (2006).

648. Chang, L., Jones, Y., Ellisman, M. H., Goldstein, L. S. B. & Karin, M. JNK1 Is Required for Maintenance of Neuronal Microtubules and Controls Phosphorylation of Microtubule-Associated Proteins. *Developmental Cell* 4, 521–533 (2003).

649. Zhao, L. *et al.* QKI Binds MAP1B mRNA and Enhances MAP1B Expression during Oligodendrocyte Development. *MBoC* 17, 4179–4186 (2006).

650. Jurewicz, A., Matysiak, M., Andrzejak, S. & Selmaj, K. TRAIL-induced death of human adult oligodendrocytes is mediated by JNK pathway. *Glia* 53, 158–166 (2006).

651. Li, Q. M. *et al.* Opposite regulation of oligodendrocyte apoptosis by JNK3 and Pin1 after spinal cord injury. *J Neurosci* 27, 8395–8404 (2007).

652. Norrmén, C. *et al.* mTORC1 Is Transiently Reactivated in Injured Nerves to Promote c-Jun Elevation and Schwann Cell Dedifferentiation. *J Neurosci* 38, 4811–4828 (2018).

653. Parkinson, D. B. *et al.* c-Jun is a negative regulator of myelination. *J Cell Biol* 181, 625–637 (2008).

654. Gonsalvez, D., Ferner, A. H., Peckham, H., Murray, S. S. & Xiao, J. The roles of extracellular related-kinases 1 and 2 signaling in CNS myelination. *Neuropharmacology* 110, 586–593 (2016).

655. Domercq, M. *et al.* Dual-specific Phosphatase-6 (Dusp6) and ERK Mediate AMPA Receptor-induced Oligodendrocyte Death*. *Journal of Biological Chemistry* 286, 11825–11836 (2011).

656. Ishii, A., Fyffe-Maricich, S. L., Furusho, M., Miller, R. H. & Bansal, R. ERK1/ERK2 MAPK Signaling is Required to Increase Myelin Thickness Independent of Oligodendrocyte Differentiation and Initiation of Myelination. *J Neurosci* 32, 8855–8864 (2012).

657. Ishii, A., Furusho, M. & Bansal, R. Sustained Activation of ERK1/2 MAPK in Oligodendrocytes and Schwann Cells Enhances Myelin Growth and Stimulates Oligodendrocyte Progenitor Expansion. *J Neurosci* 33, 175–186 (2013).

658. Newbern, J. M. *et al.* Specific functions for ERK/MAPK signaling during PNS development. *Neuron* 69, 91–105 (2011).

659. Xiao, J. *et al.* Extracellular signal-regulated kinase 1/2 signaling promotes oligodendrocyte myelination in vitro. *J Neurochem* 122, 1167–1180 (2012).

660. Fyffe-Maricich, S. L., Karlo, J. C., Landreth, G. E. & Miller, R. H. The ERK2 Mitogen-Activated Protein Kinase Regulates the Timing of Oligodendrocyte Differentiation. *J Neurosci* 31, 843–850 (2011).

661. Guardiola-Diaz, H. M., Ishii, A. & Bansal, R. Erk1/2 MAPK and mTOR Signaling Sequentially Regulates Progression Through Distinct Stages Of Oligodendrocyte Differentiation. *Glia* 60, 476–486 (2012).

662. Ishii, A., Furusho, M., Dupree, J. L. & Bansal, R. Role of ERK1/2 MAPK signaling in the maintenance of myelin and axonal integrity in the adult CNS. *J Neurosci* 34, 16031–16045 (2014).

663. Fyffe-Maricich, S. L., Schott, A., Karl, M., Krasno, J. & Miller, R. H. Signaling through ERK1/2 Controls Myelin Thickness during Myelin Repair in the Adult Central Nervous System. *J Neurosci* 33, 18402–18408 (2013).

664. Suo, N., Guo, Y., He, B., Gu, H. & Xie, X. Inhibition of MAPK/ERK pathway promotes oligodendrocytes generation and recovery of demyelinating diseases. *Glia* 67, 1320–1332 (2019).

665. Peckham, H. *et al.* Fyn is an intermediate kinase that BDNF utilizes to promote oligodendrocyte myelination. *Glia* 64, 255–269 (2016).

666. Zarubin, T. & Han, J. Activation and signaling of the p38 MAP kinase pathway. *Cell Res* 15, 11–18 (2005).

667. Bhat, N. R., Zhang, P. & Mohanty, S. B. p38 MAP Kinase Regulation of Oligodendrocyte Differentiation with CREB as a Potential Target. *Neurochem Res* 32, 293–302 (2007).

668. Fragoso, G. *et al.* p38 mitogen-activated protein kinase is required for central nervous system myelination. *Glia* 55, 1531–1541 (2007).

669. Haines, J. D., Fang, J., Mushynski, W. E. & Almazan, G. Mitogen-activated protein kinase activated protein kinase 2 (MK2) participates in p38 MAPK regulated control of oligodendrocyte differentiation. *Glia* 58, 1384–1393 (2010).

670. Chen, G., Hitomi, M., Han, J. & Stacey, D. W. The p38 pathway provides negative feedback for Ras proliferative signaling. *J Biol Chem* 275, 38973–38980 (2000).

671. Arkell, R. S. *et al.* DUSP6/MKP-3 inactivates ERK1/2 but fails to bind and inactivate ERK5. *Cellular Signalling* 20, 836–843 (2008).

672. Norrmén, C. & Suter, U. Akt/mTOR signalling in myelination. *Biochemical Society Transactions* 41, 944–950 (2013).

673. Wood, T. L. *et al.* mTOR: a link from the extracellular milieu to transcriptional regulation of oligodendrocyte development. *ASN Neuro* 5, e00108 (2013).

674. Tyler, W. A. *et al.* Activation of the Mammalian Target of Rapamycin (mTOR) Is Essential for Oligodendrocyte Differentiation. *J. Neurosci.* 29, 6367–6378 (2009).

675. Gaesser, J. M. & Fyffe-Maricich, S. L. Intracellular Signaling Pathway Regulation of Myelination and Remyelination in the CNS. *Exp Neurol* 283, 501–511 (2016).

676. Flores, A. I. *et al.* Constitutively Active Akt Induces Enhanced Myelination in the CNS. *J. Neurosci.* 28, 7174–7183 (2008).

677. Goebbels, S. *et al.* Elevated Phosphatidylinositol 3,4,5-Trisphosphate in Glia Triggers Cell-Autonomous Membrane Wrapping and Myelination. *J Neurosci* 30, 8953–8964 (2010).

678. Narayanan, S. P., Flores, A. I., Wang, F. & Macklin, W. B. Akt Signals through the Mammalian Target of Rapamycin Pathway to Regulate CNS Myelination. *J. Neurosci.* 29, 6860–6870 (2009).

679. Bercury, K. K. *et al.* Conditional Ablation of Raptor or Rictor Has Differential Impact on Oligodendrocyte Differentiation and CNS Myelination. *J. Neurosci.* 34, 4466–4480 (2014).

680. Lebrun-Julien, F. *et al.* Balanced mTORC1 Activity in Oligodendrocytes Is Required for Accurate CNS Myelination. *J Neurosci* 34, 8432–8448 (2014).

681. Wahl, S. E., McLane, L. E., Bercury, K. K., Macklin, W. B. & Wood, T. L. Mammalian target of rapamycin promotes oligodendrocyte differentiation, initiation and extent of CNS myelination. *J Neurosci* 34, 4453–4465 (2014).

682. Benardais, K. *et al.* p70S6 kinase regulates oligodendrocyte differentiation and is active in remyelinating lesions. *Brain Communications* 4, (2022).

683. Tyler, W. A. *et al.* Proteomic Identification of Novel Targets Regulated by the Mammalian Target of Rapamycin Pathway during Oligodendrocyte Differentiation. *Glia* 59, 1754–1769 (2011).

684. Aguirre, A., Dupree, J. L., Mangin, J. M. & Gallo, V. A functional role for EGFR signaling in myelination and remyelination. *Nat Neurosci* 10, 990–1002 (2007).

685. Galvez-Contreras, A. Y., Quiñones-Hinojosa, A. & Gonzalez-Perez, O. The role of EGFR and ErbB family related proteins in the oligodendrocyte specification in germinal niches of the adult mammalian brain. *Front Cell Neurosci* 7, 258 (2013).

686. Abe, Y., Namba, H., Zheng, Y. & Nawa, H. In situ hybridization reveals developmental regulation of ErbB1-4 mRNA expression in mouse midbrain: implication of ErbB receptors for dopaminergic neurons. *Neuroscience* 161, 95–110 (2009).

687. Nocita, E. *et al.* EGFR/ErbB Inhibition Promotes OPC Maturation up to Axon Engagement by Co-Regulating PIP2 and MBP. *Cells* 8, 844 (2019).

688. Kataria, H. *et al.* Neuregulin-1 promotes remyelination and fosters a pro-regenerative inflammatory response in focal demyelinating lesions of the spinal cord. *Glia* 66, 538–561 (2018).

689. Kim, J. Y., Sun, Q., Oglesbee, M. & Yoon, S. O. The role of ErbB2 signaling in the onset of terminal differentiation of oligodendrocytes in vivo. *J Neurosci* 23, 5561–5571 (2003).

690. Makinodan, M., Rosen, K. M., Ito, S. & Corfas, G. A critical period for social experience-dependent oligodendrocyte maturation and myelination. *Science* 337, 1357–1360 (2012).

691. Hu, X. *et al.* Sustained ErbB Activation Causes Demyelination and Hypomyelination by Driving Necroptosis of Mature Oligodendrocytes and Apoptosis of Oligodendrocyte Precursor Cells. *J. Neurosci.* 41, 9872–9890 (2021).

692. McKinnon, R. D., Matsui, T., Dubois-Dalcq, M. & Aaronsont, S. A. FGF modulates the PDGF-driven pathway of oligodendrocyte development. *Neuron* 5, 603–614 (1990).

693. Baron, W., Shattil, S. J. & ffrench-Constant, C. The oligodendrocyte precursor mitogen PDGF stimulates proliferation by activation of αvβ3 integrins. *The EMBO Journal* 21, 1957–1966 (2002).

694. Zeger, M. *et al.* Insulin-like growth factor type 1 receptor signaling in the cells of oligodendrocyte lineage is required for normal in vivo oligodendrocyte development and myelination. *Glia* 55, 400–411 (2007).

695. Ye, P., Hu, Q., Liu, H., Yan, Y. & D'ercole, A. J. beta-catenin mediates insulin-like growth factor-I actions to promote cyclin D1 mRNA expression, cell proliferation and survival in oligodendroglial cultures. *Glia* 58, 1031–1041 (2010).

696. Singh, J., Sharma, K., Frost, E. E. & Pillai, P. P. Role of PDGF-A-Activated ERK Signaling Mediated FAK-Paxillin Interaction in Oligodendrocyte Progenitor Cell Migration. *J Mol Neurosci* 67, 564–573 (2019).

697. Tripathi, A., Parikh, Z. S., Vora, P., Frost, E. E. & Pillai, P. P. pERK1/2 Peripheral Recruitment and Filopodia Protrusion Augment Oligodendrocyte Progenitor Cell Migration: Combined Effects of PDGF-A and Fibronectin. *Cell Mol Neurobiol* 37, 183–194 (2017).

698. Miyamoto, Y., Yamauchi, J. & Tanoue, A. Cdk5 Phosphorylation of WAVE2 Regulates Oligodendrocyte Precursor Cell Migration through Nonreceptor Tyrosine Kinase Fyn. *J Neurosci* 28, 8326–8337 (2008).

699. Luo, F., Burke, K., Kantor, C., Miller, R. H. & Yang, Y. Cyclin-Dependent Kinase 5 Mediates Adult OPC Maturation and Myelin Repair through Modulation of Akt and GsK-3β Signaling. *J Neurosci* 34, 10415–10429 (2014).

700. Yang, Y. *et al.* Cyclin dependent kinase 5 is required for the normal development of oligodendrocytes and myelin formation. *Dev Biol* 378, 94–106 (2013).

701. Dai, J., Bercury, K. K. & Macklin, W. B. Interaction of mTOR and Erk1/2 signaling to regulate oligodendrocyte differentiation. *Glia* 62, 2096–2109 (2014).

702. Bibollet-Bahena, O. & Almazan, G. IGF-1-stimulated protein synthesis in oligodendrocyte progenitors requires PI3K/mTOR/Akt and MEK/ERK pathways. *J Neurochem* 109, 1440–1451 (2009).

703. Cui, Q.-L. & Almazan, G. IGF-I-induced oligodendrocyte progenitor proliferation requires PI3K/Akt, MEK/ERK, and Src-like tyrosine kinases. *J Neurochem* 100, 1480–1493 (2007).

704. Michel, K., Zhao, T., Karl, M., Lewis, K. & Fyffe-Maricich, S. L. Translational Control of Myelin Basic Protein Expression by ERK2 MAP Kinase Regulates Timely Remyelination in the Adult Brain. *J Neurosci* 35, 7850–7865 (2015).

705. González-Fernández, E. *et al.* PTEN negatively regulates the cell lineage progression from NG2+ glial progenitor to oligodendrocyte via mTOR-independent signaling. *eLife* 7, e32021 (2018).

706. Azim, K. & Butt, A. M. GSK3β negatively regulates oligodendrocyte differentiation and myelination in vivo. *Glia* 59, 540–553 (2011).

707. Ding, Q. *et al.* Erk Associates with and Primes GSK-3β for Its Inactivation Resulting in Upregulation of β-Catenin. *Molecular Cell* 19, 159–170 (2005).

708. Shin, S., Wolgamott, L., Yu, Y., Blenis, J. & Yoon, S.-O. Glycogen synthase kinase (GSK)-3 promotes p70 ribosomal protein S6 kinase (p70S6K) activity and cell proliferation. *Proc Natl Acad Sci U S A* 108, E1204–E1213 (2011).

709. Bodini, B. *et al.* Dynamic Imaging of Individual Remyelination Profiles in Multiple Sclerosis. *Ann Neurol* 79, 726–738 (2016).

710. Patrikios, P. *et al.* Remyelination is extensive in a subset of multiple sclerosis patients. *Brain* 129, 3165–3172 (2006).

711. Spitzer, S. O. *et al.* Oligodendrocyte Progenitor Cells Become Regionally Diverse and Heterogeneous with Age. *Neuron* 101, 459-471.e5 (2019).

712. Samtani, G. *et al.* Brain region dependent molecular signatures and myelin repair following chronic demyelination. *Front Cell Neurosci* 17, 1169786 (2023).

713. Ruckh, J. M. *et al.* Rejuvenation of regeneration in the aging central nervous system. *Cell Stem Cell* 10, 96–103 (2012).

714. Lau, N. C., Lim, L. P., Weinstein, E. G. & Bartel, D. P. An abundant class of tiny RNAs with probable regulatory roles in Caenorhabditis elegans. *Science* 294, 858–862 (2001).

715. Lee, R. C., Feinbaum, R. L. & Ambros, V. The C. elegans heterochronic gene lin-4 encodes small RNAs with antisense complementarity to lin-14. *Cell* 75, 843–854 (1993).

716. Wightman, B., Ha, I. & Ruvkun, G. Posttranscriptional regulation of the heterochronic gene lin-14 by lin-4 mediates temporal pattern formation in C. elegans. *Cell* 75, 855–862 (1993).

717. Lagos-Quintana, M., Rauhut, R., Lendeckel, W. & Tuschl, T. Identification of novel genes coding for small expressed RNAs. *Science* 294, 853–858 (2001).

718. Lee, R. C. & Ambros, V. An extensive class of small RNAs in Caenorhabditis elegans. *Science* 294, 862–864 (2001).

719. Shi, J., Zhou, T. & Chen, Q. Exploring the expanding universe of small RNAs. *Nat Cell Biol* 24, 415–423 (2022).

720. Bartel, D. P. MicroRNAs: Genomics, Biogenesis, Mechanism, and Function. *Cell* 116, 281–297 (2004).

721. Filipowicz, W., Bhattacharyya, S. N. & Sonenberg, N. Mechanisms of post-transcriptional regulation by microRNAs: are the answers in sight? *Nat Rev Genet* 9, 102–114 (2008).

722. Westholm, J. O. & Lai, E. C. Mirtrons: microRNA biogenesis via splicing. *Biochimie* 93, 1897–1904 (2011).

723. Finnegan, E. F. & Pasquinelli, A. E. MicroRNA biogenesis: regulating the regulators. *Crit Rev Biochem Mol Biol* 48, 51–68 (2013).

724. Desvignes, T. *et al.* microRNA nomenclature: A view incorporating genetic origins, biosynthetic pathways, and sequence variants. *Trends Genet* 31, 613–626 (2015).

725. Bartel, D. P. MicroRNAs: target recognition and regulatory functions. *Cell* 136, 215–233 (2009).

726. Sayed, D. & Abdellatif, M. MicroRNAs in development and disease. *Physiol Rev* 91, 827–887 (2011).

727. Friedman, R. C., Farh, K. K.-H., Burge, C. B. & Bartel, D. P. Most mammalian mRNAs are conserved targets of microRNAs. *Genome Res* 19, 92–105 (2009).

728. Lewis, B. P., Burge, C. B. & Bartel, D. P. Conserved seed pairing, often flanked by adenosines, indicates that thousands of human genes are microRNA targets. *Cell* 120, 15–20 (2005).

729. Grimson, A. *et al.* MicroRNA targeting specificity in mammals: determinants beyond seed pairing. *Mol Cell* 27, 91–105 (2007).

730. Lytle, J. R., Yario, T. A. & Steitz, J. A. Target mRNAs are repressed as efficiently by microRNA-binding sites in the 5' UTR as in the 3' UTR. *Proc Natl Acad Sci U S A* 104, 9667–9672 (2007).

731. Liu, J. *et al.* Argonaute2 is the catalytic engine of mammalian RNAi. *Science* 305, 1437–1441 (2004).

732. Yekta, S., Shih, I.-H. & Bartel, D. P. MicroRNA-directed cleavage of HOXB8 mRNA. *Science* 304, 594–596 (2004).

733. Fukao, A. *et al.* MicroRNAs trigger dissociation of eIF4AI and eIF4AII from target mRNAs in humans. *Mol Cell* 56, 79–89 (2014).

734. Humphreys, D. T., Westman, B. J., Martin, D. I. K. & Preiss, T. MicroRNAs control translation initiation by inhibiting eukaryotic initiation factor 4E/cap and poly(A) tail function. *Proc Natl Acad Sci U S A* 102, 16961–16966 (2005).

735. Kiriakidou, M. *et al.* An mRNA m7G cap binding-like motif within human Ago2 represses translation. *Cell* 129, 1141–1151 (2007).

736. Standart, N. & Jackson, R. J. MicroRNAs repress translation of m7Gppp-capped target mRNAs in vitro by inhibiting initiation and promoting deadenylation. *Genes Dev* 21, 1975–1982 (2007).

737. Chendrimada, T. P. *et al.* MicroRNA silencing through RISC recruitment of eIF6. *Nature* 447, 823–828 (2007).

738. Maroney, P. A., Yu, Y., Fisher, J. & Nilsen, T. W. Evidence that microRNAs are associated with translating messenger RNAs in human cells. *Nat Struct Mol Biol* 13, 1102–1107 (2006).

739. Nottrott, S., Simard, M. J. & Richter, J. D. Human let-7a miRNA blocks protein production on actively translating polyribosomes. *Nat Struct Mol Biol* 13, 1108–1114 (2006).

740. Petersen, C. P., Bordeleau, M.-E., Pelletier, J. & Sharp, P. A. Short RNAs Repress Translation after Initiation in Mammalian Cells. *Molecular Cell* 21, 533–542 (2006).

741. Behm-Ansmant, I. *et al.* mRNA degradation by miRNAs and GW182 requires both CCR4:NOT deadenylase and DCP1:DCP2 decapping complexes. *Genes Dev* 20, 1885–1898 (2006).

742. Mathys, H. *et al.* Structural and Biochemical Insights to the Role of the CCR4-NOT Complex and DDX6 ATPase in MicroRNA Repression. *Molecular Cell* 54, 751–765 (2014).

743. Wu, L., Fan, J. & Belasco, J. G. MicroRNAs direct rapid deadenylation of mRNA. *Proceedings of the National Academy of Sciences* 103, 4034–4039 (2006).

744. Mitchell, P., Petfalski, E., Shevchenko, A., Mann, M. & Tollervey, D. The exosome: a conserved eukaryotic RNA processing complex containing multiple 3'-->5' exoribonucleases. *Cell* 91, 457–466 (1997).

745. Parker, R. & Song, H. The enzymes and control of eukaryotic mRNA turnover. *Nat Struct Mol Biol* 11, 121–127 (2004).

746. Zekri, L., Kuzuoğlu-Öztürk, D. & Izaurralde, E. GW182 proteins cause PABP dissociation from silenced miRNA targets in the absence of deadenylation. *EMBO J* 32, 1052–1065 (2013).

747. Wakiyama, M., Takimoto, K., Ohara, O. & Yokoyama, S. Let-7 microRNA-mediated mRNA deadenylation and translational repression in a mammalian cell-free system. *Genes Dev* 21, 1857–1862 (2007).

748. Jakymiw, A. *et al.* Disruption of GW bodies impairs mammalian RNA interference. *Nat Cell Biol* 7, 1267–1274 (2005).

749. Liu, J. *et al.* A role for the P-body component GW182 in microRNA function. *Nat Cell Biol* 7, 1261–1266 (2005).

750. Liu, J., Valencia-Sanchez, M. A., Hannon, G. J. & Parker, R. MicroRNA-dependent localization of targeted mRNAs to mammalian P-bodies. *Nat Cell Biol* 7, 719–723 (2005).

751. Huang, Q. *et al.* MicroRNAs associated with the pathogenesis of multiple sclerosis. *Journal of Neuroimmunology* 295, 148–161 (2016).

752. Ma, X. *et al.* Expression, Regulation and Function of MicroRNAs in Multiple Sclerosis. *Int J Med Sci* 11, 810–818 (2014).

753. Martin, N. A. & Illes, Z. Differentially expressed microRNA in multiple sclerosis: A window into pathogenesis? *Clinical and Experimental Neuroimmunology* 5, 149–161 (2014).

754. Martinez, B. & Peplow, P. V. MicroRNAs in blood and cerebrospinal fluid as diagnostic biomarkers of multiple sclerosis and to monitor disease progression. *Neural Regen Res* 15, 606–619 (2020).

755. Piket, E., Zheleznyakova, G. Y., Kular, L. & Jagodic, M. Small non-coding RNAs as important players, biomarkers and therapeutic targets in multiple sclerosis: A comprehensive overview. *Journal of Autoimmunity* 101, 17–25 (2019).

756. Jafari, N. *et al.* Overexpression of microRNA biogenesis machinery: Drosha, DGCR8 and Dicer in multiple sclerosis patients. *J Clin Neurosci* 22, 200–203 (2015).

757. Fenoglio, C. *et al.* Expression and genetic analysis of miRNAs involved in CD4+ cell activation in patients with multiple sclerosis. *Neurosci Lett* 504, 9–12 (2011).

758. Junker, A. *et al.* MicroRNA profiling of multiple sclerosis lesions identifies modulators of the regulatory protein CD47. *Brain* 132, 3342–3352 (2009).

759. Kroesen, B.-J. *et al.* Immuno-miRs: critical regulators of T-cell development, function and ageing. *Immunology* 144, 1–10 (2015).

760. Waschbisch, A. *et al.* Glatiramer Acetate Treatment Normalizes Deregulated microRNA Expression in Relapsing Remitting Multiple Sclerosis. *PLoS One* 6, (2011).

761. Zhang, J. *et al.* MicroRNA-155 modulates Th1 and Th17 cell differentiation and is associated with multiple sclerosis and experimental autoimmune encephalomyelitis. *J Neuroimmunol* 266, 56–63 (2014).

762. Sievers, C. *et al.* Altered microRNA expression in B lymphocytes in multiple sclerosis: Towards a better understanding of treatment effects. *Clinical Immunology* 144, 70–79 (2012).

763. Cuomo-Haymour, N. *et al.* Differential Expression of Serum Extracellular Vesicle miRNAs in Multiple Sclerosis: Disease-Stage Specificity and Relevance to Pathophysiology. *Int J Mol Sci* 23, 1664 (2022).

764. Ebrahimkhani, S. *et al.* Exosomal microRNA signatures in multiple sclerosis reflect disease status. *Sci Rep* 7, 14293 (2017).

765. Fenoglio, C. *et al.* Decreased circulating miRNA levels in patients with primary progressive multiple sclerosis. *Mult Scler* 19, 1938–1942 (2013).

766. Gandhi, R. *et al.* Circulating MicroRNAs as biomarkers for disease staging in multiple sclerosis. *Annals of Neurology* 73, 729–740 (2013).

767. Pietrasik, S., Dziedzic, A., Miller, E., Starosta, M. & Saluk-Bijak, J. Circulating miRNAs as Potential Biomarkers Distinguishing Relapsing–Remitting from Secondary Progressive Multiple Sclerosis. A Review. *Int J Mol Sci* 22, 11887 (2021).

768. Bergman, P. *et al.* Circulating miR-150 in CSF is a novel candidate biomarker for multiple sclerosis. *Neurology - Neuroimmunology Neuroinflammation* 3, (2016).

769. Gao, Y., Han, D. & Feng, J. MicroRNA in multiple sclerosis. *Clinica Chimica Acta* 516, 92–99 (2021).

770. Noor Eddin, A. *et al.* Cerebrospinal fluid microRNAs as potential biomarkers in Alzheimer's disease. *Front Aging Neurosci* 15, 1210191 (2023).

771. Slota, J. A. & Booth, S. A. MicroRNAs in Neuroinflammation: Implications in Disease Pathogenesis, Biomarker Discovery and Therapeutic Applications. *Noncoding RNA* 5, 35 (2019).

772. Dobricic, V. *et al.* Common signatures of differential microRNA expression in Parkinson's and Alzheimer's disease brains. *Brain Commun* 4, fcac274 (2022).

773. Wang, J., Zhao, X. & Wan, Y. Y. Intricacies of TGF-β signaling in Treg and Th17 cell biology. *Cell Mol Immunol* 1–21 (2023) doi:10.1038/s41423-023-01036-7.

774. Bernstein, E. *et al.* Dicer is essential for mouse development. *Nat Genet* 35, 215–217 (2003).

775. Chong, M. M. W., Rasmussen, J. P., Rudensky, A. Y. & Littman, D. R. The RNAseIII enzyme Drosha is critical in T cells for preventing lethal inflammatory disease. *J Exp Med* 205, 2005–2017 (2008).

776. Baumann, F. M., Yuzefpolskiy, Y., Sarkar, S. & Kalia, V. Dicer Regulates the Balance of Short-Lived Effector and Long-Lived Memory CD8 T Cell Lineages. *PLoS One* 11, e0162674 (2016).

777. Koralov, S. B. *et al.* Dicer Ablation Affects Antibody Diversity and Cell Survival in the B Lymphocyte Lineage. *Cell* 132, 860–874 (2008).

778. Xu, S., Guo, K., Zeng, Q., Huo, J. & Lam, K.-P. The RNase III enzyme Dicer is essential for germinal center B-cell formation. *Blood* 119, 767–776 (2012).

779. Varol, D. *et al.* Dicer Deficiency Differentially Impacts Microglia of the Developing and Adult Brain. *Immunity* 46, 1030-1044.e8 (2017).

780. Liu, K. *et al.* Dicer Deletion in Astrocytes Inhibits Oligodendroglial Differentiation and Myelination. *Neurosci Bull* 37, 1135–1146 (2021).

781. Tao, J. *et al.* Deletion of astroglial Dicer causes non-cell-autonomous neuronal dysfunction and degeneration. *J Neurosci* 31, 8306–8319 (2011).

782. Dugas, J. C. *et al.* Dicer1 and miR-219 Are Required for Normal Oligodendrocyte Differentiation and Myelination. *Neuron* 65, 597–611 (2010).

783. Zhao, X. *et al.* MicroRNA-Mediated Control of Oligodendrocyte Differentiation. *Neuron* 65, 612–626 (2010).

784. Shin, D., Shin, J.-Y., McManus, M. T., Ptácek, L. J. & Fu, Y.-H. Dicer ablation in oligodendrocytes provokes neuronal impairment in mice. *Ann Neurol* 66, 843–857 (2009).

785. Huo, J., Liu, T., Li, F., Song, X. & Hou, X. MicroRNA-21-5p protects melanocytes via targeting STAT3 and modulating Treg/Teff balance to alleviate vitiligo. *Mol Med Rep* 23, 51 (2021).

786. Ji, Q. *et al.* Exosomes derived from thymic stromal lymphopoietin-treated dendritic cells regulate T helper 17/regulatory T cell differentiation via miR-21/Smad7 axis. *Exp Cell Res* 398, 112393 (2021).

787. Samiei, H. *et al.* Simultaneous disruption of circulating miR-21 and cytotoxic T lymphocytes (CTLs): Prospective diagnostic and prognostic markers for esophageal squamous cell carcinoma (ESCC). *J Clin Lab Anal* 36, e24125 (2022).

788. Iliopoulos, D., Kavousanaki, M., Ioannou, M., Boumpas, D. & Verginis, P. The negative costimulatory molecule PD-1 modulates the balance between immunity and tolerance via miR-21. *Eur J Immunol* 41, 1754–1763 (2011).

789. Shi, C. *et al.* Novel evidence for an oncogenic role of microRNA-21 in colitis-associated colorectal cancer. *Gut* 65, 1470–1481 (2016).

790. Sheedy, F. J. *et al.* Negative regulation of TLR4 via targeting of the proinflammatory tumor suppressor PDCD4 by the microRNA miR-21. *Nat Immunol* 11, 141–147 (2010).

791. Lindahl, L. M. *et al.* STAT5 induces miR-21 expression in cutaneous T cell lymphoma. *Oncotarget* 7, 45730–45744 (2016).

792. van der Fits, L. *et al.* MicroRNA-21 Expression in CD4+ T Cells Is Regulated by STAT3 and Is Pathologically Involved in Sézary Syndrome. *Journal of Investigative Dermatology* 131, 762–768 (2011).

793. Wang, M., Mungur, R., Lan, P., Wang, P. & Wan, S. MicroRNA-21 and microRNA-146a negatively regulate the secondary inflammatory response of microglia after intracerebral hemorrhage. *Int J Clin Exp Pathol* 11, 3348–3356 (2018).

794. Zhang, L., Dong, L.-Y., Li, Y.-J., Hong, Z. & Wei, W.-S. miR-21 represses FasL in microglia and protects against microglia-mediated neuronal cell death following hypoxia/ischemia. *Glia* 60, 1888–1895 (2012).

795. Yin, Z. *et al.* Neuron-derived exosomes with high miR-21-5p expression promoted polarization of M1 microglia in culture. *Brain, Behavior, and Immunity* 83, 270–282 (2020).

796. Bhalala, O. G. *et al.* microRNA-21 Regulates Astrocytic Response Following Spinal Cord Injury. *J. Neurosci.* 32, 17935–17947 (2012).

797. Su, Y. *et al.* Silencing miR-21 induces polarization of astrocytes to the A2 phenotype and improves the formation of synapses by targeting glypican 6 via the signal transducer and activator of transcription-3 pathway after acute ischemic spinal cord injury. *The FASEB Journal* 33, 10859–10871 (2019).

798. Ziu, M., Fletcher, L., Rana, S., Jimenez, D. F. & Digicaylioglu, M. Temporal Differences in MicroRNA Expression Patterns in Astrocytes and Neurons after Ischemic Injury. *PLoS One* 6, e14724 (2011).

799. Zhang, F. *et al.* MicroRNA-21-5p agomir inhibits apoptosis of oligodendrocyte precursor cell and attenuates white matter injury in neonatal rats. *Brain Res Bull* 189, 139–150 (2022).

800. Cruz, L. O. *et al.* Excessive expression of miR-27 impairs Treg-mediated immunological tolerance. *J Clin Invest* 127, 530–542 (2017).

801. Guerau-de-Arellano, M. *et al.* Micro-RNA dysregulation in multiple sclerosis favours pro-inflammatory T-cell-mediated autoimmunity. *Brain* 134, 3578–3589 (2011).

802. Severin, M. E. *et al.* MicroRNAs targeting TGFβ signalling underlie the regulatory T cell defect in multiple sclerosis. *Brain* 139, 1747–1761 (2016).

803. Ahmadian-Elmi, M. *et al.* miR-27a and miR-214 exert opposite regulatory roles in Th17 differentiation via mediating different signaling pathways in peripheral blood CD4+ T lymphocytes of patients with relapsing–remitting multiple sclerosis. *Immunogenetics* 68, 43–54 (2016).

804. Dong, M. *et al.* Mir-27a-3p attenuates bronchiolitis obliterans in vivo via the regulation of dendritic cells' maturation and the suppression of myofibroblasts' differentiation. *Clin Transl Med* 10, e140 (2020).

805. Min, S. *et al.* TGF-β-associated miR-27a inhibits dendritic cell-mediated differentiation of Th1 and Th17 cells by TAB3, p38 MAPK, MAP2K4 and MAP2K7. *Genes Immun* 13, 621–631 (2012).

806. Gayen, M., Bhomia, M., Balakathiresan, N. & Knollmann-Ritschel, B. Exosomal MicroRNAs Released by Activated Astrocytes as Potential Neuroinflammatory Biomarkers. *International Journal of Molecular Sciences* 21, 2312 (2020).

807. Lv, Y., Ou-yang, A. & Fu, L. MicroRNA-27a Negatively Modulates the Inflammatory Response in Lipopolysaccharide-Stimulated Microglia by Targeting TLR4 and IRAK4. *Cell Mol Neurobiol* 37, 195–210 (2017).

808. Jennewein, C., von Knethen, A., Schmid, T. & Brüne, B. MicroRNA-27b Contributes to Lipopolysaccharide-mediated Peroxisome Proliferator-activated Receptor γ (PPARγ) mRNA Destabilization. *J Biol Chem* 285, 11846–11853 (2010).

809. Tripathi, A. *et al.* Oligodendrocyte Intrinsic miR-27a Controls Myelination and Remyelination. *Cell Rep* 29, 904-919.e9 (2019).

810. Morquette, B. *et al.* MicroRNA-223 protects neurons from degeneration in experimental autoimmune encephalomyelitis. *Brain* 142, 2979–2995 (2019).

811. Fayyad-Kazan, H. *et al.* MicroRNA profile of circulating CD4-positive regulatory T cells in human adults and impact of differentially expressed microRNAs on expression of two genes essential to their function. *J Biol Chem* 287, 9910–9922 (2012).

812. Walker, L. S. K. Treg and CTLA-4: Two intertwining pathways to immune tolerance. *J Autoimmun* 45, 49–57 (2013).

813. Fan, L. *et al.* MicroRNA-145 influences the balance of Th1/Th2 via regulating RUNX3 in asthma patients. *Exp Lung Res* 42, 417–424 (2016).

814. Xie, X. *et al.* miR-145-5p/Nurr1/TNF-α Signaling-Induced Microglia Activation Regulates Neuron Injury of Acute Cerebral Ischemic/Reperfusion in Rats. *Front Mol Neurosci* 10, 383 (2017).

815. Freilich, R. W., Woodbury, M. E. & Ikezu, T. Integrated expression profiles of mRNA and miRNA in polarized primary murine microglia. *PLoS One* 8, e79416 (2013).

816. Wang, C.-Y., Yang, S.-H. & Tzeng, S.-F. MicroRNA-145 as one negative regulator of astrogliosis. *Glia* 63, 194–205 (2015).

817. Kornfeld, S. F., Cummings, S. E., Fathi, S., Bonin, S. R. & Kothary, R. MiRNA-145-5p prevents differentiation of oligodendrocyte progenitor cells by regulating expression of myelin gene regulatory factor. *Journal of Cellular Physiology* 236, 997–1012 (2021).

818. Han, S. R. *et al.* Differential Expression of miRNAs and Behavioral Change in the Cuprizone-Induced Demyelination Mouse Model. *Int J Mol Sci* 21, 646 (2020).

819. Huang, Y., Lin, X. & Lin, X. MiR-146a-5p Contributes to Microglial Polarization Transitions Associated With AGEs. *Mol Neurobiol* 60, 3020–3033 (2023).

820. Iyer, A. *et al.* MicroRNA-146a: a key regulator of astrocyte-mediated inflammatory response. *PLoS One* 7, e44789 (2012).

821. Li, B. *et al.* miR-146a modulates autoreactive Th17 cell differentiation and regulates organ-specific autoimmunity. *J Clin Invest* 127, 3702–3716 (2017).

822. Liu, T., Zhang, L., Joo, D. & Sun, S.-C. NF-κB signaling in inflammation. *Sig Transduct Target Ther* 2, 1–9 (2017).

823. Huang, Y., Li, T., Sane, D. C. & Li, L. IRAK1 serves as a novel regulator essential for lipopolysaccharide-induced interleukin-10 gene expression. *J Biol Chem* 279, 51697–51703 (2004).

824. Maitra, U., Davis, S., Reilly, C. M. & Li, L. Differential regulation of Foxp3 and IL-17 expression in CD4 T helper cells by IRAK-1. *J Immunol* 182, 5763–5769 (2009).

825. Lu, L.-F. *et al.* Function of miR-146a in controlling Treg cell-mediated regulation of Th1 responses. *Cell* 142, 914–929 (2010).

826. Zhang, Y. *et al.* miR-146a enhances regulatory T-cell differentiation and function in allergic rhinitis by targeting STAT5b. *Allergy* 77, 550–558 (2022).

827. Wu, D. *et al.* Brain endothelial miR-146a negatively modulates T-cell adhesion through repressing multiple targets to inhibit NF-κB activation. *J Cereb Blood Flow Metab* 35, 412–423 (2015).

828. Huang, C. *et al.* MiR-146a modulates macrophage polarization by inhibiting Notch1 pathway in RAW264.7 macrophages. *International Immunopharmacology* 32, 46–54 (2016).

829. Sharma, N., Verma, R., Kumawat, K. L., Basu, A. & Singh, S. K. miR-146a suppresses cellular immune response during Japanese encephalitis virus JaOArS982 strain infection in human microglial cells. *J Neuroinflammation* 12, 30 (2015).

830. Saba, R. *et al.* MicroRNA 146a (miR-146a) Is Over-Expressed during Prion Disease and Modulates the Innate Immune Response and the Microglial Activation State. *PLoS One* 7, e30832 (2012).

831. Zhang, J. *et al.* MiR-146a promotes remyelination in a cuprizone model of demyelinating injury. *Neuroscience* 348, 252–263 (2017).

832. Zhang, J. *et al.* MiR-146a promotes oligodendrocyte progenitor cell differentiation and enhances remyelination in a model of experimental autoimmune encephalomyelitis. *Neurobiology of Disease* 125, 154–162 (2019).

833. Martin, N. A. *et al.* Absence of miRNA-146a Differentially Alters Microglia Function and Proteome. *Front Immunol* 11, 1110 (2020).

834. Martin, N. A. *et al.* Experimental Demyelination and Axonal Loss Are Reduced in MicroRNA-146a Deficient Mice. *Frontiers in Immunology* 9, (2018).

835. Zhou, B., Wang, S., Mayr, C., Bartel, D. P. & Lodish, H. F. miR-150, a microRNA expressed in mature B and T cells, blocks early B cell development when expressed prematurely. *Proc Natl Acad Sci U S A* 104, 7080–7085 (2007).

836. Xiao, C. *et al.* MiR-150 controls B cell differentiation by targeting the transcription factor c-Myb. *Cell* 131, 146–159 (2007).

837. Chen, Z. *et al.* MiR-150 regulates memory CD8 T cell differentiation via c-Myb. *Cell Rep* 20, 2584–2597 (2017).

838. Xia, S. *et al.* miR-150 promotes progressive T cell differentiation via inhibiting FOXP1 and RC3H1. *Hum Immunol* 83, 778–788 (2022).

839. Hu, Z. *et al.* Silencing miR-150 Ameliorates Experimental Autoimmune Encephalomyelitis. *Frontiers in Neuroscience* 12, (2018).

840. Li, H. *et al.* MicroRNA-150 serves as a diagnostic biomarker and is involved in the inflammatory pathogenesis of Parkinson's disease. *Mol Genet Genomic Med* 8, e1189 (2020).

841. Moore, C. S. *et al.* miR-155 as a multiple sclerosis-relevant regulator of myeloid cell polarization. *Ann Neurol* 74, 709–720 (2013).

842. Yao, R. *et al.* MicroRNA-155 modulates Treg and Th17 cells differentiation and Th17 cell function by targeting SOCS1. *PLoS One* 7, e46082 (2012).

843. Chong, M. M. W., Metcalf, D., Jamieson, E., Alexander, W. S. & Kay, T. W. H. Suppressor of cytokine signaling-1 in T cells and macrophages is critical for preventing lethal inflammation. *Blood* 106, 1668–1675 (2005).

844. Qin, H., Wilson, C. A., Lee, S. J. & Benveniste, E. N. IFN-beta-induced SOCS-1 negatively regulates CD40 gene expression in macrophages and microglia. *FASEB J* 20, 985–987 (2006).

845. Tamiya, T., Kashiwagi, I., Takahashi, R., Yasukawa, H. & Yoshimura, A. Suppressors of Cytokine Signaling (SOCS) Proteins and JAK/STAT Pathways. *Arteriosclerosis, Thrombosis, and Vascular Biology* 31, 980–985 (2011).

846. Grenningloh, R., Kang, B. Y. & Ho, I.-C. Ets-1, a functional cofactor of T-bet, is essential for Th1 inflammatory responses. *J Exp Med* 201, 615–626 (2005).

847. Hu, R. *et al.* MicroRNA-155 confers encephalogenic potential to Th17 cells by promoting effector gene expression. *J Immunol* 190, 5972–5980 (2013).

848. Moisan, J., Grenningloh, R., Bettelli, E., Oukka, M. & Ho, I.-C. Ets-1 is a negative regulator of Th17 differentiation. *J Exp Med* 204, 2825–2835 (2007).

849. Mouly, E. *et al.* The Ets-1 transcription factor controls the development and function of natural regulatory T cells. *J Exp Med* 207, 2113–2125 (2010).

850. Zhang, J. *et al.* MicroRNA-155 modulates Th1 and Th17 cell differentiation and is associated with multiple sclerosis and experimental autoimmune encephalomyelitis. *J Neuroimmunol* 266, 56–63 (2014).

851. Lu, L.-F. *et al.* Foxp3-dependent microRNA155 confers competitive fitness to regulatory T cells by targeting SOCS1 protein. *Immunity* 30, 80–91 (2009).

852. Zheng, Y. *et al.* Genome-wide analysis of Foxp3 target genes in developing and mature regulatory T cells. *Nature* 445, 936–940 (2007).

853. Kohlhaas, S. *et al.* Cutting edge: the Foxp3 target miR-155 contributes to the development of regulatory T cells. *J Immunol* 182, 2578–2582 (2009).

854. Alivernini, S. *et al.* MicroRNA-155 influences B-cell function through PU.1 in rheumatoid arthritis. *Nat Commun* 7, 12970 (2016).

855. Zheng, Y. *et al.* miR-155 Regulates IL-10-Producing CD24hiCD27+ B Cells and Impairs Their Function in Patients with Crohn's Disease. *Front Immunol* 8, 914 (2017).

856. Lopez-Ramirez, M. A. *et al.* MicroRNA-155 negatively affects blood-brain barrier function during neuroinflammation. *FASEB J* 28, 2551–2565 (2014).

857. Cardoso, A. L., Guedes, J. R., Pereira de Almeida, L. & Pedroso de Lima, M. C. miR-155 modulates microglia-mediated immune response by down-regulating SOCS-1 and promoting cytokine and nitric oxide production. *Immunology* 135, 73–88 (2012).

858. He, L. *et al.* MiR-155-5p Aggravated Astrocyte Activation and Glial Scarring in a Spinal Cord Injury Model by Inhibiting Ndfip1 Expression and PTEN Nuclear Translocation. *Neurochem Res* 48, 1912–1924 (2023).

859. Kong, H. *et al.* The Effect of miR-132, miR-146a, and miR-155 on MRP8/TLR4-Induced Astrocyte-Related Inflammation. *J Mol Neurosci* 57, 28–37 (2015).

860. Korotkov, A. *et al.* Increased expression of miR142 and miR155 in glial and immune cells after traumatic brain injury may contribute to neuroinflammation via astrocyte activation. *Brain Pathol* 30, 897–912 (2020).

861. Mor, E. *et al.* Species-specific microRNA roles elucidated following astrocyte activation. *Nucleic Acids Res* 39, 3710–3723 (2011).

862. Liu, X. *et al.* Microglia Polarization from M1 toward M2 Phenotype Is Promoted by Astragalus Polysaccharides Mediated through Inhibition of miR-155 in Experimental Autoimmune Encephalomyelitis. *Oxid Med Cell Longev* 2021, 5753452 (2021).

863. Pena-Philippides, J. C., Caballero-Garrido, E., Lordkipanidze, T. & Roitbak, T. In vivo inhibition of miR-155 significantly alters post-stroke inflammatory response. *J Neuroinflammation* 13, 287 (2016).

864. Louafi, F., Martinez-Nunez, R. T. & Sanchez-Elsner, T. MicroRNA-155 Targets SMAD2 and Modulates the Response of Macrophages to Transforming Growth Factor-β. *J Biol Chem* 285, 41328–41336 (2010).

865. Pedicone, C. *et al.* Discovery of a novel SHIP1 agonist that promotes degradation of lipid-laden phagocytic cargo by microglia. *iScience* 25, 104170 (2022).

866. Ruffell, D. *et al.* A CREB-C/EBPβ cascade induces M2 macrophage-specific gene expression and promotes muscle injury repair. *Proc Natl Acad Sci U S A* 106, 17475–17480 (2009).

867. Sly, L. M. *et al.* The role of SHIP in macrophages. *Front Biosci* 12, 2836–2848 (2007).

868. Yin, H., Song, S. & Pan, X. Knockdown of miR-155 protects microglia against LPS-induced inflammatory injury via targeting RACK1: a novel research for intracranial infection. *J Inflamm (Lond)* 14, 17 (2017).

869. Lescher, J. *et al.* MicroRNA regulation in experimental autoimmune encephalomyelitis in mice and marmosets resembles regulation in human multiple sclerosis lesions. *J Neuroimmunol* 246, 27–33 (2012).

870. Venkatesha, S. H., Dudics, S., Song, Y., Mahurkar, A. & Moudgil, K. D. The miRNA Expression Profile of Experimental Autoimmune Encephalomyelitis Reveals Novel Potential Disease Biomarkers. *Int J Mol Sci* 19, 3990 (2018).

871. Su, W. *et al.* The p53 transcription factor modulates microglia behavior through microRNA-dependent regulation of c-Maf. *J Immunol* 192, 358–366 (2014).

872. de Faria Jr., O. *et al.* Regulation of miRNA 219 and miRNA Clusters 338 and 17-92 in Oligodendrocytes. *Frontiers in Genetics* 3, (2012).

873. Nazari, B. *et al.* Overexpression of miR-219 promotes differentiation of human induced pluripotent stem cells into pre-oligodendrocyte. *Journal of Chemical Neuroanatomy* 91, 8–16 (2018).

874. Nazari, B. *et al.* Derivation of preoligodendrocytes from human-induced pluripotent stem cells through overexpression of microRNA 338. *Journal of Cellular Biochemistry* 120, 9700–9708 (2019).

875. Okado, H. *et al.* The transcriptional repressor RP58 is crucial for cell-division patterning and neuronal survival in the developing cortex. *Dev Biol* 331, 140–151 (2009).

876. Cantone, M. *et al.* A gene regulatory architecture that controls region-independent dynamics of oligodendrocyte differentiation. *Glia* 67, 825–843 (2019).

877. Noorbakhsh, F. *et al.* Impaired neurosteroid synthesis in multiple sclerosis. *Brain* 134, 2703–2721 (2011).

878. Reiprich, S. *et al.* Transcription factor Sox10 regulates oligodendroglial Sox9 levels via microRNAs. *Glia* 65, 1089–1102 (2017).

879. Wang, H. *et al.* miR-219 Cooperates with miR-338 in Myelination and Promotes Myelin Repair in the CNS. *Developmental Cell* 40, 566-582.e5 (2017).

880. Liu, S. *et al.* miR-219 attenuates demyelination in cuprizone-induced demyelinated mice by regulating monocarboxylate transporter 1. *Eur J Neurosci* 45, 249–259 (2017).

881. Li, X., Sun, L., Chen, L., Xu, Y. & Kong, X. Upregulation of microRNA-219-5p relieves ulcerative colitis through balancing the differentiation of Treg/Th17 cells. *Eur J Gastroenterol Hepatol* 32, 813–820 (2020).

882. Moyano, A. L. *et al.* microRNA-219 Reduces Viral Load and Pathologic Changes in Theiler's Virus-Induced Demyelinating Disease. *Mol Ther* 26, 730–743 (2018).

883. Nguyen, L. H. *et al.* Effects of miR-219/miR-338 on microglia and astrocyte behaviors and astrocyte-oligodendrocyte precursor cell interactions. *Neural Regen Res* 15, 739–747 (2020).

884. Lau, P. *et al.* Identification of Dynamically Regulated MicroRNA and mRNA Networks in Developing Oligodendrocytes. *J Neurosci* 28, 11720–11730 (2008).

885. Letzen, B. S. *et al.* MicroRNA Expression Profiling of Oligodendrocyte Differentiation from Human Embryonic Stem Cells. *PLoS One* 5, e10480 (2010).

886. Yin, Y. *et al.* Tumor-secreted miR-214 induces regulatory T cells: a major link between immune evasion and tumor growth. *Cell Res* 24, 1164–1180 (2014).

887. Kuypers, N. J., Bankston, A. N., Howard, R. M., Beare, J. E. & Whittemore, S. R. Remyelinating Oligodendrocyte Precursor Cell miRNAs from the Sfmbt2 Cluster Promote Cell Cycle Arrest and Differentiation. *J Neurosci* 36, 1698–1710 (2016).

888. Lin, S.-H. *et al.* Heme oxygenase-1 modulates microRNA expression in cultured astroglia: Implications for chronic brain disorders. *Glia* 63, 1270–1284 (2015).

889. Budde, H. *et al.* Control of oligodendroglial cell number by the miR-17-92 cluster. *Development* 137, 2127–2132 (2010).

890. Wang, E. & Cambi, F. MicroRNA expression in mouse oligodendrocytes and regulation of proteolipid protein gene expression. *J Neurosci Res* 90, 1701–1712 (2012).

891. Nowak, A. *et al.* The role of non-coding RNAs in neuroinflammatory process in multiple sclerosis. *Mol Neurobiol* 59, 4651–4668 (2022).

892. Perdaens, O., Dang, H. A., D'Auria, L. & van Pesch, V. CSF microRNAs discriminate MS activity and share similarity to other neuroinflammatory disorders. *Neurol Neuroimmunol Neuroinflamm* 7, (2020).

893. Ghafouri-Fard, S. *et al.* Nanoparticle-mediated delivery of microRNAs-based therapies for treatment of disorders. *Pathology - Research and Practice* 248, 154667 (2023).

894. Marangon, D., Raffaele, S., Fumagalli, M. & Lecca, D. MicroRNAs change the games in central nervous system pharmacology. *Biochem Pharmacol* 168, 162–172 (2019).

895. Murphy, D. E. *et al.* Extracellular vesicle-based therapeutics: natural versus engineered targeting and trafficking. *Exp Mol Med* 51, 1–12 (2019).

896. Ruseska, I. & Zimmer, A. Cellular uptake and trafficking of peptide-based drug delivery systems for miRNA. *Eur J Pharm Biopharm* S0939-6411(23)00232–1 (2023) doi:10.1016/j.ejpb.2023.08.019.

897. Tripathi, A. *et al.* Identifying miRNAs in multiple sclerosis gray matter lesions that correlate with atrophy measures. *Ann Clin Transl Neurol* 8, 1279–1291 (2021).

898. Reich, D. S., Lucchinetti, C. F. & Calabresi, P. A. Multiple Sclerosis. *N Engl J Med* 378, 169–180 (2018).

899. Zheleznyakova, G. Y. *et al.* Epigenetic research in multiple sclerosis: progress, challenges, and opportunities. *Physiological Genomics* 49, 447–461 (2017).

900. Dolati, S. *et al.* Dysregulated Network of miRNAs Involved in the Pathogenesis of Multiple Sclerosis. *Biomedicine & Pharmacotherapy* 104, 280–290 (2018).

901. Haghikia, A. *et al.* Regulated microRNAs in the CSF of patients with multiple sclerosis: a case-control study. *Neurology* 79, 2166–2170 (2012).

902. Teunissen, C. E. *et al.* A consensus protocol for the standardization of cerebrospinal fluid collection and biobanking. *Neurology* 73, 1914–1922 (2009).

903. Bayart, J.-L., Muls, N. & van Pesch, V. Free Kappa light chains in neuroinflammatory disorders: Complement rather than substitute? *Acta Neurologica Scandinavica* 138, 352–358 (2018).

904. Muls, N. G., Dang, H. A., Sindic, C. J. & Pesch, V. van. Regulation of Treg-associated CD39 in multiple sclerosis and effects of corticotherapy during relapse: *Multiple Sclerosis Journal* (2015) doi:10.1177/1352458514567215.

905. Teunissen, C. *et al.* Consensus definitions and application guidelines for control groups in cerebrospinal fluid biomarker studies in multiple sclerosis. *Mult Scler* 19, 1802–1809 (2013).

906. Reiber, H. Flow rate of cerebrospinal fluid (CSF) — A concept common to normal blood-CSF barrier function and to dysfunction in neurological diseases. *Journal of the Neurological Sciences* 122, 189–203 (1994).

907. Barkhof, F. *et al.* Comparison of MRI criteria at first presentation to predict conversion to clinically definite multiple sclerosis. *Brain* 120, 2059–2069 (1997).

908. Baraniskin, A. *et al.* Identification of microRNAs in the cerebrospinal fluid as marker for primary diffuse large B-cell lymphoma of the central nervous system. *Blood* 117, 3140–3146 (2011).

909. Livak, K. J. & Schmittgen, T. D. Analysis of relative gene expression data using real-time quantitative PCR and the 2(-Delta Delta C(T)) Method. *Methods* 25, 402–408 (2001).

910. Lê, S., Josse, J. & Husson, F. FactoMineR: An R Package for Multivariate Analysis. *Journal of Statistical Software* 25, 1–18 (2008).

911. Ratovitski, E. A. Tumor Protein p63/microRNA Network in Epithelial Cancer Cells. *Curr Genomics* 14, 441–452 (2013).

912. Quintana, E. *et al.* miRNAs in cerebrospinal fluid identify patients with MS and specifically those with lipid-specific oligoclonal IgM bands. *Mult Scler* 23, 1716–1726 (2017).

913. de Candia, P. *et al.* Intracellular Modulation, Extracellular Disposal and Serum Increase of MiR-150 Mark Lymphocyte Activation. *PLOS ONE* 8, e75348 (2013).

914. Cox, M. B. *et al.* MicroRNAs miR-17 and miR-20a Inhibit T Cell Activation Genes and Are Under-Expressed in MS Whole Blood. *PLoS One* 5, e12132 (2010).

915. Selmaj, I. *et al.* Global exosome transcriptome profiling reveals biomarkers for multiple sclerosis. *Annals of Neurology* 81, 703–717 (2017).

916. Iwuchukwu, I., Nguyen, D. & Sulaiman, W. MicroRNA Profile in Cerebrospinal Fluid and Plasma of Patients with Spontaneous Intracerebral Hemorrhage. *CNS Neuroscience & Therapeutics* 22, 1015–1018 (2016).

917. Kumar, S. & Reddy, P. H. Are circulating microRNAs peripheral biomarkers for Alzheimer's disease? *Biochimica et Biophysica Acta (BBA) - Molecular Basis of Disease* 1862, 1617–1627 (2016).

918. Lindberg, R. L. P., Hoffmann, F., Mehling, M., Kuhle, J. & Kappos, L. Altered expression of miR-17-5p in CD4+ lymphocytes of relapsing–remitting multiple sclerosis patients. *European Journal of Immunology* 40, 888–898 (2010).

919. Baulina, N. *et al.* Immune-related miRNA expression patterns in peripheral blood mononuclear cells differ in multiple sclerosis relapse and remission. *Journal of Neuroimmunology* 317, 67–76 (2018).

920. Liguori, M. *et al.* Dysregulation of MicroRNAs and Target Genes Networks in Peripheral Blood of Patients With Sporadic Amyotrophic Lateral Sclerosis. *Frontiers in Molecular Neuroscience* 11, (2018).

921. Nuzziello, N. *et al.* Investigating the Role of MicroRNA and Transcription Factor Co-regulatory Networks in Multiple Sclerosis Pathogenesis. *International Journal of Molecular Sciences* 19, 3652 (2018).

922. Riveros, C. *et al.* A Transcription Factor Map as Revealed by a Genome-Wide Gene Expression Analysis of Whole-Blood mRNA Transcriptome in Multiple Sclerosis. *PLOS ONE* 5, e14176 (2010).

923. Zheng, H. *et al.* PLAGL2 Regulates Wnt Signaling to Impede Differentiation in Neural Stem Cells and Gliomas. *Cancer Cell* 17, 497–509 (2010).

924. Berge, T. *et al.* Quantitative proteomic analyses of CD4+ and CD8+ T cells reveal differentially expressed proteins in multiple sclerosis patients and healthy controls. *Clin Proteomics* 16, 19 (2019).

925. Cerutti, C. *et al.* MiR-126 and miR-126* regulate shear-resistant firm leukocyte adhesion to human brain endothelium. *Sci Rep* 7, 45284 (2017).

926. Wang, Z., Han, J., Cui, Y., Zhou, X. & Fan, K. miRNA-21 inhibition enhances RANTES and IP-10 release in MCF-7 via PIAS3 and STAT3 signalling and causes increased lymphocyte migration. *Biochemical and Biophysical Research Communications* 439, 384–389 (2013).

927. Juzenas, S. *et al.* A comprehensive, cell specific microRNA catalogue of human peripheral blood. *Nucleic Acids Research* 45, 9290–9301 (2017).

928. Torri, A. *et al.* Extracellular MicroRNA Signature of Human Helper T Cell Subsets in Health and Autoimmunity *. *Journal of Biological Chemistry* 292, 2903–2915 (2017).

929. Yagi, Y. *et al.* Next-generation sequencing-based small RNA profiling of cerebrospinal fluid exosomes. *Neuroscience Letters* 636, 48–57 (2017).

930. Geraci, F. *et al.* Differences in Intercellular Communication During Clinical Relapse and Gadolinium-Enhanced MRI in Patients With Relapsing Remitting Multiple Sclerosis: A Study of the Composition of Extracellular Vesicles in Cerebrospinal Fluid. *Frontiers in Cellular Neuroscience* 12, (2018).

931. Hiltensperger, M. & Korn, T. The Interleukin (IL)-23/T helper (Th)17 Axis in Experimental Autoimmune Encephalomyelitis and Multiple Sclerosis. *Cold Spring Harb Perspect Med* 8, (2018).

932. Fletcher, J. M. *et al.* CD39 $^{+}$ Foxp3 $^{+}$ Regulatory T Cells Suppress Pathogenic Th17 Cells and Are Impaired in Multiple Sclerosis. *J Immunol* 183, 7602–7610 (2009).

933. Garavelli, S., De Rosa, V. & de Candia, P. The Multifaceted Interface Between Cytokines and microRNAs: An Ancient Mechanism to Regulate the Good and the Bad of Inflammation. *Front. Immunol.* 9, (2018).

934. D'haene, B., Mestdagh, P., Hellemans, J. & Vandesompele, J. miRNA Expression Profiling: From Reference Genes to Global Mean Normalization. in *Next-Generation MicroRNA Expression Profiling Technology: Methods and Protocols* (ed. Fan, J.-B.) 261–272 (Humana Press, 2012). doi:10.1007/978-1-61779-427-8_18.

935. Chang, L., Zhou, G., Soufan, O. & Xia, J. miRNet 2.0: network-based visual analytics for miRNA functional analysis and systems biology. *Nucleic Acids Res* 48, W244–W251 (2020).

936. Chen, Y. & Wang, X. miRDB: an online database for prediction of functional microRNA targets. *Nucleic Acids Res* 48, D127–D131 (2020).

937. Miranda, K. C. *et al.* A pattern-based method for the identification of MicroRNA binding sites and their corresponding heteroduplexes. *Cell* 126, 1203–1217 (2006).

938. Paraskevopoulou, M. D. *et al.* DIANA-microT web server v5.0: service integration into miRNA functional analysis workflows. *Nucleic Acids Res* 41, W169-173 (2013).

939. Sticht, C., De La Torre, C., Parveen, A. & Gretz, N. miRWalk: An online resource for prediction of microRNA binding sites. *PLoS One* 13, e0206239 (2018).

940. Vejnar, C. E. & Zdobnov, E. M. MiRmap: comprehensive prediction of microRNA target repression strength. *Nucleic Acids Res* 40, 11673–11683 (2012).

941. Goertsches, R. H., Hecker, M. & Zettl, U. K. Monitoring of multiple sclerosis immunotherapy. *J Neurol* 255, 48–57 (2008).

942. Hecker, M. *et al.* Interferon-beta therapy in multiple sclerosis: the short-term and long-term effects on the patients' individual gene expression in peripheral blood. *Mol Neurobiol* 48, 737–756 (2013).

943. Libertinova, J. *et al.* Myxovirus Resistance Protein A mRNA Expression Kinetics in Multiple Sclerosis Patients Treated with IFNβ. *PLOS ONE* 12, e0169957 (2017).

944. Matas, E. *et al.* MxA mRNA expression as a biomarker of interferon beta response in multiple sclerosis patients. *Journal of Neuroimmunology* 291, 73–77 (2016).

945. Matas, E. *et al.* Baseline MxA mRNA Expression Predicts Interferon Beta Response in Multiple Sclerosis Patients. *PLoS ONE* 9, e112758 (2014).

946. Serana, F. *et al.* MxA mRNA Quantification and Disability Progression in Interferon Beta-Treated Multiple Sclerosis Patients. *PLOS ONE* 9, e94794 (2014).

947. van der Voort, L. F. *et al.* Spontaneous MxA mRNA level predicts relapses in patients with recently diagnosed MS. *Neurology* 75, 1228–1233 (2010).

948. Bertolotto, A. Neutralizing antibodies to interferon beta: implications for the management of multiple sclerosis. *Curr Opin Neurol* 17, 241–246 (2004).

949. Benveniste, E. N., Liu, Y., McFarland, B. C. & Qin, H. Involvement of the Janus Kinase/Signal Transducer and Activator of Transcription Signaling Pathway in Multiple Sclerosis and the Animal Model of Experimental Autoimmune Encephalomyelitis. *J Interferon Cytokine Res* 34, 577–588 (2014).

950. Conti, L. *et al.* Th17 Cells in Multiple Sclerosis Express Higher Levels of JAK2, Which Increases Their Surface Expression of IFN-γR2. *The Journal of Immunology* 188, 1011–1018 (2012).

951. Chen, C., Liu, X., Wan, B. & Zhang, J. Z. Regulatory Properties of Copolymer I in Th17 Differentiation by Altering STAT3 Phosphorylation1. *The Journal of Immunology* 183, 246–253 (2009).

952. Rojas-Morales, E. *et al.* Differential Transcription of SOCS5 and SOCS7 in Multiple Sclerosis Patients Treated with Interferon Beta or Glatiramer Acetate. *Int J Mol Sci* 21, 218 (2019).

953. Mindur, J. E. *et al.* IL-27: a potential biomarker for responders to glatiramer acetate therapy. *Journal of Neuroimmunology* 304, 21–28 (2017).

954. Sweeney, C. M. *et al.* IL-27 mediates the response to IFN-β therapy in multiple sclerosis patients by inhibiting Th17 cells. *Brain, Behavior, and Immunity* 25, 1170–1181 (2011).

955. Namdar, A., Nikbin, B., Ghabaee, M., Bayati, A. & Izad, M. Effect of IFN-ß therapy on the frequency and function of CD4+CD25+ regulatory T cells and Foxp3 gene expression in relapsing–remitting multiple sclerosis (RRMS): A preliminary study. *Journal of Neuroimmunology* 218, 120–124 (2010).

956. Sellebjerg, F., Krakauer, M., Khademi, M., Olsson, T. & Sørensen, P. S. FOXP3, CBLB and ITCH gene expression and cytotoxic T lymphocyte antigen 4 expression on CD4+CD25high T cells in multiple sclerosis. *Clin Exp Immunol* 170, 149–155 (2012).

957. Dalla Libera, D. *et al.* T Regulatory Cells Are Markers of Disease Activity in Multiple Sclerosis Patients. *PLoS One* 6, e21386 (2011).

958. Etesam, Z. *et al.* Altered Expression of Specific Transcription Factors of Th17 (RORγt, RORα) and Treg Lymphocytes (FOXP3) by Peripheral Blood Mononuclear Cells from Patients with Multiple Sclerosis. *J Mol Neurosci* 60, 94–101 (2016).

959. Min, S. *et al.* TGF-β-associated miR-27a inhibits dendritic cell-mediated differentiation of Th1 and Th17 cells by TAB3, p38 MAPK, MAP2K4 and MAP2K7. *Genes Immun* 13, 621–631 (2012).

960. Hecker, M. *et al.* MicroRNA Expression Changes during Interferon-Beta Treatment in the Peripheral Blood of Multiple Sclerosis Patients. *Int J Mol Sci* 14, 16087–16110 (2013).

961. Ehtesham, N., Khorvash, F. & Kheirollahi, M. miR-145 and miR20a-5p Potentially Mediate Pleiotropic Effects of Interferon-Beta Through Mitogen-Activated Protein Kinase Signaling Pathway in Multiple Sclerosis Patients. *J Mol Neurosci* 61, 16–24 (2017).

962. Xie, M. *et al.* NF-κB-driven miR-34a impairs Treg/Th17 balance via targeting Foxp3. *J Autoimmun* 102, 96–113 (2019).

963. Asirvatham, A. J., Magner, W. J. & Tomasi, T. B. miRNA regulation of cytokine genes. *Cytokine* 45, 58–69 (2009).

964. Salvi, V., Gianello, V., Tiberio, L., Sozzani, S. & Bosisio, D. Cytokine Targeting by miRNAs in Autoimmune Diseases. *Front Immunol* 10, (2019).

965. Jiang, R. *et al.* Inhibition of long non-coding RNA XIST upregulates microRNA-149-3p to repress ovarian cancer cell progression. *Cell Death Dis* 12, 145 (2021).

966. Liu, G. *et al.* Silencing miR-125b-5p attenuates inflammatory response and apoptosis inhibition in mycobacterium tuberculosis-infected human macrophages by targeting DNA damage-regulated autophagy modulator 2 (DRAM2). *Cell Cycle* 19, 3182–3194 (2020).

967. Zou, Q., Yang, M., Yu, M. & Liu, C. Influences of Regulation of miR-126 on Inflammation,Th17/Treg Subpopulation Differentiation, and Lymphocyte Apoptosis through Caspase Signaling Pathway in Sepsis. *Inflammation* 43, 2287–2300 (2020).

968. Yao, R. *et al.* MicroRNA-155 Modulates Treg and Th17 Cells Differentiation and Th17 Cell Function by Targeting SOCS1. *PLoS One* 7, (2012).

969. Dong, L. *et al.* Decreased expression of microRNA-21 correlates with the imbalance of Th17 and Treg cells in patients with rheumatoid arthritis. *J Cell Mol Med* 18, 2213–2224 (2014).

970. Murugaiyan, G. *et al.* MicroRNA-21 promotes Th17 differentiation and mediates experimental autoimmune encephalomyelitis. *J Clin Invest* 125, 1069–1080 (2015).

971. Cui, B. *et al.* Brucella Omp25 Upregulates miR-155, miR-21-5p, and miR-23b to Inhibit Interleukin-12 Production via Modulation of Programmed Death-1 Signaling in Human Monocyte/Macrophages. *Front Immunol* 8, 708 (2017).

972. Lu, T. X., Munitz, A. & Rothenberg, M. E. MicroRNA-21 is up-regulated in allergic airway inflammation and regulates IL-12p35 expression. *J Immunol* 182, 4994–5002 (2009).

973. Li, B. *et al.* miR-146a modulates autoreactive Th17 cell differentiation and regulates organ-specific autoimmunity. *J Clin Invest* 127, 3702–3716 (2017).

974. Ehya, F., Abdul Tehrani, H., Garshasbi, M. & Nabavi, S. M. Identification of miR-24 and miR-137 as novel candidate multiple sclerosis miRNA biomarkers using multi-staged data analysis protocol. *Mol Biol Res Commun* 6, 127–140 (2017).

975. Vistbakka, J., Sumelahti, M.-L., Lehtimäki, T., Elovaara, I. & Hagman, S. Evaluation of serum miR-191-5p, miR-24-3p, miR-128-3p, and miR-376c-3 in multiple sclerosis patients. *Acta Neurol Scand* 138, 130–136 (2018).

976. Hadi, N. *et al.* Study of The Correlation between miR-106a, miR-125b, and miR-330 on Multiple Sclerosis Patients by Targeting TNFSF4 and SP1 in NF-κb/TNF-α Pathway: A Case-Control Study. *Cell J* 24, 403–409 (2022).

977. Søndergaard, H. B., Hesse, D., Krakauer, M., Sørensen, P. S. & Sellebjerg, F. Differential microRNA expression in blood in multiple sclerosis. *Mult Scler* 19, 1849–1857 (2013).

978. Martinelli-Boneschi, F. *et al.* MicroRNA and mRNA expression profile screening in multiple sclerosis patients to unravel novel pathogenic steps and identify potential biomarkers. *Neuroscience Letters* 508, 4–8 (2012).

979. Fancy, S. P. J., Chan, J. R., Baranzini, S. E., Franklin, R. J. M. & Rowitch, D. H. Myelin Regeneration: A Recapitulation of Development? *Annual Review of Neuroscience* 34, 21–43 (2011).

980. Wang, C. *et al.* Lesion activity and chronic demyelination are the major determinants of brain atrophy in MS. *Neurology - Neuroimmunology Neuroinflammation* 6, (2019).

981. Elliott, C. *et al.* Chronic white matter lesion activity predicts clinical progression in primary progressive multiple sclerosis. *Brain* 142, 2787–2799 (2019).

982. Piehl, F. Current and emerging disease-modulatory therapies and treatment targets for multiple sclerosis. *J Intern Med* 289, 771–791 (2021).

983. Bushati, N. & Cohen, S. M. microRNA Functions. *Annual Review of Cell and Developmental Biology* 23, 175–205 (2007).

984. Barca-Mayo, O. & Lu, Q. R. Fine-Tuning Oligodendrocyte Development by microRNAs. *Front Neurosci* 6, 13 (2012).

985. Wang, H. *et al.* miR-219 Cooperates with miR-338 in Myelination and Promotes Myelin Repair in the CNS. *Dev Cell* 40, 566-582.e5 (2017).

986. Bruinsma, I. B. *et al.* Regulator of oligodendrocyte maturation, miR-219, a potential biomarker for MS. *Journal of Neuroinflammation* 14, 235 (2017).

987. Teuber-Hanselmann, S., Meinl, E. & Junker, A. MicroRNAs in gray and white matter multiple sclerosis lesions: impact on pathophysiology. *The Journal of Pathology* 250, 496–509 (2020).

988. Louis, J. C., Magal, E., Muir, D., Manthorpe, M. & Varon, S. CG-4, a new bipotential glial cell line from rat brain, is capable of differentiating in vitro into either mature oligodendrocytes or type-2 astrocytes. *J Neurosci Res* 31, 193–204 (1992).

989. Lourenço, T. *et al.* Modulation of oligodendrocyte differentiation and maturation by combined biochemical and mechanical cues. *Sci Rep* 6, 21563 (2016).

990. O'Meara, R. W., Ryan, S. D., Colognato, H. & Kothary, R. Derivation of enriched oligodendrocyte cultures and oligodendrocyte/neuron myelinating co-cultures from post-natal murine tissues. *J Vis Exp* 3324 (2011) doi:10.3791/3324.

991. Bankhead, P. *et al.* QuPath: Open source software for digital pathology image analysis. *Sci Rep* 7, 16878 (2017).

992. McGeary, S. E. *et al.* The biochemical basis of microRNA targeting efficacy. *Science* 366, eaav1741 (2019).

993. Liu, Z. *et al.* Induction of oligodendrocyte differentiation by Olig2 and Sox10: evidence for reciprocal interactions and dosage-dependent mechanisms. *Dev Biol* 302, 683–693 (2007).

994. Meijer, D. H. *et al.* Separated at birth? The functional and molecular divergence of OLIG1 and OLIG2. *Nat Rev Neurosci* 13, 819–831 (2012).

995. Gard, A. L. & Pfeiffer, S. E. Two proliferative stages of the oligodendrocyte lineage (A2B5+O4- and O4+GalC-) under different mitogenic control. *Neuron* 5, 615–625 (1990).

996. Jurga, A. M., Paleczna, M., Kadluczka, J. & Kuter, K. Z. Beyond the GFAP-Astrocyte Protein Markers in the Brain. *Biomolecules* 11, 1361 (2021).

997. Strzalka, W. & Ziemienowicz, A. Proliferating cell nuclear antigen (PCNA): a key factor in DNA replication and cell cycle regulation. *Ann Bot* 107, 1127–1140 (2011).

998. Gaesser, J. M. & Fyffe-Maricich, S. L. Intracellular signaling pathway regulation of myelination and remyelination in the CNS. *Experimental Neurology* 283, 501–511 (2016).

999. Emery, B. & Lu, Q. R. Transcriptional and Epigenetic Regulation of Oligodendrocyte Development and Myelination in the Central Nervous System. *Cold Spring Harb Perspect Biol* 7, a020461 (2015).

1000. Coelho, R. P., Yuelling, L. M., Fuss, B. & Sato-Bigbee, C. Neurotrophin-3 targets the translational initiation machinery in oligodendrocytes. *Glia* 57, 1754–1764 (2009).

1001. Fletcher, J. L. *et al.* Targeting TrkB with a Brain-Derived Neurotrophic Factor Mimetic Promotes Myelin Repair in the Brain. *J. Neurosci.* 38, 7088–7099 (2018).

1002. Hutagalung, A. H. & Novick, P. J. Role of Rab GTPases in membrane traffic and cell physiology. *Physiological reviews* 91, (2011).

1003. Yazdankhah, M. *et al.* BNIP3L-mediated mitophagy is required for mitochondrial remodeling during the differentiation of optic nerve oligodendrocytes. *Autophagy* 17, 3140–3159 (2021).

1004. Zhang, Z., Zhao, W.-Q., Ma, F., Zhang, H. & Xu, X.-H. Rab10 Disruption Results in Delayed OPC Maturation. *Cell Mol Neurobiol* 37, 1303–1310 (2017).

1005. Fekete, C. D., Horning, R. Z., Doron, M. S. & Nishiyama, A. Cleavage of VAMP2/3 affects oligodendrocyte lineage development in the developing mouse spinal cord. *J. Neurosci.* (2023) doi:10.1523/JNEUROSCI.2206-21.2023.

1006. Lam, M. *et al.* CNS myelination requires VAMP2/3-mediated membrane expansion in oligodendrocytes. *Nat Commun* 13, 5583 (2022).

1007. Sanz-Rodriguez, M. *et al.* R-Ras1 and R-Ras2 Are Essential for Oligodendrocyte Differentiation and Survival for Correct Myelination in the Central Nervous System. *J. Neurosci.* 38, 5096–5110 (2018).

1008. Mikdache, A. *et al.* Elmo1 function, linked to Rac1 activity, regulates peripheral neuronal numbers and myelination in zebrafish. *Cell Mol Life Sci* 77, 161–177 (2020).

1009. Abdul Azeez, K. R., Knapp, S., Fernandes, J. M. P., Klussmann, E. & Elkins, J. M. The crystal structure of the RhoA-AKAP-Lbc DH-PH domain complex. *Biochem J* 464, 231–239 (2014).

1010. Klussmann, E. *et al.* Ht31: the first protein kinase A anchoring protein to integrate protein kinase A and Rho signaling. *FEBS Lett* 507, 264–268 (2001).

1011. Mendez, R. & Richter, J. D. Translational control by CPEB: a means to the end. *Nat Rev Mol Cell Biol* 2, 521–529 (2001).

1012. Mi, S. *et al.* LINGO-1 negatively regulates myelination by oligodendrocytes. *Nat Neurosci* 8, 745–751 (2005).

1013. Sacco, F. *et al.* Tumor Suppressor Density-enhanced Phosphatase-1 (DEP-1) Inhibits the RAS Pathway by Direct Dephosphorylation of ERK1/2 Kinases*. *Journal of Biological Chemistry* 284, 22048–22058 (2009).

1014. Santra, M. *et al.* Thymosin beta 4 up-regulates miR-200a expression and induces differentiation and survival of rat brain progenitor cells. *J Neurochem* 136, 118–132 (2016).

1015. Schneble, N. *et al.* The protein-tyrosine phosphatase DEP-1 promotes migration and phagocytic activity of microglial cells in part through negative regulation of fyn tyrosine kinase. *Glia* 65, 416–428 (2017).

1016. Tsuboi, N. *et al.* The tyrosine phosphatase CD148 interacts with the p85 regulatory subunit of phosphoinositide 3-kinase. *Biochem J* 413, 193–200 (2008).

1017. Yang, S. & Kim, H.-M. The RhoA-ROCK-PTEN pathway as a molecular switch for anchorage dependent cell behavior. *Biomaterials* 33, 2902–2915 (2012).

1018. Zhang, S. *et al.* AKAP13 couples GPCR signaling to mTORC1 inhibition. *PLOS Genetics* 17, e1009832 (2021).

1019. Choi, Y. J. & Anders, L. Signaling through cyclin D-dependent kinases. *Oncogene* 33, 1890–1903 (2014).

1020. Di Maio, R. *et al.* LRRK2 activation in idiopathic Parkinson's disease. *Sci. Transl. Med.* 10, eaar5429 (2018).

1021. Ridge, P. G. *et al.* Linkage, whole genome sequence, and biological data implicate variants in RAB10 in Alzheimer's disease resilience. *Genome Med* 9, 100 (2017).

1022. Huang, Y. *et al.* Tropomyosin Receptor Kinase B Expressed in Oligodendrocyte Lineage Cells Functions to Promote Myelin Following a Demyelinating Lesion. *ASN Neuro* 12, 1759091420957464 (2020).

1023. Shan, B.-Q. *et al.* miR-33-3p Regulates PC12 Cell Proliferation and Differentiation In Vitro by Targeting Slc29a1. *Neurochem Res* 46, 2403–2414 (2021).

1024. Honsho, M., Asaoku, S. & Fujiki, Y. Posttranslational Regulation of Fatty Acyl-CoA Reductase 1, Far1, Controls Ether Glycerophospholipid Synthesis*♦. *Journal of Biological Chemistry* 285, 8537–8542 (2010).

1025. Gerin, I. *et al.* Expression of miR-33 from an SREBP2 Intron Inhibits Cholesterol Export and Fatty Acid Oxidation *. *Journal of Biological Chemistry* 285, 33652–33661 (2010).

1026. Sung, H. Y. *et al.* Protective role of ABCA1 in ischemic preconditioning is mediated by downregulation of miR-33-5p and miR-135-5p. *Sci Rep* 11, 12511 (2021).

1027. Tepavčević, V. Oligodendroglial Energy Metabolism and (re)Myelination. *Life* 11, 238 (2021).

1028. Itoh, T., Itoh, A. & Pleasure, D. Bcl-2-related protein family gene expression during oligodendroglial differentiation. *J Neurochem* 85, 1500–1512 (2003).

1029. Pei, Z. *et al.* The expression and roles of Nde1 and Ndel1 in the adult mammalian central nervous system. *Neuroscience* 271, 119–136 (2014).

1030. Hu, S. *et al.* MicroRNA-34c Downregulation Ameliorates Amyloid-β-Induced Synaptic Failure and Memory Deficits by Targeting VAMP2. *J Alzheimers Dis* 48, 673–686 (2015).

1031. Pham, E. *et al.* Progressive accumulation of amyloid-β oligomers in Alzheimer's disease and APP transgenic mice is accompanied by selective alterations in synaptic scaffold proteins. *FEBS J* 277, 3051–3067 (2010).

1032. Kao, Y.-C., Wang, I.-F. & Tsai, K.-J. miRNA-34c Overexpression Causes Dendritic Loss and Memory Decline. *International Journal of Molecular Sciences* 19, 2323 (2018).

1033. Jauhari, A., Singh, T., Singh, P., Parmar, D. & Yadav, S. Regulation of miR-34 Family in Neuronal Development. *Mol Neurobiol* 55, 936–945 (2018).

1034. Miñones-Moyano, E. *et al.* MicroRNA profiling of Parkinson's disease brains identifies early downregulation of miR-34b/c which modulate mitochondrial function. *Human Molecular Genetics* 20, 3067–3078 (2011).

1035. Tu, Y. & Hu, Y. MiRNA-34c-5p protects against cerebral ischemia/reperfusion injury: involvement of anti-apoptotic and anti-inflammatory activities. *Metab Brain Dis* 36, 1341–1351 (2021).

1036. Nobs, L. *et al.* Stage-specific requirement for cyclin D1 in glial progenitor cells of the cerebral cortex. *Glia* 62, 829–839 (2014).

1037. Noble, M., Murray, K., Stroobant, P., Waterfield, M. D. & Riddle, P. Platelet-derived growth factor promotes division and motility and inhibits premature differentiation of the oligodendrocyte/type-2 astrocyte progenitor cell. *Nature* 333, 560–562 (1988).

1038. Bai, C., Gao, Y., Zhang, X., Yang, W. & Guan, W. MicroRNA-34c acts as a bidirectional switch in the maturation of insulin-producing cells derived from mesenchymal stem cells. *Oncotarget* 8, 106844–106857 (2017).

1039. Wei, H. *et al.* miR-34c-5p targets Notch1 and suppresses the metastasis and invasion of cervical cancer. *Mol Med Rep* 23, 120 (2021).

1040. Baldassarro, V. A. *et al.* Nerve growth factor promotes differentiation and protects the oligodendrocyte precursor cells from in vitro hypoxia/ischemia. *Front Neurosci* 17, 1111170 (2023).

1041. Kumar, S., Kahn, M. A., Dinh, L. & de Vellis, J. NT-3-mediated TrkC receptor activation promotes proliferation and cell survival of rodent progenitor oligodendrocyte cells in vitro and in vivo. *J Neurosci Res* 54, 754–765 (1998).

1042. Wang, Y., Wang, X., Tang, J., Su, X. & Miao, Y. The study of mechanism of miR-34c-5p targeting FLOT2 to regulate proliferation, migration and invasion of osteosarcoma cells. *Artif Cells Nanomed Biotechnol* 47, 3559–3568 (2019).

1043. Wu, Z. *et al.* Differential effects of miR-34c-3p and miR-34c-5p on the proliferation, apoptosis and invasion of glioma cells. *Oncol Lett* 6, 1447–1452 (2013).

1044. Alcover-Sanchez, B., Garcia-Martin, G., Wandosell, F. & Cubelos, B. R-Ras GTPases Signaling Role in Myelin Neurodegenerative Diseases. *International Journal of Molecular Sciences* 21, 5911 (2020).

1045. Dutta, R. *et al.* Hippocampal demyelination and memory dysfunction are associated with increased levels of the neuronal microRNA miR-124 and reduced AMPA receptors. *Ann Neurol* 73, 637–645 (2013).

1046. Cheng, L.-C., Pastrana, E., Tavazoie, M. & Doetsch, F. miR-124 regulates adult neurogenesis in the subventricular zone stem cell niche. *Nat Neurosci* 12, 399–408 (2009).

1047. Lim, L. P. *et al.* Microarray analysis shows that some microRNAs downregulate large numbers of target mRNAs. *Nature* 433, 769–773 (2005).

1048. Chen, Q. *et al.* MiR-124-5p inhibits the growth of high-grade gliomas through posttranscriptional regulation of LAMB1. *Neuro-Oncology* 16, 637–651 (2014).

1049. Wang, R.-K. *et al.* MicroRNA-124-5p delays the progression of cerebral aneurysm by regulating FoxO1. *Exp Ther Med* 22, 1172 (2021).

1050. Cohen, J. L. *et al.* Differential stress induced c-Fos expression and identification of region-specific miRNA-mRNA networks in the dorsal raphe and amygdala of high-responder/low-responder rats. *Behavioural Brain Research* 319, 110–123 (2017).

1051. Raju, C. S. *et al.* In Cultured Oligodendrocytes the A/B-type hnRNP CBF-A Accompanies MBP mRNA Bound to mRNA Trafficking Sequences. *MBoC* 19, 3008–3019 (2008).

1052. Tominaga, K. *et al.* Tip60/KAT5 Histone Acetyltransferase Is Required for Maintenance and Neurogenesis of Embryonic Neural Stem Cells. *Int J Mol Sci* 24, 2113 (2023).

1053. Aprato, J. *et al.* Myrf guides target gene selection of transcription factor Sox10 during oligodendroglial development. *Nucleic Acids Research* 48, 1254–1270 (2020).

1054. Lee, H. K. *et al.* MicroRNA-145 Is Downregulated in Glial Tumors and Regulates Glioma Cell Migration by Targeting Connective Tissue Growth Factor. *PLOS ONE* 8, e54652 (2013).

1055. Rani, S. B. *et al.* MiR-145 functions as a tumor-suppressive RNA by targeting Sox9 and adducin 3 in human glioma cells. *Neuro-Oncology* 15, 1302–1316 (2013).

1056. Yamamoto, Y. *et al.* Myelin-associated oligodendrocytic basic protein is essential for normal arrangement of the radial component in central nervous system myelin. *European Journal of Neuroscience* 11, 847–855 (1999).

1057. Chen, W. *et al.* Schwann Cell-Like Cells Derived from Human Amniotic Mesenchymal Stem Cells Promote Peripheral Nerve Regeneration through a MicroRNA-214/c-Jun Pathway. *Stem Cells Int* 2019, 2490761 (2019).

1058. Mellios, N. *et al.* MeCP2-regulated miRNAs control early human neurogenesis through differential effects on ERK and AKT signaling. *Mol Psychiatry* 23, 1051–1065 (2018).

1059. Shu, P. *et al.* MicroRNA-214 modulates neural progenitor cell differentiation by targeting Quaking during cerebral cortex development. *Sci Rep* 7, 8014 (2017).

1060. Wu, Q. *et al.* Neuroprotection of miR-214 against isoflurane-induced neurotoxicity involves the PTEN/PI3K/Akt pathway in human neuroblastoma cell line SH-SY5Y. *Archives of Biochemistry and Biophysics* 678, 108181 (2019).

1061. Zhang, M. *et al.* Up-regulating microRNA-214-3p relieves hypoxic–ischemic brain damage through inhibiting TXNIP expression. *Mol Cell Biochem* 478, 597–608 (2023).

1062. Zhang, Y. *et al.* MiR-214-3p attenuates cognition defects via the inhibition of autophagy in SAMP8 mouse model of sporadic Alzheimer's disease. *Neurotoxicology* 56, 139–149 (2016).

1063. Zhang, J. *et al.* AKT activation by N-cadherin regulates beta-catenin signaling and neuronal differentiation during cortical development. *Neural Dev* 8, 7 (2013).

1064. Tang, S.-L., Gao, Y.-L. & Chen, X.-B. MicroRNA-214 targets PCBP2 to suppress the proliferation and growth of glioma cells. *Int J Clin Exp Pathol* 8, 12571–12576 (2015).

1065. Wang, S. *et al.* Combined aberrant expression of microRNA-214 and UBC9 is an independent unfavorable prognostic factor for patients with gliomas. *Med Oncol* 31, 767 (2014).

1066. Aya-Bonilla, C. *et al.* In silico analyses reveal common cellular pathways affected by loss of heterozygosity (LOH) events in the lymphomagenesis of Non-Hodgkin's lymphoma (NHL). *BMC Genomics* 15, 390 (2014).

1067. Berset, T. A., Hoier, E. F. & Hajnal, A. The C. elegans homolog of the mammalian tumor suppressor Dep-1/Scc1 inhibits EGFR signaling to regulate binary cell fate decisions. *Genes Dev* 19, 1328–1340 (2005).

1068. Bestman, J. E. & Cline, H. T. The RNA binding protein CPEB regulates dendrite morphogenesis and neuronal circuit assembly in vivo. *Proc Natl Acad Sci U S A* 105, 20494–20499 (2008).

1069. Yin, J. *et al.* CPEB1 modulates differentiation of glioma stem cells via downregulation of HES1 and SIRT1 expression. *Oncotarget* 5, 6756–6769 (2014).

1070. Tan, D. *et al.* Inhibition of RhoA-Subfamily GTPases Suppresses Schwann Cell Proliferation Through Regulating AKT Pathway Rather Than ROCK Pathway. *Front Cell Neurosci* 12, 437 (2018).

1071. Wang, H. *et al.* Dual efficacy of Fasudil at improvement of survival and reinnervation of flap through RhoA/ROCK/PI3K/Akt pathway. *Int Wound J* 19, 2000–2011 (2022).

1072. Su, Y., Li, Z., Rang, X., Wang, Y. & Fu, J. Integrated Analysis and Identification of CSF-Derived Risk miRNAs and Pivotal Genes in Multiple Sclerosis. *J Mol Neurosci* 72, 1916–1928 (2022).

1073. Keller, A. *et al.* Multiple sclerosis: microRNA expression profiles accurately differentiate patients with relapsing-remitting disease from healthy controls. *PLoS One* 4, e7440 (2009).

1074. Rezaeepoor, M. *et al.* Semaphorin-3A as An Immune Modulator Is Suppressed by MicroRNA-145-5p. *Cell J* 20, 113–119 (2018).

1075. Sabaie, H. *et al.* Identification of potential regulatory long non-coding RNA-associated competing endogenous RNA axes in periplaque regions in multiple sclerosis. *Front Genet* 13, 1011350 (2022).

1076. Smirnova, E. V. *et al.* Comprehensive Atlas of the Myelin Basic Protein Interaction Landscape. *Biomolecules* 11, 1628 (2021).

1077. Varma-Doyle, A. V., Lukiw, W. J., Zhao, Y., Lovera, J. & Devier, D. A hypothesis-generating scoping review of miRs identified in both multiple sclerosis and dementia, their protein targets, and miR signaling pathways. *Journal of the Neurological Sciences* 420, (2021).

1078. Liu, W., Gao, Y. & Chang, N. Nurr1 overexpression exerts neuroprotective and anti-inflammatory roles via down-regulating CCL2 expression in both in vivo and in vitro Parkinson's disease models. *Biochem Biophys Res Commun* 482, 1312–1319 (2017).

1079. Xie, X. *et al.* miR-145-5p/Nurr1/TNF-α Signaling-Induced Microglia Activation Regulates Neuron Injury of Acute Cerebral Ischemic/Reperfusion in Rats. *Front Mol Neurosci* 10, 383 (2017).

1080. Montarolo, F., Perga, S., Martire, S. & Bertolotto, A. Nurr1 reduction influences the onset of chronic EAE in mice. *Inflamm Res* 64, 841–844 (2015).

1081. Pansieri, J., Pisa, M., Yates, R. L., Esiri, M. M. & DeLuca, G. C. A potential protective role of the nuclear receptor-related factor 1 (Nurr1) in multiple sclerosis motor cortex: a neuropathological study. *Brain Commun* 5, fcad072 (2023).

1082. de la Fuente, A. G. *et al.* Vitamin D receptor–retinoid X receptor heterodimer signaling regulates oligodendrocyte progenitor cell differentiation. *J Cell Biol* 211, 975–985 (2015).

1083. Gomez-Pinedo, U. *et al.* Vitamin D increases remyelination by promoting oligodendrocyte lineage differentiation. *Brain Behav* 10, e01498 (2020).

1084. Li, N. *et al.* Vitamin D Promotes Remyelination by Suppressing c-Myc and Inducing Oligodendrocyte Precursor Cell Differentiation after Traumatic Spinal Cord Injury. *Int J Biol Sci* 18, 5391–5404 (2022).

1085. Mengozzi, M., Hesketh, A., Bucca, G., Ghezzi, P. & Smith, C. P. Vitamins D3 and D2 have marked but different global effects on gene expression in a rat oligodendrocyte precursor cell line. *Mol Med* 26, 32 (2020).

1086. Furusho, M., Kaga, Y., Ishii, A., Hébert, J. M. & Bansal, R. Fibroblast Growth Factor Signaling Is Required for the Generation of Oligodendrocyte Progenitors from the Embryonic Forebrain. *J. Neurosci.* 31, 5055–5066 (2011).

1087. Tian, J. *et al.* MiR-223-3p inhibits inflammation and pyroptosis in monosodium urate-induced rats and fibroblast-like synoviocytes by targeting NLRP3. *Clin Exp Immunol* 204, 396–410 (2021).

1088. Zheng, S. *et al.* Human Umbilical Cord Mesenchymal Stem Cells Inhibit Pyroptosis of Renal Tubular Epithelial Cells through miR-342-3p/Caspase1 Signaling Pathway in Diabetic Nephropathy. *Stem Cells Int* 2023, 5584894 (2023).

1089. Galloway, D. A. *et al.* Investigating the NLRP3 inflammasome and its regulator miR-223-3p in multiple sclerosis and experimental demyelination. *Journal of Neurochemistry* 163, 94–112 (2022).

1090. Kim, D. *et al.* Anti-inflammatory Roles of Glucocorticoids Are Mediated by Foxp3+ Regulatory T Cells via a miR-342-Dependent Mechanism. *Immunity* 53, 581-596.e5 (2020).

1091. Chen, K., Fang, H. & Xu, N. LncRNA LOXL1-AS1 is transcriptionally activated by JUND and contributes to osteoarthritis progression via targeting the miR-423-5p/KDM5C axis. *Life Sci* 258, 118095 (2020).

1092. Hou, Y. *et al.* Protective mechanism of apigenin in diabetic nephropathy is related to its regulation of miR-423-5P-USF2 axis. *Am J Transl Res* 13, 2006–2020 (2021).

1093. Wu, X., Fan, D. & Chen, B. LncRNA NEAT1 Accelerates the Proliferation, Oxidative Stress, Inflammation, and Fibrosis and Suppresses the Apoptosis Through the miR-423-5p/GLIPR2 Axis in Diabetic Nephropathy. *J Cardiovasc Pharmacol* 79, 342–354 (2022).

1094. Mu, X., Wang, H. & Li, H. Silencing of long noncoding RNA H19 alleviates pulmonary injury, inflammation, and fibrosis of acute respiratory distress syndrome through regulating the microRNA-423-5p/FOXA1 axis. *Exp Lung Res* 47, 183–197 (2021).

1095. Wang, M., Guo, J., Zhao, Y.-Q. & Wang, J.-P. IL-21 mediates microRNA-423-5p /claudin-5 signal pathway and intestinal barrier function in inflammatory bowel disease. *Aging (Albany NY)* 12, 16099–16110 (2020).

1096. Chugh, P. & Dittmer, D. P. Potential Pitfalls in microRNA Profiling. *Wiley Interdiscip Rev RNA* 3, 601–616 (2012).

1097. Schwarzenbach, H., da Silva, A. M., Calin, G. & Pantel, K. Data Normalization Strategies for MicroRNA Quantification. *Clinical Chemistry* 61, 1333–1342 (2015).

1098. Mestdagh, P. *et al.* A novel and universal method for microRNA RT-qPCR data normalization. *Genome Biol* 10, R64 (2009).

1099. Takousis, P. *et al.* Differential expression of microRNAs in Alzheimer's disease brain, blood, and cerebrospinal fluid. *Alzheimer's & Dementia* 15, 1468–1477 (2019).

1100. Zhao, Y. *et al.* The Potential Markers of Circulating microRNAs and long non-coding RNAs in Alzheimer's Disease. *Aging Dis* 10, 1293–1301 (2019).

1101. Gui, Y., Liu, H., Zhang, L., Lv, W. & Hu, X. Altered microRNA profiles in cerebrospinal fluid exosome in Parkinson disease and Alzheimer disease. *Oncotarget* 6, 37043–37053 (2015).

1102. Arora, T. *et al.* Dysregulated miRNAs in Progression and Pathogenesis of Alzheimer's Disease. *Mol Neurobiol* 59, 6107–6124 (2022).

1103. Santos-Lobato, B. L., Vidal, A. F. & Ribeiro-dos-Santos, Â. Regulatory miRNA–mRNA Networks in Parkinson's Disease. *Cells* 10, 1410 (2021).

1104. Goh, S. Y., Chao, Y. X., Dheen, S. T., Tan, E.-K. & Tay, S. S.-W. Role of MicroRNAs in Parkinson's Disease. *Int J Mol Sci* 20, 5649 (2019).

1105. Piancone, F., La Rosa, F., Marventano, I., Saresella, M. & Clerici, M. The Role of the Inflammasome in Neurodegenerative Diseases. *Molecules* 26, 953 (2021).

1106. Fazeli, S. *et al.* A compound downregulation of SRRM2 and miR-27a-3p with upregulation of miR-27b-3p in PBMCs of Parkinson's patients is associated with the early stage onset of disease. *PLoS One* 15, e0240855 (2020).

1107. Kim, J. *et al.* miR-27a and miR-27b regulate autophagic clearance of damaged mitochondria by targeting PTEN-induced putative kinase 1 (PINK1). *Mol Neurodegener* 11, 55 (2016).

1108. Smith, K. M. *et al.* miR-29ab1-deficiency Identifies a Negative Feedback Loop Controlling Th1 Bias that is Dysregulated in Multiple Sclerosis. *J Immunol* 189, 1567–1576 (2012).

1109. Bolandi, Z. *et al.* In vitro naive CD4+ T cell differentiation upon treatment with miR-29b-loaded exosomes from mesenchymal stem cells. *Mol Biol Rep* (2023) doi:10.1007/s11033-023-08767-w.

1110. Satoh, J.-I., Kino, Y. & Niida, S. MicroRNA-Seq Data Analysis Pipeline to Identify Blood Biomarkers for Alzheimer's Disease from Public Data. *Biomark Insights* 10, 21–31 (2015).

1111. Han, L. *et al.* Association of the serum microRNA-29 family with cognitive impairment in Parkinson's disease. *Aging (Albany NY)* 12, 13518–13528 (2020).

1112. Bai, X. *et al.* Downregulation of blood serum microRNA 29 family in patients with Parkinson's disease. *Sci Rep* 7, 5411 (2017).

1113. Ma, W. *et al.* Serum miR-221 serves as a biomarker for Parkinson's disease. *Cell Biochemistry and Function* 34, 511–515 (2016).

1114. Wang, R., Yang, Y., Wang, H., He, Y. & Li, C. MiR-29c protects against inflammation and apoptosis in Parkinson's disease model in vivo and in vitro by targeting SP1. *Clinical and Experimental Pharmacology and Physiology* 47, 372–382 (2020).

1115. Wang, R. *et al.* miR-29c-3p inhibits microglial NLRP3 inflammasome activation by targeting NFAT5 in Parkinson's disease. *Genes Cells* 25, 364–374 (2020).

1116. Wang, W., Lv, R., Zhang, J. & Liu, Y. circSAMD4A participates in the apoptosis and autophagy of dopaminergic neurons via the miR-29c-3p-mediated AMPK/mTOR pathway in Parkinson's disease. *Mol Med Rep* 24, 540 (2021).

1117. Lei, X., Lei, L., Zhang, Z., Zhang, Z. & Cheng, Y. Downregulated miR-29c correlates with increased BACE1 expression in sporadic Alzheimer's disease. *Int J Clin Exp Pathol* 8, 1565–1574 (2015).

1118. Liu, Z., Zhang, H., Sun, L., Zhu, K. & Lang, W. miR-29c-3p Increases Cell Viability and Suppresses Apoptosis by Regulating the TNFAIP1/NF-κB Signaling Pathway via TNFAIP1 in Aβ-Treated Neuroblastoma Cells. *Neurochem Res* 45, 2375–2384 (2020).

1119. Huo, X. *et al.* LINC00667 regulates MPP+-induced neuronal injury in Parkinson's disease. *Ann Clin Transl Neurol* 9, 707–721 (2022).

1120. Zovoilis, A. *et al.* microRNA-34c is a novel target to treat dementias. *EMBO J* 30, 4299–4308 (2011).

1121. Shi, Z. *et al.* Increased miR-34c mediates synaptic deficits by targeting synaptotagmin 1 through ROS-JNK-p53 pathway in Alzheimer's Disease. *Aging Cell* 19, e13125 (2020).

1122. Starhof, C. *et al.* The biomarker potential of cell-free microRNA from cerebrospinal fluid in Parkinsonian Syndromes. *Movement Disorders* 34, 246–254 (2019).

1123. Yan, W., Chen, Z.-Y., Chen, J.-Q. & Chen, H.-M. BMP2 promotes the differentiation of neural stem cells into dopaminergic neurons in vitro via miR-145-mediated upregulation of Nurr1 expression. *Am J Transl Res* 8, 3689–3699 (2016).

1124. Ye, Y. *et al.* Downregulation of MicroRNA-145-5p in Activated Microglial Exosomes Promotes Astrocyte Proliferation by Removal of Smad3 Inhibition. *Neurochem Res* 47, 382–393 (2022).

1125. Jakaria, M. *et al.* Molecular Insights into NR4A2(Nurr1): an Emerging Target for Neuroprotective Therapy Against Neuroinflammation and Neuronal Cell Death. *Mol Neurobiol* 56, 5799–5814 (2019).

1126. Kadkhodaei, B. *et al.* Transcription factor Nurr1 maintains fiber integrity and nuclear-encoded mitochondrial gene expression in dopamine neurons. *Proc Natl Acad Sci U S A* 110, 2360–2365 (2013).

1127. Kadkhodaei, B. *et al.* Nurr1 is required for maintenance of maturing and adult midbrain dopamine neurons. *J Neurosci* 29, 15923–15932 (2009).

1128. Saucedo-Cardenas, O. *et al.* Nurr1 is essential for the induction of the dopaminergic phenotype and the survival of ventral mesencephalic late dopaminergic precursor neurons. *Proc Natl Acad Sci U S A* 95, 4013–4018 (1998).

1129. Le, W. *et al.* Decreased NURR1 gene expression in patients with Parkinson's disease. *J Neurol Sci* 273, 29–33 (2008).

1130. Le, W. *et al.* Mutations in NR4A2 associated with familial Parkinson disease. *Nat Genet* 33, 85–89 (2003).

1131. Moon, M. *et al.* Correlation between orphan nuclear receptor Nurr1 expression and amyloid deposition in 5XFAD mice, an animal model of Alzheimer's disease. *J Neurochem* 132, 254–262 (2015).

1132. Satoh, J. *et al.* Microarray analysis identifies an aberrant expression of apoptosis and DNA damage-regulatory genes in multiple sclerosis. *Neurobiol Dis* 18, 537–550 (2005).

1133. Gilli, F. *et al.* Loss of Braking Signals During Inflammation: A Factor Affecting the Development and Disease Course of Multiple Sclerosis. *Archives of Neurology* 68, 879–888 (2011).

1134. Montarolo, F. *et al.* Effects of isoxazolo-pyridinone 7e, a potent activator of the Nurr1 signaling pathway, on experimental autoimmune encephalomyelitis in mice. *PLoS One* 9, e108791 (2014).

1135. Shu, Y., Qian, J. & Wang, C. Aberrant expression of microRNA-132-3p and microRNA-146a-5p in Parkinson's disease patients. *Open Life Sci* 15, 647–653 (2020).

1136. Caggiu, E. *et al.* Differential expression of miRNA 155 and miRNA 146a in Parkinson's disease patients. *eNeurologicalSci* 13, 1–4 (2018).

1137. Guo, L. *et al.* Celastrol attenuates 6-hydroxydopamine-induced neurotoxicity by regulating the miR-146a/PI3K/Akt/mTOR signaling pathways in differentiated rat pheochromocytoma cells. *Journal of Affective Disorders* 316, 233–242 (2022).

1138. Zhan-Qiang, H. *et al.* miR-146a aggravates cognitive impairment and Alzheimer disease-like pathology by triggering oxidative stress through MAPK signaling. *Neurologia (Engl Ed)* S0213-4853(21)00022–0 (2021) doi:10.1016/j.nrl.2020.12.006.

1139. Lei, B. *et al.* NF-κB-Induced Upregulation of miR-146a-5p Promoted Hippocampal Neuronal Oxidative Stress and Pyroptosis via TIGAR in a Model of Alzheimer's Disease. *Front Cell Neurosci* 15, 653881 (2021).

1140. Chanda, K., Jana, N. R. & Mukhopadhyay, D. Receptor tyrosine kinase ROR1 ameliorates Aβ1-42 induced cytoskeletal instability and is regulated by the miR146a-NEAT1 nexus in Alzheimer's disease. *Sci Rep* 11, 19254 (2021).

1141. Fan, Y. *et al.* Epigenetic transcripts of LINC01311 and hsa-miR-146a-5p regulate neural development in a cellular model of Alzheimer's disease. *IUBMB Life* 73, 916–926 (2021).

1142. Sierksma, A. *et al.* Deregulation of neuronal miRNAs induced by amyloid-β or TAU pathology. *Mol Neurodegener* 13, 54 (2018).

1143. Prada, I. *et al.* Glia-to-neuron transfer of miRNAs via extracellular vesicles: a new mechanism underlying inflammation-induced synaptic alterations. *Acta Neuropathol* 135, 529–550 (2018).

1144. Liang, C. *et al.* MicroRNA-146a switches microglial phenotypes to resist the pathological processes and cognitive degradation of Alzheimer's disease. *Theranostics* 11, 4103–4121 (2021).

1145. Fernandes, A. *et al.* Differences in Immune-Related Genes Underlie Temporal and Regional Pathological Progression in 3xTg-AD Mice. *Cells* 11, 137 (2022).

1146. Thome, A. D., Harms, A. S., Volpicelli-Daley, L. A. & Standaert, D. G. microRNA-155 Regulates Alpha-Synuclein-Induced Inflammatory Responses in Models of Parkinson Disease. *J Neurosci* 36, 2383–2390 (2016).

1147. Lv, R. *et al.* Rosmarinic Acid Alleviates Inflammation, Apoptosis, and Oxidative Stress through Regulating miR-155-5p in a Mice Model of Parkinson's Disease. *ACS Chem Neurosci* 11, 3259–3266 (2020).

1148. Liu, D. *et al.* Inhibition of microRNA-155 Alleviates Cognitive Impairment in Alzheimer's Disease and Involvement of Neuroinflammation. *Curr Alzheimer Res* 16, 473–482 (2019).

1149. Guedes, J. R. *et al.* Early miR-155 upregulation contributes to neuroinflammation in Alzheimer's disease triple transgenic mouse model. *Hum Mol Genet* 23, 6286–6301 (2014).

1150. Wang, W. *et al.* MicroRNA-155-5p Targets SKP2, Activates IKKβ, Increases Aβ Aggregation, and Aggravates a Mouse Alzheimer Disease Model. *J Neuropathol Exp Neurol* 81, 16–26 (2022).

1151. Aloi, M. S. *et al.* The pro-inflammatory microRNA miR-155 influences fibrillar β-Amyloid1-42 catabolism by microglia. *Glia* 69, 1736–1748 (2021).

1152. Dong, H. *et al.* A panel of four decreased serum microRNAs as a novel biomarker for early Parkinson's disease. *Biomarkers* 21, 129–137 (2016).

1153. Li, L. *et al.* Long noncoding RNA BACE1-antisense transcript plays a critical role in Parkinson's disease via microRNA-214-3p/Cell death-inducing p53-target protein 1 axis. *Bioengineered* 13, 10889–10901 (2022).

1154. Liao, Y. *et al.* HSF1 inhibits microglia activation to attenuate neuroinflammation via regulating miR-214-3p and NFATc2 in Parkinson's disease. *Folia Neuropathol* 61, 53–67 (2023).

1155. Yu, D. *et al.* FREMSA: A Method That Provides Direct Evidence of the Interaction between microRNA and mRNA. *Methods Mol Biol* 2102, 557–566 (2020).

1156. Solé, A., Mencia, N., Villalobos, X., Noé, V. & Ciudad, C. J. Validation of miRNA-mRNA interactions by electrophoretic mobility shift assays. *BMC Research Notes* 6, 454 (2013).

1157. Clément, T., Salone, V. & Rederstorff, M. Dual Luciferase Gene Reporter Assays to Study miRNA Function. in *Small Non-Coding RNAs: Methods and Protocols* (ed. Rederstorff, M.) 187–198 (Springer, 2015). doi:10.1007/978-1-4939-2547-6_17.

1158. Babion, I. *et al.* miR-9-5p Exerts a Dual Role in Cervical Cancer and Targets Transcription Factor TWIST1. *Cells* 9, (2019).

1159. Zhang, Y.-C. *et al.* Genetically Determined Levels of mTOR-Dependent Circulating Proteins and Risk of Multiple Sclerosis. *Neurol Ther* 12, 751–762 (2023).

1160. Akbarian, F. *et al.* Upregulation of MTOR, RPS6KB1, and EIF4EBP1 in the whole blood samples of Iranian patients with multiple sclerosis compared to healthy controls. *Metab Brain Dis* 35, 1309–1316 (2020).

1161. Di Mitri, D. *et al.* The p38 mitogen-activated protein kinase cascade modulates T helper type 17 differentiation and functionality in multiple sclerosis. *Immunology* 146, 251–263 (2015).

1162. Noubade, R. *et al.* Activation of p38 MAPK in CD4 T cells controls IL-17 production and autoimmune encephalomyelitis. *Blood* 118, 3290–3300 (2011).

1163. Song, F. *et al.* Complexity of trophic factor signaling in experimental autoimmune encephalomyelitis: differential expression of neurotrophic and gliotrophic factors. *J Neuroimmunol* 262, 11–18 (2013).

1164. Yalın, O. Ö. *et al.* Novel SNARE Complex Polymorphisms Associated with Multiple Sclerosis: Signs of Synaptopathy in Multiple Sclerosis. *Balkan Med J* 36, 174–178 (2019).

1165. Jahanbazi Jahan-Abad, A., Salapa, H. E., Libner, C. D., Thibault, P. A. & Levin, M. C. hnRNP A1 dysfunction in oligodendrocytes contributes to the pathogenesis of multiple sclerosis. *Glia* 71, 633–647 (2023).

1166. Libner, C. D. *et al.* Autoimmunity to a ribonucleoprotein drives neuron loss in multiple sclerosis models. *Neurobiol Dis* 170, 105775 (2022).

1167. Clarke, J.-P. W. E. *et al.* Multiple Sclerosis-Associated hnRNPA1 Mutations Alter hnRNPA1 Dynamics and Influence Stress Granule Formation. *Int J Mol Sci* 22, 2909 (2021).

1168. Salapa, H. E., Hutchinson, C., Popescu, B. F. & Levin, M. C. Neuronal RNA-binding protein dysfunction in multiple sclerosis cortex. *Ann Clin Transl Neurol* 7, 1214–1224 (2020).

1169. Zhou, Y. *et al.* LncRNA BACE1-AS Promotes Autophagy-Mediated Neuronal Damage Through The miR-214-3p/ATG5 Signalling Axis In Alzheimer's Disease. *Neuroscience* 455, 52–64 (2021).

1170. Liu, J., Zhang, H., Di, K., Hou, L. & Yu, S. Circular noncoding RNA circ_0007865, serves as a competing endogenous RNA, targeting the miR-214-3p/FKBP5 axis to regulate oxygen-glucose deprivation-induced injury in brain microvascular endothelial cells. *NeuroReport* 33, 163 (2022).

1171. Wu, W. *et al.* Astrocyte-derived exosome-transported microRNA-34c is neuroprotective against cerebral ischemia/reperfusion injury via TLR7 and the NF-κB/MAPK pathways. *Brain Res Bull* 163, 84–94 (2020).

1172. Xiao, W., Jiang, Z., Wan, W., Pan, W. & Xu, J. miR-145-5p targets MMP2 to protect brain injury in hypertensive intracerebral hemorrhage via inactivation of the Wnt/β-catenin signaling pathway. *Ann Transl Med* 10, 571 (2022).

1173. Hu, S. *et al.* Long-term iTBS Improves Neural Functional Recovery by Reducing the Inflammatory Response and Inhibiting Neuronal Apoptosis Via miR-34c-5p/p53/Bax Signaling Pathway in Cerebral Ischemic Rats. *Neuroscience* 527, 37–51 (2023).

1174. Winkle, M., El-Daly, S. M., Fabbri, M. & Calin, G. A. Noncoding RNA therapeutics — challenges and potential solutions. *Nat Rev Drug Discov* 20, 629–651 (2021).

1175. Rupaimoole, R. & Slack, F. J. MicroRNA therapeutics: towards a new era for the management of cancer and other diseases. *Nat Rev Drug Discov* 16, 203–222 (2017).

1176. Biray Avcı, Ç., Özcan, İ., Balcı, T., Özer, Ö. & Gündüz, C. Design of polyethylene glycol-polyethylenimine nanocomplexes as non-viral carriers: mir-150 delivery to chronic myeloid leukemia cells. *Cell Biol Int* 37, 1205–1214 (2013).

1177. Østergaard, M. E. *et al.* Efficient Synthesis and Biological Evaluation of 5'-GalNAc Conjugated Antisense Oligonucleotides. *Bioconjug Chem* 26, 1451–1455 (2015).

1178. Tsoumpra, M. K. *et al.* Peptide-conjugate antisense based splice-correction for Duchenne muscular dystrophy and other neuromuscular diseases. *EBioMedicine* 45, 630–645 (2019).

1179. Jewell, C. M. *et al.* Oligonucleotide Delivery by Cell-Penetrating "Striped" Nanoparticles. *Angew Chem Int Ed Engl* 50, 12312–12315 (2011).

1180. Grafals-Ruiz, N. *et al.* Brain Targeted Gold Liposomes Improve RNAi Delivery for Glioblastoma. *International Journal of Nanomedicine* 15, 2809–2828 (2020).

1181. Keskin, S. *et al.* AAV5-miHTT Lowers Huntingtin mRNA and Protein without Off-Target Effects in Patient-Derived Neuronal Cultures and Astrocytes. *Mol Ther Methods Clin Dev* 15, 275–284 (2019).

1182. van Rooij, E. The Art of MicroRNA Research. *Circulation Research* 108, 219–234 (2011).

1183. Zhou, Y. *et al.* Exosome-mediated small RNA delivery for gene therapy. *WIREs RNA* 7, 758–771 (2016).

1184. Gupta, D. *et al.* Quantification of extracellular vesicles in vitro and in vivo using sensitive bioluminescence imaging. *J Extracell Vesicles* 9, 1800222.

1185. Xu, L. *et al.* Design of experiment (DoE)-driven in vitro and in vivo uptake studies of exosomes for pancreatic cancer delivery enabled by copper-free click chemistry-based labelling. *J Extracell Vesicles* 9, 1779458 (2020).

1186. Wu, A. Y.-T. *et al.* Multiresolution Imaging Using Bioluminescence Resonance Energy Transfer Identifies Distinct Biodistribution Profiles of Extracellular Vesicles and Exomeres with Redirected Tropism. *Advanced Science* 7, 2001467 (2020).

1187. Hong, D. S. *et al.* Phase 1 study of MRX34, a liposomal miR-34a mimic, in patients with advanced solid tumours. *Br J Cancer* 122, 1630–1637 (2020).

1188. Sioud, M. Induction of Inflammatory Cytokines and Interferon Responses by Double-stranded and Single-stranded siRNAs is Sequence-dependent and Requires Endosomal Localization. *Journal of Molecular Biology* 348, 1079–1090 (2005).

1189. Sioud, M. Single-stranded small interfering RNA are more immunostimulatory than their double-stranded counterparts: a central role for 2'-hydroxyl uridines in immune responses. *Eur J Immunol* 36, 1222–1230 (2006).

1190. Sledz, C. A., Holko, M., de Veer, M. J., Silverman, R. H. & Williams, B. R. G. Activation of the interferon system by short-interfering RNAs. *Nat Cell Biol* 5, 834–839 (2003).

1191. Elmén, J. *et al.* Locked nucleic acid (LNA) mediated improvements in siRNA stability and functionality. *Nucleic Acids Res* 33, 439–447 (2005).

1192. Khan, A. A. *et al.* Transfection of small RNAs globally perturbs gene regulation by endogenous microRNAs. *Nat Biotechnol* 27, 549–555 (2009).

1193. Grimm, D. *et al.* Fatality in mice due to oversaturation of cellular microRNA/short hairpin RNA pathways. *Nature* 441, 537–541 (2006).

1194. Ui-Tei, K., Naito, Y., Nishi, K., Juni, A. & Saigo, K. Thermodynamic stability and Watson-Crick base pairing in the seed duplex are major determinants of the efficiency of the siRNA-based off-target effect. *Nucleic Acids Res* 36, 7100–7109 (2008).

1195. Pisano, M. *et al.* Targeting Bcl-2 protein in treatment of melanoma still requires further clarifications. *Ann Oncol* 19, 2092–2093 (2008).

1196. Vo, D. D. *et al.* Targeting the production of oncogenic microRNAs with multimodal synthetic small molecules. *ACS Chem Biol* 9, 711–721 (2014).

1197. Avitabile, C. *et al.* Targeting pre-miRNA by Peptide Nucleic Acids. *Artif DNA PNA XNA* 3, 88–96 (2012).

1198. Hansen, T. B. *et al.* Natural RNA circles function as efficient microRNA sponges. *Nature* 495, 384–388 (2013).

1199. Murakami, K. & Miyagishi, M. Tiny masking locked nucleic acids effectively bind to mRNA and inhibit binding of microRNAs in relation to thermodynamic stability. *Biomedical Reports* 2, 509–512 (2014).

1200. Limmroth, V., Barkhof, F., Desem, N., Diamond, M. P. & Tachas, G. CD49d antisense drug ATL1102 reduces disease activity in patients with relapsing-remitting MS. *Neurology* 83, 1780–1788 (2014).

1201. Lovett-Racke, A. E. *et al.* Silencing T-bet defines a critical role in the differentiation of autoreactive T lymphocytes. *Immunity* 21, 719–731 (2004).

1202. Doi, Y. *et al.* Orphan nuclear receptor NR4A2 expressed in T cells from multiple sclerosis mediates production of inflammatory cytokines. *Proc Natl Acad Sci U S A* 105, 8381–8386 (2008).

1203. Yang, Y. *et al.* Silencing Nogo-A promotes functional recovery in demyelinating disease. *Ann Neurol* 67, 498–507 (2010).

1204. Kalantari, T. *et al.* Tolerogenic dendritic cells produced by lentiviral-mediated CD40- and interleukin-23p19-specific shRNA can ameliorate experimental autoimmune encephalomyelitis by suppressing T helper type 17 cells. *Clin Exp Immunol* 176, 180–189 (2014).

1205. Wang, C.-J. *et al.* Lingo-1 Inhibited by RNA Interference Promotes Functional Recovery of Experimental Autoimmune Encephalomyelitis. *The Anatomical Record* 297, 2356–2363 (2014).

1206. Baharlooi, H., Mansourabadi, A. H., Minbashi Moeini, M., Mohamed Khosroshahi, L. & Azimi, M. Nucleic Acids as Novel Therapeutic Modalities to Address Multiple Sclerosis Onset and Progression. *Cell Mol Neurobiol* 42, 2611–2627 (2022).

1207. Nastasijevic, B. *et al.* Remyelination induced by a DNA aptamer in a mouse model of multiple sclerosis. *PLoS One* 7, e39595 (2012).

1208. Wang, T., Larcher, L. M., Ma, L. & Veedu, R. N. Systematic Screening of Commonly Used Commercial Transfection Reagents towards Efficient Transfection of Single-Stranded Oligonucleotides. *Molecules* 23, 2564 (2018).

1209. Fiszer-Kierzkowska, A. *et al.* Liposome-based DNA carriers may induce cellular stress response and change gene expression pattern in transfected cells. *BMC Molecular Biology* 12, 27 (2011).

1210. Jin, H. Y. *et al.* Transfection of microRNA mimics should be used with caution. *Frontiers in Genetics* 6, (2015).

1211. Merrill, J. E. In Vitro and In Vivo Pharmacological Models to Assess Demyelination and Remyelination. *Neuropsychopharmacol* 34, 55–73 (2009).

1212. Demerens, C. *et al.* Induction of myelination in the central nervous system by electrical activity. *Proceedings of the National Academy of Sciences* 93, 9887–9892 (1996).

1213. Marangon, D. *et al.* Novel in vitro Experimental Approaches to Study Myelination and Remyelination in the Central Nervous System. *Frontiers in Cellular Neuroscience* 15, (2021).

1214. Lee, S., Chong, S. Y. C., Tuck, S. J., Corey, J. M. & Chan, J. R. A rapid and reproducible assay for modeling myelination by oligodendrocytes using engineered nanofibers. *Nat Protoc* 8, 771–782 (2013).

1215. Hu, B. *et al.* NF155-overexpression promotes remyelination and functional restoration in a hypoxic-ischemic mixed neonatal rat forebrain cell culture system. *Neuroscience Letters* 718, 134743 (2020).

1216. Azevedo, M. M. *et al.* Jmy regulates oligodendrocyte differentiation via modulation of actin cytoskeleton dynamics. *Glia* 66, 1826–1844 (2018).

1217. Shimizu, S., Ishino, Y., Tohyama, M. & Miyata, S. NDE1 positively regulates oligodendrocyte morphological differentiation. *Sci Rep* 8, 7644 (2018).

1218. Humpel, C. Organotypic brain slice cultures: A review. *Neuroscience* 305, 86–98 (2015).

1219. Patel, M. *et al.* The miR-183/Taok1 Target Pair Is Implicated in Cochlear Responses to Acoustic Trauma. *PLoS One* 8, e58471 (2013).

1220. Carriel, V., Campos, A., Alaminos, M., Raimondo, S. & Geuna, S. Staining Methods for Normal and Regenerative Myelin in the Nervous System. *Methods Mol Biol* 1560, 207–218 (2017).

1221. Ransohoff, R. M. Animal models of multiple sclerosis: the good, the bad and the bottom line. *Nat Neurosci* 15, 1074–1077 (2012).

1222. Matsushima, G. K. & Morell, P. The Neurotoxicant, Cuprizone, as a Model to Study Demyelination and Remyelination in the Central Nervous System. *Brain Pathology* 11, 107–116 (2001).

1223. Bottes, S. & Jessberger, S. Live imaging of remyelination in the adult mouse corpus callosum. *Proc. Natl. Acad. Sci. U.S.A.* 118, e2025795118 (2021).

1224. Nait-Oumesmar, B. *et al.* Progenitor cells of the adult mouse subventricular zone proliferate, migrate and differentiate into oligodendrocytes after demyelination. *European Journal of Neuroscience* 11, 4357–4366 (1999).

1225. Plemel, J. R. *et al.* Mechanisms of lysophosphatidylcholine-induced demyelination: A primary lipid disrupting myelinopathy. *Glia* 66, 327–347 (2018).

1226. Baxi, E. G. *et al.* Transfer of Myelin-Reactive Th17 Cells Impairs Endogenous Remyelination in the Central Nervous System of Cuprizone-Fed Mice. *J. Neurosci.* 35, 8626–8639 (2015).

1227. Gerhauser, I., Hansmann, F., Ciurkiewicz, M., Löscher, W. & Beineke, A. Facets of Theiler's Murine Encephalomyelitis Virus-Induced Diseases: An Update. *International Journal of Molecular Sciences* 20, (2019).

1228. Sun, P., Liu, D. Z., Jickling, G. C., Sharp, F. R. & Yin, K.-J. MicroRNA-based therapeutics in central nervous system injuries. *J Cereb Blood Flow Metab* 38, 1125–1148 (2018).

1229. Shamaeizadeh, N., Varshosaz, J., Mirian, M. & Aliomrani, M. Glutathione targeted tragacanthic acid-chitosan as a non-viral vector for brain delivery of miRNA-219a-5P: An in vitro/in vivo study. *International Journal of Biological Macromolecules* 200, 543–556 (2022).

1230. Wang, D. *et al.* MiR-128-3p Alleviates Spinal Cord Ischemia/Reperfusion Injury Associated Neuroinflammation and Cellular Apoptosis via SP1 Suppression in Rat. *Frontiers in Neuroscience* 14, (2020).

1231. Yang, J., Zhang, X., Chen, X., Wang, L. & Yang, G. Exosome Mediated Delivery of miR-124 Promotes Neurogenesis after Ischemia. *Mol Ther Nucleic Acids* 7, 278–287 (2017).

1232. Lee, S.-T. *et al.* miR-206 regulates brain-derived neurotrophic factor in Alzheimer disease model. *Ann Neurol* 72, 269–277 (2012).

1233. Merkler, D. *et al.* Multicontrast MRI of remyelination in the central nervous system. *NMR in Biomedicine* 18, 395–403 (2005).

1234. Deloire-Grassin, M. S. *et al.* In vivo evaluation of remyelination in rat brain by magnetization transfer imaging. *J Neurol Sci* 178, 10–16 (2000).